

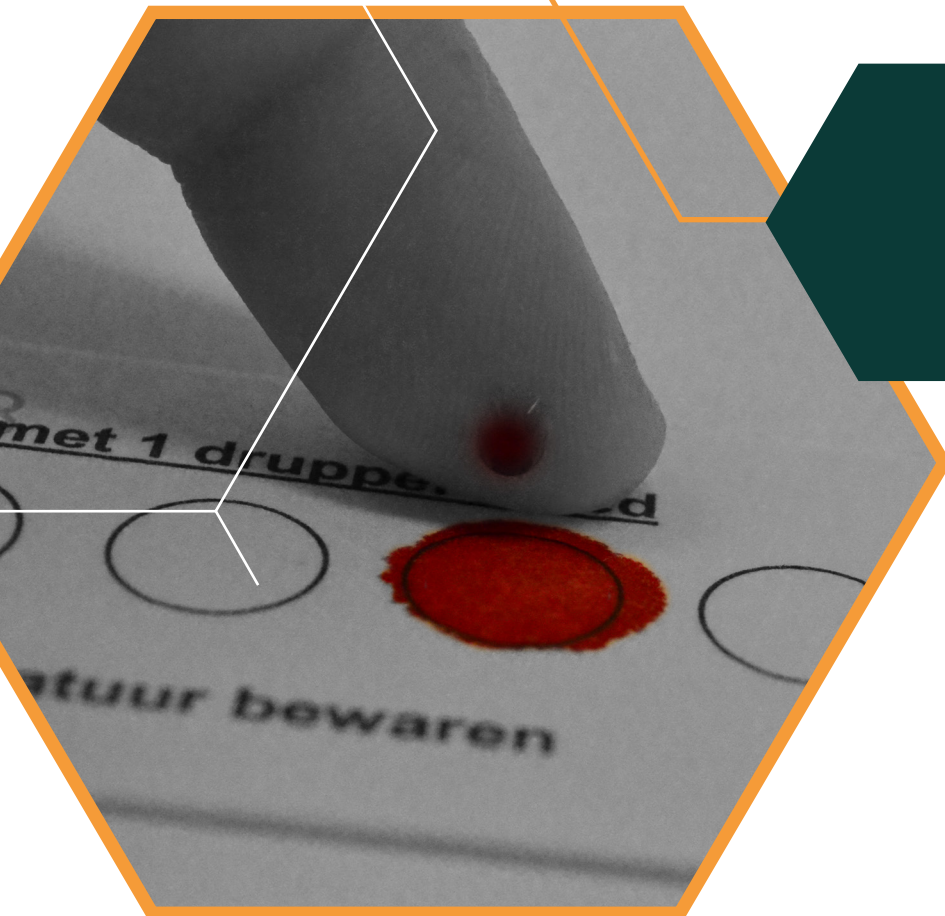


IMPORTANT INSIGHTS

FROM DISCRETE DETAILS

Hanneke Haijes

Gaining insight in pathophysiology of inborn errors of metabolism through deep metabolic phenotyping



IMPORTANT INSIGHTS FROM DISCRETE DETAILS

**Gaining insight in pathophysiology of inborn errors of metabolism
through deep metabolic phenotyping**

Hanneke Haijes

The studies described in this thesis were carried out at the metabolic diagnostic laboratory of the University Medical Centre Utrecht, the Netherlands. All studies in this thesis were financially supported by the Alexandre Suerman Stipend of the University Medical Centre Utrecht. Studies described in chapter 5-9 were financially supported by Metakids (2017-075) and studies described in chapter 13-14 were financially supported by Stofwisselkracht. The study described in chapter 4 received additional financial support from the Czech Ministry of Health (17-29423A), the Oxford National Institute for Health Research and the Health Innovation Challenge Fund (R6-388/WT100127), the Duke University Health System, the Telethon Undiagnosed Diseases Program of the Telethon Foundation (GSP15001), Mining for Miracles of the British Columbia Children's Hospital Foundation and the Clinical Assessment of the Utility of Sequencing as a Service (CAUSES) study of Genome British Columbia, the Deutsche Forschungsgesellschaft (SFB850, SFB992) and the Proteins at Work program of the Netherlands Organization for Scientific Research (NWO 184.032.201). The study described in chapter 9 received additional financial support from the Child Health Initiative Limiting Disability – Brain Research Improving Growth and Health Trajectories (CHILD-BRIGHT) of the Canadian Institutes of Health Research (CIHR-SCA-145104), the British Columbia Children's Hospital Foundation and the Michael Smith Foundation for Health Research.

ISBN: 978-90-393-7275-3
Cover design: Anika Siepel, Hanneke Haijes
Lay-out: Anika Siepel, Hanneke Haijes
Printed by: Ridderprint Alblaserdam, www.ridderprint.nl

© H.A. Haijes, 2020. All rights reserved.

No part of this thesis may be reproduced, stored in a retrieval system or transmitted in any form or by any means without prior written permission of the author.

IMPORTANT INSIGHTS FROM DISCRETE DETAILS

**Gaining insight in pathophysiology of inborn errors of metabolism
through deep metabolic phenotyping**

Belangrijke inzichten uit schijnbaar onopvallende details:
inzicht krijgen in de ziektemechanismen van metabole ziekten
door het diepgaand in kaart brengen van het metabole fenotype

(met een samenvatting in het Nederlands)

Proefschrift

ter verkrijging van de graad van doctor aan de
Universiteit Utrecht
op gezag van de
rector magnificus, prof. dr. H.R.B.M. Kummeling,
ingevolge het besluit van het college voor promoties
in het openbaar te verdedigen op

donderdag 14 mei 2020 des middags te 2.30 uur

door

Hanneke Albertine Haijes-Siepel

geboren op 11 maart 1992
te Apeldoorn

Promotor:

Prof. dr. N.M. Verhoeven-Duif

Copromotoren:

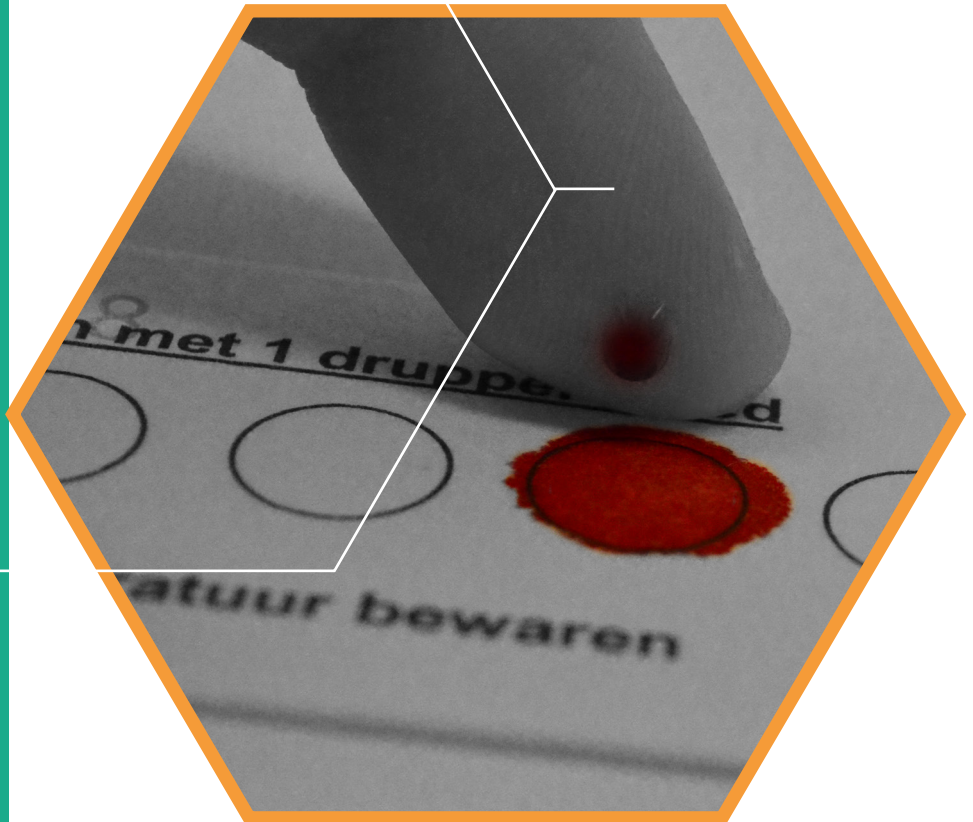
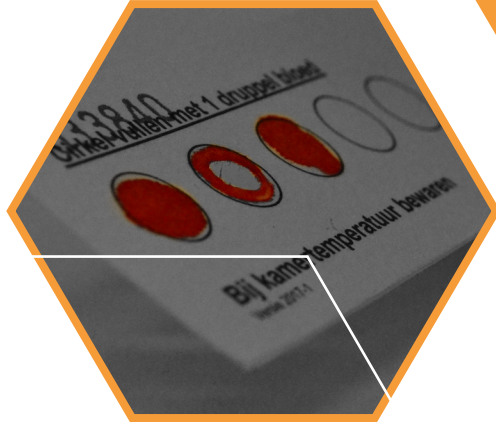
Dr. P.M. van Hasselt

Dr. J.J.M. Jans

TABLE OF CONTENTS

Chapter 1	General introduction and outline of this thesis	9
Part I	Phenomics	
Chapter 2	Hypothesis: Lobe A (COG1-4)-CDG causes a more severe phenotype than lobe B (COG5-8)-CDG	21
Chapter 3	Hypothesis: determining phenotypic specificity facilitates understanding of pathophysiology in rare genetic disorders	33
Chapter 4	<i>De novo</i> heterozygous variants in <i>POLR2A</i> cause a neuro-developmental syndrome with infantile-onset hypotonia	57
Part II	Metabolomics	
Chapter 5	Direct-infusion based metabolomics identifies metabolic disease in patients' dried blood spots and plasma	95
Chapter 6	Direct-infusion based metabolomics unveils biochemical profiles of inborn errors of metabolism in cerebrospinal fluid	113
Chapter 7	Untargeted metabolomics for metabolic diagnostic screening with automated data interpretation using a knowledge-based algorithm	127
Chapter 8	Assessing the pre-analytical stability of small-molecule metabolites in cerebrospinal fluid using direct-infusion metabolomics	143
Chapter 9	Aspartylglucosamine is a biomarker for NGLY1-CDDG, a congenital disorder of deglycosylation	161
Chapter 10	Accurate discrimination of Hartnup disorder from other aminoacidurias using a diagnostic ratio	171

Part III	Deep metabolic phenotyping	
Chapter 11	Pathophysiology of propionic and methylmalonic acidemias. Part 1: Complications	183
Chapter 12	Pathophysiology of propionic and methylmalonic acidemias. Part 2: Treatment strategies	209
Chapter 13	Retrospective evaluation of the Dutch pre-newborn screening cohort for propionic acidemia and isolated methylmalonic acidemia: what to aim, expect, and evaluate from newborn screening?	233
Chapter 14	High protein prescription in methylmalonic and propionic acidemia patients and its negative association with long-term outcome	265
Chapter 15	Understanding acute metabolic decompensation in propionic and methylmalonic acidemias: a deep metabolic phenotyping approach	289
Chapter 16	General discussion	311
Appendices	Samenvatting	332
	Summary	336
	List of abbreviations	340
	List of publications	342
	Dankwoord	344
	Curriculum vitae	348



1

General introduction

and outline of this thesis

RATIONALE AND SCOPE OF THIS THESIS

Only one year ago, a fifteen-year-old girl with perfect vision commuted to high school by bike daily, surrounded by friends. Now at sixteen, she is almost blind and needs a cab to visit a special school, on her own. She has been ambushed by optic atrophy, one of the devastating and poorly understood long-term complications of methylmalonic acidemia (MMA), an inborn error of metabolism (IEM). Despite regular outpatient visits, clinicians were not able to predict, prevent or treat the occurrence of this disastrous complication.

This serious example illustrates our lack of understanding of these types of diseases. Moreover, it formed the start of this thesis and instigated our efforts to better understand these types of diseases. IEM are rare diseases, with a prevalence of a few individuals worldwide to 1:18,000 for the most common IEM, phenylketonuria (PKU). Altogether, these rare diseases affect 10,000 Dutch families, with 800 patients per year being diagnosed with an IEM in the Netherlands, according to the Dutch patient organization. For many IEM, pathophysiology, which is the understanding of how a certain genotype could lead to a certain phenotype, is hardly understood. This lack of understanding is caused by the rarity of each individual disease and by the inherent scarcity of available data. This raises major challenges with respect to understanding and predicting a patient's disease course, and for conceiving treatment strategies, as exemplified by our blind sixteen-year-old MMA patient. The scarcity of available data for rare IEM demands for an intelligible use of available data and resources. To increase insight into pathophysiology, a more in-depth assessment of a disease, as thoroughly and as comprehensively as possible, is required. The scope of this thesis is the development of different approaches to study pathophysiology of IEM more in-depth than has been done in the past. Hereby, we aim to identify discrete details, originating either from the patient's phenotype or metabolome, that have the potential to lead to important insights into pathophysiology, to serve our ultimate aim of providing clinicians with more knowledge to predict, prevent or treat clinical problems arising in these destructive IEM.

In this chapter we introduce pathophysiology, IEM and the specific conditions addressed in this thesis. In addition, we present the three parts of this thesis: phenomics, metabolomics and deep metabolic phenotyping, by providing an outline of the following chapters.

PATHOPHYSIOLOGY: FROM GENOTYPE TO PHENOTYPE

According to the medical dictionaries, "physiology" describes processes within an organism and "pathology" describes conditions observed during a disease state. Pathophysiology then, according to the medical dictionaries, is the study of disordered physiological processes that cause, result from or are associated with disease or injury. Pathophysiology thus seeks to explain the functional changes that are occurring within an individual due to a disease. For genetic diseases, insight into pathophysiology means understanding of how a certain genotype can lead to a certain phenotype within an individual. Over the years, this has aided disease recognition, development of diagnostic methods and development of treatment strategies (as illustrated in BOX I). Even when no treatment is available, insight into pathophysiology can aid counseling of patients and families on a patient's disease course and prognosis and on decisions about reproduction.

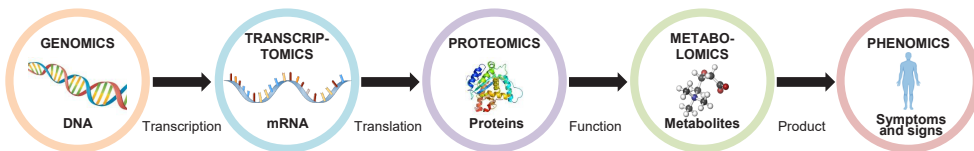
To increase insight into how a certain genotype can lead to a certain phenotype within an individual, different layers of information can be studied in great detail. Biological fields of interest termed "-omics" aim to characterize and quantify a certain group of biological molecules (Figure 1).

BOX I. The value of insight into pathophysiology

Hyperphenylalaninemia is usually due to a deficiency of the enzyme phenylalanine hydroxylase deficiency, called PKU. This disease, which is characterized by mental retardation, strongly smelling urine and increased excretion of phenylpyruvic acid in urine, was first described in 1934 by Asbjørn Følling.¹ In 1953, hepatic phenylalanine hydroxylase activity was shown to be deficient in the PKU patient² and in 1954, the pathophysiological insight that accumulating L-phenylalanine might cause the mental retardation in untreated PKU patients led to the discovery that a low phenylalanine diet could prevent hyperphenylalaninemia in PKU patients, with benefit to cognitive function.³ In 1963, a laboratory test suitable for population screening in the newborn was developed⁴ and newborn screening programs appeared worldwide to attain early diagnosis and treatment in PKU patients, to prevent mental retardation.⁵ Although to date, there is still no final cure for PKU, treatment consisting of a low phenylalanine diet, additional treatment with large neutral amino acids and in some, treatment with tetrahydrobiopterin, can prevent mental retardation to a great extent.⁵

The unraveling of the route from genotype to phenotype starts at the genome, which is studied by genomics. This includes the study of epigenomics, which is the study of modifications onto the genetic material (DNA) of a cell. DNA is transcribed into messenger RNA (mRNA), which is studied by transcriptomics. Subsequently, mRNA is translated into proteins, which is studied by proteomics. Proteins fulfill different functions in the organism, including enzymes, transporters and chaperones, affecting the concentrations of many different metabolites. These metabolites are studied by metabolomics. Lastly, changes in concentrations of metabolites can induce different symptoms and signs in an individual, which is studied by phenomics (Figure 1).

Figure 1, different -omics techniques



With each step from genomics to phenomics, the influence of the environment increases. Data interpretation gets harder, since it is difficult to determine what the influence of the genetic defect on the observed alteration is, and what the influence of the environment is. As nearly all IEM are caused by pathogenic genetic variants in single genes, genomics will be addressed to some extent throughout the thesis. However, the focus of this thesis will be on phenomics in part I, on metabolomics in part II and on the combination of phenomics and metabolomics in part III. Transcriptomics is not addressed, and proteomics will be addressed only shortly (**chapter 4**).

INBORN ERRORS OF METABOLISM

IEM are considered to be “any condition in which the impairment of a biochemical pathway is intrinsic to the pathophysiology of the disease”.⁶ These biochemical pathways concern protein, fat and carbohydrate metabolism, but also metabolism of vitamins and minerals. IEM are a large class of genetic diseases, of which the main part is monogenetic. The genes affected in IEM mostly encode enzymes that facilitate conversion of metabolic substrates into products. Clinical problems of enzyme deficiencies can either arise from accumulation of the substrate or from a deficiency of the product. IEM can also be due to transporter

deficiencies. In these IEM, a specific metabolite cannot be transported into the tissue, cell or organelle where it is supposed to perform its function in a biochemical pathway. These location-specific deficiencies can lead to a variety of clinical problems as well.

Recently, a new classification of IEM was proposed (BOX II). More than 1,000 individual IEM were listed and grouped according to their pathophysiological basis.⁶ In this thesis we discuss, according to this nosology, two categories of IEM: congenital disorders of glycosylation (CDG) and disorders of nitrogen-containing compounds.

BOX II. A proposed nosology of inborn errors of metabolism⁶

Criteria used for the inclusion of an IEM in the current nosology are: 1) The disruption of a metabolic pathway is considered necessary and sufficient for inclusion, regardless of laboratory abnormalities in standard biochemical test and regardless of an association with clinical manifestations of disease. 2) Severity alone is not considered sufficient for separation into different entries when a single gene product is involved, regardless of the mode of inheritance. 3) A different pathomechanism is considered necessary for separation into different entries when a single gene product is involved, regardless of the mode of inheritance. 4) The involvement of different gene products is considered sufficient for separation into different entries, even if the phenotype is similar. 5) The error must have been reported in more than a single family, and the involvement of the gene product must have been well characterized on an enzymatic or molecular level.

Based on these criteria, nine categories with 130 groups containing 1,105 IEM were defined. An additional 111 disease descriptions fell into the final category with lack of substantiation, until further confirmation of their validity as unique errors is established based on either enzymatic or molecular grounds, or until reports of a second individual/family are available.⁶

Congenital disorders of glycosylation: COGx-CDG and NGLY1-CDDG

In the category CDG, in the group glycosylation disorders of vesicular trafficking, we discuss COGx-CDG (**chapter 2** and **3**). This group of disorders, seven IEM in total, is caused by deficiencies of the conserved oligomeric Golgi complex (COG), subunits 1-8, except subunit 3.⁷ The COG subunits are encoded by *COG1–COG8* and are divided into two lobes, lobe A, consisting of subunit COG1-COG4 and lobe B, consisting of subunit COG5-COG8. The COG complex is a tethering protein that mediates the approach and fusion of vesicles with Golgi membranes. Correct tethering of these vesicles is essential for proper positioning of glycosyltransferases that catalyze the attachment of sugar donors onto glycans. In patients with COGx-CDG, vesicular trafficking in the Golgi apparatus is disturbed, and thereby the construction of glycans in the Golgi apparatus is affected. This leads to a phenotype that is characterized by global developmental delay, microcephaly, failure to thrive, elevated hepatic transaminases, muscular hypotonia, episodic fever and infantile death.⁷ To date, 45 COGx-CDG patients have been described (**chapter 3**), but pathophysiology of this disease is largely unknown.

Also in the category CDG, in the group congenital disorders of deglycosylation (CDDG), we introduce NGLY1-CDDG. This IEM is caused by a deficiency of the enzyme peptide:*N*-glycanase (**chapter 9**), which is encoded by *NGLY1*. In patients with NGLY1-CDDG, degradation of *N*-glycans in the endoplasmic reticulum is disturbed. This leads to a phenotype that is characterized by global developmental delay, movement disorders, muscular hypotonia, decreased deep tendon reflexes, electroencephalogram abnormalities, microcephaly, hypo- or alacrima, elevated hepatic transaminases and constipation. To date, 22 NGLY1-CDDG patients have been described, but the patient organization is aware of more than 60 patients diagnosed worldwide with NGLY1-CDDG (**chapter 9**).

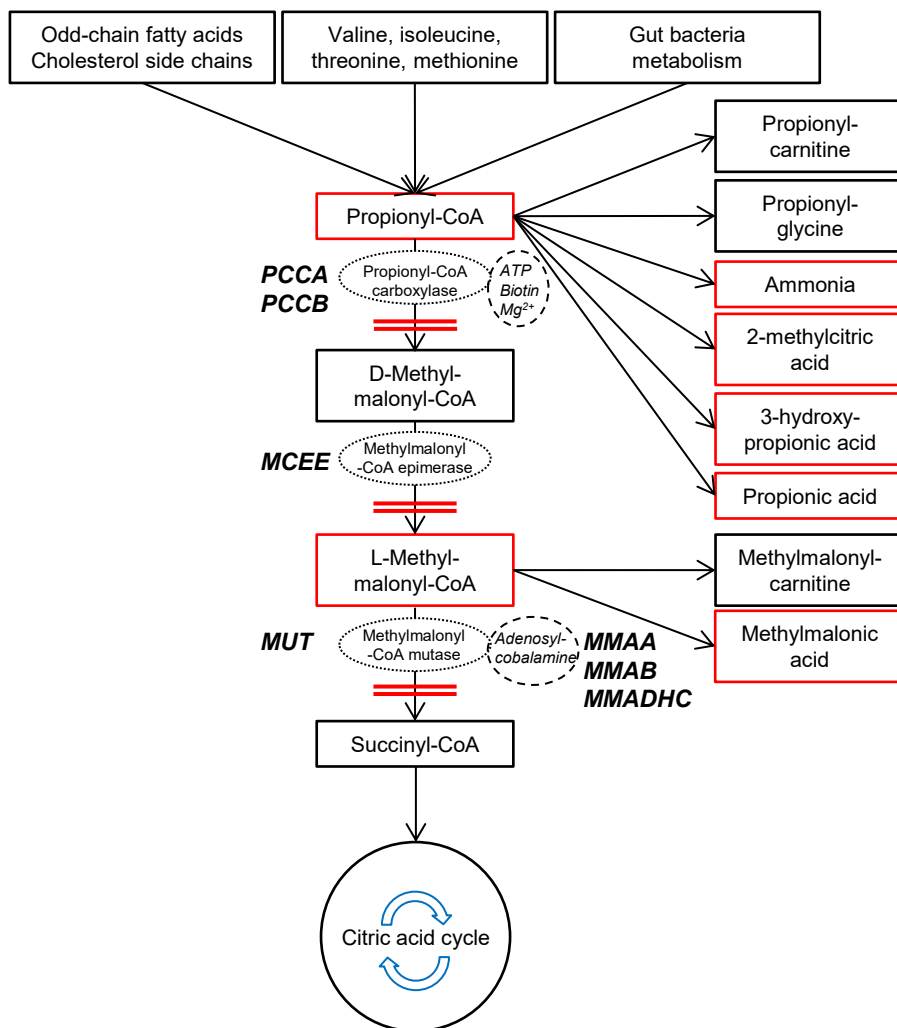
Disorders of nitrogen-containing compounds: Hartnup disease, propionic aciduria and isolated methylmalonic aciduria

In the category disorders of nitrogen-containing compounds, in the group disorders of amino acid transport, we report on Hartnup disorder, which is caused by a deficiency of the B⁰ AT1 neutral amino acid transporter (**chapter 10**). This transporter is encoded by *SLC6A19*. In patients with Hartnup disorder, excretion of a specific set of amino acids in the proximal kidney tubule is increased, due to disturbed reabsorption of these amino acids. This could result in deficiencies of these amino acids, in particular tryptophan. As tryptophan is the precursor of nicotinamide and serotonin, this transporter deficiency may lead to a phenotype similar to a nicotinamide (vitamin B3) deficiency, characterized by a pellagra-like rash, light-sensitive dermatitis, intermittent cerebellar ataxia and psychiatric symptoms as emotional instability, delirium and hallucinations.⁸ Hartnup disorder has an estimated frequency of 1:20.000,⁹ but nowadays the majority of individuals remain asymptomatic due to a protein-rich diet.^{8,10}

Also in the category disorders of nitrogen-containing compounds, in the group disorders of branched-chain amino acid metabolism, we describe propionic aciduria (PA), caused by a deficiency of propionyl-CoA carboxylase¹¹ and isolated MMA, either caused by a deficiency of methylmalonyl-CoA mutase or methylmalonyl-CoA epimerase, or by a diminished synthesis or availability of the cofactor for methylmalonyl-CoA mutase, 5'-deoxyadenosylcobalamin, which is associated with cobalamin A, B or D deficiency (Figure 2) (**chapter 11-15**).¹² Subunits of propionyl-CoA carboxylase are encoded by *PCCA* and *PCCB*,¹¹ methylmalonyl-CoA mutase is encoded by *MUT*, methylmalonyl-CoA epimerase is encoded by *MCEE* and proteins involved in cobalamin A, B and D deficiency are encoded by *MMAA*, *MMAB* and *MMADHC*, respectively.¹² The latter three disorders are categorized among disorders of vitamins, cofactors, metals and minerals, and grouped as disorders of cobalamin metabolism, as the pathophysiological mechanism leading to isolated MMA is different from *MUT* and *MCEE* type MMA.⁶

Both PA and MMA impair the biochemical pathway of breakdown of propionyl-CoA (Figure 2). Accumulation of propionyl-CoA, leading to accumulation of many other metabolites (Figure 2), is the main cause for the phenotype that PA and MMA patients demonstrate. The clinical course of these patients usually starts with an acute metabolic decompensation (AMD) in the neonatal period or thereafter. During an AMD, the acidic nature of circulating toxic metabolites rapidly causes a metabolic acidosis, with high anion-gap, hyperammonemia and lactic acidosis. Clinically, this can result in lethargy, anorexia, vomiting, dehydration, hypotonia, Kussmaul breathing, coma or even death. Oftentimes, the first symptomatic phase causes irreversible neurological damage, manifesting as for example movement disorders in varying severity and/or psychomotor retardation. This neurological damage can be visible as white matter lesions and/or basal ganglia hyperintensities on magnetic resonance imaging. Next to the neurological damage, the clinical course of PA and MMA is characterized by metabolic instability resulting in frequent AMD, by cognitive deficits and by many different long-term complications (**chapter 11-15**)^{11,12} including the sudden onset of optic atrophy, as mentioned in the first paragraph of this chapter.

Figure 2. Biochemical pathway of propionyl-CoA breakdown



Enzymatic deficiencies of propionyl-CoA carboxylase, methylmalonyl-CoA epimerase and methylmalonyl-CoA mutase are indicated by double red lines. Affected genes are depicted in bold italics. Accumulating toxic metabolites are indicated by red rectangles and decreased activity of the citric acid cycle is indicated by blue arrows.

Transcription disorder

Lastly, we discuss a disorder involving RPB1, which is the largest subunit of the RNA polymerase II complex. This subunit is encoded by *POLR2A*. This genetic disease is not an IEM, as impairment of a biochemical pathway is not intrinsic to the pathophysiology of the disease. Instead, in patients with pathogenic variants in *POLR2A*, transcription of protein-encoding genes and short non-coding RNA genes is hampered, leading to a phenotype which is characterized by profound infantile-onset muscular hypotonia, global developmental delay, strabismus, decreased endurance and feeding difficulties (**chapter 4**).

PHENOMICS

Phenomics is the systematic study of phenotypes, including all physical and biochemical traits that an organism can demonstrate. “Deep phenotyping” is being advocated to increase insight into pathophysiology of rare disorders by describing the physical state of an individual as comprehensively and thoroughly as possible.^{13,14} In **chapter 2-4** we investigate the use of several deep phenotyping approaches to use scarce data with utmost efficiency in order to unveil pathophysiology of rare genetic diseases.

In **chapter 2** we hypothesize that a deficiency of one of the subunits of lobe A of the COG complex causes a more severe phenotype than a comparable molecular defect of one of the subunits of lobe B of the COG complex. We investigate this hypothesis by studying the phenotypes of mutant COGx cell lines, by deep phenotyping of each COGx-CDG patient reported in literature and by quantification of the phenotypic severity of these patients.

In **chapter 3** we present an alternative way to increase insight into pathophysiology using deep phenotyping. Hypothesizing that clinical similarities may be indicative of shared pathophysiology, we explored whether highly specific phenotypic features could provide unsuspected understanding of underlying pathophysiology of rare genetic disorders. To test this hypothesis we extract all available data on COGx-CDG from literature. Next, we merge this data using the Human Phenotype Ontology, we retrieve the occurrence of phenotypic features in other genetic diseases from the Human Phenotype Ontology and we study pathophysiology in diseases sharing these highly specific phenotypic features. Hereby, we ultimately aim to link the most specific phenotypic features in COG-CDG to pathophysiological processes in other diseases that also present with these phenotypic features.

In **chapter 4** we study the pathogenicity of sixteen *de novo* heterozygous variants in *POLR2A* through structural evaluation of the protein, proteomics studies and studies in model systems. In addition to these functional studies, we determine the degree of phenotypic overlap in these patients, by the in-depth comparison of all clinical symptoms and signs. Moreover, by quantification of phenotypic severity, we delineate the severity of the consequence of the genetic variants.

METABOLOMICS

Metabolomics is the simultaneous and comprehensive analysis of small-molecule metabolites in a biological sample. Potentially, all intermediates and final products of a metabolic pathway in an organism can be measured in a very short amount of time. Metabolomics is considered to bridge the gap between genotype and phenotype¹⁵ (Figure 1). The recent development of robust metabolomics methods provides an unique opportunity to study rare IEM more in-depth than previously possible.

The predominant tools in the field of metabolomics are nuclear magnetic resonance spectroscopy and mass spectrometry. Mass spectrometry can be performed using gas chromatography, liquid chromatography, capillary electrophoresis, flow-injection analysis or direct-infusion, with each approach having its benefits and hindrances.¹⁵ In addition, metabolomics can be performed “targeted”, with exact identification and quantification of a subset of predefined metabolites, or “untargeted”, with no predefined subset of metabolites to analyze, no exact metabolite identification and with only relative quantification, comparing mass over charge intensities of one or multiple samples to another set of samples. Semi-targeted and semi-quantitative approaches are also often performed, combining quantitative and non-quantitative metabolic assays, in an attempt to circumvent the hindrances of non-quantitative data but maintaining the benefits of capturing a broad range of metabolites.

For IEM, metabolomics is performed for seven main purposes of which four are addressed in this thesis: (1) the development of next-generation metabolic screening platforms (NGMS),^{16,17} (2) the identification of novel single biomarkers or biochemical profiles in predefined patient cohorts, (3) as a functional read-out to aid interpretation of genetic variants of unknown significance and (4) to gain insight into pathophysiology of IEM. Other applications that are not addressed in this thesis are (5) identification of new IEM, (6) monitoring of therapeutic effects and (7) integration of metabolomics with other –omics platforms.

In **chapter 5** we describe the development of a non-quantitative direct-infusion method for NGMS and demonstrate its diagnostic value for both dried blood spots and plasma. In **chapter 6** we disclose the diagnostic value of the method for NGMS in cerebrospinal fluid and in **chapter 7** we report on the performance of a diagnostic knowledge-based algorithm with automated data interpretation, also to serve NGMS.

Metabolomics studies aiming to identify new biomarkers or new IEM or aiming to aid interpretation of genetic variants of unknown significance frequently make use of historical or multicenter cohorts. However, pre-analytical conditions, including sample storage conditions, may vary in these cohorts. This potentially affects metabolite concentrations measured. In **chapter 8** we assess whether small-molecule metabolites in cerebrospinal fluid are affected by changes in storage conditions, to serve interpretation of potential new biomarkers studied in multicenter or historical cohorts. With respect to the identification of new biomarkers in predefined patient cohorts, we demonstrate the identification of a biomarker for NGLY1-CDDG in **chapter 9**. In addition, in **chapter 5** we test whether the ratio trimethyllysine over γ -butyrobetaine supports pathogenicity of an identified variant of unknown significance in *TMLHE*.

Lastly, we study the metabolome of PA and MMA patients in **chapter 15** extensively to evaluate the biochemical processes at play during an AMD, in order to improve understanding of pathophysiology of AMD.

In contrast to the non-quantitative direct-infusion method described in **chapter 5-9** and **chapter 15**, we use in **chapter 10** a targeted metabolomics assay for the exact quantification of amino acid excretion in urine. In asymptomatic individuals, only the amino acid excretion profile might indicate Hartnup disorder, warranting proper distinction of Hartnup disorder from generalized aminoaciduria to prevent misdiagnosis. We test whether quantitative assessment rather than qualitative assessment of amino acid concentrations enhances correct discrimination of Hartnup disorder from other aminoacidurias.

DEEP METABOLIC PHENOTYPING

Deep metabolic phenotyping is the integration of phenomics and metabolomics approaches, to study pathophysiology even more in-depth. In this thesis we performed deep metabolic phenotyping to study pathophysiology of PA and isolated MMA.

Only a few decades ago, patients with PA and isolated MMA had a very poor life expectancy. Nowadays, patients tend to reach adulthood. Next to general advances in clinical care, this has been accomplished through recognition of the pathophysiological mechanisms at play in these diseases. The understanding that both diseases are caused by an enzyme deficiency in the breakdown of branched-chain amino acids (Figure 2) resulted in the implementation of a protein restricted diet.^{18,19} In addition, the recognition that MMA is caused by a deficiency of an enzyme for which cobalamin is a cofactor (Figure 2) paved the way to cobalamin supplementation²⁰ and the understanding that carnitine acts as a scavenger for

the toxic metabolites produced in PA and MMA (Figure 2) led to the introduction of carnitine supplementation.²¹

Despite these therapies, residual disease in these disorders is substantial and current treatment strategies are inadequate for prevention and treatment of the frequently occurring AMD, the neurological deficits, and of many of the complications in PA and MMA. To optimize treatment in order to improve outcome, more insight into the pathophysiology of AMD and complications is essential.

In **chapter 11** we perform an extensive systematic data-analysis of cohort studies and case-reports on PA and MMA. We investigate the prevalence of all known common and rare complications described, illustrating the severity of the phenotype of PA and MMA. We summarize the common denominators in hypotheses on pathophysiology of complications to support that a common hypothesis is that mitochondrial impairment plays a major role. We use data provided by the Human Phenotype Ontology to study which complications are overrepresented or underrepresented in monogenic mitochondrial diseases, as evidence to support a role for mitochondrial impairment in pathophysiology of the complication. We combine this line of evidence with evidence from literature to draw conclusions on the possible role of mitochondrial impairment in each complication.

In **chapter 12** we summarize the biochemical hallmarks of PA and MMA, including altered concentrations of metabolites and altered activities of enzymes. By illustrating these consequences, we display potential therapy targets. We provide a systematic overview of all current, experimental and unexplored treatment strategies in PA and MMA. We discern two approaches: (1) treat the cause, by reducing the amount of toxic metabolites and, in line with our hypothesis in **chapter 11**, (2) treat the effects, by preventing or treating mitochondrial energetic failure and increase of reactive oxygen species formation. We study the available evidence for the effectiveness of the treatment strategies to discern which of the strategies is most promising for attaining substantial improvements in overall outcome for PA and MMA patients.

In **chapter 13** we perform deep phenotyping on a national, retrospective cohort including almost all Dutch PA and MMA patients, to estimate the expected health gain of newborn screening (NBS) for PA and MMA, as NBS for PA and MMA was added to the NBS program of the Netherlands in October 2019. We explore how evaluation of NBS implementation can be performed by assessing clinical outcome parameters and we study the pre-NBS cohort to gain insights that could guide counseling and surveillance of NBS cohorts.

In **chapter 14** we study dietary treatment strategies applied in the pre-NBS cohort in relation to clinical outcome parameters, stratified for disease severity. Hereby, we aim to delineate current best practice in dietary therapy for PA and MMA patients, to guide future treatment strategies.

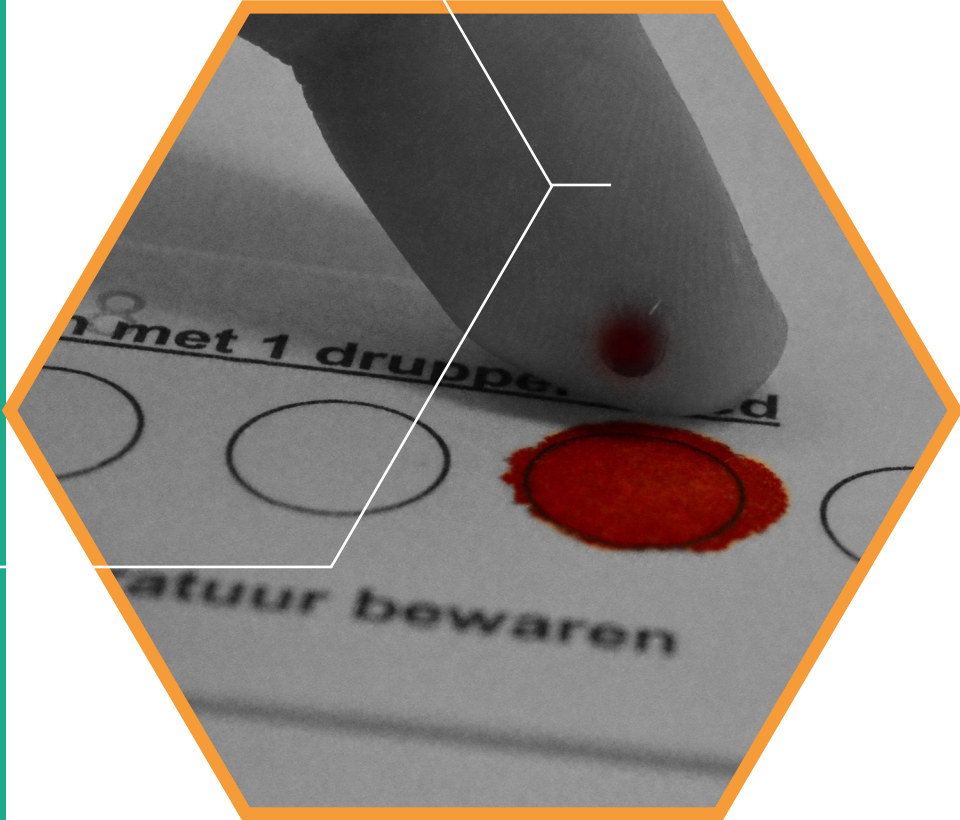
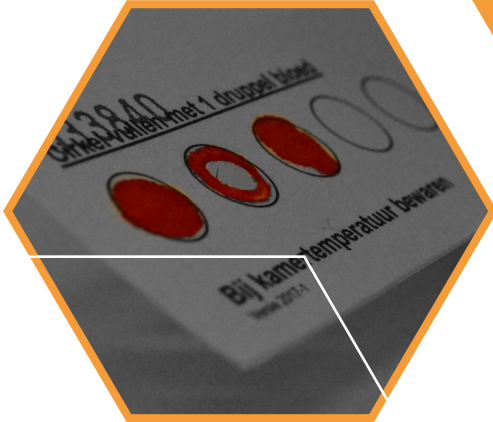
In **chapter 15** we perform deep metabolic phenotyping of PA and MMA patients, by studying the metabolomes of these patients throughout life, to increase pathophysiological understanding of AMD. Hereto, we analyze longitudinal results from targeted biochemical assays and our untargeted, non-quantitative direct-infusion metabolomics method. We integrate our findings with the results of an extensive, systematic search for biomarkers reported in literature, to draw conclusions on the potential biochemical processes at play during AMD.

IMPORTANT INSIGHTS FROM DISCRETE DETAILS

In conclusion, in this thesis we explore the value of different approaches for the in-depth study of pathophysiology in rare IEM, which can be applied despite a small number of patients and scarcity of available data. Throughout this thesis we investigate how these approaches can aid the recognition of discrete details, either from the patient's phenotype or metabolome, and how these details can lead to important insights into pathophysiology. In **chapter 16** we discuss the implications of our findings and we discuss challenges, reflections and prospects regarding our research.

REFERENCES

1. Fölling A. Über Ausscheidung von Phenylbrenztraubensäure in den Harn als Stoffwechselanomalie in Verbindung mit Imbezillität. *Hoppe Seylers Z Physiol Chem.* 1934;277:169-176.
2. Jervis GA. Phenylpyruvic oligophrenia: deficiency of phenylalanine oxidizing system. *Proc Soc Exp Biol Med.* 1953;82:514.
3. Bickel H, Gerrard J, Hickmans EM. Influence of phenylalanine intake on the chemistry and behavior of a phenylketonuric child. *Acta Paediatr.* 1954;43:64.
4. Guthrie R, Susi A. A simple phenylalanine method for detecting phenylketonuria in large populations of newborn infants. *Pediatrics* 1963;32:318-343.
5. Scriver CR. The PAH gene, phenylketonuria, and a paradigm shift. *Hum Mutat.* 2007;28:831:845.
6. Ferreira CR, van Karnebeek CDM, Vockley J, Blau N. A proposed nosology of inborn errors of metabolism. *Genet Med.* 2019;21:102-106.
7. Rymen D, Winter J, van Hasselt PM et al. Key features and clinical variability of COG6-CDG. *Mol Genet Metab.* 2015;116(3):163-70.
8. Camargo SM, Bockenbauer D, Kleta R. Aminoacidurias: clinical and molecular aspects. *Kidney Int.* 2008;73(8):918-925.
9. Levy HL. Hartnup disorder. In: Scriver CR, Sly WS, Valle D (eds) *The metabolic and molecular bases of inherited diseases.* McGraw-Hill, New York; 2001.
10. Wilcken B, Yu JS, Brown DA. Natural history of Hartnup disease. *Arch Dis Child.* 1977;51(1):38-40.
11. Shchelochkov OA, Carillo N, Venditti CP. Propionic acidemia. In: Adam MP, Ardinger HH, Pagon RA et al., eds. *GeneReviews*®. Seattle, WA: University of Washington, Seattle; 1993-2019. Updated: 2016, October 6.
12. Manoli I, Sloan JL, Venditti CP. Isolated methylmalonic acidemia. In: Adam MP, Ardinger HH, Pagon RA et al., eds. *GeneReviews*®. Seattle, WA: University of Washington, Seattle; 1993-2019. Updated: 2016, December 1.
13. Tracy RP. "Deep phenotyping": characterizing populations in the era of genomics and systems biology. *Curr Opin Lipidol.* 2008;19:151-7.
14. Haring R, Wallaschofski H. Diving through the "-omics": the case for deep phenotyping and systems epidemiology. *Omics* 2012;16:231-4.
15. Sandlers Y. The future perspective: metabolomics in laboratory medicine for inborn errors of metabolism. *Transl Res.* 2017;189:65-75.
16. Miller MJ, Kennedy AD, Eckhart AD et al. Untargeted metabolomics analysis for the clinical screening of inborn errors of metabolism. *J Inherit Metab Dis.* 2015;38(6):1029-39.
17. Coene KLM, Kluijtmans LAJ, van der Heeft E et al. Next-generation metabolic screening: targeted and untargeted metabolomics for the diagnosis of inborn errors of metabolism in individual patients. *J Inherit Metab Dis.* 2018;41(3):337-353.
18. Childs B, Nyhan WL, Borden M, Bard L, Cooke RE. Idiopathic hyperglycinemia and hyperglycinuria: a new disorder of amino acid metabolism. I. *Pediatrics* 1961;27:522-38.
19. Nyhan WL, Borden M, Childs B. Idiopathic hyperglycinemia: a new disorder of amino acid metabolism. II. The concentrations of other amino acids in the plasma and their modification by the administration of leucine. *Pediatrics* 1961;27:539-50.
20. Matsui SM, Mahoney MJ, Rosenberg LE. The natural history of the inherited methylmalonic acidemias. *N Engl J Med.* 1983;308:857-861.
21. Roe CR, Millington DS, Maltby DA, Bohan TP, Hoppel CL. L-carnitine enhances excretion of propionyl coenzyme A as propionylcarnitine in propionic acidemia. *J Clin Invest.* 1984;73:1785-1788.



Part I - Phenomics

2

Hypothesis: Lobe A (COG1-4)-CDG causes a more

severe phenotype than lobe B (COG5-8)-CDG

Journal of Medical Genetics 2018, 55(2): 137-142
DOI: 10.1136/jmedgenet-2017-104586

Hanneke A. Haijes*, Jaak Jaeken, François Foulquier, Peter M. van Hasselt

* Corresponding author

ABSTRACT

The conserved oligomeric Golgi (COG) complex consists of eight subunits organized in two lobes: lobe A (COG1–4) and lobe B (COG5–8). The different functional roles of COG lobe A and lobe B might result in distinct clinical phenotypes in patients with COG-CDG (congenital disorders of glycosylation). This hypothesis is supported by three observations. First, knock-down of COG lobe A components affects Golgi morphology more severely than knock-down of COG lobe B components. Second, nearly all of the 27 patients with lobe B COG-CDG had bi-allelic truncating mutations, as compared with only one of the six patients with lobe A COG-CDG. This represents a frequency gap which suggests that bi-allelic truncating mutations in COG lobe A genes might be non-viable. Third, in support, large-scale exome data of healthy adults (Exome Aggregation Consortium (ExAC)) underline that COG lobe A genes are less tolerant to genetic variation than COG lobe B genes. Thus, comparable molecular defects are more detrimental in lobe A COG-CDG than in lobe B COG-CDG. In a larger perspective, clinical phenotypic severity corresponded nicely with tolerance to genetic variation. Therefore, genomic epidemiology can potentially be used as a photographic negative for mutational severity.

KEY MESSAGE

Conserved oligomeric Golgi (COG) lobe A mutations with a comparable molecular defect to COG lobe B mutations cause a more severe COG-CDG (congenital disorders of glycosylation) phenotype.

INTRODUCTION

Congenital disorders of glycosylation (CDG) form a heterogeneous group of rare, mostly autosomal recessive and mostly multi-system conditions, illustrating the biological importance of glycosylation. Deficiencies of the conserved oligomeric Golgi (COG) complex are a subgroup of CDG. The COG complex, a multi-subunit tethering complex, consists of eight subunits organised in two lobes. Lobe A consists of subunits COG1 to COG4 and lobe B consists of subunits COG5 to COG8. The two lobes are bridged by an interaction between the COG1 and COG8 subunits.¹

The function of the COG complex as a whole is to facilitate tethering and fusion of Golgi vesicles in order to deliver the vesicular content to the correct compartment.² However, lobe A and lobe B appear to have different functional roles: while lobe A mainly resides on the Golgi membrane, lobe B mainly resides on non-Golgi vesicles.² In addition, while lobe A appears to be essential for maintaining overall Golgi structure, lobe B impacts recognition and vesicle tethering to the right Golgi compartment.³ Moreover, the two lobes interact differently with other trafficking-related proteins. Lobe A mainly interacts with tethering proteins and coat and motor proteins, while lobe B mainly interacts with SNAREs and Rabs.⁴ It was hypothesized that the different functional roles of COG lobes A and B might result in distinct clinical phenotypes in patients with COG-CDG.

The validity of this hypothesis was assessed in three steps: first, by studying cellular phenotypes of all different COG mutant cell lines; second, by studying clinical phenotypes of all patients with COG-CDG described in literature; third, by studying tolerance to genetic variation of human COG genes in large-scale exome data of healthy adults.

COG lobe A mutants show a more severe cellular phenotype than COG lobe B mutants

COG deficiencies were first studied in the yeast *Saccharomyces cerevisiae*. A clear distinction between COG lobe A and COG lobe B mutant phenotypes was observed. COG lobe A genes appeared to be essential genes since mutants were either inviable or showed a severe growth defect at different temperatures.⁵⁻⁹ Moreover, accumulation of internal membranes and vesicles was observed as well as greatly reduced Golgi glycosylation.¹⁰⁻¹² Conversely, all COG lobe B null strains were viable and showed normal growth rates compared with wild-types at different temperatures.^{9,11} In these strains, only mildly reduced glycosylation and protein secretion was noted.⁹

The consequences of COG deficiencies in non-mammalian multi-cellular species appeared milder, as COG lobe A deficiencies were not associated with decreased viability. Cog3-deficient and Cog8-deficient plants *Arabidopsis thaliana* exhibited short cisternae with increased widths as well as less efficient anterograde trafficking, slow growth and male sterility.¹³ In the Cog5-deficient fly *Drosophila melanogaster*, it was observed that the COG complex is necessary for changing the cellular and subcellular morphology during spermatogenesis, again resulting in male sterility.¹⁴ In the Cog1-deficient worm *Caenorhabditis elegans*, slowed growth and decreased fucosylation were observed.¹⁵ The sparse and heterogeneous data preclude any conclusions with regard to phenotypic differences between COG lobe A and B. In contrast, mammalian cell lines were studied extensively and did reveal a clear cellular phenotypic difference between COG lobes A and B. COG1 and COG2 deficiencies were studied in Chinese hamster ovary cells, Id1B and Id1C cells, respectively.¹⁶ All COG deficiencies (COG1–COG8) were studied in human cell lines: either in small interfering RNA knock-down or knock-sideways immortalised HeLa cell lines,^{3,17-23} in CRISPR/Cas9 knock-out immortalised HEK293T cell lines²⁴ and in patient fibroblasts.^{17,21,22,25-28}

Table 1. Mutation severity and clinical severity scores in COG-CDG

Study	Ethnicity	Sex	Age	Gene	DNA mutation	Effect on amino acids
Foulquier 2006 ⁸	Portuguese	F	21 m	COG1	c.2659-2660insC (HO)	p.388 frameshift, p.900 stop codon
Zeevaert 2009 ⁹	Bulgarian	M	14 Y	COG1	c.1070+5G>A (HO)	Splice defect, skipping exon 6, p.321*
Zeevaert 2009 ⁹	Greek-Turkish	M	12 Y	COG1	c.1070+5G>A (HO)	Splice defect, skipping exon 6, p.321*
Kodera 2014 ¹⁰	Japanese	M	6 Y	COG2	c.701dup	p.Tyr234*
Reynders 2009 ¹²	Portuguese	M	3 Y	COG4	c.1900T>G	p.Trp634Gly
Ng 2011 ¹³	Indian	M	2 Y	COG4	c.2185C>T No mat. COG4 gene c.697G>T	p.Arg729Trp No transcript found p.Glu233*
Paesold-Burda 2009 ¹⁴	Iraqi	F	14 Y	COG5	c.2318T>G	p.Leu773Arg
Rymen 2012 ¹⁵	Moroccan	F	15 Y	COG5	c.1669-115T>C (HO)	Splice defect, skipping exon 15 and 16, loss of 58 aa
Rymen 2012 ¹⁵	Moroccan	F	19 Y	COG5	c.2518G>T (HO)	p.Glu840*
Rymen 2012 ¹⁶	Moroccan	F	28 Y	COG5	c.2518G>T (HO)	p.Glu840*
Fung 2011 ¹⁵	Chinese	F	9 Y	COG5	(NR) c.2518G>T (HO) c.556_560delAGTAA insCT c.95T>G	(NR) p.Glu840* p.Ser186_Lys187del insLeu p.Met32Arg
Rymen 2012 ¹⁶	Italian	M	3 Y	COG5	c.1890delG (HO)	p.Cys64Valfs*6
Rymen 2012 ¹⁶	Belgian	M	3 Y	COG5	c.1780G>T (HO)	p.Val594Phe, splicing exon 16
Shaheen 2013 ¹³	Saudi-Arabian	M	12 Y	COG6	c.1167-24A>G (HO)	p.Gly390Phefs*6, intronic insertion 37 bp, novel splice site stop codon
Rymen 2015 ²⁰	Moroccan	M	21 Y	COG6	c.1646G>T	p.Gly549Val
Lübbehusen 2010 ¹⁷	Turkish-Moroccan	F	5 w	COG6	c.785A>G	p.Tyr262Cys
Rymen 2015 ²⁰	Turkish	F	15 m	COG6	c.1646G>T (HO)	p.Gly549Val
Rymen 2015 ²⁰	Turkish	M	12 m	COG6	c.1238_1239insA (HO)	p.Phe414Leufs*4
Rymen 2015 ²⁰	Moroccan	M	14 m	COG6	c.1746 + 2T>G (HO)	Splice defect
Rymen 2015 ²⁰	Turkish	F	12 Y	COG6	c.1646G>T (HO)	p.Gly549Val
Rymen 2015 ²⁰	Turkish-Moroccan	F	5 w	COG6	c.785A>G	p.Tyr262Cys
Huybr. 2011 ¹⁸	Moroccan	F	6 Y	COG6	c.1746 + 2T>G (HO)	Splice defect
Rymen 2015 ²⁰	Bulgarian	F	26 d	COG6	c.511C>T (HO)	(NR) p.Gly549Val
Zeevaert 2009 ²⁵	Moroccan	M	4 Y	COG7	(NR) c.170-7A>G (HO)	p.Arg171*
Zeevaert 2009 ²⁵	Moroccan	M	17 m	COG7	(NR) c.170-7A>G (HO)	(NR) p.56-57insAlaThr
Morava 2007 ²³	Moroccan	M	7 m	COG7	c.170-7A>G (HO)	p.56-57insAlaThr
Morava 2007 ²³	Moroccan	F	8 m	COG7	c.169+4A>C (HO)	Splice defect exon 1
Morava 2007 ²³	Moroccan	F	9 m	COG7	c.169+4A>C (HO)	Splice defect exon 1
Wu 2004 ²¹	Tunisian	M	5 w	COG7	c.169+4A>C (HO)	Splice defect exon 1
Wu 2004 ²¹	Tunisian	F	10 w	COG7	c.169+4A>C (HO)	Splice defect exon 1
Ng 2007 ²⁴	Moroccan	F	3 m	COG7	c.169+4A>C (HO)	Splice defect exon 1
Kranz 2007 ²⁷	NR	M	8 Y	COG8	c.1V53+1G>A c.1687-1688 del TT	Splice defect, stop codon, los 306 aa Premature stop codon, loss 47 aa
Foulquier 2007 ²⁶	Spanish	F	8 Y	COG8	c.1611 C.G (HO)	p.537Tyr*

Study	Functional COGx protein (%), measured by Western Blot								Severity score (*)
	COG1	COG2	COG3	COG4	COG5	COG6	COG7	COG8	
Foulquier 2006 ⁸	16±4	53±10	51±15	75±7	98±2	95±5	98±2	68±7	9
Zeevaert 2009 ⁹	23		Normal	Normal	Normal	Normal	Normal	84	9
Zeevaert 2009 ⁹									13
Kodera 2014 ¹⁰	25	Decr.	Decr.	Decr.	40	Normal	Normal	Normal	10
Reynders 2009 ¹²	Normal	40	50	20	Normal	Normal	Normal	Normal	8
Ng 2011 ¹³	Normal	Normal	Normal	34	Normal	Normal	Normal	Normal	±16
Paesold-Burda 2009 ¹⁴					Low				4
Rymen 2012 ¹⁵					±10				6
Rymen 2012 ¹⁶									7
Rymen 2012 ¹⁶									7
Fung 2011 ¹⁵					±25				10
Rymen 2012 ¹⁶					±3				11
Rymen 2012 ¹⁶					0				14
Shaheen 2013 ¹⁹						28			7
Rymen 2015 ²⁰									10
Lübbekhusen 2010 ¹⁷	97±5			100±2	55±7	21±8	62±4		±13
Rymen 2015 ²⁰									±13
Rymen 2015 ²⁰									±13
Rymen 2015 ²⁰									±14
Rymen 2015 ²⁰									15
Rymen 2015 ²⁰									±18
Huybr. 2011 ¹⁸									±18
Rymen 2015 ²⁰									±25
Zeevaert 2009 ²⁵									8
Morava 2007 ²³	Normal		Normal	Normal	42	77	68	80	±14
Morava 2007 ²³					6	27	5	29	±19
Morava 2007 ²³	Normal		Normal	Normal	6	27	5	29	±21
Wu 2004 ²¹	100±4	100±3	100±2	100±3	7±2	28±3	5±2	85±4	±22
Wu 2004 ²¹							15		±22
Ng 2007 ²⁴	55	100	89	78	1	11	1	61	±22
Kranz 2007 ²⁷	41	100	100	70	35	44	36	1	±23
Foulquier 2007 ²⁶	24±10	90±5	90±3	100±3	100±9	80±5	97±3	25±10	4

0-5 6-10 11-15 16-20 >20

*According to a clinical severity scoring system: age at onset at birth scores four points, age at onset < 3 months scores two points. Mortality < 1 year scores eight points, mortality > 1 year scores four points. Microcephaly, global developmental delay, seizures, intellectual disability, elevated hepatic transaminases, hepatomegaly, splenomegaly, failure to thrive, short stature, muscular hypotonia, abnormality of the face, abnormality of blood and blood-forming tissues, episodic fever, recurrent infections, abnormality of skeletal morphology and abnormality of the urinary system score each one additional point, to a total of 28 points. Symptom nomenclature is in accordance with the Human Phenotype Ontology. Abbreviations: aa: amino acids; bp: base pairs; d: days; decr: decreased; F: female; HO: homozygous mutation; m: months; NR: not reported and not determined (it is assumed that mutations are the same as in their siblings); y: years; †: patient died.

The cellular phenotypic difference found in mammalian cell lines is centred around Golgi morphology. In all studied COG lobe A deficiencies, Golgi structure was severely fragmented and cisternae showed dramatic dilatation in both IdIB and IdIC cells¹⁶ and in human cells.^{3,24,28} Conversely, in lobe B deficiencies, Golgi morphology phenotype varied. Normal Golgi morphology and normal growth were seen^{3,17} as well as some mildly dilated Golgi membranes organised in mini-stacks^{21,24} ranging to a more severe phenotype of cisternae dilatation and accumulation of vesicles.²² Of all lobe B deficiencies, Golgi morphology was most severely disrupted in COG7-deficient patient fibroblasts, with virtually no normally organised stacks and swollen cisternae.²⁸ The most robust comparison of COG deficiencies has been made by Blackburn et al. Assessment of all eight COG subunit deficiencies in completely knock-down HEK293T cells led to the conclusion that “defects associated with Golgi morphology were most notable in lobe A knock-downs”.²⁴

It should be noted that next to this clear cellular phenotypic difference in Golgi morphology, similar phenotypic characteristics were also observed. All COG deficiencies led to a complete block in retrograde trafficking,^{18,20,24,25,27,28} along with a partial decrease in anterograde trafficking efficiency.¹⁸⁻²⁰ Second, an accumulation of non-tethered transport vesicles appeared,¹⁸ resulting in accumulation and mislocalisation of glycosylation enzymes and decreased enzyme stability.¹⁹ This resulted in a decrease of steady-state levels of Golgi enzymes as mannosidase II,^{26,27} B4GALT13^{19,20,26,27} and ST6GAL1³ as well as decreased activity of these enzymes.²⁵ Third, in line with decreased glycosylation enzyme presence and activity, sialylation and fucosylation were equally decreased in both lobes, although it has also been observed that sialylation of N-glycans was more decreased in lobe A deficiencies.²⁰

Despite these similarities, lobe A deficiencies appear to be more detrimental to the cellular phenotype, impacting viability in yeast and severely impacting Golgi morphology in a wide range of human cell lines.

Bi-allelic truncating mutations are more detrimental in COG lobe A genes than in COG lobe B genes in patients with COG-CDG

Next, it was assessed whether the observation of a more severe cellular phenotype in COG lobe A mutants could also be discerned in patients with COG-CDG. Therefore, genotypic and phenotypic severity among patients with COG-CDG was assessed by taking mutation type and protein expression data as a proxy for genotypic severity. It should be noted that protein expression data are unknown for many patients and therefore conclusions are drawn with caution. In order to assess phenotypic severity among the different patients with COG-CDG, a clinical severity score was developed based on a severity score for Costello syndrome.²⁹ In this scoring system, most symptoms reported frequently in patients with COG-CDG are allocated a single point; important indicators for severity – age at onset and age at death – are allocated more points, to a maximum of 28 points (Table 1).

A striking difference in prevalence was observed between lobe A and lobe B COG-CDG. To date, only six unrelated patients with lobe A COG-CDG have been described,^{26,28,30-32} as opposed to 27 patients with lobe B COG-CDG from 19 different families.^{25,27,33-43} No patient with COG3-CDG has yet been described. This substantial prevalence difference cannot be explained by gene size nor by founder mutations (16 different mutations in lobe B COG-CDG, Table 1).

Table 1 demonstrates that in patients with lobe A COG-CDG, expression of the affected subunit in patients' fibroblasts was only marginally reduced to 16%-34%. This included one patient with COG1-CDG with bi-allelic truncating mutations close to the C terminus

(positions 888 and 900, while protein length is 980 amino acids). Otherwise, bi-allelic truncating mutations in patients with lobe A COG-CDG were absent as well as other mutations resulting in negligible amounts of residual protein expression. These data imply that bi-allelic truncating mutations in lobe A genes, reducing protein expression close to zero, may be inviable.

In contrast, in patients with lobe B COG-CDG, expression of the affected subunit is < 5% in at least seven patients. Moreover, almost all patients with lobe B COG-CDG have (severe) bi-allelic truncating mutations. Still, a viable COG-CDG phenotype is seen, although it should be noted that severe lobe B COG-CDG can be lethal at a young age, especially in COG7-CDG. Overall, the frequency gap in bi-allelic truncating mutations, reducing protein expression to zero, strongly suggests that these mutations may be inviable in COG lobe A genes. The detrimental effect of bi-allelic truncating mutations on COG lobe A genes might therefore explain the observed difference in prevalence between patients with lobe A and lobe B COG-CDG.

COG lobe A genes are less tolerant to variation than COG lobe B genes

To look further into the observed frequency gap in bi-allelic mutations in COG lobe A and COG lobe B genes, tolerance to genetic variation of human COG genes was studied. To this end, the variant browser of the Exome Aggregation Consortium (ExAC) was consulted (Table 2). ExAC is an initiative to collect and harmonise exome sequencing data in apparently healthy adults and is available online. Expected and observed numbers of loss of function (LoF) variants in the canonical transcript of a gene in healthy unrelated individuals are reported.⁴⁴ A gene is considered LoF intolerant if pLI score is >0.90. Strikingly, this is case for the *COG3* gene, the only gene within the COG complex that still awaits a phenotypic description in man. To further assess tolerance to variation, the ratio of observed and expected number of LoF variants – the degree to which variants within a gene are under-reported – was calculated. This ratio is considered to reflect a survival disadvantage of such variants. Surprisingly, ranking COG genes on tolerance to variation clearly demonstrates that COG lobe A genes are indeed less tolerant to variation than COG lobe B genes (Table 2).

Table 2. Tolerance to variability of human COG genes

Gene	Protein length (aa)	Expected LoF variants	Observed LoF variants	Ratio obs/exp	LoF – pLI
<i>COG3</i>	828	33.4	3	0.0898	1.00
<i>COG1</i>	980	30.7	8	0.2606	0.10
<i>COG2</i>	738	30.9	12	0.3883	0.00
<i>COG4</i>	785	30.0	14	0.4667	0.00
<i>COG7</i>	770	31.2	15	0.4808	0.00
<i>COG5</i>	839	35.6	23	0.6461	0.00
<i>COG6</i>	657	29.0	19	0.6552	0.00
<i>COG8</i>	612	12.8	9	0.7031	0.00

COG genes were sorted by ratio LoF observed/expected. pLI scores indicate the deviation from expected numbers of LoF mutations, a gene being LoF intolerant if pLI score > 0.90 (*COG3*) and tolerant if pLI < 0.10. None of the healthy subjects in the ExAC database was homozygous for a pathogenic mutation found in any patient with COG-CDG. *COG5* p.Val594Phe and *COG6* p.Arg171* were observed in three and two alleles, respectively, both with allele frequencies < 1/10,000 (last update ExAC database: August 2016). Abbreviations: aa: amino acid; ExAC: Exome Aggregation Consortium; exp: expected; LoF: loss of function; obs: observed.

COG-CDG phenotypic severity is in line with tolerance to variation of COG genes

While the small number of patients with lobe A COG-CDG does not allow for intra-lobe comparison of clinical phenotypic severity, clinical phenotypic severity of patients with lobe B COG-CDG corresponds surprisingly well with the ranking on tolerance to variation based on ExAC data. Mutations in the *COG7* gene, which is the least tolerant to variation of all COG lobe B genes, gave rise to the most severe clinical lobe B COG-CDG phenotype (Table 1) as well as the most severe disruption of Golgi morphology in patient fibroblasts.²⁸ On the other hand, mutations in the *COG8* gene, being the most tolerant to variation, were associated with a mild phenotype despite a *COG8* protein expression of only 1%.⁴³ Although the relatively small number of patients identified per subunit thus does not permit definite conclusions, these findings imply that the ratio of observed and expected number of LoF variants might give an even more subtle indication of tolerance to variation of human genes.

CONCLUSION

Observations from cellular phenotypes from completely knockdown HEK293T cell lines, the frequency gap of bi-allelic mutations in patients with lobe A and B COG-CDG, and differences in tolerance to genetic variation of the human COG genes all support the notion that comparable molecular defects are more detrimental in lobe A COG-CDG than in lobe B COG-CDG. In a larger perspective, the approach described here illustrates the potency of genomic epidemiology to be used as a photographic negative for mutational severity.

WEB RESOURCES

ExAC

<https://exac.broadinstitute.org>

REFERENCES

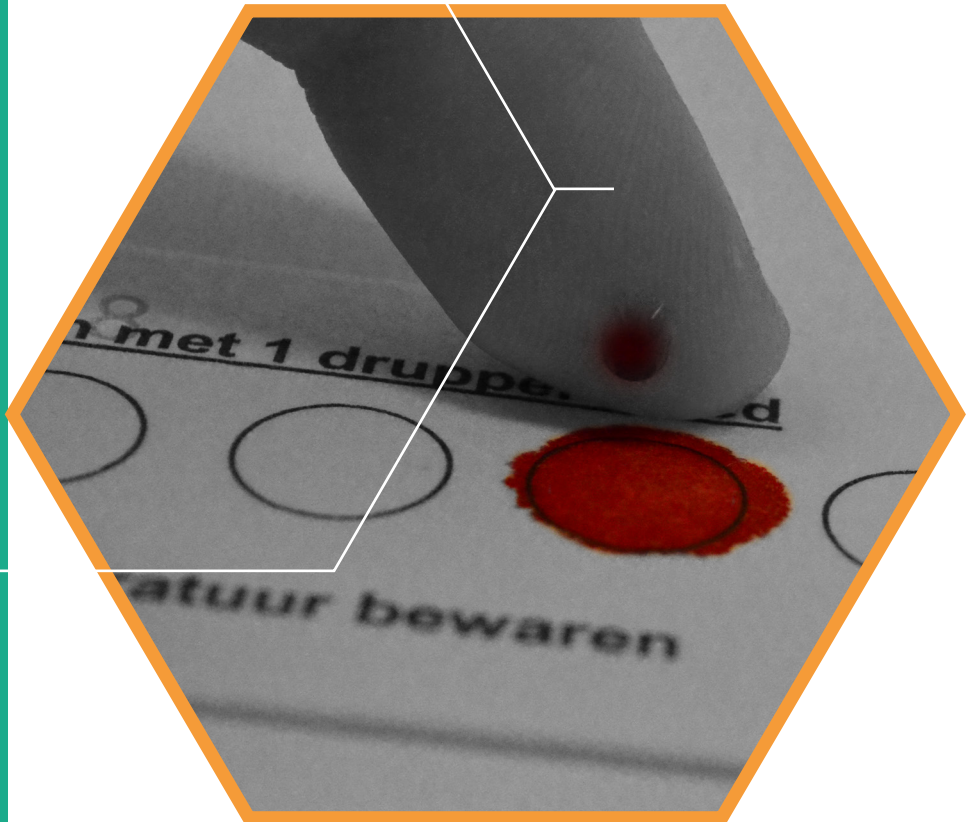
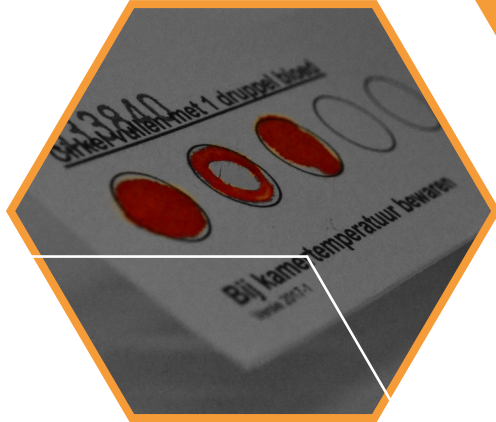
1. Ungar D, Oka T, Vasile E, Krieger M, Hughson FM. Subunit architecture of the conserved oligomeric Golgi complex. *J Biol Chem*. 2005;280:32729-35.
2. Willett R, Blackburn JB, Climer L, Pokrovskaya I, Kudlyk T, Wang W, Lupashin V. COG lobe B sub-complex engages v-SNARE GS15 and functions via regulated interaction with lobe A sub-complex. *Sci Rep*. 2016;6:29139.
3. Peanne R, Legrand D, Duvet S, Mir AM, Matthijs G, Rohrer J, Foulquier F. Differential effects of lobe A and lobe B of the conserved oligomeric Golgi complex on the stability of β -1,4-galactosyltransferase 1 and α -2,6-sialyltransferase 1. *Glycobiology* 2011;21:864-76.
4. Willett R, Ungar D, Lupashin V. The Golgi puppet master: COG complex at center stage of membrane trafficking interactions. *Histochem Cell Biol*. 2013;140:271-83.
5. VanRheenen SM, Cao X, Lupashin VV, Barlowe C, Waters MG. Sec35p, a novel peripheral membrane protein, is required for ER to Golgi vesicle docking. *J Cell Biol*. 1998;141:1107-19.
6. VanRheenen SM, Cao X, Sapperstein SK, Chiang EC, Lupashin VV, Barlowe C, Waters MG. Sec34p, a protein required for vesicle tethering to the yeast Golgi apparatus, is in a complex with Sec35p. *J Cell Biol*. 1999;147:729-42.
7. Kim DW, Sacher M, Scarpa A, Quinn AM, Ferro-Novick S. High-copy suppressor analysis reveals a physical interaction between Sec34p and Sec35p, a protein implicated in vesicle docking. *Mol Biol Cell*. 1999;10:3317-29.
8. Spelbrink RG, Nothwehr SF. The yeast GRD20 gene is required for protein sorting in the trans-Golgi network/endosomal system and for polarization of the actin cytoskeleton. *Mol Biol Cell*. 1999;10:4263-81.
9. Ram RJ, Li B, Kaiser CA. Identification of Sec36p, Sec37p, and Sec38p: components of yeast complex that contains Sec34p and Sec35p. *Mol Biol Cell*. 2002;13:1484-500.
10. Wuestehube LJ, Duden R, Eun A, Hamamoto S, Korn P, Ram R, Schekman R. New mutants of *Saccharomyces cerevisiae* affected in the transport of proteins from the endoplasmic reticulum to the Golgi complex. *Genetics* 1996;142:393-406.
11. Whyte JR, Munro S. The Sec34/35 Golgi transport complex is related to the exocyst, defining a family of complexes involved in multiple steps of membrane traffic. *Dev Cell*. 2001;1:527-37.
12. Kim DW, Massey T, Sacher M, Pypaert M, Ferro-Novick S. Sgf1p, a new component of the Sec34p/Sec35p complex. *Traffic* 2001;2:820-30.

13. Tan X, Cao K, Liu F et al. Arabidopsis COG complex subunits COG3 and COG8 modulate Golgi morphology, vesicle trafficking homeostasis and are essential for pollen tube growth. *PLoS Genet.* 2016;12:e1006140.
14. Farkas RM, Giansanti MG, Gatti M, Fuller MT. The Drosophila Cog5 homologue is required for cytokinesis, cell elongation, and assembly of specialized Golgi architecture during spermatogenesis. *Mol Biol Cell.* 2003;14:190-200.
15. Struwe WB, Reinhold VN. The conserved oligomeric Golgi complex is required for fucosylation of N-glycans in *Caenorhabditis elegans*. *Glycobiology* 2012;22:863-75.
16. Ungar D, Oka T, Brittle EE et al. Characterization of a mammalian Golgi-localized protein complex, COG, that is required for normal Golgi morphology and function. *J Cell Biol.* 2002;157:405-15.
17. Oka T, Vasile E, Penman M et al. Genetic analysis of the subunit organization and function of the conserved oligomeric golgi (COG) complex: studies of COG5- and COG7-deficient mammalian cells. *J Biol Chem.* 2005;280:32736-45.
18. Zolov SN, Lupashin VV. Cog3p depletion blocks vesicle-mediated Golgi retrograde trafficking in HeLa cells. *J Cell Biol.* 2005;168:747-59.
19. Shestakova A, Zolov S, Lupashin V. COG complex-mediated recycling of Golgi glycosyltransferases is essential for normal protein glycosylation. *Traffic* 2006;7:191-204.
20. Pokrovskaya ID, Willett R, Smith RD, Morelle W, Kudlyk T, Lupashin VV. Conserved oligomeric Golgi complex specifically regulates the maintenance of golgi glycosylation machinery. *Glycobiology* 2011;21:1554-69.
21. Kudlyk T, Willett R, Pokrovskaya ID, Lupashin V. COG6 interacts with a subset of the Golgi SNAREs and is important for the Golgi complex integrity. *Traffic* 2013;14:194-204.
22. Laufman O, Freeze HH, Hong W, Lev S. Deficiency of the Cog8 subunit in normal and CDG-derived cells impairs the assembly of the COG and Golgi SNARE complexes. *Traffic* 2013;14:1065-77.
23. Willett R, Pokrovskaya I, Kudlyk T, Lupashin V. Multipronged interaction of the COG complex with intracellular membranes. *Cell Logist.* 2014;4:e27888.
24. Bailey Blackburn J, Pokrovskaya I, Fisher P, Ungar D, Lupashin VV. COG complex complexities: detailed characterization of a complete set of HEK293T cells lacking individual COG Subunits. *Front Cell Dev Biol.* 2016;4:23.
25. Wu X, Steet RA, Bohorov O et al. Mutation of the COG complex subunit gene COG7 causes a lethal congenital disorder. *Nat Med* 2004;10:518-23.
26. Foulquier F, Vasile E, Schollen E et al. Conserved oligomeric Golgi complex subunit 1 deficiency reveals a previously uncharacterized congenital disorder of glycosylation type II. *Proc Natl Acad Sci U S A* 2006;103:3764-9.
27. Foulquier F, Ungar D, Reynnders E et al. A new inborn error of glycosylation due to a Cog8 deficiency reveals a critical role for the Cog1–Cog8 interaction in COG complex formation. *Hum Mol Genet.* 2007;16:717-30.
28. Reynnders E, Foulquier F, Leão Teles E et al. Golgi function and dysfunction in the first COG4-deficient CDG type II patient. *Hum Mol Genet.* 2009;18:3244-56.
29. McCormick EM, Hopkins E, Conway L et al. Assessing genotype–phenotype correlation in Costello syndrome using a severity score. *Genet Med.* 2013;15:554-7.
30. Zeevaert R, Foulquier F, Dimitrov B et al. Cerebrocostomandibular-like syndrome and a mutation in the conserved oligomeric Golgi complex, subunit 1. *Hum Mol Genet.* 2009;18:517-24.
31. Kodera H, Ando N, Yuasa I et al. Mutations in COG2 encoding a subunit of the conserved oligomeric Golgi complex cause a congenital disorder of glycosylation. *Clin Genet.* 2015;87:455-60.
32. Ng BG, Sharma V, Sun L, Loh E, Hong W, Tay SK, Freeze HH. Identification of the first COG-CDG patient of Indian origin. *Mol Genet Metab.* 2011;102:364-7.
33. Paesold-Burda P, Maag C, Troxler H et al. Deficiency in COG5 causes a moderate form of congenital disorders of glycosylation. *Hum Mol Genet.* 2009;18:4350-6.
34. Rymen D, Keldermans L, Race V et al. COG5-CDG: expanding the clinical spectrum. *Orphanet J Rare Dis.* 2012;7:94.
35. Fung CW, Matthijs G, Sturiale L et al. COG5-CDG with a mild neurohepatic presentation. *JIMD Rep.* 2012;3:67-70.
36. Lübbehusen J, Thiel C, Rind N et al. Fatal outcome due to deficiency of subunit 6 of the conserved oligomeric Golgi complex leading to a new type of congenital disorders of glycosylation. *Hum Mol Genet.* 2010;19:3623-33.
37. Huybrechts S, De Laet C, Bontems P et al. Deficiency of subunit 6 of the conserved oligomeric Golgi complex (COG6-CDG): second patient, different phenotype. *JIMD Rep.* 2012;4:103-8.
38. Shaheen R, Ansari S, Alshammari MJ, Alkhalidi H, Alrukban H, Eyaid W, Alkuraya FS. A novel syndrome of hypohidrosis and intellectual disability is linked to COG6 deficiency. *J Med Genet.* 2013;50:431-6.
39. Rymen D, Winter J, Van Hasselt PM et al. Key features and clinical variability of COG6-CDG. *Mol Genet Metab.* 2015;116:163-70.

40. Morava E, Zeevaert R, Korsch E et al. A common mutation in the COG7 gene with a consistent phenotype including microcephaly, adducted thumbs, growth retardation, VSD and episodes of hyperthermia. *Eur J Hum Genet.* 2007;15:638-45.
41. Ng BG, Kranz C, Hagebeuk EE et al. Molecular and clinical characterization of a Moroccan Cog7 deficient patient. *Mol Genet Metab.* 2007;91:201-4.
42. Zeevaert R, Foulquier F, Cheillan D et al. A new mutation in COG7 extends the spectrum of COG subunit deficiencies. *Eur J Med Genet.* 2009;52:303-5.
43. Kranz C, Ng BG, Sun L et al. COG8 deficiency causes new congenital disorder of glycosylation type IIh. *Hum Mol Genet.* 2007;16:731-41.
44. Lek M, Karczewski KJ, Minikel EV et al. Exome Aggregation Consortium. Analysis of protein-coding genetic variation in 60,706 humans. *Nature* 2016;536:285-91.

Hypothesis: Lobe A (COG1-4)-CDG causes a more severe phenotype than lobe B (COG5-8)-CDG

2



Part I - Phenomics

3

Hypothesis: determining phenotypic specificity

facilitates understanding of pathophysiology in rare genetic disorders

*Journal of Inherited Metabolic Diseases 2019, Epub ahead of print
DOI: 10.1002/jimd.12201*

Hanneke A. Haijes*, Jaak Jaeken, Peter M. van Hasselt*

* Corresponding authors

ABSTRACT

In the rapidly growing group of rare genetic disorders, data scarcity demands an intelligible use of available data, in order to improve understanding of underlying pathophysiology. We hypothesize, based on the principle that clinical similarities may be indicative of shared pathophysiology, that determining phenotypic specificity could provide unsuspected insights in pathophysiology of rare genetic disorders. We explored our hypothesis by studying subunit deficiencies of the Conserved Oligomeric Golgi (COG) complex, a subgroup of Congenital Disorders of Glycosylation (CDG). In this systematic data assessment, all 45 reported patients with COG-CDG were included. The vocabulary of the Human Phenotype Ontology (HPO) was used to annotate all phenotypic features and to assess occurrence in other genetic disorders. Gene occurrence ratios were calculated by dividing the frequency in the patient cohort over the number of associated genes according to HPO. Prioritization based on phenotypic specificity was highly informative and captured phenotypic features commonly associated with glycosylation disorders. Moreover, it captured features not seen in any other glycosylation disorder, among which episodic fever, likely reflecting underappreciated other cellular functions of the COG complex. Interestingly, the COG complex was recently implicated in the autophagy pathway, as are more than half of the genes underlying disorders that present with episodic fever. This suggests that whereas many phenotypic features in these patients are caused by disrupted glycosylation, episodic fever might be caused by disrupted autophagy. Thus, we here demonstrate support for our hypothesis that determining phenotypic specificity could facilitate understanding of pathophysiology in rare genetic disorders.

KEY MESSAGE

Determining phenotypic specificity could facilitate understanding of pathophysiology in rare genetic disorders, despite data scarcity.

INTRODUCTION

Whole-exome sequencing has induced an explosion of newly discovered rare genetic disorders. Understanding the underlying pathophysiology of each of these disorders would improve disease recognition, would allow insight in a patient's disease course and would create the opportunity for conceiving treatment strategies. However, the small number of patients and the inherent scarcity of data pose a new and significant challenge which demands for an intelligible use of available data.

Attempting to meet this challenge, "deep phenotyping" is being advocated to increase insight into pathophysiology of rare disorders, by describing the physical state of a single patient as comprehensively and thoroughly as possible.¹⁻² To enable interpretation, these in-depth phenotypic descriptions of single patients should be pooled. To facilitate this process, a standard vocabulary of phenotypic abnormalities is provided by the Human Phenotype Ontology (HPO).³ Its openly accessible unambiguous terminology allows aligning in-depth heterogeneous phenotypic descriptions. HPO thereby effectively enhances specificity of phenotypic description, so that slightly different symptoms can be better distinguished. Moreover, it allows trustworthy delineation of the frequency of phenotypic features.⁴

Deep phenotyping using HPO results in a large list of disease phenotypic features and their frequencies. To gain insight in pathophysiology, this list requires prioritization. However, as exemplified by developmental delay and failure to thrive, prioritization based on frequency alone is insufficient, as it may merely reflect the commonness of a feature across a range of genetic disorders. In contrast, features that are pathognomonic for a disease tend to reflect underlying pathophysiology. This is exemplified by the "Kayser-Fleischer ring" in Wilson disease, indicating the copper depositions in the cornea that arise as a result of excessive copper accumulation, caused by defective copper transport. Interestingly, as illustrated by mucopolysaccharidoses, a group of disorders involving one degradation pathway, striking clinical similarities between different diseases may be indicative of shared pathophysiology. By analogy, we here hypothesize that prioritization based on highly specific phenotypic features in poorly understood rare genetic disorders combined with a search for better understood disorders sharing these features, would allow us to extrapolate pathophysiological insights from known diseases to less known diseases. We here test our hypothesis, by exploring a strategy focusing on systematically assessing phenotypic specificity and shared pathophysiology to improve understanding of underlying pathophysiology.

We use COG-CDG (deficiencies in the Conserved Oligomeric Golgi complex, causing a Congenital Disorder of Glycosylation) to illustrate this strategy, as COG-CDG patients illustrate the problem of data scarcity and vocabulary heterogeneity in rare genetic disorders. Along with the increase in the number of identified COG-CDG patients in the past fifteen years, some insights in the pathophysiology of COG-CDG have been gained,⁵ but it still remains largely unknown how the clinical picture of COG-CDG patients evolves. In the most recent case series about COG-CDG, all available clinical data was assembled.⁶ However, distilling a relevant phenotypic description from different case reports of many different authors was seriously impeded by an ambiguous nomenclature. For example, facial dysmorphism was noted in 70% of patients,⁶ implying phenotypic overlap, but do all patients look the same?

METHODS

Study population

In this systematic data assessment, all reported patients with a deficiency of one of the eight subunits of the COG complex were included. The COG complex is a tethering protein

complex in the Golgi apparatus and is crucial for proper glycosylation. Since the first reported patient in 2004,⁷ 45 patients from 32 families have been reported^{5,8-11} in 22 case series and case reports, with mutations in all but one (*COG3*) of the eight subunits (MIM: #611209, #606974, #613489, #613612, #614576, #608779 and #611182 respectively for COG1-CDG to COG8-CDG).

Phenotypic frequency

Phenotypic traits were aligned using the openly accessible terminology of HPO. HPO has placed all phenotypic features in a tree-like hierarchical structure. For each reported phenotypic feature in the case series and case reports included in this study, the most specifically described HPO code was retrieved. Signs and symptoms not specifically addressed in phenotypic descriptions of COG-CDG patients were considered absent. All first and corresponding authors of the case-series and case-reports were contacted to confirm the presence and absence of phenotypic features. For each of the HPO codes and all their associated super classes, the number of patients that presented with that feature was counted. Next, phenotypic frequency was calculated, dividing the number of patients that present with a phenotypic feature over the total number of patients ($n = 45$).

Phenotypic specificity

Phenotypic specificity was assessed by determining occurrence of the phenotypic feature in other genetic diseases. In HPO it is noted for each phenotypic feature with which genetic diseases and corresponding genes it is associated. For each phenotypic feature this number of associated genes and the list of associated genes were retrieved. HPO was last consulted on November 1st, 2018.

Subsequently, for each phenotypic feature a “gene occurrence ratio” was calculated, dividing the frequency in the COG-CDG patient cohort over the number of associated genes. To meet a minimum sensitivity, a cut-off value of how many patients in the cohort should at least present with a phenotypic feature was needed. To explore the best cut-off value, for each percentage of patients presenting with a phenotypic feature, the number of phenotypic features was noted, and the differences between these counts were studied. In addition, a “specificity ratio” was calculated for each percentage of patients presenting with a phenotypic feature, dividing the median gene occurrence ratio of the top 10 phenotypic features over the median gene occurrence ratio of all other phenotypic features. Data analysis was performed in R programming language. R code is supplied in Supplemental Notes 1.

Studying pathophysiology

Phenotypic features with the ten highest occurrence ratios were studied in detail. For all genes that were associated with any of the ten selected features, gene encoded protein functions were derived from GeneCards. Protein functions were classified into data-driven categories. Since glycosylation is expected to play an important role in pathophysiology of COG-CDG, these categories included the category “glycosylation”. The number of genes per category was noted to assess differences in distribution over categories for the different phenotypic features. Hereby, a special interest was in the category “glycosylation”, to assess if specific phenotypic features also occur in other glycosylation disorders.

RESULTS

Aligning phenotypic descriptions using HPO

All reported signs and symptoms in COG-CDG patients were aligned and pooled by using the HPO vocabulary, allowing a multi-faceted but unambiguous phenotypic description (Table S1, Table S2). Accuracy of the pooled data was confirmed by the corresponding author of 1/45 cases. From the aligned and pooled phenotypic data, listing 666 phenotypic features, recurrent features in COG-CDG were delineated. Largely in line with the report of Rymen et al.⁶, the nervous system is the most frequently affected organ system, affected in all COG-CDG patients. This comprises amongst others of microcephaly (76%), global developmental delay (73%) and intellectual disability (53%) (Table S1). The second most frequently affected organ is the abdomen (67%), mainly due to abnormalities of the liver (60%) (Table S1).

The enhanced specificity of phenotypic description provided by HPO allowed us to differentiate whether or not a common phenotype at a higher aggregation level reflected true clinical overlap. Facial dysmorphism (present in 71%) turned out to include abnormalities of the mouth (29%), nose (27%), orbital region (27%) and skull (27%) (Table S1). This can be further distinguished in a list of many different characteristic features (Table S2). Thus, the use of an unambiguous nomenclature confirmed that COG-CDG patients with facial dysmorphisms do not look the same at all.

Despite the harmonization of all phenotypic descriptions using HPO, the most frequently observed features (microcephaly and global developmental delay) fail to be discriminatory, nor do they contribute to an increased pathophysiological understanding of COG-CDG.

Determining phenotypic specificity to prioritize phenotypic features

In contrast to ascertaining phenotypic frequency, ascertaining phenotypic specificity provided more relevant prioritization. A sliding scale was noted, ranging from one phenotypic feature that is described in all COG-CDG patients (e.g. abnormality of the nervous system, Table S1), towards >250 phenotypic features that are described only in a single COG-CDG patient (e.g. gingival bleeding, Table S2) (Figure S1). The best trade-off between frequency and specificity was explored. We noted that for features described in at least six COG-CDG patients the number of phenotypic features added to the total list per added patient frequency is very constant (Figure S1), suggesting that zooming in on features described in at least six COG-CDG patients is optimal. The calculated specificity ratio (the ratio of the median gene occurrence ratio of the top ten phenotypic features over the median gene occurrence ratio of all other phenotypic features) supported this cut-off value of at least six patients presenting with a certain phenotype (Figure S2). A wider zoom (at least four patients) resulted in a longer list of less relevant features (Figure S3) while a narrower zoom (at least eight patients) resulted in missing relevant features (Figure S4).

Plotting all occurrence ratios of phenotypic features present in at least six COG-CDG patients illustrated the diversity in phenotypic specificity and clearly highlighted the top ten of very specific phenotypes (Figure 1A). Features with the highest occurrence ratios were severe hearing impairment (present in 7 patients, associated with only 5 genetic diseases) and episodic fever (present in 20 patients, associated with only 22 genetic diseases), contrasting with for example global developmental delay (present in 33 patients, but associated with 1123 other genetic diseases). Strikingly, for episodic fever even its two super classes (fever (HP:0001945) and abnormality of temperature regulation (HP:0004370)) stood out as highly specific phenotypic features (Figure 1A).

Figure 1. Phenotypic specificity in COG-CDG

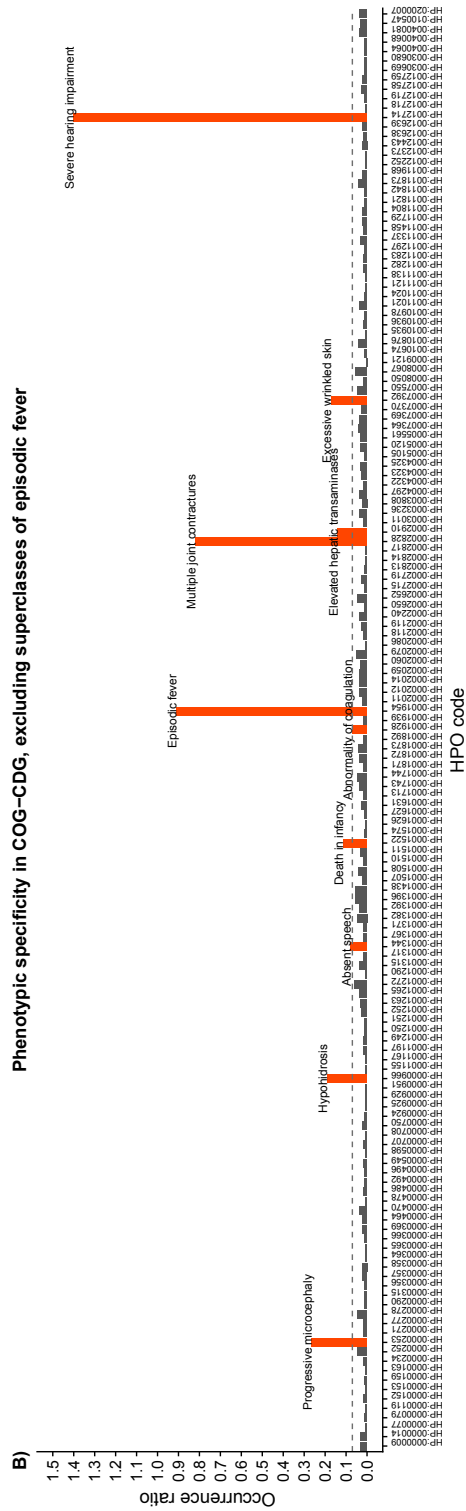
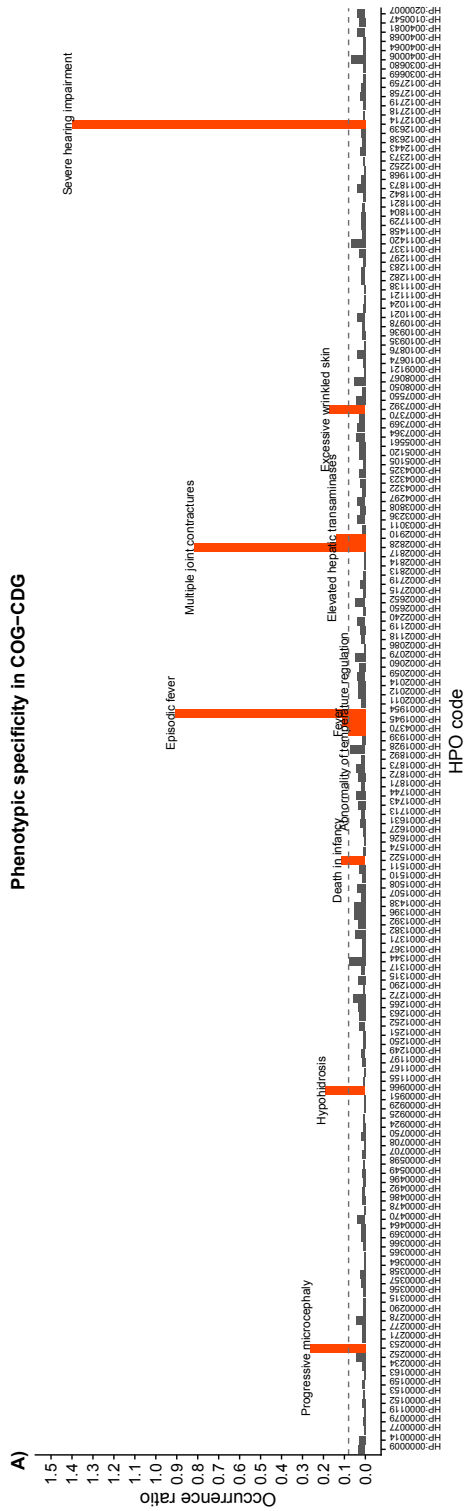


[Figure 1 continued] The ratio of the number of COG-CDG patients over the number of HPO associated genes is depicted on the y-axis, while all the different phenotypic features, indicated by their HPO code, are depicted on the x-axis. A) In red, the ten most specific COG-CDG phenotypic features. B) In red, the ten most specific COG-CDG phenotypic features after excluding “Fever” and “Abnormality of temperature regulation” as super classes of “Episodic fever”. Now “Absent speech” and “Abnormality of coagulation” reach top ten. Abbreviations: CDG: congenital disorder of glycosylation; COG: conserved oligomeric Golgi; HPO: Human Phenotype Ontology.

Studying pathophysiology in diseases sharing highly specific phenotypic features

Next, we assessed potential shared pathophysiology among diseases sharing highly specific phenotypic features. Hereto, the super classes of episodic fever were excluded (Figure 1B). Gene encoded protein functions of all 677 genes associated with the ten most specific phenotypic features (Figure 1B) were classified into 26 data-driven categories, including the category “glycosylation” (Table 1). Demonstrating the power of this approach, seven out of the ten extracted highly specific phenotypic features were clearly associated with other CDG (Table 1; bottom lines). This included the features elevated hepatic transaminases and abnormality of coagulation, features that are commonly associated with classical CDG and are mainly seen in CDG affecting N-glycosylation (Figure S5). It also included absent speech, a feature described in a subset of non-classical CDG affecting O-mannosylation and glycosylphosphatidylinositol anchoring (Figure S5). These findings corroborate the known importance of the tethering function of the COG complex for proper glycosylation and provide support for its suspected involvement in solid glycosylphosphatidylinositol anchoring. Altogether, these findings demonstrate the relevance of prioritizing phenotypic features based on phenotypic specificity.

Two out of the ten extracted highly specific phenotypic features, severe hearing impairment and excessive wrinkled skin, are not linked to any other CDG according to HPO. However, their super classes (hearing impairment (HP:0000365) and abnormally lax or hyperextensible skin (HP:0008067)) have poor specificity (969 and 109 associated genes, ratios 0.007 and 0.055, respectively) and are associated with other CDG. According to HPO, hearing impairment has been described in seven CDG (MIM #212066, #610768, #616721, #617082, #606056, #612015 and #613661) and abnormally lax or hyperextensible skin has been described in four (MIM #612379, #219200, #617403 and #617402) (Table S3).

In contrast, one of the ten extracted highly specific phenotypic features, episodic fever, is not linked to any other CDG. According to HPO, its highly specific super classes (fever (HP:0001945) and abnormality of temperature regulation (HP:0004370) are linked to only one other CDG, *TMEM165*-CDG (MIM #614727) (Table S3). *TMEM165* encodes a protein which is considered an ion transporter and is presumed to play a key role in manganese homeostasis, and to influence calcium and pH homeostasis of the Golgi apparatus.¹² Manganese is considered a cofactor for several glycosyltransferases in the glycosylation process.¹² To date, five *TMEM165*-CDG patients have been described, of which two presented with recurrent episodes of unexplained fever.^{13,14}

The scarcity of clinical overlap with other CDG suggests a function of the COG-complex other than glycosylation. To explore this hypothesis, we focused on other genetic diseases that present with episodic fever, to extrapolate pathophysiological knowledge from other, better understood diseases that present with episodic fever to COG-CDG.

Table 1. Ten highly specific phenotypic features in COG-CDG associated with other genetic diseases according to HPO

	Severe hearing impairment	Episodic fever	Multiple joint contractures	Progressive microcephaly	Hypohidrosis	Excessive wrinkled skin	Elevated hepatic transaminases	Death in infancy	Absent speech	Abnormality of coagulation	Total
Number of COG-CDG patients	7	20	9	14	11	6	22	15	6	9	
Number of associated genes	5	22	11	53	58	35	157	132	77	127	677
Ratio COG-CDG patients/genes	1.400	0.909	0.818	0.264	0.190	0.171	0.140	0.114	0.078	0.071	
Purine and pyrimidine metab.		1				1	2	3	2	1	12
DNA			1	4	1	1	12	14	4	1	38
Transcription			1	2	14	3	14	10	10	7	62
RNA				12		1	8	4	4	7	36
Amino acid metabolism		3		3		2	2	5	2	1	19
Protein metabolism		1	1	1	1		2	1		1	9
Mitosis	2		1	3	1	5	1	1	5	8	27
Cell proliferation	1	4		2	3	4	10	12	4	6	46
Cell adhesion					1		1	4			6
Cell cilia				1			6		2	1	10
Cytoskeleton	1		2	1	7		6	9	2	3	32
Cell signaling	1	1		2	7	3	5	5	5	8	337
Cargo trafficking		1		3		1	6	3	1	5	25
Cell homeostasis		4		5	4	3	12	6	7	7	49
Mitoch. homeost./energy met.				5			27	14	6	6	58
Peroxisome biogenesis							2	13		13	28
Sterol and bile acid metab.		2		1	1		9			6	18
Glycosaminoglycan metab.				1				3	1		5
Ectodermal development		2		1	10	1		2	3	1	23
Mesodermal development				1	3	8		10	2	1	27
Neurotransmitters and synaps			3	2	3			1	3		12
Muscle cell homeostasis			1			1	2	4	1	1	9
Immune system		3					6	1		3	14
Coagulation							1			23	24
Other				1		1	7	2		1	12
Glycosylation	0%	0%	9.1%	5.7%	3.4%	0%	9.6%	3.8%	10.4%	13.3%	71.4%
Glycosylation percentage	0%	0%	9.1%	5.7%	3.4%	0%	9.6%	3.8%	10.4%	13.3%	71.4%

Abbreviations: CDG: congenital disorder of glycosylation; COG: conserved oligomeric Golgi; metab: metabolism; mitoch. homeost./energy met.: mitochondrial homeostasis and energy metabolism.

Studying pathophysiology in diseases presenting with episodic fever

All but two (*CYP11B2* and *LPIN2*) of the proteins encoded by the 22 genes associated with episodic fever have an established function in temperature regulation, implying involvement of the COG complex in temperature regulation. Aspects ranged from inflammation induction and control to cytokine response, second messenger function, neuronal pathways, neurotransmitter synthesis and calcium signaling (Table 2), which at first glance appear unrelated to known functions of the COG complex. However, we noted that autophagy is thought to play a considerable role in pathophysiology in more than half of the diseases presenting with episodic fever (Table 2).¹⁵⁻²⁴ This is of interest, since the COG complex has recently been shown to be involved in the non-selective autophagy pathway.²⁵⁻²⁷ Specifically, in the cytoplasm-to-vesicle pathway in yeast, the COG complex is expected to promote vesicle fusion to form double-membrane autophagosomes and/or to deliver *Atg9* to the post-Golgi compartment.²⁵⁻²⁷

The links between episodic fever and autophagy, and autophagy and the COG complex suggest that episodic fever in COG-CDG patients, unlike other COG-CDG phenotypic features caused by the disrupted glycosylation process, might be caused by disruption of its function in the autophagy pathway. The veracity of this hypothesis remains to be further elucidated.

DISCUSSION

Since improving understanding of underlying pathophysiology in the rapidly growing group of rare genetic disorders demands for an intelligible use of available data, we here explored a strategy focusing on systematically assessing phenotypic specificity and shared pathophysiology. Our results confirm the power of HPO in reliably aligning heterogeneous phenotypic information from multiple case series and case reports. We showed that calculating phenotypic frequency, while revealing the most prevalent phenotypic features, did not aid pathophysiological understanding. In contrast, determining phenotypic specificity did lead the way towards features easily linked to the underlying pathophysiology. Seven features could be linked to the major known pathophysiological process glycosylation, whereas episodic fever could be linked to disturbances of cellular processes (e.g. autophagy) of which the importance was previously uncertain. Thus, we here provide support for our hypothesis that phenotypic specificity could facilitate progress in understanding underlying pathophysiology of rare genetic disorders.

We note four important limitations of our approach, all regarding the risk of reporting bias. Due to importance of reporting bias for the validity of the conclusions, we here urge awareness of these limitations when our approach will be used in daily practice. Firstly, there is a risk that phenotypic features noted in case series and case reports are incorrectly attributed to a certain disease. This could be the case in genetically isolated populations, or in patients from consanguineous parents, who may harbor more than one genetic disease. As the risk for incorrectly attributed phenotypic features decreases when the number of patients increases, this limitation should be considered especially in case series with a limited sample size. Secondly, reporting bias might be introduced by the potential inclination of authors of case series and case reports to include phenotypic features that are in line with related genetic disorders, and to reduce emphasis on phenotypic features that are not known to overlap with related genetic disorders. This might cause overrepresentation of phenotypic features commonly associated with a certain disease, and underrepresentation of less usual phenotypic features.

Table 2. Genes associated to one of the most specific phenotypic features in COG-CDG, episodic fever (HP:0001954)

Gene	Gene name	Disease name	OMIM	Protein function	Autophagy associated	Protein effect on autophagy
<i>ELP1</i>	Elongator Complex Protein 1	Neuropathy, hereditary sensory and autonomic, type III	#223900		No	
<i>PSMB8</i>	Proteasome Subunit Beta 8	Autoinflammation, lipodystrophy and dermatosis syndr.	#256040	Inflammation induction	No	
<i>STXBP2</i>	Syntaxin Binding Protein 2	Familial hemophagocytic lymphohistiocytosis V	#613101		No	
<i>MVK</i>	Mevalonate Kinase	Mevalonic aciduria	#610377		Yes ¹⁵	Impaired RhoA transloc.
<i>MEFV</i>	MEFV, Pyrin Innate Immunity Regulator	Familial Mediterranean fever	#249100	Inflammation control	Yes ^{15,16}	No NLRP3 degradation
<i>NLRP3</i>	NLR Family Pyrin Domain Containing 3	Familial cold autoinfl. syndrome I	#120100		No	
<i>NLRP12</i>	NLR Family Pyrin Domain Containing 12	Familial cold autoinfl. syndrome II	#611762		No	
<i>CRLF1</i>	Cytokine Receptor Like Factor 1	Cold-induced sweating syndrome I	#272430		No	
<i>LIFR</i>	LIF Receptor Alpha	Stuve-Wiedemann syndrome	#601559		No	
<i>SLC29A3</i>	Solute Carrier Family 29 Member 3	Histiocytosis-lymphadenopathy plus syndrome	#602782	Cytokine response	No	
<i>TNFAIP3</i>	TNF Alpha Induced Protein 3	Familial autoinflammatory syndrome, Behcet-like	#616744		Yes ¹⁷	mTORC1 inactivation
<i>TNFRSF1A</i>	TNF Receptor Superfamily Member 1A	Familial periodic fever, AD	#142680		Yes ¹⁷	No NF- κ B pathway act.
<i>GALC</i>	Galactosylceramidase	Krabbe disease	#245200	Second messenger	Yes ^{18,19}	LC3-II overexpression
<i>NGF</i>	Nerve Growth Factor	Neuropathy, hereditary sensory and autonomic, type V	#608654		Yes ²⁰	PI3K signalling
<i>NTRK1</i>	Neurotrophic Receptor Tyrosine Kinase 1	Congenital insensitivity to pain, with anhidrosis	#256800	Neuronal cell growth	Yes ²¹	PI3K signalling
<i>PTS</i>	6-Pyruvoyltetrahydropterin Synthase	BH4-deficient hyperPhe. type A	#261640		Yes ²²	mTORC1 inactivation
<i>GCH1</i>	GTP Cyclohydrolase 1	BH4-deficient hyperPhe. type B	#233910	Tetrahydrobiop- terin synthesis	Yes ²³	mTORC1 inactivation
<i>ODPR</i>	Quinoid Dihydropteridine Reductase	BH4-deficient hyperPhe. type C	#261630		Yes ²³	mTORC1 inactivation
<i>ORAI1</i>	ORAI Calcium Release-Activated Calcium Modulator 1	Immunodeficiency 9	#612782	Calcium signaling	Yes ²⁴	mTORC1 inactivation
<i>STIM1</i>	Stromal Interaction Molecule 1	Immunodeficiency 10	#612783		Yes ²⁴	mTORC1 inactivation
<i>LIPIN2</i>	Lipin 2	Majeed syndrome	#609628	Adipose tiss. met.	No	
<i>CYP11B2</i>	Cytochrome P450 Family 11 Subfamily B Member 2	Corticosterone methyloxidase type I deficiency	#203400	Aldosterone synthesis	No	

Abbreviations: AD: autosomal dominant; adipose tiss. met.: adipose tissue metabolism; hyperPhe: hyperphenylalaninemia; OMIM: Online Mendelian Inheritance in Man; syndr.: syndrome.

For example, when reporting on COG-CDG patients, authors might be more inclined to report on features such as elevated hepatic transaminases and abnormality of coagulation, because these features are commonly associated with CDG. This might cause overrepresentation of CDG among genes associated with these features. Thirdly, although HPO provides a standard vocabulary, enhancing reliable alignment and pooling of phenotypic data, ascertaining phenotypic frequency and specificity heavily relies on the extent, specificity and completeness of the initial phenotypic description. We illustrate this limitation using two examples. According to HPO, the phenotypic feature abnormally lax or hyperextensible skin (HP:0008067) is defined as “abnormally loose or stretchable skin” or “abnormally loose or hyperelastic skin”. This feature is associated to 109 genes (Table S3) and when mentioned in case series and case reports, it can be readily recognized. However, it might be hard to distinguish the three underlying subclasses, excessive wrinkled skin (HP:0007392, 35 genes), cutis laxa (HP:0000973 73 genes, defined as “inelastic skin, cutaneous laxity, generalized elastolysis, hanging skin, lax skin, dermatochalasia, skin laxity, hypoeelastic skin, loose skin, chalazoderma or dermatomegaly) and increased number of skin folds (HP:0007522, 3 genes), based on phenotypic descriptions in case series and case reports. For COG-CDG, three patients were described as having “loose, wrinkled skin”.^{7,28} These patients were noted to have both cutis laxa and excessive wrinkled skin. Three other patients were described to have “wrinkled skin”.²⁹ For these patients, only excessive wrinkled skin was noted (Table S2). Similarly, while episodes of recurrent fever described in COG-CDG patients were noted as episodic fever in HPO, episodes of recurrent, unexplained fever, described in TMEM165-CDG patients,^{13,14} were noted as unexplained fever in HPO. Altogether, these examples illustrate the need for an unambiguous terminology in case series and case reports, which would allow for a more trustworthy delineation of phenotypic features, especially when features are described in much detail. In addition, it illustrates the need for further improvements of the residual unambiguity of the HPO vocabulary. We advocate that when classification is still ambiguous, both HPO classifications should be noted, rather than making an arbitrary decision. Fourth and lastly, the strategy presented here depends on the completeness of HPO. Unfortunately, the HPO database is incomplete, especially in subclasses most distant from the root of the HPO-tree. This is illustrated by the phenotypic feature hearing impairment (HP:0000365). This phenotypic feature is associated to 969 genes, according to HPO (Table S3). However, while hearing impairment is well-specified based on the type in either conductive or sensorineural hearing loss (810/969 genes), only a few genes are further classified based on other characteristics of hearing impairment: only 15/969 genes on severity (mild/moderate/severe/profound hearing impairment), 9/969 genes on frequency (low/mid/high frequency hearing impairment) and 50/969 genes on the course (transient/progressive hearing impairment), clearly demonstrating the incompleteness of HPO. This is important, as this incompleteness can potentially lead to underestimation of the denominator of the gene occurrence ratio, and thus an overestimation of the degree of phenotypic specificity. Likely as a consequence of the underestimation of the number of associated genes, in COG-CDG patients hearing impairment has poor specificity (ratio 0.0007), while severe hearing impairment has very high specificity (1.400). To overcome this limitation, we assessed whether the superclasses of highly specific phenotypic features were also highly specific, and whether these superclasses were associated to other CDG. This revealed that hearing impairment was associated to seven CDG, whereas the two superclasses of episodic fever were associated to only one CDG, underlining a potential function of the COG complex other than glycosylation.

Taking into account these limitations, phenotypic specificity can be determined as reliably as possible if (1) an unambiguous vocabulary is used, (2) when classification is debatable, both HPO classifications are noted, (3) a cut-off value of how many patients in the cohort should at least present with a phenotypic feature to meet a minimum sensitivity is calculated, (4) superclasses of potentially highly specific phenotypic features are also assessed and (5) if potentially relevant findings are confirmed using the available literature. To further improve the validity of our approach, we advocate the use of an unambiguous vocabulary in case series and case reports, as it enhances the reliability of the type of systematic data assessment as we present here. Perhaps even more importantly, we encourage to include detailed phenotypic descriptions of all patients included in case series and case reports, for example as Supplemental Material. Moreover, we urge curation and completion of HPO, to better serve deep phenotyping approaches.

Interestingly, we had the opportunity to assess the effect of the addition of newly described patients on the results of the approach, when during the development of our strategy four additional case reports were published and HPO was updated. This necessitated us to retake our steps, now including the twelve newly described COG-CDG patients.⁸⁻¹¹ Both analyses, including first 33 and now 45 patients, were strikingly similar and both put forward episodic fever as highly specific feature not associated with any other CDG, supporting the soundness of our approach.

The approach that we present here can be performed relatively easy and rapidly by anyone with access to medical literature, HPO and GeneCards. For this reason, we anticipate that our approach could readily find its way to daily research and clinical practice, when the problem of data scarcity hampering pathophysiological understanding of a rare genetic disease is faced. We invite anyone interested to test our hypothesis that determining phenotypic specificity could facilitate understanding of pathophysiology for their own rare genetic disorder of interest. To facilitate this, we provide a standard operating procedure, explaining the here described approach step by step (Supplemental Notes 2).

CONCLUSION

In summary, we here demonstrate support for our hypothesis that despite data scarcity, determining phenotypic specificity allows relevant prioritization of phenotypic features in rare genetic disorders, thereby facilitating progress in understanding underlying pathophysiology in a hypothesis-free manner.

WEB RESOURCES

GeneCards	https://www.genecards.org
Human Phenotype Ontology	http://compbio.charite.de/hpweb/
OMIM	https://www.omim.org

REFERENCES

1. Haring R, Wallaschofski H. Diving through the “-omics”: the case for deep phenotyping and systems epidemiology. *Omics* 2012;16:231-4.
2. Tracy RP. “Deep phenotyping”: characterizing populations in the era of genomics and systems biology. *Curr Opin Lipidol.* 2008;19:151-7.
3. Köhler S, Vasilevsky N, Engelstad M et al. The Human Phenotype Ontology in 2017. *Nucl Acids Res.* 2017;45:865-876.
4. Westbury SK, Turro E, Greene D et al. Human phenotype ontology annotation and cluster analysis to unravel genetic defects in 707 cases with unexplained bleeding and platelet disorders. *Genome Med.* 2015;7:36.
5. Haijes HA, Jaeken J, Foulquier F, van Hasselt PM. Hypothesis: lobe A (COG1-4)-CDG causes a more severe phenotype than lobe B (COG5-8)-CDG. *J Med Genet.* 2018;55:137-142.

6. Rymen D, Winter J, van Hasselt PM et al. Key features and clinical variability of COG6-CDG. *Mol Genet Metab*. 2015;116:163-170.
7. Wu X, Steet RA, Bohorov O et al. Mutation of the COG complex subunit gene COG7 causes a lethal congenital disorder. *Nat Med*. 2004;10:518-23.
8. Kim YO, Yun M, Jeong JH et al. A mild form of COG5 defect showing early-childhood-onset Friedreich's-ataxia-like phenotypes with isolated cerebellar atrophy. *J Korean Med Sci*. 2017;32:1885-1890.
9. Alsubhi S, Alhashen A, Faqih E et al. Congenital disorders of glycosylation: the Saudi experience. *Am J Med Genet. A* 2017;173:2614-2621.
10. Althonaia N, Alsultan A, Morava E, Alfadhel M. Secondary hemophagocytic syndrome associated with COG6 gene defect: report and review. *JIMD Rep*. 2018;42:105-111.
11. Yang A, Cho SY, Jang JH et al. Further delineation of COG8-CDG: a case with novel compound heterozygous mutations diagnosed by targeted exome sequencing. *Clin Chim Acta* 2017;471:191-195.
12. Dulary E, Potelle S, Legrand D, Foulquier F. TMEM165 deficiencies in congenital disorders of glycosylation type II (CDG-II): clues and evidences for roles of the protein in Golgi functions and ion homeostasis. *Tissue Cell* 2017;49:150-156.
13. Foulquier F, Amyere M, Jaeken J et al. TMEM165 deficiency causes a congenital disorder of glycosylation. *Am J Hum Genet*. 2012;91:15-26.
14. Zeevaert R, de Zegher F, Sturiale L et al. Bone dysplasia as a key feature in three patients with a novel congenital disorder of glycosylation (CDG) type II due to a deep intronic splice mutation in TMEM165. *JIMD Rep*. 2013;8:145-52.
15. Kwak SS, Suk J, Choi JH et al. Autophagy induction by tetrahydrobiopterin deficiency. *Autophagy* 2011;7:1323-1334.
16. Si Q, Sun S, Gu Y. A278C mutation of dihydropteridine reductase decreases autophagy via mTOR signaling. *Acta Biochim Biophys Sin*. 2017;49:706-712.
17. Tanwar J, Motiani RK. Role of SOCE architects STIM and Orai proteins in cell death. *Cell Calcium* 2018;69:19-27.
18. Ohashi Y, Munro S. Membrane delivery to the yeast autophagosome from the Golgi-Endosomal system. *Mol Biol Cell* 2010;21:3998-4008.
19. Yen WL, Shintani T, Nair U et al. The conserved oligomeric Golgi complex is involved in double-membrane vesicle formation during autophagy. *J Cell Biol*. 2010;188:101-114.
20. Wang IH, Chen YJ, Hsu JW, Lee FJS. The Arl3 and Arl1 GTPases co-operate with Cog8 to regulate selective autophagy via Atg9 trafficking. *Traffic* 2017;18:580-589.
21. Hua Y, Shen M, McDonald C, Yao Q. Autophagy dysfunction in autoimmune diseases. *J Autoimmun*. 2018;88:11-20.
22. Aslan D. Leukopenia in Familial Mediterranean Fever: Case series and literature review with special emphasis on pathogenesis. *Ped Hem Onc*. 2014;31:120-128.
23. Matsuzawa Y, Oshima S, Takahara M et al. TNFAIP3 promotes survival of CD4 T cells by restricting mTOR and promoting autophagy. *Autophagy* 2015;11:1052-1062.
24. Ribbens JJ, Moser AB, Hubbard WC, Bongarzone ER, Maegawa GH. Characterization and application of a disease-cell model for a neurodegenerative lysosomal disease. *Mol Genet Metab*. 2014;111:172-183.
25. Del Grosso A, Antoninin S, Angella L, Tonazzini I, Signore G, Cecchini M. Lithium improves cell viability in psychosine-treated MO3.13 human oligodendrocyte cell line via autophagy activation. *J Neurosci Res*. 2016;94:1246-1260.
26. Xue L, Fletcher GC, Tolkovsky AM. Autophagy is activated by apoptotic signalling in sympathetic neurons: an alternative mechanism of death execution. *Mol Cell Neurosci*. 1999;14:180-198.
27. Franco ML, Melero C, Sarasola E et al. Mutations in TrkA causing congenital insensitivity to pain with anhidrosis (CIPA) induce misfolding, aggregation, and mutation-dependent neurodegeneration by dysfunction of the autophagic flux. *J Biol Chem*. 2016;291:21363-21374.
28. Rymen D, Keldermans L, Race V et al. COG5-CDG: expanding the clinical spectrum. *Orphanet J Rare Dis*. 2012;7:94.
29. Morava E, Zeevaert R, Korsch E et al. A common mutation in the COG7 gene with a consistent phenotype including microcephaly, adducted thumbs, growth retardation, VSD and episodes of hyperthermia. *Eur J Hum Genet*. 15(6):638-45.

SUPPLEMENTAL DATA

Supplemental Notes 1. R code to create figures

```

library('ggplot2')
library('cowplot')

setwd("~/Promotietraject/3) COG-CDG/A) Change of focus")
color<-c('TRUE'='orangered', 'FALSE'='gray34')

# Load files
AllRatios<-read.csv("COG_AllRatios_CSV.csv", sep=";", stringsAsFactors=FALSE)
AllRatios$HPOcode<-factor(AllRatios$HPOcode, levels=unique(AllRatios$HPOcode))
SelRatios<-read.csv("COG_SelRatios_CSV.csv", sep=";", stringsAsFactors=FALSE)
SelRatios$HPOcode<-factor(SelRatios$HPOcode, levels=unique(SelRatios$HPOcode))

# Figure 1A and 1B
p1<-ggplot()+
  geom_bar(data=AllRatios[which(AllRatios[,5]>5),],
  stat='identity', aes(x=HPOcode, y=Ratio, fill=Ratio>=0.08))+
  geom_text(data=AllRatios[which(AllRatios[,6]>=0.08 & AllRatios[,5]>5),],
  aes(x=HPOcode, y=Ratio, label=Feature), size=3, vjust=0)+
  geom_hline(yintercept=0.08, col='gray43', linetype=2)+
  scale_fill_manual(values=color)+
  scale_y_continuous(breaks=seq(0, 1.5, 0.1), limits=c(0, 1.5))+
  labs(x='HPO code', y='Occurrence ratio', title='Phenotypic specificity in
  COG-CDG')+
  theme(axis.text.x=element_text(angle=90, hjust=1, size=7),
  legend.position='none')

p2<-ggplot()+
  geom_bar(data=SelRatios[which(SelRatios[,5]>5),],
  stat='identity', aes(x=HPOcode, y=Ratio, fill=Ratio>=0.07))+
  geom_text(data=SelRatios[which(SelRatios[,6]>=0.07 & SelRatios[,5]>5),],
  aes(x=HPOcode, y=Ratio, label=Feature), size=3, vjust=0)+
  geom_hline(yintercept=0.07, col='gray43', linetype=2)+
  scale_fill_manual(values=color)+
  scale_y_continuous(breaks=seq(0, 1.5, 0.1), limits=c(0, 1.5))+
  labs(x='HPO code', y='Ratio COG-CDG patients over HPO associated genes',
  title='Phenotypic specificity in COG-CDG, excluding super classes of
  episodic fever')+
  theme(axis.text.x=element_text(angle=90, hjust=1, size=7),
  legend.position='none')

plot_grid(p1, p2, ncol=1, axis='r|bt', rel_heights=c(1, 1))
rm(p1, p2)

# Figure S1
Diff<-read.csv("COG_difference_CSV.csv", sep=";", stringsAsFactors=FALSE)
ggplot(Diff)+
  geom_line(aes(x=Patients, y=Difference, col=Patients<5), size=2)+
  geom_line(aes(x=Patients, y=Difference, col=Patients>=6), size=2)+
  geom_vline(xintercept=6, col='gray43', linetype=2)+
  scale_color_manual(values=color)+
  scale_y_continuous(breaks=seq(-10, 160, 10), limits=c(-10, 160))+
  scale_x_continuous(breaks=seq(0, 45, 3), limits=c(0, 45))+
  labs(x='Number of COG-CDG patients', y='Difference in number of phenotypic
  features', title='Number of phenotypic features versus phenotypic frequency
  in COG-CDG')+
  theme(legend.position='none')

# Figure S2
AllRatios<-AllRatios[order(-AllRatios$Ratio),]
Spec<-setNames(data.frame(matrix(ncol=3, nrow=45)),
  c('MedianTop10', 'MedianNoise', 'MedianRatio'))
for(freq in 1:40) {

```

```
Spec[freq,1]<-median(as.numeric(AllRatios[which(AllRatios[,5]>
(freq-1)),6][1:10]),na.rm=TRUE)
Spec[freq,2]<-median(as.numeric(AllRatios[which(AllRatios[,5]>
(freq-1)),6][11:length(AllRatios[which(AllRatios[,5]>
(freq-1)),6])]),na.rm=TRUE)
Spec[freq,3]<-(Spec[freq,1]/Spec[freq,2])
}

Spec$Patients<-as.numeric(as.character(rownames(Spec)))
ggplot(Spec)+
  geom_line(aes(x=Patients,y=MedianRatio,col=Patients<5),size=2)+
  geom_line(aes(x=Patients,y=MedianRatio,col=Patients>=6),size=2)+
  geom_vline(xintercept = 6,col='gray43',linetype=2)+
  scale_color_manual(values=color)+
  scale_x_continuous(breaks=seq(0,45,3),limits=c(0,45))+
  scale_y_continuous(breaks=seq(0,70,5),limits=c(0,70))+
  labs(x='Number of COG-CDG patients',y='Specificity ratio',
  title='Specificity ratio versus phenotypic frequency in COG-CDG')+
  theme(legend.position='none')
```

Figure S3

```
ggplot()+
  geom_bar(data=AllRatios[which(AllRatios[,5]>3)],,
  stat='identity',aes(x=HPOcode,y=Ratio,fill=Ratio>=0.28))+
  geom_text(data=AllRatios[which(AllRatios[,6]>=0.08 & AllRatios[,5]>3)],,
  aes(x=HPOcode,y=Ratio,label=Feature),size=3,vjust=0)+
  geom_hline(yintercept=0.08,col='gray43',linetype=2)+
  scale_fill_manual(values=color)+
  scale_y_continuous(breaks=seq(0,1.5,0.1),limits=c(0,1.5))+
  labs(x='HPO code',y='Occurrence ratio', title='Phenotypic specificity in
  COG-CDG')+
  theme(axis.text.x=element_text(angle=90,hjust=1,size=7),
  legend.position='none')
```

Figure S4

```
ggplot()+
  geom_bar(data=AllRatios[which(AllRatios[,5]>7)],,
  stat='identity',aes(x=HPOcode,y=Ratio,fill=Ratio>=0.06))+
  geom_text(data=AllRatios[which(AllRatios[,6]>=0.08 & AllRatios[,5]>7)],,
  aes(x=HPOcode,y=Ratio,label=Feature),size=3,vjust=0)+
  geom_hline(yintercept=0.08,col='gray43',linetype=2)+
  scale_fill_manual(values=color)+
  scale_y_continuous(breaks=seq(0,1.5,0.1),limits=c(0,1.5))+
  labs(x='HPO code',y='Occurrence ratio', title='Phenotypic specificity in
  COG-CDG')+
  theme(axis.text.x=element_text(angle=90,hjust=1,size=7),
  legend.position='none')
```

Supplemental Notes 2. Standard Operating Procedure “Determining phenotypic specificity to facilitate understanding of underlying pathophysiology in rare genetic disorders

A Standard Operation Procedure for the identification of highly specific phenotypic features in rare genetic disorders, to study shared pathophysiology.

Listing all phenotypic features

1. Perform a literature study. Identify all described cases and collect all data from case-reports and case-series. If you need additional information, do not hesitate to contact the authors.
Example: 45 COG-CDG patients from 32 families, reported in 22 case-reports and case-series.
2. Choose a single case to start with, preferably the one described in most detail
3. For this case, list all described phenotypic features (preferably in an Excel-like program).

Example:

Pregnancy and delivery of the female patient were uncomplicated and at term. The patient suffered from intractable focal seizures, vomiting and loss of consciousness due to intracranial bleedings. Biochemical investigations revealed a normal level for albumin and mildly elevated values for lactate, aspartate aminotransferase and creatine kinase. Metabolic investigations revealed cholestasis and subsequent vitamin K deficiency, explaining in part her intracranial bleedings. The patient died due to brain edema at 5 weeks of age. Since the clinical phenotype of the patient was suspect for a CDG syndrome, initial CDG diagnosis was established by isoelectric focusing (IEF) of the patient's serum transferrin.

Lübbehusen et al. 2010, Human Molecular Genetics

List: intractable focal seizures, vomiting, intracranial bleeding, elevated lactate, elevated aspartate aminotransferase, elevated creatine kinase, cholestasis, vitamin K deficiency

4. For each phenotypic feature, list the most appropriate HPO-term and the associated HPO-code. In the search bar you can type the phenotypic feature to see the possible HPO-terms. Primary ID on the left renders the HPO-code. In the middle text block, synonyms for the feature are listed and on the right a textual definition is provided. Super classes and subclasses are listed below. Always be as precise as possible, if a subclass is applicable, it is preferred over its superclass.

Example:

Intractable focal seizures	Focal seizures	HP:0002358
Vomiting	Vomiting	HP:0002013
Intracranial bleeding	Intracranial hemorrhage	HP:0002170
Elevated lactate	Increased serum lactate	HP:0002151

5. Expand the list of phenotypic features by listing the super classes of each of the phenotypic features that you listed. For the patient that you started with, score each phenotypic feature and all super classes. If you do this, you will preserve the tree-like hierarchical structure of HPO.

Example:

		P1	
0.	Phenotypic abnormality	HP:0000118	1
1.	Abnormality of the nervous system	HP:0000707	1
2.	Abnormality of nervous system physiology	HP:0012638	1
3.	Seizures	HP:0001250	1
4.	Focal seizures	HP:0002358	1

When more super classes are applicable, list the most appropriate one. If you cannot choose, list both.

6. When you finished this for the first patient, you can add the second:

Example: add the phenotypic feature "profound intellectual disability" to your list:

		P1	P2
0.	Phenotypic abnormality	HP:0000118	1 1
1.	Abnormality of the nervous system	HP:0000707	1 1
2.	Abnormality of nervous system physiology	HP:0012638	1 1
3.	Neurodevelopmental abnormality	HP:0012759	0 1
4.	Intellectual disability	HP:0001249	0 1
5.	Intellectual disability, profound	HP:0002187	0 1
3.	Seizures	HP:0001250	1 0
4.	Focal seizures	HP:0002358	1 0

7. Retake step 3-6 until you listed all phenotypic features as detailed as possible for all your patients. Be meticulous in also scoring all appropriate super classes of the phenotypic features.

Example: Table S2

Calculating gene occurrence ratios

8. Sum the total number of patients for each listed phenotypic feature.

Example: Table S2

9. Calculate the phenotypic frequency by dividing the total number of patients that present with a phenotypic feature over the total number of included patients

Example: Table S1

10. Retrieve from HPO for each phenotypic feature the number of associated genes and note this number for each of the phenotypic features and all super classes.

The associated number of genes can be found below the number of associated diseases. HPO is frequently updated, so note the date you last consulted HPO and during your assessment, regularly check if nothing has changed.

11. Calculate the **gene occurrence ratio** by dividing the frequency in the patient cohort over the number of associated genes.
Example: episodic fever was noted in 20 patients (Table 1) and the feature is associated with 22 genes. Occurrence ratio is $20/22 = 0.909$. For all occurrence ratios, see Table S1.
Example: Table S1

Determine the cut-off value to meet a minimum sensitivity

12. Order all phenotypic features on the total number of patients that present with the phenotypic feature and calculate the number of phenotypic features that were noted in only one patient, the number of phenotypic features that were noted in only two patients, etc. and tabulate this.
Example: Figure S1
13. Calculate and plot the differences between these numbers. The cut-off value is the number of patients from whereon the difference in number of phenotypic features is fairly stable.
Example: Figure S1
14. This cut-off value can be checked by calculating the specificity ratio. This is the ratio of the median occurrence ratio of the top ten phenotypic features over the median occurrence ratio of all phenotypic features.
 - If no cut-off value is used, calculate the median occurrence ratio of the ten phenotypic features with the highest occurrence ratios. In addition, calculate the median occurrence of all other phenotypic features. The specificity ratio is calculated by dividing the median occurrence ratio of the top ten phenotypic features over the median occurrence ratio of all phenotypic features.
 - Exclude all phenotypic features that are noted in only one patient and calculate the second specificity ratio.
 - Exclude all phenotypic features that are noted in one or two patients and calculate the third specificity ratio.
 - Calculate specificity ratios for all possible phenotypic frequencies and plot this. This should support the cut-off value from step 13.*Example: Figure S2*

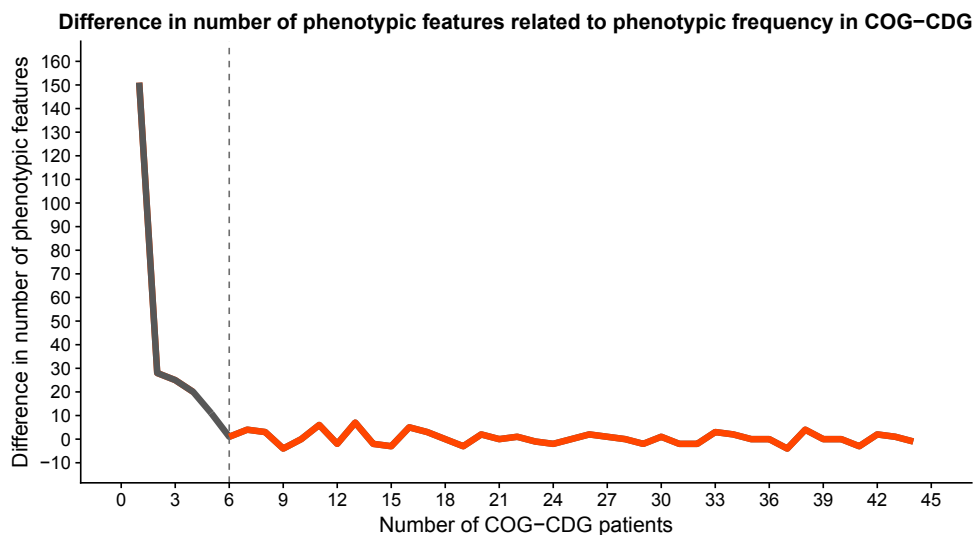
Study highly specific phenotypic features

15. To study the top XX highly specific phenotypic features of a given disease (in the paper top 10 phenotypic features), retrieve the list of associated genes from HPO (Figure 2, Export to Excel).
Example: Table 2
16. Derive the gene encoded protein functions from GeneCards.com or other resources.
Example: for episodic fever one of the genes is ELP1. According to GeneCards this is Elongator Protein Complex 1, a scaffold protein and regulator for three different kinases involved in proinflammatory signaling.
17. Classify the protein functions into – data-driven – categories.
Example: Table 2. ELP1 was categorized in the category “Immune system”.
18. Note the number of genes per category to assess differences in distribution over the categories from the different phenotypic features.
Example: Table 1.
19. Based on your research question, decide what might be an interesting phenotypic feature to look into.
Example: for episodic fever even its two super classes (fever (HP:0001945) and abnormality of temperature regulation (HP:0004370)) stood out as highly specific phenotypic features and it was not associated to any other glycosylation disorder, so this phenotypic feature was chosen to (first) look into.
20. Perform literature studies for each of the associated genes and see if you can establish one or multiple pathophysiological pathways where genes are related to. This way you can conceive a hypothesis on the possible function in this pathway of the gene you are studying.

Disclaimer

Please bear in mind that the systematic assessment of phenotypic specificity and shared pathophysiology as described here heavily relies on the extent, specificity and completeness of the initial phenotypic description, and also on the accuracy and completeness of the used open access databases: HPO and GeneCards. For HPO, be aware that it is regularly updated, not always with adjustment of the version.

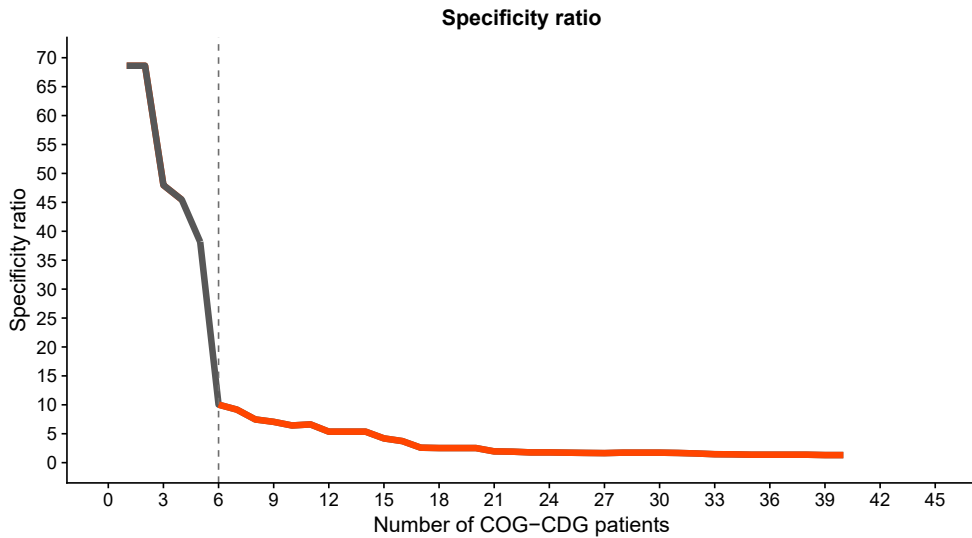
Figure S1. Number of phenotypic features versus phenotypic frequency in COG-CDG



Pat.	Feat.	Diff.
1	253	
2	102	151
3	74	28
4	50	25
5	29	21
6	18	11
7	17	1
8	13	4
9	10	3
10	14	-4
11	14	0
12	8	6
13	10	-2
14	3	7
15	5	-2
...
Total	666	

A sliding scale was noted of only one phenotypic feature that is described in all patients, towards many phenotypic features that are described in only one COG-CDG patient (table, column “features”). For features described in at least six COG-CDG patients the number of phenotypic features added to the total list per added patient frequency is very constant (Figure). This suggests that zooming in on features described in at least six COG-CDG patients provides the most relevant focus. Abbreviations: CDG: congenital disorder of glycosylation; COG: conserved oligomeric Golgi; diff.: difference; feat.: features; pat.: patients.

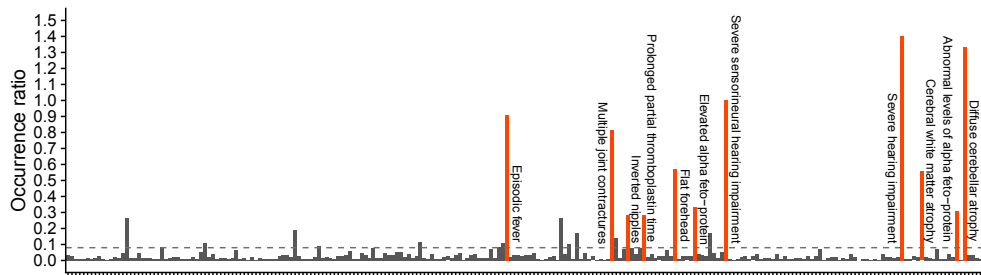
Figure S2. Specificity ratio versus phenotypic frequency in COG-CDG



3

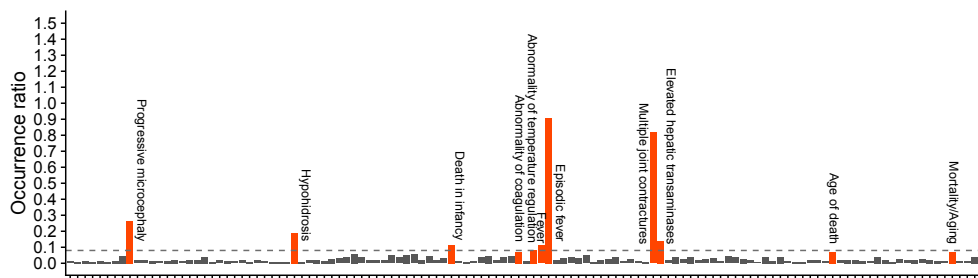
A “specificity ratio” was calculated: the ratio of the median occurrence ratio of the top 10 phenotypic features over the median occurrence ratio of all other phenotypic features. This specificity ratio in relation to the number of COG-CDG patients presenting with a phenotypic feature supported the cut-off value of at least six patients presenting with a certain phenotypic feature. Abbreviations: CDG: congenital disorder of glycosylation; COG: conserved oligomeric Golgi.

Figure S3. Phenotypic specificity when assessing features present in at least four patients



A wider zoom than the cut-off value of a phenotypic feature being present in at least six COG-CDG patients, namely being present in at least four COG-CDG patients, results in a longer list of less relevant features.

Figure S4. Phenotypic specificity when assessing features present in at least eight patients

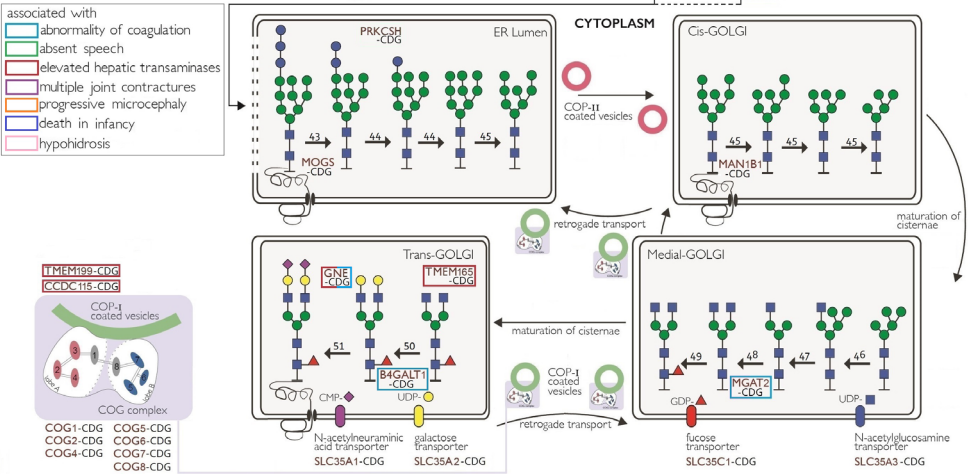
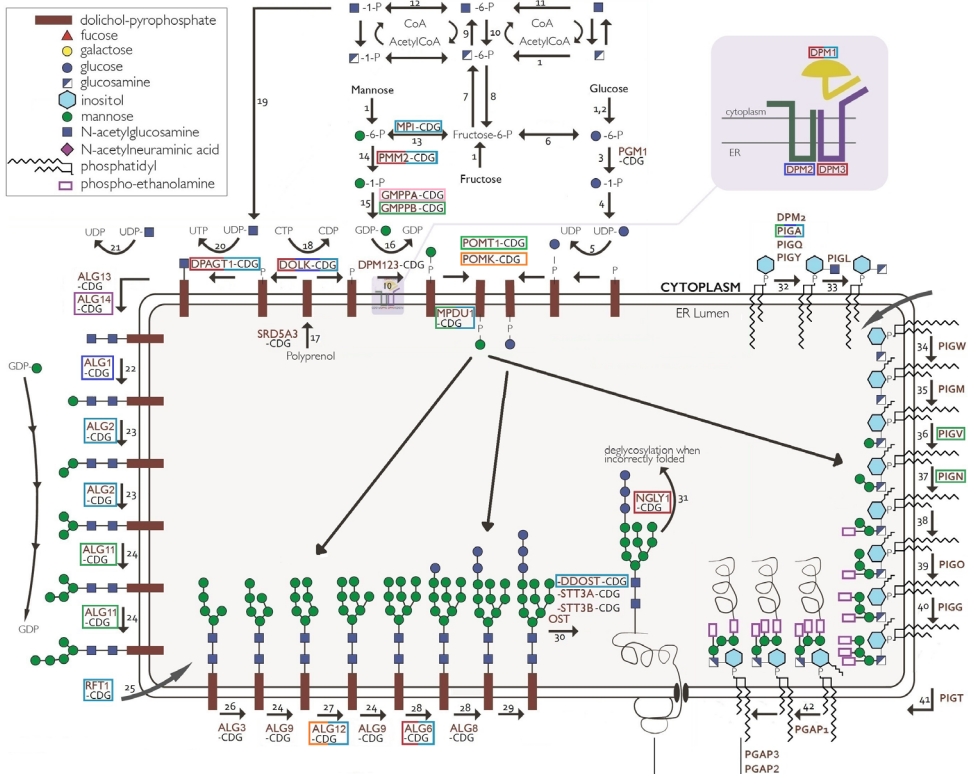


A narrower zoom than the cut-off value of a phenotypic feature being present in at least six COG-CDG patients, namely being present in at least eight COG-CDG patients, results in missing relevant features.

Figure S5. Specific phenotypic features in COG-CDG associated with other CDG

Figure S5 is depicted on the right page and demonstrates the glycosylation process. Black text: metabolites. Red text: known CDG, caused by a deficiency of the gene encoding the required enzyme. Seven of the ten extracted highly specific phenotypic features are clearly associated with other CDG, depicted in the different colors surrounding the known CDG. For example, abnormality of coagulation and elevated hepatic transaminases are mainly seen in CDG affecting N-glycosylation (process drawn on the left of the endoplasmatic reticulum), while absent speech is seen in CDG affecting O-mannosylation and glycosylphosphatidylinositol anchoring (process drawn on the right of the endoplasmatic reticulum). Abbreviations: CDG: congenital disorder of glycosylation; COG: conserved oligomeric Golgi; ER: endoplasmatic reticulum.

Hypothesis: determining phenotypic specificity facilitates understanding of pathophysiology in rare genetic disorders



Enzymes:

1. Hexokinase	12. Phosphoglucomutase 3	26. Alpha-1,3-mannosyltransferase	40. Ethanolamine phosphate transferase III
2. Glucokinase	13. Mannose-6-phosphate isomerase	27. Alpha-1,6-mannosyltransferase	41. GPI transamidase (PIGT)
3. Phosphoglucomutase 1	14. Phosphomannomutase	28. Alpha-1,3-glucosyltransferase	42. Inositol deacetylase (PGAP1)
4. UDP-glucose-hexose-2-phosphate uridylyltransferase	15. Mannose-3-phosphate guanylyltransferase	29. Alpha-1,2-glucosyltransferase	43. Mannosyl-oligosaccharide glucosidase
5. Dolichyl-phosphate beta-glucosyltransferase	16. Dolichyl-phosphate mannosyltransferase	30. Dolichyl-diphospho-oligosaccharide-protein-glycosyltransferase	44. Alpha-1,3-glucosidase
6. Glucose-6-phosphate isomerase	17. Steroid 5 alpha-reductase 3	31. N-glycanase 1	45. Mannosyl-oligosaccharide alpha-1,2-mannosidase
7. Glucosamine-fructose-6-phosphate aminotransferase	18. Dolichol kinase	32. UDP-phosphatidyl-alpha-1,6-N-acetylglucosaminyltransferase	46. Alpha-1,3-mannosyl-glycoprotein beta-1,2-N-acetylglucosaminyltransferase
8. N-acetylglucosamine-6-phosphate deacetylase	19. UDP-N-acetylglucosamine pyrophosphorylase	33. Phosphatidylglucosaminyl de-N-acetylase	47. Mannosyl-oligosaccharide alpha-1,3/alpha-1,6-mannosidase
9. Glucosamine-phosphate N-acetyltransferase	20. UDP-N-acetylglucosamine-dolichyl-phosphate N-acetylglucosaminophosphotransferase	34. Inositol acyltransferase	48. Alpha-1,6-mannosyl-glycoprotein beta-1,2-N-acetylglucosaminyltransferase
10. N-acetylglucosamine-6-phosphate deacetylase	21. Beta-1,4-N-acetylglucosaminyltransferase	35. Mannosyltransferase I	49. GDP-alpha-1,6-fucosyltransferase
11. N-acetylglucosamine kinase	22. Dolichyl-1,4-mannosyltransferase	36. Mannosyltransferase II	50. UDP-beta-1,4-galactosyltransferase
	23. Alpha-1,3/alpha-1,6-mannosyltransferases	37. Ethanolamine phosphate transferase I	51. CMP-alpha-2,6-sialyltransferase
	24. Alpha-1,2-mannosyltransferase	38. Mannosyltransferase III	
	25. Dolichyl-diphospho-di-N-acetylglucosamine-pentamannose flippase	39. Ethanolamine phosphate transferase II	

Table S1. Aligning phenotypic descriptions to assess phenotypic frequency using the Human Phenotype Ontology in COG-CDG – Summarized table

Clinical features	HPO code	COG subunit								Total	
		1 n=3	2 n=1	4 n=2	5 n=10	6 n=18	7 n=8	8 n=3	n=	%	
Abn. of the nervous system	HP:0000707	3	1	2	10	18	8	3	45	100	
Microcephaly	HP:0000252	3	1	1	7	15	6	1	34	76	
Global developm. delay	HP:0001263	3	1	2	6	16	4	1	33	73	
Intellectual disability	HP:0001249	2	1		10	9		2	24	53	
Seizures	HP:0001250		1	2	1	4	5	2	15	33	
Cerebral atrophy	HP:0002059	2	1	2	1	4	2	1	13	29	
Cerebellar atrophy	HP:0001272	2			5	1	2	2	12	27	
Reduced tendon refl.	HP:0001315				4	1	5	2	12	27	
Abn. of the abdomen	HP:0001438	1	1	2	3	12	8	3	30	67	
Abnormality of the liver	HP:0001392	1	1	2	2	12	7	2	27	60	
Elev. hepatic transam.	HP:0002910			2	1	12	5	2	22	49	
Hepatomegaly	HP:0002240	1		1	2	6	5		15	33	
Splenomegaly	HP:0001744	1		1	1	8	2		13	29	
Growth abnormality	HP:0001507	3		1	6	14	8	2	34	76	
Failure to thrive	HP:0001508	1		1	3	12	8	1	26	58	
Short stature	HP:0004322	2		1	5	3	3	1	15	33	
Muscular hypotonia	HP:0001252	1		2	7	11	8	3	32	71	
Abnormality of the face	HP:0000271	3	1	1	4	15	6	2	32	71	
Abn. of the mouth	HP:0000153	2			1	6	4		13	29	
Abnormality of the nose	HP:0000366	1			2	5	3	1	12	27	
Abn. of orbital region	HP:0000315	2				6	3	1	12	27	
Abnormality of the skull	HP:0000929	1			1	4	5	1	12	27	
Abn. of skeletal morphol.	HP:0011842	2			6	11	5	1	25	56	
Episodic fever	HP:0001954					11	8	1	20	44	
Abn. of blood or blood-forming tissues	HP:0001871	1	1	2	1	9	2	1	17	38	
Abnormality of limbs	HP:0040064	3			2	4	4	2	15	33	
Abn. of eye physiology	HP:0012373	1		1	3	5	2	2	14	31	
Abnormality of the ear	HP:0000598	2			4	1	6		13	29	
Recurrent infections	HP:0002719	1		2	1	7	2		13	29	
Abn. of the urinary system	HP:0000079	2			4	3	3	1	13	29	
Abn. of circ. protein level	HP:0010876			1	1	5	3	2	12	27	
Abn. of the cardiovas. syst.	HP:0001626	2				6	4		12	27	
Death in infancy	HP:0001522								15	33	
Neonatal death	HP:0003811								1		

25-40% 41-55% 56-70% 71-85% 86-100%

Abbreviations: Abn: abnormality; COG: conserved oligomeric Golgi; HPO: Human Phenotype Ontology.

Table S2. Aligning phenotypic descriptions to assess phenotypic frequency using the Human Phenotype Ontology in COG-CDG – Full table

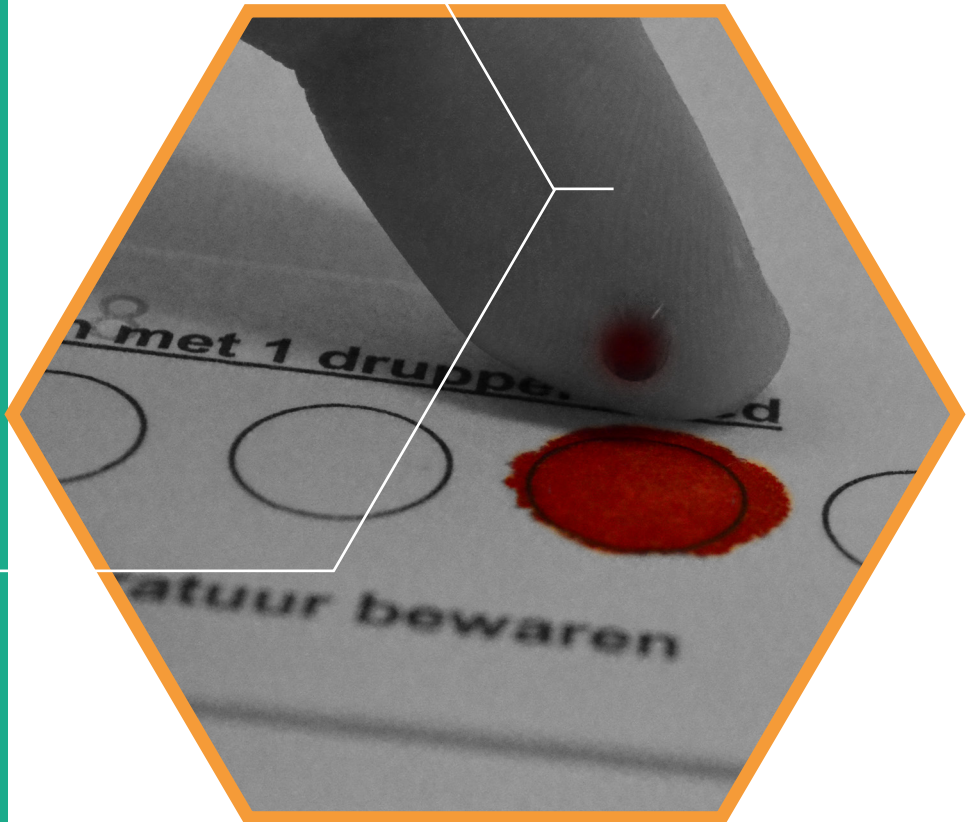
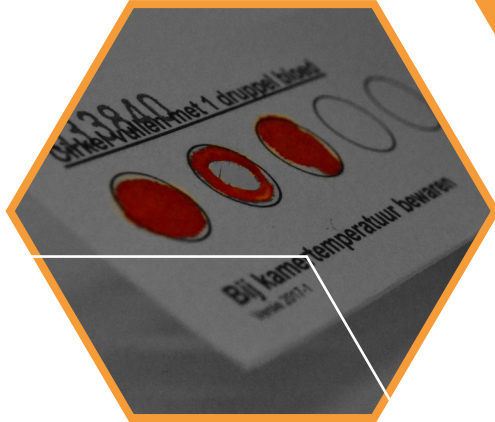
Due to its size, this table is only available online.

Table S3. Genes associated to phenotypic features discussed throughout the manuscript

Due to its size, this table is only available online.

Hypothesis: determining phenotypic specificity facilitates understanding of pathophysiology in rare genetic disorders

3



De novo heterozygous variants in *POLR2A* cause a

neurodevelopmental syndrome with profound
infantile-onset hypotonia

The American Journal of Human Genetics 2019, 105(2): 283-301
DOI: 10.1016/j.ajhg.2019.06.016

Hanneke A. Haijes[†], Maria J.E. Koster[†], Holger Rehmann, Dong Li, Hakon Hakonarson, Gerarda Cappuccio, Miroslava Hancarova, Daphne Lehalle, Willie Reardon, G. Bradley Schaefer, Anna Lehman, Ingrid M.B.H. van de Laar, Coranne D. Tesselaar, Clesson Turner, Alice Goldenberg, Sophie Patrier, Julien Thevenon, Michele Pinelli, Nicola Brunetti-Pierri, Darina Prchalová, Markéta Havlovicová, Markéta Vlckova, Zdeněk Sedláček, Elena Lopez, Vassilis Ragoussis, Alistair T. Pagnamenta, Usha Kini, Harmjan R. Vos, Robert M. van Es, Richard F.M.A. van Schaik, Ton A.J. van Essen, Maria Kibaek, Jenny C. Taylor, Jennifer Sullivan, Vandana Shashi, Slave Petrovski, Christina Fagerberg, Donna M. Martin, Koen L.I. van Gassen, Rolph Pfundt, Marni J. Falk, Elizabeth M. McCormick, H.T. Marc Timmers[#], Peter M. van Hasselt^{#,*}

[†] These authors contributed equally to this article

[#] These authors contributed equally to this article

* Corresponding author

ABSTRACT

The RNA polymerase II complex (pol II) is responsible for transcription of all ~21,000 human protein-encoding genes. Here, we describe sixteen individuals harboring *de novo* heterozygous variants in *POLR2A*, encoding RPB1, the largest subunit of pol II. An iterative approach combining structural evaluation and mass spectrometry analyses, the use of *S. cerevisiae* as a model system, and the assessment of cell viability in HeLa cells allowed us to classify eleven variants as probably disease-causing and four variants as possibly disease-causing. The significance of one variant remains unresolved. By quantification of phenotypic severity, we could distinguish mild and severe phenotypic consequences of the disease-causing variants. Missense variants expected to exert only mild structural effects led to a malfunctioning pol II enzyme, thereby inducing a dominant-negative effect on gene transcription. Intriguingly, individuals carrying these variants presented with a severe phenotype dominated by profound infantile-onset hypotonia and developmental delay. Conversely, individuals carrying variants expected to result in complete loss of function, thus reduced levels of functional pol II from the normal allele, exhibited the mildest phenotypes. We conclude that subtle variants that are central in functionally important domains of *POLR2A* cause a neurodevelopmental syndrome characterized by profound infantile-onset hypotonia and developmental delay through a dominant-negative effect on pol-II-mediated transcription of DNA.

KEY MESSAGE

Heterozygous *de novo* variants in *POLR2A* cause a neurodevelopmental syndrome characterized by profound infantile-onset hypotonia and developmental delay. The clinical consequences are dependent on their effect on pol-II-mediated transcription, as *POLR2A* variants predicted to result in loss of RPB1 are better tolerated than missense variants, which we propose cause a dominant-negative effect on pol-II-mediated transcription.

INTRODUCTION

Human *POLR2A* (MIM #180660) encodes the highly conserved RPB1 protein, which is the largest of twelve subunits of the essential RNA polymerase II (pol II) enzyme.^{1,2} This protein complex is responsible for the transcription of all protein-encoding genes, as well as several long and short non-coding RNA genes.³ Due to its central role in gene expression, pol II and the regulation of its activity have been studied in depth since its discovery fifty years ago.⁴ Biochemical and structural studies have shown that transcription initiation by pol II requires a set of basal (or general) transcription factors. After assembly of the pol II initiation complex at the promoter region, these factors are exchanged for transcription elongation factors including TFIIIS, DSIF, and P-TEFb to allow processive RNA synthesis by pol II.⁵ Detailed structural analysis of the pol II of *Saccharomyces cerevisiae* (*S. cerevisiae*)⁶ revealed different aspects of RNA synthesis, including initiation,⁷⁻¹⁰ nucleotide binding,¹¹ chain elongation,¹²⁻¹⁶ error correction, and backtracking.¹⁷⁻²⁰ For example, during the elongation cycle, the incorporation of the incoming nucleotide involves movement of the so-called RPB1 trigger loop, which induces the forward movement of pol II over the DNA template strand coincident with nucleotide selection. *In vivo* dynamics of pol II during initiation and promoter pausing were studied in GFP-RPB1 knock-in cells, and this research demonstrated that the continuous release and reinitiation of promoter-bound pol II is important for transcriptional regulation.²¹ Mutational studies focusing on *S. cerevisiae* and human RPB1 indicated that residues in the trigger loop region are controlling the rate of RNA synthesis.^{22,23} Experiments in *S. cerevisiae* indicated that the phenotypic consequences of *rpb1* variants in yeast might be concealed by transcript buffering²⁴ and might only become apparent under conditions of environmental or nutrient stress.²⁵ Experiments in *Arabidopsis* mutants that encode truncated RPB1 with different sizes of shortened C-terminal domain (CTD) show disturbed cell cycling control, demonstrating its importance in transcriptional regulation of cell cycle genes.²⁶ Despite its critical role in transcription, *POLR2A* has not been implicated in human disease thus far.

Here, we describe 16 individuals harboring *de novo* heterozygous genetic variants in *POLR2A*. We acknowledge that, although the occurrence of *de novo* variants provides an important clue toward variant pathogenicity,²⁷ this is not decisive²⁸ because large-scale sequencing of individuals without severe pediatric disease has revealed that protein-changing genetic variants are present in all ~21,000 protein-encoding genes.²⁹ Similarly, as individuals carrying a variant in a certain gene are increasingly found through gene-matching initiatives,³⁰ phenotypic overlap might merely reflect the general characteristics of individuals undergoing whole-exome or whole-genome sequencing (WES, WGS). In addition, neither the presence nor the absence of evidence from functional analyses can be used to prove or refute pathogenicity. This transition of genetics from a dichotomous field to an exciting but puzzling world full of shades of gray also offers new avenues of study. Deep phenotyping analyses might help to accurately expose the extent of the phenotypic overlap to support pathogenicity and so might severity metrics from population genetics. We here apply an iterative process wherein we combine several lines of evidence, including a detailed phenotypic analysis, an assessment of variant severity metrics, and structural biology and functional analyses in both *S. cerevisiae* and HeLa cells to assess the pathogenicity of the 16 identified variants in *POLR2A* in detail.

METHODS

Phenotypes of affected individuals

The cohort was assembled through the GeneMatcher initiative.³⁰ The inclusion criterion was the detection of a *de novo* heterozygous variant in *POLR2A* (GenBank: NM_000937.4) confirmed by either clinical or research trio WES or WGS or by confirming the exclusion of the heterozygous variant in both parents. Physicians first provided a detailed phenotypic description of the individual. In a second round, questions were asked regarding the specific clinical features of the individual to further define the clinical overlap among individuals. Additionally, doctors and parents together performed a thorough evaluation of the individuals' attained milestones by using items of the Denver Scale.³¹ We used these data to assess both the rate of development over time and developmental-domain-specific delays. To assess these focus points, we calculated Z-scores. The Denver Scale provides information on the fiftieth (p50) and ninetieth (p90) percentiles of the age in months, at which the normal population attains developmental milestones. The ninetieth percentile corresponds to 1.28 standard deviations (SDs). SD was calculated by $(p90 - p50)/1.28$. Z-scores were calculated as $(x - p50)/SD$, wherein x is the month the individual attained the developmental milestone. We performed the statistical analysis in R programming language by using log10 transformation. All procedures followed were in accordance with the Helsinki Declaration of 1975, as revised in 2000. The legal guardians for all individuals agreed to the participation of their child in the study and signed the appropriate consent forms, in agreement with institutional and national legislation for the different centers. Permission for publication of pictures was given separately.

Metrics of variant severity

Probability of intolerance to loss of function (pLI) scores for loss-of-function variants and Z-scores for synonymous and missense variants were retrieved from the Genome Aggregation Database (gnomAD) for *POLR2A*, as well as for the genes encoding other pol II subunits. High pLI scores are indicative of intolerance of loss-of-function variation, and Z-scores are indicative of intolerance of synonymous or missense variation.²⁹ Additionally, ratios of observed and expected variants were retrieved and acted as a reflection of the degree to which variants within a gene are underreported, indicative of a survival disadvantage.

The CADD score is a tool for scoring the deleteriousness of single-nucleotide variants and insertion and/or deletion variants in the human genome.³² It integrates multiple annotations into one metric by contrasting variants that survived natural selection with simulated variants. CADD scores were obtained for all missense variants in gnomAD, as well as for the missense and nonsense variants of the included individuals. A CADD score > 20 suggests pathogenicity because it indicates that the variant is predicted to be among the 1% of most deleterious substitutions that can be done to the human genome.

The distribution of genetic variants throughout *POLR2A* was assessed on the basis of all *POLR2A* variants from gnomAD. The interval length (number of amino acid positions) between two sequential missense variants was calculated. A larger interval size signifies a stretch devoid of missense variants and was considered a possible index of pathogenicity for variants found within such an interval. The mean and SD were calculated. The "desert Z-score", indicating to which degree stretches within the gene are devoid of missense variants, was calculated by the formula: $(\text{stretch length} - \text{mean stretch length})/SD$ of stretch length.

Structural evaluation of *POLR2A* variants in *pol II*

Pol II of *S. cerevisiae* is extensively studied by X-ray crystallography and cryo-electron microscopy.^{7-11,13,14,16-20} Sequence conservation between human *POLR2A* and *S. cerevisiae rpb1* is high, and thus the available structures can serve as a model for the human protein. To evaluate the putative consequences of *POLR2A* variants, the structures of RNA polymerase from Protein Data Bank entries PDB: 1i6h, 1r5u, 1r9s, 1twf, 1y1v, 1y1w, 1y1y, 2e2h, 2nvq, 2nvz, 3gtj, 3gtm, 3how, 3hoy, 3po2, 3po3, 4a3l, 4a93, 4bbr, 4gwp, 4v1m, 4v1n, 4v1o, 5sva, 5xog, and 5xon were superimposed by overlaying the coordinates for *rpb1* with the algorithm provided by BRAGI.³³ Variants were mapped onto the structures and evaluated for their putative impact on local protein folding and enzymatic activity. Figures were prepared in the programs Molscript³⁴ and raster3D.³⁵

Functional evaluation of variants in *pol II*: *POLR2A* variants expressed in *S. cerevisiae*

Six *POLR2A* variants were matched through GeneMatcher at the time the experiment in *S. cerevisiae* was initiated; therefore six *POLR2A* variants were functionally evaluated in *S. cerevisiae*. Plate phenotyping of *rpb1* mutants was performed as described before.²² All of the *S. cerevisiae* strains that we used in this study are listed in Table S1. They were derived from CKY283, CKY718, and CKY721. Shortly, to generate mutant *rpb1*, point mutations in *S. cerevisiae rpb1* were introduced by PCR mutagenesis into the *CEN LEU2* plasmid pRS315H3alt-RPB1* XmaI 1122-1123 T69 corrected. The *CEN LEU2* plasmids, containing mutant *rpb1*, were transformed into an appropriate Leu⁻ strain with corresponding endogenous *rpb1* deletion and complemented with a *CEN URA3 WT rpb1* subunit gene expressing wild-type (WT) RPB1. Leu⁺ transformants were patched on solid medium that lacked leucine and replica-plated to medium that lacked leucine but contained 5-fluoroorotic acid (Thermo Scientific) to select against cells maintaining RPB1 WT *URA3* plasmids. $\Delta sub1$ or $\Delta dst1 + rpb1$ mutant strains for direct testing of double mutant phenotypes were constructed based on CKY721 or CKY718, respectively, and analyzed in the same fashion as *rpb1* single mutants. Assays were performed in biological triplicate in three different backgrounds: WT background, absence of TFIIIS ($\Delta dst1$ background), and absence of the SUB1 transcription elongation factor ($\Delta sub1$ background). Transcriptional activity and genetic interactions were determined. The assays with c.1592A>G (p.Asn531Ser) (p.Asn517Ser_{yeast}) and c.2207C>T (p.Thr736Met) (p.Ser713Met_{yeast}) in the WT background were performed in sextuplicate to increase the consistency of the results. p.Ala301Asp_{yeast} was used as a positive control for reduced transcriptional activity,^{36,37} and p.Glu1230Lys_{yeast} was used as a positive control for reduced genetic interaction with TFIIIS.³⁸

For spot assays, overnight yeast peptone dextrose (YPD) cultures from single colonies grown at 30°C were diluted to an OD₆₀₀ of 0.15. Five-fold serial dilutions were prepared and spotted on indicated plates and grown for 3 to 6 days at 30°C or 37°C when indicated. YPD medium contained yeast extract (1% w/v final, Biosciences), peptone (2% w/v final, Biosciences), dextrose (2% w/v final), and bacto agar (2% w/v final, Biosciences). Alternative-carbon-source YP media were YP raffinose (2% final w/v) and YP raffinose (2% w/v final) plus galactose (1% w/v final). Synthetic complete medium lacking leucine (SC-Leu) contained: 2 gr/l drop-out mix minus leucine (US Biological) and 6.71 gr/l Yeast Nitrogen Base (YNB) without amino acids and carbohydrate and with ammonium sulfate (US Biological) with 2% dextrose. Mycophenolic acid (MPA, Sigma-Aldrich) was added to SC-Leu at 20 µg/mL final concentration from a 10 mg/mL stock in ethanol.

Functional evaluation of variants in pol II: POLR2A variants expressed in HeLa Cells

Nine *POLR2A* variants were matched through GeneMatcher at the time the experiment in HeLa cells was initiated, therefore nine *POLR2A* variants could be functionally evaluated in HeLa cells. The open reading frame of human RPB1 was amplified by PCR with a plasmid expressing RPB1 fusion with a B10 epitope, EGFP, hRPB1, and six His residues³⁶ and introduced into the pDONR201 cloning vector. The *POLR2A* coding sequence contained a point mutation (AAC>GAC), which resulted in the replacement of asparagine 792 by aspartate and resistance to α -amanitin.³⁹ The observed *POLR2A* point mutations in the included individuals were introduced through the Quickchange protocol (Stratagene) and verified by DNA sequencing. p.Lys812* was used as a representative of c.2098C>T (p.Gln700*) and c.2203C>T (p.Gln735*). These two variants could not be designed because amino acid residues Gln700 and Gln735 are localized in front of the built-in resistance to α -amanitin (residue 792). p.Lys812* is expected to result in a similar truncated version of the protein as p.Gln700* and p.Gln735*. All RPB1 mutant proteins were tagged by GFP at the N terminus. We created the stable doxycycline inducible cell lines by transfecting pCDNA5/FRQT/TO and pOG44 into HeLa FRT cells carrying the TET repressor by using polyethyleneimine (PEI) and then antibiotic selection. HeLa cells were maintained in DMEM containing 4.5 g/l glucose (GIBCO) supplemented with 10% v/v heat-inactivated fetal bovine serum (FBS, Sigma-Aldrich) and 10 mM L-Glutamine (Sigma-Aldrich) under blasticidin (5 μ g/ml) (InvivoGen) and hygromycin B (400 μ g/ml) (Roche Diagnostics) selection.

The expression of GFP-tagged RPB1 was induced by treatment with 1 μ g/ml doxycycline for 24 hours. Cells were spun down for 5 minutes at 400 g and washed with PBS. Next, cells were lysed in whole-cell lysate buffer (50 mM Tris-HCl [pH 8.0], 420 mM NaCl, 10 mM MgCl₂, 10% glycerol, 0.1% NP40, 0.5 mM DTT, containing protease inhibitor cocktail), and lysates were subjected to centrifugation at 400 g for 10 minutes. The supernatant was harvested and stored at -80°C. For the MTT (3-(4,5-dimethylthiazolyl-2)-2,5-diphenyltetrazoliumbromide, Sigma-Aldrich) assay, doxycycline-inducible GFP-RPB1^{amanitin resistant}-expressing mutant HeLa FRT cells were cultured for 3 to 5 days in the presence of 1 μ g/ml doxycycline to induce the expression of the mutants. Cells were seeded at 3,000 cells per well in 100 ml normal DMEM in the presence of doxycycline in 96-well plates. After a few hours, the medium was replaced by DMEM with doxycycline, and when indicated, 2.5 μ g/ml α -amanitin (Boehringer Mannheim) was added. After 72 hours of incubation, MTT was added to a final concentration of 0.5 mg/ml.⁴⁰ Cells were incubated for 4 hours under normal culturing conditions, then the medium was carefully removed, and 100 μ L DMSO was added to dissolve the formazan crystals. The absorbance was measured at 570- and 630-nm wavelengths. Relative growth was calculated with the equation $(A_{570, \text{sample}} - A_{630, \text{sample}}) / (A_{570, \text{untreated}} - A_{630, \text{untreated}})$.

GST pull-down

A GST-TFIIIS recombinant expression construct⁴¹ was transformed in BL21DE3; single colonies were picked, grown in LB + ampicillin, and induced for 3 hours with 1 mM IPTG when cells reached an OD₆₀₀ of 0.6. Cells were pelleted by centrifugation and resuspended in lysis buffer (50 mM Tris-HCl [pH 7.0], 300 mM KCl, 2 mM EDTA, 20% sucrose, 0.1% Triton X-100, 0.5 mM PMSF, and 1 mM DTT) containing 50 μ L lysozyme (25 mg/ml) and incubated for 10 minutes on ice. The suspension was freeze-thawed three times and sonicated three times for 20 seconds. Cells were spun down at 25,000 rpm for 45 minutes at 4°C, and the supernatant was harvested and stored at -80°C.

Glutathione-agarose beads (50% slurry) were washed three times with binding buffer (20 mM Tris-HCl [pH 8.0], 50 mM NaCl, 1 mM EDTA, 10% glycerol, 0.1 mM ZnCl₂, 1 mM DTT, and 0.5 mM PMSF). 20 µL glutathione-agarose beads (Sigma-Aldrich) per reaction were coated with 25 µL GST-TFIIS lysate per reaction for 1 hour at 4°C. After this, the glutathione-agarose beads were washed three times with binding buffer and incubated with 300 µg HeLa FRT whole-cell lysates (unless otherwise stated) in a final volume of 800 µL (50 mM NaCl at final concentration) for 2 hours at 4°C while rotating. Beads were washed three times and proteins were eluted in 15 µL sample buffer by a 5 minute incubation at 95°C. Samples were lysed in sample buffer (160 mM Tris-HCl [pH 6.8], 4% SDS, 20% glycerol, and 0.05% bromophenol blue), run on an 8% SDS-PAGE, and transferred onto a PVDF membrane. The membrane was developed with the appropriate antibodies and ECL. Antibodies came from the following sources: α-Tubulin (DM1A, CP06, Calbiochem) and GFP (#632381, JL-8 Clontech).

Interactome analysis with mass spectrometry

For interactome analysis, HeLa cells were grown, and nuclear extracts were prepared as described.⁴² The protein concentration was determined with a Bradford assay. GFP affinity purification was essentially performed as described.⁴² Protein extracts were incubated with GFP-trap beads (Chromotek) or with blocked agarose beads (Chromotek) as a negative control on a rotating wheel at 4°C with 1 mg input protein. Peptides were eluted from the beads by 2 hour trypsin incubation in elution buffer (100 mM Tris-HCl [pH 7.5], 2 M urea, and 10 mM DTT). Eluate was collected, and beads were eluted for a second time. Eluates were combined, and trypsin digested overnight. Tryptic digests were desalted with stage tips.⁴³

The samples were cleaned up with in-house-made stage tips. Peptides were separated on a 30-cm pico-tip column (50 µm ID, New Objective) in-house packed with 3 µm aquapur gold C-18 material by applying a gradient (7%–80%ACN0.1% FA, 140 min), delivered by an easy-nLC 1000 system (LC120, Thermo Scientific), and electro-sprayed directly into an LTQ Orbitrap Mass Spectrometer (Velos, Thermo Scientific). Raw files were analyzed with the MaxQuant software version 1.5.1.0.; oxidation of methionine was set as variable and carbamidomethylation of cysteine was set as fixed modification. The human protein database of UniProt was searched with the peptide and protein false discovery rate set to 1%.

Assessing phenotype-genotype correlation

To assess phenotype-genotype correlation, we evaluated the *POLR2A* variants for which support for pathogenicity was obtained from positional and functional analyses and the variants for which support for pathogenicity was obtained solely from positional analysis. These variants were considered “probable” to be disease causing, indicating that we are strongly convinced that the individuals’ genotypes are causing the individuals’ phenotypes. We used the phenotypic features of the individuals harboring these variants to delineate the phenotypic spectrum. For the remaining variants, pathogenicity was assessed by determining the degree of overlap. Phenotypic similarity was defined as the presence of at least three phenotypic features of the five most prevalent phenotypic features found in individuals harboring “probable” disease-causing variants in *POLR2A*. If the overlap in phenotypic features was sufficient, these variants were considered to be “possibly” disease-causing. If the phenotypic overlap was not sufficient or could not be determined, the variant

was classified as “unknown” whether this variant is disease-causing or not.

To correlate phenotypic severity to the predicted consequences of the *POLR2A* variant and to find an explanation for the wide phenotypic spectrum, an *ad hoc* severity score was conceived.⁴⁴ It was calculated as follows: each tabulated item that was present (+) in the individual scored 1 point and each absent item (–) scored 0 points (Table 1). The items “sit without support”, “walk well” and “brain magnetic resonance imaging (MRI) abnormalities” were calculated as follows: “sit without support” at < 12 months scored 0 points, at 13–18 months scored 1 point, at 19–30 months scored 2 points, and at > 30 months scored 3 points; “walk well” at < 24 months scored 0 points, at 25–30 months scored 1 point, at 31–48 months scored 2 points, and at > 48 months scored 3 points; no brain abnormalities scored 0 points, wide ventricles and/or delayed myelination scored 1 point, and white matter abnormalities scored 2 points. A severity score of < 12 points indicated the phenotype was mild, a score of 12–17 indicated moderate, a score of 18–23 indicated severe, and a score of > 23 points indicated profound.

RESULTS

Phenotypes of affected individuals

Sixteen individuals, all harboring ultra-rare, *de novo* heterozygous variants in *POLR2A*, were located via GeneMatcher.³⁰ Other (genetic) causes of the phenotypes of the included individuals were thoroughly excluded. The cohort included three individuals with truncating variants (two stop codons and one frameshift), three individuals with in-frame deletions (IF deletion), and ten individuals with missense variants. Portraits of the individuals are shown in Figure 1A, clinical characteristics of all individuals are summarized in Table 1, and extended individual reports can be found in the Supplemental Note. In summary, eleven individuals were born after a generally uneventful pregnancy and delivery at term and had a normal birth weight and normal perinatal events. Decreased fetal movements were noted in three pregnancies, and one female was born preterm at 28 weeks. One pregnancy carrying a male fetus (individual 3, p.Asn531Ser) was terminated because of corpus callosum agenesis, frontonasal dysplasia, and a cleft lip.

The most frequent early and usually striking phenotypic feature was hypotonia. It was noted in fourteen individuals and was profound in nine (Figure S1), evidenced by decreased muscle tone, a frog-like posture in infancy, and reduced spontaneous movements but normal tendon reflexes. Muscles were considered atrophic in four individuals. A muscle biopsy, on suspicion of a myopathy, was performed in four individuals, but the results were inconclusive. In addition, there were symptoms and signs commonly associated with hypotonia; these signs included brachyplagiocephaly (in five individuals), a high arched palate (in five individuals), pectus excavatum (in three individuals), recurrent respiratory tract infections (in eight individuals), and inguinal hernia (in four individuals). The majority of individuals (ten) had feeding difficulties, with gastro-esophageal reflux (in six individuals), resulting in failure to thrive (in three individuals). Ocular signs included strabismus (in eleven individuals) and delayed visual maturation (in six individuals), resulting in decreased vision (in five individuals). Moderate to severe sensorineural hearing loss was reported in two individuals, and conductive hearing loss due to recurrent respiratory tract infections was reported in one individual. Dysmorphic features were generally mild and non-distinctive; these included a high forehead (in seven individuals), hypertelorism (in six individuals), and tooth misalignment (in five individuals), which is defined as an abnormal spacing of the teeth without missing any teeth. Brain MRI performed in eleven individuals revealed white matter

abnormalities (in ten individuals), ranging from delayed myelination (in five individuals) to wide lateral ventricles, putatively due to white-matter loss (in four individuals). A thin corpus callosum, a feature consistent with the loss of white matter was noted in two individuals. Additionally, three individuals had cerebellar abnormalities. Severe epilepsy was reported in three individuals. Eight individuals had sleeping difficulties. Autistic (in four individuals) and aggressive (in four individuals) behavior, including extreme behavior such as pica (eating dung), was reported. Hypotonia tended to improve over time, albeit slowly. Later in life, endurance was diminished (in ten individuals).

A delayed development involving all domains was noted in all individuals and ranged from mild to severe. The severity of the delay was evaluated by calculating Z-scores on the basis of the acquisition of developmental milestones, with higher Z-scores indicating later acquisition of milestones. The individuals' developmental Z-scores were stable over time, consistent with a gradual development without developmental catch-up or decline. The Z-scores between domains were similar, arguing against developmental-domain-specific delays (Figure 1B). The degree of delay appeared to correlate with the degree of hypotonia. Temporary loss of milestones was reported in four individuals, usually following an infection. Additional metabolic investigations ruled out known inborn errors of metabolism.

Variant severity metrics

Large-scale genetic data retrieved from gnomAD from individuals without severe pediatric disease indicate that *POLR2A* is intolerant of deleterious, heterozygous, protein-changing variants. This is evidenced by a maximal pLI score (1.0) and a very low observed/expected ratio (0.08), indicating intolerance of loss of function variants (Table S2). Moreover, the Z-score (7.13) for missense variants is one of the highest of all human protein-coding genes, suggesting that subtle heterozygous changes can also cause a survival disadvantage (Table S2).

An assessment of conservation across species (Figure 2A) revealed that nine out of ten missense variants affect highly conserved amino acid residues (Figure 2B). However, this variant property fails to be discriminatory because the overall degree of conservation of *POLR2A* is extremely high (Figure 2). In the pol II core, roughly 50% of residues are identical, and an additional 20% are highly similar between humans and yeast. Similarly, the CADD scores of the individuals' variants were all above the arbitrary cut-off of 20, indicating that these variants are predicted to be in the 1% of the most deleterious substitutions that can be done to the human genome and thereby suggesting pathogenicity;³² however, most of the CADD scores of the variants observed in the gnomAD cohort of individuals without severe pediatric disease (Figure S2) were also above the cut-off. Thus, these indices of pathogenicity at the amino-acid level lack discriminative power.

Next, we evaluated whether pathogenicity was related to the variants' positions within *POLR2A*. The observation that the individuals' variants were found throughout the gene argued against a domain-specific deleteriousness. In line with Lelieveld et al. and Havrilla et al.,^{45,46} we hypothesized that the distribution of protein-changing *POLR2A* variants observed in the gnomAD cohort of individuals without severe pediatric disease – apparently tolerated well enough and therefore more likely to be found at positions tolerant to change – could conversely unveil areas intolerant to change. *S. cerevisiae* tolerates truncations of the CTD region comprising up to 50% of its 26 heptad repeats in *rpb1*, the ortholog of *POLR2A*.^{47,48}

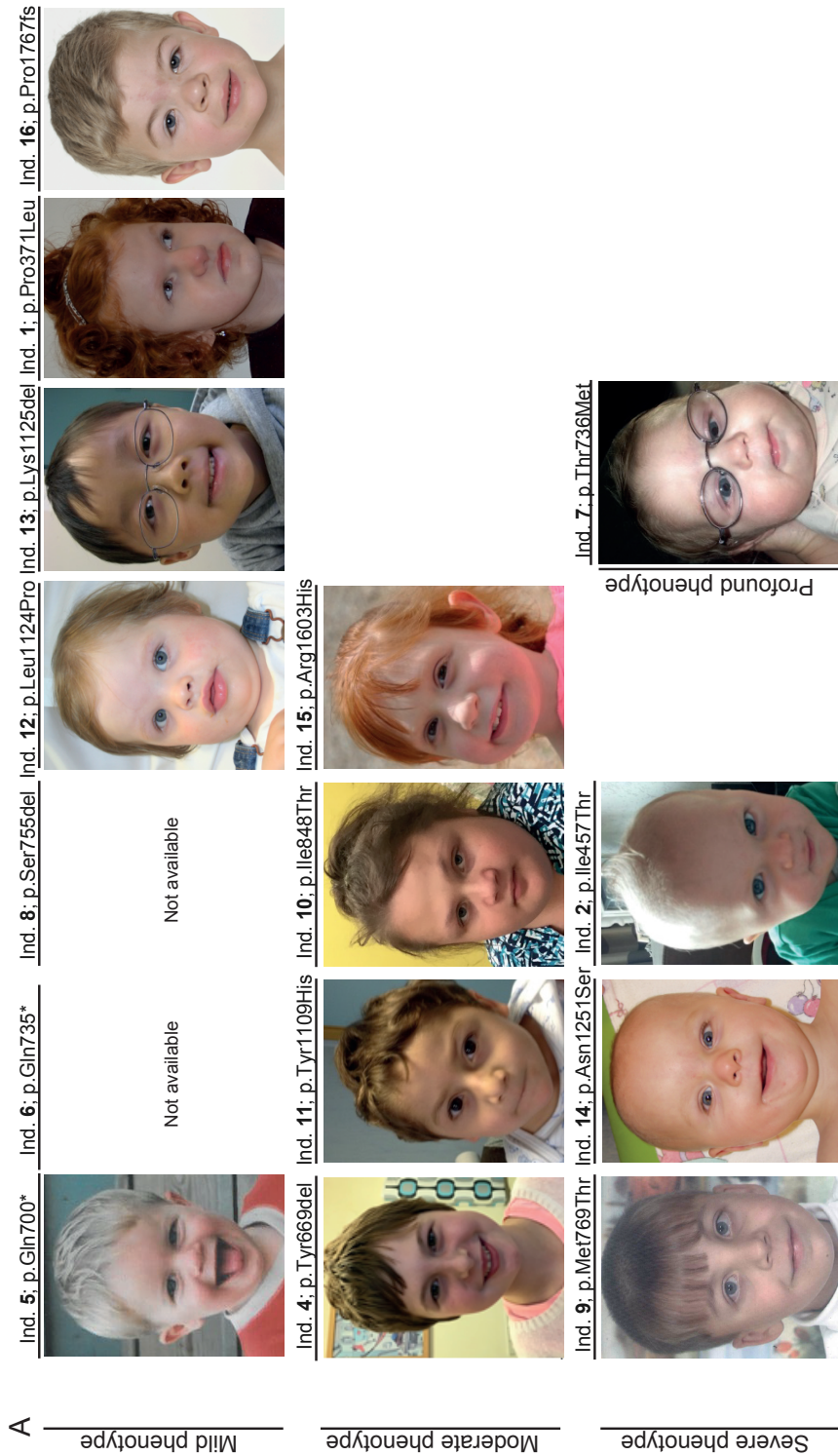
Table 1. Characteristics of individuals harboring a heterozygous *de novo* variant in *POLR2A*

Individual Variant	5	6	8	12	13	1	16	4
	p.Gln700*	p.Gln735*	p.Ser755del	p.Leu1124Pro	p.Lys1125del	p.Pro371Leu	p.Pro1767fs	p.Tyr669del
Sex	M	F	M	F	M	F	M	F
Gestation (weeks)	42	28	Term	38	37	41	41	41
Age (years)	17	13	3	4	7	7	9	11
General hypotonia	-	+	+	+	+	+	+	+
Strabismus	-	+	+	+	+	+	+	+
Frog position infancy	-	-	+	+	-	-	-	+
Decreased endurance	-	-	+	+	+	-	+	+
Feeding difficulties	-	+	+	+	-	+	+	+
Recurrent RTI	-	-	+	+	-	-	+	-
High forehead	+	+	+	+	+	-	+	-
Disturbed sleeping	+	-	-	-	-	-	-	+
Gastro-esoph. reflux	+	+	-	-	-	-	-	+
High palate	+	-	-	-	+	-	-	+
Delayed visual matur.	+	-	-	-	-	-	-	+
Microcephaly	-	-	-	-	-	-	-	-
Brachyplagiocephaly	-	-	-	-	+	-	-	-
Muscle atrophy	-	-	-	-	-	-	-	-
Hypertelorism	-	-	-	-	+	+	+	-
Teeth misalignment	-	+	-	+	+	+	+	+
Decreased vision	+	-	-	-	-	+	-	+
Stagnation episodes	-	-	-	-	-	-	-	+
Inguinal hernia	-	-	-	-	-	-	-	-
Decreased fetal movem.	-	-	NA	+	-	-	-	-
Autistic behavior	+	-	-	NA	-	-	-	+
Aggressive behavior	-	-	-	-	-	-	-	+
Failure to thrive	-	-	-	-	-	+	-	-
Pectus excavatum	-	-	-	-	-	-	-	+
Epilepsy	-	-	-	-	-	-	-	-
Sit, no support (months)	7	12	NA	12	18	24	24	11
Walk well (months)	18	30	>36	23	24	72	28	26
Brain MRI abnormalities	-	Yes*	Yes*	Yes*	Yes*	-	-	-
Severity score	6	9	9	9	10	11	11	14
Severity class	Mild	Mild	Mild	Mild	Mild	Mild	Mild	Moderate

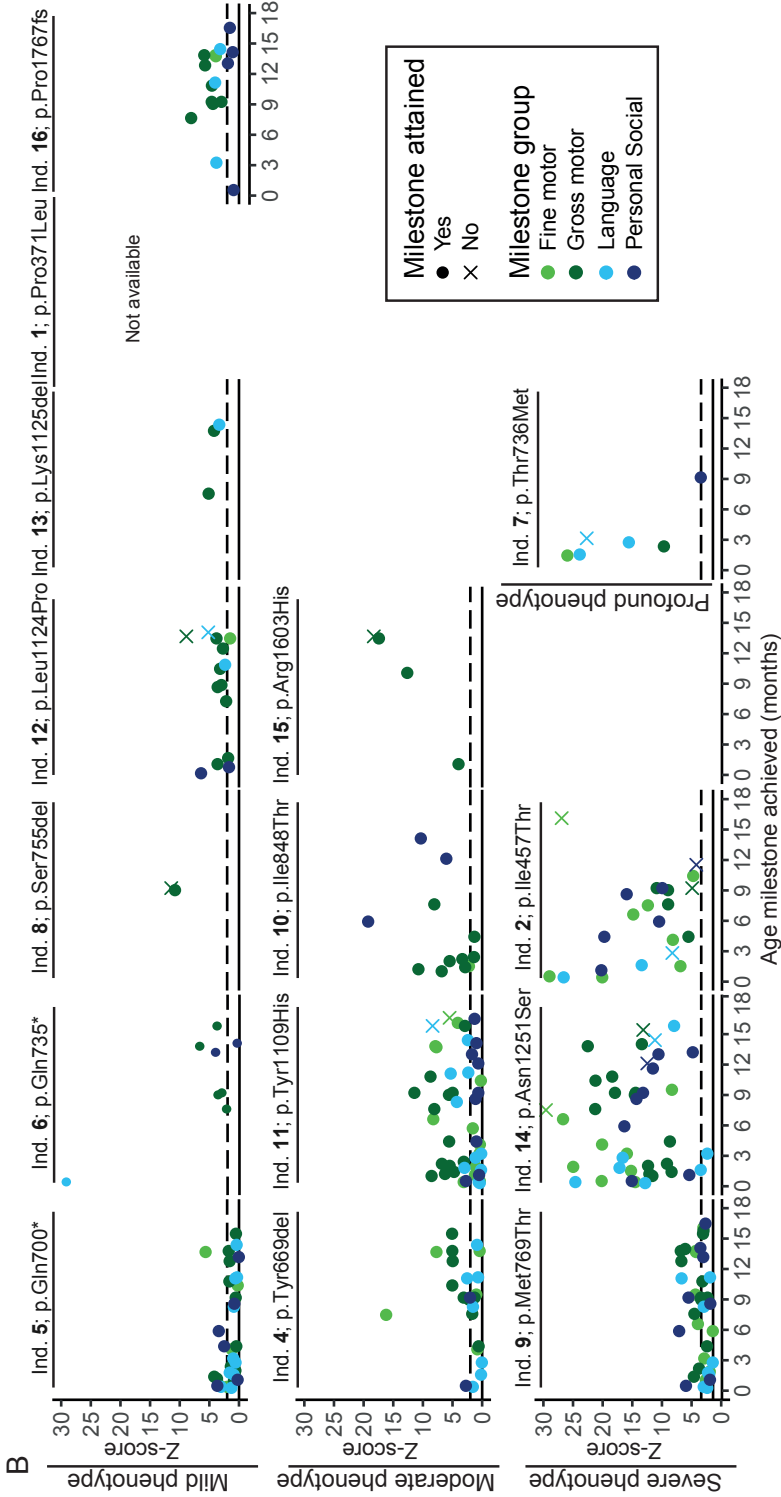
Individual Variant	11 p.Tyr1109His	10 p.Ile848Thr	15 p.Arg1603His	9 p.Met769Thr	14 p.Asn1251Ser	2 p.Ile457Thr	7 p.Thr736Met	3 p.Asn531Ser
Sex	M	F	F	M	F	M	F	M
Gestation (weeks)	40	41	Term	41	40	40	39	30 †
Age (years)	6	13	7	18	6	4	9	0
General hypotonia	+	+	+	+	+	+	+	
Strabismus	+	-	+	+	+	+	+	
Frog position infancy	+	+	+	+	+	+	+	
Decreased endurance	NA	+	-	+	+	+	+	
Feeding difficulties	-	+	-	+	+	+	+	
Recurrent RTI	+	-	+	-	+	+	+	
High forehead	-	-	+	+	-	+	-	-
Disturbed sleeping	-	-	+	+	-	+	-	-
Gastro-esoph. reflux	-	+	-	+	+	+	+	
High palate	-	-	-	+	-	+	+	
Delayed visual matur.	-	-	+	+	-	+	+	
Microcephaly	+	-	+	+	-	+	+	
Brachyplagiocephaly	-	+	-	+	+	-	+	
Muscle atrophy	-	+	-	+	+	+	+	
Hypertelorism	-	-	-	+	-	+	-	+
Teeth misalignment	-	-	-	+	-	-	-	-
Decreased vision	-	-	+	+	-	-	+	
Stagnation episodes	+	-	-	+	-	+	+	
Inguinal hernia	-	-	-	+	-	+	+	
Decreased fetal movem.	-	-	-	-	+	+	-	
Autistic behavior	-	-	+	+	-	-	-	-
Aggressive behavior	-	+	+	-	+	-	+	
Failure to thrive	-	-	-	-	+	-	+	
Pectus excavatum	-	-	-	+	+	-	-	
Epilepsy	+	-	+	-	-	-	-	
Sit, no support (months)	24	24	Attained	14	48	23	>108	
Walk well (months)	>72	>156	56	27	65	>55	>108	
Brain MRI abnormalities	Yes*	Yes*	Yes*	Yes*	Yes*	Yes*	Yes*	Yes*
Severity score	14	15	16	19	21	23	25	NA
Severity class	Moderate	Moderate	Moderate	Severe	Severe	Severe	Profound	NA

*Brain MRI abnormalities: ind. 6: cerebellar atrophy, inferior vermis, small pons, megacisterna magna, slightly small corpus callosum; ind. 8, 12, 13 and 9: delayed myelination; ind. 11: wide ventricles, increased T2 signals in nuclei pallidii; ind. 10: wide ventricles, cystic area in periventricular white matter; ind. 15: wide ventricles, thin corpus callosum, bilateral loss white matter; ind. 14: megacisterna magna; ind. 2: delayed myelination, wide ventricles; ind. 7: wide ventricles and sulci, cerebellar volume loss, abnormal globus pallidus; ind. 3: corpus callosum agenesis. † Termination of pregnancy. Abbreviations: f: female; m: male; NA: not available; RTI: respiratory tract infections.

Figure 1. Photos and attainment of developmental milestones of individuals with *POLR2A* variants

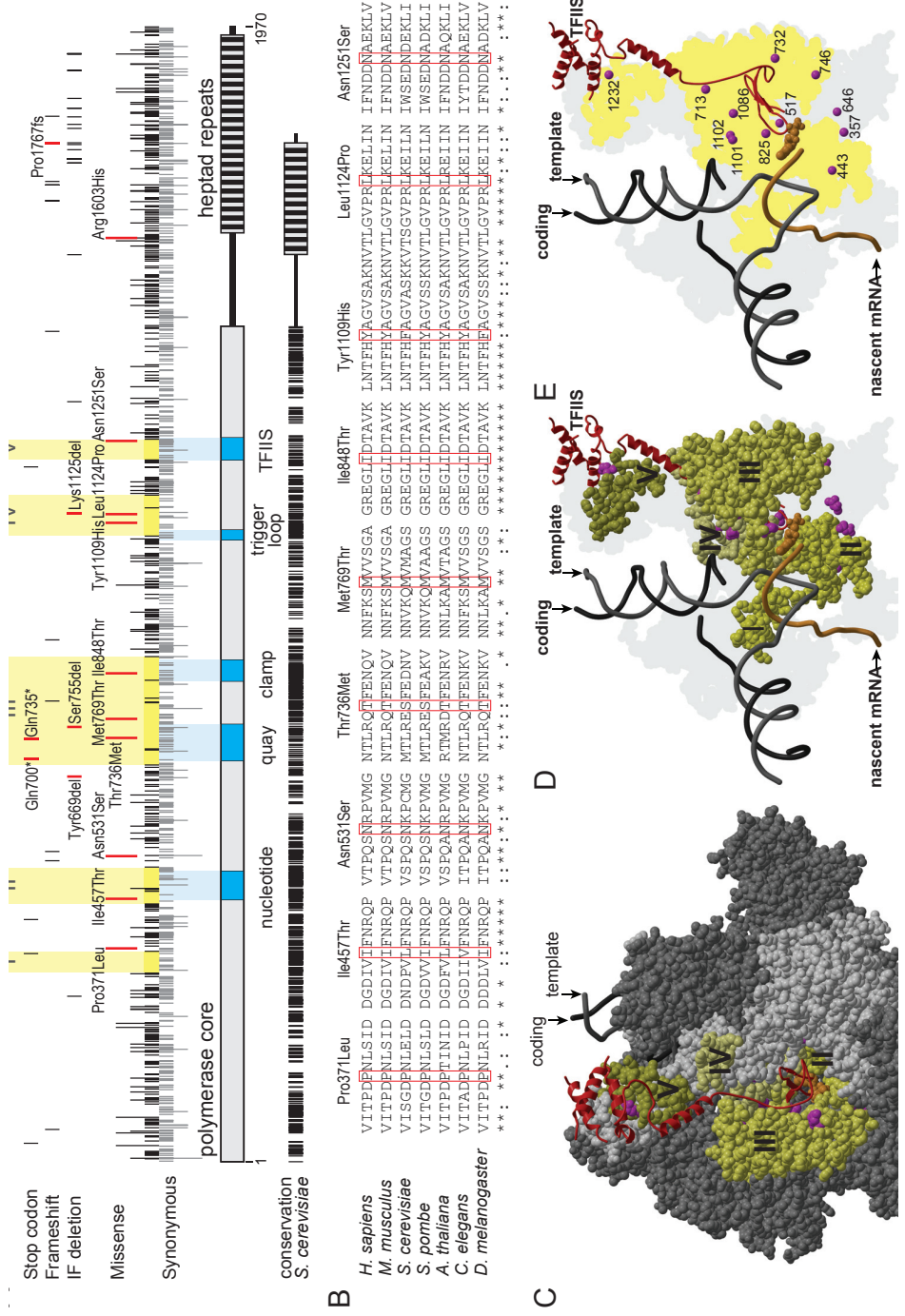


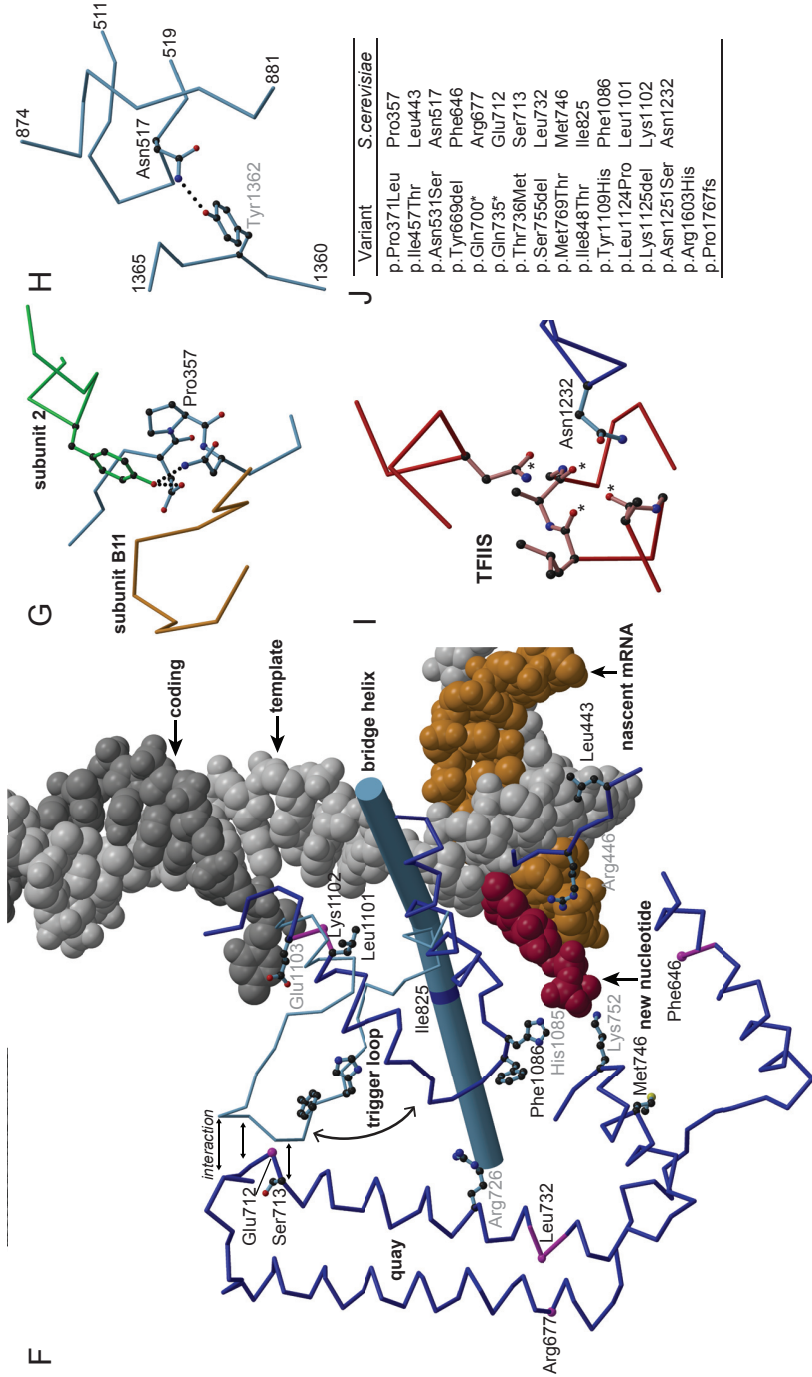
Ind. 7: p.Thr736Met
 Profound phenotype



A) Photos of 13 of the 16 individuals harboring a *de novo* variant in *POLR2A*, in order of severity score. B) Attained and unattained developmental milestones during the first 18 months of life for 14 of the 16 individuals harboring a *de novo* variant in *POLR2A*, in order of severity score. For each milestone, Z-scores were calculated indicating the delay in attaining that milestone. The higher the Z-scores, the greater the developmental delay. The figure demonstrates that in individuals with a mild phenotype, developmental Z-scores are mostly < 10, in individuals with a moderate phenotype, developmental Z-scores are < 20, and in individuals with a severe phenotype, developmental Z-scores can even reach 30. In addition, among the individuals with a severe phenotype, relatively more (and more early) developmental milestones were not attained by the individual. Individual 3 (p.Asn531Ser) was not included in this figure because the pregnancy was terminated. Abbreviations: ind: individual.

Figure 2. Structural evaluation of *POLR2A* variants





A) RPB1 is represented; the core and the C-terminal heptad repeats are shown as bars. Functional elements are highlighted in dark blue and are labeled underneath. The positions of gained stop codons, frameshifts, in-frame (IF) deletions, missense and synonymous mutations, as reported in the gnomAD database, are indicated by vertical black strokes. The length of the stroke represents the number of different mutations at the DNA level in the corresponding codon. The individuals' variants are indicated by red strokes and are labeled. Stretches devoid of missense mutations are highlighted in yellow and are labeled by Roman numerals. The degree of conservation in humans and *S. cerevisiae* is depicted underneath, whereby each identical amino acid is represented by a vertical black stroke. B) Conservation across species of amino acid residues that are changed in the individuals

[Figure 2 continued] affected by missense mutations. Arg1603 is not conserved and is localized in the region between the pol II core and the heptad repeats. For this region, alignment is not reliable. C) Space-filling model of the elongating form of pol II from *S. cerevisiae* with TFIS in ribbon representation in red. Subunits other than RPB1 are shown in dark gray. RPB1 is shown in light gray; the positions of the variants are highlighted in magenta, and stretches devoid of missense variants are shown in shades of yellow labeled by Roman numerals as in A). The incoming nucleotide is shown as space-filling model in orange. The template strand, the coding strand, and the nascent mRNA are shown as backbone trace in gray, black and orange, respectively. D) Same as in C), but omitting subunits other than RPB1. Only the RPB1 stretches devoid of missense variants and the positions of individuals' variants are shown, and all other parts of RPB1 have been omitted. The 3D-envelope of RPB1 is projected in light gray on the background plane. E) Same as in D), but additionally omitting the RPB1 stretches devoid of missense variants. The α -atoms of amino acid residues affected in individuals' variants are shown as magenta spheres. F) Detailed view at the catalytic center of pol II. The coding strand in dark gray, the template strand in light gray, the nascent mRNA in orange, and the incoming nucleotide in red are shown as a space-filling model. The bridge helix is shown as a rod, and selected other parts of RPB1 as backbone trace. The trigger loop is shown in its open and closed conformation in light and dark blue, respectively. Side chains of amino acid residues affected in individuals with a missense variant and of some residues known to be of catalytic importance are shown in ball-and-stick representation. The α -atoms of amino acid residues affected by IF deletions or the gain of a stop codon are shown as spheres in magenta. G) Environment of residue Pro357. Elements from RPB1, subunit 2, and the pol II subunit RPB11 are depicted in light blue, green, and orange, respectively. Hydrogen bonds are indicated by dotted lines. H) Environment of residue Asn517. Elements of RPB1 are shown in blue. I) Environment of residue Asn1232. Elements of RPB1 and TFIS are shown in blue and red, respectively. Putative hydrogen bonding partners for Asn1232 in TFIS are marked by an asterisk. J) A table assigning human amino acid residues to the corresponding residues in *S. cerevisiae*.

This strongly suggests that the human *POLR2A* CTD region, consisting of 52 repeats, might be equally tolerant to the loss of a proportion of the heptad repeats. Indeed, the majority of the truncating variants reported in gnomAD – and none of the truncations found in these individuals – are positioned in the distal portion of the CTD region (Figure 2A). In addition, the density of *POLR2A* missense variants reported in gnomAD is also highest in the CTD region, not only in the distal part but throughout the whole repeat region, indicating that a putative functional loss of a single heptad repeat is tolerated, regardless of its position. Within the remaining part of *POLR2A*, missense variants are strikingly unevenly distributed when compared with synonymous variants (Figure 2A). In line with our hypothesis, although the median distance between variants is only two amino acid residues, several stretches, the longest of which spans about 80 amino acid residues, that are devoid of missense variants are observed (Figure 2A). These stretches devoid of missense variants correspond to a number of known functionally important regions of the protein. Nine out of ten missense variants from our individuals, two out of three in-frame deletions, and two out of three truncating variants were positioned within these stretches with desert Z-scores that fell between 2.9 and 11.9, indicating intolerance to change in these regions and thereby supporting pathogenicity (Figure 2A and Table 2).

Structural evaluation of POLR2A variants in pol II

Most of the amino residues affected in the individuals have identical or similar residues in the *S. cerevisiae* counterpart (Figures 2A, 2B, and 2J), for which high-resolution structural information is available. This allows for structural evaluation of the variants in pol II. Variants p.Gln700* and p.Gln735* result in a truncation that leads to missing more than half of the protein. If translation is not already prevented by nonsense-mediated decay, the truncated protein is still not expected to form a stable fold with the second largest and core subunit of pol II, RPB2, and it lacks binding sites for several other subunits (Table 2). It is therefore most likely that effects observed with p.Gln700* and p.Gln735* result from RPB1 haploinsufficiency. In support of this, mass spectrometry analyses showed that

the variant p.Lys812* (which we used as a representative of p.Gln700* and p.Gln735* because p.Lys812* is similarly truncated, see Material and Methods) could only associate with RPABC3 (*POLR2H*) but not with any of the other pol II subunits (Figure 3C). Variant c.5298dup (p.Pro1767fs) is located in the proximal half of the CTD and results in the loss of the last 200 amino acids, corresponding to about 50% of the heptad repeats. The folding of the polymerase core is not expected to be affected by this truncation.^{49,50} Therefore, p.Pro1767fs is expected to form pol II, but because the CTD region of RPB1 is too short, pol II function might be affected.

The IF deletions c.2006_2008delACT (p.Tyr669del) (p.Phe646_{yeast}) and c.2262_2264delCTC (p.Ser755del) (p.Leu732_{yeast}) are localized in close proximity to the quay, whereas the IF deletion c.3373_3375delAAG (p.Lys1125del) (p.Lys1102_{yeast}) is localized in the trigger loop (Figures 2C–2F). The deletions are predicted to alter the local protein fold and to have a strong impact on catalytic activity. It is difficult to predict to what extent the overall protein fold and the ability to assemble into pol II are impaired, but such impairment would shift the properties from severe dominant-negative to mild haploinsufficiency. In case of p.Ser755del, mass spectrometry data showed that the interaction with other pol II subunits is largely unaltered, showing that formation of the pol II complex is not affected (Figure 3C).

Interestingly, most missense variants are centered around the catalytic site (Figures 2C–2F and Table 2): c.3325T>C (p.Tyr1109His) (p.Phe1086_{yeast}) and c.3371T>C (p.Leu1124Pro) (p.Leu1101_{yeast}) are positioned in the trigger loop, p.Thr736Met (p.Ser713_{yeast}) in the opposing quay, c.1370T>C (p.Ile457Thr) (p.Leu443_{yeast}) and c.2306T>C (p.Met769Thr) (p.Met746_{yeast}) in the nucleotide binding site, c.1112C>T (p.Pro371Leu) (p.Pro357_{yeast}) in the funnel (Figure 2G), and c.2543T>C (p.Ile848Thr) (p.Ile825_{yeast}) in the bridge helix (Figures 2C–2F and Table 2). These *POLR2A* variants are likely to reduce the transcriptional pausing, elongation, and/or back-tracking activities of pol II without affecting transcription initiation. Indeed, all tested missense RPB1 variants were found to interact with other pol II subunits, indicating that complex formation is largely unaltered (Figure 3C).

The missense mutation c.3752A>G (p.Asn1251Ser) (p.Asn1232_{yeast}) is located distantly from the catalytic site, but it is localized in the interaction surface for transcription-elongation factor TFIIS, which is required for back-tracking of pol II due to elongation blocks or nucleotide mis-incorporation (Figure 2I). TFIIS interaction mutants of pol II would have both an increased error rate and reduced elongation rates. The consequences of the missense variants p.Asn531Ser (p.Asn517_{yeast}) (Figure 2H) and c.4808G>A (p.Arg1603His) are more difficult to predict. p.Asn531 is not directly associated with a structural element involved in catalysis (Figure 2H). p.Arg1603His is localized in the region that connects the RPB1 core to the heptad repeats (Figure 2A). No structural information is available for this region, and it is only partially conserved between human and *S. cerevisiae* RPB1 (Figure 2A).

Altogether, structural evaluation of *POLR2A* variants resulted in the expected haploinsufficiency for p.Gln700* and p.Gln735*, putative haploinsufficiency for the IF deletions, and an expected dominant-negative effect for the missense variants p.Ile457Thr, p.Thr736Met, p.Met769Thr, p.Tyr1109His, and p.Leu1124Pro (Table 2).

Functional evaluation of *POLR2A* variants in pol II

The consequences of *POLR2A* variants on pol II function were investigated in *S. cerevisiae* and HeLa cells for six and nine of the individuals' variants, respectively, representing the whole clinical spectrum (Table 2).

Table 2. Lines of evidence for pathogenicity of *POLR2A* variants

Individual Variant cDNA change	1 p.Pro371Leu c.1112C>T	2 p.Ile457Thr c.1370T>C	3 p.Asn531Ser c.1592A>G	4 p.Tyr669del c.2006_2008 delACT	5 p.Gln700* c.2098C>T	6 p.Gln735* c.2203C>T	7 p.Thr736Met c.2207C>T	8 p.Ser753del c.2262_2264 delCTC
Phenotype	11 Mild	23 Severe		14 Moderate	6 Mild	9 Mild	25 Profound	9 Mild
Variant severity metrics								
Yeast conservation	Identical	Similar	Identical	NA	NA	NA	Similar	NA
Amino acid stretch	366-375	448-470	523-532	664-671	689-715	689-715	717-797	717-797
Stretch length	9	22	9	7	26	26	80	80
Desert Z-score	0.8	2.9	0.8	0.5	3.5	3.5	11.9	11.9
Structural evaluation								
Position	Funnel	Catalytic site		Close to quay Locally altered	Quay Loss	Quay Loss	Quay Expected	Quay Locally altered
Protein folding		Expected		Putative	Expected	Expected	Expected	Putative
Dominant negative								
Haploinsufficiency								
Functional evaluation								
Yeast mutation		Leu443Thr	Asn517Ser				Ser713Met	Leu732del
Yeast growth (WT)		Normal	Normal				Normal	Normal
Yeast growth (Δ dst1: Δ sub1)		Aberrant	Normal				Aberrant	Aberrant
Yeast galactose sensitivity		Yes	No				Yes	Yes
Yeast MPA sensitivity		Yes	No				Yes	Yes
HeLa cell viability		=	=		↓ ↓ ↓ ↓	↓ ↓ ↓ ↓	↓ ↓ ↓ ↓	↓ ↓ ↓ ↓
Disease causing variant	Possible	Probable	<i>Unknown</i>	Possible	Probable	Probable	Probable	Probable

Individual Variant cDNA change	9 p.Met769Thr c.2306T>C	10 p.Ile848Thr c.2543T>C	11 p.Tyr1109His c.3325T>C	12 p.Leu1124Pro c.3371T>C	13 p.Lys1125del c.3373_3375 delAAG	14 p.Asn1251Ser c.3752A>G	15 p.Arg1603His c.4808G>A	16 p.Pro1767fs c.5298dup
Phenotype	19 Severe	15 Moderate	14 Moderate	9 Mild	10 Mild	21 Severe	16 Moderate	11 Mild
Severity score								
Severity class								
Variant severity metrics								
Yeast conservation	Identical	Identical	Similar	Identical	NA	Identical	Other	NA
Amino acid stretch	717-797	836-877	1086-1135	1086-1135	1086-1135	1218-1254	1603-1604	1766-1769
Stretch length	80	41	49	49	49	36	1	3
Desert Z-score	11.9	5.8	7.1	7.1	7.1	5.0	-0.4	-0.1
Structural evaluation								
Position	Catalytic site	Bridge helix	Trigger loop	Trigger loop	Trigger loop Locally altered	TFIS interact.		Hepta repeats Core normal
Protein folding			Expected	Expected				
Dominant negative	Expected							
Haploinsufficiency					Putative			
Functional evaluation								
Yeast mutation				Leu1101Pro				
Yeast growth (WT)				Aberrant		Asn1232Ser		
Yeast growth (Δ dst1; Δ sub1)				Aberrant		Normal		
Yeast galactose sensitivity				Yes		Normal		
Yeast MPA sensitivity				Yes		No		
HeLa cell viability				↓↓↓		No		
Disease causing variant	Probable	Possible	Probable	Probable	Probable	Probable	Possible	Probable

Abbreviations: MPA: mycophenolic acid; NA: not available; WT: wild-type.

[Figure 3 continued] A) A growth assay in *S. cerevisiae* of six *rpb1* mutants, compared to wild-type (WT). p.Ala301Asp demonstrates a positive control for reduced transcriptional activity, and p.Glu1230Lys demonstrates a positive control for reduced genetic interaction with TFIIS. YPD 30°C depicts growth under normal circumstances, and YPD 37°C depicts growth under stress induced by increased temperature. YPRaf/Gal day 4 and day 6 depict growth under stress induced by increased inappropriate GAL 3' termination on day 4 and day 6 of culture, respectively. SC-LEU + MPA day 4 and day 6 depict growth under stress induced by the lack of leucine and the addition of mycophenolic acid (MPA) on day 4 and day 6 of culture, respectively. B) HeLa cell viability. The individuals' variants were introduced in an α -amanitin-resistant version of *POLR2A* (*ama*^R) and expressed from a doxycycline-inducible promoter as a GFP fusion construct in HeLa cells. After the induction of expression, endogenous pol II was left untreated (dark gray bars) or inhibited by the application of α -amanitin (light gray bars), and cell viability was determined. Error bars represent the standard deviation. p.Lys812* was used as a representative of p.Gln700* and p.Gln735* because it is similarly truncated (see Material and Methods). C) Interactome analysis of wild-type (WT) and mutant versions of RPB1 using mass spectrometry. Nuclear extracts from HeLa cells expressing GFP-tagged WT or mutant versions of RPB1 were used for precipitations with control agarose beads (-) or GFP-affinity beads (+) in triplicate. In total, 1,133 proteins were identified by more than two peptides via intensity-based absolute quantification (iBAQ) mass spectroscopy. Known members of pol II (highlighted) and a random selection of 5% of the other proteins are shown. The summed peptide intensities of identified proteins were logarithmically transformed to the basis of ten and are represented by shades of gray. Note, intensities smaller than 10⁴ are not obtained due to technical constraints. p.Lys812* was used as a representative of p.Gln700* and p.Gln735*.

In *S. cerevisiae*, in a WT genetic background, normal growth was observed in all but one variant (p.Leu1124Pro [p.Leu1101Pro_{yeast}]) under optimal conditions, as well as under temperature stress conditions (YPD at 37°C) (Table 2 and Figure S3). In genetic backgrounds lacking transcription factors *Dst1* (yeast ortholog of TFIIS) or *Sub1* (yeast ortholog of PC4), aberrant growth surfaced in four out of six variants (p.Leu1124Pro [p.Leu1101Pro_{yeast}], p.Ile457Thr [p.Leu443Thr_{yeast}], p.Thr736Met [p.Ser713Met_{yeast}], and p.Ser755del [p.Leu732del_{yeast}]) when compared with WT and the positive controls for Δ *dst1* (p.Glu1230Lys_{yeast}) (Table 2 and Figure S3) and Δ *sub1* (p.Ala301Asp_{yeast}) (Figure 3A and Table 2). A read-through transcription assay, in which GAL7 production is inhibited in WT (*gal10 Δ 56*) cells, causing galactose sensitivity on YPRaf/Gal,²³ also shows aberrant growth for these four variants (Figures 3A and S3 and Table 2). Although milder, these four variants also exhibited aberrant growth when exposed to the nucleotide synthesis inhibitor mycophenolic acid (MPA) in one or both of these genetic backgrounds (Figures 3A and S3 and Table 2). Disturbances in both genetic backgrounds (Δ *dst1* and Δ *sub1*) are suggestive of reduced transcriptional fidelity.

Cell viability was assessed with an MTT assay in doxycycline-inducible GFP-RPB1^{amanitin resistant}-expressing mutant HeLa FRT cells, in which the endogenous WT RPB1 was annihilated with the pol-II-specific drug α -amanitin. Cell viability was grossly reduced in mutants expressing variants p.Thr736Met, p.Ser755del, p.Lys812*, and p.Leu1124Pro (Figure 3B), supporting the pathogenicity of these variants. No significant effects were seen for the variants p.Ile457Thr, p.Asn531Ser, p.Asn1251Ser, and p.Arg1603His (Figure 3B). For all mutants, the amounts of RPB1 protein were similar to the protein amount of WT RPB1 (Figure S4). Binding affinity toward TFIIS, a key transcription factor, was unaffected for all mutants. This included the p.Asn1251Ser mutant, despite its location in the TFIIS binding site (Figure 4). Taken together, the characterization in *S. cerevisiae* and MTT cell viability in HeLa cells provide evidence for pathogenicity of variants located close to the catalytic core, but not for p.Asn531Ser, p.Asn1251Ser, and p.Arg1603His (Table 2).

Assessing phenotype-genotype correlation

To delineate the phenotypic spectrum that could be attributed to *POLR2A* variants, we focused on variants considered to be probable to cause disease. Positional and functional evaluation of the *POLR2A* variants' effects on pol II function supported pathogenicity of the

missense variants p.Ile457Thr, p.Thr736Met, and p.Leu1124Pro, as well as of the IF deletion p.Ser755del and the truncated variants p.Gln700* and p.Gln735* (Table 2), and solely positional evaluation supported pathogenicity for the missense variants p.Met769Thr, p.Ile848Thr, p.Tyr1109His, and p.Asn1251Ser and for the IF deletion p.Lys1125del (Table 2). The phenotypic features of the eleven individuals harboring these variants were used to delineate the *POLR2A* phenotypic spectrum (Table 2). These phenotypic features included profound general hypotonia (in ten individuals), as evidenced by a frog position in infancy (in eight individuals), strabismus (in nine individuals), decreased endurance (in eight individuals), and feeding difficulties (in seven individuals) (Table 1). The pathogenicity of the remaining variants was assessed by determining the degree of phenotypic overlap. Individual 1 (p.Pro371Leu), individual 4 (p.Tyr669del), individual 15 (p.Arg1603His), and individual 16 (p.Pro1767fs) presented with clinical phenotypes clearly fitting the phenotypes of the other *POLR2A* individuals because all had at least three of the five most prevalent *POLR2A* symptoms (Table 1), and therefore these variants were considered to be possibly disease-causing (Table 2). For individual 3 (p.Asn531Ser), the phenotypic overlap could not be assessed because the pregnancy had been terminated, and it is thus unknown whether this variant is disease-causing (Table 2).

We noted that the degree of developmental delay correlated with the predicted consequences of the variant: in the individuals with variants predicted to cause haploinsufficiency, we noted relatively low Z-scores (mean Z-score 1.74 \pm 3.13), but variants expected to cause a dominant-negative effect were associated with appreciably higher Z-scores (median Z-score 4.23 \pm 3.96, $p < 0.0001$) and thus with more severe delays (Figure 1B). To assess this further, we calculated a severity score that summarizes the severity of the clinical phenotype for *POLR2A*. The severity scores of individuals harboring variants with expected or putative haploinsufficiency (mean severity score 10, range 6–14 points) were lower than in individuals harboring variants with expected dominant-negative effects (mean severity score 17, range 6–25 points, Table 1). This suggests that a missense mutation exerting a dominant-negative effect is more likely to result in a severe phenotype (severity score > 15) than a mutation inducing haploinsufficiency.

DISCUSSION

In this study, we applied an iterative approach to assess the pathogenicity of identified variants in *POLR2A*. The main argument supporting the pathogenicity of the identified variants is that all variants occurred *de novo*.²⁷ In addition, *POLR2A* is, overall, very intolerant of deleterious, heterozygous, protein-changing variants. Furthermore, nine out of ten missense variants affected highly conserved amino acid residues that are localized at important functional regions of the gene. Functional analyses support pathogenicity of the variants p.Ile457Thr, p.Thr736Met, p.Gln700*, p.Gln735*, p.Ser755del, and p.Leu1124Pro, although we note that both yeast and HeLa cells are model systems that might not fully recapitulate the complex developmental disease of the individuals reported here. Although we did not demonstrate support from functional analyses for the variants p.Asn531Ser and p.Asn1251Ser, the pathogenicity of p.Asn1251Ser is strongly supported by the conservation of the amino acid residue and the importance of the region for interaction with TFIIIS. Altogether, on the basis of the results of both predictive and functional analyses, eleven variants were classified as probably disease-causing (Table 2).

Deep phenotyping, including quantification of phenotypic severity of the individuals, allowed us to delineate the phenotypic spectrum that could be ascribed to the pathogenic

POLR2A variants. The severe end of the spectrum is characterized by profound infantile-onset hypotonia and developmental delay, and is further accompanied by strabismus, decreased endurance, and feeding difficulties. Determining the degree of clinical overlap between the individuals harboring probably disease-causing variants and the remaining individuals allowed us to classify four additional variants as possibly disease-causing. Additional support for the pathogenicity of the variant p.Asn531Ser, other than its *de novo* occurrence, conservation across species, and a severe phenotype, could not be determined, so this variant was classified as of unknown significance.

Thus, the iterative process described here allowed us to delineate pathogenicity for the majority – but not all – of the individuals' variants. Given the current knowledge, evidence that either confirms or excludes pathogenicity for four possibly disease-causing variants and the one variant of unknown significance will be hard to obtain. This is illustrated by the variant p.Arg1603His. Support for its pathogenicity is obtained from its *de novo* occurrence and from the phenotypic overlap of individual 15 with individuals harboring probably disease-causing variants in *POLR2A*; this overlap includes symptoms such as extreme hypotonia with a frog-like positioning of the legs, developmental delay, strabismus, recurrent respiratory tract infections, and wide ventricles, a thin corpus callosum, and bilateral white-matter loss on brain MRI. However, arguments against its pathogenicity are that the variant has been reported three times in gnomAD and that it is part of a poorly conserved region with no known functional importance. We stress the importance of including these unresolved issues when describing novel disease-causing genes because this aids the subsequent resolution of variant pathogenicity when more individuals are described.

In our search for lines of evidence to support pathogenicity, we found an extra line of evidence to support pathogenicity of the variants in *POLR2A* in the design of a desert Z-score. While the CADD score,³² which is usually seen as an estimate of the likelihood of a variant being pathogenic, did not differentiate between variants reported in gnomAD and the missense variants reported here, the variants that we report appeared to cluster within *POLR2A* in large regions devoid of apparently harmless variants reported in gnomAD. We calculated the desert Z-score to reflect this property for all variants within *POLR2A*. This score confirmed not only that the size of these regions exceeded the size that would be expected by chance (the largest region had a Z-score of 11.9), but also confirmed the clustering of individuals' variants within these regions. The relevance of this finding was supported by subsequent structural analyses that unveiled the functional importance of these “desert regions”. We therefore anticipate, in line with Lelieveld et al. and Havrilla et al.,^{45,46} that this property might be helpful to identify within-gene regions that are relatively intolerant of genetic variants and are likely to be of functional importance.

The quantification of phenotypic severity unveiled that individuals harboring heterozygous truncating variants that are incapable of proper pol II formation presented with a mild phenotype, whereas individuals harboring heterozygous missense variants that allow the formation of pol II exhibited the most severe phenotype. This observation implies that the presence of a malfunctioning species of pol II is more detrimental than the reduced availability of pol II alone. We propose that the aberrant pol II enzymes are capable of the proper assembly of the pol II machinery at the transcription start sites, but subsequent elongation of the nascent RNA occurs at reduced rates and possibly with an increased error rate, blocking access to and progression of WT pol II on the same DNA strand. Altogether, this could greatly influence the dynamics of pol II initiation and release, both of which are essential components of transcriptional regulation.²¹ The results reported here direct

further mechanistic studies to investigate this defective elongation hypothesis.

Malfunctioning pol II has deleterious consequences on transcription. To date, none of the eleven other pol II subunits have been implicated in human disease. Interestingly, we noticed some phenotypic overlap between individuals harboring variants in *POLR2A* and individuals harboring variants in subunits of pol III. Mutations in *POLR1C* (MIM #610060, encoding a subunit that is part of both pol III and pol I), *POLR3A* (MIM #614258), and *POLR3B* (MIM #614366) have been described to cause hypomyelinating leukodystrophy 11 (HLD11, MIM #616494), 7 (HLD7, MIM #607694), and 8 (HLD8, MIM #614381), respectively. These three diseases are summarized under the name POLR3-related leukodystrophy.⁵¹ Recently, two individuals with HLD were reported to harbor mutations in *POLR3K*,⁵² thereby expanding the list of potential genetic defects underlying POLR3-related leukodystrophy. In addition to hypomyelination on brain imaging, the clinical phenotype of POLR3-related leukodystrophy is characterized by progressive cerebellar dysfunction and cognitive dysfunction. Non-neurological features are abnormal dentition and hypogonadotropic hypogonadism. Phenotypic features of POLR3-related leukodystrophy that are also noted in *POLR2A* individuals are delayed myelination (5/15), white-matter loss (6/15), and tooth misalignment (5/15). However, the cellular functions of the three nuclear RNA polymerases are different; pol III and pol II are responsible for tRNA and mRNA synthesis, respectively. This can be reconciled by the proposal that mutations in both pol II and pol III subunits can affect protein synthesis via different mechanisms, and this can result in similar clinical phenotypes.

In addition to POLR3-related leukodystrophy, *POLR1A* has been associated with both acrofacial dysostosis⁵³ (MIM #616462) and severe neurodegenerative disease with ataxia, psychomotor retardation, cerebellar and cerebral atrophy, and leukodystrophy;⁵⁴ *POLR3A* is also, in addition to HLD7, associated with Wiedemann-Rautenstrauch syndrome, a neonatal progeroid syndrome⁵⁵ (MIM #264090), and has been discussed as potential cause of hereditary ataxia and spastic paraparesis,^{56,57} implying a broader phenotypic range for *POLR3A* mutations.

CONCLUSION

In summary, we here report that heterozygous *de novo* variants in *POLR2A*, which is indispensable for the synthesis of mRNA and several non-coding RNAs as it encodes the RPB1 subunit of pol II, can result in a neurodevelopmental syndrome characterized by profound infantile-onset hypotonia and developmental delay. We conclude that the clinical consequences of probably disease-causing variants in *POLR2A* are dependent on their effect on pol-II-mediated transcription because *POLR2A* variants predicted to result in loss of RPB1 protein are better tolerated than missense variants, which we propose can cause a dominant-negative effect on pol-II-dependent transcription.

WEB RESOURCES

GeneMatcher	https://www.genematcher.org
gnomAD	https://gnomad.broadinstitute.org
OMIM	https://www.omim.org
Protein Data Bank	http://www.rcsb.org
UniProt	https://www.uniprot.org

REFERENCES

1. Wintzerith M, Acker J, Vicaire S, Vigneron M, Kedinger C. Complete sequence of the human RNA polymerase II largest subunit. *Nucleic Acids Res.* 1992;20:910.

2. Mita K, Tsuji H, Morimyo M et al. The human gene encoding the largest subunit of RNA polymerase II. *Gene* 1995;159:285-286.
3. Kornberg RD. Eukaryotic transcriptional control. *Trends Cell Biol.* 1999;9:M46-M49.
4. Roeder RG, Rutter WJ. Multiple forms of DNA-dependent RNA polymerase in eukaryotic organisms. *Nature* 1969;224:234-237.
5. Thomas MC, Chiang CM. The general transcription machinery and general cofactors. *Crit Rev Biochem Mol Biol.* 2006;41:105-178.
6. Sainsbury S, Bernecky C, Cramer P. Structural basis of transcription initiation by RNA polymerase II. *Nat Rev Mol Cell Biol.* 2015;16:129-143.
7. Bushnell DA, Westover KD, Davis RE, Kornberg RD. Structural basis of transcription: An RNA polymerase II-TFIIB cocystal at 4.5 Angstroms. *Science* 2004;303:983-988.
8. Sainsbury S, Niesser J, Cramer P. Structure and function of the initially transcribing RNA polymerase II-TFIIB complex. *Nature* 2013;493:437-440.
9. Plaschka C, Larivière L, Wenzek L et al. Architecture of the RNA polymerase II-Mediator core initiation complex. *Nature* 2015;518:376-380.
10. Robinson PJ, Trnka MJ, Bushnell DA, Davis RE, Mattei PJ, Burlingame AL, Kornberg RD. Structure of a complete mediator-RNA polymerase II pre-initiation complex. *Cell* 2016;166:1411-1422.
11. Westover KD, Bushnell DA, Kornberg RD. Structural basis of transcription: Nucleotide selection by rotation in the RNA polymerase II active center. *Cell* 2004;119:481-489.
12. Cramer P. RNA polymerase II structure: From core to functional complexes. *Curr Opin Genet Dev.* 2004;14:218-226.
13. Cheung AC, Sainsbury S, Cramer P. Structural basis of initial RNA polymerase II transcription. *EMBO J.* 2011;30:4755-4763.
14. Gnatt AL, Cramer P, Fu J, Bushnell DA, Kornberg RD. Structural basis of transcription: An RNA polymerase II elongation complex at 3.3 Å resolution. *Science* 2001;292:1876-1882.
15. Jonkers I, Lis JT. Getting up to speed with transcription elongation by RNA polymerase II. *Nat Rev Mol Cell Biol.* 2015;16:167-177.
16. Ehara H, Yokoyama T, Shigematsu H, Yokoyama S, Shirouzu M, Sekine SI. Structure of the complete elongation complex of RNA polymerase II with basal factors. *Science* 2017;357:921-924.
17. Kettenberger H, Armache KJ, Cramer P. Complete RNA polymerase II elongation complex structure and its interactions with NTP and TFIS. *Mol Cell* 2004;16:955-965.
18. Sydow JF, Brueckner F, Cheung AC et al. Structural basis of transcription: Mismatch-specific fidelity mechanisms and paused RNA polymerase II with frayed RNA. *Mol Cell* 2009;34:710-721.
19. Cheung AC, Cramer P. Structural basis of RNA polymerase II backtracking, arrest and reactivation. *Nature* 2001;471:249-253.
20. Walmacq C, Cheung AC, Kireeva ML et al. Mechanism of translesion transcription by RNA polymerase II and its role in cellular resistance to DNA damage. *Mol Cell* 2012;46:18-29.
21. Steurer B, Janssens RC, Geverts B et al. Live-cell analysis of endogenous GFFRBP1 uncovers rapid turnover of initiating and promoter paused RNA Polymerase II. *Proc Natl Acad Sci USA* 2018;115:E4368-E4376.
22. Wang D, Bushnell DA, Westover KD, Kaplan CD, Kornberg RD. Structural basis of transcription: Role of the trigger loop in substrate specificity and catalysis. *Cell* 2006;127:941-954.
23. Kaplan CD, Jin H, Zhang IL, Belyanin A. Dissection of Pol II trigger loop function and Pol II activity dependent control of start site selection *in vivo*. *PLoS Genet.* 2012;8:e1002627.
24. Timmers HTM, Tora L. Transcription buffering: A balancing act between mRNA synthesis and mRNA degradation. *Mol Cell* 2018;72:10-17.
25. Sugaya K. Amino acid substitution of the largest subunit of yeast RNA polymerase II: Effect of a temperature sensitive mutation related to G1 cell cycle arrest. *Curr Microbiol.* 2003;47:159-162.
26. Zhang QQ, Li F, Fu ZY et al. Intact Arabidopsis RPB1 functions in stem cell niches maintenance and cell cycling control. *Plant J* 2018;95:150-167.
27. Richards S, Aziz N, Bale S et al. Standards and guidelines for the interpretation of sequence variants: A joint consensus recommendation of the American College of Medical Genetics and Genomics and the Association for Molecular Pathology. *Genet Med.* 2015;17:405-424.
28. Lelieveld SH, Reijnders MRF, Pfundt R et al. Meta-analysis of 2,104 trios provides support for 10 new genes for intellectual disability. *Nat Neurosci.* 2016;19:1194-1196.
29. Lek M, Karczewski KJ, Minikel EV et al. Analysis of protein-coding genetic variation in 60,706 humans. *Nature* 2016;536:285-291.
30. Sobreira N, Schiettecatte F, Valle D, Hamosh A. GeneMatcher: A matching tool for connecting investigators with an interest in the same gene. *Hum Mutat.* 2015;36:928-930.
31. Gray OP. The Denver scale. *Dev Med Child Neurol.* 1972;14:666-667.

32. Kircher M, Witten DM, Jain P, O’Roak BJ, Cooper GM, Shendure J. A general framework for estimating the relative pathogenicity of human genetic variants. *Nat Genet.* 2014;46:310-315.
33. Schomburg D, Reichelt J. BRAGI – A comprehensive protein modeling program system. *J Mol Graph.* 1988;6:161-165.
34. Kraulis PJ. Molscript – A program to produce both detailed and schematic plots of protein structures. *J Appl Cryst.* 1991;24:946-950.
35. Merritt EA, Murphy MEP. Raster3D Version 2.0. A program for photorealistic molecular graphics. *Acta Crystallogr D Biol Crystallogr.* 1994;50:869-873.
36. Sugaya K, Vigneron M, Cook PR. Mammalian cell lines expressing functional RNA polymerase II tagged with the green fluorescent protein. *J Cell Sci.* 2000;113:2679-2683.
37. Sugaya K, Sasanuma S, Cook PR, Mita K. A mutation in the largest (catalytic) subunit of RNA polymerase II and its relation to the arrest of the cell cycle in G(1) phase. *Gene* 2001;274:77-81.
38. Malagon F, Kireeva ML, Shafer BK, Lubkowska L, Kashlev M, Strathern JN. Mutations in the *Saccharomyces cerevisiae* RPB1 gene conferring hypersensitivity to 6-azauracil. *Genetics* 2006;172:2201-2209.
39. Nguyen VT, Giannoni F, Dubois MF, Seo SJ, Vigneron M, Kédinger C, Bensaude O. *In vivo* degradation of RNA polymerase II largest subunit triggered by alpha-amanitin. *Nucleic Acids Res.* 1996;24:2924-2929.
40. Baas R, Lelieveld D, van Teeffelen H et al. A novel microscopy-based high-throughput screening method to identify proteins that regulate global histone modification levels. *J Biomol Screen.* 2014;19:287-296.
41. Pereira LA, van der Knaap JA, van den Boom V, van den Heuvel FA, Timmers HTM. TAF(II)170 interacts with the concave surface of TATA-binding protein to inhibit its DNA binding activity. *Mol Cell Biol.* 2001;21:7523-7534.
42. Baymaz HI, Spruijt CG, Vermeulen M. Identifying nuclear protein-protein interactions using GFP affinity purification and SILAC-based quantitative mass spectrometry. *Methods Mol Biol.* 2014;1188:207-226.
43. Rappsilber J, Ishihama Y, Mann M. Stop and go extraction tips for matrix-assisted laser desorption/ionization, nanoelectrospray, and LC/MS sample pretreatment in proteomics. *Anal Chem.* 2003;75:663-670.
44. Haijes HA, Jaeken J, Foulquier F, van Hasselt PM. Hypothesis: Lobe A (COG1-4)-CDG causes a more severe phenotype than lobe B (COG5-8)-CDG. *J Med Genet.* 2018;55:137-142.
45. Lelieveld SH, Wiel L, Venselaar H et al. Spatial clustering of *de novo* missense mutations identifies candidate neurodevelopmental disorder-associated genes. *Am J Hum Genet.* 2017;101:478-484.
46. Havrilla JM, Pedersen BS, Layer RM, Quinlan AR. A map of constrained coding regions in the human genome. *Nat Genet.* 2019;51:88-95.
47. Scafe C, Chao D, Lopes J, Hirsch JP, Henry S, Young RA. RNA polymerase II C-terminal repeat influences response to transcriptional enhancer signals. *Nature* 1990;347:491-494.
48. Eick D, Geyer M. The RNA polymerase II carboxy-terminal domain (CTD) code. *Chem Rev.* 2013;113:8456-8490.
49. Nonet M, Sweetser D, Young RA. Functional redundancy and structural polymorphism in the large subunit of RNA polymerase II. *Cell* 1987;50:909-915.
50. Rosonina E, Blencowe BJ. Analysis of the requirement for RNA polymerase II CTD heptapeptide repeats in pre-mRNA splicing and 30-end cleavage. *RNA* 2004;10:581-589.
51. Bernard G, Vanderver A. POLR3-related leukodystrophy. In: Adam MP, Ardinger HH, Pagon PA et al., eds. *GeneReviews*®. Seattle, WA: University of Washington, Seattle; 1993-2019. Updated: 2017, May 11.
52. Dorboz I, Dumay-Odelot H, Boussaid K. Mutation in POLR3K causes hypomyelinating leukodystrophy and abnormal ribosomal RNA regulation. *Neurol Genet* 2018;4:e289.
53. Weaver KN, Watt KEN, Hufnagel RB et al. Acrofacial dysostosis, Cincinatti type, a mandibulofacial dysostosis syndrome with limb anomalies, is caused by POLR1A dysfunction. *Am J Hum Genet.* 2015;96:765-774.
54. Kara B, Köröglu C, Peltonen K et al. Severe neurodegenerative disease in brothers with homozygous mutation in POLR1A. *Eur J Hum Genet.* 2017;25:315-323.
55. Jay AM, Conway RL, Thiffault I, Saunders C, Farrow E, Adams J, Toriello HV. Neonatal progeroid syndrome associated with biallelic truncating variants in POLR3A. *Am J Med Genet A.* 2016;170:3343-3346.
56. Rydning SL, Koht J, Sheng Y et al. Biallelic POLR3A variants confirmed as a frequent cause of hereditary ataxia and spastic paraparesis. *Brain* 2019;142:e12.
57. Minnerop M, Kurzwelly D, Wagner H, Schüle R, Ramirez A. Reply: Biallelic POLR3A variants confirmed as a frequent cause of hereditary ataxia and spastic paraparesis. *Brain* 2019;142:e13.

SUPPLEMENTAL DATA

Supplemental Note. Case reports of individuals harboring *POLR2A de novo* variants

Mild phenotype

Individual 5; p.Gln700* – heterozygous de novo c.2098C>T – Ann Arbor, Michigan, USA

Individual p.Gln700*, a 17-year old boy, is the first and only child of non-consanguineous American parents. Family history was unremarkable. Pregnancy was uncomplicated. The boy was born by Caesarean section at 42 weeks, with good Apgar scores. Birth weight was 3884g. During childhood, the boy had mild global developmental delay. He spoke words at 15 months and walked at 18 months of age. There was some intellectual disability, however he was able to complete 8th grade at 14 years of age. His tendon reflexes were normal. Except for a high frontal hairline and a high arched palate, there were no dysmorphic features. During childhood, there was no hypotonia and there were no feeding difficulties. At present, he wears glasses due to bilateral myopia and he wears hearing aids due to bilateral moderate high frequency sensorineural hearing loss. He has a blonde fundus and a poor vision: 20/200 and 20/60. He has frequent headaches. He has difficulty sleeping, waking up at night between 2 and 5 a.m. He has been diagnosed with PDD-NOS and has social communication difficulties, diminished eye contact, inappropriate behavior and attention difficulties. He enjoys bowling and other social interactions. His parents report that he is always hungry. He has a BMI of 48, however no endocrinological abnormalities were found.

Individual 6; p.Gln735* – heterozygous de novo c.2203C>T – Oxford, United Kingdom

Individual p.Gln735* is a 13-year old girl, born to non-consanguineous Caucasian parents. Family history was unremarkable. Pregnancy was complicated by preterm birth at 28 weeks' gestational age. She has a high forehead, teeth misalignment and strabismus. There are no other dysmorphic features. During childhood, she had generalized hypotonia, but no muscle atrophy. There were feeding difficulties and a gastro-esophageal reflux, but no failure to thrive. She sat without support at age twelve months, began standing at age eighteen months and walked well at thirty months. She could jump at 50 months and cycle a tricycle at 60 months of age. Brain MRI demonstrated cerebellar atrophy, inferior vermis, a very small pons, heterotopia, a right frontal porencephalic cyst, a megacisterna magna and a slightly small corpus callosum.

Individual 8; p.Ser755del – heterozygous de novo c.2262_2264delCTC – Bethesda, Maryland, USA

Individual p.Ser755del, a 3-year old boy, is the first child of healthy, non-consanguineous Caucasian American parents. Family history was unremarkable. Pregnancy was complicated by polycystic ovarian syndrome prior to pregnancy. He was born at term, birth weight was 2584g. Despite a high forehead, there were no dysmorphic features. There were no feeding difficulties, no failure to thrive, no food allergies. There was no reflux, no inguinal hernia, no constipation. The boy was referred to a geneticist at 1 year of age due to global developmental delay and severe congenital hypotonia. He had a hypomimic face, hypokinesia and a frog position. Brain MRI performed at 13 and at 20 months of age showed decreased myelination. He suffered from recurrent ear infections. He has conductive hearing loss, though this is thought to be associated to the recurrent ear infections. He has had surgery to correct strabismus. At present, he is 3 years old. He is easily tired. There are no sleeping problems. He walks with the assistance of a walker and he is not able to speak, but communicates through a communication device.

Individual 12; p.Leu1124Pro – heterozygous de novo c.3371T>C – Dublin, Ireland

Individual p.Leu1124Pro, a 4-year old girl, is the first child of non-consanguineous Irish Caucasian parents. Family history was unremarkable. At 12 weeks' gestational age nuchal translucency was noted but parents decided to do nothing further. Fetal growth slowed from 34 weeks' gestational age and at 38 weeks a Caesarean section, was performed since fetal movements were not reassuring. Birth weight was 2610g. The girl looked "unusual" according to parents and dysmorphic features included epicanthus, macrostomia and full lips. Skin and nails were normal. Trisomy 21 was suspected, but karyotype was normal. The girl did not feed well on breast, but bottle feeding went fine. There was no failure to thrive. There was hypotonia and a frog position. There was a motor developmental delay, at 4 months there was some head control and at 9 months gross motor development was described as "poor". However, she responded to physical therapy. She sat without support and crawled at 12 months, stood at 18 months and walked at 23 months. At 3.5 years of age she was good at tasks requiring gross motor skills, but she still needed support with cutting and glueing, buttons and zippers. Speech-language development was also delayed. She smiled at 4 months, made sounds at 24 months and at 2.5 years of age she used eight single words, however with poor comprehension. She made two-word sentences at 30 months and three-word sentences at 36 months, but speech was unclear. Verbal IQ was 78, non-verbal IQ was 99, according to the Stanford Binet Intelligence Scale 5. She was hospitalized twice for infections. There were no seizures. Brain MRI showed delayed myelination. Differential diagnosis was Kleefstra syndrome or Pitt-Hopkins syndrome but DNA assays, including the intellectual disability panel, were normal. Trio WES revealed a *POLR2A* mutation. At present, she is a happy child, however easily tired. She sleeps 16 hours a day. She has some strabismus, especially when she is tired. She does not like loud noises and is routine driven, but autism has not been diagnosed. She continues to make progress in motor skills, especially fine motor skills, but her greatest deficit is in language acquisition.

Individual 13; p.Lys1125del – heterozygous de novo c.3373_3375delAAG – Vancouver, Canada

Individual p.Lys1125del, a 7-year old boy, is the first child of healthy, non-consanguineous Chinese parents. Family history was unremarkable. The boy has a healthy younger sister. Pregnancy was uncomplicated, there were normal fetal movements and at 37 weeks' gestational age, the boy was born with good Apgar scores. Birth weight was 2780g. At 6 months of age, global developmental delay was identified. The boy had hypotonia since birth. Dysmorphic features include plagiocephaly and brachycephaly without any craniosynostosis, a high hairline with frontal bossing, broad round face with flat malar eminences, hypoplastic supraorbital ridges, hypertelorism, flat nose with anteverted nares, a high and long palate, dental crowding, posteriorly rotated ears, bilateral single palmar creases and bilateral clinodactyly. He has mild velopharyngeal dysfunction with nasal speech. Brain MRI showed delayed myelination. There were no feeding difficulties. The boy walked at 22 months and started to speak single words at 2 years of age. At age 6, he could run with immature gait, he could barely jump with two feet and he could balance on one foot for only 3 seconds. He mainly spoke in 2-4 word phrases or simple sentences. A mild intellectual disability was diagnosed. He has had surgery for strabismus. At present, he suffers from constipation. He has joint hypermobility and continues to have hypotonia. His endurance is significantly decreased. There is no vision or hearing loss. The boy does not have autistic or aggressive behavior; he is a social and pleasant boy. There are no food allergies, although the boy has eczema.

Individual 1; p.Pro371Leu – heterozygous de novo c.1112C>T – Prague, Czech Republic

Individual p.Pro371Leu, a 7-year old girl, is the first child from the second pregnancy of young healthy non-consanguineous Czech parents. Family history was unremarkable. The pregnancy was uncomplicated and no reduced fetal movements were noted. The girl was born at 41 weeks' gestational age with good Apgar scores. Birth weight was 3050g. In the newborn period, feeding difficulties, poor suck, failure to thrive and periods of hypothermia and fever were present. The girl was able to sit without support at the age of 2 years and was able to walk without support at the age of 6.5 years. Speech and language development was also delayed. She was able to speak single words at the age of 4 years and simple sentences at the age of 6 years. The girl had frontal bossing, hypertelorism, large dysplastic ears, short philtrum, thick lips and strabismus. MRS of brain was normal. At present, she is obese and on growth hormone therapy. No behavioral abnormalities, sleeping disturbances or seizures are present.

Individual 16; p.Pro1767fs – heterozygous de novo c.5298dup – Odense, Denmark

Individual p.Pro1767fs, a 9-year old boy, is the first child of non-consanguineous Caucasian parents. Family history revealed that the younger sister has hearing impairment. On the mother's side of the family, hypermobility, epicanthus and myopia are more common. Mother has 3 café-au-lait spots. Pregnancy was uncomplicated and the boy was born at 41+3 weeks' gestational age with good Apgar scores. Birth weight was 3690g. Oral motor function was slightly affected, resulting in swallowing his food and avoiding chewing. Motor development was moderately delayed. The boy sat without support at 12 months and walked at 27 months. Also speech and language development was delayed. At 5 years of age, WPPSI-R testing showed a verbal IQ of 77 and a performance IQ of 63, with a total IQ below 66. Brain MRI was normal. Dysmorphic features included flat occiput, a broad forehead, marked arched eyebrows, broad nasal bridge, hypertelorism, slightly downslanting palpebral fissures, slight ptosis, epicanthus, slight midfacial hypoplasia, anteverted nares, bulbous nasal tip, full lower lip, high peaks of the upper vermilion border and six light brown café-au-lait spots. At age 6 years, he had surgery for significant bilateral pes planus and pes valgus, with implantation of graft from the hip. However, at age 9, the graft on the left foot has not healed and repeat surgery is planned. Also his knees are in valgus position. He has a progressing myopia, -2.0/-2.0 at 4 years of age and -4.0/-3.5 at 8 years of age. There is no blonde fundus. He is learning to read. He is very sociable and functions well in a social context, however he is shy with strangers. He has special interests in trains and food and has a very well developed geographic memory, he finds his way in places that he has been to years ago. He has a tactile shyness resulting in problems eating solid food and in avoiding touching special materials. He is not fond of being touched. He still has enuresis nocturna. There is a slight hypotonia and hypermobility and a poor balance. He has a discrete cerebral palsy with a foot clonus, hyperactive patellar reflexes and achilles tendon reflexes. He has eruption of canines before the incisors.

*Moderate phenotype***Individual 4; p.Tyr669del – heterozygous de novo c.2006_2008delACT – Rotterdam, the Netherlands**

Individual p.Tyr669del, an 11-year old girl, is the first child of non-consanguineous Dutch Caucasian parents. She has two younger, healthy siblings. Family history was unremarkable. Pregnancy was uncomplicated. The girl was born at 41+4 weeks with Apgar scores of 9 and 10. Birth weight was 3950g. Examination at birth showed no abnormalities. During the first year of life, the girl was very quiet, she did not move much and did not cry much. There were feeding problems: she got dehydrated since she did not have the strength for breastfeeding. Feeding problems persisted with bottle feeding. She had weak oral motor skills, could not suck strongly, could not prevent

milk falling out of her mouth, there was excessive drooling and there was gastro-esophageal reflux. Fine and gross motor development started normally, but slowed down during the first year of life. She was able to roll at 6 months and to creep at 9 months, however for a long time she was not able to sit independently, due to hypotonia. She had physiotherapy twice a week from 15 months of age. She started to walk independently at 26 months, but she only walked when she really had to. When the surface changed, she first sat down to test the “new” surface, and then proceeded to walk, over and over again. At the age of 3, during two infection episodes, there was regression of motor and speech and language development. She had no stamina. When she was 5 years old, after 1-1.5 kilometer she started limping. Most of the time her parents used a buggy. It took a long time before she learned more words. At 5 years of age she was diagnosed with autism. She laughs very hard, she asks many questions, she does not have fantasy-play, she is in need of structure and she is socially awkward. However, she is interested and kind towards other children. At 6 years of age she was operated on for an inguinal hernia. At present, her joints are very flexible. Her balance is limited and she is afraid to fall. Normally she corrects her imbalance with her visus, but when this is not possible she gets nauseous. Vision and hearing are good. There are sleeping problems, difficulty going to sleep and early waking in the morning. Her frontal incisors are widely spaced. She has a mild pectus excavatum. She now has a moderate intellectual disability with an IQ of 44.

Individual 11; p.Tyr1109His – heterozygous *de novo* c.3325T>C – Naples, Italy

Individual p.Tyr1109His, a 6-year old boy, is the third child of healthy, Caucasian Italian non-consanguineous parents. Family history was unremarkable. Pregnancy was uncomplicated and the child was born after 40 weeks of gestation with Apgar scores of 6 and 9 at 1 and 5 minutes, respectively. At birth his weight was 3440g, his length 49 cm and head circumference 34.5 cm. Tremors were noted at birth. He was noted to have hypotonia from the first months of life, although this improved slightly over time. He had no feeding problems and no gastro-esophageal reflux. His growth and weight were normal, but he developed microcephaly. During the first years of life, he had recurrent episodes of respiratory tract infections and during these episodes, he became severely lethargic and poorly responsive. He was suspected to have an inborn error of metabolism, but an extensive metabolic work-up was negative. At 5 years of age, he developed generalized tonic-clonic seizures. At the last evaluation at 6 years of age, he was able to sit without support but he could neither stand up nor was he able to walk. He had not developed any language. He had strabismus, but no signs of reduced vision or hearing loss. He had bilateral cryptorchidism. Brain MRI showed enlarged ventricles and bilateral increase of T2 signals in the nuclei pallidi. Cardiac echo and abdominal ultrasound did not reveal any abnormalities. Array CGH and methylation testing for Angelman/Prader-Willi region were both negative.

Individual 10; p.Ile848Thr – heterozygous *de novo* c.2543T>C – Durham, North Carolina, USA

Individual p.Ile848Thr is a 14 year old girl. She is the second child of non-consanguineous, Northern European, Caucasian parents. Family history was notable for a full sister with trisomy 21. Pregnancy was complicated by first trimester spotting, with normal ultrasound imaging. Maternal exposures included an antidepressant for the first 2 weeks of pregnancy and vitamin B12 injections for nausea. The girl was born at 41 weeks’ gestational age by emergency Cesarean section for failure to progress and fetal cardiac decelerations to a G2P2 to a 36 year old mother. Birth weight was 3440g. Apgar scores were 4 (-2 for respiratory rate, -2 tone, -1 reflex, -1 color) and 7 (-1 respiratory rate, -1 tone, -1 color). At delivery, amniotic fluid was meconium stained. Bulb suctioning was performed followed by two-minute, bag-mask ventilation for poor respiratory effort. A chest x-ray was consistent with congenital pneumonia and she was treated at a tertiary care facility until her discharge at the 9th day of life. Her parents report that at 3-4 months of age, she did not have yet good head control and developmental delay was discussed with the pediatrician. Torticollis was mentioned in early infancy, but resolved before age 9 months. At 9 months of age her first developmental evaluation confirmed global delay. Head lag was present until 11 months. She rolled over at 9 months, but at that age had difficulty sustaining an upright truck posture when seated in her mother’s lap. Severe hypotonia and joint flexibility were noted by on clinical exam at both at 12 and 18 months old. At almost 18 months, she could push to a sitting position. At 21 months she could bear weight and pull to stand. She took steps with assistance at around 30 months. Brain MRI completed at 3 and 6 years did not show any myelination or cerebellar changes.

Presently at age 14 she has a square appearance to the face, with a broad forehead and plagiocephaly with flattening on the right side of the occiput and truncal obesity. She has a wide based gait with no ataxia. She can take about 6 independent steps, but most often will crawl, scoot or walk with assistance (hand rails at home, walker, holding a hand). Walking appears to be limited by poor trunk tone. She will exhibit fatigue while sitting and will slouch within a few moments of sitting upright. The family uses a stroller or wheelchair for long distances outside the home. She does not like to walk on grass or sand. She is not yet toilet trained. She can finger feed and use a spoon with assistance. She has some pincer grip abilities and can undress and assists with dressing. She has very limited language (receptive more than expressive), but vocalizes almost constantly when awake, with louder volume when agitated. She presently uses 6 words with meaning, 10 consistent signs and can shake her

head yes and no. She is interested in play and social interaction but has difficulty engaging appropriately. She has been diagnosed with poor sensory processing and engages in increasingly aggressive behavior as her arousal escalates. She will grab clothing, hair and other body parts with equal (hard) strength in her attempts to engage and pull others toward her. When highly agitated she will scream, grab, punch and bite, especially in environments or situations undesirable to her. She will calm herself quickly when removed from undesirable environments. No regression has been appreciated.

Individual 15; p.Arg1603His – heterozygous *de novo* c.4808G>A – Little Rock, Arkansas, USA

Individual p.Arg1603His, a 7-year old girl, is the first child of non-consanguineous Caucasian Northern-European parents. Family history was unremarkable. The girl has a healthy younger sibling. Pregnancy was uncomplicated and at term the girl was born with good Apgar scores. Birth weight was 3060g. There was a severe (supranuclear) congenital hypotonia from birth that improved very slowly. She had mild retrognathia, but no other notable facial dysmorphisms. She exhibited severe global developmental delay, especially in speech-language development. She would make only limited eye-contact and she has never acquired much meaningful expressive language. There is severe cognitive impairment. At the age of 6 she was assessed as having a development scores consistent with normal ranges for 5-9 months of age. She suffers from epilepsy with her EEG showing a slow background and sharply contoured wave forms. She experiences sleep disturbances. She has been diagnosed with autism and other behavioral problems as head banging, stereotypy and chewing walls. She frequently suffers from otitis media and respiratory tract infections. She has constipation and has had recurrent episodes of enterocolitis. She has cortical visual impairment and astigmatism. She has normal hearing. Despite the retrognathia, she has normal dentition and alignment. She has some seasonal allergies. She has been diagnosed as having a sinus tachycardia. Her brain MRI showed a thin corpus callosum, enlarged ventricles and bilateral loss of white matter. She had a muscle biopsy which was interpreted as being consistent with a cytochrome C oxidase deficiency. A mitochondrial disorder was considered. As such she was placed on a mitochondrial cocktail of high dose vitamins. Empirically she seemed to be healthier and have better developmental progress. Overall her development remained markedly delayed with very slow progress in all of her areas of development. She continues to have almost no expressive language.

Severe phenotype

Individual 9; p.Met769Thr – heterozygous *de novo* c.2306T>C – Prague, Czech Republic

Individual p.Met769Thr, an 18-year old boy, is the first child (second pregnancy) of healthy Caucasian Czech parents. The first pregnancy resulted in mola hydatidosa. Family history revealed that father's brother had strabismus and a sister from father showed multiple congenital anomalies and died at the age of 4 days. A nephew from father had an atrial septal defect. This pregnancy was uncomplicated and no reduced fetal movements were noted. The boy was born at 41+2 weeks with good Apgar scores. The birth weight was 3100g. At 4 months of age he presented with moderate hypotonia and weak muscles. He had feeding difficulties and poor suck. He showed psychomotor delay. He was able to sit without support at the age of 1 year and walk without support at the age of 2 years; however his gait was unsteady. Speech and language development was also delayed. He was able to speak single words at the age of 1 years and simple sentences at the age of 4.5 years. The boy had frontal bossing, hypertelorism, high arched palate and pedes planovalgi. At the age of 6 years he had surgery for an inguinal hernia. At present he shows a hypomimic face, a narrow chest, pectus excavatum, a marfanoid habitus, long fingers and toes, hypermobility of joints, dyslalia and echolalia. He is easily defatigable, asks repeating questions and has some autistic traits. He is able to initiate a conversation, but not to maintain it. He finished primary education and is able to read, write and count, however he reads without understanding the content. The boy also has strabismus, hypermetropia and reduced vision. He suffers from sleep disturbances. Diazepam medication was used since EEG showed high voltage theta bursts, which later improved. Brain MRI demonstrated bilateral frontal subcortical delayed myelination.

Individual 14; p.Asn1251Ser – heterozygous *de novo* c.3752A>G – Groningen, the Netherlands

Individual p.Asn1251Ser, a 6-year old girl, is the first child of healthy non-consanguineous Dutch Caucasian parents. Family history was unremarkable. Mother has another, healthy son from a former relationship. Pregnancy was complicated by diminished fetal movements. At 40 weeks' gestational age, the girl was born with good Apgar scores. Birth weight was 3310 g. However, after birth, she turned very blue. In the first hours, the girl barely moved, did not open her eyes and she barely cried. On the first and fourth day of life, she was hospitalized due to hypothermia. There was severe hypotonia, with hypokinesia, hypomimic face and frog position. There were feeding difficulties since she could not suck very well, had gastro-esophageal reflux and frequently choked. She drank very slowly and vomited frequently until 2 years of age. To eat solid foods without choking, she needs to eat small pieces of food and she has to concentrate very hard. Dysmorphic features include brachiocephaly and plagiocephaly, thin, sparse, slow growing blond hair, strong upslant of eyes, full nasal tip, flat philtrum, thin lips, clinodactyly of 5th fingers and pectus excavatum. Motor development was severely delayed. She did not have enough head control until 3 years of age. At the age of 4.5 years, she was able to sit without support. She crawled till she was 5 years old. She

could sit up straight from the age of 5.5 years. By then, she was also able to walk without support, though she had an unsteady gait and needed to walk very concentrated. At the age of 6, she is able to walk 100 meters. Muscle strength is good, she is very strong. Speech and language development was also severely delayed. At the age of 15 months she started to make eye contact. At 3.5 years she started to smile and at 5.5 years she started to make sounds. Since she was 5 years of age, she seems to understand small tasks. At the age of 6, she is learning gestures to express herself. She had frequent unexplained fevers and episodes of hyperthermia. During the first years of life she could get ill very quickly, with high fevers and febrile convulsions. There was no epilepsy. Due to respiratory tract infections and urinary tract infections because of vesico-urethral reflux, she needed to be hospitalized every winter. During episodes of illness there was no stagnation of development. There is no hearing loss or vision loss. There only is convergent strabismus when she is tired. There are sleeping disturbances, she wakes up every night and lies awake for 2-4 hours, most of the time happy. In first years of life however, she seemed to be in trance when she woke up, she cried loudly for hours, without making any contact. The girl has a short attention span and always wants multiple things at the same time. She needs to be entertained throughout the day. At times, she can be very frustrated and she bites, claws and pinches herself and others, sometimes also out of happiness. There is inappropriate behavior, she sometimes tries to eat her faeces and she tries to undress all the time, even when she is asleep. Brain MRI showed despite a megacisterna magna, no abnormalities.

Individual 2; p.Ile457Thr – heterozygous *de novo* c.1370T>C – Utrecht, the Netherlands

Individual p.Ile457Thr, a 4-year old boy, is the second child of non-consanguineous Dutch Caucasian parents. He has an older, healthy sister. Family history was unremarkable. Pregnancy was complicated by polyhydramnion and few fetal movements. The boy was born at term (40+4) with Apgar scores of 8 and 9. Birth weight was 3925g. At 3 days of age, he was hospitalized because of feeding difficulties and choking incidents with dropping saturation and blue turning. Despite thickening, choking persisted. At 5 weeks, he had surgery for an inguinal hernia. Parents noted general hypotonia, a preferred head position, a frog position of the hips and only little mimicry and consulted a physiotherapist at 7 weeks of age. Gross and fine motor skills developed very slowly, he had a weak cry and a weak cough. He had three episodes of respiratory infections by the time he was 8 months of age, necessitating antibiotics. During these episodes, his motor development stagnated or regressed for weeks. He was referred to a tertiary center, specialized in developmental delay. He presented with plagiocephaly, a hypomimic face and axial and peripheral hypotonia which was more pronounced in his legs than in his arms. Muscle weakness was more pronounced proximally. He had a dystrophic muscle mass. There was a head lag, minimal head balance, a positive scarf sign, slipping through, frog position and minimal spontaneous movements. He scored 46 points out of 64 points on the CHOP INTEND (Children's Hospital of Philadelphia Infant Test of Neuromuscular Disorders). There were normal tendon reflexes and Babinski sign on both feet. Breathing pattern was normal, thorax was symmetrical and there were no dysmorphic features, despite a high frontal hairline and a high arched palate. Vision and hearing development was normal. Brain MRI only demonstrated wide ventricular spaces, normal for his age. Differential diagnosis was a congenital myopathy, Pompe disease, congenital myotonic dystrophy type 1 or congenital myasthenia. Spinal muscular atrophy was considered less likely. Plasma creatine kinase was normal, muscle ultrasound showed no abnormalities, metabolic diagnostics tests were all normal and DNA showed a normal male array profile. Muscle biopsy showed no structural, enzyme or immune abnormalities. However, by electron microscopy an increase of nerve tissue and a slightly abnormal structure was seen, possibly due to a disorder in the motor endplate. A single fiber electromyography showed increased jitter, which pointed towards a disorder in the neuromuscular junction. Baseline measurement at 17 months of age for experimental treatment with pyridostigmine demonstrated that motor development improved, he scored 62 out of 64 points on the CHOP INTEND. Pyridostigmine was stopped after two weeks since it did not improve symptoms and motor development stagnated. At 20 months of age, strabismus of the left eye and choreatic movements were noted. He could sleep in easily but could not sleep through the night. He always had a warm head, but cold hands and feet. He made sounds, but no words. He started to make eye contact. He had a delayed reaction: it takes a minute for he starts to smile at a funny face. At 3 years of age, his motor development was still progressing, however slowly. He was able to sit for 1.5-2 hours and he was able to stand on his own. He made more sounds and tried to imitate. He made more eye contact. He had frequent middle ear infections with high fevers. He had misaligned teeth and hyperlaxity of skin. At present, he is easily tired, but he is still developing at his own pace.

Profound phenotype

Individual 7; p.Thr736Met – heterozygous *de novo* c.2207C>T – Philadelphia, Philadelphia, USA

Individual p.Thr736Met, a 4 year old girl, is the third child of non-consanguineous Caucasian parents. Despite hypothyroidism and Celiac disease, family history was unremarkable. Pregnancy was uncomplicated and the girl was born at term (39 weeks) with good Apgar scores. Birth weight was 3033g. Hypotonia and bilateral contractures of the middle fingers were noted at birth. Examination at 4 years old was significant for a round and full face, sparse lateral eyebrows, mildly low nasal root, a slightly high palate, a small mouth, long, tapered fingers, hyperextensible

elbows and wrists and a proximally placed anus. There was general truncal hypotonia and myopathy, and frog position of the hips. She was minimally active. During the neonatal period, there were severe feeding problems and failure to thrive due to gastro-esophageal reflux, demanding a G-tube placement at 3 months of age and a Nissen at 5 months of age. At 5 months of age, she also had surgery for a hiatal hernia. She had chronic constipation with increasing episodic abdominal pains. She had an atrial septal defect which closed spontaneously and there was a mildly impaired diastolic function of her left ventricle. There was a very severe developmental delay. There is still no head control and there is no speech and language development. However, she is able to communicate somewhat by iPad. She suffered from recurrent respiratory tract infections with several hospitalizations for pneumonia. She also had recurrent urinary tract infections and a thickened bladder wall. She had wide fluctuations in temperature, with cold and blue extremities followed by warmth of the opposite extremity. There was strabismus, hyperopia, there were delayed visual responses on VER and bilateral optic nerve pallor. However, there is good tracking and visual function and a color preference. She had a congenital moderate to severe sensorineural hearing loss, right more than left. At 3 years of age, she developed generalized tonic-clonic seizures, which are now in good control on Keppra, except during high fevers. She had a scoliosis requiring surgery at 7 years of age. Teeth alignment is normal. Muscle ultrasound was normal. Muscle biopsy showed that type I fibers were smaller, though not more numerous, which was suggestive of congenital fiber type disproportion. MRI showed prominent ventricles and sulci, cerebellar volume loss, and an abnormal globus pallidus signal, more on the right than on the left.

Unclassified phenotype

Individual 3; p.Asn531Ser – heterozygous *de novo* c.1592A>G – Rouen, France

Individual p.Asn531Ser, a male fetus, is the first child of healthy, non-consanguineous parents. Family history was unremarkable. The second child of parents, born a year later, was healthy. During pregnancy, growth parameters were normal. Fetal movements were normal. However, on intrauterine imaging frontonasal dysplasia, a cleft lip and corpus callosum agenesis was seen. At 30 weeks of gestational age the pregnancy was terminated and the fetus died. Postmortem a severe median cleft lip and palate and a bifid nose without any fusion of the nasal buds was seen. Also hypertelorism, a widow peak, thymus hyperplasia and hypotrophic genitalia were noted. There was no evidence for hypotonia in utero, there were no contractures. No muscle biopsy was performed.

Figure S1. Pictures of Individuals showing profound infantile hypotonia

*Moderate phenotype: Individual 11; p.Tyr1109His – heterozygous *de novo* c.3325T>C – Naples, Italy*

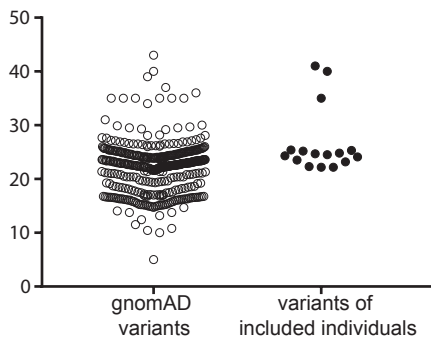


Severe phenotype: Individual 2; p.Ile457Thr – heterozygous de novo c.1370T>C – Utrecht, the Netherlands



4

Figure S2. CADD scores of variants observed in gnomAD and CADD scores of variants included in this study

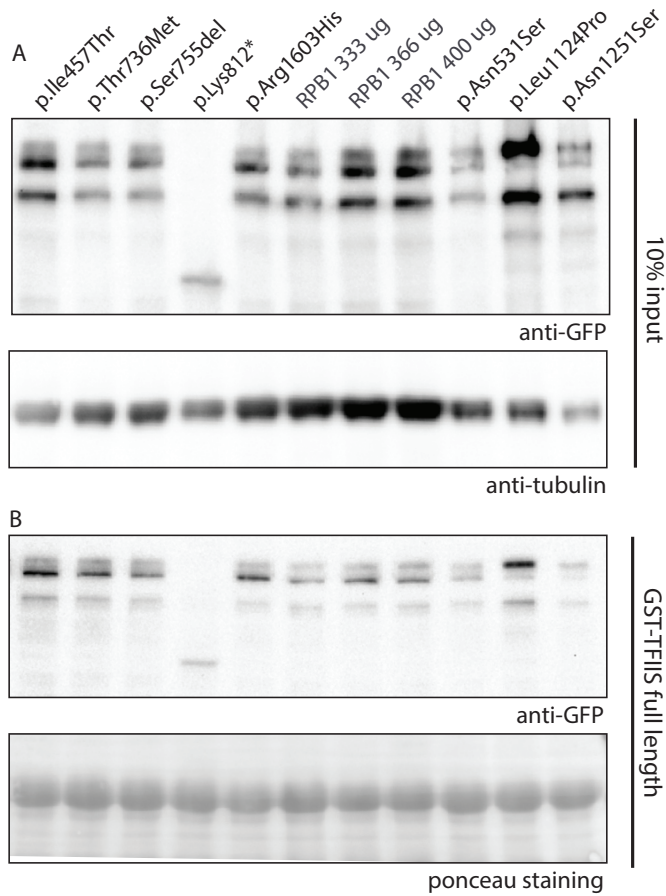


The y-axis depicts the height of the CADD scores of the *POLR2A* variants observed in the cohort from gnomAD and of the variants observed in the sixteen individuals included in this study, both depicted on the x-axis.

Figure S3. Characterization of the included *POLR2A* variants in *S. cerevisiae*

As in Figure 3A, functional evaluation of six *rbp1* mutants in *S. cerevisiae*: p.Leu443Thr (p.Ile457Thr), p.Asn517Ser (p.Asn531Ser), p.Ser713Met (p.Thr736Met), p.Leu732del (p.Ser755del), p.Leu1101Pro (p.Leu1124Pro) and p.Asn1232Ser (p.Asn1251Ser) are compared to wild type (WT). p.Ala301Asp demonstrates a positive control for reduced transcriptional activity and p.Glu1230Lys demonstrates a positive control for reduced genetic interaction with TFIIIS. YPD 30°C depicts growth under normal circumstances, YPD 37°C depicts growth under stress induced by increased temperature. YPRaf/Gal day 4 and day 6 depict growth under stress induced by increased inappropriate GAL 3' termination, on day 4 and day 6 of culture, respectively. SC-LEU + MPA day 4 and day 6 depict growth under stress induced by lack of leucine and addition of mycophenolic acid (MPA), on day 4 and day 6 of culture, respectively.

Figure S4. Interaction efficiency of RPB1 variants with TFIIIS as tested by GST pull-down



A) demonstrates whole cell lysates (10% input) and in B) demonstrates the interaction of GFP-tagged RPB1 mutants with GST-TFIIIS measured by a GST pull-down assay. In the anti-GFP blot, the bands represent both unphosphorylated and phosphorylated (at one, two or more positions) forms of RPB1 (~220 kD). Bands in the anti-tubulin plot represent loading controls.

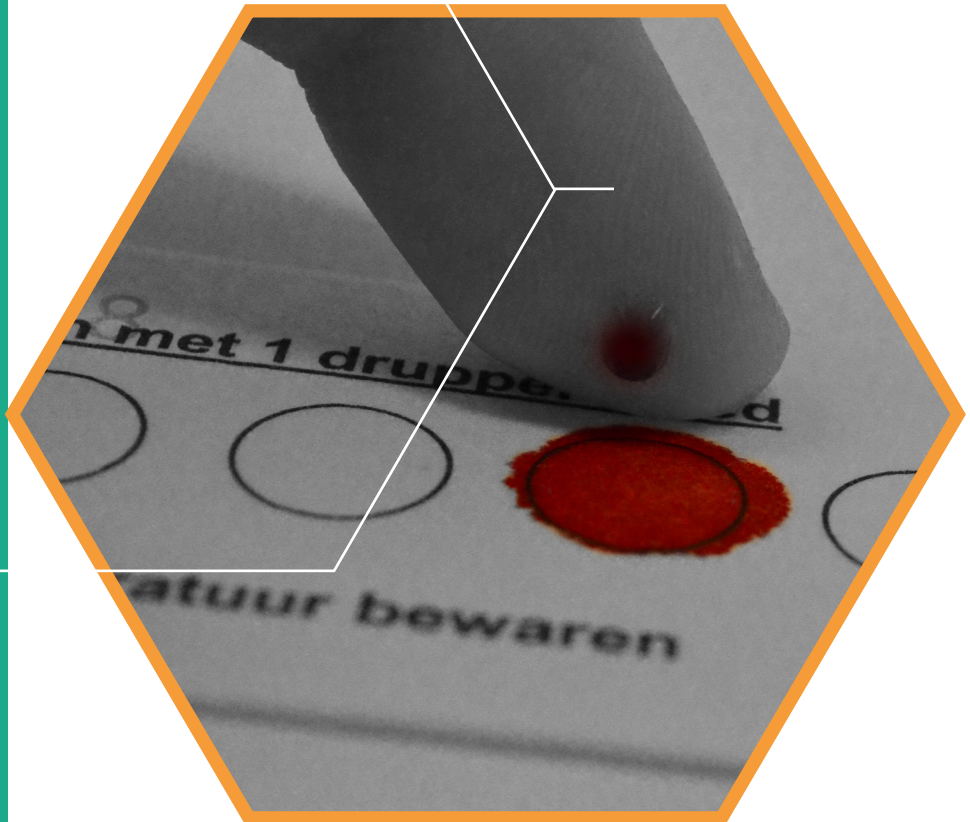
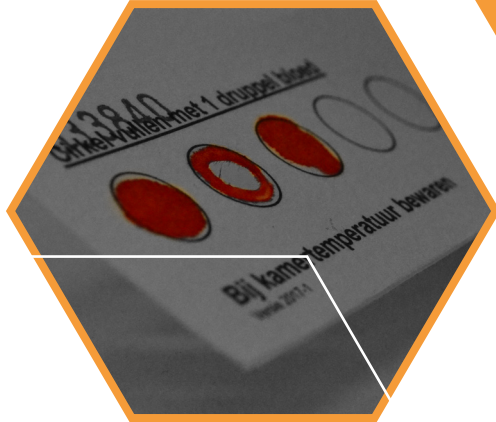
Table S1. List of *S. cerevisiae* strains used in this study

Name	Genotype	Source
CKY283	MA7a ura3-52 his3Δ200 leu2Δ1 or Δ0 trp1Δ63 met15A0 lys2-1280 gal10A56 rpb1A::CLONATMX RPB3::TAP::KlactRP1 [pRP112 RPB1 CEN URA3]	C. Kaplan
CKY718	MA7a ura3-52 his3Δ200 leu2Δ1 or Δ0 trp1Δ63 met15A0 lys2-1280 gal10A56 rpb1A::CLONATMX RPB3::TAP::KlactRP1 dst1A::KANMX [pRP112 RPB1 CEN URA3]	C. Kaplan
CKY721	MA7a ura3-52 his3Δ200 leu2Δ1 or Δ0 trp1Δ63 met15A0 lys2-1280 gal10A56 rpb1A::CLONATMX RPB3::TAP::KlactRP1 sub1A::KANMX [pRP112 RPB1 CEN URA3]	C. Kaplan
YMK73	MA7a ura3-52 his3Δ200 leu2Δ1 or Δ0 trp1Δ63 met15A0 lys2-1280 gal10A56 rp1A::CLONATMX RPB3::TAP::KlactRP1 [pCDNA5 N-GFP hRPB1 amar]	This study
YMK74	MA7a ura3-52 his3Δ200 leu2Δ1 or Δ0 trp1Δ63 met15A0 lys2-1280 gal10A56 rp1A::CLONATMX RPB3::TAP::KlactRP1 [pCDNA5 N-GFP hRPB1 amar A301D]	This study
YMK75	MA7a ura3-52 his3Δ200 leu2Δ1 or Δ0 trp1Δ63 met15A0 lys2-1280 gal10A56 rp1A::CLONATMX RPB3::TAP::KlactRP1 [pCDNA5 N-GFP hRPB1 amar L443T]	This study
YMK76	MA7a ura3-52 his3Δ200 leu2Δ1 or Δ0 trp1Δ63 met15A0 lys2-1280 gal10A56 rp1A::CLONATMX RPB3::TAP::KlactRP1 [pCDNA5 N-GFP hRPB1 amar N517S]	This study
YMK77	MA7a ura3-52 his3Δ200 leu2Δ1 or Δ0 trp1Δ63 met15A0 lys2-1280 gal10A56 rp1A::CLONATMX RPB3::TAP::KlactRP1 [pCDNA5 N-GFP hRPB1 amar S713M]	This study
YMK78	MA7a ura3-52 his3Δ200 leu2Δ1 or Δ0 trp1Δ63 met15A0 lys2-1280 gal10A56 rp1A::CLONATMX RPB3::TAP::KlactRP1 [pCDNA5 N-GFP hRPB1 amar L732del]	This study
YMK79	MA7a ura3-52 his3Δ200 leu2Δ1 or Δ0 trp1Δ63 met15A0 lys2-1280 gal10A56 rp1A::CLONATMX RPB3::TAP::KlactRP1 [pCDNA5 N-GFP hRPB1 amar L1101P]	This study
YMK80	MA7a ura3-52 his3Δ200 leu2Δ1 or Δ0 trp1Δ63 met15A0 lys2-1280 gal10A56 rp1A::CLONATMX RPB3::TAP::KlactRP1 [pCDNA5 N-GFP hRPB1 amar E1230K]	This study
YMK81	MA7a ura3-52 his3Δ200 leu2Δ1 or Δ0 trp1Δ63 met15A0 lys2-1280 gal10A56 rp1A::CLONATMX RPB3::TAP::KlactRP1 [pCDNA5 N-GFP hRPB1 amar N1232S]	This study
YMK82	MA7a ura3-52 his3Δ200 leu2Δ1 or Δ0 trp1Δ63 met15A0 lys2-1280 gal10A56 rp1A::CLONATMX RPB3::TAP::KlactRP1 dst1A::KANMX [pCDNA5 N-GFP hRPB1 amar]	This study
YMK83	MA7a ura3-52 his3Δ200 leu2Δ1 or Δ0 trp1Δ63 met15A0 lys2-1280 gal10A56 rp1A::CLONATMX RPB3::TAP::KlactRP1 dst1A::KANMX [pCDNA5 N-GFP hRPB1 amar L443T]	This study
YMK84	MA7a ura3-52 his3Δ200 leu2Δ1 or Δ0 trp1Δ63 met15A0 lys2-1280 gal10A56 rp1A::CLONATMX RPB3::TAP::KlactRP1 dst1A::KANMX [pCDNA5 N-GFP hRPB1 amar L443T]	This study
YMK85	MA7a ura3-52 his3Δ200 leu2Δ1 or Δ0 trp1Δ63 met15A0 lys2-1280 gal10A56 rp1A::CLONATMX RPB3::TAP::KlactRP1 dst1A::KANMX [pCDNA5 N-GFP hRPB1 amar N517S]	This study
YMK86	MA7a ura3-52 his3Δ200 leu2Δ1 or Δ0 trp1Δ63 met15A0 lys2-1280 gal10A56 rp1A::CLONATMX RPB3::TAP::KlactRP1 dst1A::KANMX [pCDNA5 N-GFP hRPB1 amar S713M]	This study
YMK87	MA7a ura3-52 his3Δ200 leu2Δ1 or Δ0 trp1Δ63 met15A0 lys2-1280 gal10A56 rp1A::CLONATMX RPB3::TAP::KlactRP1 dst1A::KANMX [pCDNA5 N-GFP hRPB1 amar L732del]	This study
YMK88	MA7a ura3-52 his3Δ200 leu2Δ1 or Δ0 trp1Δ63 met15A0 lys2-1280 gal10A56 rp1A::CLONATMX RPB3::TAP::KlactRP1 dst1A::KANMX [pCDNA5 N-GFP hRPB1 amar L1101P]	This study
YMK89	MA7a ura3-52 his3Δ200 leu2Δ1 or Δ0 trp1Δ63 met15A0 lys2-1280 gal10A56 rp1A::CLONATMX RPB3::TAP::KlactRP1 dst1A::KANMX [pCDNA5 N-GFP hRPB1 amar E1230K]	This study
YMK90	MA7a ura3-52 his3Δ200 leu2Δ1 or Δ0 trp1Δ63 met15A0 lys2-1280 gal10A56 rp1A::CLONATMX RPB3::TAP::KlactRP1 dst1A::KANMX [pCDNA5 N-GFP hRPB1 amar N1232S]	This study
YMK91	MA7a ura3-52 his3Δ200 leu2Δ1 or Δ0 trp1Δ63 met15A0 lys2-1280 gal10A56 rp1A::CLONATMX RPB3::TAP::KlactRP1 sub1A::KANMX [pCDNA5 N-GFP hRPB1 amar]	This study
YMK92	MA7a ura3-52 his3Δ200 leu2Δ1 or Δ0 trp1Δ63 met15A0 lys2-1280 gal10A56 rp1A::CLONATMX RPB3::TAP::KlactRP1 sub1A::KANMX [pCDNA5 N-GFP hRPB1 amar A301D]	This study
YMK93	MA7a ura3-52 his3Δ200 leu2Δ1 or Δ0 trp1Δ63 met15A0 lys2-1280 gal10A56 rp1A::CLONATMX RPB3::TAP::KlactRP1 sub1A::KANMX [pCDNA5 N-GFP hRPB1 amar L443T]	This study
YMK94	MA7a ura3-52 his3Δ200 leu2Δ1 or Δ0 trp1Δ63 met15A0 lys2-1280 gal10A56 rp1A::CLONATMX RPB3::TAP::KlactRP1 sub1A::KANMX [pCDNA5 N-GFP hRPB1 amar N517S]	This study
YMK95	MA7a ura3-52 his3Δ200 leu2Δ1 or Δ0 trp1Δ63 met15A0 lys2-1280 gal10A56 rp1A::CLONATMX RPB3::TAP::KlactRP1 sub1A::KANMX [pCDNA5 N-GFP hRPB1 amar S713M]	This study
YMK96	MA7a ura3-52 his3Δ200 leu2Δ1 or Δ0 trp1Δ63 met15A0 lys2-1280 gal10A56 rp1A::CLONATMX RPB3::TAP::KlactRP1 sub1A::KANMX [pCDNA5 N-GFP hRPB1 amar L732del]	This study
YMK97	MA7a ura3-52 his3Δ200 leu2Δ1 or Δ0 trp1Δ63 met15A0 lys2-1280 gal10A56 rp1A::CLONATMX RPB3::TAP::KlactRP1 sub1A::KANMX [pCDNA5 N-GFP hRPB1 amar L1101P]	This study
YMK98	MA7a ura3-52 his3Δ200 leu2Δ1 or Δ0 trp1Δ63 met15A0 lys2-1280 gal10A56 rp1A::CLONATMX RPB3::TAP::KlactRP1 sub1A::KANMX [pCDNA5 N-GFP hRPB1 amar E1230K]	This study
YMK99	MA7a ura3-52 his3Δ200 leu2Δ1 or Δ0 trp1Δ63 met15A0 lys2-1280 gal10A56 rp1A::CLONATMX RPB3::TAP::KlactRP1 sub1A::KANMX [pCDNA5 N-GFP hRPB1 amar N1232S]	This study

Table S2. Tolerance to variability of the human *POLR2x* genes according to gnomAD

	SYNONYMOUS			MISSENSE			LOSS OF FUNCTION					
	Expected	Observed	Z-score	Ratio o/e	Expected	Observed	Z-score	Ratio o/e	Expected	Observed	pLI score	Ratio o/e
<i>POLR2A</i>	483.4	625	-5.06	1.29	1210	512	7.13	0.42	82.8	7	1.00	0.08
<i>POLR2B</i>	212.6	194	1.01	0.91	660.7	182	6.62	0.28	63.5	14	0.52	0.22
<i>POLR2C</i>	66.8	55	1.14	0.82	164.3	97	1.86	0.59	19.4	8	0.00	0.41
<i>POLR2D</i>	25.8	23	0.43	0.89	78.4	39	1.58	0.50	7.0	2	0.21	0.29
<i>POLR2E</i>	57.7	80	-2.31	1.39	140.8	129	0.35	0.92	13.9	13	0.00	0.94
<i>POLR2F</i>	33.4	30	0.46	0.90	83.8	61	0.89	0.73	12.0	5	0.01	0.42
<i>POLR2G</i>	35.8	36	-0.02	1.00	99.6	41	2.09	0.41	11.9	10	0.00	0.84
<i>POLR2H</i>	32.6	32	0.08	0.98	84.6	44	1.57	0.52	7.7	1	0.65	0.13
<i>POLR2I</i>	31.6	32	-0.06	1.01	82.1	44	1.49	0.54	8.9	2	0.36	0.23
<i>POLR2J</i>	25.7	35	-1.44	1.36	61.8	33	1.30	0.53	6.6	4	0.01	0.60
<i>POLR2K</i>	9.2	10	-0.21	1.09	31.4	22	0.60	0.70	3.5	4	0.00	1.13
<i>POLR2L</i>	17.6	30	-2.33	1.71	40.5	39	0.08	0.96	2.2	4	0.00	1.79

Tolerance to variability of the human *POLR2x* genes, retrieved from gnomAD (version 2.1.1). Abbreviations: e: expected; o: observed.



Direct-infusion based metabolomics identifies

metabolic disease in patients' dried blood spots and plasma

Metabolites 2019, 9(1)
DOI: 10.3390/metabo9010012

Hanneke A. Haijes*, Marcel Willemsen, Maria van der Ham,
Johan Gerrits, Mia L. Pras-Raves, Hubertus C.M.T. Prinsen,
Peter M. van Hasselt, Monique G.M. de Sain-van der Velden,
Nanda M. Verhoeven-Duif†, Judith J.M. Jans†,*

† These authors contributed equally to this article

* Corresponding authors

ABSTRACT

In metabolic diagnostics, there is an emerging need for a comprehensive test to acquire a complete view of metabolite status. Here, we describe a non-quantitative direct-infusion high-resolution mass spectrometry (DI-HRMS) based metabolomics method and evaluate the method for both dried blood spots (DBS) and plasma. 110 DBS of 42 patients harboring 23 different inborn errors of metabolism (IEM) and 86 plasma samples of 38 patients harboring 21 different IEM were analyzed using DI-HRMS. A peak calling pipeline developed in R programming language provided Z-scores for ~1,875 mass peaks corresponding to ~3,835 metabolite annotations (including isomers) per sample. Based on metabolite Z-scores, patients were assigned a “most probable diagnosis” by an investigator blinded for the known diagnoses of the patients. Based on DBS sample analysis, 37/42 of the patients, corresponding to 22/23 IEM, could be correctly assigned a “most probable diagnosis”. Plasma sample analysis, resulted in a correct “most probable diagnosis” in 32/38 of the patients, corresponding to 19/21 IEM. The added clinical value of the method was illustrated by a case wherein DI-HRMS metabolomics aided interpretation of a variant of unknown significance identified by whole-exome sequencing. In summary, non-quantitative DI-HRMS metabolomics in DBS and plasma is a very consistent, high-throughput and nonselective method for investigating the metabolome in genetic disease.

KEY MESSAGE

Non-quantitative DI-HRMS metabolomics in DBS and plasma is a very consistent, high-throughput and nonselective method for investigating the metabolome in genetic disease.

INTRODUCTION

With unprecedented pace, the number of known inborn errors of metabolism (IEM) is expanding. It is a challenge to diagnose this diverse spectrum of diseases in a timely manner. Thus, there is an emerging need for a comprehensive test to acquire a complete view of metabolite status.¹ To meet this need, metabolomics – the parallel determination of thousands of small-molecule metabolites – is regarded as the way forward. Using metabolomics, all intermediates and final products of metabolic pathways in the body can potentially be measured. Metabolomics with exact quantification of a subset of predefined metabolites has been used for small-scale diagnostic screening²⁻⁴ and for biomarker identification in predefined patient groups.⁵ While broad quantitative metabolomics assays are already a big step forward compared to the focused targeted assays currently used in metabolic diagnostics, semi- and non-quantitative metabolomics can potentially detect an even larger range of metabolites. Non-quantitative metabolomics has mainly been performed in toxicology, neurology, cardiovascular, and cancer research. However, also in the IEM field, both combined approaches of quantitative and non-quantitative metabolomics⁶⁻¹⁰ as well as exclusively non-quantitative metabolomics have been used to study predefined patient groups.¹¹⁻²⁰

Recently, two studies reported a metabolomics approach for metabolic diagnostics in individual patients and argued their potential applicability in clinical diagnostics of IEM.^{1,21} The workflow presented by Miller et al. is semi-quantitative and involves three separate mass spectrometry (MS) platforms run in parallel.²¹ The workflow of Coene et al. is non-quantitative and involves a single-platform MS analysis.¹ Both workflows make use of chromatographic separation as they are based on either (high-resolution) gas chromatography MS (GC-MS) or (high-resolution) liquid chromatography MS (LC-MS).^{1,21}

The optimal configuration for semi- and non-quantitative metabolomics in diagnostic applications is not known yet. In direct-infusion high-resolution MS (DI-HRMS), no chromatographic separation is performed, circumventing the need to create an experimental library containing metabolite masses and retention times and avoiding the problem of chromatographic alignment. For DI-HRMS, sample preparation is technically uncomplicated and only a very small amount of sample is needed (3 mm dried blood spot (DBS) or 20 μ L plasma).²² Thus, DI-HRMS is in potential a powerful technique for the development of a high-throughput²³⁻²⁴ broad test requiring limited patient material. DI-HRMS has been used in a quantitative and non-quantitative fashion for biomarker identification.²⁵⁻³⁰ Moreover, Denes et al. started to explore its use for metabolic diagnostics by studying phenylketonuria, medium-chain acyl-coenzyme A dehydrogenase deficiency and homocystinuria.¹² However, in contrast to GC-MS and LC-MS approaches,^{1,21} the use of non-quantitative DI-HRMS has not been explored for a broad range of IEM.

In most metabolomics studies, the main focus is on plasma. However, DBS have the advantage of being easy to obtain (even at home), easy to store and easy to send and share. DBS have been used in some quantitative and non-quantitative chromatography based metabolomics approaches focusing on IEM.^{4,8,12,23} Here, we describe a non-quantitative DI-HRMS metabolomics method for metabolic diagnostics. For the first time, we evaluate the use of a non-quantitative metabolomics method for both DBS and plasma by analyzing samples of patients with a broad range of IEM. As an example of the added clinical value, we present a case wherein DI-HRMS metabolomics aided interpretation of a variant of uncertain significance (VUS) identified by whole-exome sequencing (WES).

METHODS

Sample collection

Blood samples were initially drawn for routine metabolic diagnostics or follow-up. Blood samples were collected by venous puncture in heparin-containing tubes. For DBS, aliquots of the blood sample were aspirated or a blood sample was collected by a finger prick. Blood samples were spotted onto Guthrie card filter paper (Whatman no. 903 Protein saver TM cards). The papers were left to dry for at least four hours at room temperature. DBS were stored at -80°C in a foil bag with desiccant package pending further analysis. For plasma, blood samples were centrifuged at room temperature. The plasma was collected and stored at -80°C pending further analysis.

Patient inclusion and sample selection

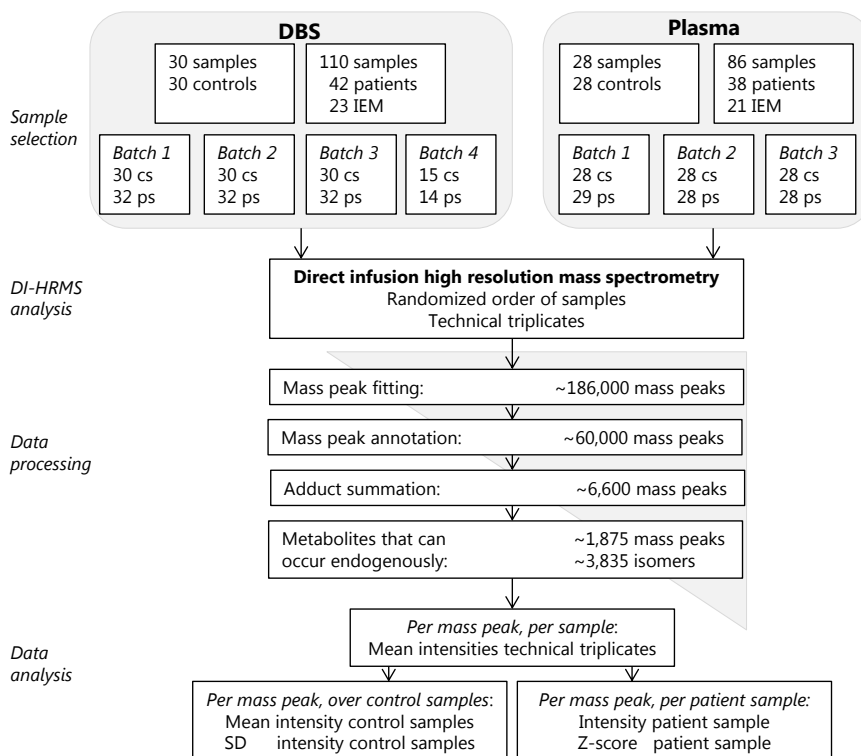
IEM of interest for this study were IEM with one or more known small-molecule biomarkers in blood, such as urea cycle disorders, organic acidurias, amino acid metabolism disorders, amino acid transport disorders, fatty acid oxidation disorders and disorders of creatine biosynthesis. Patients harboring such IEM were included when one or more residual DBS or plasma samples were available in the metabolic diagnostics laboratory of the University Medical Centre Utrecht, with a maximum of two patients per IEM. All patients or their legal guardians approved the possible use of their remnant samples for method development and validation, in agreement with institutional and national legislation. All procedures followed were in accordance with the ethical standards of the University Medical Centre Utrecht and with the Helsinki Declaration of 1975, as revised in 2000.

Patient samples were included based on availability, and noteworthy, they were specifically neither selected based on whether a patient was under clinical management at time of sampling or not, nor based on presence of abnormal biochemical findings. 110 DBS from 42 patients with 23 different IEM and 86 plasma samples from 38 patients with 21 different IEM could be included (Figure 1). To serve as control samples, samples of individuals in whom an IEM was excluded after a thorough routine diagnostic work-up, were selected out of banked DBS and plasma samples. For DBS, 30 samples of 30 control individuals could be included. For plasma, 28 samples of 28 control individuals could be included (Figure 1). Control samples varied in age (including both neonates and elderly), sex, time of day at sampling, diets, supplements, drugs, storage time, and for control plasma samples degree of hemolysis, in order to take into account considerable variation in factors that might influence an individual's metabolome. Patient DBS samples were analyzed in four different batches, with each batch including all control DBS samples. Patient plasma samples were analyzed in three different batches, with each batch including all control plasma samples (Figure 1). In each batch, the samples were analyzed in randomized order.

Sample preparation

In order to be able to assess within batch variation, a working solution containing stable isotope-labeled compounds (sILC) was prepared in methanol achieving concentrations of $^{15}\text{N};2\text{-}^{13}\text{C}$ -glycine, $20.0\ \mu\text{M}$ $^2\text{H}_4$ -alanine, $^2\text{H}_3$ -leucine, $^2\text{H}_3$ -methionine, $^{13}\text{C}_6$ -phenylalanine, $^{13}\text{C}_6$ -tyrosine, $^2\text{H}_3$ -aspartate, $^2\text{H}_3$ -glutamate, $^2\text{H}_2$ -ornithine, $^2\text{H}_2$ -citrulline and $^2\text{H}_4,^{13}\text{C}$ -arginine, $6.08\ \mu\text{M}$ $^2\text{H}_9$ -carnitine, $1.52\ \mu\text{M}$ $^2\text{H}_3$ -acetylcarnitine, $0.304\ \mu\text{M}$ $^2\text{H}_3$ -propionylcarnitine, $^2\text{H}_3$ -butyrylcarnitine, $^2\text{H}_9$ -isovalerylcarnitine, $^2\text{H}_3$ -octanoylcarnitine, $^2\text{H}_9$ -myristoylcarnitine and $0.608\ \mu\text{M}$ $^2\text{H}_3$ -palmitoylcarnitine (Cambridge Isotope Laboratories, Buchem b.v., Apeldoorn, The Netherlands).

Figure 1. Flowchart of the non-quantitative direct-infusion high-resolution MS (DI-HRMS) method



Abbreviations: cs: control samples; DBS: dried blood spots; DI-HRMS: direct infusion high resolution mass spectrometry; IEM: inborn error of metabolism; ps: patient samples; SD: standard deviation.

For DBS, this working solution was diluted 1:4. For plasma, sILC working solution was used undiluted. DBS sample extraction (3 mm, ~3.1 μ L whole blood) was performed by addition of 140 μ L sILC working solution, followed by a twenty minute ultra-sonication step. DBS samples were diluted with 60 μ L 0.3% formic acid (Emsure, Darmstadt, Germany). Plasma samples were thawed to room temperature. Twenty μ L of the plasma sample was added to 140 μ L sILC working solution. This solution was centrifuged for five minutes at 17,000 g. One hundred and five microliters of supernatant was diluted with 45 μ L 0.3% formic acid. Both DBS and plasma solutions were filtered using a methanol preconditioned 96 well filter plate (Acro prep, 0.2 μ m GHP, NTRL, 1 mL well; Pall Corporation, Ann Arbor, MI, USA) and a vacuum manifold. The sample filtrate was collected in a 96 well plate (Advion, Ithaca, NY, USA).

DI-HRMS analysis

A TriVersa NanoMate system (Advion, Ithaca, NY, USA) controlled by Chipsoft software (version 8.3.3, Advion) was mounted onto the interface of a Q-Exactive high-resolution mass spectrometer (Thermo Scientific™, Bremen, Germany). This system is a combined automatic sampler and nano-electrospray ionization (ESI) source. It houses a rack of 384

disposable conductive pipette tips and a 96-well microtiter plate that holds the samples to be analyzed. The electrospray ionization chip contains four hundred nozzles with nominal internal diameter of 5 μm . Samples (13 μL) were automatically aspirated sequentially into a pipette tip followed by an air gap (2 μL). For each sample, technical triplicates were analyzed, infusing each sample three times into the mass spectrometer (Figure 1). Pipette tips were engaged with the electrospray ionization chip to deliver the sample using nitrogen gas pressure at 0.5 psi and a spray voltage of 1.6 kV. For each sample new pipette tips and nozzles were used to prevent any cross-contamination or carryover. The Q-Exactive high-resolution mass spectrometer was operated in positive and negative ion mode in a single run, with automatic polarity switching. There were two time segments of 1.5 min with a total run time of 3.0 min. Scan range was 70 to 600 mass to charge ratio (m/z), resolution was 140,000 at $m/z = 200$ for optimal separation of m/z , automatic gain control target value was $3e6$, maximum injection time was 200 ms, capillary temperature was 275°C , the sample tray was kept at 18°C and for the S-lens RF level factor 70 was used. In the positive segment, the sodium adduct of $^{13}\text{C}_6$ -Phenylalanine (m/z 194.0833) was used as a lock mass and in the negative segment $^2\text{H}_9$ -myristoylcarnitine (m/z 381.36733) was used as lock mass.

Data processing

Data acquisition was performed using Xcalibur software (version 3.0, Thermo Scientific™, Waltham, MA, USA). Using MSConvert15 (ProteoWizard Software Foundation, Palo Alto, CA, USA), raw data files containing scanning time, m/z and peak intensity were converted to mzXML format in Profile mode. A peak calling pipeline was developed in R programming language. Peak calling of raw mass spectrometry data resulted in $\sim 186,000$ mass peaks per batch (Figure 1), with for each mass peak the mean intensity of the technical triplicate (Figure 1), excluding miss infusions. Detected mass peaks were annotated by matching the m/z of the mass peak with a range of two parts per million to metabolite masses present in the Human Metabolome Database (HMDB), version 3.6.³⁴ Taking into account isomers and adduct ions, $\sim 60,000$ mass peaks could be annotated with one or more possible identifications (Figure 1).

Since during electrospray ionization adduct ions are formed, each of the $\sim 60,000$ annotated mass peaks may account for a metabolite without adduct ion, or with one or more adduct ions. This means that one metabolite can be detected with different adduct ions, thus different mass peaks. To facilitate interpretation, metabolite annotations without adduct ions in negative or positive mode ($[\text{M}-\text{H}]^-$, $[\text{M}+\text{H}]^+$), or with the single adduct ions $[\text{M}+\text{Na}]^+$, $[\text{M}+\text{K}]^+$ and $[\text{M}+\text{Cl}]^-$ were selected. For each sample, the intensities of these five mass peaks were summed, resulting in one (summed) mass peak intensity per metabolite annotation: $\sim 6,600$ summed mass peaks in total. Next, exogenous and drug metabolite annotations were excluded by manual curation of the database by four trained clinical laboratory geneticists. Metabolites that can occur endogenously and metabolites with still unknown function were included, resulting in $\sim 1,875$ summed mass peaks in total, corresponding to $\sim 3,835$ metabolite annotations (Figure 1), since mass peaks can account for several isomers. Data and R code can be supplied upon request.

Data analysis

Data processing provided the mean intensity of the technical triplicate per mass peak, per sample (Figure 1). Since non-quantitative metabolomics provides relative comparisons between samples, interpretation of the mass peak intensities was enabled by calculating

the mean intensity and the standard deviation of the intensities of the control samples in the same batch for each mass peak (Figure 1). For each mass peak per patient sample, the deviation from the intensities in control samples was indicated by a Z-score, calculated by: $Z\text{-score} = (\text{intensity patient sample} - \text{mean intensity control samples}) / \text{standard deviation intensity control samples}$ (Figure 1). For each sample, metabolite annotations were ranked on Z-score: positive Z-scores were ranked from rank 1 onwards from the highest Z-scores to a Z-score of 0.0, and negative Z-scores were ranked from rank (-)1 onwards from the lowest Z-scores to a Z-score of 0.0.

Evaluation of the clinical value of the method

For each patient, mean intensity and mean Z-score were calculated over the included patient samples. Each patient was assigned a "most probable diagnosis" based on metabolite Z-score and rank per patient sample and mean metabolite Z-score and rank. The investigator assigning these diagnoses was blinded for the patient's true diagnosis, and for the list of 23 included IEM. Furthermore, neither information regarding patient characteristics (sex, age), nor clinical information was provided to the researcher.

Reproducibility assessment

To monitor variability within each batch, twenty sILC were added to each sample. For each sILC, the relative standard deviation (RSD) was calculated over all samples in a batch, calculated by: $\text{standard deviation intensity} / \text{mean intensity}$. A median RSD below 0.25 was considered satisfactory. To monitor variability between batches and to assess the variability in Z-scores, three DBS samples of three patients, one with PA, one with LPI and one with PKU were analyzed in seven batches. For PA, metabolites of interest were propionylcarnitine, glycine, and propionylglycine. For LPI, metabolites of interest were citrulline, glutamine, and lysine and for PKU the metabolite of interest was phenylalanine. For each of these seven metabolites, the RSD was calculated over all seven samples measurements, calculated by: $\text{standard deviation Z-score} / \text{mean Z-score}$. A median RSD below 0.25 was considered satisfactory.

RESULTS

Reproducibility assessment

The variability within and between batches was analyzed to assess reproducibility of the acquired data. The samples of patients and controls were analyzed in seven batches by DI-HRMS (Figure 1). Between these batches there was limited variation in the number of mass peaks and metabolite annotations in the successive steps of data processing (Table 1). To monitor variability within each batch, a solution containing twenty sILC was added to each sample. Variability within each batch was satisfactory, with median RSDs of 0.20, 0.16, 0.16, 0.20, 0.21, 0.21, and 0.20, respectively (Table 2). To monitor variability between batches and to assess the variability in Z-scores, three DBS samples of three patients with IEM were analyzed in seven independent batches. Variability between batches was also satisfactory, with a median RSD of 0.24 for the seven compounds assessed. RSDs of the individual compounds were 0.19, 0.30, and 0.24 for propionylcarnitine, glycine and propionylglycine in the sample of the patient with propionic aciduria (PA), 0.15, 0.26 and 0.09 for citrulline, glutamine and lysine in the sample of the patient with lysinuric protein intolerance (LPI) and 0.33 for phenylalanine in the sample of the patient with phenylketonuria (PKU) (Table 3). Many other compounds annotated in these three patients, representing major chemical

classes of metabolites such as acylcarnitines, amino acids, and organic acids, were found to have satisfactory RSDs (all data is available on request). Altogether, the reproducibility of the results pointed out by the limited variability within a batch and between different batches, indicates that all the components of the non-quantitative DI-HRMS metabolomics method, including resolution and sensitivity of the system, are stable over time.

Table 1. Variation in number of mass peaks and metabolite annotations in data processing steps

	DBS				PLASMA		
	Batch 1	Batch 2	Batch 3	Batch 4	Batch 1	Batch 2	Batch 3
Mass peak fitting	185,661	176,934	197,681	190,172	192,198	177,879	185,642
Mass peak annotation	59,543	56,250	63,360	60,979	62,503	58,212	60,450
Adduct summation	6,580	6,625	6,598	6,611			
Endogenous mass peaks*	1,874	1,885	1,874	1,875	1,875	1,867	1,868
Endogenous metabolite annotations*	3,822	3,863	3,826	3,839	3,832	3,847	3,817

* Mass peaks and annotations corresponding to metabolites that can occur endogenously. Abbreviations: DBS: dried blood spots.

Table 2. Within-batch variation: relative standard deviation of stable isotope-labeled compounds

	DBS				PLASMA		
	Batch 1	Batch 2	Batch 3	Batch 4	Batch 1	Batch 2	Batch 3
¹⁵ N, ²⁻¹³ C-glycine	0.23	0.16	0.18	0.24	0.22	0.21	0.79
² H ₄ -alanine	0.20	0.14	0.16	0.20	0.20	0.21	0.19
² H ₃ -leucine	0.18	0.14	0.15	0.18	0.60	0.55	0.50
² H ₃ -methionine	0.31	0.30	0.36	0.39	1.70	0.22	0.20
¹³ C ₆ -phenylalanine	0.19	0.16	0.14	0.18	0.21	0.20	0.19
¹³ C ₆ -tyrosine	0.19	0.17	0.16	0.20	0.22	0.21	0.18
² H ₃ -aspartate	0.24	0.22	0.22	0.25	0.23	0.24	0.26
² H ₃ -glutamate	0.17	0.15	0.14	0.18	0.20	0.21	0.15
² H ₃ -ornithine	0.21	0.19	0.17	0.21	0.14	0.17	0.12
² H ₃ -citrulline	0.16	0.16	0.14	0.18	0.18	0.19	0.14
² H ₄ , ¹³ C-arginine	0.21	0.17	0.16	0.20	0.17	0.18	0.16
² H ₆ -valine	0.18	0.14	0.15	0.18	0.20	0.19	0.18
² H ₉ -carnitine	0.27	0.21	0.22	0.30	0.22	0.24	0.21
² H ₃ -acetylcarnitine	0.89	0.21	0.82	0.92	0.46	0.46	0.74
² H ₃ -propionylcarnitine	0.21	0.16	0.16	0.20	0.19	0.20	0.20
² H ₃ -butyrylcarnitine	3.39	0.63	1.34	1.53	0.77	0.92	1.08
² H ₉ -isovalerylcarnitine	0.20	0.13	0.15	0.17	0.19	0.20	0.19
² H ₃ -octanoylcarnitine	0.18	0.12	0.14	0.17	0.16	0.21	0.20
² H ₉ -myristoylcarnitine	0.20	0.14	0.14	0.17	0.20	0.22	0.20
² H ₃ -palmitoylcarnitine	0.19	0.16	0.15	0.18	0.23	0.23	0.21
5th percentile	0.16	0.13	0.14	0.17	0.16	0.18	0.14
Median	0.20	0.16	0.16	0.20	0.21	0.21	0.20
95th percentile	2.96	0.30	0.79	0.89	0.76	0.55	0.79

Abbreviations: DBS: dried blood spots.

Evaluation of the clinical value of the method

For each patient sample, Z-scores were calculated for all mass peaks annotated with metabolites that can occur endogenously (~3,835) (Figure 1). Based on these Z-scores and their ranking, a “most probable diagnosis” was assigned to each patient (Table 4). The assigned diagnoses corresponded to the known diagnoses in 37/42 (88%) of patients based on DBS samples and in 32/38 (84%) of patients based on plasma samples. Figure 2 exemplifies Z-scores of biomarkers that had a very high Z-score and thus contributed to the “most probable diagnoses” (Figure 2).

Table 3. Between-batch variation: Z-scores and relative standard deviations of positive control samples

	Batch 1	Batch 2	Batch 3	Batch 4	Batch 5	Batch 6	Batch 7	RSD
<i>Propionic aciduria</i>								
Propionylcarnitine	40.23	66.57	47.17	70.07	61.18	52.29	52.66	0.19
Glycine	12.99	20.75	17.28	16.42	23.48	24.54	10.12	0.30
Propionylglycine	7.89	7.69	9.26	7.54	12.69	9.09	6.10	0.24
<i>Lysinuric protein int.</i>								
Citrulline	23.86	26.55	18.98	29.23	24.10	30.03	22.51	0.15
Glutamine	3.32	3.40	3.56	4.68	3.39	4.81	2.07	0.26
Lysine	-2.07	-2.13	-1.89	-2.07	-2.25	-1.97	-1.71	0.09
<i>Phenylketonuria</i>								
Phenylalanine	34.29	17.93	16.79	23.13	21.74	16.21	14.19	0.33

Abbreviations: RSD: relative standard deviation.

In the five patients in whom the assigned diagnosis was incorrect based on DBS samples, the biochemical profile had (almost) normalized due to treatment, as confirmed by routine targeted diagnostics in corresponding plasma samples of the patients. For example, a patient with 3-phosphoglycerate dehydrogenase deficiency presented with normalized serine due to serine supplementation (188, 234, and 83 $\mu\text{mol/mL}$, reference range 70–194 $\mu\text{mol/mL}$) and glycine (368, 213, and 161 $\mu\text{mol/mL}$, reference range 107–343 $\mu\text{mol/mL}$) in plasma. Serine Z-score in this patient's DBS was 0.8, glycine Z-score -0.1 (Table 4).

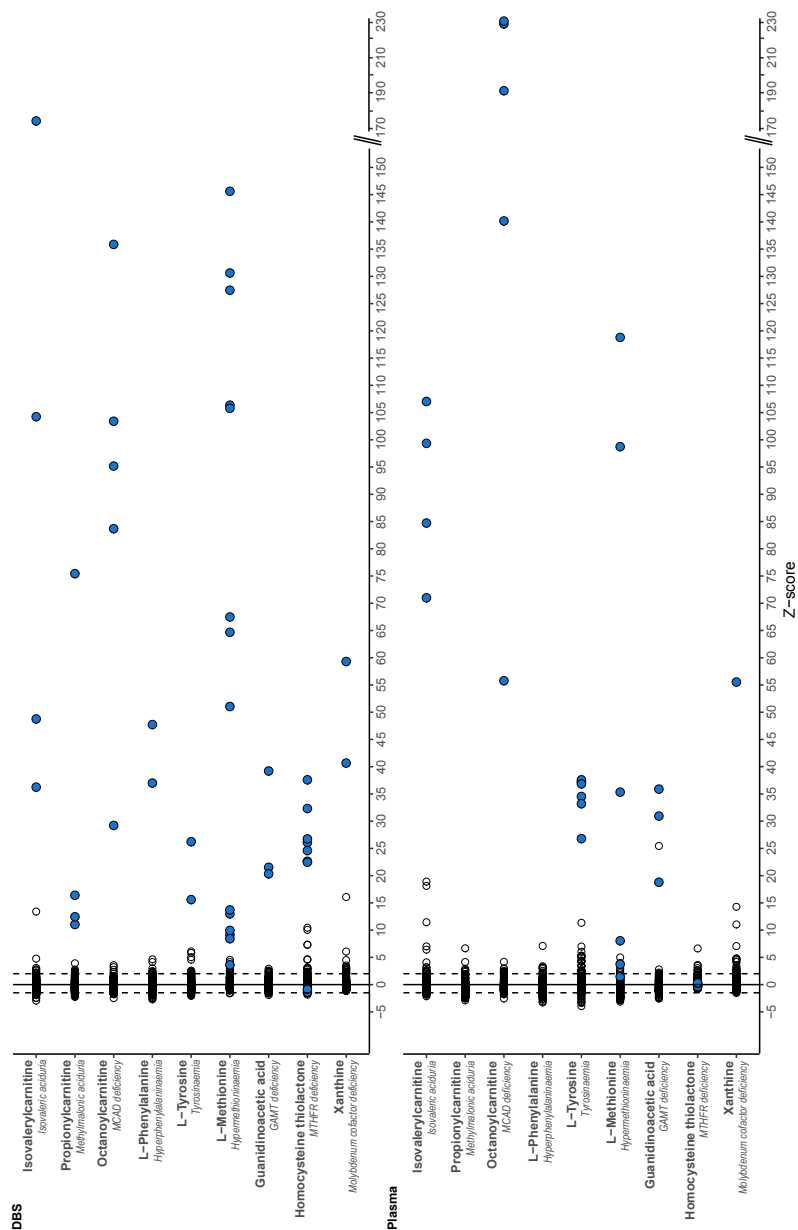
When not taking into account samples in which the biochemical profiles approximated the normal range due to treatment, the “most probable diagnoses” were correct in all patients. Moreover, for all but one of the 23 included IEM we demonstrated that the IEM is correctly diagnosable in DBS using DI-HRMS.

In six patients the assigned diagnosis was incorrect based on plasma samples. In one patient the diagnosis 3-methylcrotonylglycinuria was missed, due to normal values of methylcrotonylglycine and hydroxyisovalerylcarnitine. In two patients with methylenetetrahydrofolate reductase (MTHFR) deficiency the intensity of the biomarker homocysteine was normal, not reflecting the concentration measured using targeted diagnostics. In a patient with non-ketotic hyperglycinaemia the biochemical profile had (almost) normalized due to treatment and lastly, in two patients carnitine palmitoyltransferase (CPT) I deficiency was missed since plasma might be a less adequate matrix than DBS for diagnosing these patients.^{31,32}

Direct-Infusion based metabolomics in metabolic diagnostics

As an example of the added clinical value of direct-infusion based metabolomics in metabolic diagnostics, we present a case wherein DI-HRMS metabolomics aided interpretation of a VUS identified by WES. A 16-year-old patient was referred by his psychiatrist to the genetics department because of a combination of an autism spectrum disorder, therapy resistant psychoses, intellectual disability (IQ 62-77), and some mild facial dysmorphisms. Routine targeted metabolic diagnostics revealed a severely decreased plasma L-carnitine (1.5 $\mu\text{mol/L}$, reference range 21.6–57.4 $\mu\text{mol/L}$). WES revealed a missense variant in the gene *TMLHE*, located on the X-chromosome (c.230G > A, p.R77Q, a hemizygous VUS). *TMLHE* encodes trimethyllysine hydroxylase (TMLHE), an enzyme that converts trimethyllysine into 3-hydroxytrimethyllysine. Mutations in *TMLHE* cause susceptibility to X-linked autism, type 6 (MIM #300872). To support this possible diagnosis, we analyzed five DBS sampled at five different time points.

Figure 2. Representative examples of important biomarkers for the diagnosed IEM



For both dried blood spots and plasma three acylcarnitine biomarkers, three amino acids and three other metabolites are demonstrated as representative examples of compounds with high Z-scores that contributed to the assigned “most probable diagnosis”. Each dot represents a unique sample. Black open circles represent both control samples and samples of other IEM patients, blue filled circles represent patients with that specific IEM. Abbreviations: DBS: dried blood spots; GAMT: guanidinoacetate methyltransferase; MCAD: medium-chain acyl-CoA dehydrogenase; MTHFR: methylenetetrahydrofolate reductase.

Table 4. Assigned "most probable diagnoses" based on metabolite Z-scores in DBS and plasma.

Urea cycle	Patient diagnosis	Diagnostic metabolite*	DBS #1			DBS #2			PLASMA #1			PLASMA #2		
			Z-s.c.	Rank	Corr diag	Z-s.c.	Rank	Corr diag	Z-s.c.	Rank	Corr diag	Z-s.c.	Rank	Corr diag
Urea cycle	OTC def.	Orotic acid	5.7	1	Yes (n=2)	-0.5		No (n=3)	11.7	2	Yes (n=2)	2.3		Yes (n=1)
		Uridine	1.6			-0.5			7.1			39.2	6	
		5-Oxoproline	-0.7			0.2			0.4			9.0		
		Uracil	-0.8			-0.7			4.0			4.0		
		Orotidine	0.1			-0.5			-1.1			4.0		
		L-lysine	0.0			-0.2			0.3			3.3		
Branched amino acid metabolism	MSUD	Citrulline	-0.3			-1.8			-0.6			-2.8		
		Ketoleucine	23.3	2	Yes (n=4)	3.0	20	Yes (n=3)	65.0	7	Yes (n=4)	13.3	17	Yes (n=3)
		(Is)oleucine	12.4	6		0.4			37.4	10		24.7	7	
		2-OH-3-methylbutyric acid	9.4	8		-0.4			579.1	1		234.8	1	
		Alpha-ketoisovaleric acid	4.8			2.2			39.5	9		21.2	9	
		Isovalerylcarnitine	137.9	1	Yes (n=2)	42.5	2	Yes (n=2)	84.7	1	Yes (n=1)	92.5	1	Yes (n=3)
		3-Hydroxyisovaleric acid	0.0			-0.1			0.4			0.1		
		3-Hydroxyisovaleric acid	5.4	1	Yes (n=2)	33.2	1	Yes (n=2)	17.8	4	No (n=1)	825.8	1	Yes (n=2)
		3-Methylcrotonylglycine	0.7			22.9	2		-0.1			2.7		
		Isovalerylcarnitine	0.6			0.3			7.0	11		0.7		
Lysine metabolism	GA-1	3-OH-isovalerylcarnitine	0.6			-1.6			-0.2			0.0		
		Propionylcarnitine	13.3	2	Yes (n=3)	75.4	1	Yes (n=1)						
		Methylcitric acid	7.3	4		4.3								
		Methylmalonic acid	0.2			16.6	4							
		Methylmalonylcarnitine	1.1			0.7								
		Glutaryl carnitine	18.6	2	Yes (n=4)	4.9	10	Yes (n=2)	26.3	1	Yes (n=3)	27.9	5	Yes (n=3)
Phenylalanine and tyrosine metabolism	PKU	Glutaric acid	7.9	3		-0.9			6.4	17		71.6	3	
		3-hydroxyglutaric acid	-0.3			0.2			10.5	8		8.2	11	
		Glutaconic acid	-1.6			27.9	2	Yes (n=1)						
		Phenylalanine	47.7	1	Yes (n=1)	37.0	3							
		Hydroxyphenylacetic acid	10.9	4		1.9								
		N-acetylphenylalanine	6.3	9		7.0	22							
Tyrosinaemia		Tyrosine	-1.0			-0.1								
		4-OH-phenyllactic acid	150.7	1	Yes (n=1)	125.6	2	Yes (n=1)	206.5	1	Yes (n=3)	263.5	1	Yes (n=3)
		Tyrosine	26.2	3		15.6	6		35.0	3		33.7	3	
		4-OH-phenylacetic acid	4.6			6.3	9		2.2			2.0		
		4-OH-phenylpyruvic acid	0.2			2.0			10.4	8		6.8		
Succinylacetone	-1.5			-1.2			0.2			1.1				

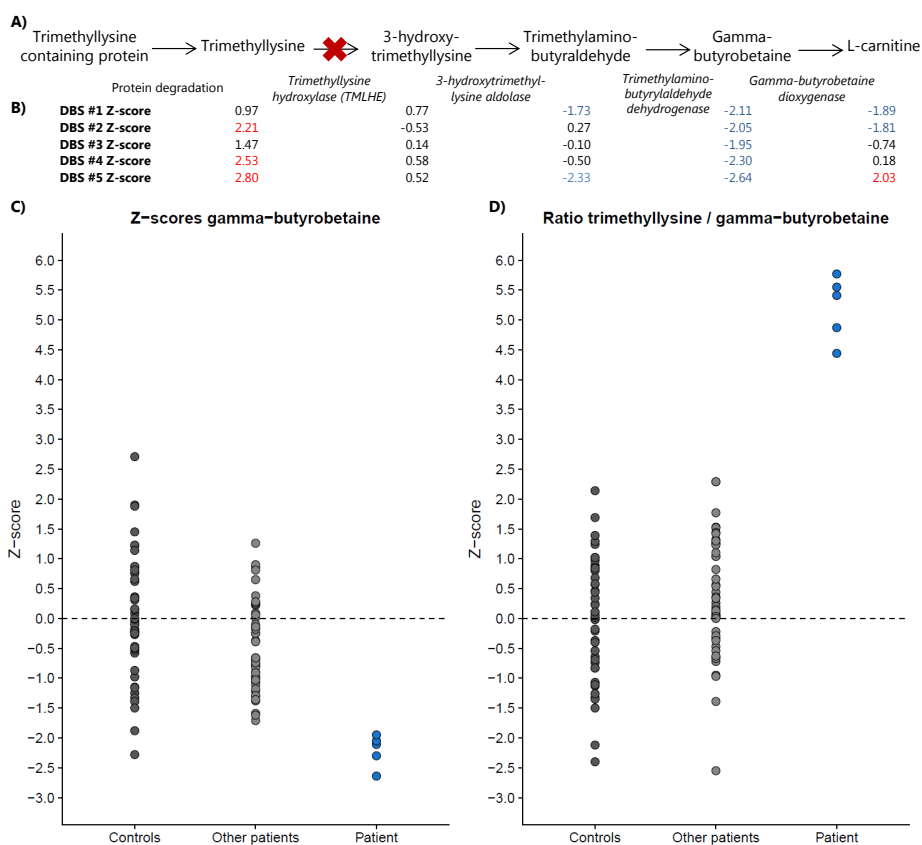
Sulphur amino acid metabolism	MATIA deficiency	Methionine sulfoxide	72.2	1	Yes (n=5)	53.4	2	Yes (n=5)	1106.7	1	Yes (n=1)	632.2	1	Yes (n=3)
		Methionine	57.1	2		96.4	1		118.8	4		47.4	6	
		S-adenosylmethionine	0.5			-0.3			0.1			0.3		
		S-adenosylhomocysteine	-0.8			0.4			0.4			0.1		
		Methionine sulfoxide	22.4	2	Yes (n=4)				778.9	1	Yes (n=2)			
		Methionine	31.1	3					2.6					
		Homocysteine	3.2	7					1.3					
		Homocysteine	2.6	12					2.2					
		Homocysteine thiolactone	28.0	1	Yes (n=6)	7.5	3	Yes (n=3)	-0.3		No (n=1)	0.1		No (n=3)
		Homocysteine	1.1			4.8	9		-0.2			0.3		
		Methionine	0.2			0.0			-2.4	-20		-2.3		
		Xanthine	59.3	1	Yes (n=1)	40.7	3	Yes (n=1)	55.5	7	Yes (n=1)			
		A-amino adipic semialdehydic cofactor deficiency	-0.9			0.6			11.8	22				
		Cysteine	-1.0			-2.6			-2.1	-14				
		Uric acid	-1.4			-0.8			-2.6	-5				
Serine & glycine metabolism	NKH	Glycine	3.7	18	Yes (n=2)	2.0		No (n=3)	3.4		Yes (n=3)	2.2		No (n=3)
		Serine	5.1	1	No (n=3)	0.8		No (n=3)	-2.5	4	Yes (n=2)	-2.4		Yes (n=3)
		Glycine	2.1			-0.1			-1.6			-1.8		
Proline metabolism	OAT deficiency	Proline	4.0	11	Yes (n=6)				4.0		Yes (n=5)			
		Ornithine	2.8	18					-0.8					
Amino acid transport	LPI	Citrulline	8.5	2	Yes (n=3)				16.1	13	Yes (n=3)			
		Serine	6.2	3				2.4						
		Proline	6.4	4					0.2					
		Threonine	5.7	7					0.6					
		Lysine	-2.0	-7					-1.3					
		Ornithine	-1.5						0.6					
		Arginine	-1.0						-1.0					

Fatty acid oxidation	VLCAD deficiency	C14:1 carnitine	28.9	1	Yes (n=1)	0.6	No (n=3)	7.3	34	Yes (n=1)	5.8	Yes (n=1)
		C14:2 carnitine	15.7	2	Yes (n=1)	1.4		7.6	33		2.8	
		C14-carnitine	3.7			1.5		1.4			2.4	
		C14-OH carnitine	3.1	35	Yes (n=1)			8.3	14	Yes (n=2)	8.2	Yes (n=2)
		C16-OH carnitine	3.0	37				22.7	2		37.3	12
		C16-OH:1 carnitine	1.5					23.8	1		41.6	11
		C18-OH carnitine	0.7					21.9	3		29.8	17
		C8-carnitine	56.5	1	Yes (n=2)	111.5	1	189.3	1	Yes (n=3)	143.4	1
		C6-carnitine	7.3	6		16.0	3	51.7	2		55.7	2
		C10:1-carnitine	1.7			8.1	7	24.9	4		11.6	5
		C10-carnitine	1.1			2.6		7.3	12		3.2	
		L-Carnitine	-2.0		Yes (n=1)	-1.3		-2.4	-3	Yes (n=2)	-2.3	Yes (n=1)
		Acetylcarnitine	-1.9			-0.9		-2.5	-1		-2.5	-9
		C16-carnitine	-1.7			-1.3		-1.1			-0.3	
		C16:1-carnitine	-2.6	-5		-1.1		-1.3			-1.8	
		C18-carnitine	-1.7			-1.7	-2	-0.6			-0.9	
		C18:1-carnitine	-2.3	-12		-1.8	-1	-1.1			-1.0	
		L-Carnitine	19.0	1	Yes (n=2)	19.0	1	-2.7	-84	No (n=2)	1.8	No (n=2)
		C0/(n=C16+C18) ratio	10.3	3		8.4	3	-1.6			-0.3	
		C16-carnitine	-3.1	-1		-1.8	-5	-2.7	-82		-0.2	
		C18-carnitine	-2.6	-3		-2.2	-2	-1.1			-0.6	
		C18:1-carnitine	-2.6	-4		-2.5	-1	0.0			1.1	
		C16+C18:1/C2 ratio	2.2	25	Yes (n=2)	4.8	1	-1.4		Yes (n=4)	0.1	Yes (n=2)
		Acetylcarnitine	-1.7	-8		-2.4	-1	8.8	9		6.5	6
		C16-carnitine	-0.6			-1.4		9.3	8		6.7	5
		C18-carnitine	-0.6			-1.7		4.1			3.1	
		C18:1-carnitine	-0.7			-1.8						
		Guanidoacetic acid	20.9	1	Yes (n=2)	39.2	2	25.1	1	Yes (n=3)	35.9	1
		Creatine	-1.4			-1.2		1.8			-1.7	Yes (n=1)

Metabolites that contributed most to assigning the “most probable diagnosis” are reported, although more metabolites have influenced the final decision. *For each mass peak, only one metabolite annotation is reported, the one that influenced the final decision. Metabolites that are not reported were either less relevant for assigning “most probable diagnosis” or were normal. All data is available on request. Z-sc. is the average Z-score of the included samples. The rank is the metabolite rank in the list of metabolites ordered on highest to lowest Z-score. A negative rank is the rank from bottom to top of the list. Abbreviations: 3-MCC: 3-methylcrotonylglycinuria; 3-PGDH: 3-phosphoglycerate dehydrogenase; CBS: cystathionine beta-synthase; CPT1: carnitine palmitoyltransferase I; CPT2: carnitine palmitoyltransferase II; DBS: dried blood spot; def.: deficiency; GA-1: glutaric acidemia type I; GAMT: guanidinoacetate methyltransferase; IVA: isovaleric acidemia; LCHAD: long-chain hydroxyacyl-CoA dehydrogenase; LPI: lysinuric protein intolerance; MAT1A: methionine adenosyltransferase I; MCAD: medium-chain acyl-CoA dehydrogenase; MMA: methylmalonic acidemia, isolated; MSUD: maple syrup urine disease; MTHFR: methylenetetrahydrofolate reductase; NKKH: non-ketotic hyperglycaemia; OAT: ornithine aminotransferase; OCTN2: organic cation transporter 2; OTC: ornithine transcarbamylase; PKU: phenylketonuria; VLCAD: very long chain acyl-CoA dehydrogenase.

The first two DBS were sampled prior to carnitine supplementation, DBS #3 and #4 during supplementation with 1000 mg levocarnitine and DBS #5 during supplementation with 1500 mg levocarnitine. At 3/5 time points trimethyllysine was significantly increased (Figure 3). Interestingly, at 5/5 time points, γ -butyrobetaine, a metabolite downstream of TMLHE and the precursor of L-carnitine, was significantly decreased (Figure 3). The substrate/(downstream-)product ratio trimethyllysine/ γ -butyrobetaine was significantly increased in all five patient samples, clearly separating this patient from control samples and samples of other patients and thereby supporting pathogenicity of the identified VUS in the *TMLHE* gene (Figure 3).

Figure 3. DI-HRMS metabolomics pathway analysis of the pathway of trimethyllysine hydroxylase



A) Metabolic pathway of trimethyllysine hydroxylase, in italic the enzyme responsible for the metabolite conversion depicted by the arrow. **B)** Z-scores of the five included dried blood spots (DBS) for each of the metabolites included in the pathway. Z-scores in red are significantly increased, Z-scores in blue are significantly decreased. **C)** Z-scores of control samples, other patient samples and the samples of this patient for γ -butyrobetaine, the metabolite decreased in all patient samples. **D)** Z-scores of control samples, other patient samples and the samples of this patient for the ratio of trimethyllysine over γ -butyrobetaine. De ratio is significantly increased in all patient samples and clearly separates this patient from control samples and samples of other patients, thereby supporting pathogenicity of the identified variant of uncertain significance in *TMLHE*.

DISCUSSION

We here present the first non-quantitative DI-HRMS metabolomics method for metabolic diagnostics and demonstrate its consistency and accuracy for both DBS and plasma. Using this method, 37/42 of the included patients could be correctly assigned a “most probable diagnosis” based on DBS samples, corresponding to 22/23 of included IEM. In addition, 32/38 included patients could be assigned a correct diagnosis based on plasma samples, corresponding to 19/21 of included IEM. For 3-phosphoglycerate dehydrogenase deficiency we could not demonstrate the accuracy of the method in DBS, as the sample was drawn under serine supplementation, normalizing the level of serine. However, decreased concentrations of amino acids can be detected by this method, as illustrated by the repeatedly decreased concentration of lysine in a sample of a patient affected with LPI (Tables 3 and 4). Our method failed to detect MTHFR deficiency and CPT1 deficiency in plasma. Methanol-based sample extraction as performed here only captures the unbound fraction of homocysteine, which is not a good representative of the total homocysteine concentration in blood, and therefore MTHFR deficiency was missed in plasma. Interestingly, in DBS MTHFR deficiency was correctly diagnosed since homocysteine thiolactone, an intramolecular thioester of homocysteine, was significantly increased (Table 2). CPT1 deficiency was missed in plasma, since we and others already demonstrated that DBS is a more suitable matrix to diagnose CPT1 deficiency,^{31,32} although diagnosis based on ratios may be possible in plasma.^{31,33} In direct infusion, an observed mass can account for multiple metabolite annotations, since a specific *m/z* can account for multiple isomers (Figure 1). Here, this did not result in any data interpretation problems nor in any incorrect diagnosis, probably since most *m/z* are dominated by a single metabolite of significant abundance. Still, semi-quantitative metabolomics always produces tentative results. When used in daily practice, we advocate confirmation of the results with second-tier testing, using targeted diagnostic platforms or genetic tests.

Direct infusion is superior to LC-MS methods in being nonselective and very sensitive and it allows the identification of many mass peaks. Even after strict metabolite selection, ~1,875 mass peaks corresponding to metabolites that can occur endogenously remained, compared to ~400 or ~340 clinically relevant metabolites in LC-MS and/or GC-MS based metabolomics methods.^{1,21} The method of Miller et al. did not identify guanidinoacetic acid, methylmalonic acid and C14:1 and C14:2 carnitine.²¹ In our method, these four metabolites were annotated, demonstrated by the correct diagnosis of guanidinoacetic acid methyltransferase deficiency, methylmalonic aciduria and very long-chain acyl-CoA dehydrogenase deficiency. The method of Coene et al. could not identify guanidinoacetic acid, argininosuccinic acid and dimethylglycine and thus could not recognize guanidinoacetic acid methyltransferase deficiency, argininosuccinic aciduria, and dimethylglycine dehydrogenase deficiency.¹ These last two IEM were not included in our study, but both argininosuccinic acid and dimethylglycine were annotated in every batch, suggesting that we should be able to correctly diagnose these IEM. Lastly, the method of Coene et al. could not recognize LPI due to strict criteria for the statistical tests.¹ We demonstrate that using our method we could diagnose LPI based on the combined decrease of lysine (mean Z-score -2.0, rank 7th from below) and increase of citrulline (mean Z-score 8.5, rank 2nd).

A strength of our study is that the assignment of the “most probable diagnosis” was performed blindly, as the investigator was blinded to clinical data and to diagnoses included in the study. In addition, we demonstrate for the first time that next to plasma, as used in the studies of Miller and Coene et al.,^{1,21} DBS are also suitable material to use for non-

quantitative metabolomics for metabolic diagnostics. Also, in contrast to Coene et al., who considered four peaks individually for each metabolite,¹ we sum mass peak intensities of single adduct ions, leaving only one peak per metabolite to assess, facilitating data interpretation to a great extent.

Potential clinical applications of non-quantitative metabolomics are numerous. We exemplified this by demonstrating a case in which DI-HRMS metabolomics aided interpretation of a VUS identified by WES. In addition, non-quantitative metabolomics can be used for generating hypotheses for new disease biomarkers, for studying pathophysiology in pre-defined patient groups and for studying the complete metabolome of cases suspected of an IEM that remained unresolved after routine metabolic diagnostics.

CONCLUSION

In summary, we demonstrate a very consistent, nonselective, high-throughput DI-HRMS metabolomics method for investigating the metabolome in genetic disease, which requires only small amounts of patient material. We demonstrated the value of this method for both DBS and plasma by blindly assigning a correct “most probable diagnosis” to patients with a wide range of IEM.

WEB RESOURCES

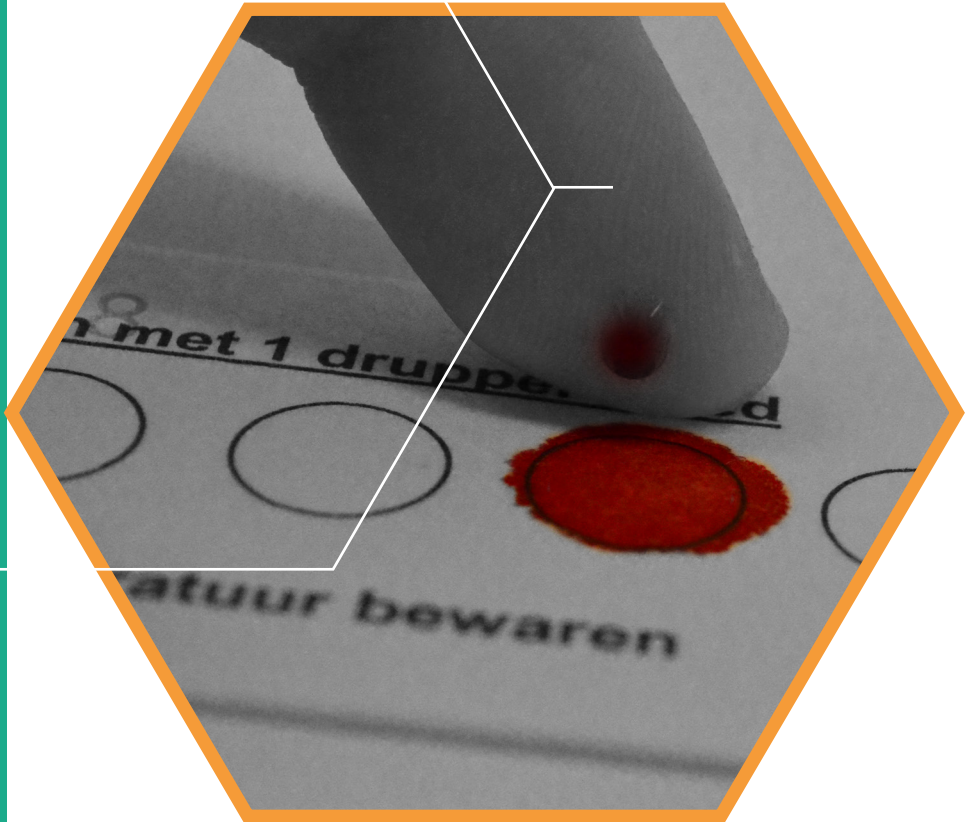
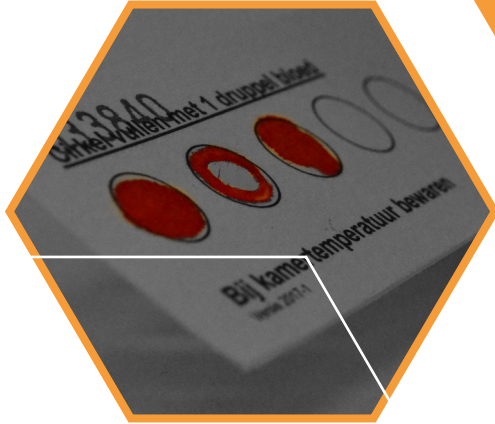
HMDB

<https://hmdb.ca>

REFERENCES

1. Coene KLM, Kluijtmans LAJ, van der Heeft E et al. Next-generation metabolic screening: Targeted and untargeted metabolomics for the diagnosis of inborn errors of metabolism in individual patients. *J Inher Metab Dis*. 2018;41:337-353.
2. Janeckova H, Hron K, Wojtowicz P et al. Targeted metabolomic analysis of plasma samples for the diagnosis of inherited metabolic disorders. *J Chromatogr A* 2012;1226:13-17.
3. Pitt JJ, Eggington M, Kahler SG. Comprehensive screening of urine samples for inborn errors of metabolism by electrospray tandem mass spectrometry. *Clin Chem*. 2002;48:1970-1980.
4. Jacob M, Malkawi A, Albast N, Al Bougha S, Lopata A, Dasouki M, Abdel Rahman AM. A targeted metabolomics approach for clinical diagnosis of inborn errors of metabolism. *Analyt Chim Acta* 2018;1025:141-153.
5. Kurko J, Tringham M, Tanner L et al. Imbalance of plasma amino acids, metabolites and lipids in patients with lysinuric protein intolerance. *Metabolism* 2016;65:1361-1375.
6. Dercksen M, Koekemoer G, Duran M, Wanders RJA, Mienie LJ, Reinecke CJ. Organic acid profile of isovaleric acidemia: A comprehensive metabolomics approach. *Metabolomics* 2013;9:765-777.
7. Smuts I, van der Westhuizen FH, Louw R et al. Disclosure of a putative biosignature for respiratory chain disorders through a metabolomics approach. *Metabolomics* 2013;9:379-391.
8. Najdekr L, Gardlo A, Madrova L et al. Oxidized phosphatidylcholines suggest oxidative stress in patients with medium-chain acyl-CoA dehydrogenase deficiency. *Talanta* 2015;139:62-66.
9. Tebani A, Schmitz-Afonso I, Abily-Donval L et al. Urinary metabolic phenotyping of mucopolysaccharidosis type I combining untargeted and targeted strategies with data modeling. *Clin Chim Acta* 2017;475:7-14.
10. Wangler MF, Huber L, Donti TR et al. A metabolomics map of Zellweger spectrum disorders reveals novel disease biomarkers. *Genet Med*. 2018;20:1274-1283.
11. Wikoff WR, Gangoiti JA, Barshop BA, Siuzdak G. Metabolomics identifies perturbations in human disorders of propionate metabolism. *Clin Chem*. 2007;53:2169-2176.
12. Denes J, Szabo E, Robinette SL et al. Metabonomics of newborn screening dried blood spot samples: A novel approach in the screening and diagnostics of inborn errors of metabolism. *Anal Chem*. 2012;84:10113-10120.
13. Peretz H, Watson DG, Blackburn G et al. Urine metabolomics reveals novel physiologic functions of human aldehyde oxidase and provides biomarkers for typing xanthinuria. *Metabolomics* 2012;8:951-959.
14. Atwal PS, Donti TR, Cardon AL et al. Aromatic L-amino acid decarboxylase deficiency diagnosed by clinical metabolomics profiling of plasma. *Mol Genet Metab*. 2015;115:91-94.
15. Venter L, Lindeque Z, Jansen van Rensburg P, van der Westhuizen F, Smuts I, Louw R. Untargeted urine metabolomics reveals a biosignature for muscle respiratory chain deficiencies. *Metabolomics* 2015;11:111-121.

16. Abela L, Simmons L, Steindl K et al. N(8)-acetylspermidine as a potential plasma biomarker for Snyder-Robinson syndrome identified by clinical metabolomics. *J Inherit Metab Dis.* 2016;39:131-137.
17. Donti TR, Cappuccio G, Hubert L et al. Diagnosis of adenylosuccinate lyase deficiency by metabolomic profiling in plasma reveals a phenotypic spectrum. *Mol Genet Metab Rep.* 2016;8:61-66.
18. Miller MJ, Bostwick BL, Kennedy AD, Donti TR, Sun Q, Sutton VR, Elsea SH. Chronic oral L-carnitine supplementation drives marked plasma TMAO elevations in patients with organic acidemias despite dietary meat restrictions. *JIMD Rep.* 2016;30:39-44.
19. Abela L, Spiegel R, Crowther LM et al. Plasma metabolomics reveals a diagnostic metabolic fingerprint for mitochondrial aconitase (ACO2) deficiency. *PLoS ONE* 2017;12.
20. Glinton KE, Benke PJ, Lines MA et al. Disturbed phospholipid metabolism in serine biosynthesis defects revealed by metabolomic profiling. *Mol Genet Metab.* 2018;123:309-316.
21. Miller MJ, Kennedy AD, Eckhart AD et al. Untargeted metabolomic analysis for the clinical screening of inborn errors of metabolism. *J Inherit Metab Dis.* 2015;38:1029-1039.
22. de Sain-van der Velden MGM, van der Ham M, Gerrits J et al. Quantification of metabolites in dried blood spots by direct infusion high resolution mass spectrometry. *Anal Chim Acta* 2017;979:45-50.
23. Kertesz V, Van Berkel GJ. Fully automated liquid extraction-based surface sampling and ionization using a chip-based robotic nanoelectrospray platform. *J Mass Spectrom.* 2010;45:252-260.
24. Kirwan JA, Broadhurst DI, Davidson RL, Viant MR. Characterising and correcting batch variation in an automated direct infusion mass spectrometry (DIMS) metabolomics workflow. *Anal Bioanal Chem.* 2013;405:5147-5157.
25. González-Domínguez R, García-Barrera T, Gómez-Ariza JL. Using direct infusion mass spectrometry for serum metabolomics in Alzheimer's disease. *Anal Bioanal Chem.* 2014;406:7137-7148.
26. Likhov PG, Trifonova OP, Maslov DL et al. Diagnosing impaired glucose intolerance using direct infusion mass spectrometry of blood plasma. *PLoS ONE* 2014;9:e105343.
27. Koulman A, Prentice P, Wong MCY et al. The development and validation of a fast and robust dried blood spot based lipid profiling method to study infant metabolism. *Metabolomics* 2014;10:1018-1025.
28. Anand S, Barnes JM, Young SA, Garcia DM, Tolley HD, Kauwe JSK, Graves SW. Discovery and confirmation of diagnostic serum lipid biomarkers for Alzheimer's disease using direct infusion mass spectrometry. *J Alzheimers Dis.* 2017;59:277-290.
29. Anand S, Young S, Esplin MS et al. Detection and confirmation of serum lipid biomarkers for preeclampsia using direct infusion mass spectrometry. *J Lipid Res.* 2017;57:687-696.
30. Ramos RJ, Pras-Raves ML, Gerrits J et al. Vitamin B6 is essential for serine *de novo* biosynthesis. *J Inherit Metab Dis.* 2017;40:883-891.
31. Sain-van der Velden MGM, Diekman EF, Jans JJ, van der Ham M, Prinsen BT, Visser G, Verhoeven-Duif NM. Differences between acylcarnitine profiles in plasma and bloodspots. *Mol Genet Metabol.* 2013;110:116-121.
32. Primassin S, Spiekerkoetter U. ESI-MS/MS measurement of free carnitine and its precursor γ -butyrobetaine in plasma and dried blood spots from patients with organic acidurias and fatty acid oxidation disorders. *Mol Genet Metabol.* 2010;101:145-150.
33. Heiner-Fokkema MR, Vaz FM, Maatman R, Kluijtmans LAJ, van Spronsen FJ, Reijngoud DJ. Reliable diagnosis of carnitine palmitoyltransferase type IA deficiency by analysis of plasma acylcarnitine profiles. *JIMD Rep.* 2016;32:33-39.
34. Wishart DS, Jewison T, Guo AC et al. HMDB 3.0 – The Human Metabolome Database in 2013. *Nucleic Acids Res.* 2013;41:801-807.



Direct-infusion based metabolomics unveils

biochemical profiles of inborn errors of metabolism in cerebrospinal fluid

Molecular Genetics and Metabolism 2019, 127(1): 51-57
DOI: 10.1016/j.ymgme.2019.03.005

Hanneke A. Haijes*, Maria van der Ham, Johan Gerrits,
Peter M. van Hasselt, Hubertus C.M.T. Prinsen,
Monique G.M. de Sain-van der Velden,
Nanda M. Verhoeven-Duif, Judith J.M. Jans*

* Corresponding authors

ABSTRACT

Background: For inborn errors of metabolism (IEM), metabolomics is performed for three main purposes: (1) development of next-generation metabolic screening platforms, (2) identification of new biomarkers in predefined patient cohorts and (3) for identification of new IEM. To date, plasma, urine and dried blood spots are used. We anticipate that cerebrospinal fluid (CSF) holds additional – valuable – information, especially for IEM with neurological involvement. To expand metabolomics to CSF, we here tested whether direct-infusion high-resolution mass spectrometry (DI-HRMS) based non-quantitative metabolomics could correctly capture the biochemical profile of patients with an IEM in CSF.

Methods: Eleven patient samples, harboring eight different IEM, and thirty control samples were analyzed using DI-HRMS. First we assessed whether the biochemical profile of the control samples represented the expected profile in CSF. Next, each patient sample was assigned a “most probable diagnosis” by an investigator blinded for the known diagnoses of the patients.

Results: the biochemical profile identified using DI-HRMS in CSF samples resembled the known profile, with – among others – the highest median intensities for mass peaks annotated with glucose, lactic acid, citric acid and glutamine. Subsequent analysis of patient CSF profiles resulted in correct “most probable diagnoses” for all eleven patients, including non-ketotic hyperglycinaemia, propionic aciduria, purine nucleoside phosphorylase deficiency, argininosuccinic aciduria, tyrosinaemia type I, hyperphenylalaninemia and hypermethioninaemia.

Conclusion: We here demonstrate that DI-HRMS based non-quantitative metabolomics accurately captures the biochemical profile of this set of patients in CSF, opening new ways for using metabolomics in CSF in the metabolic diagnostic laboratory.

KEY MESSAGE

Non-quantitative DI-HRMS accurately captures the biochemical profile of this set of patients in CSF, opening new ways for using metabolomics in CSF in the metabolic diagnostic laboratory.

INTRODUCTION

With unprecedented pace, metabolomics is implemented in the diagnostic laboratory. For inborn errors of metabolism (IEM), metabolomics is performed for three main purposes: (1) development of next-generation metabolic screening (NGMS) platforms,^{7,13,19} (2) identification of new biomarkers in predefined patient cohorts,^{1-3,9-11,20,23,29,30} and (3) for identification of new IEM.²⁸ To this aim, plasma, urine and dried blood spots are generally used.

The use of cerebrospinal fluid (CSF) for metabolomics analyses is lagging behind in these developments. As CSF circulates in the subarachnoidal space, surrounding brain and spinal cord, CSF is the closest possible read-out of body fluids of metabolite concentrations in the brain. For this reason, metabolomics in CSF has been used for biomarker studies for a variety of neurodegenerative diseases and cerebral infections.^{4-6,12,14,16,18,24,26} However, for IEM, metabolomics studies only recently expanded to CSF. Kennedy et al. determined the molecular composition of CSF and identified the biochemical pathways represented in CSF, in order to understand the potential for untargeted screening of IEM.¹⁵ In their study, they included one patient harboring an IEM, dihydropteridine reductase deficiency (MIM #261630), and demonstrated that they could indeed capture the biochemical signature of this disease in CSF of this patient. They conclude that further validation will illustrate the power of this technology.

In line with Kennedy et al., we acknowledge the potential power of metabolomics in CSF. We anticipate that CSF holds additional valuable information to plasma, urine and dried blood spots, especially for IEM with neurological involvement. First of all, – if CSF is available – it could add a new level of information to NGMS. Secondly, it provides the opportunity to identify biomarkers in neurometabolic IEM, for diagnostic or prognostic purposes or for treatment follow-up. Lastly, analysis of CSF could be an additional opportunity to find a diagnosis in patients that have remained without a diagnosis so far.

Here we describe the investigation of direct-infusion based non-quantitative metabolomics as a method to correctly capture the biochemical profile of patients with an IEM in CSF.

METHODS

Sample collection and patient inclusion

We used remnant CSF samples which were initially drawn for routine metabolic diagnostics or follow-up. CSF samples were collected by lumbar puncture in a standardized procedure in which six separate fractions (0.5, 1.0, 1.0, 1.5, 1.0 and 2.0 mL) were drawn and immediately put on ice at bedside. Each fraction was protected from light and stored at -80°C . Patients with a known IEM were included when a remnant CSF sample was available in the metabolic diagnostics laboratory of the University Medical Centre Utrecht. CSF samples visually contaminated with blood were excluded. Eleven samples from eleven patients could be included. To serve as control samples, thirty samples of individuals in whom an IEM was excluded after a thorough routine diagnostic work-up turned back negative, were selected. Different fractions were available to serve as patient and control samples (fraction I in 4/41, II in 3/41, III in 1/41, IV in 10/41, V in 4/41 and VI in 19/41 samples), with a comparable distribution over the patient and control groups. All procedures followed were in accordance with the ethical standards of the University Medical Centre Utrecht and with the Helsinki Declaration of 1975, as revised in 2000. In agreement with institutional and national legislation, all included individuals, or their legal guardians, had approved the possible use of their remnant samples for method development and validation.

Sample preparation and DI-HRMS analysis

Metabolomics analysis was performed as previously described.¹³ In short, samples were thawed to room temperature. 10 μL of CSF was added to 140 μL a working solution containing stable isotope-labeled compounds (sILC) achieving concentrations similar to plasma.¹³ The solution was centrifuged for five minutes at 17,000 g and 105 μL of supernatant was diluted with 45 μL 0.3% formic acid (Emsure, Darmstadt, Germany). The solution was filtered using a methanol preconditioned 96 well filter plate (Acro prep, 0.2 μm GHP, NTRL, 1 mL well; Pall Corporation, Ann Arbor, MI, USA) and a vacuum manifold. The sample filtrate was collected in a 96 well plate (Advion, Ithaca, NY, USA).

Direct-infusion high resolution mass spectrometry analysis was performed using a TriVersa NanoMate system (Advion, Ithaca, NY, USA) controlled by Chipsoft software (version 8.3.3, Advion), mounted onto the interface of a Q-Exactive Plus high-resolution mass spectrometer (Thermo Scientific™, Bremen, Germany). Samples (13 μL) were automatically aspirated sequentially into a pipette tip followed by an air gap (2 μL). For each sample, technical triplicates were analyzed, infusing each sample three times into the mass spectrometer. Pipette tips were engaged with the electrospray ionization chip to deliver the sample using nitrogen gas pressure at 0.5 psi and a spray voltage of 1.6 kV. For each sample new pipette tips and nozzles were used to prevent any cross-contamination or carryover. The Q-Exactive Plus high-resolution mass spectrometer was operated in positive and negative ion mode in a single run, with automatic polarity switching. There were two time segments with a total run time of 3.0 min. Scan range was 70 to 600 mass to charge ratio (m/z), resolution was set at 140,000 at $m/z = 200$ for optimal separation of m/z , automatic gain control target value was $3e6$, maximum injection time was 200 ms, capillary temperature was 275°C, sample tray was kept at 18°C and for the S-lens RF level factor 70 was used. In the positive segment, the sodium adduct of $^{13}\text{C}_6$ -Phenylalanine (m/z 194.0833) was used as a lock mass and in the negative segment $^2\text{H}_9$ -myristoylcarnitine (m/z 381.36733) was used as lock mass.

Data processing and data analysis

Data acquisition and data processing was performed using a peak calling pipeline developed in R programming language.¹³ In this pipeline, detected mass peaks were annotated by matching the m/z value of the mass peak with a range of two parts per million to monoisotopic metabolite masses present in the Human Metabolome Database (HMDB), version 3.6.³² According to the Metabolomics Standards Initiative, the level of certainty in metabolite identification is 2, as we putatively annotate compounds based on the matched m/z value of the mass peak.²⁷ Mass peak intensities of mass peaks annotated without adduct ion or with a single adduct ion in negative ($[\text{M}-\text{H}]^-$, $[\text{M}+\text{Cl}]^-$) or positive ($[\text{M}+\text{H}]^+$, $[\text{M}+\text{Na}]^+$ and $[\text{M}+\text{K}]^+$) mode were summed. Hereof, annotations of metabolites that could occur endogenously and annotations of metabolites with still unknown function were manually curated by four trained clinical laboratory geneticists.¹³ For each mass peak per patient sample, the deviation from the intensities in control samples was indicated by a Z-score, calculated by: $\text{Z-score} = (\text{intensity patient sample} - \text{mean intensity control samples}) / \text{standard deviation intensity control samples}$. For each sample, metabolite annotations were ranked on Z-score: positive Z-scores were ranked from rank 1 onwards from the highest Z-scores to a Z-score of 0.0, and negative Z-scores were ranked from rank (-)1 onwards from the lowest Z-scores to a Z-score of 0.0. Z-scores are considered aberrant when > 2.0 (as a Z-score of 1.96 corresponds to a p-value of 0.05) or < -1.5 , since decreases are often more subtle than increases. Ratios

were calculated by dividing the mass peak intensities and by subsequently calculating the Z-scores. Data and R code can be supplied upon request.¹³

Assessing the biochemical profiles of control and patient samples

To assess whether the biochemical profile of control samples identified with DI-HRMS represents the expected biochemical profile of CSF, it was determined whether metabolites that are enlisted in HMDB as “detected and quantified in CSF” were identified using our method. Next, metabolites measured with the highest median intensities in the control samples were listed. The most abundant metabolites in CSF, as previously described,³¹ were expected to have relatively high intensities.

Next, to assess whether the patient biochemical profile identified with DI-HRMS represents the expected patient biochemical profile, each patient was assigned a “most probable diagnosis” by an investigator blinded for the patient’s known diagnosis. This assigned “most probable diagnosis” was based on the ranked metabolite list as provided by the workflow. For all metabolite annotations with aberrant Z-scores (> 2.0 and < -1.5), association to any known IEM was assessed. Next, Z-scores of all annotated intermediates of the involved pathways were inquired, to confirm or confute a possible diagnosis. Neither information regarding patient characteristics (sex, age), nor clinical information was provided to the investigator.

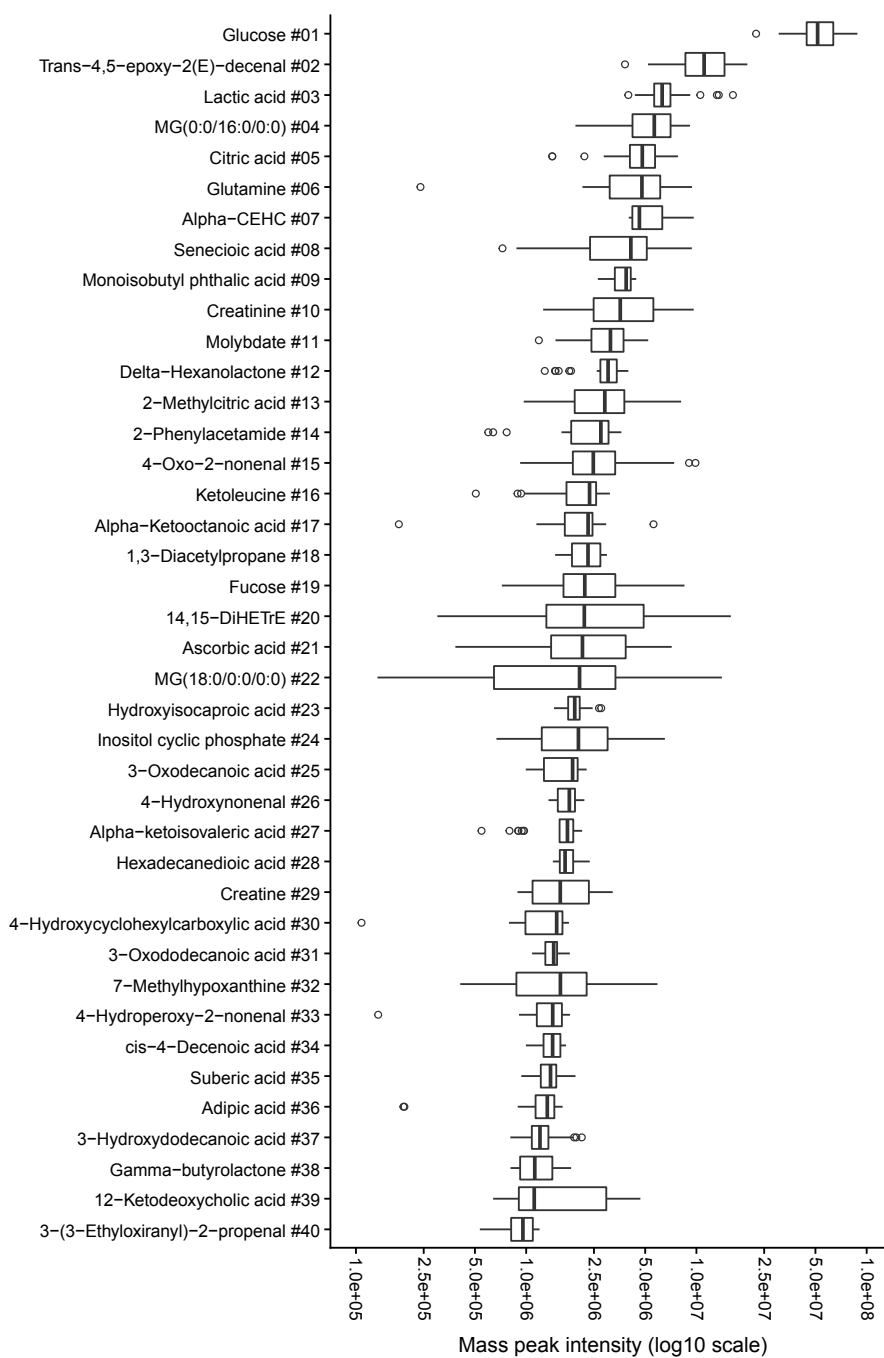
Per included IEM, a list was composed, comprising expected increases and decreases of metabolites, based on whether it is the substrate or product of the defective enzyme, and on reported increases or decreases in CSF, plasma, dried blood spots or urine in OMIM and additional literature.^{8,13,17}

RESULTS

Biochemical profile of control samples

The biochemical profile of control samples identified with DI-HRMS represented the expected biochemical profile of CSF.³¹ In our peak calling pipeline, 1,811 mass peaks were annotated with 3,676 metabolites that could occur endogenously (Table S1). The relative standard deviation of the within-run variation was 0.17, thus satisfactory. We compared our results to the metabolites enlisted as “detected and quantified in CSF” in the HMDB. This HMDB list comprises 448 metabolites, of which 70 metabolites have masses < 70 m/z or > 600 m/z and were therefore not detectable using the m/z range selected for this study. Furthermore, we classified 34/448 metabolites as exogenous metabolites and 13/448 metabolites as drug metabolites and excluded these compounds. Of the remaining 331 metabolites, our method annotated 321 (97%) metabolites to 210 mass peaks. Interestingly, our method identified 1,601 additional mass peaks with endogenous metabolite identifications in CSF (Table S1). The forty mass peaks with the highest median intensities in thirty CSF control samples are shown in Figure 1. As expected, these mass peaks include mass peaks annotated with hexoses or cyclohexanes (glucose, fructose, galactose and/or myo-inositol, #1), lactic acid (#3), citric acid (#5), glutamine (#6) and ascorbic acid (#21). More metabolites described to be abundant in CSF were annotated: creatinine (#10) and creatine (#29), pyroglutamic acid (#52), ribitol (#73), glycerol (#79), 2-hydroxybutyric acid (#85), succinic acid (#100), glutamate (#128), serine (#141) and alanine (#146) (Table S1).³¹

Figure 1. Forty mass peaks with the highest median intensities in CSF control samples



Boxplots of mass peak intensities of forty mass peaks with the highest median intensities in thirty cerebrospinal fluid control samples. The y-axis displays the mass peaks with for each mass peak, one of the annotated metabolites. For the full list, see Table S1. Mass peaks are ordered on median mass peak intensity. The x-axis displays the measured mass peak intensity on a logarithmic scale.

Interesting metabolites present among the forty metabolites with the highest intensities in CSF, are metabolites of the degradation pathway of branched-chain amino acids (BCAA): senecioic acid (#8), ketoleucine (#16), 2-hydroxy-3-methylpentanoic acid (#23) and alphaketoisovaleric acid (#27) and the free fatty acid oxidation products trans-4,5-epoxy-2(E)-decenal (#2), 4-oxo-2-nonenal (#15), 4-hydroxynonenal (#26, described to be present in CSF), 4-hydroperoxy-2-nonenal (#33) and 3-(3-ethyloxiranyl)-2-propenal (#40).

Biochemical profile of patient samples

The biochemical profiles of the patient CSF samples analyzed by DIHRMS, all showed abnormalities in line with the genetic defects of the patients. Of all eleven included patients, the “most probable diagnosis” assigned to the patient based on the metabolomics profile was correct, including non-ketotic hyperglycinaemia, propionic aciduria, purine nucleoside phosphorylase deficiency, argininosuccinic aciduria, tyrosinaemia, non-tetrahydrobiopterin deficient hyperphenylalaninaemia and hypermethioninaemia. Figure 2 demonstrates the Z-scores of a selection of relevant biomarkers on which assigned diagnoses were based, for patients compared to controls. Table 1 lists Z-scores of the most important and interesting metabolites for these IEM.

Non-ketotic hyperglycinaemia is an IEM that generally presents with severe epileptic encephalopathy and hypotonia in the neonatal period. It is due to an enzyme deficiency of the glycine cleavage system. The diagnosis is mainly based on an increase of glycine in CSF. We could identify this IEM in one patient (P1), based on an isolated significant increase of glycine (Table 1, Figure 2). Metabolites associated with diseases that also can present with an increase of glycine all had normal Z-scores.

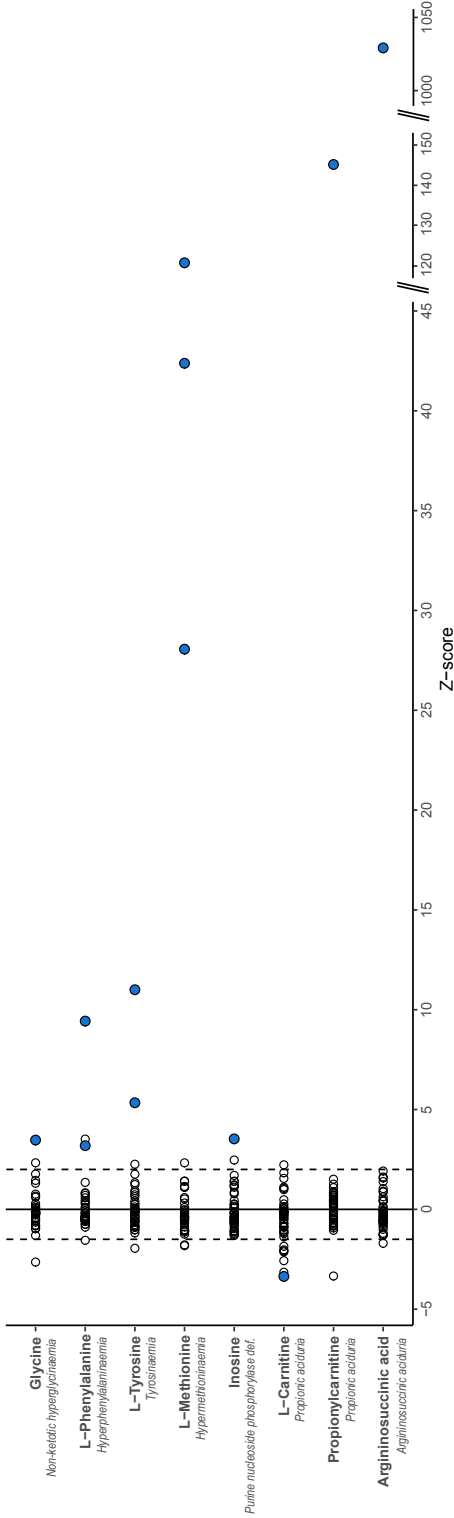
We identified propionic aciduria, a deficiency of propionyl-CoA carboxylase, in one patient (P2), based on a significant increase of propionylcarnitine, 2-methylcitric acid, propionylglycine and 3-hydroxypropionic acid, which all are products of the reactive enzymatic substrate propionyl-CoA, and on a significant decrease of L-carnitine, a scavenger of propionyl-CoA (Table 1, Figure 2). Methylmalonic acid and methylmalonylcarnitine, which are expected to be increased in methylmalonic acidemia, a closely related IEM, were both normal (Z-scores 0.02 and -0.51, respectively).

Purine nucleoside phosphorylase deficiency is a progressive neurological disorder which presents with spasticity, movement disorders and retardation. This IEM was identified in one patient (P3), based on the combined significant increases of inosine, one of the substrates of purine nucleoside phosphorylase (Figure 2), and a significant decrease of uric acid, a downstream metabolite in the affected pathway (Table 1).

Argininosuccinic aciduria was identified in one patient (P4), based on a stunning increase of argininosuccinic acid, the substrate of the enzyme. Argininosuccinic acid is normally very low in CSF (mean mass peak intensity 28,857; standard deviation 2,928), and was found vastly increased (mass peak intensity 4,997,820). In support, citrulline and orotidine, metabolites upstream in the affected metabolic pathway, also show a significant increase. In untreated samples, arginine (the product of the enzymatic reaction) is expected to be decreased, but due to arginine supplementation, which is the appropriate therapy for this disease, this patient demonstrates a significant increase of arginine in CSF.

Tyrosinaemia, without specifying the type of tyrosinaemia, was identified in two patients with tyrosinaemia type I (P5, P6). Tyrosinaemia type I is due to a deficiency of fumarylacetoacetase, which converts fumarylacetoacetate into fumarate and acetoacetate.

Figure 2. Distribution of Z-scores of a selection of relevant biomarkers on which patient “most probable diagnoses” were based



Four amino acids and four other metabolites are demonstrated as representative examples of compounds annotated to a mass peak with increased or decreased Z-scores that contributed to the assigned probable diagnosis. Each dot represents a unique sample. Black open circles represent both control samples and samples of other IEM patients, blue filled circles represent patients with that specific IEM. The dashed lines depict the cut-off values for aberrant Z-scores: > 2.0 for positive values and < -1.5 for negative values.

Table 1. Assigned “most probable diagnoses” based on diagnostic metabolites in CSF

Most probable diagnosis	Metabolite*	Expected change**	P	Rank	Z-score	P	Rank	Z-score	P	Rank	Z-score
Non-ketotic hyperglycaemia (MIM #605899)	Glycine	Increase, substrate	P1	8	3.47						
			P2	1	144.68						
Propionic aciduria (MIM #606054)	Propionylcarnitine	Increase		18	5.60						
	2-Methylcitric acid	Increase		40	3.96						
	3-Hydroxypropionic acid	Increase		41	3.96						
	Propionylglycine	Increase ⁷		63	2.70						
	Heptadecanoylcarnitine	Increase		175	-0.13						
	Glycine	Increase		78	-1.11						
	Propionic acid	Decrease		2	-3.36						

Purine nucleoside phosphorylase deficiency (MIM #613179)	Inosine	26	3.53										
	Guanosine	146	-0.30										
	Deoxyinosine	172	0.72										
	Deoxyguanosine	175	-0.01										
	Guanine	242	0.02										
	Hypoxanthine	107	-0.69										
	Uric acid	26	-1.61										
	Argininosuccinic acid	1	1032.1										
	Citrulline	14	7.13										
	Orotidine	42	3.55										
Argininosuccinic aciduria (MIM #207900)	Glutamine	147	1.16										
	Uracil	178	-0.04										
	Orotic acid	77	-1.05										
	Arginine	22	5.50										
	L-Tyrosine	1	11.00										
	Hydroxyphenyllactic acid	2	6.64										
	Hydroxyphenylacetic acid	113	-0.74										
	4-Hydroxyphenylpyruvic acid	100	-0.87										
	5-Aminolevulinic acid	57	-1.32										
	4-Fumarylacetoacetic acid	11	3.06										
Tyrosinaemia (type not specified)	Succinylacetone	162	0.17										
	Fumaric acid	90	-0.97										
	Acetoacetic acid	122	-0.65										
	Phenylalanine/Tyrosine ratio	6	3.95										
	L-Phenylalanine	11	3.19										
	Phenylpyruvic acid	171	0.19										
	Phenylacetic acid	118	-0.63										
	Phenyllactic acid	39	-1.47										
	Tyrosine	124	-0.57										
	Methionine	1	121.94										
#1 PAH (MIM #261600)	Homocysteine	216	-0.06										
	Homocysteine thiolactone	89	-1.01										
	S-Adenosylmethionine	68	-1.24										
#2 DNAJC12 (MIM #606060)	Increase, substrate	1	121.94	P10									
	Increase ⁸	155	-0.22										
	Increase ¹³	89	-1.01										
	Decrease, product	68	-1.24										
Hyperphenylalaninaemia, non-tetrahydropterin deficient (genetic defect not specified)	Increase, substrate (#1)	6	3.95	P8									
	Increase	11	3.19										
	Increase	171	0.19										
	Increase	118	-0.63										
	Increase	39	-1.47										
	Decrease, product (#1)	124	-0.57										
	Increase, substrate	1	121.94	P10									
	Increase ⁸	155	-0.22										
	Increase ¹³	89	-1.01										
	Decrease, product	68	-1.24										
#1 PAH (MIM #261600)	Increase, substrate (#1)	6	3.95	P8									
	Increase	11	3.19										
	Increase	171	0.19										
	Increase	118	-0.63										
	Increase	39	-1.47										
	Decrease, product (#1)	124	-0.57										
	Increase, substrate	1	121.94	P10									
	Increase ⁸	155	-0.22										
	Increase ¹³	89	-1.01										
	Decrease, product	68	-1.24										
#2 DNAJC12 (MIM #606060)	Increase, substrate (#1)	6	3.95	P8									
	Increase	11	3.19										
	Increase	171	0.19										
	Increase	118	-0.63										
	Increase	39	-1.47										
	Decrease, product (#1)	124	-0.57										
	Increase, substrate	1	121.94	P10									
	Increase ⁸	155	-0.22										
	Increase ¹³	89	-1.01										
	Decrease, product	68	-1.24										
Hypermethioninaemia (MIM #250850)	Increase, substrate (#1)	6	3.95	P8									
	Increase	11	3.19										
	Increase	171	0.19										
	Increase	118	-0.63										
	Increase	39	-1.47										
	Decrease, product (#1)	124	-0.57										
	Increase, substrate	1	121.94	P10									
	Increase ⁸	155	-0.22										
	Increase ¹³	89	-1.01										
	Decrease, product	68	-1.24										
Hyperphenylalaninaemia, non-tetrahydropterin deficient (genetic defect not specified)	Increase, substrate (#1)	6	3.95	P8									
	Increase	11	3.19										
	Increase	171	0.19										
	Increase	118	-0.63										
	Increase	39	-1.47										
	Decrease, product (#1)	124	-0.57										
	Increase, substrate	1	121.94	P10									
	Increase ⁸	155	-0.22										
	Increase ¹³	89	-1.01										
	Decrease, product	68	-1.24										
Hypermethioninaemia (MIM #250850)	Increase, substrate (#1)	6	3.95	P8									
	Increase	11	3.19										
	Increase	171	0.19										
	Increase	118	-0.63										
	Increase	39	-1.47										
	Decrease, product (#1)	124	-0.57										
	Increase, substrate	1	121.94	P10									
	Increase ⁸	155	-0.22										
	Increase ¹³	89	-1.01										
	Decrease, product	68	-1.24										
Hyperphenylalaninaemia, non-tetrahydropterin deficient (genetic defect not specified)	Increase, substrate (#1)	6	3.95	P8									
	Increase	11	3.19										
	Increase	171	0.19										
	Increase	118	-0.63										
	Increase	39	-1.47										
	Decrease, product (#1)	124	-0.57										
	Increase, substrate	1	121.94	P10									
	Increase ⁸	155	-0.22										
	Increase ¹³	89	-1.01										
	Decrease, product	68	-1.24										

Metabolite annotations that were expected to be increased or decreased in patient samples are reported, although more metabolite annotations have influenced the final decision. For each mass peak, only one metabolite annotation is reported, the annotation that influenced the final decision. Metabolite annotations that are not reported were either less relevant for assigning the most probable diagnosis, or were normal. All data is available on request. Expected change indicates whether a metabolite can be expected to be increased or decreased in the patient samples, based on whether it is the substrate or product of the defective enzyme, and on increases or decreases in CSF, plasma, dried blood spots or urine reported in OMIM and additional literature. Abbreviations: MIM: Mendelian Inheritance in Man; P: patient.

The diagnosis is generally based on a significant increase of tyrosine (Table 1, Figure 2), a metabolite upstream in this metabolic pathway. In both patients hydroxyphenyllactic acid – a tyrosine derivative – was significantly increased as well. Succinylacetone, the most toxic metabolite produced in tyrosinaemia type I, distinguishing type I from type II and III, was not increased, since both patients were treated with a tyrosine restricted diet and nitisinone at the moment of sampling. Interestingly, in one patient sample (P5), the substrate of fumarylacetoacetase was increased: 4-fumarylacetoacetic acid ranked 11th with a Z-score of 3.06 (Table 1), providing additional information that this patient, is, indeed, affected with tyrosinaemia type I.

Non-tetrahydrobiopterin deficient hyperphenylalaninaemia is most often caused by a deficiency of phenylalanine hydroxylase, which converts phenylalanine into tyrosine. Untreated, the disease is characterized by severe brain damage with intellectual disability, spasticity and seizures. Non-tetrahydrobiopterin deficient hyperphenylalaninaemia was identified in two patients (P7,P8), based on a significant increase of the substrate of phenylalanine hydroxylase: phenylalanine, combined with a significant increase of the substrate/product ratio: the ratio of phenylalanine over tyrosine (Table 1, Figure 2) and normal pterines and neurotransmitters. The substrate/product ratio is very important for recognition of an IEM, as phenylalanine can also be increased due to a general surplus of amino acids. In Figure 2 it is shown that also one control sample has a significant increase of phenylalanine (Z-score 3.52), but it ranks at 38 only (pointing to many increased metabolites) and the phenylalanine/tyrosine ratio is much lower than in both patients (Z-score 2.82, rank 73), making a genetic defect causing the observed hyperphenylalaninaemia in this control sample unlikely. The affected gene in P7 is *PAH*, the affected gene in P8 is *DNAJC12*.

Lastly, hypermethioninaemia, an IEM characterized by demyelination and intellectual disability, is caused by a deficiency of methionine adenosyltransferase I. This IEM was correctly identified in three patients (P9-P11), based on a significant increase of methionine, the substrate of the deficient enzyme (Table 1, Figure 2). In two patients (P10, P11), homocysteine thiolactone was also increased, and in one patient (P11) S-adenosylmethionine, the enzyme's product, demonstrated a significant decrease (Table 1).

DISCUSSION

This is the first study using DI-HRMS for non-quantitative metabolomics in CSF. The method is fast, requires only 10 μ L of CSF and it correctly captures the biochemical profile of CSF in control samples. We could annotate 97% of the 331 metabolites that could occur endogenously (m/z 70–600) enlisted in HMDB as “detected and quantified in CSF”. The unselective nature of the method even allowed for annotation of 1811 mass peaks with metabolites that could occur endogenously, with a level of certainty of 2, according to the Metabolomics Standards Initiative.²⁷ Among the mass peaks with the highest median intensities were, as expected, mass peaks annotated with glucose, lactic acid, citric acid, glutamine, creatinine, ascorbic acid and creatine. In addition, we observed metabolite groups that were not reported in CSF before. Interestingly, several metabolites of the BCAA degradation pathway were also among the mass peaks with the highest median intensities. Ketoleucine and 3-methyl-2-oxoisovaleric acid (#16, isomers) are the direct products of reversible transamination of leucine and isoleucine, and alpha-ketoisovaleric acid (#27) is the direct product of reversible transamination of valine. These transaminations provide nitrogen for the concurrently occurring conversion of alpha-ketoglutarate into glutamate, an important neurotransmitter in the brain. Yudkoff recently reviewed these interactions of

the glutamine/glutamate cycle and the BCAA and keto acids in the central nervous system. BCAA transamination is responsible for approximately one third of glutamine synthesis, the latter part being provided by leucine.³³ The importance of this glutamate-BCAA cycle could explain the relative abundance of keto-acids in CSF.

Another set of metabolites found with relatively high median intensities were free fatty acid oxidation products as 4-hydroxy-2-nonenal. This metabolite is produced during peroxidation of omega-6-polyunsaturated fatty acids as arachidonic acid and linoleic acid.²⁵ It is considered to be a biomarker of lipid peroxidation *in vivo*.²⁵ Lipid peroxidation in the brain has been associated with many pathophysiological processes in a wide range of neurological disorders.²⁵ Therefore, the relative abundance of the free fatty acid oxidation products that we found in control samples might reflect the underlying neurological conditions in these patients that initially required additional investigations in CSF, and might not resemble the abundance of free fatty acid oxidation products of a truly healthy population.

The eight mass peaks of the HMDB list that we could not identify in this CSF series were molybdenum (m/z 96.9400), palladium (m/z 106.4200), triphosphate (m/z 257.9550), thiamine (m/z 265.3550), 8-isoprostane (m/z 280.5316), 7- and 8- dehydrocholesterol (m/z 384.6377), adenine diphosphate (m/z 427.2011) and guanosine diphosphate (m/z 443.2005). However, we repeatedly have identified all these mass peaks in plasma and dried blood spots (data available on request). Furthermore, in another CSF dataset we did identify palladium, triphosphate and 7- or 8-dehydrocholesterol, albeit with intensities just above the detection limit (data available on request). Thus, the reason for missing these metabolites is not in sample preparation, sample analysis or data processing, so it is most likely due to metabolite concentrations being just below the detection limit.

DI-HRMS metabolomics also correctly captured the biochemical profile of IEM patients. In all eleven included patients the known patient diagnosis was correctly identified, so we can conclude that these IEM biochemical profiles are accurately captured with our DI-HRMS workflow. However, a limitation of our study is the still limited set of patient samples and different IEM included in the study. It was not possible to test other IEM, due to limited availability of samples of – preferably untreated – patients with known IEM. We are open to receiving more samples for further validation.

We here demonstrate, that next to nuclear magnetic resonance, gas chromatography and liquid chromatography mass spectrometry,³¹ DI-HRMS is a suitable method to display the biochemical profile of CSF. In very limited amounts of patient material, only 10 μ L, we detect > 1,800 mass peaks, with metabolite concentrations ranging from millimolars for glucose (2.960 ± 1.110 mM³¹) to nanomolars for L-cysteine (58 nM²²) and methylguanidine (< 50 nM²¹). To our knowledge, mass peak identification in CSF to this extent has not been described before.

In theory, DI-HRMS based metabolomics in CSF can meet three main purposes: (1) NGMS, (2) biomarker identification and (3) identification of yet unknown IEM. A fourth potential application of CSF metabolomics is evaluation of treatment effects. We demonstrated that we captured both treatment (increase of arginine in a patient with argininosuccinic aciduria, treated with arginine) and treatment effects (normal succinylacetone in a patient with tyrosinaemia type I, treated with a tyrosine restricted diet and nitisinone). However, one should always weigh the expected benefit of this way of evaluating treatment effectiveness against the burden of a very invasive procedure, so we expect the use of CSF metabolomics for evaluation of treatment effectiveness only when specific information on the brain effect of treatment is needed. We expect that metabolomics in CSF will have most added value for

NGMS, for the identification of new biomarkers and for the identification of yet unknown IEM. For the identification of biomarkers for neurometabolic IEM for which a biochemical hallmark is not yet known, CSF samples of a cohort of patients with a specific IEM could be compared to control samples. In addition, for the identification of new biomarkers for neurometabolic IEM that are – biochemically – difficult to distinguish from another IEM, cohorts of patients with these IEM can be compared. Next to diagnostic purposes, identification of new biomarkers for neurometabolic IEM could elucidate pathophysiological mechanisms in neurometabolic IEM that are not yet fully understood.

To serve NGMS and the identification of yet unknown IEM, we anticipate that in patients suspected of a neurometabolic disease, metabolomics in CSF could hold additional information on increased and decreased metabolite annotations of many different metabolic pathways that might provide a diagnostic lead, for both known and yet unknown IEM. This diagnostic lead can subsequently be evaluated by targeted diagnostics, analysis of enzymatic activity and/or genetic testing. Thus, in summary, DI-HRMS metabolomics in CSF – as the closest possible read-out of body fluids of metabolite concentrations in the brain – could serve both improvements in metabolic diagnostics as well as it could provide new insights in pathophysiological mechanisms in neurometabolic IEM.

CONCLUSION

By correctly assigning a “most probable diagnosis” to all included patients harboring an IEM, we here demonstrate that direct-infusion based non-quantitative metabolomics accurately captures the biochemical profile of patients in CSF. This opens new ways for using metabolomics in CSF for NGMS, for biomarker identification in IEM, and for finding a diagnosis in the yet undiagnosed patients suspected of a neurometabolic disease.

WEB RESOURCES

HMDB
OMIM

<https://hmdb.ca>

<https://www.omim.org>

REFERENCES

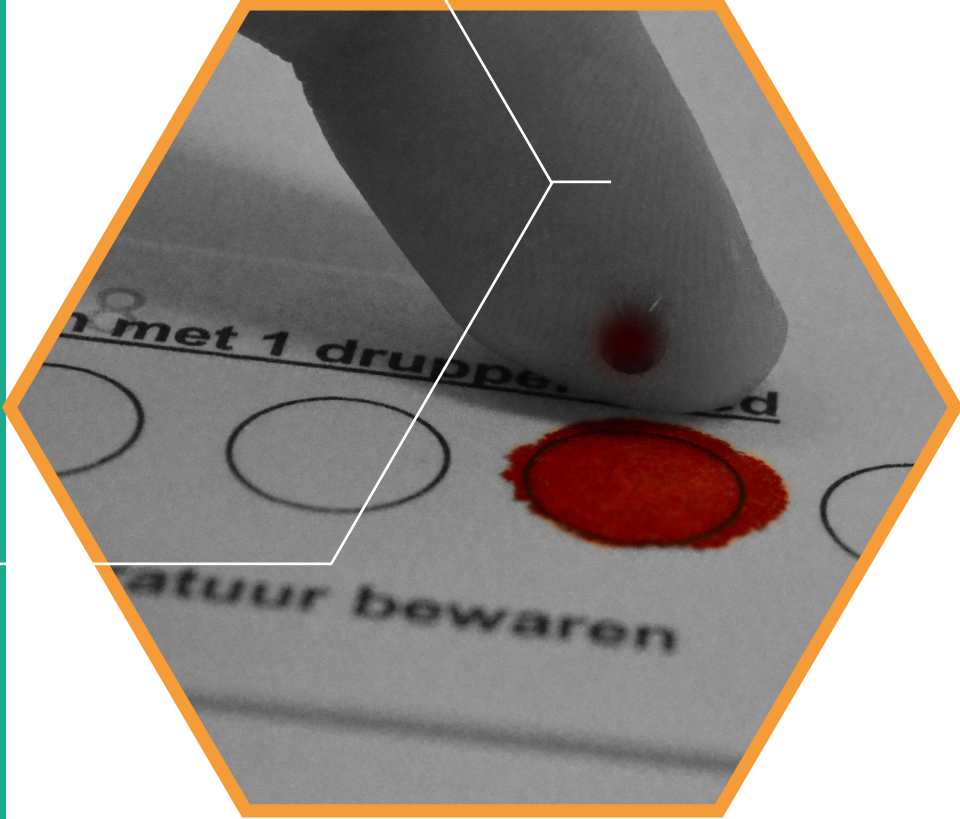
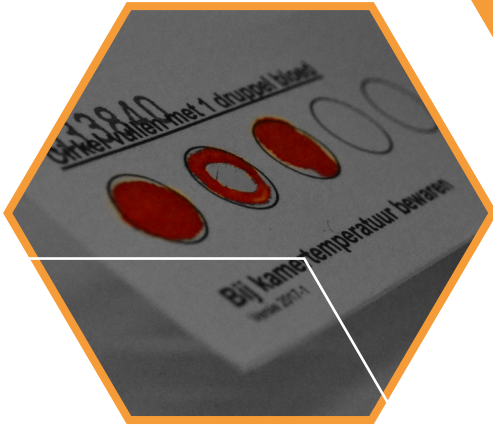
1. Abela L, Simmons L, Steindl K et al. N(8)-acetylspermidine as a potential plasma biomarker for Snyder-Robinson syndrome identified by clinical metabolomics. *J Inherit Metab Dis.* 2016;39:131-137.
2. Abela L, Spiegel R, Crowther LM et al. Plasma metabolomics reveals a diagnostic metabolic fingerprint for mitochondrial aconitase (ACO2) deficiency. *PLoS ONE* 2017;12.
3. Atwal PS, Donti TR, Cardon AL et al. Aromatic L-amino acid decarboxylase deficiency diagnosed by clinical metabolomics profiling of plasma. *Mol Genet Metab.* 2015;115:91-94.
4. Blasco H, Corcia P, Pradat PF et al. Metabolomics in cerebrospinal fluid of patients with amyotrophic lateral sclerosis: an untargeted approach via high-resolution mass spectrometry. *J Proteome Res.* 2013;12(8): 3746-3754.
5. Blasco H, Nadal-Desbarats L, Pradat PF et al. Untargeted 1H-NMR metabolomics in CSF: toward a diagnostic biomarker for motor neuron disease. *Neurology* 2014;82(13):1167-1174.
6. Cassol E, Misra V, Dutta A, Morgello S, Gabuzda D. Cerebrospinal fluid metabolomics reveals altered waste clearance and accelerated aging in HIV patients with neurocognitive impairment, *AIDS* 2014;28(11):1579-1591.
7. Coene KLM, Kluijtmans LAJ, van der Heeft E et al. Next-generation metabolic screening: Targeted and untargeted metabolomics for the diagnosis of inborn errors of metabolism in individual patients. *J Inherit Metab Dis.* 2018;41:337-353.
8. Couce ML, Boveda MD, Garcia-Jimenez C. et al. Clinical and metabolic findings in patients with methionine adenosyltransferase I/III deficiency detected by newborn screening. *Mol Genet Metab.* 2013;110(3):218-221.
9. Denes J, Szabo E, Robinette SL et al. Metabonomics of newborn screening dried blood spot samples: A novel approach in the screening and diagnostics of inborn errors of metabolism. *Anal Chem.* 2012;84:10113-10120.
10. Donti TR, Cappuccio G, Hubert L et al. Diagnosis of adenylosuccinate lyase deficiency by metabolomic profiling

- in plasma reveals a phenotypic spectrum. *Mol Genet Metab Rep.* 2016;8:61-66.
11. Grinton KE, Benke PJ, Lines MA et al. Disturbed phospholipid metabolism in serine biosynthesis defects revealed by metabolomic profiling. *Mol Genet Metab.* 2018;123:309-316.
 12. Gonzalo H, Brieval L, Tatzber F et al. Lipidome analysis in multiple sclerosis reveals protein lipoxidative damage as potential pathogenic mechanism. *J. Neurochem.* 2012;123(4):622-634.
 13. Haijes HA, Willemsen M, van der Ham M et al. Direct-infusion based non-quantitative metabolomics identifies metabolic disease in patients' dried blood spots and plasma. *Metabolites* 2019;9:12.
 14. Karlikova R, Micova K, Najdekr L et al. Metabolic status of CSF distinguishes rats with tauopathy from controls. *Alzheimers Res Ther.* 2017;9(1):78.
 15. Kennedy AD, Pappan KL, Donti TR et al. Elucidation of the complex metabolic profile of cerebrospinal fluid using an untargeted biochemical profiling assay. *Mol Genet Metab.* 2017;121(2):83-90.
 16. Lamour SD, Alibu VP, Holmes A, Sternberg JM. Metabolic profiling of central nervous system disease in *Trypanosoma brucei rhodesiense* infection. *J Infect Dis.* 2017;216(10):1273-1280.
 17. Malvagia S, Haynes CA, Grisotto L et al. Heptadecanoylcarnitine (C17) a novel candidate biomarker for newborn screening of propionic and methylmalonic acidemias. *Clin Chim Acta* 2015;450:342-348.
 18. Mason S, Reinecke C, Solomons R et al. Cerebrospinal fluid amino acid profiling of pediatric cases with tuberculous meningitis. *Front Neurosci.* 2017;11:534.
 19. Miller MJ, Kennedy AD, Eckhart AD et al. Untargeted metabolomic analysis for the clinical screening of inborn errors of metabolism. *J Inherit Metab Dis.* 2015;38:1029-1039.
 20. Miller MJ, Bostwick BL, Kennedy AD, Donti TR, Sun Q, Sutton VR, Elsea SH. Chronic oral L-carnitine supplementation drives marked plasma TMAO elevations in patients with organic acidemias despite dietary meat restrictions. *JIMD Rep.* 2016;30:39-44.
 21. Mizutani N, Hayakawa C, Ohya Y, Watanabe K, Watanabe Y, Mori A. Guanidino compounds in hyperargininaemia. *Tohoku J Exp Med.* 1987;153(3):197-205.
 22. Obeid R, Kasoha M, Knapp JP, Kostopoulos P, Becker G, Fassbender K, Herrmann W. Folate and methylation status in relation to phosphorylated tau protein (181P) and beta-amyloid (1-42) in cerebrospinal fluid. *Clin Chem.* 2007;53(6):1129-1136.
 23. Peretz H, Watson DG, Blackburn G et al. Urine metabolomics reveals novel physiologic functions of human aldehyde oxidase and provides biomarkers for typing xanthinuria. *Metabolomics* 2012;8:951-959.
 24. Pieragostino D, D'Alessandro M, di Iorio M et al. An integrated metabolomics approach for the research of new cerebrospinal fluid biomarkers of multiple sclerosis. *Mol BioSyst.* 2015;11(6):1563-1572.
 25. Shichiri M. The role of lipid peroxidation in neurological disorders. *J Clin Biochem Nutr.* 2014;54(3):151-160.
 26. Stoessel D, Schulte C, Teixeira Dos Santos MC et al. Promising metabolite profiles in the plasma and CSF of early clinical Parkinson's disease. *Front Aging Neurosci.* 2018;10:51.
 27. Sumner LW, Amberg A, Barrett D et al. Proposed minimum reporting standards for chemical analysis Chemical Analysis Working Group (CAWG) Metabolomics Standards Initiative (MSI). *Metabolomics* 2007;3:211-221.
 28. van Karnebeek CD, Bonafe L, Wen XY et al. NANS-mediated synthesis of sialic acid is required for brain and skeletal development. *Nat Genet.* 2016;48(7):777-784.
 29. Venter L, Lindeque Z, Jansen van Rensburg P, van der Westhuizen F, Smuts I, Louw R. Untargeted urine metabolomics reveals a biosignature for muscle respiratory chain deficiencies. *Metabolomics* 2015;11:111-121.
 30. Wikoff WR, Gangoiti JA, Barshop BA, Siuzdak G. Metabolomics identifies perturbations in human disorders of propionate metabolism. *Clin Chem.* 2007;53:2169-2176.
 31. Wishart DS, Lewis MJ, Morrissey JA et al. The human cerebrospinal fluid metabolome. *J Chromatogr B Analyt Technol Biomed Life Sci* 2008;871(2):164-173.
 32. Wishart DS, Jewison T, Guo AC et al. HMDB 3.0 – The Human Metabolome Database in 2013. *Nucleic Acids Res.* 2013;41:801-807.
 33. Yudkoff M. Interactions in the metabolism of glutamate and the branched-chain amino acids and ketoacids in the CNS. *Neurochem Res.* 2017;42:10-18.

SUPPLEMENTAL DATA

Table S1. Mass peaks corresponding to endogenous metabolites identified in cerebrospinal fluid

Due to its size, this table is only available online.



Untargeted metabolomics for metabolic diagnostic

**screening with automated data interpretation using a
knowledge-based algorithm**

*International Journal of Molecular Sciences 2020, 21(3)
DOI: 10.3390/ijms21030979*

Hanneke A. Haijes*, Maria van der Ham, Hubertus C.M.T. Prinsen,
Melissa H. Broeks, Peter M. van Hasselt,
Monique G.M. de Sain-van der Velden,
Nanda M. Verhoeven-Duif, Judith J.M. Jans*

* Corresponding authors

ABSTRACT

Background: Untargeted metabolomics may become a standard approach to address diagnostic requests, but, at present, data interpretation is very labor-intensive. To facilitate its implementation for metabolic diagnostic screening, we developed a method for automated data interpretation that preselects the most likely inborn errors of metabolism (IEM).

Methods: A knowledge-based algorithm was developed for 119 different IEM. Input parameters were (1) weight scores assigned to 268 unique metabolites based on literature and expert opinion, and (2) metabolite Z-scores and ranks based on direct-infusion high resolution mass spectrometry. The output was a ranked list of differential diagnoses (DD) per sample. The algorithm was first optimized using a training set of 110 dried blood spots (DBS) comprising 23 different IEM and 86 plasma samples comprising 21 different IEM. Further optimization was performed using a set of 96 DBS consisting of 53 different IEM. The diagnostic value was validated in a set of 115 plasma samples including 58 different IEM.

Results: In the validation set, the correct diagnosis was included in the DD in 72% of the samples, comprising 44 different IEM. The median length of the DD was 10 IEM, and the correct diagnosis ranked first in 37% of the samples.

Discussion: We demonstrate the accuracy of the diagnostic algorithm in preselecting the most likely IEM, based on untargeted metabolomics of a single sample. We show as a proof of principle that automated data interpretation has the potential to facilitate implementation of untargeted metabolomics for metabolic diagnostic screening, and we provide suggestions for further optimization of the algorithm, to improve diagnostic accuracy.

KEY MESSAGE

Automated interpretation of untargeted metabolomics data could potentially facilitate implementation of untargeted metabolomics for metabolic diagnostic screening.

INTRODUCTION

Untargeted metabolomics is readily finding its way into the metabolic diagnostic laboratory. In the near future, next-generation metabolic screening (NGMS) through untargeted metabolomics may become the preferred approach to address diagnostic requests for patients referred to the metabolic diagnostic laboratory for basic metabolic screening, as advocated by studies that demonstrated the diagnostic value of untargeted metabolomics for NGMS.¹⁻⁴ However, data interpretation of untargeted metabolomics analyses is labor-intensive, due to the extensive amounts of data that are generated, the non-quantitative nature of the data, the lack of metabolite reference ranges and the large number of metabolite alterations of which the diagnostic significance remains to be elucidated.¹⁻⁴ This prevents metabolic laboratories from implementing a potentially powerful technique for NGMS.

In addition, most untargeted metabolomics analyses are developed to detect hydrophilic, small-molecule metabolites, in either plasma,¹⁻³ dried blood spots (DBS)³ or cerebrospinal fluid (CSF).⁴ Therefore, these methods are currently only capable of correctly identifying inborn errors of metabolism (IEM) with hydrophilic small-molecule biomarkers in blood or CSF.¹⁻⁴ Many IEM, such as several lysosomal and peroxisomal disorders, lack these types of biomarkers and thus, these IEM cannot be detected (yet) using these methods. For this reason it is not yet possible to exclude all IEM based on current NGMS methods.

To facilitate further implementation of untargeted metabolomics as NGMS method, we developed an automated data interpretation approach that preselects the most likely IEM, by designing a knowledge-based algorithm. As a proof of principle, we here demonstrate its diagnostic value.

METHODS

Development of an IEM-panel and automated data interpretation

We developed a diagnostic knowledge-based algorithm. The first input parameter for this algorithm was an “expected library”, consisting of current knowledge about metabolite alterations for the IEM included in the IEM panel. The second input parameter, here called “observed”, consisted of the results of the untargeted metabolomics method. The output of the algorithm was a ranked list of differential diagnoses (DD), per patient sample. An overview of the algorithm is visualized in Figure 1.

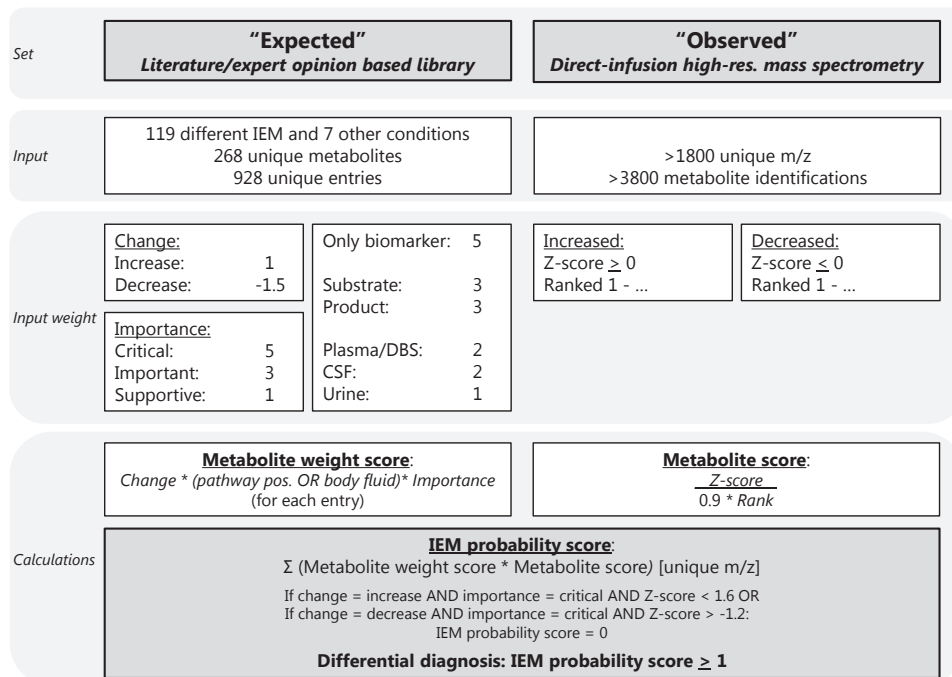
The algorithm, including the expected library, was developed in six phases (Figure 2). First, a preliminary version of the algorithm was developed, followed by testing of the diagnostic value using a training set containing both DBS and plasma samples. Next, the algorithm was further optimized, again followed by testing of the diagnostic value, now using an optimization set of DBS samples. Finally, the algorithm was again optimized, followed by a final assessment of the preselection accuracy using a validation set consisting of plasma samples (Figure 2). All presented results were determined using the final version of the algorithm (Figure 2).

Patient inclusion

IEM of interest for this study were IEM with one or more known small-molecule biomarkers in blood (Table S1). This included mainly disorders of nitrogen-containing compounds, disorders of vitamins, cofactors, metals and minerals, disorders of carbohydrates and disorders of lipids, according to the nosology of Ferreira et al. (Table S1).⁵

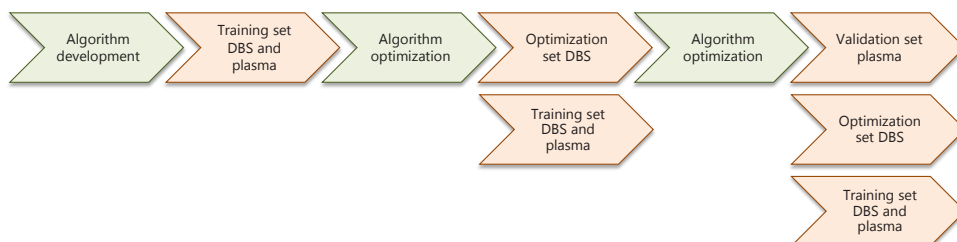


Figure 1. Overview of the diagnostic algorithm



Abbreviations: CSF: cerebrospinal fluid; DBS: dried blood spots; IEM: inborn error of metabolism; m/z: mass to charge ratio.

Figure 2. Flowchart of the six phases of the development and optimization of the diagnostic algorithm with in-between assessments of the performance of the algorithm in the training sets, DBS optimization set and plasma validation set



Abbreviations: DBS: dried blood spots.

Patients affected with these IEM were included when at least one remnant DBS or plasma sample was available in the metabolic diagnostic laboratory of the University Medical Centre Utrecht. All patients or their legal guardians approved the possible use of their remaining samples for method validation, in agreement with institutional and national legislation. All followed procedures were in accordance with the ethical standards of the University Medical Centre Utrecht and with the Helsinki Declaration of 1975, as revised in 2000.

Sample inclusion

Up to three samples per patient per IEM were included in each sample set. The training set consisted of the samples that were used for the development of our previously published untargeted metabolomics method.³ This set included 110 DBS of 42 patients harboring 23 different IEM and 86 plasma samples of 38 patients harboring 21 different IEM. In addition, this set included 105 DBS of 30 individuals and 84 plasma samples of 28 individuals that served as control samples, defined as samples from individuals in whom an IEM was excluded after a thorough routine diagnostic work-up.³ All included samples are listed in Table S2 (Table S2).

For the DBS optimization and for the plasma validation set, one sample per patient per IEM was included. Preferably, samples of patients who did not receive relevant treatment at time of sampling were selected. When these samples were not available, samples were selected in which metabolite alterations diagnostic for an IEM were measured by targeted diagnostics before inclusion. The DBS optimization set consisted of 96 DBS of 96 patients harboring 53 different IEM. This set also included 66 DBS of 48 individuals that served as control samples. None of the patient DBS samples included in the optimization set were included in the training set. The plasma validation set included 115 plasma samples of 115 patients harboring 58 different IEM, and 83 plasma samples of 28 individuals that served as control samples. None of the patient plasma samples included in the validation set were included in the training set. Control samples of the optimization and validation sets were identical to the control samples used in the training set. All included samples are listed in Table S2 (Table S2).

Input parameter: expected library

Based on extensive literature research, the Online Mendelian Inheritance in Man (OMIM), IEMbase version 1.4.3, the database of the Metabolic and Genetic Information Center and expert opinions of four trained laboratory specialists, a database was constructed containing the expected metabolite alterations of 268 unique metabolites, assigned to 119 different IEM and 7 other common conditions and interferences, with a total of 928 entries (Figure 1, Table S1). These other conditions and interferences included liver failure, renal failure, fasting, hemolysis, prolonged plasma storage, dietary cobalamin deficiency and folate deficiency (Table S1). For each of the 119 IEM we noted the following: disease category and disease group according to the nosology of Ferreira et al.,⁵ disease, gene and protein function; the OMIM number including a link; a link to the clinical phenotype from the Human Phenotype Ontology; the estimated incidence of the disease, which was retrieved from OMIM, Orphanet and from literature research and we noted an artefact disclaimer, which describes potential artefacts that might cause alterations of the diagnostic metabolites (Table S1). Each of the 928 metabolite entries contained the metabolite name; the Human Metabolome Database (HMDB) code⁶ including a link; the mass to charge ratio (m/z); whether there were any endogenous isomers for the compound; the names of the endogenous isomers; and the expected metabolite alteration (increased or decreased) (Table S1). In addition, we also noted the following information per metabolite entry: in which body fluid the metabolite alteration is known to occur; whether the metabolite is either a substrate or product of the affected enzyme; whether the metabolite is the only known biomarker; whether the metabolite is known to be increased or decreased; and the importance of the metabolite alteration (Table S1).



A metabolite alteration in either plasma, DBS or CSF was considered more important than a metabolite alteration in urine, as the algorithm was optimized and tested for plasma and DBS samples. Therefore, plasma, DBS and CSF were assigned a value of 2 and urine was assigned a value of 1 (Figure 1). To ensure that the most important metabolites are correctly valued, metabolites that were products or substrates of the affected enzymes were valued 3, and metabolites that were the only biomarker of the IEM were valued 5 (Figure 1, Table S1). To ensure that decreases, which are often more subtle than increases, were properly valued, an increase was valued 1 and a decrease was valued -1.5 . Lastly, the importance of the metabolite alteration for the IEM diagnosis was noted in three categories: supportive was valued 1, important influence was valued 3 and critical was valued 5 (Figure 1, Table S1). Metabolite alterations considered to be critical for the diagnosis were labelled as indispensable for the diagnosis, indicating that when, for example, a decrease of serine is considered critical for the diagnosis of a serine deficiency, a serine deficiency cannot be in the DD if no decrease of serine is observed (Figure 1, Table S1).

Input parameter: observed metabolite alterations using untargeted metabolomics

Sample collection, sample preparation and untargeted metabolomics analysis were performed as previously described.³ In short, direct-infusion high resolution mass spectrometry was performed using a TriVersa NanoMate system (Advion, Ithaca, NY, USA) controlled by Chipsoft software (version 8.3.3, Advion), mounted onto the interface of a Q-Exactive high-resolution mass spectrometer (Thermo Scientific™, Bremen, Germany). For each sample, technical triplicates were analyzed, infusing each sample three times into the mass spectrometer. Scan range was 70 to 600 m/z in positive and negative mode. Mass peak annotation was performed by matching the m/z value of the mass peak with a range of two parts per million to monoisotopic metabolite masses present in the HMDB, version 3.6.⁶ Annotations of metabolites that can occur endogenously were selected: $>1,800$ unique m/z per batch, corresponding to $>3,800$ metabolite identifications, in line with previous analyses.^{3,4} For each mass peak per patient sample, the deviation from the intensities in the control samples was indicated by a Z-score, calculated by: $Z\text{-score} = (\text{intensity patient sample} - \text{mean intensity control samples}) / \text{standard deviation intensity control samples}$. Z-scores were calculated for both patient and control samples. For each sample, positive Z-scores were ranked from the maximum Z-score to zero (the highest Z-score observed ranked at position 1), and negative Z-scores were ranked from the minimum Z-score (ranking at 1) to zero (Figure 1).

Automated data interpretation

Automated data interpretation was performed as follows: for each metabolite entry in the expected library a “metabolite weight score” was calculated. This score was the product of the weights for increase (1) or decrease (-1.5); only biomarker (5), substrate or product (3), plasma, DBS or CSF (2) or urine (1); and critical (5), important (3) or supportive (1) (Figure 1, Table S1). In addition, for all observed metabolite alterations measured by direct-infusion high-resolution mass spectrometry a “metabolite score” was calculated as follows: $Z\text{-score} / (\text{rank} * 0.9)$, as the rank was considered slightly less important than the Z-score. Next, for each of the 119 IEM and 7 other conditions or interferences, an “IEM probability score” was calculated, summing the product of the metabolite weight score and the metabolite score for all metabolite entries with a unique m/z :

$$IEM \text{ probability score} = \sum_{\text{unique } m/z} \left(\text{weight score} \times \frac{Z - \text{score}}{\text{rank} * 0.9} \right)$$

After the calculation of the IEM probability score, two scenarios were considered: 1) when a metabolite expected to be increased and considered critical for the diagnosis, was not found increased (defined as Z-score < 1.6), the IEM probability score was set to zero, and likewise, 2) when a metabolite expected to be decreased and considered critical for the diagnosis, was not decreased (defined as Z-score > -1.2), the IEM probability score was also set to zero (Figure 1).

All 119 IEM included in this algorithm, as well as the 7 common conditions and interferences, were classified based on the IEM probability score. An IEM was considered “very likely” when the IEM probability score was >50, “likely” when >10 and ≤50, “possible” when >1 and ≤10, “unlikely” when >0 and ≤1 and “very unlikely” when ≤0. The DD consisted of IEM classified as “very likely”, “likely” or “possible”, corresponding to an IEM probability score of ≥1 (Figure 1).

All arbitrary assigned values used in the diagnostic algorithm, including the metabolite weight scores, the consideration of the metabolite rank with factor 0.9, the Z-score cut-off values of < 1.6 and > -1.2 and the ranges for the probability scores were defined based on trial and error in the algorithm development phase (Figure 2), by trying to achieve optimal results using both the DBS and plasma training sets.

R Shiny app to aid automated data interpretation

To aid the use of the diagnostic algorithm, an R Shiny application was developed. The expected library and the data file containing the untargeted metabolomics results were used as input files. The output of the application was an interface wherein a sample and an IEM in the DD can be selected. The calculations of the algorithm could be demonstrated for each sample and for each IEM in the DD. The R code for the R Shiny application is available in the Supplementary Information. The results of the untargeted metabolomics analysis of all IEM and control samples analyzed in the test, optimization and validation sets are available in Table S3-S8.

RESULTS

Training and optimization sets, patient samples

Automated data interpretation resulted in the correct diagnosis being present in the DD in 78% of the 110 DBS samples in the training set and in 79% of the 86 plasma samples in the training set (Table 1, Table S2). The correct diagnosis ranked first in 42% (DBS) and 33% (plasma) of the samples, and the median lengths of the DD were 8 (DBS) and 12 (plasma) IEM (Table 1, Table S2). In the DBS training set, the correct diagnosis was absent in the DD in 24 samples of 12 patients harboring 9 IEM (Table S2). For each sample, the reason for not correctly preselecting the diagnosis is explained in Table S2. In 14/24 samples this was due to the sample selection: the sample was drawn when the patient was under treatment and the diagnostic biochemical alterations had normalized. In 5/24 samples this was as a result of the detection method: Z-scores were in the normal range while targeted analyses demonstrated the presence of – often subtle – diagnostic biochemical alterations. In another 5/24 samples this was caused by a combination of sample selection and the method: targeted analyses showed only mild biochemical alterations, resulting in normal



Z-scores (Table S2). In the plasma training set, the correct diagnosis was not in the DD in 18 samples of 11 patients harboring 8 IEM (Table S2). In line with the missed diagnoses in DBS, this was either due to the sample selection (7/18), the method (8/18) or by a combination thereof (3/18) (reasons listed in Table S2).

In the DBS optimization set, automated data interpretation resulted in the correct diagnosis in the DD in 71% of the 96 samples (Table 1), including 38 different IEM of which 19 IEM were not included in the DBS training set (Table S2). The correct diagnosis ranked first in 40%, and the median length of the DD was 8 IEM (Table 1, Table S2). The correct diagnosis was not in the DD in 28 samples of 28 patients harboring 20 IEM (and reasons for not correctly preselecting these diagnoses were listed in Table S2 (Table S2). These reasons included the diagnostic algorithm (1/28), a combination of the algorithm and the method (4/28), the method (14/28) and a combination of sample selection and the method (2/28). For 7/28 samples the reason for missing the correct diagnosis was not known, as the diagnostic metabolites that the algorithm is based on were not quantified using targeted analyses (Table S2).

Table 1. Performance automated data interpretation for patient sample sets

	Training sets		Optimization set	Validation set
	DBS	Plasma	DBS	Plasma
Matrix				
Samples	110	86	96	115
Patients	42	38	96	115
IEM	23	21	53	58
Correct IEM in DD (<i>n</i> ; %)	86/110; 78%	68/86; 79%	68/96; 71%	83/115; 72%
Correct IEM in top 3 of DD (<i>n</i> ; %)	74/110; 67%	36/86; 42%	60/96; 63%	65/115; 57%
Correct IEM ranked first (<i>n</i> ; %)	46/110; 42%	28/86; 33%	38/96; 40%	43/115; 37%
Length DD (median; [5 th -95 th])	8; [2–14]	12; [3–25]	8; [1–23]	10; [3–22]

Abbreviations: 5th: fifth percentile; 95th: ninety-fifth percentile; DBS: dried blood spots; DD: differential diagnosis; IEM: inborn error of metabolism; *n*: total number.

Validation set, patient samples

In the plasma validation set, automated data interpretation included the correct diagnosis in the DD in 72% (Table 1), comprising 44 different IEM of which 24 IEM were not included in the plasma training set. The correct diagnosis ranked first in 37% of the samples and top 3 in 57% of the samples, and the median length of the DD was 10 IEM (Table 1). In 32 samples of 32 patients harboring 21 IEM, the diagnosis was not in the DD (Table S2). This was either due to the diagnostic algorithm (10/32) to a combination of the method and the algorithm (3/32), to the method (12/32) or to the sample selection (1/32). For 6/32 samples the reason for missing the correct diagnosis could not be determined, as the diagnostic metabolites that the algorithm is based on were not quantified using targeted analyses (all reasons have been explained in Table S2). Proposed further changes to the expected library based on the results of the validation set, as listed in Table S2, could improve the diagnostic yield of the algorithm to 77%, as they would result in the correct diagnosis in the DD in another 6 samples, comprising 4 IEM (demonstrated in Table S2, Patient validation set plasma).

Performance assessment of all patient samples

Automated data interpretation included the correct diagnosis in the DD in 75% (*n* = 305/407 of all included patient samples), comprising 53 different IEM. The correct diagnosis ranked first in 26% (*n* = 155/407) and top 3 in 59% (*n* = 240/407) of the patient samples. The categories storage disorders and disorders of peroxisomes and oxalate had a true positive

rate of 100%, but both these categories only included two samples (Table S2). The diagnostic algorithm performed best among disorders of nitrogen-containing compounds and among disorders of lipids (80.3% and 79.8% true positive samples, respectively). The algorithm performed worse among the other common conditions and interferences, mitochondrial disorders of energy metabolism and among disorders of carbohydrates (Table S2).

Control samples

For control samples, the median length of the DD was 2 IEM for DBS in both the training and optimization set, and 3 IEM for plasma in both the training and validation set (Table 2). In control DBS samples, IEM that were frequently noted in the DD of the training and optimization sets included aromatic L-amino acid decarboxylase deficiency ($n = 17/171$), Hartnup disorder ($n = 12/171$) and the condition “fasting” ($n = 11/171$) (Table S2). In control plasma samples, IEM that frequently arose in the DD of the training and validation sets included Hartnup disorder ($n = 23/167$), 3-phosphoserine phosphatase deficiency ($n = 20/167$) and the condition “fasting” ($n = 20/167$) (Table S2). None of the individuals whose samples were selected as control samples experienced any clinical problems that could in retrospect be related to any of the IEM included in the DD of these patients.

R Shiny app to aid insight in automated data interpretation

The accessibility of the R Shiny app that was developed is demonstrated in Video S1. This video shows how the app provides an interface to select patient samples and IEM in the DD, in order to see how the data was valued, which data was valued, and how the DD was created in the automated data interpretation (Video S1).



Table 2. Performance automated data interpretation for control sample sets

	Training sets		Optimization set	Validation set	
	DBS	Plasma	DBS	Plasma	
Matrix					
Samples	105	84	66	83	
Individuals	30	28	48	28	
Length DD (median; [5 th –95 th])	2; [0–12]	3; [0–11]	2; [0–8]	3; [0–10]	

Abbreviations: 5th: fifth percentile; 95th: ninety-fifth percentile; DBS: dried blood spots; DD: differential diagnosis.

DISCUSSION

New all-encompassing technologies, such as untargeted metabolomics, are finding their way to clinical applications. Interpretation of the extensive data sets, however, is laborious and should preferably be automated. Here, we provide a proof of principle, demonstrating that automated data interpretation using a knowledge-based algorithm has added value in the diagnostic use of untargeted metabolomics. The algorithm that we developed correctly reduces a list of 119 IEM and 7 other conditions and interferences to a DD consisting of approximately 10 IEM, in 72% of the plasma samples. In 37% of the samples, the correct diagnosis ranked first and in 57% of the samples, the correct diagnosis ranked top 3. As expected, the diagnostic algorithm performs best among disorders of nitrogen-containing compounds and disorders of lipids, achieving a true positive rate of approximately 80%. Moreover, we showed that we were able to correctly preselect 44 different IEM, very rapidly and based on only one sample. Interestingly, in the DBS optimization set and in the plasma validation set, respectively 19 and 24 IEM were correctly preselected while these IEM were not included in the training set. This demonstrates that even without prior testing, IEM can be correctly preselected by the diagnostic algorithm, solely based on literature and expert

knowledge on diagnostic metabolite alterations.

We envision that interpretation of the preselection that the diagnostic algorithm provides, should be performed by trained laboratory specialists, in line with the current workflow for results of targeted diagnostic platforms. Provided that these laboratory specialists are specialized in IEM, they can appraise the significance of the observed biochemical alterations, and relate them to the patient's phenotype, in order to judge for each IEM in the DD whether the clinical phenotype potentially fits the diseases, and whether this IEM should indeed be considered as a diagnosis in the patient. Based on this judgement, laboratory specialists could recommend second-tier tests, to confirm or refute IEM in the DD.

Many IEM share the same biomarker or set of biomarkers critical for the diagnosis. However, as the specific defect varies between these IEM, other metabolites have the potential to corroborate a certain diagnosis, although these metabolites are in general not able to confirm or refute a diagnosis with absolute certainty. This is exemplified by disorders of the phenylalanine and tetrahydrobiopterin metabolism. We included three IEM, all characterized by an increase of phenylalanine: phenylketonuria, dihydropteridine reductase deficiency and DNAJC12 deficiency (Table S2). All disorders of the phenylalanine and tetrahydrobiopterin metabolism are present in the DD of the included samples, as none of the additional metabolites are able to confirm or refute a diagnosis with certainty. However, these metabolites can provide supportive evidence to corroborate a diagnosis. In the DD of all these samples, phenylketonuria ranks first, as the weight of phenylalanine in this IEM is the highest (Table S1). However, a decrease of homovanillic acid (Z-score 2.95, rank 3) in P038.1 with dihydropteridine reductase deficiency and a decrease of 5-hydroxyindoleacetic acid (Z-score -1.64, rank 24) in P070.1 with DNAJC12 deficiency, ensure that in both these samples DNAJC12 deficiency ranks second and dihydropteridine reductase deficiency ranks third. In contrast, in samples of patients with phenylketonuria, these metabolites were normal and DNAJC12 deficiency and dihydropteridine reductase deficiency can also rank fourth or fifth. This example demonstrates that next to the main biomarker(s) for a disease, additional biomarkers – captured by untargeted metabolomics and considered by the diagnostic algorithm – can support the likeliness of a certain diagnosis.

For a first-tier test for patients referred for basic metabolic screening, a diagnostic value of ~70% of the preselection algorithm for untargeted metabolomics is still insufficient. However, routine targeted basic metabolic diagnostic screening, the current gold standard for metabolic diagnostics, is not perfect either, as IEM diagnoses can be overlooked as well when only assessing a selection of biomarkers in a single blood sample. This imperfection of the current gold standard is corroborated by the annual report of 2017 of the European Research Network for evaluation and improvement of screening, Diagnosis and treatment of Inherited disorders of Metabolism, that reports that 82.9% of participating laboratories obtained satisfactory performance in all of the external quality assessment schemes they participated in.⁷ False-negative findings of the diagnostic algorithm, i.e. IEM that were incorrectly left out of the IEM preselection in the DBS optimization set and the plasma validation set, were for example galactosaemia type I and methyltetrahydrofolate reductase deficiency (Table S2). For galactosaemia type I this is most likely due to the fact that in direct infusion, an observed m/z can account for multiple metabolite annotations, since metabolites can have multiple isomers. In general, this does not result in any data interpretation problems or incorrect diagnoses, since most m/z are dominated by a single metabolite of significant abundance.³ However, the m/z of galactose and galactose-1-phosphate are most likely dominated by glucose and glucose-1-phosphate, thereby masking the increases of

galactose and galactose-1-phosphate. The reason for not including methyltetrahydrofolate reductase deficiency in the DD is that a methanol-based sample extraction only captures the unbound fraction of homocysteine, which is not an accurate representation of the total homocysteine concentration in blood.³

Conversely, some IEM in the DD of control samples were more common than others (Table S2). These IEM could be considered false-positive findings. However, slight alterations of amino acids, organic acids and acylcarnitines that do not correspond to any specific IEM diagnosis are also frequently detected using routine targeted basic metabolic diagnostic screening, but these insignificant findings in general do not cause any diagnostic dilemmas. The diagnostic algorithm frequently included aromatic L-amino acid decarboxylase deficiency. The presence of this IEM in the DD might be an artefact caused by the use of L-Dopa, which is frequently used in pediatric patients for its inotropic function. We noted this potential artefact in the “artefact disclaimer” (Table S1). Likewise, for Hartnup disorder we noted in the artefact disclaimer that this disease is caused due to a defective urinary transporter, and that this disease is hard, although not impossible (Table S2, Plasma validation set, Patient P054.1), to detect in blood (Table S1). Also, the diagnosis of Hartnup disorder, as well as those of fasting and malnutrition and serine synthesis defects are mainly based on amino acid decreases. The frequent detection of amino acid decreases is explained by the fact that many samples were drawn when patients were in a fasting state and like in targeted diagnostics, this is not expected to cause any diagnostic dilemmas.

A limitation of this study comprises the sample selection. The algorithm was designed using both DBS and plasma samples that were also used for the development of our method.³ With the aim to validate the designed algorithm, DBS and plasma samples were collected for the validation set. However, during the analysis of the DBS validation samples, it was noted that more optimization could be done that would improve the algorithm to a significant extent. It was then decided that the DBS set would serve as optimization set, and that the plasma sample set would serve as final validation set. Ideally, one would collect a new DBS validation set, but due to the rarity of IEM and considering the preference for samples drawn when patients were not under treatment, this was not feasible. In addition, although a sample size of 407 IEM samples is impressive, a sample size of 3 samples per IEM is rather small. For more common IEM, more samples were available, but it was decided to not include these samples as inclusion would skew the robustness of the model, since these IEM would influence the model more than rarer IEM. Lastly, despite a sample size of 407 IEM samples, we were not able to validate the preselection accuracy of the diagnostic algorithm for every IEM included in the IEM panel, since we did not have samples of all IEM. Based on a thorough analysis of the successes and failures of the diagnostic algorithm, we propose six ways to further improve the robustness of the diagnostic algorithm. First, we advocate (1) expanded testing of the algorithm, also including samples of IEM that were not tested yet, and subsequent further optimization of the algorithm including the proposed changes in Table S2 (Table S2, Patient validation set plasma). The potential value of expanded testing is exemplified by carbamoylphosphate synthase I deficiency. This IEM was not incorporated in the training or optimization sets, but only in the validation set. In the expected library, an increase of L-glutamine was considered indispensable for the diagnosis. However, this resulted in missing this IEM in the preselection, while changing the importance of L-glutamine from critical to important influence resulted in correct inclusion of this diagnosis in the DD (Table S2, Patient validation set plasma). We showed that the proposed further changes to the expected library based on the results of the validation



set, could theoretically improve the diagnostic yield of the algorithm to 77% (Table S2, Patient validation set plasma), corroborating that the algorithm can be further optimized by expanded testing of additional IEM samples. Second, to reduce the number of false-negative findings, we suggest (2) investigating whether a metabolite-specific Z-score cut-off value for increases and decreases could lead to a reduction of the DD provided by the algorithm. For most diagnostic metabolites a higher Z-score cut-off value than 1.6, or lower than -1.2, would increase the specificity of the algorithm. However, accurate implementation of this improvement requires expanded testing of the range of metabolite increases per IEM for common IEM as well as for rarer IEM, requiring a large sample size per IEM. Third, (3) the addition of phenotypic data to the algorithm could theoretically lead to a reduction of the DD provided by the algorithm. Computational phenotype analysis has been proven successful in exome prioritization^{8,9} and is likely to also have great potential for prioritization of IEM, provided that a patient's phenotype is described as comprehensively as possible. Fourth, we support the (4) addition of biomarkers that are identified by untargeted metabolomics studies to the library^{3,10-13}, (5) inclusion of additional⁵ or newly discovered IEM and (6) testing of the algorithm in other body fluids, like CSF⁴ or urine.¹⁴

An important strength of our study is that the diagnostic algorithm is based on an IEM panel. In line with gene panels in genetic screening approaches, this could facilitate a conclusion such as "NGMS did not reveal any indication of an IEM included in the IEM panel", provided that the diagnostic value is sufficiently high. A second strength of the diagnostic algorithm is its independence of the type of untargeted metabolomics method that is used. Any metabolic diagnostic laboratory can test, use and improve the diagnostic algorithm, as long as metabolite identification can be converted to HMDB codes⁶ and metabolite intensities can be converted to Z-scores. Moreover, the development of the R Shiny application ensures that we can present the algorithm as an easily accessible diagnostic tool for NGMS. In addition, since the number of known IEM is expanding with unprecedented pace,⁵ and in parallel, the number of potential biomarkers for IEM as well,^{3,10-13} it gets increasingly hard for laboratory specialists to keep knowledge up-to-date. The expected library, which serves as the input for the diagnostic algorithm, can be easily expanded with newly discovered IEM as well as new biomarkers, provided that markers included in the library are validated and that the algorithm can correctly preselect the IEM in a patient sample.

CONCLUSION

In conclusion, we here demonstrate as a proof of principle that a diagnostic algorithm can correctly reduce a differential diagnosis of 119 IEM and 7 other conditions and interferences, to a median of 10 IEM in 72% of the plasma samples in the validation set. Moreover, we show that the algorithm can correctly preselect 44 different IEM, very rapidly based on only a single sample. Although automated data interpretation is not yet flawless and still needs to be further optimized, we demonstrate that it could potentially facilitate the implementation of untargeted metabolomics for NGMS to a great extent.

WEB RESOURCES

HMDB	https://hmdb.ca
Human Phenotype Ontology	http://compbio.charite.de/hpweb/
IEMbase	http://iembase.org
Metagene	https://metagene.de
OMIM	https://www.omim.org
Orphanet	https://www.orpha.net/consor4.01/www/cgi-bin/Disease.php?Ing=EN

REFERENCES

1. Miller MJ, Kennedy AD, Eckhart AD et al. Untargeted metabolomic analysis for the clinical screening of inborn errors of metabolism. *J Inherit Metab Dis.* 2015;38:1029-1039.
2. Coene KLM, Kluijtmans LAJ, van der Heeft E et al. Next-generation metabolic screening: targeted and untargeted metabolomics for the diagnosis of inborn errors of metabolism in individual patients. *J Inherit Metab Dis.* 2018;41(3):337-353.
3. Haijes HA, Willemsen M, van der Ham M et al. Direct-infusion based non-quantitative metabolomics identifies metabolic disease in patients' dried blood spots and plasma. *Metabolites* 2019;9:12.
4. Haijes HA, van der Ham M, Gerrits J et al. Direct-infusion based metabolomics unveils biochemical profiles of inborn errors of metabolism in cerebrospinal fluid. *Mol Genet Metab.* 2019;127:51-57.
5. Ferreira CR, van Karnebeek CDM, Vockley J, Blau N. A proposed nosology of inborn errors of metabolism. *Genet Med.* 2019;21:102-106.
6. Wishart DS, Jewison T, Guo AC et al. HMDB 3.0 – The Human Metabolome Database in 2013. *Nucleic Acids Res.* 2013;41:801-807.
7. European Research Network for evaluation and improvement of screening, diagnosis and treatment of inherited disorders of metabolism. Annual report 2017. Available online: <https://www.erndim.org/store/docs/DOC4322ERNDIMAnnualRepor-HETAEBUV245881-19-10-2018.pdf>
8. Aitken S, Firth HV, McRae J et al. Finding diagnostically useful patterns in quantitative phenotypic data. *Am J Hum Genet.* 2019;105:933-946.
9. Smedley D, Robinson PN. Phenotype-driven strategies for exome prioritization of human Mendelian disease genes. *Genome Med.* 2015;7(1):81.
10. Haijes HA, de Sain-van der Velden MGM, Prinsen HCMT et al. Aspartylglycosamine is a biomarker for NGLY1-CDDG, a congenital disorder of glycosylation. *Mol Genet Metab.* 2019;127(4):368-372.
11. Abela L, Simmons L, Steindl K et al. N(8)-acetylspermidine as a potential biomarker for Snyder-Robinson syndrome identified by clinical metabolomics. *J Inherit Metab Dis.* 2016;39(1):131-7.
12. Kennedy AD, Pappan KL, Donti T et al. 2-Pyrrolidinone and succinimide as clinical screening biomarkers for GABA-transaminase deficiency: anti-seizure medications impact accurate diagnosis. *Front Neurosci.* 2019;13:394.
13. Burrage LC, Thistlethwaite L, Stroup BM et al. Untargeted metabolomics profiling reveals multiple pathway perturbations and new clinical biomarkers in urea cycle disorders. *Genet Med.* 2019;21(9):1977-1986.
14. González-Domínguez R, Castilla-Quintero R, García-Barrera T, Gómez-Ariza JL. Development of a metabolomics approach based on urine samples and direct infusion mass spectrometry. *Anal Biochem.* 2014;15(465):20-27.

SUPPLEMENTAL DATA

Table S1. Expected library, input for the automated data interpretation

Due to its size, this table is only available online.

Table S2. Results of the automated data interpretation for the different sample sets

Due to its size, this table is only available online.

Table S3. Results of the untargeted metabolomics analysis of the dried blood spots of patients included in the DBS training and optimization set

Due to its size, this table is only available online.

Table S4. True diagnoses of the patients included in the DBS training and optimization set

Due to its size, this table is only available online.

Table S5. Results of the untargeted metabolomics analysis of the dried blood spots of control individuals included in the DBS training and optimization set

Due to its size, this table is only available online.



Table S6. Results of the untargeted metabolomics analysis of the plasma samples of patients included in the plasma training and validation set

Due to its size, this table is only available online.

Table S7. True diagnoses of the patients included in the plasma training and validation set

Due to its size, this table is only available online.

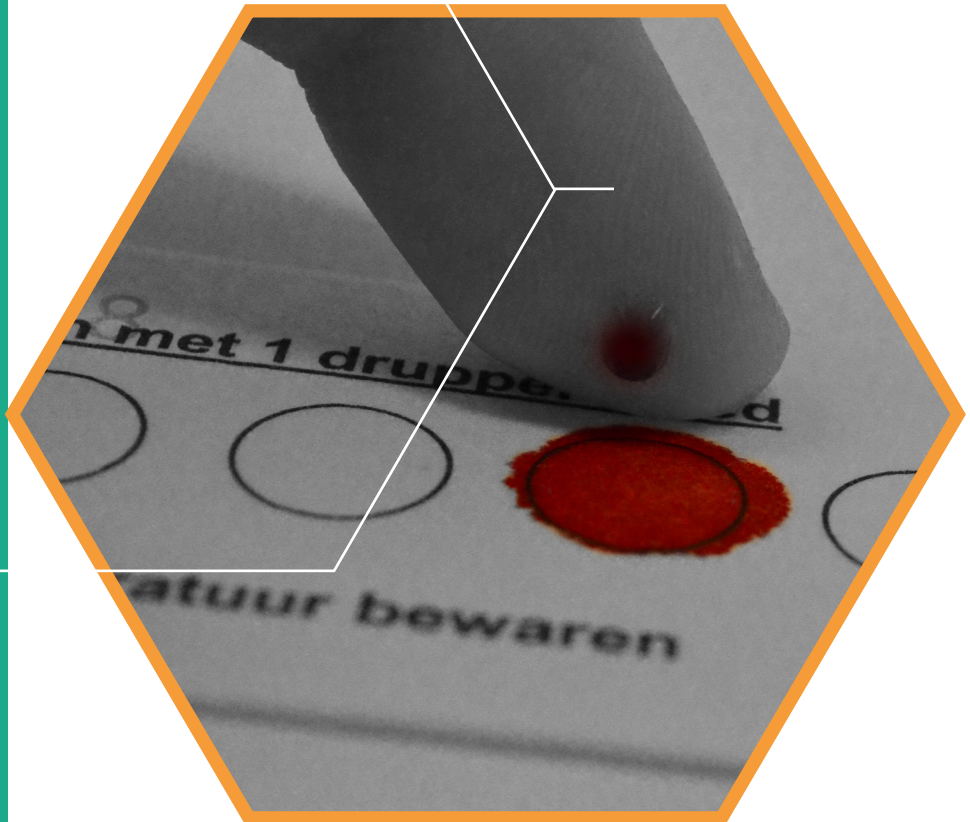
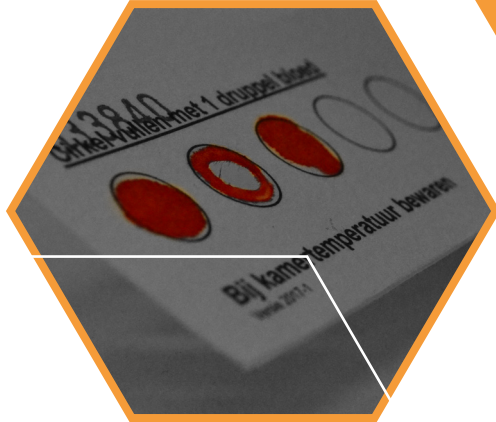
Table S8. Results of the untargeted metabolomics analysis of the plasma samples of control individuals included in the plasma training and validation set

Due to its size, this table is only available online.

Video S1. Demonstration of the R Shiny application for automated data interpretation

This video is only available online.





Assessing the pre-analytical stability of small-
molecule metabolites in cerebrospinal fluid using
direct-infusion metabolomics

Metabolites 2019, 9(10)
DOI: 10.3390/metabo9100236

Hanneke A. Haijes*, Eline A.J. Willemse, Johan Gerrits,
Wiesje M. van der Flier, Charlotte E. Teunissen,
Nanda M. Verhoeven-Duif, Judith J.M. Jans*

* Corresponding authors

ABSTRACT

Metabolomics studies aiming to find biomarkers frequently make use of historical or multicenter cohorts. These samples often have different pre-analytical conditions that potentially affect metabolite concentrations. We studied the effect of different storage conditions on the stability of small-molecule metabolites in cerebrospinal fluid to aid a reliable interpretation of metabolomics data. Three cerebrospinal fluid pools were prepared from surplus samples from the Amsterdam Dementia Cohort biobank. Aliquoted pools were exposed to different storage conditions to assess the temperature and freeze/thaw stability before final storage at $-80\text{ }^{\circ}\text{C}$: storage up to four months at $-20\text{ }^{\circ}\text{C}$ and up to one week at either $5\text{--}8\text{ }^{\circ}\text{C}$ or $18\text{--}22\text{ }^{\circ}\text{C}$ and exposure to up to seven freeze/thaw cycles. Direct-infusion high-resolution mass spectrometry was performed, resulting in the identification of 1852 m/z peaks. To test the storage stability, principal component analyses, repeated measures analysis of variance, Kruskal–Wallis tests, and fold change analyses were performed, all demonstrating that small-molecule metabolites in the cerebrospinal fluid are relatively unaffected by 1–3 freeze/thaw cycles, by storage at $-20\text{ }^{\circ}\text{C}$ up to two months, by storage at $5\text{--}8\text{ }^{\circ}\text{C}$ for up to 72 h, or by storage at $18\text{--}22\text{ }^{\circ}\text{C}$ for up to 8 h. This suggests that these differences do not affect the interpretation of potential small-molecule biomarkers in multicenter or historical cohorts and implies that these cohorts are suitable for biomarker studies.

KEY MESSAGE

Minor differences in pre-analytical storage conditions do not affect the interpretation of potential small-molecule biomarkers in multicenter or historical cohorts, implying that these cohorts are suitable for biomarker studies.

INTRODUCTION

The cerebrospinal fluid (CSF) is the closest possible read-out of all body fluids of metabolite concentrations in the brain, as it circulates in the subarachnoid space and is in direct contact with the brain parenchyma, meninges, and spinal cord.¹ For this reason, CSF has been studied to identify biomarkers to aid diagnostics for a variety of neurological disorders, from neurodegenerative diseases and cerebral infections to inborn errors of metabolism. Since studies aiming to identify biomarkers generally require large sample sizes, they frequently make use of historical or multicenter cohorts. However, the pre-analytical conditions in these cohorts, including the collection, processing, and storage of these samples, often vary.¹ These differences potentially affect the metabolite concentrations, resulting in bias.¹ Whereas studies on the effects of pre-analytical conditions on CSF often focus on protein stability,¹ only a few studies have focused on the stability of small-molecule metabolites.²⁻⁴ For example, one study found that the CSF concentrations of four amino acids (glutamic acid, glycine, aspartic acid, and taurine) were not affected by storage at -20°C or -80°C , provided that the sample was deproteinized and neutralized before storage.² Another study demonstrated that storage for 72 h at room temperature, compared to immediate storage at -70°C , resulted in decreased levels of citrate and increased levels of lactate, glutamine, creatine, and creatinine, whereas the levels of myo-inositol, glucose, pyruvate, acetate, and alanine were unaffected.³ Others showed that storage for 30 or 120 min at room temperature, compared to immediate storage at -80°C , significantly increased the concentrations of 10/17 amino acids measured in porcine CSF.⁴ In addition, the majority of other measured small-molecule metabolites ($n = 79$) in this study⁴ also demonstrated increased concentrations after 30 min and/or 120 min at room temperature, indicating that residual enzymatic activity in CSF after collection may lead to altered metabolite levels, possibly by the degradation of proteins,⁴ indicating that the storage conditions indeed affect the stability of small-molecule metabolites in CSF.

Although the studies performed to date give some indication of the potential effects of differences in pre-analytical storage conditions on the stability of small-molecule metabolites, only a limited number of metabolites were included in these studies, while targeted and untargeted metabolomics studies can potentially identify many more small-molecule metabolites. Thus, as targeted and untargeted metabolomics studies are more frequently performed for the identification of biomarkers in CSF, we studied the effect of different storage conditions on the stability of small-molecule metabolites in CSF to aid a reliable interpretation of metabolomics data.

METHODS

Sample collection and storage

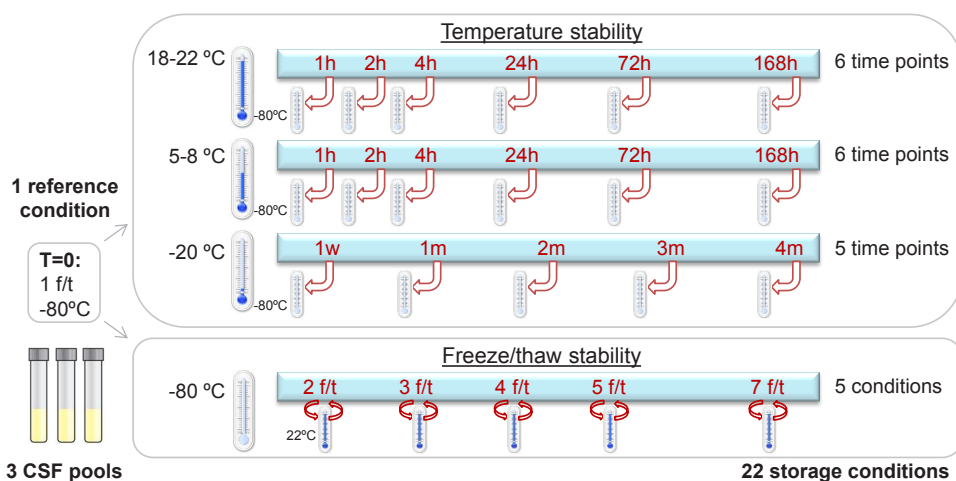
Surplus CSF samples from the Amsterdam Dementia Cohort biobank (e.g., samples having incomplete clinical information for use in clinical validation studies), collected between 2000 and 2017, were used.⁵ For the biobank, CSF was collected by lumbar puncture in 10 mL polypropylene tubes (Sarstedt, Nümbrecht, Germany) and centrifuged at $1,800\text{--}2,100\times g$ for 10 min at 4°C within 2 h, using a predefined procedure, according to international guidelines.⁶ The CSF was divided into polypropylene tubes (1.5 or 2.0 mL; Sarstedt) in 500 μL volumes and was stored at -80°C .^{5,6}

The biobanking protocol of the Amsterdam Dementia Cohort was approved by the review board of the Vrije Universiteit Medical Center of Amsterdam. All procedures followed were in accordance with the ethical standards of the institution and with the Helsinki Declaration

of 1975, as revised in 2000. All subjects provided written consent.

Aliquots of 0.5 mL per sample from multiple CSF samples from three to six different individuals were merged into a CSF pool in 50-mL polypropylene tubes. In total, three CSF pools with different compositions were acquired. Aliquots of 500 μ L of these three CSF pools were stored in 1.5 mL polypropylene tubes with screw caps (Sarstedt). The aliquoted CSF pools were exposed to storage conditions as described in the standard operating procedure for sample stability⁷ and as depicted in Figure 1, i.e., to assess the temperature stability of storage for up to four months at -20 °C and up to one week at either 5 – 8 °C or 18 – 22 °C before final storage at -80 °C; and to assess freeze/thaw stability exposure to up to seven freeze/thaw cycles (Figure 1). One reference aliquot of each pool was stored at -80 °C directly at time point 0. This sample had thus undergone one freeze/thaw cycle.

Figure 1. Overview of the different storage conditions analyzed to assess the temperature and freeze/thaw stability of small-molecule metabolites in cerebrospinal fluid



Three pools of cerebrospinal fluid were analyzed. For each pool, one reference sample and 22 samples for the different storage conditions were analyzed. Abbreviations: CSF: cerebrospinal fluid, f/t: freeze/thaw cycle, h: hours, m: months, w: week.

Sample preparation and analysis

Metabolomics analysis of CSF was performed as previously described by our group.^{8,9} Samples were thawed to room temperature. Five microliters of the sample were added to 140 μ L of a working solution containing stable isotope-labeled compounds (sILC), with fixed concentrations as previously described.⁹ The solution was centrifuged for five minutes at $17,000\times g$ and 105 μ L of supernatant was diluted with 45 μ L 0.3% formic acid (Emsure, Darmstadt, Germany). The solution was filtered using a methanol preconditioned 96-well filter plate (Acro prep, 0.2 μ m GHP, NTRL, 1 mL well; Pall Corporation, Ann Arbor, MI, USA) and a vacuum manifold. The sample filtrate was collected in a 96-well plate (Advion, Ithaca, NY, USA). Direct-infusion high-resolution mass spectrometry was performed using a TriVersa NanoMate system (Advion), controlled by Chipsoft software (version 8.3.3, Advion), that was mounted onto the interface of a Q-Exactive high-resolution mass spectrometer (Thermo Scientific™, Bremen, Germany), with a scan range of 70 – 600 mass over charge (m/z).⁹ For

each sample, technical triplicates were analyzed, infusing each sample three times into the mass spectrometer. Samples were analyzed in a randomized order.

Data processing

Data acquisition and processing were performed using a peak calling pipeline developed in the R programming language.^{8,9} In this pipeline, mass peak identification and annotation was conducted by matching the m/z value of the mass peak with a range of two parts per million to metabolite masses present in the Human Metabolome Database, version 3.6.¹⁰ According to the Metabolomics Standards Initiative, the level of certainty of metabolite annotation is 2, as we putatively annotate compounds based on the matched m/z value of the mass peak.¹¹ Taking into account isomers and adduct ions, ~60,000 m/z peaks could be annotated with one or more possible annotations.⁸ Metabolite annotations without adduct ions in negative or positive mode ($[M - H]^-$, $[M + H]^+$) or with single adduct ions $[M + Na]^+$, $[M + K]^+$ and $[M + Cl]^-$ were selected. For each sample, intensities of the five selected m/z peaks were added together, resulting in one summed m/z peak intensity per metabolite annotation: ~6,600 summed m/z peaks in total, per sample. Endogenous metabolite annotations and metabolite annotations with unknown function were selected.⁵ No normalization of mass peak intensities was performed. The R code is available online (<https://github.com/UMCUGenetics/DIMS>).

Metabolite groups

To study metabolites known or expected to be important in neurometabolic diagnostics in CSF in detail (www.metagene.de),¹² 106 m/z peaks corresponding to neurometabolic metabolites were selected and grouped into different categories (Table 1).

Data analysis

To assess which part of the identified variability is due to technical aspects of the analysis, the variability within the run was monitored by the addition of sILC to each sample during the sample analysis. For each sILC, the coefficient of variation was calculated over all samples in the run by standard deviation intensity/mean intensity. To assess the most extreme conditions of each series, these samples were compared to the reference sample by calculating the median absolute variation of the sILC as follows: (1) calculation of the fold change: intensity of the most extreme condition/intensity of the reference sample; (2) fold change – 1; (3) conversion to absolute numbers; (4) calculation of the median absolute variation: median of the absolute variation of the three CSF pools.

For the total number of m/z peaks, as well as for the 106 m/z peaks corresponding to neurometabolic metabolites, for each series a principal component analysis was performed to visualize whether there was any clustering of different freeze/thaw cycles or time points, or of the three CSF pools. In addition, for each series a repeated measures analysis of variance (ANOVA) for all storage conditions was performed for each of the m/z peaks, as well as a non-parametric Kruskal–Wallis test comparing the most extreme condition to the reference sample for each of the m/z peaks. To control the familywise error rate in order to prevent any type I errors, all p -values were adjusted according to the Bonferroni method.

To assess which part of the identified variability is due to the different storage conditions, for each sample (except the reference sample), the fold change (FC) was calculated as the intensity of the sample divided by the intensity of the reference sample. For each condition, the median absolute variation and 95% CI of the three CSF pools were calculated. Next, to

correct for variability that can solely be attributed to the analysis, metabolites were defined as possibly affected by the storage condition when the lower limit of 95% CI was above the range attributed to the analysis variability (calculated by: FC 1.000 + median absolute variation of sILC), or when the upper limit of 95% CI was below the range attributed to the analysis variability (calculated by: FC 1.000 – median absolute variation of sILC). For each series, the median and 95% CI were plotted for the most extreme condition. This was performed for the total number of *m/z* peaks (data not shown), as well as for the 106 *m/z* peaks corresponding to neurometabolic metabolites. To assess whether mass peak intensities were affected in specific groups of neurometabolic metabolites, metabolites were colored according to the metabolite group (Table 1). Data analysis was performed in the R programming language.

Table 1. 106 *m/z* peaks corresponding to metabolites important for neurometabolic diagnostics in the cerebrospinal fluid

Amino acids (24)	Neurotransmitters (21)	Purines, pyrimidines (20)	Organic Acids (16)
Alanine	3-Methoxytyrosine/ 3-OMD/ Methylidopa	5-Hydroxymethyluracil	N-Acetylaspartylglut. acid
Arginine		Adenine	2-Methylcitric acid
Asparagine	5-Hydroxyindoleacetic acid	Adenosine/Deoxyguanos.	3-Hydroxybutyric acid
Aspartic acid	5-Hydroxytryptophan	AICAR	3-Hydroxyisovaleric acid
Cysteine	5-Methyltetrahydrofolic ac.	Deoxyadenosine	4-Guanidinobutanoic acid
Cystine	Dopamine	Deoxyinosine	Acetoacetic acid
Glutamic acid	Dopamine 4-sulfate	Dihydrothymine	Cis-Aconitic acid
Glutamine	Dopamine glucuronide	Dihydrouracil	Citric acid
Glycine	Epinephrine	Guanosine	Fumaric acid
Histidine	Epinephrine glucuronide	Hypoxanthine	Lactic acid/
Homoarginine	Homovanillic acid/	Inosine	3-OH-propionic acid
Homocarnosine	3-OH-phenyllactic acid	Orotic acid	Malic acid
(Iso)leucine	Epinephrine sulfate	SAICAR	N-Acetylaspartic acid
Lysine	Gamma-aminobutyric acid	Succinyladenosine	Oxalacetic acid
Methionine	Glutamic acid	Thymidine	Propionic acid
Phenylalanine	L-Dopa/Dihydroxyphenylal.	Thymine	Pyruvic acid
Proline	Methoxyhydroxyphenylglyc.	Uracil	Succinic acid/
Serine	N-Acetylserotonin	Uric acid	Methylmalonic acid
Threonine	Norepinephrine	Uridine	
Tryptophan	Norepinephrine sulfate	Xanthine	
Tyrosine	Serotonin		
Ornithine	Vanillic acid	Other (1)	Methyl donor (2)
Taurine	Vanillylmandelic acid	Saccharopine	s-Adenosylhomocysteine
Valine			s-Adenosylmethionine
Creatine metab. (5)	Vitamins (5)	Pterines (6)	Vitamin B6 vitamins (8)
Creatine	Folic acid	7,8-Dihydroneopterin	Pipecolic acid
Creatinine	Thiamine	Dihydrobiopterin	Pyridoxal
Guanidoacetic acid	Thiamine monophosphate	Neopterin	Pyridoxal 5'-phosphate
Phosphocreatine	Thiamine pyrophosphate	Biopterin/Sepiapterin/	Pyridoxamine
Phosphocreatinine	Thiamine triphosphate	Primapterin/6-Pyruvoil-tetrahydropterin	Pyridoxamine 5'-phosph.
		Tetrahydroneopterin	Pyridoxine
		Tetrahydroneopterin	Pyridoxine 5'-phosphate
		Tetrahydrobiopterin	Alpha-amino adipic acid
			delta-semialdehyde

Groups of neurometabolic metabolites are depicted in bold. Abbreviations: 3-OH: 3-hydroxy; 3-OMD: 3-O-methylidopa; ac: acid; AICAR: 5-aminoimidazole-4-carboxamide ribonucleotide; metab: metabolism; SAICAR: succinyl-aminoimidazole-4-carboxamide ribonucleotide.

RESULTS

Untargeted metabolomics using direct-infusion high-resolution mass spectrometry resulted in a list of 1,852 unique *m/z* peaks, corresponding to 3806 unique annotations of metabolites that can occur endogenously, including isomers. This was in line with previous analyses.^{8,9}

In four out of 69 samples, direct infusion was hampered, resulting in the exclusion of the following samples: one of freeze/thaw cycle 1 (second CSF pool), one of freeze/thaw cycle 7 (first CSF pool), one of 5–8 °C for 168 h, and one of 18–22 °C for 2 h (both in the third CSF pool). In total, 65/69 samples were used for statistical analyses. An overview of the different pre-analytical storage conditions assessed is given in Figure 1.

Analysis of variability

To assess which part of the identified variability is solely due to technical aspects of the analysis, the variability within the run was monitored by the addition of sILC to each sample during the sample preparation. The median coefficient of variation of the sILCs was 0.166 (95% confidence interval: 0.127–1.565), in line with previous analyses^{8,9} (Table 2).

As the sILCs were added during the sample preparation, the median absolute variation of the most extreme storage conditions was calculated as a reflection of the variation in the sample that can be solely attributed to analysis variability, and not to variability due to the different storage conditions tested. The median absolute variation of the sILCs was 0.384, 0.072, 0.171, and 0.188 for the samples that experienced the most extreme storage conditions: freeze/thaw cycle 7, storage at –20 °C for four months, storage at 5–8 °C for 168 h, and storage at 18–22 °C for 168 h, respectively (Table 2).

Freeze/thaw stability

To assess whether the metabolome changed due to multiple freeze/thaw cycles, principal component analysis was performed for the 1,852 m/z peaks as well as for the selection of 106 m/z peaks corresponding to metabolites marked as important for neurometabolic diagnostics (Table 1). This did not reveal any clustering of the different freeze/thaw cycles (Figure S1), indicating that the metabolome as a whole did not change upon multiple freeze/thaw cycles. In addition, no clustering of the samples from the three different CSF pools was observed, suggesting that the three CSF pools had comparable metabolomes (Figure S1).

Repeated measures ANOVA assessing all 1,852 m/z peaks for all freeze/thaw cycles revealed no significant differences; nor did Kruskal–Wallis tests comparing freeze/thaw cycle 7 to freeze/thaw cycle 1. When assessing the selection of 106 m/z peaks corresponding to neurometabolic metabolites, neither the repeated measures ANOVA comparing all freeze/thaw cycles nor the Kruskal–Wallis tests comparing freeze/thaw cycle 7 to freeze/thaw cycle 1 revealed any significant differences, suggesting that the stability of individual m/z peaks is unaffected by multiple freeze/thaw cycles.

To detect more subtle changes in metabolite stability, the freeze/thaw stability was further assessed by an analysis of FC. After correction for the median absolute variation reflecting the analysis variability, 119 of the 1,852 m/z peaks were considered to be affected by the most extreme storage condition, of which six were neurometabolic metabolites (Table 3, Figure 2). There was no specific group of neurometabolic metabolites that was more affected than another group (Figure 2). The six metabolites that were possibly affected by multiple freeze/thaw cycles were visually assessed (Figure S2). Remarkably, adenine concentrations showed a decrease of more than 50% after more than four freeze/thaw cycles and glycine concentrations showed a more than five-fold increase after more than five freeze/thaw cycles (Figure S2).

Table 2. Coefficient of variation of the analysis and median absolute variation of stable isotope-labeled compounds for the most extreme storage conditions

Stable isotope-labelled compound	CV	MEDIAN ABSOLUTE VARIATION			
		Freeze/thaw cycle 7	-20 °C, 4 months	5-8 °C, 168 hours	18-22 °C, 168 hours
¹⁵ N; ²⁻¹³ C-glycine	0.580	0.975	1.732	6.999	1.855
² H ₄ -alanine	0.161	0.371	0.070	0.171	0.188
² H ₄ -leucine	0.166	0.411	0.037	0.158	0.265
² H ₃ -methionine	0.775	3.388	0.188	0.607	0.359
¹³ C ₆ -phenylalanine	0.149	0.374	0.050	0.142	0.204
¹³ C ₆ -tyrosine	0.150	0.349	0.043	0.098	0.206
² H ₃ -aspartate	0.160	0.349	0.137	0.110	0.155
² H ₃ -glutamate	0.126	0.247	0.099	0.110	0.074
² H ₂ -ornithine	0.183	0.540	0.014	0.108	0.168
² H ₂ -citrulline	0.134	0.231	0.070	0.131	0.038
² H ₄ / ¹³ C-arginine	0.163	0.380	0.105	0.190	0.170
² H ₄ -valine	0.155	0.377	0.042	0.124	0.222
² H ₈ -carnitine	0.202	0.580	0.072	0.179	0.162
² H ₃ -acetylcarnitine	1.058	432.707	689.785	0.567	0.999
² H ₃ -propionylcarnitine	0.194	0.384	0.038	0.225	0.161
² H ₃ -butyrylcarnitine	2.914	42.155	0.164	92.851	0.277
² H ₃ -isovalerylcarnitine	0.217	0.519	0.103	0.215	0.173
5th percentile	0.127	0.244	0.033	0.106	0.067
Median	0.166	0.384	0.072	0.171	0.188
95th percentile	1.565	120.266	139.343	24.170	1.170

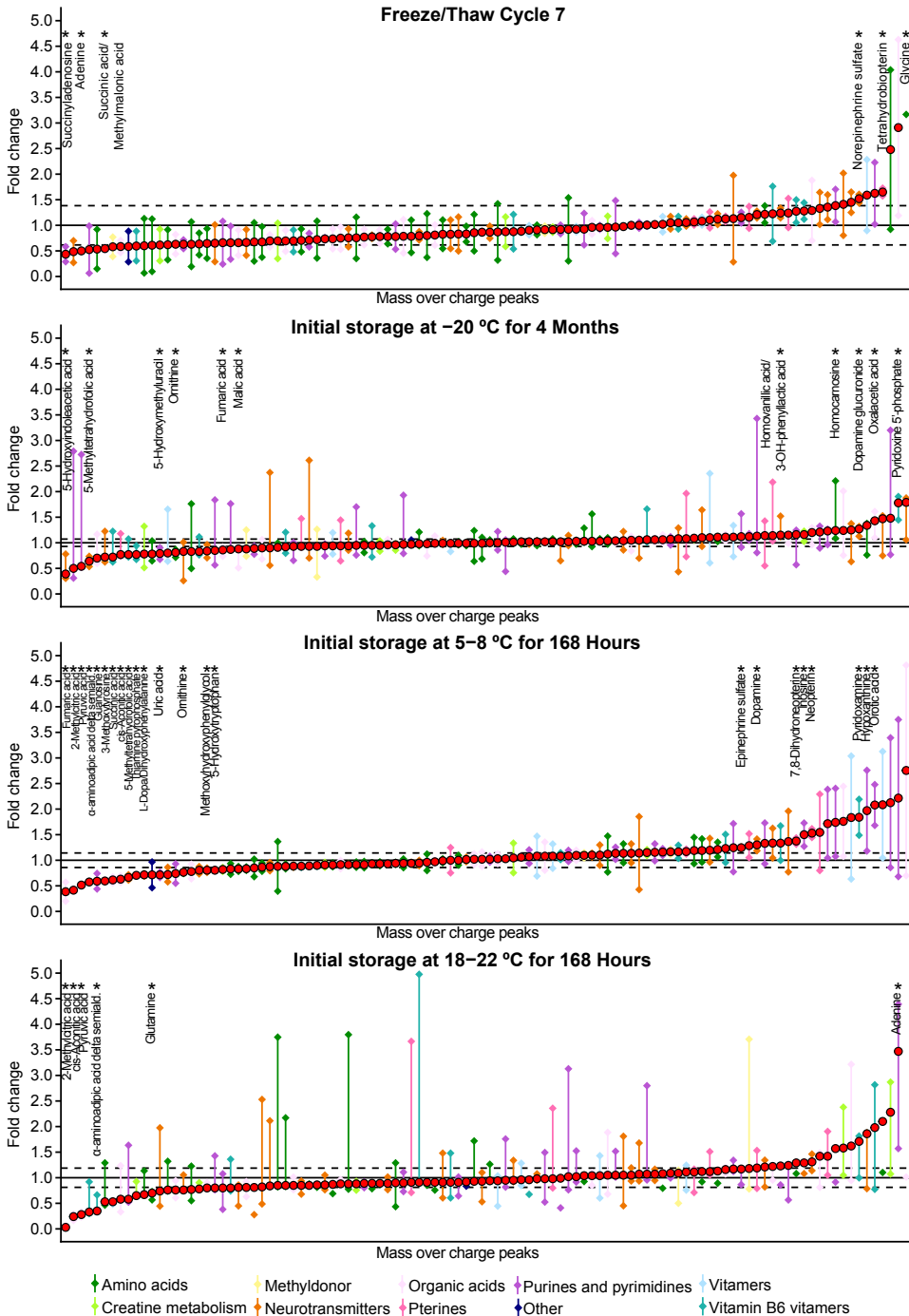
CV: coefficient of variation of all 65 samples, calculated by: standard deviation intensity/mean intensity. Median absolute variation for the most extreme storage condition was calculated by: (1) calculation of the fold change: intensity of the most extreme condition/intensity of the reference sample; (2) fold change - 1; (3) conversion to absolute numbers; (4) calculation of the median absolute variation: median of the absolute variation of the three CSF pools.

Table 3. Number of metabolites possibly affected by the most extreme storage condition, after correction for the analysis variability

	Freeze/thaw cycle 7	-20 °C, 4 months	5-8 °C, 168 hours	18-22 °C, 168 hours
Median absolute variation sILC	0.384	0.072	0.171	0.188
Range analysis variability	0.616-1.384	0.928-1.072	0.829-1.171	0.812-1.188
1,852 m/z peaks				
<i>m/z peaks with decreased intensities</i>	45	142	206	67
<i>m/z peaks with increased intensities</i>	74	134	213	54
106 m/z peaks corresponding to neurometabolic metabolites				
<i>m/z peaks with decreased intensities</i>	3	5	8	1
<i>m/z peaks with increased intensities</i>	3	6	15	5

Groups of *m/z* peaks are depicted in bold. The median absolute variation of the sILC, as demonstrated in Table 2, reflects the variability in the sample that can be attributed to technical aspects of the analysis. The range of the analysis variability is calculated by a fold change of $1 \pm$ median absolute variation of the sILC. *m/z* peaks were considered decreased when the upper limit of the 95% confidence interval of the *m/z* peak was below the range of the analysis variability, and increased when the lower limit of 95% confidence interval of the *m/z* peak was above the range of the analysis variability. Abbreviations: sILC: stable isotope-labeled compound.

Figure 2. *m/z* peaks corresponding to metabolites important for neurometabolic diagnostics that are possibly affected by the most extreme storage conditions compared to the reference sample, after correction for the analysis variability



[Figure 2 continued] The y-axis depicts the fold change of the most extreme storage condition compared to the reference sample; the x-axis depicts the 106 m/z peaks corresponding to metabolites important for neurometabolic diagnostics (as listed in Table 1). Colored diamonds depict the upper and lower limit of the 95% confidence intervals; colored lines depict the range of the 95% confidence interval. Red filled circles depict the mean fold change. Colors depict the group of neurometabolic metabolites, as listed in the legend. The horizontal black line depicts fold change = 1, horizontal dashed lines indicate the range of the analysis variability: fold change plus or minus the median absolute variation of the stable isotope-labeled compounds for the analysis series. Asterisks depict the metabolites for which the lower limit of 95% confidence interval was above the upper dashed line and metabolites for which the upper limit of the 95% confidence interval was below the lower dashed line. For these, metabolite names are indicated below the asterisks. These metabolites correspond to the metabolites illustrated in Figures S2–S5.

Temperature stability

For all three temperature stability series, i.e., storage at $-20\text{ }^{\circ}\text{C}$, at $5\text{--}8\text{ }^{\circ}\text{C}$ or at $18\text{--}22\text{ }^{\circ}\text{C}$ for different periods of time (Figure 1), principal component analysis, performed to assess whether the metabolome changed due to the storage conditions, did not reveal any clustering of the different time points (Figure S1), suggesting that the metabolome as a whole was not affected by the different storage conditions. In addition, no clustering of CSF pools was observed, indicating the comparable metabolic compositions of the pools (Figure S1).

Repeated measures ANOVA assessing all time points and Kruskal–Wallis tests comparing the most extreme time points to the reference samples revealed no significant differences. For the selection of 106 m/z peaks corresponding to neurometabolic metabolites, Kruskal–Wallis tests comparing the most extreme time points to the reference samples did not display any significant differences, and repeated measures ANOVA only disclosed a significant change in mass peak intensity for cis-aconitic acid when stored at $18\text{--}22\text{ }^{\circ}\text{C}$, suggesting that the stability of individual m/z peaks is unaffected by the different storage conditions, except for cis-aconitic acid when stored at $18\text{--}22\text{ }^{\circ}\text{C}$.

To detect more subtle changes, the temperature stability was further assessed by analysis of FCs. After correction for the median absolute variation reflecting the analysis variability, 276 of the 1852 m/z peaks were considered to be affected by storage for four months at $-20\text{ }^{\circ}\text{C}$, 419 m/z peaks were considered to be affected by storage for a week at $5\text{--}8\text{ }^{\circ}\text{C}$ and 121 m/z peaks were considered to be affected by storage for a week at $18\text{--}22\text{ }^{\circ}\text{C}$ (Table 3). Of these peaks, 11, 23, and six (25 unique m/z peaks) were among the 106 m/z peaks corresponding to neurometabolic metabolites (Table 3, Figure 2). No specific group of neurometabolic metabolites was more affected than another group (Figure 2). Metabolites that were possibly affected by prolonged storage at $-20\text{ }^{\circ}\text{C}$, $5\text{--}8\text{ }^{\circ}\text{C}$, and $18\text{--}22\text{ }^{\circ}\text{C}$ were visually assessed (Figure S3–S5). 5-methyltetrahydrofolic acid concentrations were decreased after storage for more than two months at $-20\text{ }^{\circ}\text{C}$ and dopamine glucuronide concentrations were increased after storage for more than three months at $-20\text{ }^{\circ}\text{C}$ (Figure S3). Prolonged storage at $5\text{--}8\text{ }^{\circ}\text{C}$ resulted in a decrease in cis-aconitic acid, pyruvic acid, 2-methylcitric acid, and α -aminoadipic acid delta-semialdehyde concentrations and an increase in orotic acid and neopterin concentrations (Figure S4). Lastly, prolonged storage at $18\text{--}22\text{ }^{\circ}\text{C}$ resulted in a decrease in cis-aconitic acid, pyruvic acid, 2-methylcitric acid, α -aminoadipic acid delta-semialdehyde, and glutamine concentrations, and an increase in adenine concentrations (Figure S5).

DISCUSSION

We studied the effect of different storage conditions on the stability of small-molecule

metabolites in CSF to aid a reliable interpretation of metabolomics results. We present two main findings. First, the majority of small-molecule metabolites seems to be relatively unaffected by multiple freeze/thaw cycles, as clustering analysis as well as repeated measures ANOVA comparing the different conditions and Kruskal–Wallis tests comparing the most extreme condition to the reference sample revealed no significant differences in metabolite intensities. Analysis of FCs revealed that adenine levels decreased more than 50% after more than four freeze/thaw cycles, and that glycine levels showed a five-fold increase after more than five freeze/thaw cycles (Figure S2). Two studies reported stable glycine concentrations in CSF after three freeze/thaw cycles, but these studies did not investigate the effects of more freeze/thaw cycles on glycine concentrations.^{13,14} Altogether, we conclude that different numbers of freeze/thaw cycles in a single cohort are not expected to influence levels of small-molecule metabolites, but we suggest reticence in interpretation of potential biomarker concentrations in samples with more than four freeze/thaw cycles, especially with respect to adenine and glycine.

The second main finding is that the majority of small-molecule metabolites seems relatively unaffected by the time and temperature at which they were stored. For temperature stability analyses, clustering analysis as well as repeated measures ANOVA and Kruskal–Wallis tests revealed no significant differences, except for cis-aconitic acid when stored at 18–22 °C. Analysis of FCs revealed that the levels of some metabolites, including 5-methyltetrahydrofolic acid, dopamine glucuronide, cis-aconitic acid, pyruvic acid, 2-methylcitric acid, α -aminoadipic acid delta-semialdehyde, orotic acid, neopterin, glutamine and adenine might be affected by prolonged storage at –20 °C, 5–8 °C, or 18–22 °C (Figure S3–S5). In another study, our group investigated the stability of 5-methyltetrahydrofolic acid in CSF samples and demonstrated decreased concentrations after a week of storage at room temperature, but, contrasting with our findings in this study, there were stable levels after storage for a week at 4 °C.¹⁵ In the study previously performed by our group, storage at –20 °C was not included.¹⁵ Another group found an increase of glutamine at 18–22 °C,³ whereas we report a decrease of glutamine levels at this time point. Moreover, we did not observe decreased levels of citrate, nor increased levels of lactate, creatine, and creatinine. We observed decreased levels of pyruvic acid when stored at 18–22 °C, while Levine et al. reported stable levels of pyruvic acid.³ Although Levine et al. used proton NMR analyses to detect potential differences, there were no other important differences in the study design that could explain these differences.³ Thus, the effects of prolonged storage at –20 °C, 5–8 °C, or 18–22 °C before final storage at –80 °C are debatable. We suggest being cautious by including samples stored at –20 °C for more than two months (Figure S3), samples stored at 5–8 °C for more than 72 h (Figure S4), and samples stored at 18–22 °C for more than 8 h (Figure S5) in a cohort study for biomarker identification.

There are a few limitations to this study. First, while a wide range of pre-analytical conditions was studied, the sample size per condition was relatively small ($n = 3$), hampering the power of the analysis. For this reason, the relative stability of small-molecule metabolites in CSF might be overestimated, as biologically relevant changes in metabolite concentrations might not have reached statistical significance. Second, due to the exploratory nature of this study, surplus CSF samples were used that needed an extra thawing cycle for pooling. The reference sample thus underwent one freeze/thaw cycle instead of zero freeze/thaw cycles, hampering the interpretation of the effects of one freeze/thaw cycle on the concentrations of small-molecule metabolites.

Despite these limitations, an important strength of this study is that multiple statistical

analyses were performed, including unsupervised clustering analysis, repeated measures ANOVA for comparing all storage conditions for each identified *m/z* peak, Kruskal–Wallis tests for comparing the most extreme storage condition to the reference sample for each identified *m/z* peak, and analysis of FCs with correction for the analysis variability to assess the more subtle differences in mass peak intensities. All these analyses pointed towards the same conclusion: concentrations of small-molecule metabolites are relatively unaffected by most pre-analytical storage conditions. Moreover, the nature of this study was untargeted, hypothesis-free, and broad, as the stability of more than 1,800 *m/z* peaks was tested.

CONCLUSION

In conclusion, we report that small-molecule metabolites in CSF are relatively unaffected by 1–3 freeze/thaw cycles, by storage at –20 °C for up to two months, by storage at 5–8 °C up to 72 h, or by storage at 18–22 °C up to 8 h, suggesting that minor differences in pre-analytical storage conditions in multicenter or historical cohorts used for the identification of biomarkers will not affect the interpretation of potential biomarkers, and implying that these cohorts are suitable for biomarker studies. We recommend caution when including samples with more extreme pre-analytical storage conditions. In addition, prior to using a biomarker for clinical decision-making, we recommend that the effects of pre-analytical conditions on the concentrations of any newly identified potential biomarker are tested.

WEB RESOURCES

R code <https://github.com/UMCUGenetics/DIMS>
Metagene <https://metagene.de>

REFERENCES

1. Cameron S, Gillio-Meina C, Ranger A, Choong K, Fraser DD. Collection and analyses of cerebrospinal fluid for pediatric translational research. *Pediatr Neurol.* 2019;98:3-17.
2. Anesi A, Rondanelli M, d’Eiril GM. Stability of neuroactive amino acids in cerebrospinal fluid under various conditions of processing and storage. *Clin Chem.* 1998;44:2359-2360.
3. Levine J, Panchalingam K, McClure RJ, Gershon S, Pettegrew JW. Stability of CSF metabolites measured by proton NMR. *J Neural Transm.* 2000;107:843-848.
4. Rosenling T, Slim CL, Christin C et al. The effect of preanalytical factors on stability of the proteome and selected metabolites in cerebrospinal fluid (CSF). *J Proteome Res.* 2009;8:5511-5522.
5. Van der Flier WM, Pijnenburg YA, Prins N et al. Optimizing patient care and research: The Amsterdam Dementia Cohort. *J Alzheimers Dis.* 2014;41:313-27.
6. Del Campo M, Mollenhauer B, Bertolotto A et al. Recommendations to standardize pre-analytical confounding factors in Alzheimer’s and Parkinson’s disease cerebrospinal fluid biomarkers: An update. *Biomark Med.* 2012;6:419-430.
7. Andreasson U, Perret-Liaudet A, van Waalwijk van Doorn LJ et al. A practical guide to immunoassay method validation. *Front Neurol.* 2015;19:179.
8. Haijes HA, Willemsen M, van der Ham M et al. Direct-infusion based non-quantitative metabolomics identifies metabolic disease in patients’ dried blood spots and plasma. *Metabolites* 2019;9:12.
9. Haijes HA, van der Ham M, Gerrits J et al. Direct-infusion based metabolomics unveils biochemical profiles of inborn errors of metabolism in cerebrospinal fluid. *Mol Genet Metab* 2019;127:51-57.
10. Wishart DS, Jewison T, Guo AC et al. HMDB 3.0 – The Human Metabolome Database in 2013. *Nucleic Acids Res.* 2013;41:801-807.
11. Sumner IW, Amberg A, Barrett D et al. Proposed minimum reporting standards for chemical analysis, Chemical Analysis Working Group (CAWG), Metabolomics Standards Initiative (MSI). *Metabolomics* 2007;3:211-221.
12. Batllori M, Molero-Luis M, Casado M, Sierra C, Artuch R, Armazabal A. Biochemical analyses of cerebrospinal fluid for the diagnosis of neurometabolic conditions. What can we expect? *Semin Pediatr Neurol.* 2016;23:273-284.
13. Fuchs SA, de Sain-van der Velden MG, de Barse MM et al. Two mass-spectrometric techniques for quantifying serine enantiomers and glycine in cerebrospinal fluid: Potential confounders and age-dependent ranges. *Clin*

Chem. 2008;54:1443-50.

14. Wilson SF, James CA, Zhu X, Davis MT, Rose MJ. Development of a method for the determination of glycine in human cerebrospinal fluid using pre-column derivatization and LC-MS/MS. *J Pharm Biomed Anal.* 2011;56:315-23.
15. Willemse EAJ, Vermeiren Y, Garcia-Ayllon MS et al. Pre-analytical stability of novel cerebrospinal fluid biomarkers. *Clin Chim Act.* 2019;497:204-211.

SUPPLEMENTAL DATA

Figure S1. Principal component analysis of the different storage conditions

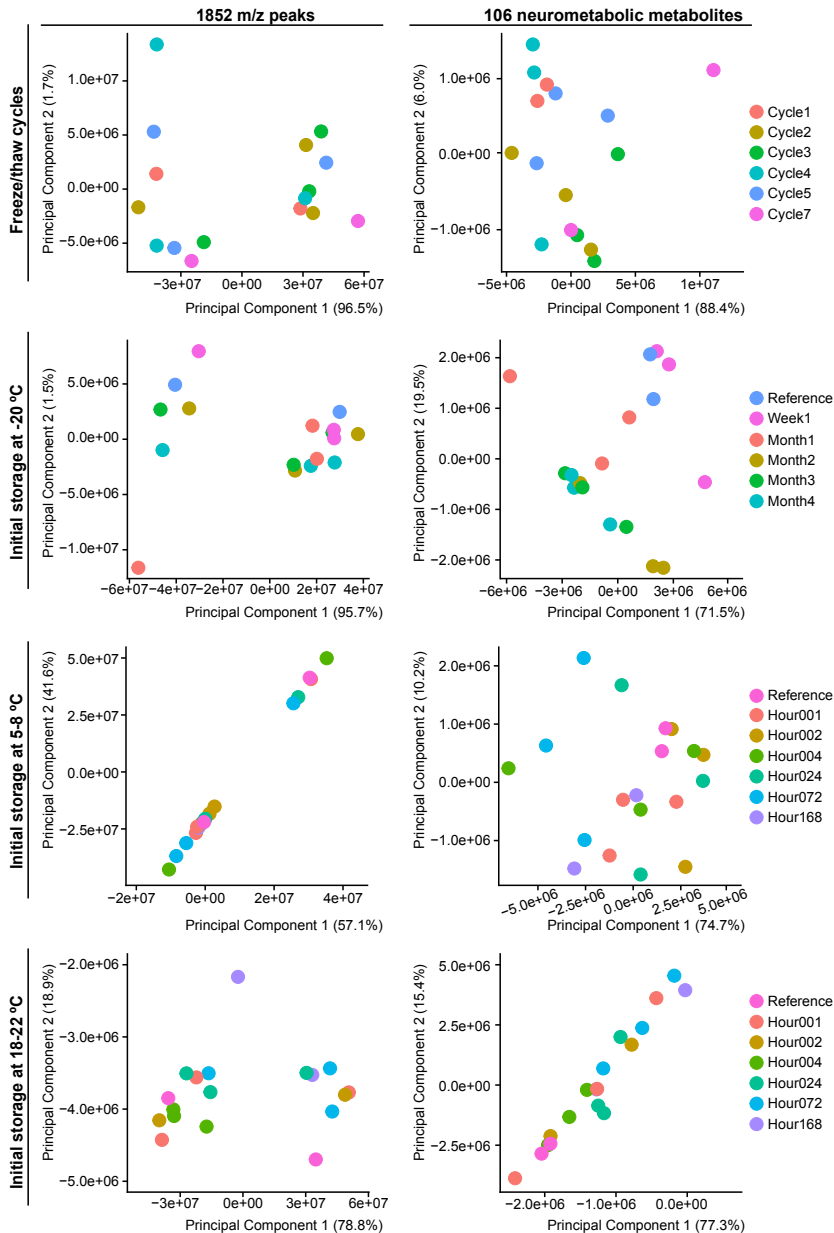
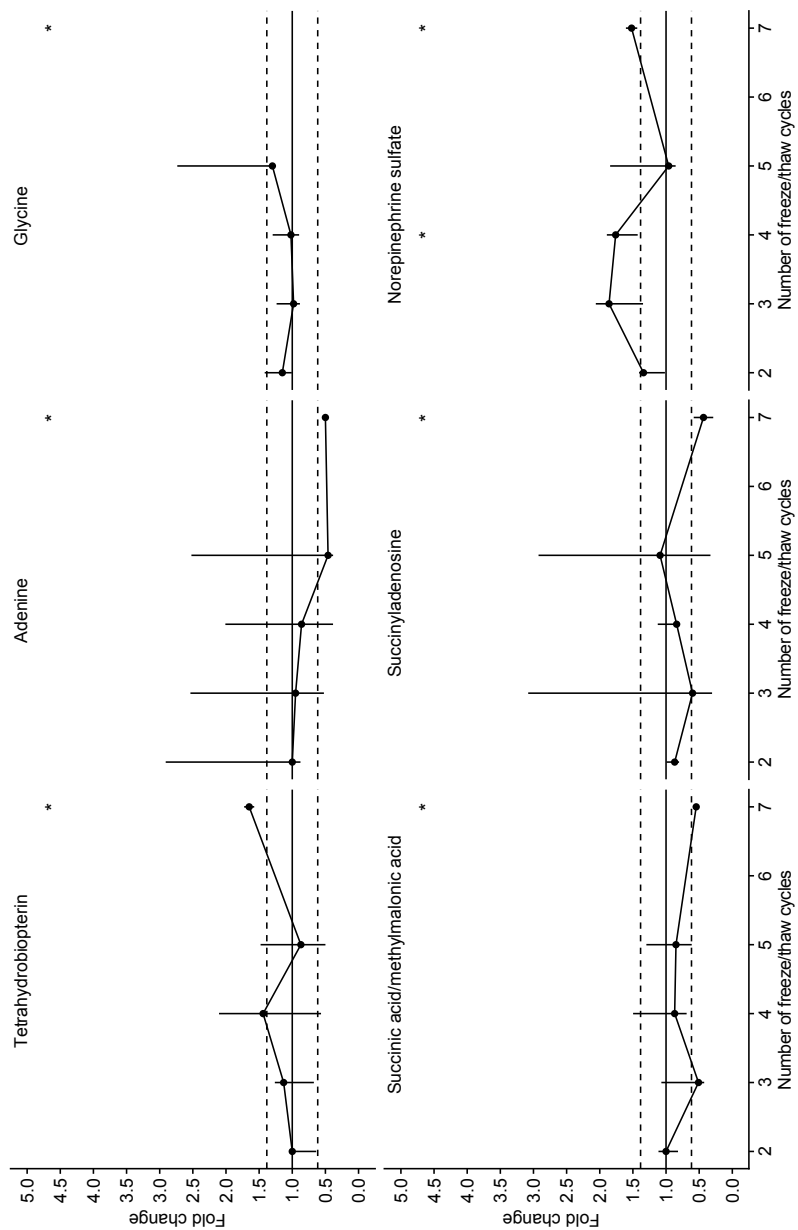
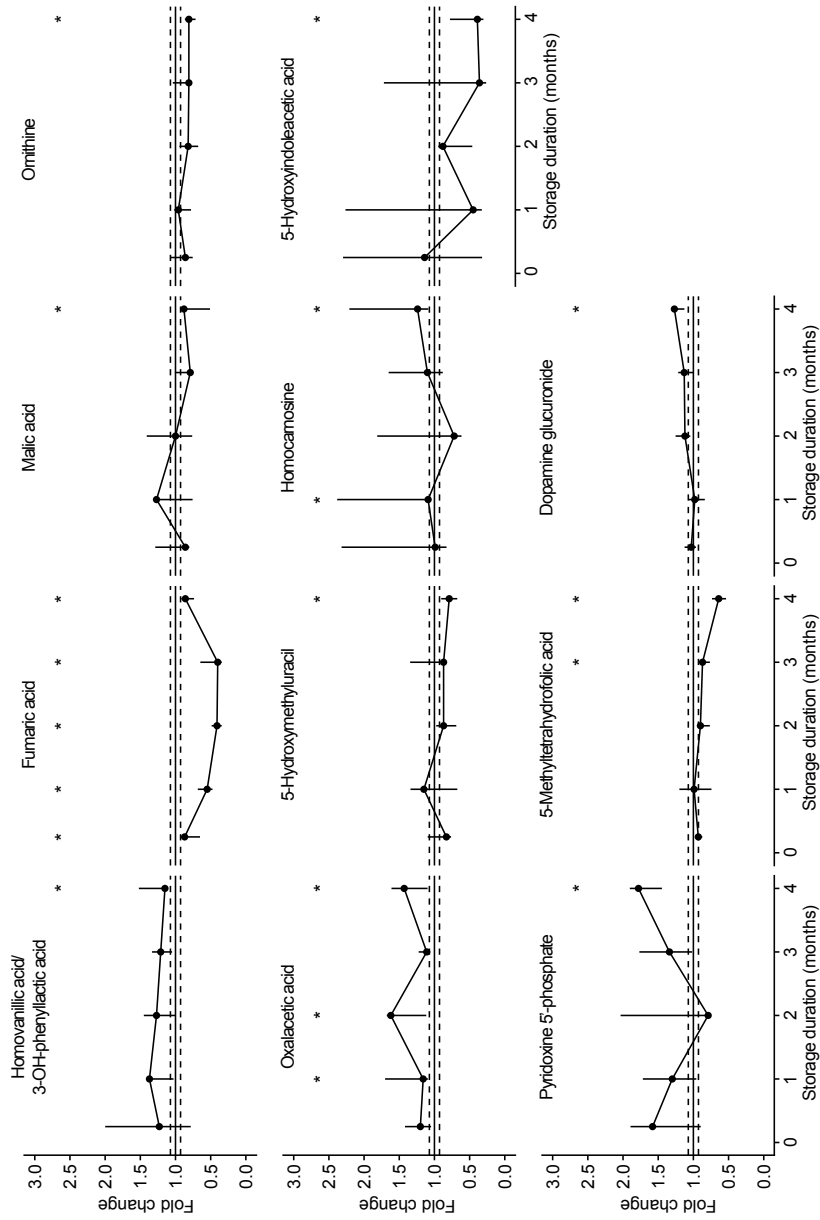


Figure S2. Fold changes of metabolites potentially affected by multiple freeze/thaw cycles



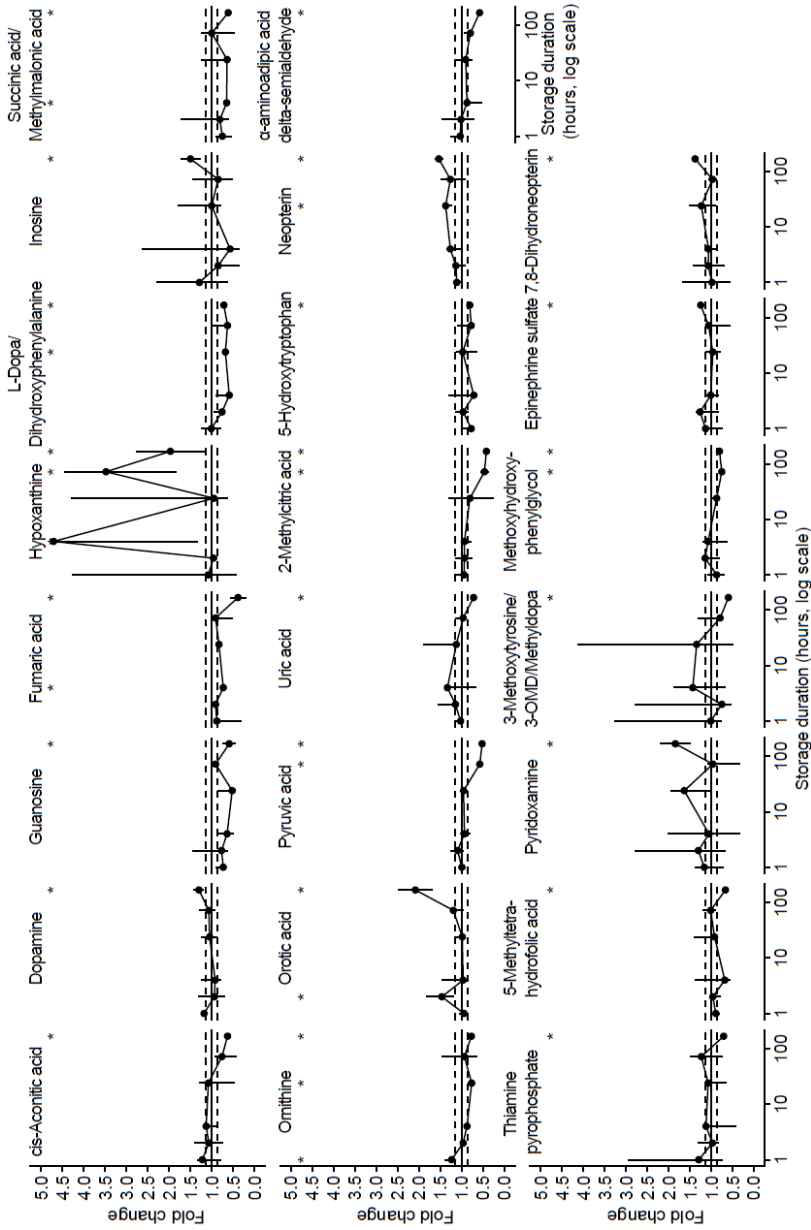
The y-axis depicts the fold change, the x-axis depicts the number of freeze/thaw cycles. The filled black circle depicts the mean fold change, the line depicts the range of the confidence interval. The horizontal black line depicts fold change = 1, horizontal dashed lines indicate the variability that is solely attributed to the analysis, as in Figure 2. Asterisks depict the storage condition for which the lower limit of the confidence interval was above the upper dashed line, and for which the upper limit of the confidence interval was below the lower dashed line.

Figure S3. Fold changes of metabolites potentially affected by prolonged storage at -20 °C



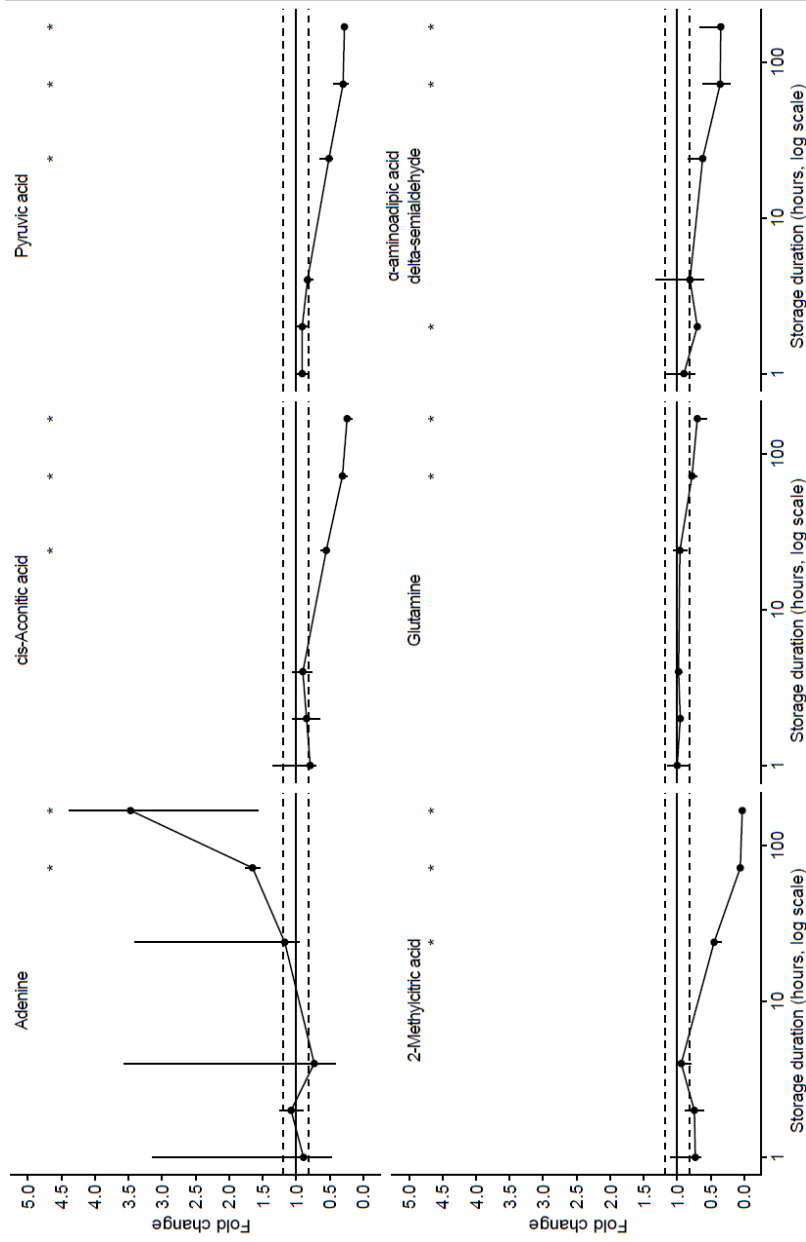
The y-axis depicts the fold change, the x-axis depicts the storage duration at -20 °C in months. The filled black circle depicts the mean fold change, the line depicts the range of the confidence interval. The horizontal black line depicts fold change = 1, horizontal dashed lines indicate the variability that is solely attributed to the analysis, as in Figure 2. Asterisks depict the storage condition for which the lower limit of the confidence interval was above the upper dashed line, and for which the upper limit of the confidence interval was below the lower dashed line.

Figure S4. Fold changes of metabolites potentially affected by prolonged storage at 5-8 °C

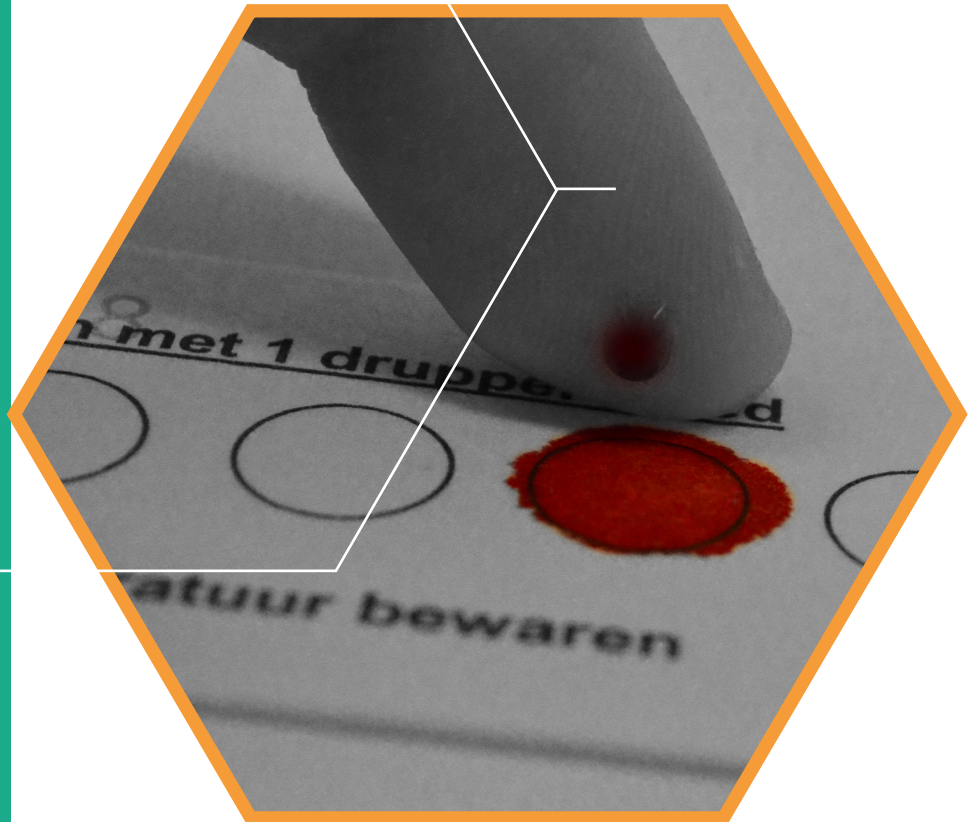
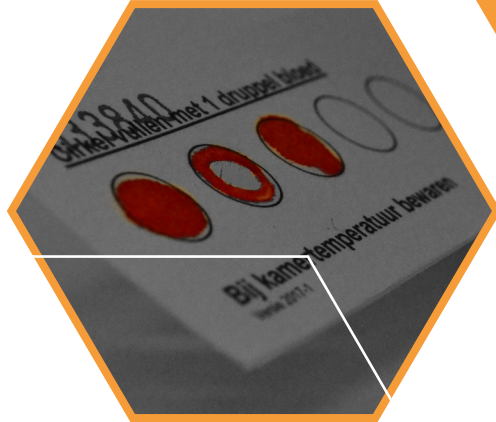


The y-axis depicts the fold change, the x-axis depicts the storage duration at 5-8 °C in hours. The filled black circle depicts the mean fold change, the line depicts the range of the confidence interval. The horizontal black line depicts fold change = 1, horizontal dashed lines indicate the variability that is solely attributed to the analysis, as in Figure 2. Asterisks depict the storage condition for which the lower limit of the confidence interval was above the upper dashed line, and for which the upper limit of the confidence interval was below the lower dashed line.

Figure S5. Fold changes of metabolites potentially affected by prolonged storage at 18-22 °C



The y-axis depicts the fold change, the x-axis depicts the storage duration at 18-22 °C in hours. The filled black circle depicts the mean fold change, the line depicts the range of the confidence interval. The horizontal black line depicts fold change = 1, horizontal dashed lines indicate the variability that is solely attributed to the analysis, as in Figure 2. Asterisks depict the storage condition for which the lower limit of the confidence interval was above the upper dashed line, and for which the upper limit of the confidence interval was below the lower dashed line.



Aspartylglucosamine is a biomarker for

NGLY1-CDDG, a congenital disorder of deglycosylation

Molecular Genetics and Metabolism 2019, 127(4): 368-372
DOI: 10.1016/j.ymgme.2019.07.001

Hanneke A. Haijes*, Monique G.M. de Sain-van der Velden,
Hubertus C.M.T. Prinsen, Anke P. Willems, Maria van der Ham,
Johan Gerrits, Madeline H. Couse, Jan M. Friedman,
Clara D.M. van Karnebeek, Kathryn A. Selby, Peter M. van Hasselt,
Nanda M. Verhoeven-Duif, Judith J.M. Jans*

* Corresponding authors

ABSTRACT

Background: NGLY1-CDDG is a congenital disorder of deglycosylation caused by a defective peptide:N-glycanase (PNG). To date, all but one of the reported patients have been diagnosed through whole-exome or whole-genome sequencing, as no biochemical marker was available to identify this disease in patients. Recently, a potential urinary biomarker was reported, but the data presented suggest that this marker may be excreted intermittently.

Methods: In this study, we performed untargeted direct-infusion high-resolution mass spectrometry metabolomics in seven dried blood spots (DBS) from four recently diagnosed NGLY1-CDDG patients, to test for small-molecule biomarkers, in order to identify a potential diagnostic marker. Results were compared to 125 DBS of healthy controls and to 238 DBS of patients with other diseases.

Results: We identified aspartylglycosamine as the only significantly increased compound with a median Z-score of 4.8 (range: 3.8 – 8.5) in DBS of NGLY1-CDDG patients, compared to a median Z-score of -0.1 (range: -2.1 – 4.0) in DBS of healthy controls and patients with other diseases.

Discussion: The increase of aspartylglycosamine can be explained by lack of function of PNG. PNG catalyzes the cleavage of the proximal N-acetylglucosamine residue of an N-glycan from the asparagine residue of a protein, a step in the degradation of misfolded glycoproteins. PNG deficiency results in a single N-acetylglucosamine residue left attached to the asparagine residue which results in free aspartylglycosamine when the glycoprotein is degraded. Thus, we here identified aspartylglycosamine as the first potential small-molecule biomarker in DBS for NGLY1-CDDG, making a biochemical diagnosis for NGLY1-CDDG potentially feasible.

KEY MESSAGE

Aspartylglycosamine is the first potential small-molecule biomarker in DBS for NGLY1-CDDG, making a biochemical diagnosis for NGLY1-CDDG potentially feasible.

INTRODUCTION

NGLY1-CDDG is the first congenital disorder of deglycosylation described (MIM #615273). It is an autosomal recessive disorder affecting peptide:N-glycanase (PNG), which is a cytosolic enzyme that catalyzes the cleavage of the amide bond between the proximal (β -aspartylglycosylamine)N-acetylglucosamine residue of glycans and the asparagine residue of a glycoprotein.¹² Non-functional PNG is expected to cause dysregulation of endoplasmic reticulum-associated degradation, the quality control system for newly synthesized proteins.⁶ This results in accumulation of misfolded N-glycoproteins in the cytosol, which may cause the various symptoms observed in NGLY1-CDDG patients.

To date, eighteen patients with pathogenic variants in *NGLY1* have been reported in literature^{1,2,4,5,8,9} and the NGLY1-CDDG patient association was aware of a total of 63 NGLY1-CDDG patients in January 2018 (NGLY1 deficiency handbook, www.NGLY1.org). Affected individuals present with global developmental delay, movement disorders, hypotonia, decreased deep tendon reflexes, EEG abnormalities and microcephaly. In addition, patients may demonstrate hypo- or alacrima (the absence of tears), elevated liver transaminases and constipation. NGLY1-CDDG is a progressive condition, for which no cure is available yet.⁶ Identification of NGLY1-CDDG is challenging, owing to the clinical heterogeneity, broad differential diagnosis, and lack of diagnostic biochemical markers. As no reliable biomarker has been available to identify this disease, all but one of the currently known patients were diagnosed through whole-exome sequencing (WES) or whole-genome sequencing (WGS). Recently, a potential urinary biomarker was reported, with a structure of Neu5Ac1Hex1GlcNAc1-Asn (Asn-N).⁴ This compound was identified by oligosaccharide analysis in urine using MALDI-TOF mass spectrometry.⁴ One additional NGLY1-CDDG patient was identified based on an increased concentration of this marker in urine. The authors report a sensitivity of 92.3% and a specificity of 99.6%, but they note that the relative amounts of Asn-N can vary over time, suggesting intermittent excretion of this metabolite.⁴ In this study, we performed untargeted direct-infusion high-resolution mass spectrometry (DI-HRMS) metabolomics in dried blood spots (DBS) of four recently diagnosed NGLY1-CDDG patients to test for small-molecule biomarkers. We identified aspartylglycosamine as a potential small-molecule biomarker for NGLY1-CDDG.

METHODS

A total of seven DBS from four NGLY1-CDDG patients (sampled at ages ranging from 1.1 to 16.5 years old) were included. Two DBS from a patient affected with aspartylglucosaminuria, obtained after stem cell transplantation (SCT), were also included. Thirty samples from individuals in whom an inborn error of metabolism (IEM) was excluded after thorough routine diagnostic work-up were selected to serve as control samples. All individuals or their legal guardians approved the use of their remnant samples for this research. All procedures followed were in accordance with the ethical standards of the University Medical Centre Utrecht and with the Helsinki Declaration of 1975, as revised in 2000. Studies on P4 were approved by the University of British Columbia Research Ethics Board (project reference H16-02126).

Blood samples were initially drawn for routine metabolic diagnostics or follow-up. Blood samples were collected by venous puncture in heparin-containing tubes where after aliquots of the blood sample were aspirated, or blood samples were collected by a finger prick. The sample was spotted onto Guthrie card filter paper (Whatman no. 903 Protein saver TM cards). Papers were left to dry for at least four hours at room temperature and were

subsequently stored at -80°C in a foil back with desiccant package pending further analysis. DBS sample extraction was performed as previously described.³ DI-HRMS was performed on DBS using a TriVersa NanoMate system (Advion, Ithaca, NY, USA), controlled by Chipsoft software (version 8.3.3, Advion), that is mounted onto the interface of a Q-Exactive high-resolution mass spectrometer (Thermo Scientific™, Bremen, Germany), with an m/z scan range of 70–600 m/z .³

For each mass peak per patient sample, the deviation from the intensities in the thirty control samples was indicated by a Z-score, calculated by: $Z\text{-score} = (\text{intensity patient sample} - \text{mean intensity control samples}) / \text{standard deviation intensity control samples}$.³ Z-scores were calculated to be able to compare results of individual samples from different batches.³ Z-scores were calculated for both patient and control samples. Z-scores were considered aberrant when > 2.0 or < -1.5 , since metabolite decreases are often more subtle than increases in IEM.

Z-scores of the patients with NGLY1-CDDG and aspartylglucosaminuria were compared to the Z-scores of the thirty control samples included in this study. To test the specificity of the potentially identified biomarker, patient Z-scores were also compared to results obtained for other research projects, reported as well as ongoing.³ For these projects, both 95 additional control samples and 238 samples from 154 patients were analyzed in other batches. The 95 control samples were also obtained from individuals in whom an IEM was excluded after thorough routine diagnostic work-up. In the 154 patients, DI-HRMS metabolomics was performed either to find a diagnosis for a yet unsolved phenotype expected to be caused by an IEM ($n = 100$), or to identify biomarkers for a variety of known IEMs ($n = 54$). A Mann-Whitney U test was performed comparing Z-scores of all 125 control samples (30 + 95 samples) and the 238 samples from other patients combined, to the 7 NGLY1-CDDG patient samples. All p-values were adjusted according to the Bonferroni method. A p-value < 0.05 was considered statistically significant. Data analysis was performed in R programming language.

RESULTS

Patients

Patient 1 is an eighteen-year old Caucasian male, the third child of consanguineous parents of Moroccan descent. He presented with psychomotor retardation and a movement disorder with involuntary movements and choreo-athetosis. His development was severely delayed, but he did not show any regression. He walked at the age of fifteen months, but he frequently fell due to insufficient balance. He spoke two-word sentences at the age of two years. He was continent for urine and defecation at the age of eleven years and learned to ride a bike at the age of thirteen years. Over the last years, his development stagnated. Currently, he is not able to read, write or calculate. He is able to dress and undress himself but he needs help with preparing food. He scored 55 on the Wechsler Non-Verbal NL IQ test, and his passive vocabulary was < 56 on the Peabody Picture Vocabulary Test-III-NL. Magnetic resonance imaging (MRI) of the brain at the age of sixteen years was normal, and vision and hearing are both normal.

His 26-year old sister presented similarly, with psychomotor retardation and a movement disorder with involuntary movements and choreo-athetosis. She also had hypolacrimea, corneal ulcerations and chalazions. No brain MRI was performed in this patient. In both patients, there is no microcephaly and no epileptic encephalopathy. There were no signs of liver problems. DBS samples of the affected sister were not available for this study.

Trio-WES revealed the homozygous variant *NGLY1* c.247-2A > G (p.?) in both patients. This variant affects the splice acceptor site of intron 3 and probably leads to an in-frame skipping of exon 4. The variant was classified as likely pathogenic, class 4, according to the American College of Medical Genetics and Genomics.¹¹ Both parents are heterozygous carriers of this variant. In patient 1, a heterozygous *de novo* *CTNNA2* c.494A > G (p.Asn165Ser) variant of unknown significance (VUS) was detected, but this variant was not detected in his affected sister. Two other siblings demonstrate normal development.

Patient 2 is an eleven-year old Caucasian male, the first child of consanguineous parents of Turkish descent. He presented with intrauterine growth retardation, microcephaly, extreme hypertension, global developmental delay with regression, and epileptic encephalopathy. MRI of the brain at the age of three years was normal, but at the age of eleven years atrophy of the pons, mesencephalon and cervical spinal cord was noted. Concurrent magnetic resonance spectroscopy revealed a decrease of N-acetylaspartic acid. In addition, the patient presented with ocular apraxia, hypolacrimation and corneal ulcerations, elevated liver transaminases, constipation and scoliosis. His younger sister, patient 3, is a six-year old girl who presented similarly, but without intrauterine growth retardation, ocular apraxia and scoliosis. She demonstrated hypotonia and decreased deep tendon reflexes.

Trio-WES revealed the homozygous variant *NGLY1* c.1756C > T (p.Arg586*) in both patients, and both parents are heterozygous carriers of this variant. The variant was classified as pathogenic, class 5.¹¹ In both patients a homozygous *GLDC* c.2027 T > C (p.Ile676Thr) VUS was also identified; both parents are heterozygous carriers of this variant. Mutations in *GLDC* are associated with non-ketotic hyperglycinemia, but the symptoms in P2 and P3 do not fit the phenotypic spectrum non-ketotic hyperglycinemia and glycine concentrations in cerebrospinal fluid (CSF) and plasma were repeatedly normal in both patients (patient 2: CSF 4.8 µmol/L (reference range 2.9–7.9 µmol/L), plasma 254, 20 and 250 µmol/L (reference range 107–343 µmol/L) and patient 3: CSF 6.0 µmol/L (reference range 3.7–7.6 µmol/L), plasma 227, 267 and 215 µmol/L (reference range 107–343 µmol/L)), making it highly unlikely that the identified variant in *GLDC* is pathogenic.

Patient 4 is a fifteen-year old female, the second child of non-consanguineous parents. Her older brother is healthy. She was born after a pregnancy that was complicated by low maternal serum estriol, indicative of increased risk for Smith-Lemli-Opitz syndrome. Later in the pregnancy, fetal movement decreased and fetal growth began to fail. She was born approximately two weeks prematurely by caesarean section for fetal distress, with poor fetal heart rate and intrauterine growth retardation. Her birth weight was less than the 3rd percentile, birth length less than the 10th percentile and birth head circumference just below the 50th percentile.

She was hospitalized for the first three weeks of life for neonatal jaundice and poor feeding. At fifteen years of age she has microcephaly (–2.3 SD), profound intellectual disability, intractable myoclonic epilepsy, spastic quadriplegia, elevated liver transaminases, chronic constipation, recurrent urinary tract infections, scoliosis and bilateral equinovarus deformities. In addition, she has posterior embryotoxon, strabismus, poor visual attention and chalazions, but no hypolacrimation or corneal ulcerations. MRI of the brain was normal at the ages of one and three years but demonstrated cerebellar atrophy at the age of nine years. Concurrent magnetic resonance spectroscopy at the age of nine years showed normal metabolites.

Trio-WGS revealed two heterozygous variants in *NGLY1*, both classified as likely pathogenic:¹¹ the nonsense variant c.1853 T > G (p.Leu618*) inherited from the father and the frameshift

variant c.1612-1_1614dupGGTA (p.Tyr539Glyfs) inherited from the mother. None of the variants reported here has yet been reported in any NGLY1-CDDG patient.^{1,2,5,8,9}

DI-HRMS analysis

DI-HRMS metabolomics resulted in identification of 1,592 m/z features in the analyzed batch that could be annotated with 3,299 metabolites that are expected to occur endogenously.³ A Mann-Whitney U test comparing the samples of NGLY1-CDDG patients to the control samples and samples of other patients revealed one mass peak (m/z 335.132865) corresponding to aspartylglycosamine, with a Bonferroni corrected statistically significant p-value of 0.012. The median Z-score in NGLY1-CDDG patient samples was 4.83 (range: 3.79 to 8.45), while the Z-scores in control and other patient samples ranged from -2.11 to 3.99 (Table 1, Figure 1). Interestingly, in two DBS of a patient with aspartylglucosaminuria (obtained post-SCT), Z-scores of aspartylglycosamine were 2.54 and 2.90, thus increased, but not to the extent of Z-scores in NGLY1-CDDG patient samples. None of the control individuals ($n = 7$) or other patients ($n = 10$) in whom we identified a Z-score > 2.0 for aspartylglycosamine were reported to have phenotypic features of NGLY1-CDDG, but in most of these individuals, no WES or WGS has been performed.

Table 1. Median Z-scores and Z-score ranges of aspartylglycosamine for all samples

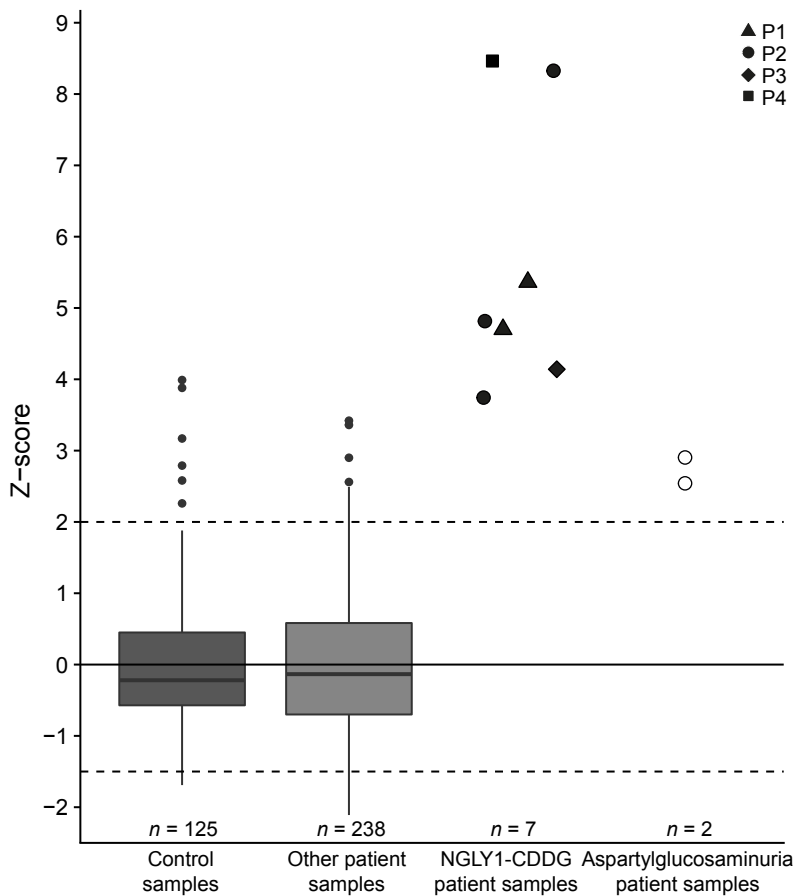
Samples	Number of patients	Patient age (years)	Z-scores Median (range)
Control samples	$n = 125$		-0.16 (-1.76 – 3.99)
Other patient samples	$n = 238$		-0.05 (-2.11 – 3.42)
Aspartylglucosaminuria	$n = 2$		2.72 (2.54 – 2.90)
NGLY1-CDDG	$n = 7$		4.83 (3.79 – 8.45)
P1.1		16.5	4.66
P1.2		16.9	5.41
P2.1		6.2	4.83
P2.2		7.4	8.31
P2.3		11.6	3.79
P3.1		1.1	4.09
P4.1		14.5	8.45

Next, we assessed whether the separation of NGLY1-CDDG patients from control and other patient samples could be improved by calculating metabolite ratios or using combinations of multiple metabolites that approximated statistical significance, but this did not result in identification of an NGLY1-CDDG biomarker that was more specific than aspartylglycosamine. Lastly, it was assessed whether we could identify biomarkers associated with disease severity, by excluding the samples of P1, who has a very mild phenotype. A Bonferroni corrected Mann-Whitney U test comparing the samples of NGLY1-CDDG patients to the control samples and samples of other patients revealed that still only the mass peak annotated with aspartylglycosamine again had a statistically significant p-value.

DISCUSSION

Next-generation sequencing has led to an enormous increase in the discovery and understanding of genetic diseases. In 2012, the first NGLY1-CDDG patient was identified,⁹ and only six years later more than sixty patients have joined the NGLY1-CDDG patient association (NGLY1 deficiency handbook, www.NGLY1.org). Despite its significance, next-generation sequencing also poses challenges, regarding both costs and diagnostic delays, but also regarding our ability to predict the phenotypic consequences of a genetic variant.

Figure 1. Z-scores of aspartylglucosamine for all samples

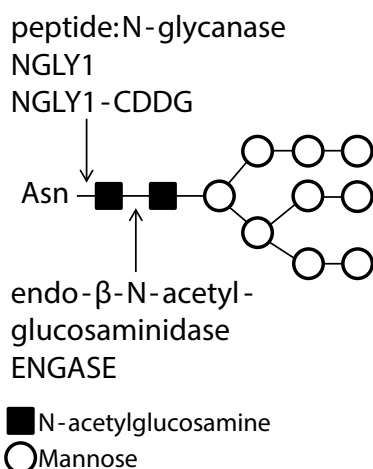


On the y-axis, Z-scores are depicted, on the x-axis, the four groups of samples are depicted. The dark gray boxplot reflects the median, 25th and 75th percentile of the Z-scores of control samples ($n = 125$), the light gray boxplot reflects the median, 25th and 75th percentile of the Z-scores of the samples of other patients ($n = 238$). In black, the Z-scores of the samples of the four NGLY1- CDDG patients ($n = 7$) are depicted with different shapes for each patient, and in open white circles the Z-scores of the samples of the aspartylglucosaminuria patient obtained after stem cell transplantation ($n = 2$) are depicted. The dashed lines depict the cut-off values for Z-scores to be considered aberrant: > 2 or < -1.5 .

Large numbers of VUS are identified through next-generation sequencing and functional assessment is often required to determine the consequences of these VUS. Easy accessible, reliable biomarkers can serve in the challenge of resolving VUS in genes encoding enzymes and transporters.³ In this study we demonstrate that aspartylglucosamine is increased in DBS of patients with NGLY1-CDDG compared to both control samples and samples of other patients. The identification of aspartylglucosamine as biomarker for NGLY1-CDDG signifies that a biochemical diagnosis, rather than a diagnosis resulting from WES, is potentially feasible for NGLY1-CDDG. In addition, it holds the promise of validating VUS in *NGLY1* and thereby possibly a further expansion of the number of patients diagnosed with NGLY1-CDDG.

Biologically, the identification of aspartylglycosamine as biomarker for NGLY1-CDDG is intelligible. The cytoplasmic PNG catalyzes the cleavage of the amide bond between the proximal (β -aspartylglycosylamine) N-acetylglucosamine residue and the asparagine residue of glycoproteins in the endoplasmatic reticulum-associated degradation of N-linked glycans. Endo- β -N-acetylglucosaminidase catalyzes the cleavage of the β -1,4-glycosidic bond between the two proximal N-acetylglucosamine residues in the N-glycan, leaving one N-acetylglucosamine residue attached to the asparagine residue of the protein (Figure 2).⁶ Thus, the activity of endo- β -N-acetylglucosaminidase in the absence of functional PNG in glycoprotein breakdown explains why we could identify aspartylglycosamine at elevated levels in DBS of patients with NGLY1-CDDG.

Figure 2. Function of peptide:N-glycanase and endo- β -N-acetylglucosaminidase



Adapted from Huang et al., figure 6⁶. Peptide:N-glycanase (PNG), encoded by *NGLY1*, catalyzes the cleavage of the amide bond between the proximal (β -aspartylglycosylamine)N-acetylglucosamine residue of N-glycans and the asparagine (Asn) residue of the protein in the endoplasmatic reticulum associated degradation of N-linked glycans. In the absence of functional PNG, endo- β -N-acetylglucosaminidase (ENG) catalyzes the cleavage of the β -1,4-glycosidic bond between the two N-acetylglucosamine residues in the N-glycan, leaving one N-acetylglucosamine residue attached to the protein.

In line with the first identified biomarker for NGLY1-CDDG,⁴ we speculate that aspartylglycosamine might also be a biomarker for aspartylglycosaminuria. In aspartylglycosaminuria, mutations in *AGA* affect the function of aspartylglucosaminidase. This is an important enzyme in the catabolism of N-glycans in the lysosomes, where it catalyzes the cleavage of the same amide bond between the proximal (β - aspartylglycosylamine) N-acetylglucosamine residue of N-glycans and the asparagine residue of the protein as PNG. The biochemical phenotype in urine of the aspartylglucosaminuria patient was partly resolved by SCT, as oligosaccharide analysis by thin layer chromatography was only minimally abnormal post-SCT. Interestingly, even after SCT, the two samples of this patient demonstrated Z-scores > 2.0 for aspartylglycosamine. These findings are in line with previous studies, reporting increased aspartylglycosamine in urine, cerebrospinal fluid and plasma of patients with aspartylglucosaminuria.^{7,10} However, we cannot draw solid conclusions on the presence of aspartylglycosamine in DBS of patients with aspartylglucosaminuria, since

Z-scores overlap with control samples and samples of other patients, and the sample size is too small (1 patient, 2 DBS) and only post-SCT.

We were not able to identify the urinary marker detected by Hall et al. in the DBS of the patients, as the mass of Asn-N exceeds 600 m/z, the maximum m/z that we identify using DI-HRMS.

This work demonstrates that DI-HRMS metabolomics is suitable for identification of new potential small-molecule biomarkers for inborn errors of metabolism, as discussed before.³ To prospectively assess the diagnostic value of aspartylglucosamine as a biomarker for NGLY1-CDDG, we are anxious to test DBS from additional patients clinically suspected to have NGLY1-CDDG, with biallelic genetic variants in *NGLY1* including *VUS*, or both. We are especially interested in testing neonatal DBS samples, to assess whether aspartylglucosamine in DBS could potentially be a biomarker for newborn screening for NGLY1-CDDG, in case a treatment for NGLY1-CDDG becomes available.

CONCLUSION

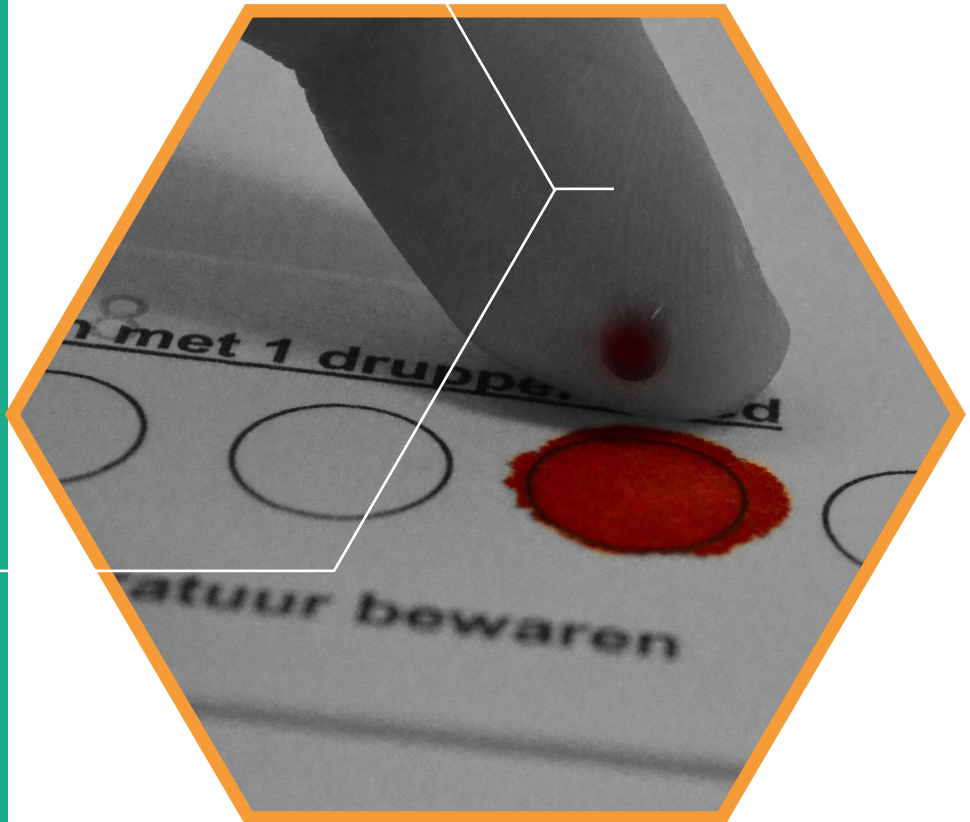
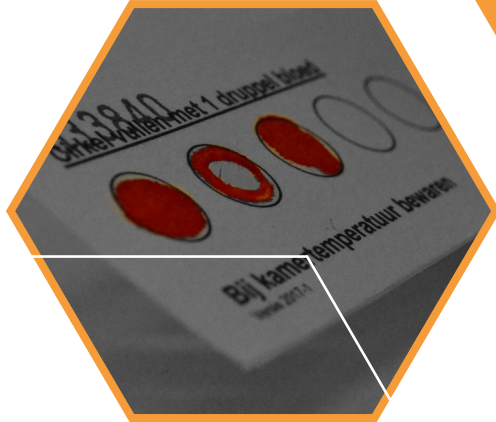
In summary, we here report aspartylglucosamine as the first small-molecule biomarker in DBS for NGLY1-CDDG, which makes a biochemical diagnosis for NGLY1-CDDG potentially feasible.

WEB RESOURCES

NGLY1-CDDG patient association <https://www.ngly1.org>

REFERENCES

1. Caglayan AO, Comu S, Baranoski JF et al. NGLY1 mutation causes neuromotor impairment, intellectual disability, and neuropathy. *Eur J Med Genet* 2015;58(1): 39-43.
2. Enns GM, Shashi V, Bainbridge M et al. Mutations in NGLY1 cause an inherited disorder of the endoplasmic reticulum-associated degradation pathway. *Genet Med* 2014;16(10):751-758.
3. Haijes HA, Willemsen M, van der Ham M et al. Direct-infusion based non-quantitative metabolomics identifies metabolic disease in patients' dried blood spots and plasma. *Metabolites* 2019;9:12.
4. Hall PL, Lam C, Alexander JJ et al. Urine oligosaccharide screening by MALDI-TOF for the identification of NGLY1 deficiency. *Mol Genet Metab*. 2018;124(1):82-86.
5. Heeley J, Shinawi M. Multi-systemic involvement in NGLY1-related disorder caused by two novel mutations. *Am J Med Genet A* 2015;167A(4):816-820.
6. Huang C, Harada Y, Hosomi A et al. Endo- β -N-acetylglucosaminidase forms N-GlcNAc protein aggregates during ER-associated degradation in Ngly1-defective cells. *Proc Natl Acad Sci USA*. 2015;112(5):1398-1403.
7. Jenner FA, Pollitt RJ. Large quantities of 2-acetamido-1-(β' -L-aspartamido)-1,2-dideoxyglucose in the urine of mentally retarded siblings. *Biochem J*. 1967;103:48-49.
8. Lam C, Ferreira C, Krasnewich D et al. Prospective phenotyping of NGLY1-CDDG, the first congenital disorder of deglycosylation. *Genet Med* 2016;19(2):160-168.
9. Need AC, Shashi V, Hitomi Y et al. Clinical application of exome sequencing in undiagnosed genetic conditions. *J Med Genet*. 2012;49(6):353-361.
10. Pollitt RJ, Jenner FA, Merskey H. Aspartylglucosaminuria, an inborn error of metabolism associated with mental defect. *Lancet* 1968;2(7562):253-255.
11. Richards S, Aziz N, Bale S et al. Standards and guidelines for the interpretation of sequence variants: A joint consensus recommendation of the American College of Medical Genetics and Genomics and the Association for Molecular Pathology. *Genet Med*. 2015;17:405-424.
12. Suzuki T, Seko A, Kitajima K, Inoue Y, Inoue S. Identification of peptide:N-glycanase activity in mammalian-derived cultured cells, *Biochem Biophys Res Commun*. 1993;194(3):1124-1130.



**Accurate discrimination of Hartnup disorder from
other aminoacidurias using a diagnostic ratio**

*Molecular Genetics and Metabolism Reports 2019, eCollection 2020 March
DOI: 10.1016/j.ymgmr.2019.100551*

Hanneke A. Haijes, Hubertus C.M.T. Prinsen,
Monique G.M. de Sain-van der Velden, Nanda M. Verhoeven-Duif,
Peter M. van Hasselt[†], Judith J.M. Jans^{†,*}

[†] These authors contributed equally to this article
^{*} Corresponding author

ABSTRACT

Introduction: Hartnup disorder is caused by a deficiency of the sodium dependent B⁰ AT1 neutral amino acid transporter in the proximal kidney tubules and jejunum. Biochemically, Hartnup disorder is diagnosed via amino acid excretion patterns. However, these patterns can closely resemble amino acid excretion patterns of generalized aminoaciduria, which may induce a risk for misdiagnosis and preclusion from treatment. Here we explore whether calculating a diagnostic ratio could facilitate correct discrimination of Hartnup disorder from other aminoacidurias.

Methods: 27 amino acid excretion patterns from 11 patients with genetically confirmed Hartnup disorder were compared to 68 samples of 16 patients with other aminoacidurias. Amino acid fold changes were calculated by dividing the quantified excretion values over the upper limit of the age-adjusted reference value.

Results: Increased excretion of amino acids is not restricted to amino acids classically related to Hartnup disorder (“Hartnup amino acids”, HAA), but also includes many other amino acids, not classically related to Hartnup disorder (“other amino acids”, OAA). The fold change ratio of HAA over OAA was 6.1 (range: 2.4 – 9.6) in the Hartnup cohort, versus 0.2 (range: 0.0 – 1.6) in the aminoaciduria cohort (p <0.0001), without any overlap observed between the cohorts.

Discussion: Excretion values of amino acids not classically related to Hartnup disorder are frequently elevated in patients with Hartnup disorder, which may cause misdiagnosis as generalized aminoaciduria and preclusion from vitamin B3 treatment. Calculation of the HAA/OAA ratio improves diagnostic differentiation of Hartnup disorder from other aminoacidurias.

KEY MESSAGE

The fold change ratio of Hartnup amino acids over other amino acids ensures correct diagnostic differentiation of Hartnup disorder from other aminoacidurias.

INTRODUCTION

Aminoacidurias are caused by defective amino acid transport across the renal epithelium. Inborn errors of amino acid transporters include lysinuric protein intolerance (LPI) (MIM #222700), cystinuria (MIM #220100), iminoglycinuria (MIM #242600), dicarboxylic amino aciduria (MIM #222730) and Hartnup disorder (MIM #234500). Next to defective amino acid transporters, transport of amino acids can also be impaired by general dysfunction of the renal tubule, as occurs for example in Fanconi syndrome¹ and Lowe syndrome.² Aminoacidurias are biochemically classified according to their specific amino acid excretion pattern.

Hartnup disorder has an estimated frequency of 1:20.000³ and is caused by a deficiency of the sodium dependent B⁰ AT1 neutral amino acid transporter, encoded by *SLC6A19*. This transporter is mainly expressed in the brush border membrane of the proximal kidney tubules and in the jejunum.⁴⁻⁶ The disorder is biochemically characterized by increased excretion of neutral amino acids including alanine, serine, threonine, valine, leucine, isoleucine, phenylalanine, tyrosine, asparagine, glutamine, tryptophan, histidine and citrulline, whereas excretion of other amino acids is reported to be less affected.^{7,8}

The impaired renal and intestinal transport of neutral amino acids is a risk factor for developing amino acid deficiencies, tryptophan deficiency in particular. As tryptophan is the precursor for serotonin and nicotinamide, also known as vitamin B3, the clinical symptoms of Hartnup disorder are those of a nicotinamide deficiency. Reported symptoms include dermatological symptoms, particularly a pellagra-like rash and light-sensitive dermatitis, intermittent cerebellar ataxia and psychiatric symptoms as emotional instability, delirium and hallucinations.⁹ All symptoms respond well to treatment with vitamin B3.¹⁰

To date, many individuals remain asymptomatic,¹¹ likely because of a sufficiently high intake of protein, tryptophan, vitamin B3 or a combination thereof.⁹ However, even in asymptomatic patients, accurate diagnosis of Hartnup disorder is essential,^{11,12} to ensure correct differentiation of Hartnup disorder from other aminoacidurias, which would demand alternative diagnostic trajectories. Biochemically, Hartnup disorder is diagnosed based on the amino acid excretion profile. Here, we demonstrate that patients with Hartnup disorder may present with an amino acid excretion pattern that closely resembles generalized aminoaciduria.^{9,13,14} We show that this potential misdiagnosis can be overcome by quantification, visualization and computation of urinary amino acids, enabling us to correctly discriminate Hartnup disorder from other causes of aminoaciduria.

METHODS

Patient inclusion

Twenty-seven urine samples of 11 patients with Hartnup disorder were analyzed. Four of these patients were included at the University Medical Centre Utrecht. Hartnup disorder was confirmed through PCR amplification followed by Sanger sequencing of *SLC6A19*. Patient 1 is compound heterozygous for the pathogenic *SLC6A19* c.517G>A (p.Asp173Asn) and c.1173+2T>G (p.?) mutations.⁶ Patient 2, 3 and 4 are homozygous for the common *SLC6A19* c.517G>A (p.Asp173Asn) mutation. Patient 3 and 4 are siblings. To extend the Hartnup disorder cohort, amino acid excretion patterns of seven patients with Hartnup disorder previously published by Potter et al. were included.¹⁵ Hartnup disorder was genetically confirmed in these patients by Seow et al.⁶ One patient (patient 2/II) was excluded, because of heterozygosity for cystinuria type II. In the patients from Potter et al., amino acid excretion patterns were quantified using a Beckman 6300 amino acid analyzer.¹⁵

To differentiate Hartnup disorder from other aminoacidurias, 10 samples of 7 patients with generalized aminoaciduria, 16 samples of 2 patients with LPI and 42 samples of 7 patients with cystinuria were included, coming to a combined aminoaciduria cohort of 68 samples of 16 patients, all from the University Medical Centre Utrecht. All diagnoses were genetically confirmed.

Quantification of amino acid excretion

Amino acid excretion was quantified at the University Medical Centre Utrecht using a Biochrom amino acid analyzer (Isogen Life Sciences, de Meern, the Netherlands) according to diagnostic standards. Amino acid excretion was expressed in mmol/mol creatinine. Age adjusted reference values were obtained from literature, taking into account seven age groups: first week (1), first week till first month (2), first month till four months (3), four months till two years (4), two years till ten years (5), ten years till eighteen years (6) and above eighteen years (7).¹⁶

Statistical analysis

Amino acid fold changes were calculated by dividing the quantified excretion values over the upper limit of the age-adjusted reference value. Amino acids were grouped into Hartnup amino acids (HAA) versus other amino acids (OAA). HAA included alanine, serine, threonine, valine, leucine, isoleucine, phenylalanine, tyrosine, asparagine, glutamine, tryptophan, histidine and citrulline,^{7,8} and OAA included arginine, lysine, aspartic acid, glutamic acid, glycine, cysteine, methionine, proline, ornithine, taurine and alpha-aminobutyric acid. Statistical analyses were performed using R programming language. Results were visualized in both heatmaps and scatter plots. Data files and R code are available upon request.

RESULTS

Amino acid excretion patterns of the patients with Hartnup disorder in the Utrecht cohort are presented in Table 1. This table displays that increased excretion of amino acids is not restricted to HAA, but also includes many OAA, including cystine (in all 20 samples), alpha-aminobutyric acid (in 19/20), glycine and lysine (both in 17/20), citrulline and glutamic acid (both in 15/20), aspartic acid (in 14/20) and arginine (in 12/20). This precludes discrimination of Hartnup disorder from other aminoacidurias and induces the risk of misclassification as generalized aminoaciduria (Figure 1A).

We assessed whether the degree of increase could aid differentiation of Hartnup disorder from other aminoacidurias. Indeed, quantification of amino acid excretion values and computation of amino acid fold changes enabled visual discrimination between Hartnup disorder and generalized aminoaciduria (Figure 1B). The heatmap demonstrating the fold changes shows that, unlike in patients with generalized aminoaciduria, in both Hartnup disorder cohorts the fold changes of HAA were strikingly higher than the fold changes of OAA. LPI and cystinuria could also be recognized easily: LPI based on clear increases of arginine, lysine and ornithine and cystinuria based on the additional increase of cystine (Figure 1B).

In patients with Hartnup disorder, the mean fold change of HAA ranged from 8.1 for phenylalanine to even 49.7 for valine. Histidine, an amino acid classically related to Hartnup disorder, was unexpectedly only slightly elevated, with a mean fold change of 3.1. Surprisingly, this was even lower than in generalized aminoaciduria, for which a mean fold change of 7.8 was calculated.

Table 1. Amino acid excretion of patients with Hartnup disorder

Age group	Upper limits age groups			Patient 1					Patient 2				
	05	06	07	1.1	1.2	1.3	1.4	1.5	2.1	2.2	2.3	2.4	
Alanine	80	85	59	1099	1443	1102	539	969	407	264	472	479	
Serine	95	78	69	1471	2015	1220	724	1145	754	536	700	655	
Threonine	45	36	48	826	1180	608	556	734	348	325	455	423	
Valine	12	11	7	344	1094	329	381	550	500	560	653	663	
Leucine	12	9	6	98	776		141	281	193	259	287	332	
Isoleucine	7	7	5	155	510		143	262	131	175	197	229	
Phenylalanine	20	17	11	119	353	95	122	156	151	134	161	175	
Tyrosine	42	37	27	623	949	536	432	616	299	233	254	249	
Asparagine	29	27	9	760	972		520	569	317	316	437	357	
Glutamine	137	98	57	2658	4684	3176	1190	1873	1571	1859	1257	1793	
Histidine	216	184	153	836	1259	732		804	436	424	396	443	
Citrulline	18	5	2	38	134		34	90	54	51	44	53	
Arginine	9	8	7	14	57	8	18	34	11	6	8	8	
Lysine	64	20	52	237	751	154	202	359	67	59	80	103	
Aspartic acid	21	7	5		47		3	4	40	12	15	23	
Glutamic acid	31	6	3	63	258			73	107	89	178	88	
Glycine	201	252	199	562	739	377	297	488	224	111	169	195	
Cysteine	17	16	19	24	71	22	26	34	65	31	45	46	
Ornithine	7	6	5	5	24	2	4	8	5	6	5	9	
Taurine	79	79	80	17	100		13	25	13	21	12	32	
α-amino-butyric acid	7	7	7	28	56		43	50	25	38	32	35	

Age group	Upper limits age groups						Patient 3						Patient 4															
	05		06		07		3.1		3.2		3.3		3.4		3.5		3.6		4.1		4.2		4.3		4.4		4.5	
	05	06	06	07	07	07	05	06	05	06	06	06	06	06	06	06	07	07	05	05	05	05	05	05	05	05	05	05
Alanine	80	85	1026	621	1020	988	1041	1108	988	474	590	585	460	1429														
Serine	95	78	1550	1002	1108	1154	997	988	736	745	892	672	1631															
Threonine	45	36	891	724	506	564	567	567	513	376	485	374	854															
Valine	12	11	605	388	363	338	416	389	441	349	377	243	803															
Leucine	12	9	199	220	81	117	151	138	181	67	87	33	189															
Isoleucine	7	7	189	168	88	88	115	131	192	105	135	50	199															
Phenylalanine	20	17	152	128	84	76	96	101	109	95	110	37	123															
Tyrosine	42	37	717	488	377	431	521	272	375	327	436	231	656															
Asparagine	29	27	504	382	417	430	389	388	388	355	441	312	492															
Glutamine	137	98	3009	1422	1858	1560	2030	1443	1052	1197	1272	997	879															
Histidine	216	184	58	710	602	656	640	515	489	557	587	477	713															
Citrulline	18	5	50	50	23	31	18	14	8	2	1	8	26															
Arginine	9	8	9	14	9	11	6	6	11	2	5	2	11															
Lysine	64	20	118	208	57	70	59	57	87	37	40	32	84															
Aspartic acid	21	7	42	42	26	34	18	18	29	19	26	43	19															
Glutamic acid	31	6	622	622	31	65	12	62	36	20	31	37	35															
Glycine	201	252	475	365	437	647	718	730	334	309	356	311	877															
Cysteine	17	16	66	60	28	24	21	20	32	20	26	25	40															
Ornithine	7	6	9	9	5	7	4	4	5	2	3	2	6															
Taurine	79	79	75	22	475	40	19	22	71	193	78	17	46															
α -amino-butyric acid	7	7	54	48	22	35	24	25	44	42	42	23	53															

Amino acid excretion patterns of patients with Hartnup disorder in mmol/mmol creatinine. Age group: age adjusted reference values were obtained from literature, taking into account seven age groups: first week (1), first month till first month (2), first month till four months (3), four months till two years (4), two years till ten years (5), ten years till eighteen years (6) and above eighteen years (7)¹⁶. Hartnup amino acids: alanine to glutamine. Other amino acids: arginine to α -aminobutyric acid.

Figure 1. Visualization of amino acid excretion in Hartnup disorder

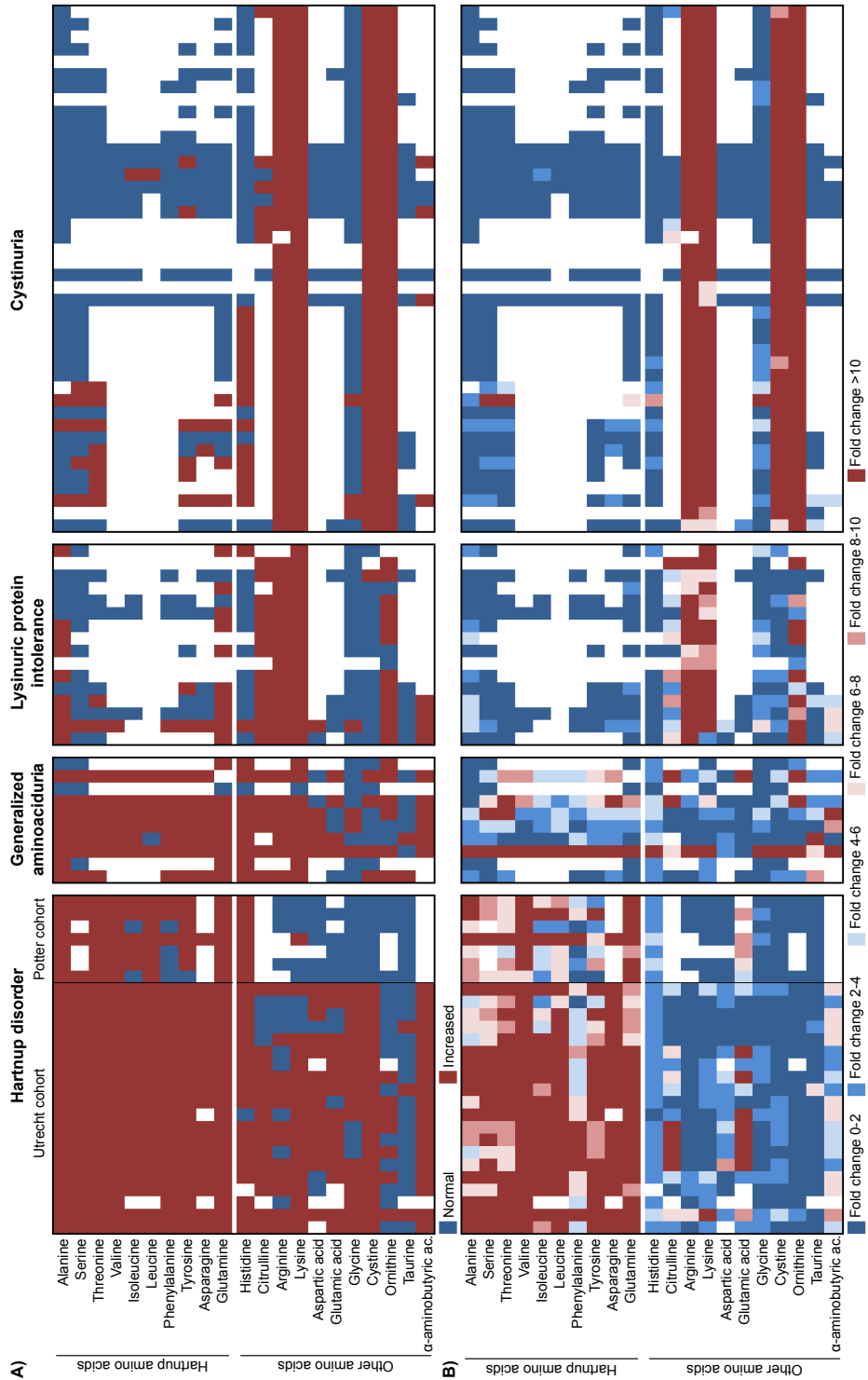
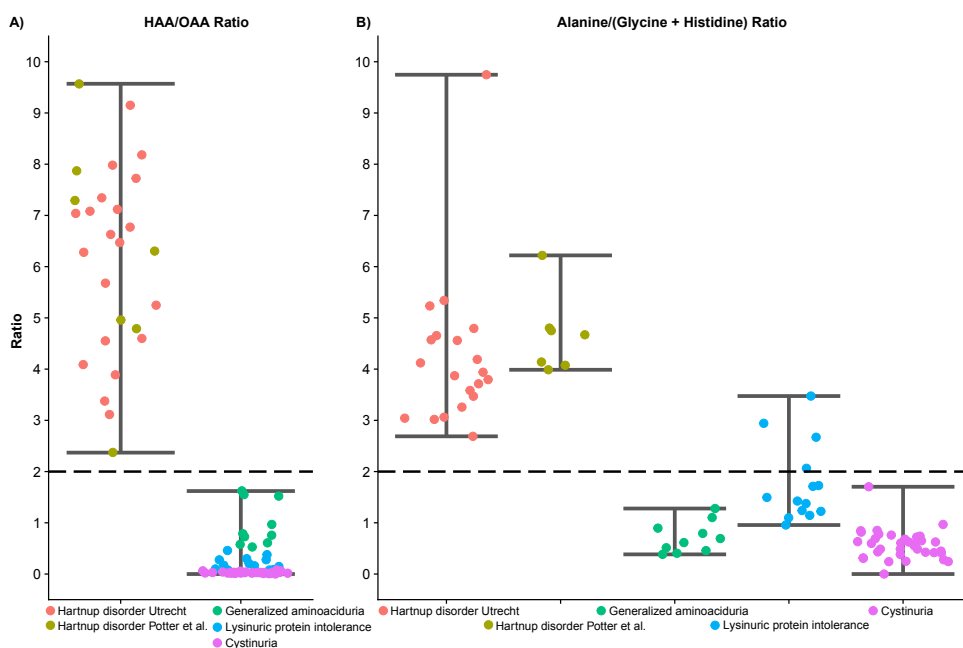


[Figure 1 continued] A) Heatmap of amino acid excretion values. Normal excretion values are depicted in blue, and excretion values higher than age-adjusted upper reference values are depicted in red. White indicates that excretion values of that amino acid were not quantified. B) Heatmap of the fold changes of the urinary amino acid concentrations over the age-adjusted upper reference value, allowing visual differentiation of Hartnup disorder from generalized aminoaciduria, lysinuric protein intolerance and cystinuria.

Histidine excretion, while increased in 18/20 samples, seemed similar to the excretion of OAA (range mean fold change 0.9 – 13.1). Computation of the ratio of the mean fold change of HAA over OAA (including histidine) clearly distinguished Hartnup disorder from other aminoacidurias (Table 2, Figure 2A). The mean HAA/OAA ratio in the Hartnup cohort was 6.1, whereas the mean HAA/OAA ratio in the aminoaciduria cohort was only 0.2 (Mann-Whitney U test $p < 0.0001$). Moreover, no overlap was observed between the two cohorts, as the minimum value of the HAA/OAA ratio in Hartnup disorder was 2.4, while the maximum value of the HAA/OAA ratio in other aminoacidurias was 1.6 (Table 2, Figure 2A).

Figure 2. HAA/OAA ratio and Ala/(Gly+His) ratio in Hartnup disorder versus other aminoacidurias



The Hartnup disorder cohort from Utrecht is depicted in orange, the Hartnup disorder cohort of Potter et al. is depicted in brown. Generalized aminoaciduria is depicted in green, lysinuric protein intolerance is depicted in blue and cystinuria is depicted in magenta. The error bar depicts the minimum and maximum values of the presented group. A) The y-axis depicts the HAA/OAA ratio. The x-axis distinguishes patients with Hartnup disorder from patients with other aminoacidurias. The dashed line at ratio = 2 depicts the cut-off value between Hartnup disorder and other aminoacidurias. B) The y-axis depicts the Ala/(Gly+His) ratio. The x-axis distinguishes the five patient groups. The dashed line at ratio = 2 depicts the cut-off value between Hartnup disorder and generalized aminoaciduria. Abbreviations: Ala: alanine; FC: fold change; Gly: glycine; HAA: Hartnup amino acids; His: histidine; OAA: other amino acids.

Table 2. HAA/OAA ratio and Ala/(Gly+His) ratio in Hartnup disorder versus other aminoacidurias

	Patients	Samples	FULL RATIO: HAA/OAA		FC Alanine	LIMITED RATIO: ALA/(GLY+HIS)	
			Mean FC HAA	Mean FC OAA		Mean FC Gly and His	Ala/(Gly+His) ratio (mean (range))
Hartnup disorder – Utrecht	4	20	19.7	3.7	10.5	2.5	4.2 (2.7–9.8)
Hartnup disorder – Potter et al.	7	7	12.0	1.9	11.9	2.5	4.7 (4.0–6.2)
Hartnup disorder – Combined	11	27	17.7	3.2	10.9	2.5	4.3 (2.7–9.8)
Generalized aminoaciduria	7	10	7.2	6.2	4.7	7.2	0.7 (0.4–1.3)
Lysinuric protein intolerance	2	16	1.6	10.5	2.5	1.7	1.8 (1.0–3.5)
Cystinuria	7	42	1.2	37.0	0.7	1.6	0.6 (0.2–1.7)
Aminoaciduria – Combined	16	68	2.3	25.7	1.8	2.6	0.9 (0.2–3.5)

Abbreviations: Ala: alanine; FC: fold change; Gly: glycine; HAA: Hartnup amino acids; His: histidine; OAA: other amino acids

Computation of the HAA/OAA ratio required quantification of all included amino acids (Table 2). Acknowledging that this is not standard practice in many metabolic diagnostic laboratories, we also evaluated the performance of a ratio using a limited set of amino acids, specifically aiming to distinguish Hartnup disorder from generalized aminoaciduria. Only six amino acids were quantified in all samples of patients with generalized aminoaciduria: serine, alanine, glycine, histidine, cystine and lysine. Of these amino acids, the differences in fold changes between these two patients groups were the largest for alanine, glycine and histidine. The ratio of the fold change of alanine over the mean fold change of glycine and histidine clearly discriminated Hartnup disorder from generalized aminoaciduria, with a mean Ala/(Gly+His) ratio in the Hartnup cohort of 4.3, contrasting with a mean Ala/(Gly+His) ratio of only 0.7 in the generalized aminoaciduria cohort. Even for this limited ratio, there was no overlap between the two cohorts, as the minimum value in the Hartnup cohort was 2.7, while the maximum value for the ratio in generalized aminoaciduria was 1.3 (Table 2, Figure 2B).

DISCUSSION

In this study we demonstrated that quantitative assessment of the degree of the increases, rather than qualitative assessment of increases of amino acid excretion, enhances correct discrimination of Hartnup disorder from other aminoacidurias. We introduce the HAA/OAA ratio as a new and easily applicable diagnostic tool to discriminate Hartnup disorder from other aminoacidurias. Moreover, we demonstrate that even the limited Ala/(Gly+His) ratio, requiring quantification of only three amino acids, can distinguish Hartnup disorder from generalized aminoaciduria.

Quantification of all urinary amino acid concentrations revealed that, in addition to the amino acids reported to be excreted excessively in Hartnup disorder,^{7,8} cystine, alpha-aminobutyric acid, glycine, lysine, citrulline, glutamic acid, aspartic acid and arginine can be increased as well in the urine of patients with Hartnup disorder.^{9,13,14} Unexpectedly, the excretion of histidine, an amino acid of which the intestinal uptake and tubular reabsorption is expected to be affected,^{7,8} was increased only modestly in 18/20 samples, contrasting with the extent of the excretion of HAA. Whether the complete range of amino acids excreted by patients with Hartnup disorder can be explained by a broader substrate specificity of the B⁰AT1 transporter than currently described, or whether the aberrant transport of amino acids in the proximal tubule of patients with Hartnup disorder affects (saturation of) other amino acid transporters remains to be elucidated.

It is of interest that the Hartnup disorder cohort derived from Potter et al. described a less generalized aminoaciduria in their patients, even though the same reference values were used.¹⁵ We speculate that differences in the patient age at time of sampling (all adults in Potter et al.) may affect the amino acid excretion pattern. Moreover, differences in nutrition, particularly a higher protein intake, could have contributed to the here observed more pronounced generalized aminoaciduria.⁹ Still, despite these differences, the distribution of the calculated ratios is comparable, corroborating the accuracy of these ratios in discriminating Hartnup disorder from other aminoacidurias. However, given the relatively small sample sizes of the two cohorts, it would be of interest to assess the generalizability of the calculated ratio in another, independent cohort of patients with Hartnup disorder.

As nutritional intake, including protein intake, has been increasing in many countries over the past decades,⁹ the degree to which individuals with Hartnup disorder demonstrate amino acid excretion patterns mimicking generalized aminoaciduria might increase as well,

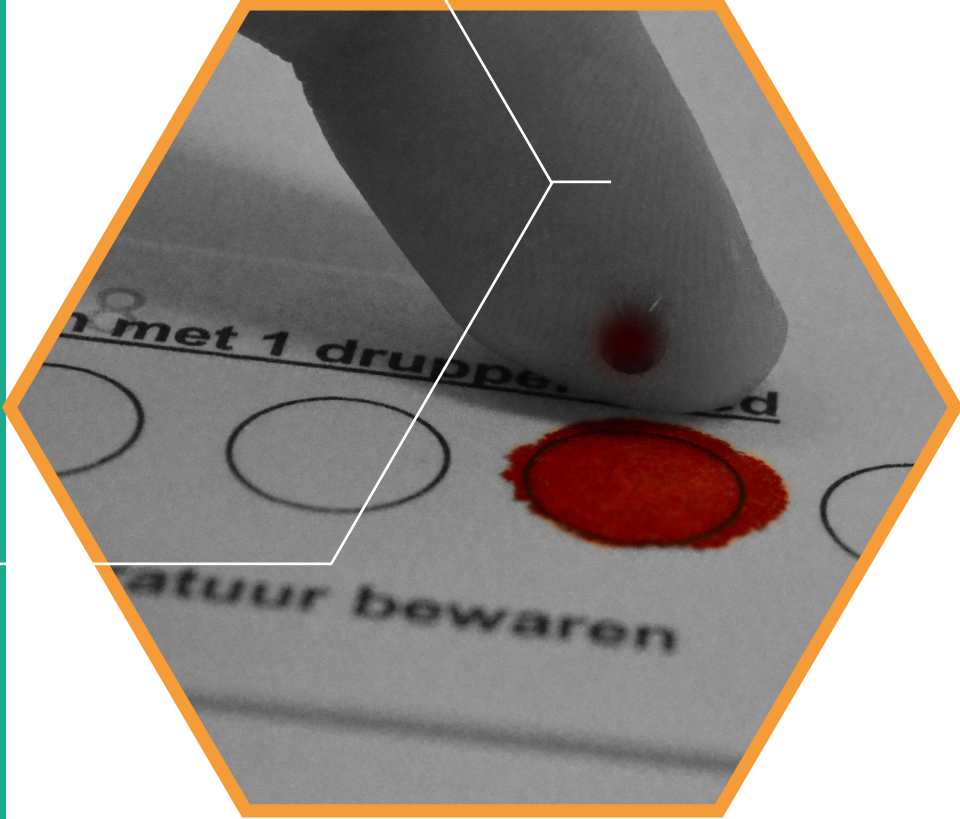
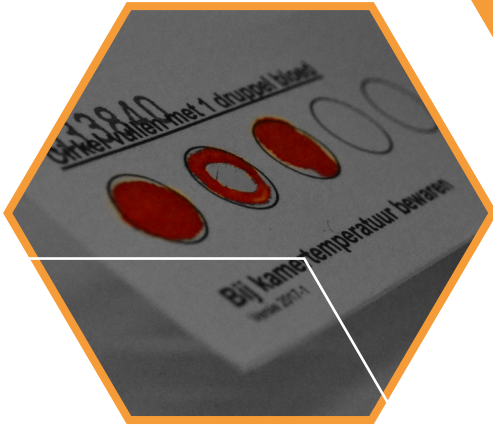
explaining why quantification of urinary amino acid concentrations was not required in the past, but is expedient now.

CONCLUSION

In conclusion, we here report that excretion values of amino acids not classically related to Hartnup disorder, are frequently elevated in patients with Hartnup disorder. This may induce a risk of misdiagnosis as generalized aminoaciduria and preclusion from vitamin B3 treatment. By changing the focus from absolute to relative increase of amino acid excretion and by calculating the HAA/OAA ratio, we introduce a diagnostic tool that enhances correct discrimination of Hartnup disorder from other aminoacidurias.

REFERENCES

1. Foreman JW. Fanconi syndrome. *Pediatr Clin North Am.* 2019;66(1):159-167.
2. Kleta R. Fanconi or not Fanconi? Lowe syndrome revisited. *Clin J Am Soc Nephrol.* 2008;3(5):1244-45.
3. Levy HL. Hartnup disorder. In: Scriver CR, Sly WS, Valle D (eds) *The metabolic and molecular bases of inherited diseases.* McGraw-Hill, New York, 2001.
4. Romeo E, Dave MH, Bacic D et al. Luminal kidney and intestine SLC6 amino acid transporters of B0AT-cluster and their tissue distribution in *Mus musculus*. *Am J Physiol Renal Physiol.* 2006;209(2):376-83.
5. Kleta R, Romeo E, Ristic Z et al. Mutations in SLC6A19, encoding B0AT1, cause Hartnup disorder. *Nat Genet.* 2004;36(9):999-1002.
6. Seow HF, Bröer S, Bröer A et al. Hartnup disorder is caused by mutations in the gene encoding the neutral amino acid transporter SLC6A19. *Nat Genet.* 2004;36(9):1003-1007.
7. Näntö-Salonen K, Niinikoski H, Simell OG. Transport defects of amino acids at the cell membrane: Cystinuria, Lysinuric Protein Intolerance and Hartnup Disorder. In: Saudubray JM, van den Berghe G, Walter JH (eds) *Inborn Metabolic Diseases.* Springer-Verlag, Berlin-Heidelberg, 2012.
8. Zschocke J, Hoffmann GF. *Vademecum Metabolicum. Milupa Metabolics, Friedrichsdorf, 2011.*
9. Camargo SM, Bockenhauer D, Kleta R. Aminoacidurias: clinical and molecular aspects. *Kidney Int.* 2008;73(8):918-925.
10. Wong PW, Lambert AM, Pillai PM, Jones PM. Observations on nicotinic acid therapy in Hartnup disease. *Arch Dis Child.* 1967;42(226):642-6.
11. Wilcken B, Yu JS, Brown DA. Natural history of Hartnup disease. *Arch Dis Child.* 1977;51(1):38-40.
12. Cheon CK, Lee BH, Ko JM, Kim HJ, Yoo HW. Novel mutation in SLC6A19 causing late-onset seizures in Hartnup disorder. *Pediatr Neurol* 2010;42(5):369-71.
13. Bröer S. The role of the neutral amino acid transporter B0AT1 (SLC6A19) in Hartnup disorder and protein nutrition. *IUBMB Life* 2009;61(6):591-9.
14. Javed K, Cheng Q, Carroll AJ, Truong TT, Bröer S. Development of biomarkers for inhibition of SLC6A19 (B0AT1)-A potential target to treat metabolic disorders. *Int J Mol Sci.* 2018;19(11).
15. Potter SJ, Lu A, Wilcken B, Green K, Rasko JE. Hartnup disorder: polymorphisms identified in the neutral amino acid transporter SLC1A5. *J Inher Metab Dis.* 2002;25(6):437-48.
16. Blau N, Duran M, Gibson KM. *Laboratory guide to the methods in biochemical genetics.* Springer-Verlag, Berlin-Heidelberg, 2008.



Pathophysiology of propionic and methylmalonic

acidemias. Part 1: Complications

Journal of Inherited Metabolic Diseases 2019, 42(5): 730-744
DOI: 10.1002/jimd.12129

Hanneke A. Haijes, Judith J.M. Jans, Simone Y. Tas,
Nanda M. Verhoeven-Duif[†],*, Peter M. van Hasselt[†]

[†] These authors contributed equally to this article

* Corresponding author

ABSTRACT

Over the last decades, advances in clinical care for patients suffering from propionic acidemia (PA) and isolated methylmalonic acidemia (MMA) have resulted in improved survival. These advances were possible thanks to new pathophysiological insights. However, patients may still suffer from devastating complications which largely determine the unsatisfying overall outcome. To optimize our treatment strategies, better insight in the pathophysiology of complications is needed. Here, we perform a systematic data-analysis of cohort studies and casereports on PA and MMA. For each of the prevalent and rare complications, we summarize the current hypotheses and evidence for the underlying pathophysiology of that complication. A common hypothesis on pathophysiology of many of these complications is that mitochondrial impairment plays a major role. Assuming that complications in which mitochondrial impairment may play a role are overrepresented in monogenic mitochondrial diseases and, conversely, that complications in which mitochondrial impairment does not play a role are underrepresented in mitochondrial disease, we studied the occurrence of the complications in PA and MMA in mitochondrial and other monogenic diseases, using data provided by the Human Phenotype Ontology. Lastly, we combined this with evidence from literature to draw conclusions on the possible role of mitochondrial impairment in each complication. Altogether, this review provides a comprehensive overview on what we, to date, do and do not understand about pathophysiology of complications occurring in PA and MMA and about the role of mitochondrial impairment herein.

INTRODUCTION

Over the last decades, advances in clinical care for patients suffering from branched-chain organic acidemias like propionic acidemia (PA) and isolated methylmalonic acidemia (MMA) have resulted in improved survival. These advances were based on new insights in pathophysiology. The understanding that both diseases are caused by an enzyme deficiency in the breakdown of branched-chain amino acids resulted in the implementation of a protein restricted diet.^{1,2} In addition, the recognition that MMA is caused by a deficiency of an enzyme for which cobalamin is a cofactor paved the way to cobalamin supplementation³ and the understanding that carnitine acts as a scavenger for the toxic metabolites produced in PA and MMA led to the introduction of carnitine supplementation.⁴ By virtue of these therapies – and general advances in clinical care – patients now tend to reach adulthood. However, it is increasingly recognized that residual disease in these disorders is substantial. Quite frequently, devastating complications may occur suddenly. These complications largely determine the unsatisfying overall outcome of patients. Current treatment strategies are thus inadequate for prevention and treatment of many complications in PA and MMA. To improve outcome, we need to optimize treatment, for which we have to gain insight in the pathophysiology of complications.

For this review we performed a systematic data-analysis of cohort studies and case-reports on PA and MMA to identify common denominators in the hypotheses on pathophysiology of complications occurring in PA and MMA. A broad PubMed literature search resulted in 2,176 records. A total of 181 publications were included based on full text, including 20 cohort studies, 34 studies on brain imaging, 16 studies on kidney failure, 12 studies on cardiomyopathy and 99 other case-series and reports covering a wide range of complications occurring in PA and MMA (Figure S1). For each of the frequent complications in PA and MMA that have been assessed in cohort studies we extracted the prevalence of the complication, and for each of the rare complications that have been described in case-reports, we extracted the number of patients reported with that complication (Figure 1). Furthermore, we summarized the current hypotheses and evidence for the underlying pathophysiology of each reported complication.

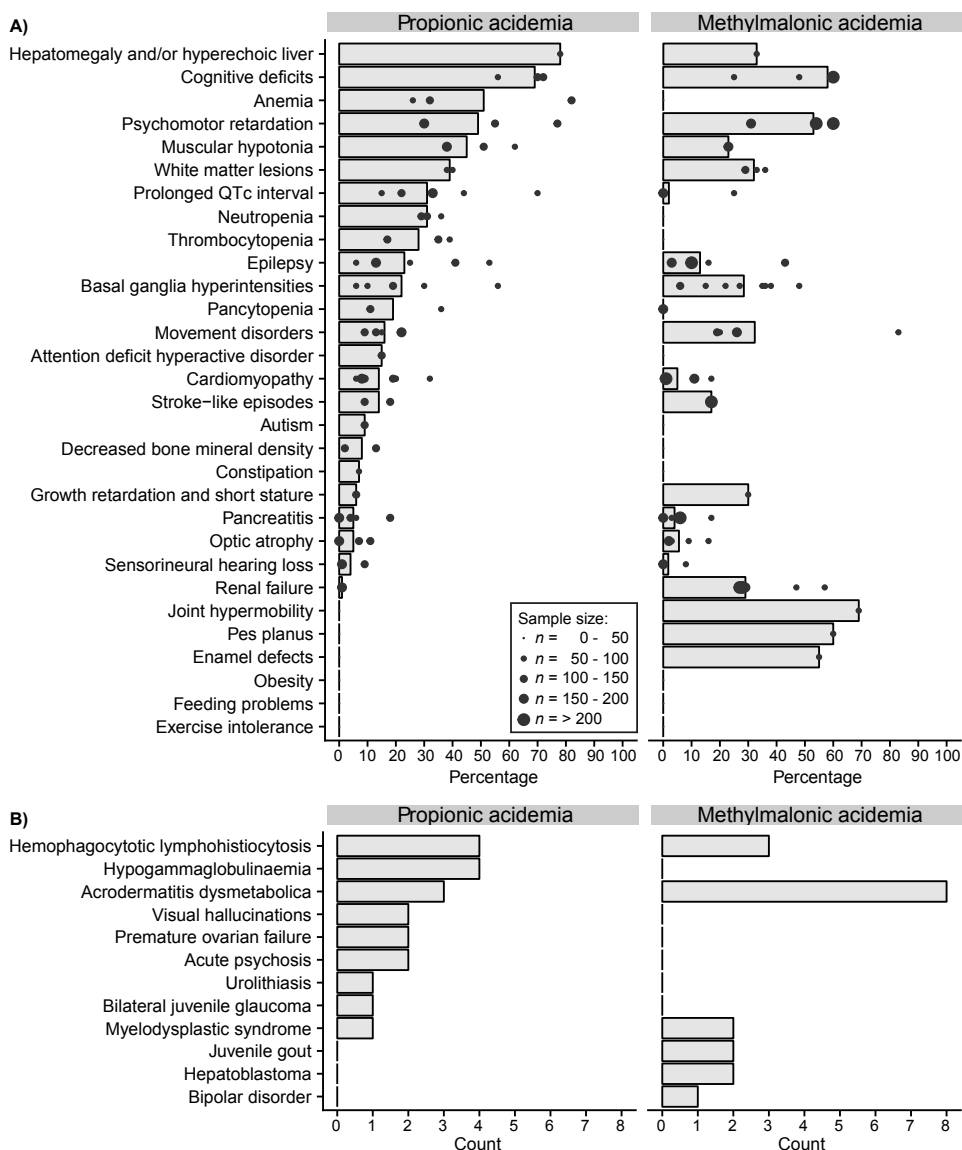
A common hypothesis on pathophysiology of many complications is that mitochondrial impairment plays a major role. We assumed that these mitochondria associated complications are overrepresented in monogenic mitochondrial diseases and, conversely, that complications in which mitochondrial impairment does not play a role are underrepresented in mitochondrial disease. We studied, for all prevalent and rare complications described in PA and MMA patients, the occurrence of these complications in monogenic mitochondrial diseases and in other monogenic diseases, using data on occurrence of a phenotypic feature in genetic diseases provided by the Human Phenotype Ontology (HPO). Altogether, this review aims to provide an overview on what we, to date, do and do not understand about pathophysiology of complications occurring in PA and MMA and about the role of mitochondrial impairment herein.

ENZYME DEFICIENCIES CAUSING PA AND MMA

PA and MMA are both caused by deficiencies of mitochondrial enzymes. PA is caused by a deficiency of propionyl-CoA carboxylase (encoded by *PCCA* and *PCCB*). Isolated methylmalonic acidemia (MMA) is either caused either by a deficiency of methylmalonyl-CoA mutase (MCM, encoded by *MUT*), by diminished synthesis or availability of its cofactor 5'-deoxyadenosylcobalamin which is associated with cobalamin A, B or D deficiency

(encoded by *MMAA*, *MMAB* or *MMADHC*, respectively), or by a deficiency of methylmalonyl-CoA epimerase (MCE, encoded by *MCEE*). Biochemically, both PA and MMA result in accumulation of propionyl-CoA, propionic acid, 3-hydroxypropionic acid, propionylcarnitine, propionylglycine and 2-methylcitrate.

Figure 1. Prevalence of complications occurring in PA and MMA



A) Complications are listed on the y-axis. The x-axis depicts the percentage in either propionic acidemia or methylmalonic acidemia. Dark-gray dots depict the percentages reported in the different cohort studies, the size of the dot indicating the sample size of the study. Light-gray bars depict the sample size-weighted percentage. B) Complications are listed on the y-axis. The x-axis depicts the number of patients with either propionic acidemia or methylmalonic acidemia that were reported to have this complication, indicated by the light gray bars.

Accumulation of methylmalonic acid and often methylmalonylcarnitine in MMA discriminates MMA biochemically from PA.⁵ An important differential diagnosis of PA is biotin deficiency, either caused by biotinidase deficiency or holocarboxylase deficiency. Due to deficiency of biotin as cofactor for carboxylases, the activity of propionyl-CoA carboxylase is hampered, as well as the activities of 3-methylcrotonyl carboxylase, acetyl-CoA carboxylase and pyruvate carboxylase. PA can be distinguished from biotin deficiency by enzyme studies on biotinidase and holocarboxylase activities. An important differential diagnosis of isolated methylmalonic aciduria is combined methylmalonic aciduria and homocystinuria which can be caused by cobalamin C, D, F or cobalamin J deficiency. Isolated methylmalonic aciduria can be distinguished from combined methylmalonic aciduria and homocystinuria by determination of total plasma homocysteine.⁵

Within isolated MMA, the cause and range of accumulation of toxic metabolites, the natural history and the prognosis differ between the different types.^{6,7} MMA caused by deficiency of MCM is often distinguished in cobalamin unresponsive patients (*mut*⁰) and cobalamin responsive patients (*mut*⁻). Cobalamin A deficient patients are usually cobalamin responsive, cobalamin B deficient patients can either be cobalamin unresponsive or responsive. *Mut*⁰ and cobalamin B deficient patients are considered severely affected regarding morbidity and mortality, whereas *mut*⁻ and cobalamin A deficient patients are considered to present with a milder form of MMA. Cobalamin D deficiency can either result in combined methylmalonic aciduria and homocystinuria, in isolated homocystinuria (variant 1) or in isolated MMA (variant 2). This type of isolated MMA is very rare compared to MCM deficiency and cobalamin A and B deficiency, and results in a cobalamin responsive phenotype similar to *mut*⁻ and cobalamin A deficiency.⁸ MCE deficiency is also very rare and its natural history is very variable, with asymptomatic patients, patients presenting with acute metabolic decompensations and patients having also a sepiapterin reductase deficiency.⁹ Despite the differences between the different forms of isolated MMA, many publications assemble research data on MCM, cobalamin A and cobalamin B deficiency, and discuss isolated MMA as one disease entity. Therefore, in this review we consider isolated MMA as one disease entity as well, but discuss the different types of MMA separately whenever possible.

ACUTE METABOLIC DECOMPENSATIONS

PA and MMA are typically diagnosed in early childhood, usually in the neonatal period (65% for PA, 48% for MMA) and frequently after an acute metabolic decompensation.¹⁰ To date, patients also come to clinical attention through newborn screening, enabling early initiation of treatment. However, despite this early initiation of treatment, patients are still prone to developing metabolic decompensations throughout life.¹¹ The predominant trigger for metabolic decompensation is catabolism, which can be induced by an increased energy demand (acute trauma, infection, fever, too much exercise or psychological stress), by reduced energy supply (fasting, vomiting), by a relatively high protein intake (inactivity) or by medication. Irrespective of the trigger, the breakdown of branched-chain amino acids acutely increases the amount of circulating toxic metabolites. The acidic nature of these metabolites rapidly causes a metabolic acidosis by decreasing the pool of bicarbonate. Oftentimes, also lactic acidosis and hyperammonemia are encountered. Clinically, patients present with vomiting and anorexia, followed by dehydration, weight loss, lethargy, hypothermia, hypotonia, and convulsions, possibly resulting in coma, multi-organ failure and even death. Metabolic decompensations can range from very mild to very severe, and likewise, triggering events can range from minor holiday stress to severe bacterial infections. It is thought

that both trigger sensitivity and severity of decompensations are mainly determined by the amount of residual activity of the affected enzyme.¹² The most important therapeutic intervention, regardless of the severity of the decompensation, is limiting protein intake and increasing the caloric intake, to stop protein catabolism. The extent to which protein intake is limited and the necessity of subsequent additional therapies is determined by the severity of the decompensation. Treatment can be immediately initiated when parents, patients and doctors recognize a decompensation and therefore, with the available therapies at hand, it is in most patients possible to prevent severe metabolic decompensations.

COMPLICATIONS

Despite current care, patients with PA and MMA are prone to develop a broad range of complications, with varying prevalence, and these complications seem to occur despite apparent good metabolic control.¹² Pathophysiology of each of these complications is not well understood. Studying the prevalent complications that have been assessed in cohort studies and calculating the weighted percentage based on sample size of the cohort studies (Figure 1, Table S1)¹³⁻²⁸ revealed that in PA, hepatomegaly and/or a hyperechoic liver, cognitive deficits and anemia, psychomotor retardation and muscular hypotonia are the five most prevalent complications. In MMA, the five most prevalent complications are joint hypermobility, pes planus, cognitive deficits, enamel defects and psychomotor retardation. Despite being highly prevalent, hepatomegaly and/or a hyperechoic liver in PA and joint hypermobility, pes planus and enamel defects in MMA were each assessed in only one study (Table S1) and these complication are not the most devastating ones. Complications considered important in both diseases, as indicated by the number of studies assessing these complications, are basal ganglia hyperintensities, epilepsy, pancreatitis, renal failure (in MMA) and cardiomyopathy (in PA) (Table S1).

For each of the prevalent complications occurring in PA and MMA that have been assessed in cohort studies, and for each of the rare complications that have been described in case-reports (Table S2), we summarize the current hypotheses and evidence and we assess the potential role of mitochondrial impairment for the underlying pathophysiology (Table 1).

Brain

Many of the complications occurring in PA and MMA arise from brain damage. On magnetic resonance imaging, both white matter lesions and basal ganglia hyperintensities are found, with comparable prevalence in PA and MMA (Figure 1, Table S1). These lesions, that are often permanent, can lead to a variety of clinical problems like psychomotor retardation, movement disorders (MMA > PA), cognitive deficits (PA > MMA) and psychiatric problems including attention deficit hyperactive disorder and autism (PA > MMA) (Figure 1, Table S1).²⁹⁻³¹ Schreiber et al. reviewed neurological complications in PA and state that these complications are partly induced by acute metabolic decompensations, often at initial presentation. Hyperammonemia leads to vulnerability of the astrocytes and causes cerebral edema and hypoperfusion. In addition, hypoglycemia, lactic acidosis, an increased anion gap, increased propionic acid, increased glycine and ketosis might also induce brain damage during acute metabolic decompensations.³² It is hypothesized that due to implementation of newborn screening and early initiation of treatment, neurological damage due to the first presentation might be prevented,¹¹ but reports on the effect of newborn screening in PA and MMA are still scarce.^{11,33-35}

Table 1. Evidence for the role of mitochondrial impairment in pathophysiology of complications in PA and MMA

HPO CODE	HPO NAME	Hypothesis	LITERATURE Evidence	% mit.	P-value	HPO Conclusion	CONCLUSION Mitochondrial pathophysiology?
HP:0001638	Cardiomyopathy	Mitochondrial	Patient treatment	22.3	<0.0001	Mitochondrial	Probably
HP:0000648	Optic atrophy	Mitochondrial	Patient histology	17.1	<0.0001	Mitochondrial	Probably
HP:0001392	Abnormality of the liver	Mitochondrial	Patient histology; Animal studies	9.7	0.0339	Mitochondrial	Probably
HP:0003546	Exercise intolerance	Mitochondrial	Patient histology	51.4	<0.0001	Mitochondrial	Probably
HP:0001733	Pancreatitis	Mitochondrial	Animal studies	26.8	<0.0001	Mitochondrial	Probably
HP:0002134	Abnormality of the basal ganglia	Mitochondrial	Animal studies	20.0	0.0306	Mitochondrial	Probably
HP:0001250	Seizures	Mitochondrial	Animal studies	11.6	<0.0001	Mitochondrial	Probably
HP:0000717	Autism	Mitochondrial	Cell lines	14.3	0.0284	Mitochondrial	Probably
HP:0012622	Chronic kidney disease	Mitochondrial	Patient histology; Animal studies	2.9	NS	NS	Possibly
HP:0001903	Anemia	Mitochondrial	Patient histology	7.8	NS	NS	Possibly
HP:0001875	Neutropenia	Mitochondrial	Patient histology	2.3	NS	NS	Possibly
HP:0001873	Thrombocytopenia	Mitochondrial	Patient histology	3.3	NS	NS	Possibly
HP:0001876	Pancytopenia	Mitochondrial	Patient histology	3.8	NS	NS	Possibly
HP:0001297	Stroke	Mitochondrial	No evidence	22.2	<0.0001	Mitochondrial	Possibly
HP:0000709	Psychosis	Mitochondrial	No evidence	21.8	0.0001	Mitochondrial	Possibly
HP:0000407	Sensorineural hearing impairment	Inhibited potassium flow	No evidence	12.0	0.0001	Mitochondrial	Possibly
HP:0011968	Feeding difficulties	Multifactorial	Cell lines	13.9	<0.0001	Mitochondrial	Possibly
HP:0001252	Muscular hypotonia	NA	No evidence	12.7	<0.0001	Mitochondrial	Possibly
HP:0001657	Prolonged QT interval	Inhibited potassium flow	Cell lines	5.9	NS	NS	Unknown
HP:0008209	Premature ovarian insufficiency	Mitochondrial	No evidence	4.7	NS	NS	Unknown
HP:0002019	Constipation	Multifactorial	No evidence	11.0	NS	NS	Unknown
HP:0000682	Abnormality of dental enamel	Chronic acidosis	No evidence	1.5	NS	NS	Unknown
HP:0001513	Obesity	NA	NA	1.4	0.0084	Non-mitochondrial	Unlikely
HP:0001997	Gout	Chronic (renal) acidosis	Patient histology	0.0	NS	NS	Unlikely
HP:0000787	Nephrolithiasis	Dehydration; Chronic acidosis; Protein restriction	Patient histology	3.4	NS	NS	Unlikely
HP:0000964	Eczema	Isoleucine restriction	Patient treatment	1.7	NS	NS	Unlikely
HP:0004349	Reduced bone mineral density	Protein restriction; Chronic acidosis	Patient treatment	2.5	NS	NS	Unlikely
HP:0004322	Short stature	Protein restriction	Patient treatment	3.8	NS	NS	Unlikely

Evidence from literature is categorized in five categories: patient treatment, patient histology, animal studies, cell lines or no evidence. NA is listed when no hypothesis for the complication on pathophysiology has been described in literature. Conclusion from HPO-data is categorized in two categories: mitochondrial, if a statistical significant P-value is indicating overrepresentation in mitochondrial disease, or nonmitochondrial, if a statistical significant P-value is indicating underrepresentation in mitochondrial disease. The final conclusion whether mitochondrial impairment might play a role in the pathophysiology of the complication is categorized in five categories: “probably” if both literature and HPO data indicate a role for mitochondrial impairment, “possibly” if literature or HPO data indicate a role for mitochondrial impairment, “unknown” if results are inconclusive and

[Table 1 continued] “unlikely” when either literature or HPO data indicate that their might be another pathophysiological process at play than mitochondrial impairment. In theory, a complication would be classified “highly unlikely” when both literature and HPO data would indicate that pathophysiology is not related to mitochondrial impairment. Abbreviations: HPO: human phenotype ontology; MMA: methylmalonic acidemia; NS: not significant; PA: propionic acidemia. % mit. is the percentage of the mitochondrial genes in the number of associated genes to the complication, according to HPO (see Table S3 for full table). P-value is the P-value resulting from a Bonferroni corrected Fisher’s exact test comparing the complication to “phenotypic abnormality” (Table S3).

However, in patients with apparent good metabolic control, neurological complications can still arise over time, possibly caused by persistently increased levels of propionic acid, 2-methylcitrate, lactate and ammonia, that inhibit and deplete enzymes in the Krebs cycle³² (reviewed in Haijes et al.³⁶). In support, increased brain lactate on magnetic resonance spectroscopy during periods of apparent good metabolic control has been demonstrated in PA children.³⁷ Furthermore, Frye et al.³⁸ demonstrated an association between autism spectrum disorders and altered propionic acid metabolism affecting mitochondrial function in lymphoblastoid cell lines. For MMA the same mechanism of accumulating toxic metabolites leading to mitochondrial oxidative stress and acidosis in neurons and astrocytes ultimately leading to cellular necrosis has been proposed.³⁹ This claim is supported by several rat studies in which injection of anti-oxidants prevented the occurrence of neurological complications that were induced by either propionic acid or methylmalonic acid (reviewed in Haijes et al.³⁶). The involvement of the basal ganglia, especially the globus pallidus, is probably due to its high energy demand, rich vascularization and elevated metabolism in that location in the first year of life.³⁹ The substantia nigra is histologically and functionally similar to the globus pallidus, explaining its susceptibility to the same toxic metabolites.⁴⁰ In contrast to these permanent lesions, stroke-like episodes can also occur (Figure 1, Table S1). In a stroke-like episode the process is still reversible, not leading to permanent damage.⁴¹⁻⁴⁴ These stroke-like episodes most often occur somewhat later in life, but it is suggested that they might share the same pathophysiological process.⁴³ However, no studies or hypotheses regarding the pathophysiology of stroke-like episodes have been described. Rare complications caused by brain damage, described in case-reports, are visual hallucinations, episodes of acute psychosis and bipolar disorder with psychotic features (Figure 1, Table S2). Pathophysiology of these rare complications is not clear and may be multifactorial, for example, genetic vulnerability, the burden of a chronic disease and distressing life-events.⁴⁵ However, the toxic compounds associated to PA and MMA also appear to play a role, as therapies inducing metabolic stability contributed to recovery of psychiatric symptoms.⁴⁶

Another important complication induced by brain damage is epilepsy, which is more prevalent in PA than in MMA (Figure 1, Table S1). There seem to be two types of epilepsy in PA and MMA. First, patients can develop epilepsy independently of acute metabolic decompensations. This type of epilepsy requires life-long anti-epileptic medication. It can be induced by structural brain lesions that arose during acute metabolic decompensations. Secondly, convulsions and even status epilepticus can arise during acute metabolic decompensations, particularly in the neonatal period. The pathophysiology of this second type of epilepsy involves two separate routes, leading to activation of the *N*-methyl-D-aspartate (NMDA) receptor and excitotoxicity. First, hyperammonemia results in inhibition of glutamate uptake and subsequent accumulation of extracellular glutamate.^{47,48} This activates the NMDA-receptors⁴⁹ and leads to excessive Ca²⁺ accumulation, inducing mitochondrial depolarization in neurons and astrocytes.^{47,50,51} Additionally, propionic acid,

methylmalonic acid and ammonia all induce inhibition of glutamate decarboxylase. Less glutamate is converted into GABA, leading to NMDA-receptor activation and promoting excitotoxicity.^{52,53} In addition to these two routes, two more processes contribute to excitotoxicity. First, glutamate dehydrogenase activity is inhibited by 2-methylcitric acid.⁵⁴ Glutamate oxidation is reduced, ATP production is reduced and the glutamine/glutamate ratio is altered, also inducing excitotoxicity.⁵⁴ Second, oxidative stress (both reactive oxygen species (ROS) and reactive nitrogen species) leads to decreased Na⁺/K⁺-ATPase activity,^{55,56} mitochondrial depolarization and decreased ATP synthesis,⁵³ again promoting excitotoxicity.

Eye

Optic atrophy is equally prevalent in PA and MMA (Figure 1, Table S1). For two reasons it is hypothesized that mitochondrial impairment plays an important role.⁵⁷ First, optic atrophy occurring in MMA and PA patients resembles the clinical profile of Leber hereditary optic neuropathy and other mitochondrial optic neuropathies in terms of age at onset, presentation and progression.^{57,58} Second, despite normal plasma levels, supplementation of coenzyme Q10 and α -tocopherol seems to have a beneficial effect on sight in patients suffering from optic atrophy.⁵⁹ Bilateral glaucomatous optic atrophy that resolved after antiglaucomatous surgery has been reported in a single PA patient. The juvenile glaucoma was thought to be caused by an altered chamber angle. As this has been described only once,⁶⁰ it is doubtful whether glaucomatous optic atrophy is due to PA.

Ear

Sensorineural hearing loss is slightly more prevalent in PA than in MMA (Figure 1, Table S1). Interestingly, in one MMA patient (*MUT* type), it has been observed to occur only 3 months after the patient developed optic atrophy,⁵⁷ suggesting a shared underlying pathophysiology. Pathophysiology of sensorineural hearing loss in PA has been addressed by Grünert et al. by comparing PA to Jervell and Lange-Nielsen syndrome, a syndrome that also presents with sensorineural hearing loss and prolonged QTc interval.⁶¹ The authors propose that sensorineural hearing loss and prolonged QTc interval share a pathogenic mechanism involving potassium channels carrying the potassium current I_{Ks} (encoded by *KCNQ1* or *KCNE1*). I_{Ks} is essential for cardiac repolarization and important for luminal secretion of potassium into the endolymphatic space in the inner ear. Potassium flow via this channel is inhibited by propionic acid.⁶¹ Therefore, the authors propose that sensorineural hearing loss is the direct effect of accumulating toxic metabolites in propionic acidemia. To date, no role for mitochondrial impairment has been discussed.

Skeletal muscle

Muscular hypotonia is more prevalent in PA than in MMA patients (Figure 1, Table S1). It tends to be worse during acute metabolic decompensations, or during chronic instability. Despite its prevalence, hypotheses on pathophysiology have not been described. Exercise intolerance, or impaired stamina, is reported in one MMA patient (*MUT* type)⁶² and occurs mostly in the second decade of life. It can be very hindering in daily activities. Exercise intolerance also tends to be worse during acute metabolic decompensations, or during chronic instability. It is hypothesized that occurrence of exercise intolerance is related to inhibition of mitochondrial energy metabolism by toxic metabolites.⁶² In a muscle biopsy of this MMA patient, subsarcolemmal accumulation of mitochondria was found,⁶² and in a muscle biopsy of a PA patient, decreased activities of respiratory chain complex III and IV

were observed,⁶³ supporting a role for mitochondrial energy failure in the pathogenesis of exercise intolerance.

Heart

Cardiomyopathy, most often hypertrophic, is more frequent in PA than in MMA patients (Figure 1, Table S1). Mitochondrial impairment is suggested to play a major role in pathophysiology of cardiomyopathy.⁶⁴ Baruteau et al. describe a patient with severe cardiomyopathy in whom myocardial biopsy showed endocardial fibrosis and enlarged mitochondria with atypical cristae and a slightly low respiratory chain complex IV activity. Myocardial coenzyme Q10 was found to be markedly decreased. Strikingly, a high dose of coenzyme Q10 supplementation slowly led to improved cardiac function, allowing removal of mechanical cardiac support after 2 months.⁶⁴ There are no other reports addressing the possible pathophysiology of cardiomyopathy in PA and MMA.

Prolonged QTc interval (defined as >440 ms) is quite prevalent in PA, but not in MMA, although quite some variation in prevalence has been reported (Figure 1, Table S1). A prolonged QTc interval indicates prolonged repolarization over the myocardium. Pathophysiology of prolonged QTc interval has been investigated in one study, by Bodi et al. They suggest that acute reduction of the repolarizing potassium currents in cardiomyocytes, induced by toxic metabolites in propionic acidemia, are responsible for the prolonged QTc interval.⁶⁵ To date, no role for mitochondrial impairment has been proposed.

Kidneys

Renal failure is much more prevalent in MMA patients than in PA patients (Figure 1, Table S1). Patients harboring a defect in *MUT* (without residual enzymatic activity, *mut*⁰) or *MMAB* develop more frequently renal failure (61% and 66%, respectively) than patients harboring a defect in *MUT* (with residual enzymatic activity, *mut*⁻) or *MMAA* (0% and 21%, respectively). In MMA patients, renal length decreases significantly over time in comparison to kidneys of healthy individuals, indicating stagnating kidney growth.⁶⁶ Histologically, extensive interstitial fibrosis, chronic inflammation and tubular atrophy are observed in patients' renal tissue. In addition, strikingly large, circular, pale mitochondria with diminished cristae are observed, with reduced cytochrome C enzyme activity and multiple OXPHOS deficiencies.^{63,67,68} The decreasing glomerular filtration rate observed in MMA patients is suggested to be protective, initiated by mitochondrial dysfunction of the proximal tubule cells, to reduce the absorptive load on these cells.⁶⁷ Manoli et al.⁶⁷ created a *Mut*^{-/-} mouse model in which MCM was expressed in liver only. In the kidneys of these mice, large numbers of mitochondria with electron-dense matrices and abnormal cristae were observed in the proximal tubules. In another *Mut*^{-/-} mouse model in which MCM was expressed in the skeletal muscle, proliferated and enlarged mitochondria were also observed in kidney tissue.⁶⁹ Altogether, it can be concluded that mitochondrial impairment plays a significant role in the pathophysiology of renal failure. This is further underlined by the observation that mice, treated with the antioxidants coenzyme Q10 and α -tocopherol showed improved glomerular filtration rate and decreased oxidative stress in renal tissue.⁶⁷

Urolithiasis is described in a single PA patient who presented with an ammonium acid urate calculus, formed through a combination of dehydration, chronic acidotic state and the low-protein diet.⁷⁰ It has not been described in more PA patients, nor in any MMA patient (Figure 1, Table S2), but it might not have been recognized as a complication of the disease.

Pancreas

Pancreatitis is equally prevalent in PA as in MMA patients (Figure 1, Table S1). Pathophysiology of pancreatitis in PA and MMA is scarcely addressed in literature. Kahler et al.⁷¹ suggested two potential mechanisms: either activation of pancreatic enzymes in inappropriate locations, or inability of the pancreas to withstand normal metabolic stress. The inability to withstand metabolic stress might be caused by free radical formation and deficiencies of carnitine, methionine and antioxidants. This latter theory was supported by Chandler et al., who found megamitochondria in pancreatic tissue of *Mut*^{-/-} mice. In contrast to hepatocytes, megamitochondria in pancreatic tissue developed only later in life.⁷² It is not reported whether these mice had suffered from pancreatitis. Megamitochondria formation is an adaptive process to unfavorable environments and is often induced by free radicals, as illustrated by the observation that formation of megamitochondria is successfully suppressed by anti-oxidants.⁷³ If intracellular ROS can be decreased, mitochondria can normalize both structurally and functionally, but if concentrations of free radicals become too high, apoptosis is induced.⁷³ Thus, the presence of megamitochondria in pancreatic tissue of *Mut*^{-/-} mice might suggest a role for mitochondrial failure in pathophysiology of pancreatitis.

Liver

Hepatomegaly and/or hyperechoic liver are reported in PA patients more often than in MMA patients (Figure 1, Table S1). In addition, Kölker et al. describe that the mean concentration of alanine aminotransferase is 12% above the reference range in MMA and 16% in PA patients. For aspartate aminotransferase this is 20% in MMA and 19% in PA patients and for gamma-glutamyl transferase the reported value is 9% and 33% in MMA and 10% and 25% in PA patients.^{74,75} Fibrosis/cirrhosis diagnosed by liver biopsy is described in three patients, with decreased respiratory chain activities.⁷⁴ Chandler et al.⁷² described megamitochondria with dysmorphic and shortened cristae, and a less electron-dense mitochondrial matrix in hepatocytes of *Mut*^{-/-} mice with MMA, already early in life. They found similar morphological changes in the hepatocytes of a MMA patient (*MUT* type). In line with this, in a *Mut*^{-/-} mouse model in which MCM was expressed in the skeletal muscle, megamitochondria with shortened or no cristae were observed in hepatocytes. These findings were accompanied by decreased activity of the respiratory chain complex and reduced oxidation rates of substrates that depend on mitochondrial function for their metabolism.⁶⁹ These findings suggest a prominent role for mitochondrial failure in pathophysiology of liver involvement in PA and MMA.

Two MMA patients (both *MUT* type) presented with a hepatoblastoma (Figure 1, Table S1). The first was a patient who received growth hormone therapy for 10 months and immunosuppressive therapy after a kidney transplant at 9.7 years. The patient developed a hepatoblastoma at the age of 11 years and died during the first weeks of chemotherapy.^{76,77} The second patient also developed a hepatoblastoma, but is in remission since he received an orthotopic split-liver-kidney transplant.⁷⁸ In this report it was speculated that increased levels of ROS led to DNA damage, affecting oncogenes or tumor-suppressor genes, although no supporting evidence was presented.⁷⁸

Gastro-intestinal system

Touati et al. describe 55% of PA and MMA patients having intermediate or major feeding disorders at 3 years of age, improving with age (35% at 6 years, 12% at 11 years). A total

of 60% of patients were tube-fed overnight or continuously, decreasing with age (48% at 6 years, 27% at 11 years), although a significant part of the patients remains dependent on tube-feeding throughout life.^{79,80} Pathophysiology of feeding problems is hard to assess and likely multi-factorial, with an important role for the strict protein-restricted diet, the constant focus on feeding and the need for continuous tube-feeding in the first years of life to prevent catabolism.

Constipation is described as an important problem in PA and MMA patients,^{12,81} but its prevalence has been described in only one study among PA patients (Figure 1, Table S1). Constipation is known to contribute to metabolic instability and requires treatment upon occurrence.^{12,81} However, the reason for its (presumed) increased prevalence and the pathophysiology in PA and MMA is not addressed in literature. Accumulating toxic metabolites might play a role through affected bowel innervation and mitochondrial energy deficiency, resulting in decreased peristalsis, but a relative lack of fibers and fluids, a relative lack of physical exercise, impaired cognition and psychosocial stress might also contribute to constipation.

Ovaries

Premature ovarian failure is described in two PA patients (Figure 1, Table S2). Lam et al.⁸² suggest that since premature ovarian failure is associated with mitochondrial diseases, with oxidative stress playing an important role, mitochondrial failure might also cause premature ovarian failure in PA, but this has not been studied yet.

Bone marrow

Anemia, neutropenia, thrombocytopenia and pancytopenia are quite frequent in PA patients, but in MMA cohort studies, the prevalence of these complications has not been assessed (Figure 1, Table S1). Kölker et al. describe that the mean level of hemoglobin is 40% below the reference range in MMA patients and 22% in PA patients. Leukocytes are on average 7% below the reference range in MMA patients and 18% in PA patients. Thrombocytes are on average 6% below the reference range in MMA patients and 18% in PA patients.⁷⁵ Severe decreases of hemoglobin, leukocytes and thrombocytes can occur during acute metabolic decompensations, and milder decreases occur also in a more chronic fashion.⁸³

Rare complications, described in case-reports, are hemophagocytotic lymphohistiocytosis and myelodysplastic syndrome (Figure 1, Table S2). Proliferation and maturation of bone marrow stem cells is affected by propionic acid and methylmalonic acid.⁸³⁻⁸⁵ Also, accumulation of intracellular propionic acid and/or methylmalonic acid or changes in membrane lipid composition may lead to erythrophagocytosis, hence shortened survival of erythrocytes. A role for mitochondrial dysfunction, leading to compromised aerobic respiration and inflammasome activation by oxidative stress is proposed as well.⁸⁶ Ineffective erythropoiesis caused by mitochondrial dysfunction is further supported by the observation of mitochondrial iron accumulation represented by ring sideroblasts in myelodysplastic syndrome in an MMA patient (*MUT* type).⁸⁷ Hypogammaglobulinemia, described in four PA patients (Figure 1, Table S2) might be caused concordantly, by affected proliferation and maturation of bone marrow cells due to a combination of energetic failure and oxidative stress, but there is no evidence to support this hypothesis.

Bone

Decreased bone mineral density (BMD) is widely accepted to be a complication of the life-

long protein restricted diet in combination with the accumulating acids, rather than being the direct, specific effect of toxic metabolites accumulating in PA and MMA. Decreased BMD has been described in PA patients but has not systematically been assessed in MMA patients (Figure 1, Table S1). A severely decreased BMD can result in pathological fractures.^{88,89} Medical food containing the allowed amino acids cannot fully prevent decreased BMD. Instead, it is suggested that amino acid mixtures might even contribute to decreased BMD, since they increase the – already high – acid load for the kidneys, inducing buffering of H⁺ ions in the bone. This evokes increased bone resorption and lowers BMD. In addition, due to subtle deficiencies of amino acids such as proline and lysine, biosynthesis of collagen might be impaired, reducing the tensile strength of the bone matrix.⁹⁰ Instead of amino acid mixtures, it is proposed that intact protein supplementation, lacking the amino acids isoleucine, valine, methionine and threonine, might be more effective in preventing decreased BMD.⁹⁰

Joints

Joint hypermobility and pes planus are both described in only one cohort study of MMA patients,⁷⁹ but the prevalence (69% joint hypermobility and 60% pes planus) suggests that both complications are more prevalent than previously acknowledged (Figure 1, Table S1), although severe patients might be over-represented in this cohort.⁷⁹

Juvenile gout has been described in two MMA patients (both *MMAB* type) (Figure 1, Table S2). Both patients presented with chronic kidney disease due to renal tubular acidosis. In the proximal tubule, the acidosis may compete with the uric acid excretion, causing long-lasting hyperuricemia in plasma and the formation of monosodium-urate crystals.⁹¹ This has not been described in any PA patient, nor in any MMA patient without chronic kidney disease.

Growth

Growth retardation, resulting in a short stature is more frequent in MMA patients than in PA patients (Figure 1, Table S1). Growth retardation is most likely secondary to the protein restricted diet rather than a direct effect of PA and MMA.⁹² In *Mut*^{-/-} mice in which MCM was expressed in the skeletal muscle, and which were on a diet resembling the diet used for the management of MMA patients, growth failure was observed throughout their life span.⁶⁹ Proteins, especially in early life, are essential for normal growth and a relative lack of protein results in impaired growth.

Feillet et al.⁹³ reported a resting energy expenditure (REE) of 80% compared to the prediction of the Schofield height and weight equation, in both PA and MMA patients. They speculate that mitochondrial impairment could contribute to the decreased REE, but they do not present any evidence. The finding of a decreased REE in PA and MMA was supported by Thomas et al.,⁹⁴ but van Hagen et al.⁹⁵ did not find a decreased REE in PA and MMA patients. They suggested that adequate caloric intake, and possibly the intake of synthetic amino acid mixtures might result in a normal REE. To test this hypothesis, Hauser et al.⁹⁶ normalized measured REE to fat free mass for MMA patients and found that normalized REE is decreased in MMA patients and that it is influenced by both creatinine clearance and body length.

The prevalence of obesity, which is mainly in the adult population an important complication of the diet used to treat PA and MMA, has not been systematically assessed (Figure 1, Table S1). Hauser et al.⁹⁶ report that fat free mass is decreased, and BMI is increased in some MMA

patients. It is expected that the prevention of catabolism through a hypercaloric diet, often with continuous overnight feeding, takes place at the expense of weight gain. Attempts to lose extra weight go along with the risk of protein catabolism. Although it differs from patient to patient, the balance between overweight and acute metabolic decompensations can be very tight.

Skin

Skin problems, often described as acrodermatitis dysmetabolica, are described in both PA and MMA patients (Figure 1, Table S2) and also in patients with other organic acidemias. It is presumed to be the result of an isolated isoleucine deficiency since symptoms can resolve quickly upon isoleucine supplementation,⁹⁷⁻¹⁰⁰ but it has also been considered the result of a more complex multideficiency syndrome.¹⁰¹ In one patient with MMA, erythema nodosum is described, which resolved in a few days upon high dose vitamin B12 treatment¹⁰² and in one patient with PA, necrolytic migratory erythema is described, which is considered to be the result of zinc deficiency in this patient.¹⁰³

Teeth

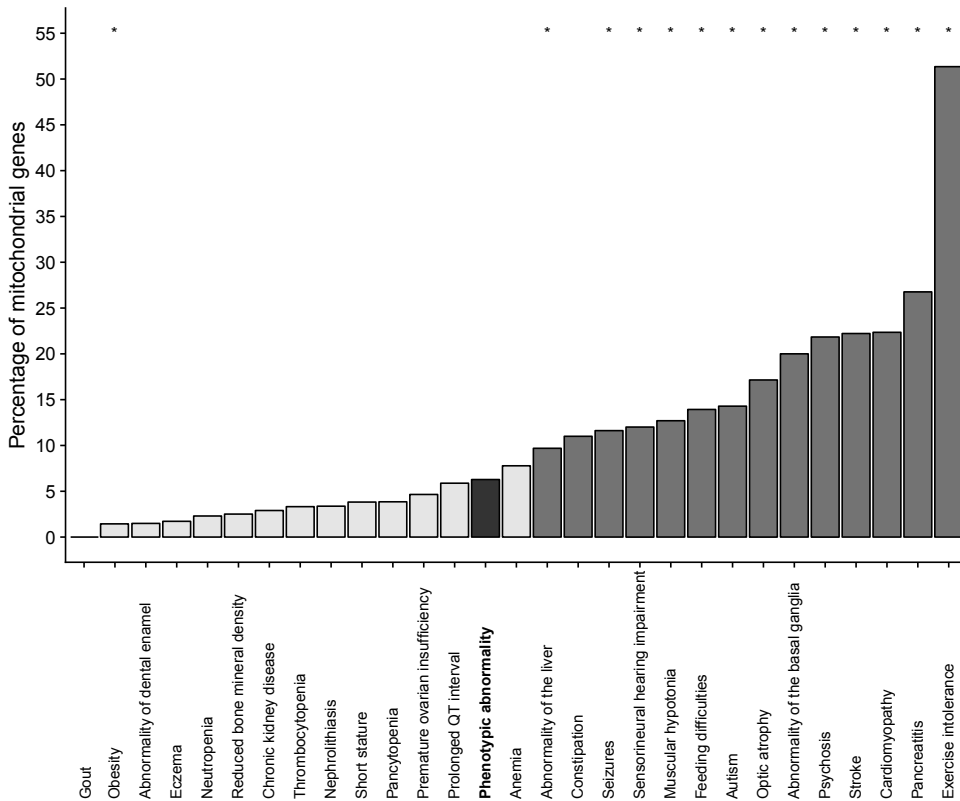
Bassim et al. describe that enamel defects occur significantly more often in the MMA patients included in their study than in the matched control patients (Figure 1, Table S1). The higher the methylmalonic acid, the more enamel defects, especially in patients harboring the *MUT* type. Pathophysiology is unknown, but it is hypothesized that enamel defects are caused by severe pediatric disease, by renal insufficiency, or by local influence of methylmalonic acid on tooth genesis.¹⁰⁴ Enamel defects have not been assessed in PA patients.

OCCURRENCE OF COMPLICATIONS IN PA AND MMA IN OTHER MONOGENIC MITOCHONDRIAL DISEASES

For many complications, it is hypothesized that mitochondrial impairment contributes to their pathophysiology (Table 1). Next to what is reported in literature, we here add an extra line of evidence using data on occurrence of a phenotypic feature in genetic diseases, provided by HPO. We assume that complications resulting from mitochondrial impairment are overrepresented in monogenetic mitochondrial diseases and conversely, that complications not caused by mitochondrial impairment are underrepresented in mitochondrial disease. Based on this assumption, we studied the occurrence of the complications in PA and MMA in both monogenetic mitochondrial diseases and in other monogenetic diseases. We used data provided by HPO and an extensive review on monogenetic mitochondrial disorders, listing all genes associated with mitochondrial disease, both nuclear and mitochondrial.¹⁰⁵ For each complication we identified the number of genes associated with this complication according to HPO. Of these genes, we determined the number of genes causing monogenetic mitochondrial disease (both nuclear and mitochondrial genes).¹⁰⁵ Next, we calculated the percentage of mitochondrial genes within the group of genes associated with the complication (Table S3). Using the phenotypic feature “phenotypic abnormality” (HP:0000118) as a reference, a Fisher’s exact test was performed to compare for each complication the percentage of mitochondrial genes to this reference (6.3% mitochondrial genes, Table S3). P-values were corrected for multiple testing according to the Bonferroni method. Figure 2 demonstrates the underrepresentation and overrepresentation of the different complications occurring in PA and MMA in mitochondrial disease and the conclusions retrieved from these calculations are presented in Table 1.

Underlining the mitochondrial nature of these complications, the complications exercise intolerance, pancreatitis, cardiomyopathy, stroke, psychosis, abnormality of the basal ganglia, optic atrophy, autism, feeding problems, muscular hypotonia, sensorineural hearing impairment, seizures and abnormality of the liver are symptoms that are significantly overrepresented in monogenic mitochondrial diseases (Table 1 and Figure 2), suggesting that indeed mitochondrial impairment plays a role in pathophysiology of these complications. For anemia the percentage of mitochondrial diseases was increased compared to “phenotypic abnormality”, but not significantly. Contrary, the complication obesity is significantly underrepresented in monogenic mitochondrial diseases, suggesting that indeed its pathophysiology is not associated with mitochondrial impairment (Table 1 and Figure 2). For gout, abnormality of dental enamel, acrodermatitis dysmetabolica, reduced bone mineral density, nephrolithiasis and short stature, the percentage of mitochondrial diseases was decreased compared to “phenotypic abnormality”, but not significantly.

Figure 2. Association to mitochondrial disease for complications occurring in PA and MMA



Complications significantly overrepresented in mitochondrial disease are depicted in dark gray. Complications not significantly overrepresented in mitochondrial disease are depicted in light gray. *P-value < 0.05 determined by a Fisher’s exact test with multiple testing correction according to the Bonferroni method, comparing the percentage of the complication to the reference phenotype “phenotypic abnormality”, which is depicted in dark gray.

Not all complications are as overrepresented among monogenic mitochondrial diseases as expected: chronic kidney disease, anemia, neutropenia, thrombocytopenia, pancytopenia and premature ovarian insufficiency are not more frequent in mitochondrial disease, while a mitochondrial role in pathophysiology is expected (Table 1). It should be noted that the validity of this extra line of evidence supporting the hypothesis that pathophysiology of many complications in PA and MMA is related to mitochondrial failure is limited. This approach relies on the accuracy and completeness of HPO and has not been validated for other (mitochondrial) diseases yet. Still, the results of this extra line of evidence are reasonably similar to what has been reported in literature (Table 1).

THE ROLE OF MITOCHONDRIAL IMPAIRMENT IN PATHOPHYSIOLOGY OF COMPLICATIONS IN PA AND MMA

Based on reports of patients treated with anti-oxidants, histology of patient tissue, animal studies and studies in cell lines, combined with supporting evidence from the occurrence of complications in other monogenic mitochondrial diseases, we conclude that mitochondrial impairment probably plays a role in pathophysiology of cardiomyopathy, optic atrophy, abnormality of the liver, exercise intolerance, pancreatitis, abnormality of the basal ganglia, seizures and autism (Table 1). Contrary, we consider a role for mitochondrial impairment unlikely for short stature, reduced BMD, acrodermatitis dysmetabolica, nephrolithiasis, gout and obesity (Table 1).

Interestingly, to date there is no evidence suggesting that mitochondrial impairment plays a role in the pathophysiology of prolonged QTc interval, nor is it overrepresented in monogenic mitochondrial diseases (Table 1). In contrast, sensorineural hearing loss is overrepresented in mitochondrial disease (Table 1), although a shared pathophysiological process involving inhibited potassium flow due to propionic acid is suspected.⁶¹ This might implicate that in hearing loss in mitochondrial disease another pathophysiological process might be at play, that both complications do not share the same pathophysiology, or that prolonged QTc is underreported or underdiagnosed in monogenic mitochondrial diseases.

KNOWING THE UNKNOWNNS

Mitochondrial failure is likely to play a major role in pathophysiology of many devastating PA and MMA complications. However, despite this knowledge, we still cannot predict for any given patient when these complications will occur, which tissue will be affected and whether that effect will be reversible or permanent, while this is crucial knowledge for determining the therapeutic window of opportunity and the target tissue(s). Questions that need answers in the (near) future include: What is the nature of the differences in age of onset, why do patients develop complications during periods with (seemingly) good metabolic control and what determines reversibility of the different mitochondrial complications? Is this solely determined by residual enzymatic activity or does the strictness of and compliance to the protein restriction and other therapies play a role? What is the influence of the number, severity and duration of metabolic decompensations? Next to these questions addressing interpatient differences, what determines in one patient the intertissue differences in susceptibility for complications if there are no differences in enzymatic activity, therapy compliance or metabolic decompensations? Answers to these questions might be the key towards therapy improvements including the determination of the therapeutic window of opportunity and the target tissue(s).

CONCLUSION

Current treatment strategies are inadequate to prevent or treat most complications in PA and MMA. To optimize treatment strategies, insight in the pathophysiology of complications in PA and MMA is crucial. Here we summarized the current hypotheses and evidence on underlying pathophysiology of these complications, we assessed the occurrence of these complications in (other) monogenic mitochondrial diseases and we report whether mitochondrial impairment might play a role in the pathophysiology of the complication (Table 1). Altogether, this is a comprehensive overview on what we, to date, do and do not understand about pathophysiology of complications occurring in PA and MMA and about the role of mitochondrial impairment herein.

WEB RESOURCES

Human Phenotype Ontology <http://compbio.charite.de/hpweb/>

REFERENCES

- Childs B, Nyhan WL, Borden M, Bard L, Cooke RE. Idiopathic hyperglycinemia and hyperglycinuria: a new disorder of amino acid metabolism I. *Pediatrics*. 1961;27:522-538.
- Nyhan WL, Borden M, Childs B. Idiopathic hyperglycinemia: a new disorder of amino acid metabolism. II. The concentrations of other amino acids in the plasma and their modification by the administration of leucine. *Pediatrics*. 1961;27:539-550.
- Matsui SM, Mahoney MJ, Rosenberg LE. The natural history of the inherited methylmalonic acidemias. *N Engl J Med*. 1983;308: 857-861.
- Roe CR, Millington DS, Maltby DA, Bohan TP, Hoppel CL. L-Carnitine enhances excretion of propionyl coenzyme a as propionylcarnitine in propionic acidemia. *J Clin Invest*. 1984;73:1785-1788.
- Fowler B, Leonard JV, Baumgartner MR. Causes of and diagnostic approach to methylmalonic acidurias. *J Inherit Metab Dis*. 2008;31:350-360.
- Hörster F, Baumgartner MR, Viardot C et al. Long-term outcome in methylmalonic acidurias is influenced by the underlying defect (mut0, mut-, clbA, clbB). *Pediatr Res*. 2007;62:225-230.
- Manoli I, Sloan JL, Venditti CP. Isolated methylmalonic acidemia. In: Adam MP, Ardinger HH, Pagon RA et al., eds. *GeneReviews*®. Seattle, WA: University of Washington, Seattle; 1993-2019. Updated: 2016, December 1.
- Parini R, Furlan F, Brambilla A et al. Severe neonatal metabolic decompensation in methylmalonic acidemia caused by CblD defect. *JIMD Rep*. 2013;11:133-137.
- Abily-Donval L, Torre S, Samson A et al. Methylmalonyl-CoA epimerase deficiency mimicking propionic aciduria. *Int J Mol Sci*. 2017;18(11):2294.
- Kölker S, Garcia Cazorla A, Valayannopoulos V et al. The phenotypic spectrum of organic acidurias and urea cycle disorders. Part 1: the initial presentation. *J Inherit Metab Dis*. 2015a;38: 1041-1057.
- Grünert SC, Müllerleile S, de Silva L et al. Propionic acidemia: neonatal versus selective metabolic screening. *J Inherit Metab Dis*. 2012;35:41-49.
- Baumgartner MR, Hörster F, Dionisi-Vici C et al. Proposed guidelines for the diagnosis and management of methylmalonic and propionic acidemia. *Orphanet J Rare Dis*. 2014;9:130.
- AlGhamdi A, Alrifai MT, Al Hammad AI et al. Epilepsy in propionic acidemia: case series of 14 Saudi patients. *J Child Neurol*. 2018;33(11):713-717.
- Baumgartner ER, Viardot C. Long-term follow-up of 77 patients with isolated methylmalonic acidemia. *J Inherit Metab Dis*. 1995;18(2):138-142.
- Baumgartner D, Scholl-Burgi S, Sass JO et al. Prolonged QTc intervals and decreased left ventricular contractility in patients with propionic acidemia. *J Pediatr*. 2007;150:192-197.
- Brismar J, Ozand PT. CT and MR of the brain in disorders of the propionate and methylmalonate metabolism. *AJNR Am J Neuroradiol*. 1994;15(8):1459-1473.
- Cosson MA, Benoist JF, Touati G et al. Long-term outcome in methylmalonic aciduria: a series of 30 French patients. *Mol Genet Metab*. 2009;97:172-178.
- Gokce M, Unal O, Hismi B et al. Secondary hemophagocytosis in 3 patients with organic acidemia involving propionate metabolism. *Pediatr Hematol Oncol*. 2012;29:92-98.
- Griffin TA, Hostoffer RW, Tserng KY. Parathyroid hormone resistance and B cell lymphopenia in propionic acidemia. *Acta Paediatr*. 1996;85:875-878.
- Grotto S, Sudrié-Arnaud B, Drouin-Garraud V. Dilated cardiomyopathy and premature ovarian failure unveiling propionic aciduria. *Clin Chem*. 2018;64:752-754.

21. Grünert SC, Müllerleile S, de Silva L et al. Propionic acidemia: clinical course and outcome in 55 pediatric and adolescent patients. *Orphanet J Rare Dis.* 2013;8:6.
22. Haberlandt E, Canestrini C, Brunner-Krainz M et al. Epilepsy in patients with propionic acidemia. *Neuropediatrics.* 2009;40:120-125.
23. Hörster F, Garbade SF, Zwickler T et al. Prediction of outcome in isolated methylmalonic acidurias: combined use of clinical and biochemical parameters. *J Inher Metab Dis.* 2009;32:630-639.
24. Karimzadeh P, Jafari N, Ahmad Abadi F et al. Methylmalonic acidemia: diagnosis and neuroimaging findings of this neurometabolic disorder (an Iranian pediatric case series). *Iran J Child Neurol.* 2013;7(3):63-66.
25. Karimzadeh P, Jafari N, Ahmad Abadi F et al. Propionic acidemia: diagnosis and neuroimaging findings of this neurometabolic disorder. *Iran J Child Neurol.* 2014;8(1):58-61.
26. Kasapkara CS, Kangin M, Ozmen BO et al. Secondary hemophagocytosis in propionic acidemia. *Iran J Pediatr.* 2015; 25:e339.
27. Ma X, Zhang Y, Yang Y et al. Epilepsy in children with methylmalonic acidemia: electroclinical features and prognosis. *Brain Dev.* 2011;33:790-795.
28. MacFarland S, Hartung H. Pancytopenia in a patient with methylmalonic acidemia. *Blood.* 2015;125:1840.
29. Al-Owain M, Kaya N, Al-Shamrani H et al. Autism spectrum disorder in a child with propionic acidemia. *JIMD Rep.* 2013;7: 63-66.
30. Dejean de la Batie C, Barbier V, Roda C et al. Autism spectrum disorders in propionic acidemia patients. *J Inher Metab Dis.* 2018;41:623-629.
31. Witters P, Debbold E, Crivelly K et al. Autism in patients with propionic acidemia. *Mol Genet Metab.* 2016;119:317-321.
32. Schreiber J, Chapman KA, Summar ML. Neurologic considerations in propionic acidemia. *Mol Genet Metab.* 2012;105:10-15.
33. Couce ML, Castiñeiras DE, Bóveda MD et al. Evaluation and long-term follow-up of infants with inborn errors of metabolism identified in an expanded newborn screening programme. *Mol Genet Metab.* 2011;104(4):470-475.
34. Dionisi-Vici C, Deodato F, Röschinger W, Rhead W, Wilcken B. "Classical" organic acidurias, propionic aciduria, methylmalonic aciduria and isovaleric aciduria: long-term outcome and effects of expanded newborn screening using tandem mass spectrometry. *J Inher Metab Dis.* 2006;29(2-3):383-389.
35. Heringer J, Valayannopoulos V, Lund AM et al. Impact of age at onset and newborn screening on outcome in organic acidurias. *J Inher Metab Dis.* 2016;39(3):341-353.
36. Haijes HA, van Hasselt PM, Jans JJM, Verhoeven-Duif NM. Pathophysiology of propionic and methylmalonic acidemias. Part 2: Complications. *J Inher Metab Dis.* 2019.
37. Chemelli AP, Schocke M, Sperl W, Trieb T, Aichner F, Felber S. Magnetic resonance spectroscopy (MRS) in five patients with treated propionic acidemia. *J Magn Reson Imaging.* 2000;11: 596-600.
38. Frye RE, Rose S, Chacko J et al. Modulation of mitochondrial function by the microbiome metabolite propionic acid in autism and control cell lines. *Transl Psychiatry.* 2016;6:e927.
39. Andreula CM, De Blasi R, Carella A. CT and MR studies of methylmalonic acidemia. *AJNR Am J Neuroradiol.* 1991;12: 410-412.
40. Baker EH, Sloan JL, Hauser NS et al. MRI characteristics of globus pallidus infarcts in isolated methylmalonic acidemia. *AJNR Am J Neuroradiol.* 2015;36:194-201.
41. Chakrapani A, Sivakumar P, McKiernan PJ, Leonard JV. Metabolic stroke in methylmalonic acidemia five years after liver transplantation. *J Pediatr.* 2002;140:261-263.
42. Heidenreich R, Natowicz M, Hainline BE et al. Acute extrapyramidal syndrome in methylmalonic acidemia: "metabolic stroke" involving the globus pallidus. *J Pediatr.* 1988;113(6):1022-1027.
43. Karall D, Haberlandt E, Schimmel M et al. Cytotoxic not vasogenic edema is the cause for stroke-like episodes in propionic acidemia. *Neuropediatrics.* 2011;42:210.
44. Scholl-Burgi S, Haberlandt E, Gotwald T et al. Stroke-like episodes in propionic acidemia caused by central focal metabolic decompensation. *Neuropediatrics.* 2009;40(2):76-81.
45. Dejean de la Batie C, Barbier V, Valayannopoulos V et al. Acute psychosis in propionic acidemia: 2 case reports. *J Child Neurol.* 2014;29:274-279.
46. Sheikhmoonesi F, Shafaat A, Moarefian S, Zaman T. Affective disorder as the first manifestation of methylmalonic acidemia: a case report. *Iran J Pediatr.* 2013;23:245-246.
47. Felipo V, Kosenko E, Miñana MD, Marcaida G, Grisolia S. Molecular mechanism of acute ammonia toxicity and of its prevention by L-carnitine. *Adv Exp Med Biol.* 1994;368:65-77.
48. Zhou BG, Noremborg MD. Ammonia downregulates GLAST mRNA glutamate transporter in rat astrocyte cultures. *Neurosci Lett.* 1999;276:145-148.
49. Lai JC, Cooper AJ. Neurotoxicity of ammonia and fatty acids: differential inhibition of mitochondrial dehydrogenases by ammonia and fatty acyl coenzyme a derivatives. *Neurochem Res.* 1991;16:795-803.

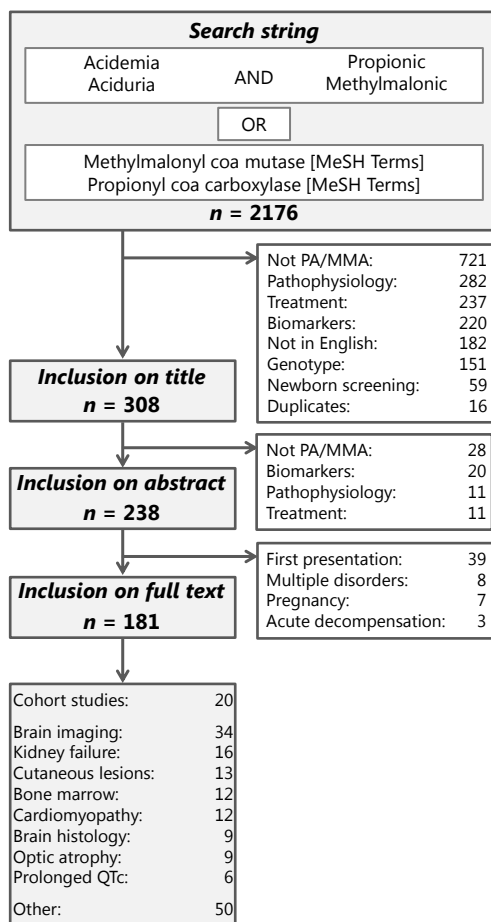
50. Schinder AF, Olson EC, Spitzer NC, Montal M. Mitochondrial dysfunction is a primary event in glutamate neurotoxicity. *J Neurosci.* 1996;16:6125-6133.
51. White RJ, Reynolds JJ. Mitochondrial depolarization in glutamate-stimulated neurons: an early signal specific to excitotoxin exposure. *J Neurosci.* 1996;16:5688-5697.
52. Malfatti CRM, Perry MLS, Schweigert ID et al. Convulsions induced by methylmalonic acid are associated with glutamic acid decarboxylase inhibition in rats: a role for GABA in the seizures presented by methylmalonic acidemia patients? *Neuroscience.* 2007;146:1879-1887.
53. Royes LFF, Gabbi P, Ribeiro LR et al. A neuronal disruption in redox homeostasis elicited by ammonia alters the glycine/glutamate (GABA) cycle and contributes to MMA-induced excitability. *Amino Acids.* 2016;48:1373-1389.
54. Amaral AU, Cecatto C, Castilho RF, Wajner M. 2-Methylcitric acid impairs glutamate metabolism and induces permeability transition in brain mitochondria. *J Neurochem.* 2016;137:62-75.
55. Malfatti CRM, Royes LF, Francescato L et al. Intrastratial methylmalonic acid administration induces convulsions and TBARS production, and alters Na⁺,K⁺-ATPase activity in the rat striatum and cerebral cortex. *Epilepsia.* 2003;44:761-767.
56. Wyse AT, Streck EL, Barros SV, Brusque AM, Zugno AI, Wajner M. Methylmalonate administration decreases Na⁺, K⁺-ATPase activity in cerebral cortex of rats. *Neuroreport.* 2000;11: 2331-2334.
57. Traber G, Baumgartner MR, Schwarz U, Pangalu A, Donath MY, Landau K. Subacute bilateral visual loss in methylmalonic acidemia. *J Neuroophthalmol.* 2011;31:344-346.
58. Sadun AA. Mitochondrial optic neuropathies. *J Neurol Neurosurg Psychiatry.* 2002;72:424-426.
59. Pinar-Sueiro S, Martínez-Fernández R, Lage-Medina S, Aldamiz-Ecchevarria L, Vecino L. Optic neuropathy in methylmalonic acidemia: the role of neuroprotection. *J Inherit Metab Dis.* 2010; 33:199-203.
60. Rosentreter A, Gaki S, Dinslage S, Dietlein TS. Juvenile glaucoma in propionic acidemia. *Ophthalmologie.* 2012;109:1211-1213.
61. Grünert SC, Bodi L, Odening KE. Possible mechanisms for sensorineural hearing loss and deafness in patients with propionic acidemia. *Orphanet J Rare Dis.* 2017;12:30.
62. Østergaard E, Wibrand F, Ørningreen MC, Vissing J, Horn N. Impaired energy metabolism and abnormal muscle histology in mut-methylmalonic aciduria. *Neurology.* 2005;65(6):931-933.
63. de Keyzer Y, Valayannopoulos V, Benoist JF et al. Multiple OXPHOS deficiency in the liver, kidney, heart and skeletal muscle of patients with methylmalonic aciduria and propionic aciduria. *Pediatr Res.* 2009;66(1):91-95.
64. Baruteau J, Hargreaves I, Krywawych S et al. Successful reversal of propionic acidemia associated cardiomyopathy: evidence for low myocardial coenzyme Q10 status and secondary mitochondrial dysfunction as an underlying pathophysiological mechanism. *Mitochondrion.* 2014;17:150-156.
65. Bodi I, Grünert SC, Becker N et al. Mechanisms of acquired long QT syndrome in patients with propionic acidemia. *Heart Rhythm.* 2016;13:1335-1345.
66. Kruszka PS, Manoli I, Sloan JL, Kopp JB, Venditti CP. Renal growth in isolated methylmalonic acidemia. *Genet Med.* 2013;15: 990-996.
67. Manoli I, Sysol JR, Li L. Targeting proximal tubule mitochondrial dysfunction attenuates the renal disease of methylmalonic acidemia. *Proc Natl Acad Sci U S A.* 2013;110:13552-13557.
68. Zsengellér ZK, Aljinovic N, Teot LA et al. Methylmalonic acidemia: a megamitochondrial disorder affecting the kidney. *Pediatr Nephrol.* 2014;29:2139-2146.
69. Manoli I, Sysol JR, Epping MW et al. FGF21 underlies a hormetic response to metabolic stress in methylmalonic acidemia. *JCI Insight.* 2018;3(23):e124351.
70. Yilmaz AC, Kiliç M, Büyükkaragöz B, Tayfur AC, Koçak M. Urolithiasis in an infant with propionic acidemia: answer. *Pediatr Nephrol.* 2015;30:77-78.
71. Kahler SG, Sherwood WG, Woolf D et al. Pancreatitis in patients with organic acidemias. *J Pediatr.* 1994;124(2):239-243.
72. Chandler RJ, Zervas PM, Shanske S et al. Mitochondrial dysfunction in mut methylmalonic acidemia. *FASEB J.* 2009;23: 1252-1261.
73. Wakabayashi T. Megamitochondria formation – physiology and pathology. *J Cell Mol Med.* 2002;6:497-538.
74. Imbard A, Garcia Segarra N, Tardieu M et al. Long-term liver disease in methylmalonic and propionic acidemias. *Mol Genet Metab.* 2018;123:433-440.
75. Kölker S, Valayannopoulos V, Burlina AB et al. The phenotypic spectrum of organic acidurias and urea cycle disorders. Part 2: the evolving clinical phenotype. *J Inherit Metab Dis.* 2015b;38:1059-1074.
76. Brassier A, Boyer O, Valayannopoulos V et al. Renal transplantation in 4 patients with methylmalonic aciduria: a cell therapy for metabolic disease. *Mol Genet Metab.* 2013;110:106-110.
77. Cosson MA, Touati G, Lacaille F et al. Liver hepatoblastoma and multiple OXPHOS deficiency in the follow-up of a patient with methylmalonic aciduria. *Mol Genet Metab.* 2008;95:107-109.

78. Chan R, Mascarenhas L, Boles RG, Kerkar N, Genyk Y, Venkatramani R. Hepatoblastoma in a patient with methylmalonic aciduria. *Am J Med Genet A*. 2014;167:635-638.
79. Ktena YP, Paul SM, Hauser NS et al. Delineating the spectrum of impairments, disabilities and rehabilitation needs in methylmalonic acidemia (MMA). *Am J Med Genet*. 2015;167A(9): 2075-2084.
80. Touati G, Valayannopoulos V, Mention K et al. Methylmalonic and propionic acidurias: management without or with a few supplements of specific amino acid mixture. *J Inherit Metab Dis*. 2006;29:288-298.
81. Prasad C, Nurko S, Borovoy J, Korson MS. The importance of gut motility in the metabolic control of propionic acidemia. *J Pediatr*. 2004;144:532-535.
82. Lam C, Desviat LR, Perez-Cerda C, Ugarte M, Barshop BA, Cederbaum S. 45-year-old female with propionic acidemia, renal failure, and premature ovarian failure; late complications of propionic acidemia? *Mol Genet Metab*. 2011;103:338-340.
83. Stork LC, Ambruso DR, Wallner SF et al. Pancytopenia in propionic acidemia: hematologic evaluation and studies of hematopoiesis *in vitro*. *Pediatr Res*. 1986;20:783-788.
84. Corazza F, Blum D, Clercx A, Mardens Y, Fondou P. Erythroblastopenia associated with methylmalonic aciduria. *Case Rep in vitro Stud Biol Neonate*. 1996;70(5):304-310.
85. Inoue S, Krieger I, Sarnaik A, Ravindranath Y, Fracassa M, Ottenbreit MJ. Inhibition of bone marrow stem cell growth *in vitro* by methylmalonic acid: a mechanism for pancytopenia in a patient with methylmalonic acidemia. *Pediatr Res*. 1981;15: 95-98.
86. Sulaiman RA, Shaheen MY, Al-Zaidan H et al. Hemophagocytic lymphohistiocytosis: a rare cause of recurrent encephalopathy. *Intract Rare Dis Res*. 2016;5:227-230.
87. Bakshi NA, Al-Anzi T, Mohamed S et al. Spectrum of bone marrow pathology and hematological abnormalities in methylmalonic acidemia. *Am J Med Genet A*. 2018;176:687-691.
88. Inoue F, Terada N, Nukina S, Kodo N, Kinugasa A, Sawada T. Methylmalonic aciduria with pathological fracture. *J Inherit Metab Dis*. 1993;16(6):1052-1053.
89. Talbot JC, Gummerson NW, Kluge W, Shaw DL, Groves C, Lealman GT. Osteoporotic femoral fracture in a child with propionic acidemia presenting as non-accidental injury. *Eur J Pediatr*. 2006;165(7):496-497.
90. Ney DM, Etzel MR. Designing medical foods for inherited metabolic disorders: why intact protein is superior to amino acids. *Curr Opin Biotechnol*. 2017;44:39-45.
91. Charuvanij S, Pattaragarn A, Wisuthsarewong W, Vatanavicharn N. Juvenile gout in methylmalonic acidemia. *Pediatr Int*. 2016;58:501-503.
92. Yannicelli S. Nutrition therapy of organic acidemias with amino acid-based formulas: emphasis on methylmalonic and propionic acidemia. *J Inherit Metab Dis*. 2006;29(2-3):281-287.
93. Feillet F, Bodamer OA, Dixon MA, Sequeira S, Leonard JV. Resting energy expenditure in disorders of propionate metabolism. *J Pediatr*. 2000;136(5):659-663.
94. Thomas JA, Bernstein LE, Greene CL, Koeller DM. Apparent decreased energy requirements in children with organic acidemias: preliminary observations. *J Am Diet Assoc*. 2000;100 (9):1074-1076.
95. van Hagen CC, Carbasius Weber E, van den Hurk TE et al. Energy expenditure in patients with propionic and methylmalonic acidemias. *J Inherit Metab Dis*. 2004;27(1):111-112.
96. Hauser NS, Manoli I, Graf JC, Sloan J, Venditti CP. Variable dietary management of methylmalonic acidemia: metabolic and energetic correlations. *Am J Clin Nutr*. 2011;93(1):47-56.
97. Blecker U, de Meirleir L, de Raevae L, Ramet J, Vandenplas Y. Acrodermatitis-like syndrome in organic aciduria. *Pediatrics*. 1994;93(3):537.
98. Lane TN, Spraker MK, Parker SS. Propionic acidemia manifesting with low isoleucine generalized exfoliative dermatosis. *Pediatr Dermatol*. 2007;24:508-510.
99. Rosa J, Fraga AB, de Carvalho R, Maia AL, Rodrigues AL, Gomes MF. Acrodermatitis dysmetabolica as a sign of methylmalonic aciduria decompensation. *Clin Case Rep*. 2018;6(6): 1048-1050.
100. Tabanlıoğlu D, Ersoy-Evans S, Karaduman A. Acrodermatitis enteropathica-like eruption in metabolic disorders: acrodermatitis dysmetabolica is proposed as a better term. *Pediatr Dermatol*. 2009;26:150-154.
101. Bodemer C, de Prost Y, Bachollet B et al. Cutaneous manifestations of methylmalonic and propionic acidemia: a description based on 38 cases. *Br J Dermatol*. 2011;131(1):93-98.
102. Karamizadeh Z, Dalili S, Karamifar H, Hossein Amirhakimi G. Association of methylmalonic acidemia and erythema nodosum. *Iran J Med Sci*. 2011;36(1):65-66.
103. Al-Rikabi AC, Al-Homsy HI. Propionic acidemia and zinc deficiency presenting as necrolytic migratory erythema. *Saudi Med J*. 2004;25(5):660-662.
104. Bassim CW, Wright JT, Guadagnini JP et al. Enamel defects and salivary methylmalonate in methylmalonic acidemia. *Oral Dis*. 2009;15:196-205.
105. Koopman WJH, Willems PHGM, Smeitink JAM. Monogenic mitochondrial disorders. *N Engl J Med*. 2012;366: 1132-1141.
106. Maguire CA, Chong H, Ramachandran R, Popoola J, Akhras V, Singh M. Acrodermatitis acidemia. *Clin Exp*

- Dermatol. 2018;43(3):315-318.
107. Nizon M, Ottolenghi C, Valayannopoulos V et al. Long-term neurological outcome of a cohort of 80 patients with classical organic acidurias. *Orphanet J Rare Dis.* 2013;23(8):148.
 108. O'Shea CJ, Sloan JL, Wiggs EA et al. Neurocognitive phenotype of isolated methylmalonic acidemia. *Pediatrics.* 2012;129(6): e1541-e1551.
 109. Pena L, Burton BK. Survey of health status and complications among propionic acidemia patients. *Am J Med Genet A.* 2012; 158A(7):1641-1646.
 110. Radmanesh A, Zaman T, Ghanaati H, Molaei S, Robertson RL, Zamani AA. Methylmalonic acidemia: brain imaging findings in 52 children and a review of the literature. *Pediatr Radiol.* 2008; 38(10):1054-1061.
 111. de Raeve L, De Meirleir L, Ramet J, Vandenplas Y, Gerlo E. Acrodermatitis enteropathica-like cutaneous lesions in organic aciduria. *J Pediatr.* 1994;124:416-420.
 112. Rafique M. Propionic acidemia: demographic characteristics and complications. *J Pediatr Endocrinol Metab.* 2013;26(5-6):497-501.
 113. Romano S, Valayannopoulos V, Touati G et al. Cardiomyopathies in propionic aciduria are reversible after liver transplantation. *J Pediatr.* 2010;156:128-134.
 114. Scott Schwoerer J, Clowes Candadai S, Held PK. Long-term outcomes in Amish patients diagnosed with propionic acidemia. *Mol Genet Metab Rep.* 2018;16:36-38.
 115. Shuaib T, Al-Hashmi N, Ghaziuddin M et al. Propionic acidemia associated with visual hallucinations. *J Child Neurol.* 2012;27: 799-803.
 116. Sipahi T, Yilmaz D, Tavil B. Propionic acidemia with myelodysplasia and neutropenia in a Turkish child. *J Pediatr Hematol Oncol.* 2004;26:154-155.
 117. Tu WJ. Methylmalonic acidemia in mainland China. *Ann Nutr Metab.* 2011;58:281.

SUPPLEMENTAL DATA

Figure S1. Flowchart for inclusion of studies in systematic review



Abbreviations: MMA: methylmalonic acidemia; PA: propionic acidemia.

Table S1. Prevalence of common complications occurring in PA and MMA, assessed in cohort studies

Complication	PROPIONIC ACIDEMIA			METHYLMALONIC ACIDEMIA		
	SS	%	References	SS	%	References
White matter lesions	16	38	Nizon et al. 2013	52	29	Radmanesh et al. 2008
	10	40	Karimzadeh et al. 2014	30	33	Cosson et al. 2009
				28	36	Nizon et al. 2013
			39 <i>Sample size-weighted mean</i>	32		<i>Sample size-weighted mean</i>
Basal ganglia hyperintensities	20	10	Brismar and Ozand 1994	23	22	Brismar and Ozand 1994
	55	19	Grünert et al. 2012, 2013	52	6	Radmanesh et al. 2008
	16	56	Nizon et al. 2013	30	27	Cosson et al. 2009
	10	30	Karimzadeh et al. 2014	43	35	O'Shea et al. 2012
	16	6	Imbard et al. 2018	28	36	Nizon et al. 2013
			20	15	Karimzadeh et al. 2013	
			40	48	Baker et al. 2015	
			37	38	Ktena et al. 2015	

		22	<i>Sample size-weighted mean</i>		28	<i>Sample size-weighted mean</i>
Movement disorders	58	13	Pena et al. 2012	52	19	Baumgartner, Viardot 1995
	55	9	Grünert et al. 2012, 2013	30	20	Cosson et al. 2009
	101	22	Kölker et al. 2015b	129	26	Kölker et al. 2015b
	20	15	Scott Schwoerer et al. 2018	37	83	Ktena et al. 2015
	16		<i>Sample size-weighted mean</i>	32		<i>Sample size-weighted mean</i>
Psychomotor retardation	58	77	Pena et al. 2012	273	54	Hörster et al. 2007, 2009
	55	55	Grünert et al. 2012, 2013	354	60	Tu et al. 2011
	101	30	Kölker et al. 2015b	129	31	Kölker et al. 2015b
	49		<i>Sample size-weighted mean</i>	53		<i>Sample size-weighted mean</i>
Cognitive deficits	58	72	Pena et al. 2012	30	48	Cosson et al. 2009
	55	70	Grünert et al. 2012, 2013	354	60	Tu et al. 2011
	16	56	Imbard et al. 2018	12	25	Imbard et al. 2018
	69		<i>Sample size-weighted mean</i>	58		<i>Sample size-weighted mean</i>
Attention deficit hyperactive disorder	58	15	Pena et al. 2012			
Autism	58	9	Pena et al. 2012			
Stroke-like episodes	58	18	Pena et al. 2012	273	17	Hörster et al. 2007, 2009
	55	9	Grünert et al. 2012, 2013			
	14		<i>Sample size-weighted mean</i>			
Epilepsy	17	53	Haberlandt et al. 2009	273	10	Hörster et al. 2007, 2009
	58	41	Pena et al. 2012	63	43	Ma et al. 2011
	26	13	Rafique 2013	43	16	O'Shea et al. 2012
	101	13	Kölker et al. 2015b	129	3	Kölker et al. 2015b
	14	6	AlGhamdi et al. 2018			
	20	25	Scott Schwoerer et al. 2018			
	23		<i>Sample size-weighted mean</i>	13		<i>Sample size-weighted mean</i>
Optic atrophy	58	11	Pena et al. 2012	30	3	Cosson et al. 2009
	55	7	Grünert et al. 2012, 2013	43	9	O'Shea et al. 2012
	101	0	Kölker et al. 2015b	129	2	Kölker et al. 2015b
	5		<i>Sample size-weighted mean</i>	37	16	Ktena et al. 2015
Muscular hypotonia	55	51	Grünert et al. 2012, 2013	129	23	Kölker et al. 2015b
	26	62	Rafique 2013			
	101	38	Kölker et al. 2015b			
	45		<i>Sample size-weighted mean</i>			
Exercise intolerance						
Anemia	58	32	Pena et al. 2012			
	55	82	Grünert et al. 2012, 2013			
	26	26	Rafique 2013			
	51		<i>Sample size-weighted mean</i>			
Neutropenia	58	31	Pena et al. 2012			
	55	29	Grünert et al. 2012, 2013			
	26	36	Rafique 2013			
	31		<i>Sample size-weighted mean</i>			
Thrombocytopenia	58	17	Pena et al. 2012			
	55	35	Grünert et al. 2012, 2013			
	26	39	Rafique 2013			
	28		<i>Sample size-weighted mean</i>			
Pancytopenia	55	11	Grünert et al. 2012, 2013	129	0	Kölker et al. 2015b
	26	36	Rafique 2013			
	19		<i>Sample size-weighted mean</i>			
Renal failure	101	1	Kölker et al. 2015b	52	27	Baumgartner, Viardot 1995
				30	47	Cosson et al. 2009
				273	28	Hörster et al. 2007, 2009
				354	27	Tu et al. 2011
				129	29	Kölker et al. 2015b
				12	57	Imbard et al. 2018
				29		<i>Sample size-weighted mean</i>
Pancreatitis	26	0	Kahler et al. 1994	30	17	Kahler et al. 1994
	58	18	Pena et al. 2012	52	0	Baumgartner, Viardot 1995
	55	4	Grünert et al. 2012, 2013	273	6	Hörster et al. 2007, 2009
	101	0	Kölker et al. 2015b	30	3	Cosson et al. 2009
	16	6	Imbard et al. 2018	129	0	Kölker et al. 2015b
	5		<i>Sample size-weighted mean</i>	4		<i>Sample size-weighted mean</i>

Hepatomegaly and/or hyperechoic liver	16	78	Imbard et al. 2018	12	33	Imbard et al. 2018
Cardiomyopathy	19	32	Massoud et al. 1994	273	1	Hörster et al. 2007, 2009
	30	20	Romano et al. 2010	129	11	Kölker et al. 2015b
	58	19	Pena et al. 2012	12	17	Imbard et al. 2018
	55	9	Grünert et al. 2012, 2013			
	101	8	Kölker et al. 2015b			
	16	6	Imbard et al. 2018			
	20	20	Scott Schwoerer et al. 2018			
		14	<i>Sample size-weighted mean</i>		5	<i>Sample size-weighted mean</i>
Prolonged QTc interval	10	70	Baumgartner et al. 2007	129	0	Kölker et al. 2015b
	55	22	Grünert et al. 2012, 2013	12	25	Imbard et al. 2018
	101	33	Kölker et al. 2015b			
	16	44	Imbard et al. 2018			
	20	15	Scott Schwoerer et al. 2018			
		31	<i>Sample size-weighted mean</i>		2	<i>Sample size-weighted mean</i>
Sensorineural hearing loss	55	9	Grünert et al. 2012, 2013	129	0	Kölker et al. 2015b
	101	1	Kölker et al. 2015b	37	8	Ktena et al. 2015
		4	<i>Sample size-weighted mean</i>		2	<i>Sample size-weighted mean</i>
Constipation	26	7	Rafique 2013			
Feeding problems						
Obesity						
Growth retardation and short stature	55	6	Grünert et al. 2012, 2013	30	30	Cosson et al. 2009
Decreased bone mineral density	58	13	Pena et al. 2012			
	55	2	Grünert et al. 2012, 2013			
		8	<i>Sample size-weighted mean</i>			
Enamel defects				22	55	Bassim et al. 2009
Joint hypermobility				37	69	Ktena et al. 2015
Pes planus				37	60	Ktena et al. 2015

Table S2. Rare complications occurring in PA and MMA, described in case reports

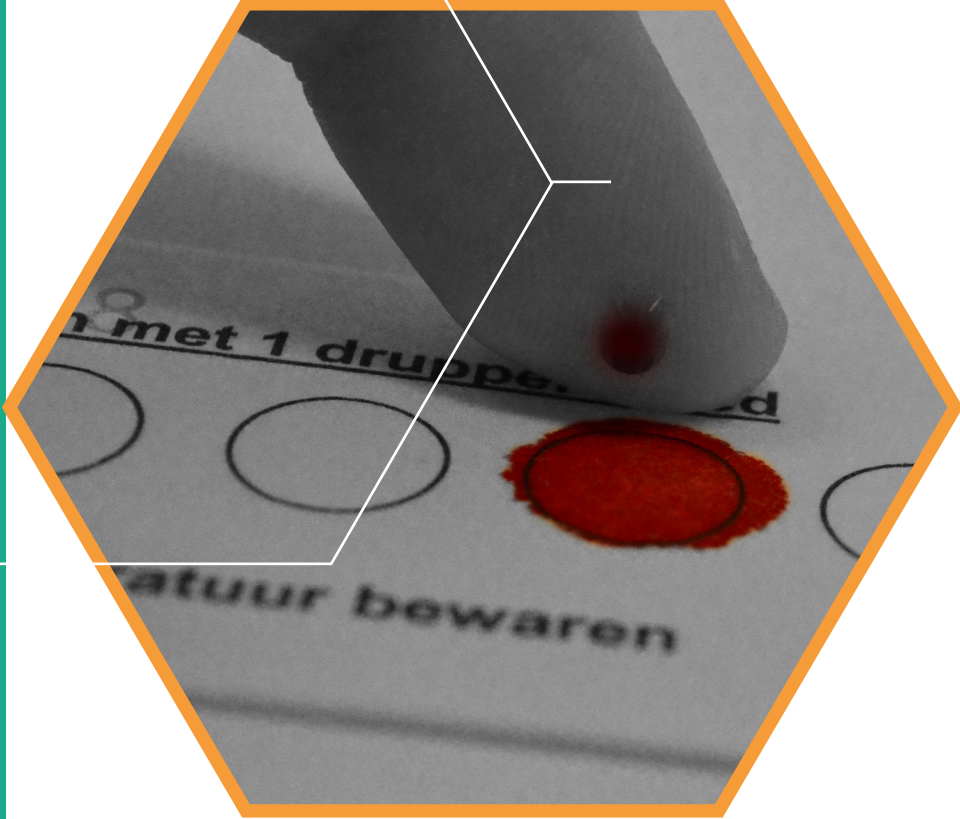
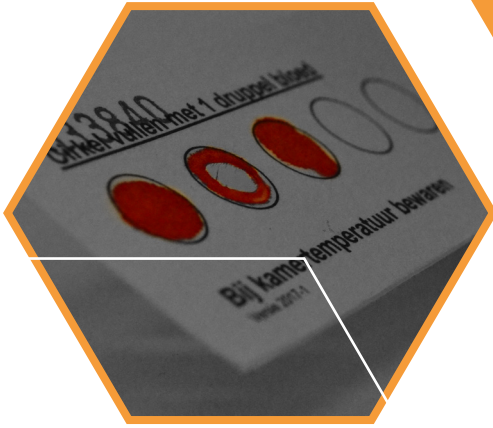
Complication	PROPIONIC ACIDEMIA		METHYLMALONIC ACIDEMIA	
	N	References	N	References
Acrodermatitis dysmetabolica	3	de Raeve et al. 1994, Lane, Spraker and Parker 2007, Tabanlıoğlu, Ersoy-Evans and Karaduman 2009	8	de Raeve et al. 1994, Blecker et al. 1994, Tabanlıoğlu, Ersoy-Evans and Karaduman 2009, Maguire et al. 2018, Rosa et al. 2018
Hemophagocytotic lymphohistiocytosis	4	Gokce et al. 2012, Kasapkara et al. 2015, Sulaiman et al. 2016	3	Gokce et al. 2012, Bakshi et al. 2018
Hypogammaglobulinaemia	4	Childs et al. 1961, Brandt et al. 1974, Muller et al. 1980, Griffin et al. 1996		
Myelodysplastic syndrome	1	Sipahi, Yilmaz and Tavil 2004	2	MacFarland and Hartung 2015, Bakshi et al. 2018
Hepatoblastoma			2	Cosson et al. 2008, Brassier et al. 2013, Chan et al. 2014
Premature ovarian failure	2	Lam et al. 2011, Grotto et al. 2018		
Juvenile gout			2	Charuvani et al. 2016
Acute psychosis	2	Dejean de la Batie et al. 2014		
Visual hallucinations	2	Shuaib et al. 2012		
Bipolar disorder			1	Sheikhmoonesi et al. 2013
Bilateral juvenile glaucoma	1	Rosentreter et al. 2012		
Urolithiasis	1	Yilmaz et al. 2015		

Abbreviations: N: number of patients reported.

Table S3. Association to mitochondrial disease for complications occurring in PA and MMA

HPO CODE	HPO NAME	NUMBER OF GENES			% Mito-chon.	P-VALUE
		Asso-ciated	Mito-chondrial	Non-mito-chondrial		
HP:0000118	Phenotypic abnormality	3676	231	3445	6.3	
HP:0003546	Exercise intolerance	74	38	36	51.4	<0.0001
HP:0001733	Pancreatitis	71	19	52	26.8	<0.0001
HP:0001638	Cardiomyopathy	349	78	271	22.3	<0.0001
HP:0001297	Stroke	99	22	77	22.2	<0.0001
HP:0000709	Psychosis	87	19	68	21.8	0.0001
HP:0002134	Abnormality of the basal ganglia	50	10	40	20.0	0.0306
HP:0000648	Optic atrophy	414	71	343	17.1	<0.0001
HP:0000717	Autism	133	19	114	14.3	0.0284
HP:0011968	Feeding difficulties	524	73	451	13.9	<0.0001
HP:0001252	Muscular hypotonia	1118	142	976	12.7	<0.0001
HP:0000407	Sensorineural hearing impairment	608	73	535	12.0	0.0001
HP:0001250	Seizures	1170	136	1034	11.6	<0.0001
HP:0002019	Constipation	209	23	186	11.0	NS
HP:0001392	Abnormality of the liver	764	74	690	9.7	0.0339
HP:0001903	Anemia	360	28	332	7.8	NS
HP:0001657	Prolonged QT interval	34	2	32	5.9	NS
HP:0008209	Premature ovarian insufficiency	43	2	41	4.7	NS
HP:0001876	Pancytopenia	52	2	50	3.8	NS
HP:0004322	Short stature	917	35	882	3.8	NS
HP:0000787	Nephrolithiasis	89	3	86	3.4	NS
HP:0001873	Thrombocytopenia	211	7	204	3.3	NS
HP:0012622	Chronic kidney disease	69	2	67	2.9	NS
HP:0004349	Reduced bone mineral density	358	9	349	2.5	NS
HP:0001875	Neutropenia	87	2	85	2.3	NS
HP:0000964	Eczema	116	2	114	1.7	NS
HP:0000682	Abnormality of dental enamel	134	2	132	1.5	NS
HP:0001513	Obesity	277	4	273	1.4	0.0084
HP:0001997	Gout	10	0	10	0.0	NS

Abbreviations: HPO: Human Phenotype Ontology; NS: not significant; P-value: p-value of Fisher's exact test.



Pathophysiology of propionic and methylmalonic

acidemias. Part 2: Treatment strategies

Journal of Inherited Metabolic Diseases 2019, 42(5): 745-761
DOI: 10.1002/jimd.12128

Hanneke A. Haijes, Peter M. van Hasselt,
Judith J.M. Jans[†], Nanda M. Verhoeven-Duif^{†,*}

[†] These authors contributed equally to this article
^{*} Corresponding author

ABSTRACT

Despite realizing increased survival rates for propionic acidemia (PA) and methylmalonic acidemia (MMA) patients, the current therapeutic regimen is inadequate for preventing or treating the devastating complications that still can occur. The elucidation of pathophysiology of these complications allows us to evaluate and rethink treatment strategies. In this review we display and discuss potential therapy targets and we give a systematic overview on current, experimental and unexplored treatment strategies in order to provide insight in what we have to offer PA and MMA patients, now and in the future. Evidence on the effectiveness of treatment strategies is often scarce, since none were tested in randomized clinical trials. This raises concerns, since even the current consensus on best practice treatment for PA and MMA is not without controversy. To attain substantial improvements in overall outcome, gene, mRNA or enzyme replacement therapy is most promising since permanent reduction of toxic metabolites allows for a less strict therapeutic regime. Hereby, both mitochondrial-associated and therapy induced complications can theoretically be prevented. However, the road from bench to bedside is long, as it is challenging to design a drug that is delivered to the mitochondria of all tissues that require enzymatic activity, including the brain, without inducing any off-target effects. To improve survival rate and quality of life of PA and MMA patients, there is a need for systematic (re-)evaluation of accepted and potential treatment strategies, so that we can better determine *who* will benefit *when* and *how* from *which* treatment strategy.

INTRODUCTION

Whereas only a few decades ago patients with propionic acidemia (PA) and methylmalonic acidemia (MMA) had a very poor life expectancy, patients now tend to reach adulthood. Next to general advances in clinical care, this has been accomplished through the implementation of a protein-restricted diet, carnitine supplementation and the supplementation of the cofactor cobalamin in MMA. These therapies were conceived when pathophysiological mechanisms at play in these diseases were recognized.¹⁻⁴

However, PA and MMA patients are still greatly at risk for developing debilitating complications, and the overall outcome remains unsatisfying. The currently available therapies are inadequate for prevention or treatment of these complications. Despite extensive research, no new therapies have been implemented over the past decade, while there is an urgent need for improved treatment.

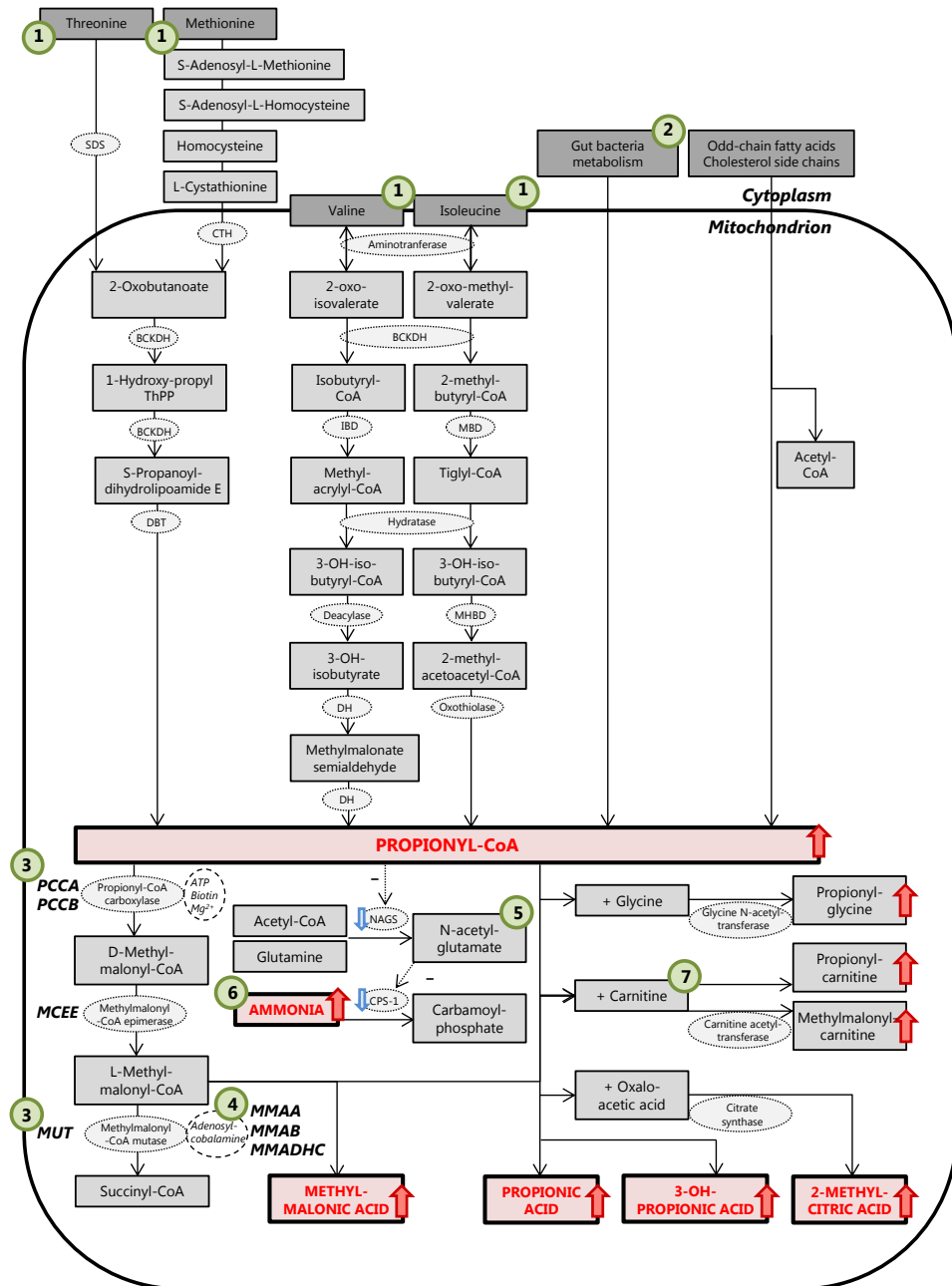
In the coming decade, the tide may turn. Pathophysiology of complications in PA and MMA is studied more and more and thereby gradually elucidated (reviewed in Haijes et al.⁵). Improved understanding of pathophysiology allows us to evaluate and rethink our treatment strategies. In this review we summarize the biochemical consequences of PA and MMA to display potential therapy targets and we provide a systematic overview on current, experimental and unexplored treatment strategies in PA and MMA in order to provide insight in what we have to offer PA and MMA patients, now and in the future.

METABOLITE ACCUMULATION IN PA AND MMA

The genes harboring mutations that give rise to PA and MMA all encode mitochondrial enzymes. PA is caused by a deficiency of propionyl-CoA carboxylase (PCC, EC 6.4.1.3), a protein complex of which the two subunits are encoded by *PCCA* and *PCCB*. Isolated methylmalonic acidemia (MMA) is either caused either by a deficiency of methylmalonyl-CoA mutase (MCM, EC 5.4.99.2, encoded by *MUT*), by diminished synthesis or availability of its cofactor 50-deoxyadenosylcobalamin which is associated with cobalamin A, B or D deficiency (encoded by *MMAA*, *MMAB* or *MMADHC*, respectively), or by a deficiency of methylmalonyl-CoA epimerase (MCE, EC 5.1.99.1, encoded by *MCEE*). The protein encoded by *MMAA* is reported to act as a reactivating factor for MCM by promoting the replacement of the inactive cofactor hydroxycobalamin by the active cofactor adenosylcobalamin.⁶ *MMAB* encodes the adenosyltransferase (EC 2.5.1.17) that converts cobalamin into adenosylcobalamin and the protein encoded by *MMADHC* is proposed to act as a trafficking chaperone that delivers processed cobalamin to its target enzymes, including MCM.⁷ The biochemical pathway harboring PCC, MCM, MCE, and adenosylcobalamin is illustrated in Figure 1.

Within isolated MMA, the cause and range of accumulation of toxic metabolites, the natural history and the prognosis differ between the different types.⁸⁻¹⁰ MMA caused by deficiency of MCM is often distinguished in cobalamin unresponsive patients (*mut*⁰) and cobalamin responsive patients (*mut*⁻). Cobalamin A deficient patients are usually cobalamin responsive, cobalamin B deficient patients can either be cobalamin unresponsive or responsive. *Mut*⁰ and cobalamin B deficient patients are considered severely affected regarding morbidity and mortality, whereas *mut*⁻ and cobalamin A deficient patients are considered to present with a milder form of MMA. Cobalamin D deficiency can either result in combined methylmalonic aciduria and homocystinuria, in isolated homocystinuria (variant 1) or in isolated MMA (variant 2).

Figure 1. Metabolite accumulation in PA and MMA, and associated therapy targets



Metabolites are depicted in light gray rectangles, toxic metabolites are depicted in red rectangles. Enzymes are depicted in light gray ovals. Cofactors for enzymes are depicted in white ovals. Primary supply routes of the propionate pathway are depicted in dark gray rectangles. Increased concentrations of metabolites are depicted by the larger red arrows, decreased enzyme activities are depicted by the smaller blue arrows. Targets for current and experimental treatment strategies are depicted by green circles, the numbers correspond to the numbers

[Figure 1 continued] of the therapy targets in Table 1 and throughout the text. Abbreviations: BCKDH: branched-chain α -keto acid dehydrogenase; CPS-1: carbamoylphosphate synthetase 1; CTH: cystathionine gamma-lyase; dihydrolipoamide branched chain transacylase E2; DH: dehydrogenase; IBD: isobutyryl-CoA dehydrogenase; MBD: 2-methylbutyryl-CoA dehydrogenase; MHBD: 2-methyl-3-hydroxy-butryl-CoA dehydrogenase; NAGS: N-acetylglutamate synthase; SDS: L-serine dehydratase.

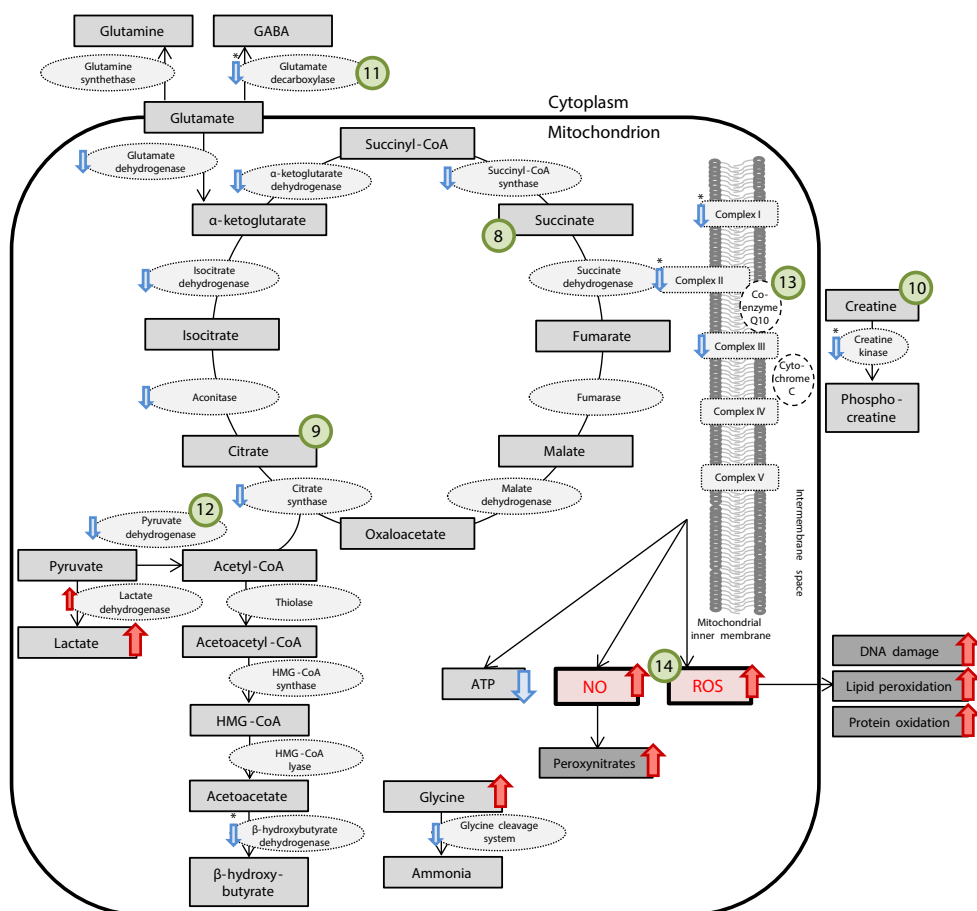
This type of isolated MMA is very rare compared to MCM deficiency and cobalamin A and B deficiency, and results in a cobalamin responsive phenotype similar to *mut*⁻ and cobalamin A deficiency.¹¹ MCE deficiency is also very rare and its natural history is very variable, with asymptomatic patients, patients presenting with acute metabolic decompensations and patients having also a sepiapterin reductase deficiency.¹² Despite the differences between the different forms of isolated MMA, many publications assemble research data on MCM, cobalamin A and cobalamin B deficiency, and discuss isolated MMA as one disease entity. Therefore, in this review we consider isolated MMA as one disease entity as well, but discuss the different types of MMA separately whenever possible.

The enzymes deficient in PA and MMA have an indispensable role in the breakdown of the branched-chain amino acids valine and isoleucine, and threonine and methionine. In addition, they act in the catabolism of propionyl-CoA that is formed in anaerobic fermentation of carbohydrates by gut bacteria and in the breakdown of odd-chain fatty acids and cholesterol side chains (Figure 1). The shares of each of these three supply routes are approximately 50%-25%-25%.^{13,14} Blockade of the conversion of propionyl-CoA into methylmalonyl-CoA and succinyl-CoA results in accumulation of the toxic metabolite propionyl-CoA. Propionyl-CoA is converted through glycine N-methylacetyltransferase into the nontoxic metabolite propionylglycine and through carnitine acetyltransferase into the – presumably – nontoxic metabolite propionylcarnitine. However, propionyl-CoA is also converted into propionic acid, hydroxypropionic acid and through citrate synthase into 2-methylcitrate, all toxic metabolites. In addition, propionyl-CoA – as competitive inhibitor of N-acetylglutamate synthase – inhibits N-acetylglutamate synthesis, resulting in a lack of stimulation of carbamoylphosphate synthase. As a consequence, detoxification of ammonia by the urea cycle is decreased, resulting in increased ammonia levels.¹⁵ In MMA patients, accumulation of methylmalonyl-CoA results in accumulation of the toxic metabolite methylmalonic acid and often in accumulation of methylmalonylcarnitine (Figure 1). The extent to which methylmalonic acid is increased in MMA patients differs between the different subtypes. Fowler et al. reported that urinary concentrations of methylmalonic acid are between 5,000 and more than 10,000 mmol/mol creatinine for *mut*⁰ and cobalamin B deficient patients, whereas *mut*⁻ and cobalamin A deficient patients have methylmalonic acid urinary concentrations between 1,000 and 9,000 mmol/mol creatinine. This range in cobalamin D deficient patients is between 500 and 10,000, and in MCE deficient patients the concentrations are between 100 and 1,000 mmol/mol creatinine,¹⁶ demonstrating important differences in severity of the metabolic defect, and thus, expected toxicity.

EFFECTS OF ACCUMULATING TOXIC METABOLITES

In PA patients the toxic metabolites propionyl-CoA, 2-methylcitric acid, ammonia, propionic acid and 3-hydroxypropionic acid accumulate. In MMA patients, also methylmalonyl-CoA and methylmalonic acid are increased. Presumed effects of these metabolites are illustrated in Figure 2.

Figure 2. Effects of toxic metabolites in PA and MMA, and associated therapy targets



Metabolites are depicted in light gray rectangles, toxic metabolites are depicted in red rectangles. Enzymes are depicted in light gray ovals. Cofactors for enzymes are depicted in white ovals. Cellular processes are depicted in dark gray rectangles. Increased concentrations of metabolites are depicted by the larger red arrows, increased enzyme activities are depicted by smaller red arrows. Decreased concentrations of metabolites are depicted by the larger blue arrows, decreased enzyme activities are depicted by the smaller blue arrows. Targets for current or experimental treatment strategies are depicted by green circles, the numbers correspond to the numbers of the therapy targets in Table 1 and throughout the text. Asterisks indicate the effects of toxic metabolites that are expected to be present in MMA patients, but not in PA patients, according to the available literature. Abbreviations: GABA: gamma-aminobutyric acid; HMG: 3-hydroxy-methylglutaryl; NO: nitric oxide; ROS: reactive oxygen species.

Propionyl-CoA

Propionyl-CoA induces secondary deficiencies of a range of mitochondrial enzymes. In rat liver mitochondria, it was demonstrated that propionyl-CoA is a competitive inhibitor of N-acetylglutamate synthetase.¹⁵ Propionyl-CoA is a substrate for this enzyme and is converted into N-propionylglutamate, which is a competitive inhibitor of carbamoylphosphate synthase.¹⁵ These inhibitions result in a secondary deficiency of the urea cycle and hyperammonemia. It has been suggested that propionyl-CoA, by inhibiting urea synthesis, also prevents the consumption of NADPH which will inhibit the glycine cleavage system. This

mechanism may explain the increase of glycine in body fluids of PA and MMA patients,^{17,18} although it has not been confirmed in other studies. Bremer demonstrated that propionyl-CoA (as well as acetyl-CoA) inhibits activity of soluble pyruvate dehydrogenase from pig heart and kidney and suggests that inhibition occurs through competition of propionyl-CoA with CoA.¹⁹ Gregersen confirmed the findings of Bremer and the suggested competition of propionyl-CoA with CoA in pig kidney tissue, but adds that inhibition of succinyl-CoA synthetase activity could also contribute to reduced oxidation of pyruvate, as suggested by Stumpe et al.^{20,21} Brock and Buckel²² demonstrated in fungi that propionyl-CoA (and not propionate) inhibits not only pyruvate dehydrogenase activity, but also citrate synthase activity and, indeed, succinyl-CoA synthetase activity. Schwab et al.²³ established that propionyl-CoA (as well as acetyl-CoA) accumulation indeed results in an inhibition of purified porcine pyruvate dehydrogenase activity. In addition, they demonstrated a propionyl-CoA induced inhibition of respiratory chain complex III and α -ketoglutarate dehydrogenase in muscle tissue of two PA patients. In summary, propionyl-CoA has a broad impact on metabolism, influencing the urea cycle, the citric acid cycle and related enzymes, the respiratory chain complex and the glycine cleavage system (Figure 2).

2-Methylcitric acid

In rat liver mitochondria, 2-methylcitric acid was demonstrated to compromise the citric acid cycle by inhibition of citrate synthase, aconitase and isocitrate dehydrogenase.²⁴ It was also shown that 2-methylcitric acid competes with citrate for the mitochondrial tricarboxylate carrier that exports citrate from mitochondria into cytosol.²⁴ In 3D organotypic rat brain cell cultures, Jafari et al.²⁵ demonstrated that exposure to 2-methylcitric acid, even in low concentrations, resulted in a significant decrease in astrocyte fiber density, an enlargement of astrocytic bodies and a swelling of proximal fibers, whereas treatment with propionic or methylmalonic acid did not show any significant changes compared to controls. In addition, it was demonstrated that 2-methylcitric acid exposure resulted in diminished axonal outgrowth, retarded neuronal differentiation or axonal degeneration, and retarded differentiation of oligodendrocytes.²⁵ Biochemically, 2-methylcitric acid led to an increase in ammonia levels and a decrease in glutamine levels in the medium of the brain cells. In a subsequent study, all effects of 2-methylcitric acid reported by Jafari et al. were confirmed.²⁶ Moreover, it was demonstrated that the earliest event was ammonium accumulation, occurring even after exposure to a single dose of 2-methylcitric acid. The authors suggest that ammonia accumulation may be the first pathogenic event that triggers further cellular and metabolic responses. This might imply that an increase of 2-methylcitric acid above a critical threshold, even for a short duration, might induce brain damage. Jafari et al.²⁵ observed an increase in the number of apoptotic cells in brain cell cultures exposed to 2-methylcitric acid, making 2-methylcitrate an important pathogenic player in PA and MMA. Cudré-Cung et al.²⁶ further demonstrated that 2-methylcitric acid led to a 40% decrease of glutamine synthetase activity, affecting ammonia detoxification in brain cells. They observed a decrease of extracellular glutamine levels, but an increase of intracellular glutamine levels, implicating that brain cells may be exposed to higher glutamine concentrations than predicted by blood glutamine levels.²⁶

Whereas Amaral et al.²⁷ could not confirm an altered glutamine synthetase activity; they demonstrated that 2-methylcitric acid inhibited glutamate dehydrogenase activity towards the formation of α -ketoglutarate in rat brain mitochondria, through competition with glutamate. This affects the availability of α -ketoglutarate for proper functioning of the

citric acid cycle. In addition, Amaral et al.²⁷ demonstrated that 2-methylcitric acid induced mitochondrial permeability transition pore opening, that ultimately led to mitochondrial energy dysfunction, as illustrated by decreased ATP synthesis.

In summary, 2-methylcitric acid leads to hyperammonemia and the risk for brain cell apoptosis and it decreases both enzymatic activities and substrate availability of the citric acid cycle, thereby leading to mitochondrial energy impairment.

Ammonia

The toxic effects of ammonia accumulation in brain were reviewed by Braissant et al.²⁸ An important effect of ammonia accumulation in patients with urea cycle disorders, is glutamine increase through activation of glutamine synthetase, which is expected to be the cause of the observed astrocyte swelling. In contrast to patients with urea cycle defects, PA and MMA patients have normal or even decreased concentrations of glutamine in plasma during acute metabolic decompensation.^{29,30}

Ammonia accumulation also activates the $\text{Na}^+\text{-K}^+\text{-Cl}^-$ cotransporter, increasing water entry into astrocytes. This might explain the observed astrocyte swelling in normoglutaminergic hyperammonemia. In astrocyte cultures exposed to ammonia, synthesis of nitric oxide is stimulated. These cultures show opening of the mitochondrial permeability transition pore, which leads to altered oxidative phosphorylation, diminished ATP synthesis, production of reactive oxygen species (ROS) and cell death. It is expected that these effects are the result of the interaction between nitric oxide and superoxide anions, leading to the formation of highly toxic peroxynitrites. This might also contribute to altered permeability of the blood-brain barrier, thereby contributing to vasogenic edema,²⁸ which is often observed in patients with hyperammonemia.

Propionic acid

Propionic acid is considered a toxic metabolite since in the brain of rats exposed to concentrations of propionic acid that simulate concentrations in PA patients, a 30% inhibition of $\text{Na}^+/\text{K}^+\text{-ATPase}$ was demonstrated,³¹ as well as an increase of lipid and protein peroxidation and a decrease of antioxidant potential,^{32,33} a reduction of ganglioside species,³⁴ increased phosphorylation of cytoskeletal proteins possibly via *N*-methyl-D-aspartate (NMDA) receptor activation,³⁵ an induction of long-term behavioral and cognitive deficits^{33,36} and an induction of convulsions possibly via NMDA receptor activation.³⁷ In peripheral leukocytes incubated with propionic acid, it was demonstrated that propionic acid induces DNA damage, possibly via formation of free radicals.³⁸

3-Hydroxypropionic acid

Little is known on the toxic effects of 3-hydroxypropionic acid. There is one report, demonstrating that 3-hydroxypropionic causes increases of CoA esters and thereby overloading of the citric acid cycle and inducing proteolysis.³⁹

Methylmalonyl-CoA

In MMA patients, methylmalonyl-CoA is increased. Methylmalonyl-CoA is reported to be a mild inhibitor of N-acetylglutamate synthetase¹⁵ and an inhibitor of carbamoylphosphate synthase,⁴⁰ thereby inhibiting the urea cycle. In addition, methylmalonyl-CoA has been demonstrated to inhibit pyruvate dehydrogenase activity in rat hepatocytes.⁴⁰

Methylmalonic acid

In MMA patients, also the toxic metabolite methylmalonic acid is increased. In brains and livers of rats exposed to concentrations of methylmalonic acid similar to those in MMA patients, a decreased activity of β -hydroxybutyrate dehydrogenase was observed,⁴¹ as well as a decreased activity of Na^+/K^+ -ATPase,⁴² mitochondrial creatine kinase,⁴³ the respiratory chain complexes I-III,³⁶ a decreased transport of succinate through membranes⁴⁴ and a decreased activity of glutamate decarboxylase which negatively correlated with the duration of methylmalonic acid-induced seizures, that possibly occurred through the activation of NMDA receptor activation.⁴⁵ Melo et al.⁴⁶ confirmed the finding of a methylmalonic acid-induced decreased activity of glutamate decarboxylase in rat brain mitochondria, but this inhibition was only minor, whereas α -ketoglutarate dehydrogenase was more profoundly inhibited by methylmalonic acid. Moreover, the exchange of methylmalonic acid for α -ketoglutarate seems to deplete mitochondria from α -ketoglutarate, but this could not be confirmed *in vivo*.⁴⁶ In addition, a methylmalonic acid-induced increase of lipid and protein peroxidation and decrease of superoxide dismutase activity was observed in rat brain⁴⁷ and kidney tissue, which was further amplified by the induction of renal failure.⁴⁸

Simultaneous and synergistic toxicity

The various effects of the toxic metabolites occur simultaneously and are synergistic. Altogether, based on the best available evidence from studies performed on the consequences of accumulation of the toxic metabolites in PA and MMA, one could expect in PA and MMA patient tissues decreased activities of N-acetylglutamate synthetase, carbamoylphosphate synthase, pyruvate dehydrogenase, citrate synthase, aconitase, isocitrate dehydrogenase, α -ketoglutarate dehydrogenase, succinyl-CoA synthetase, respiratory chain complex III, glutamate dehydrogenase and the glycine cleavage system and an increased activity of lactate dehydrogenase. In addition, one could expect in PA patient tissues a decrease in glucose concentrations and an increase in lactate and ammonia concentrations, as well as the formation of NO, ROS, peroxynitrites, and peroxidized lipids and proteins, the induction of DNA damage, reduced anti-oxidant potential and diminished ATP synthesis (Figure 2). In MMA patients, but not in PA patients, one could additionally expect decreased activities of β -hydroxybutyrate dehydrogenase, creatine kinase, glutamate decarboxylase and respiratory chain complex I and II (Figure 2, marked with an asterisk).

The presented evidence, despite being the best available, should be interpreted with caution, since nearly all studies were performed *in vitro*, mostly on mammalian – but not human – cells. It is not clear to what extent the conditions in the experiments are similar to physiological conditions in PA and MMA patients, and whether the concentrations of toxic metabolites that animals or cell lines were exposed to reflect their *in vivo* concentrations. Furthermore, exposure of cells to metabolites, requiring uptake and accumulation to reflect the disease state fundamentally differs from the true disease situation in which cells endogenously accumulate these metabolites. Moreover, especially in the studies covering the toxic effects of propionic acid and methylmalonic acid, the concentrations of the other potentially toxic metabolites were not measured. Therefore, it is not clear whether the observed effects are the direct result of propionic or methylmalonic acid, or indirect and resulting from secondary metabolites like propionyl-CoA, methylcitric acid or any other toxic metabolite. Thus, it cannot be concluded that the toxic effects attributed to methylmalonic acid, that might be specific for MMA patients, are not present in PA patients.

While these limitations are critical for the interpretation of the presented data, it can still be

concluded that the combined results of all changes induced by toxic metabolites formed in PA and MMA, are mitochondrial energetic failure and increase of ROS formation leading to oxidative stress.

OTHER THERAPY TARGETS AND TREATMENT STRATEGIES

Each step in the biochemical cascade, as illustrated in Figures 1 and 2, ultimately contributing to mitochondrial energetic failure and oxidative stress, is a potential target for treatment. We discern two main treatment strategies. The first strategy is aimed to reduce the amount of accumulating toxic metabolites. This aim can be attained by decreasing supply, improving enzyme activity or increasing disposal. Therapeutic targets for this treatment strategy are displayed in Figure 1 and listed in Table 1. The second treatment strategy is aimed to prevent or treat mitochondrial energetic failure and to prevent or treat the increase of ROS formation. Therapy targets for this treatment strategy are displayed in Figure 2 and also listed in Table 1. We will discuss the current, experimental and unexplored treatment strategies in PA and MMA (Table 1).

Treatment strategy 1: reduce the amount of toxic metabolites

Current treatment strategies

To lessen the most important supply of toxic metabolites, patients follow a life-long protein restricted diet, with limited amounts of isoleucine, valine, threonine, and methionine¹ (Figure 1 and Table 1, therapy target number 1 (TT#1)). In addition, to reverse catabolism, a high caloric diet is provided, in acute situations often with i.v. glucose.⁵¹ To tackle the second source of toxic metabolites, antibiotics (particularly metronidazole) are prescribed to diminish propionyl-CoA from gut bacteria through selective bowel decontamination.^{14,52} Laxatives, stimulating the intestinal flow in constipated patients, also aim to reduce propionyl-CoA from gut bacteria⁵³ (TT#2).

To stimulate residual enzyme activity, hydroxycobalamin is prescribed to cobalamin responsive MMA patients: *mut*–, cobalamin A and cobalamin D deficient patients² (TT#4). In very severely affected patients, solid organ transplantation is considered (liver transplantation in PA and MMA, or liver-kidney transplantation in MMA), since normal activity of the enzyme in the donor organ can (partly) compensate for the patient's enzyme deficiency^{54,55} (TT#3). Kidney transplantation is also performed, solely in MMA patients, in order to treat chronic kidney disease. The primary intent is not to provide additional enzymatic activity, although it might serve as such.¹⁰⁶

To increase disposal of toxic metabolites, L-carnitine is prescribed, which stimulates conversion of propionyl-CoA into the nontoxic propionylcarnitine, and in limited amounts in MMA patients into methylmalonylcarnitine⁴ (TT#7). Supplementation of L-carnitine restores intracellular carnitine levels and thereby it restores the impaired fatty acid oxidation due to the relative carnitine deficiency.¹⁰⁷ During acute or chronic metabolic decompensations, when ammonia accumulates, N-carbamylglutamate is prescribed to stimulate carbamoylphosphate synthase thereby optimizing detoxification of ammonia by the urea cycle^{80,81} (TT#5). Additionally, the ammonia scavenger sodium benzoate is used, which acts by promoting conjugation with glycine to form hippuric acid⁸² (TT#6). Another possibility to reduce ammonia levels in acute phases is extracorporeal detoxification, in infants via continuous venous-venous hemodiafiltration and in adults either via continuous venous-venous hemodiafiltration or via hemodialysis.¹⁰⁸

Table 1. Therapy targets and current, experimental and unexplored treatment strategies in PA and MMA

Treatment strategy	Substrategy	Therapy target	Treatment	Current status	Referen.	
Reduce amount of toxic metabolites	Reduce supply	Fig. 1 #1	Isoleucine, valine, threonine and methionine restriction (with or without amino acid supplementation)	In clinical guideline	1,49,50	
		Fig. 1 #1	High caloric diet during illness	In clinical guideline	49,51	
		Fig. 1 #2	Antibiotics	In clinical guideline	14,49,52	
	Increase enzyme activity	Fig. 1 #2	Laxatives	In clinical guideline	49,53	
		Fig. 1 #4	Reduce odd-chain fatty acids and cholesterol	Unexplored	2,49	
	Prevent or treat mitochondrial energetic failure and increase of ROS formation	Increase disposal	Fig. 1 #3	Hydroxycobalamin	In clinical guideline for cobalamin-responsive MMA patients	49,54,55
			Fig. 1 #3	Solid organ transplantation (liver or combined liver-kidney transplantation)	In clinical guideline; advice to consider in severely affected patients	56-70
			Fig. 1 #3	Gene therapy	Experimental in animal models	71-73
			Fig. 1 #3	Promotion of premature stop codon read-through	Experimental in cell lines	74
			Fig. 1 #3	Messenger RNA therapy	Experimental in animal models	75
Fig. 1 #3			Pharmacological stabilization of enzyme activity	Experimental in cell lines	76-78	
Fig. 1 #3			Enzyme replacement therapy	Experimental in animal models	79	
Fig. 1 #3			Hepatocyte transplantation	Experimental in animal models	49,80,81	
Energetic supply		Fig. 1 #5	N-carbamylglutamate	In clinical guideline	49,82	
		Fig. 1 #6	Sodium benzoate	In clinical guideline	49,51	
Cofactor supplementation	Fig. 1 #6	Extracorporeal detoxification	In clinical guideline	4,49		
	Fig. 1 #7	L-Carnitine	In clinical guideline	49		
	Fig. 1 #8	Sodium bicarbonate	Unexplored			
	Anti-oxidants	Induce N-acetyltransferase activity	Unexplored			
		Scavenger for methylmalonic acid, propionic acid, 3-hydroxypropionic acid or 2-methylcitric acid	Unexplored			
	Electron transfer med. NMDA-receptor antagonists	Energetic supply	Fig. 2 #8	Succinate	Experimental in animal models	83,84
			Fig. 2 #9	Citric acid	Experimental in patients	85
		Cofactor supplementation	Fig. 2 #10	Creatine	Experimental in animal models	83,84
			Fig. 2 #11	Fumarate, malate, alpha-ketoglutarate, glutamate	Unexplored	
		Anti-oxidants	Fig. 2 #11	Pyridoxine (vitamin B6)	Experimental in animal models	45
Fig. 2 #12			Thiamine (vitamin B1)	Experimental in patients with lactic acidosis	86,87	
Electron transfer med. NMDA-receptor antagonists		Fig. 2 #13	Coenzyme Q10	Experimental in patients	88-90	
		Fig. 2 #14	Ascorbic acid (vitamin C)	Experimental in animal models and in patients with lactic acidosis	33,91-94	
Electron transfer med. NMDA-receptor antagonists		Fig. 2 #14	Alpha-tocopherol (vitamin E)	Experimental in animal models and in patients with lactic acidosis	47,91,92,95-97	
		Fig. 2 #14	CB agonist WIN, S-allylcysteine, glutathione, GM1 ganglioside, melatonin, mitoQ, resveratrol, tiron, trolox. Uric acid, lipoic acid, retinol (vitamin A), β -carotene	Experimental in animal models and in patients with optic atrophy	42,47,98-102	
Electron transfer med. NMDA-receptor antagonists	Electron transfer med. NMDA-receptor antagonists	Fig. 2 #14	Methylene blue	Unexplored	103	
		Fig. 2 #14	Celecoxib, fish oil, kynurenic acid, MK-801	Experimental in animal models	37,45,77,83,84, 98,99,104,105	

[Table 1 continued] Abbreviations: Fig: figure; NMDA, N-methyl-D-aspartate; ROS, reactive oxygen species.

Sodium bicarbonate (TT #8) is used to reduce the acidic load of all the formed organic acids. In addition, it might induce forced diuresis and alkalinization of urine, aiding renal clearance of methylmalonic acid in MMA patients.⁴⁹

Each of these treatment strategies are applied in PA and MMA patients, are discussed in the most recent and most comprehensive guideline⁴⁹ and are considered to be best practice (Table 1). However, none of these treatment strategies have been tested in randomized clinical trials since it is unethical to test an intervention that is considered beneficial (and thereby withholding the intervention from some patients) and since conducting a randomized clinical trial in rare inborn errors of metabolism is very challenging¹⁰⁹. Hence, clinical evidence supporting the currently implemented treatment strategies is limited. We will give three examples of treatment strategies that have raised controversy and that could individually be emphasized in a full review. First, since the identification of PA and MMA as inborn errors of metabolism,¹ there has been controversy about the added value of amino acid-based formulas in the dietary treatment of PA and MMA patients.^{9,10,110-113} This debate is based on the relatively high amount of leucine in these formulas that might induce deficiencies of isoleucine and valine.^{1,9,10,114} Still, in many metabolic clinics the use of amino acid-based formulas is common practice.⁴⁹ Second, solid organ transplantation (liver or combined liver-kidney transplantation) is performed in metabolically unstable patients to provide additional enzymatic activity. The most recently reported outcomes are promising,¹¹⁵ but it remains questionable who to transplant, and when.¹¹⁶ In addition, since transplantation is not the only available treatment option, nor a curative treatment, the utility of performing solid organ transplantations in PA and MMA is questioned because of the scarcity of available donor organs.¹¹⁷ Decision-making for individual patients would benefit from a world-wide registry, enabling larger cohort studies into long-term benefits, risks, success rates and complications. Third, there is controversy about the use of N-carbamylglutamate in acute and chronic hyperammonemia. While acute amelioration of hyperammonemia due to N-carbamylglutamate is unequivocal,¹¹⁸ and no serious side effects due to N-carbamylglutamate are noted,¹¹⁹ other toxic metabolites do not decrease concurrently with ammonia.¹²⁰ Since ammonia is the main biochemical parameter indicating acute metabolic decompensation, there is a risk of not recognizing and hence not managing (impending) acute metabolic decompensations adequately. It is surprising that N-carbamylglutamate is already recommended for treatment of acute management of hyperammonemia,⁴⁹ while there is no data available on the long-term neurological outcomes of these patients. Efforts to obtain this data have unfortunately failed¹⁰⁹, but the added value of N-carbamylglutamate in acute and chronic hyperammonemia on long-term neurological outcomes can only be substantiated by cohort studies investigating these outcomes.

Experimental treatment strategies

Experimental strategies aiming to reduce the amount of accumulating toxic metabolites mainly focus on improving enzyme activity, either by gene therapy, supplementation of mRNA encoding the defective enzyme, enzyme replacement therapy or hepatocyte transplantation (TT#3).

In 1992, gene transfer using a retroviral vector resulted in correction of the metabolic defect in fibroblasts of patients with MMA.⁵⁶ Next, short-term overexpression of MCM was demonstrated after intravenous administration of plasmids expressing recombinant *Mut*

using asialoglycoprotein/polylysine/DNA targeted delivery to the livers of healthy mice.⁵⁷ Chandler et al.⁵⁸ demonstrated in both fetal murine fibroblasts and hepatocytes of two MMA patients that *Mut* gene delivery using a recombinant adenoviral vector was feasible, and resulted in correction of the enzymatic defect, suggesting that hepatocyte-directed gene delivery may be an effective treatment strategy. Subsequent studies in a *Mut*^{-/-} mouse model demonstrated that gene therapy is a promising treatment option for MMA. Whereas intramuscular injection of adenovirus carrying the *Mut* gene was not effective, intrahepatic injection resulted in rescue of neonatal lethality.⁵⁹ Intrahepatic injection with recombinant adenoassociated virus (rAAV) serotype 8 resulted in improved survival of the mice beyond one year, although there was still a gradual loss of transgene expression.⁶⁰ Carillo-Carrasco et al.⁶¹ demonstrated that the gene delivery in mice resulted in long-term phenotypic correction, but, in line with solid organ transplantation, it did not provide curative treatment. Senac et al.⁶² tested rAAV serotype 9, as this serotype might be superior in tropism for both liver and kidney tissues, and demonstrated that gene delivery by this serotype also resulted in improved survival, using a 10-fold lower dose than used with rAAV serotype 8 vectors. In order to work towards clinical testing, efficacy and dosing of the rAAV serotype 8 vector were tested. In addition, the finding that AAV antibody titers are low in 21/24 MMA patients is encouraging and supports further development of systemic gene delivery as treatment for severely affected MMA patients.⁶⁴ However, concerns have been raised about the safety of using rAAV vectors, since a dose-dependent increase in hepatocellular carcinoma is seen in *Mut*^{-/-} mice treated with intrahepatic injection of rAAV vectors.⁶⁷

Wong et al.⁶⁵ demonstrated that intravenous injection of a lentiviral vector in *Mut*^{-/-} mice could also result in effective *Mut* gene transfer, as significant but incomplete biochemical correction of the phenotype was observed.

Gene therapy for PA was studied in a *Pcca*^{-/-} mouse model. Both adenoviral and AAV serotype 8 vectors⁶⁶ carrying *Pcca* were tested, and were administered via intraperitoneal injection. It resulted in an increased lifespan from 36 hours to 70 hours, indicating only a transient effect.⁶⁶ A subsequent study using AAV serotype 8 vector delivered via intrahepatic injection resulted in a rescue of neonatal lethality in 64% of the mice and amelioration of the biochemical phenotype.⁶⁷ These findings were confirmed by Guenzel et al.,⁶⁸ who generated a *Pcca*^{-/-} mouse model that was partially rescued using a transgene, resulting in 2% residual enzymatic activity. These mice survived into adulthood and demonstrated the PA phenotype. It was demonstrated that adenovirus serotype 5 resulted only in a transient effect, whereas systemic administration of AAV serotype 8 resulted in more persistent correction of the biochemical phenotype.⁶⁸ Next, the effectiveness of systemic therapy with AAV serotype 1 (muscle tropism), serotype 8 (liver tropism) and serotype rh10 (broad tropism) was studied and revealed that AAV serotype 8 in combination with a transthyretin promotor resulted in the most promising correction of the biochemical phenotype.⁶⁹ The authors assume that gene therapy concurrently directed to hepatocytes and muscle cells would result in even better correction, as all tissues require PCC activity. They suggest that treatment of a wide array of tissues would represent the best option for PA disease correction.⁶⁹ In a subsequent study, it was demonstrated that AAV-mediated expression of *Pcca* resulted in long-term phenotypic correction, although transgene expression decreased in the liver and in skeletal muscle. Surprisingly, tissue-specific loss of expression was only present in females.⁷⁰

Next to gene therapy, there are more efforts to increase enzyme activity of PA and MMA patients. For patients harboring nonsense mutations, some drugs may promote premature termination codon read-through. For MMA patients, two studies were reported that

achieved a slight increase in MCM activity *in vitro*.^{71,79} For PA patients, restoration of *in vitro* PCC activity to a level of 10%-15% was demonstrated.⁷³ Though, protein function can only be restored in a fraction of patient cells with nonsense mutations, there is no information regarding the *in vivo* effectiveness and the clinical relevance of the attained effects is unclear. An et al.⁷⁴ demonstrate that for MMA, intravenous administration of mRNA encoding *Mut* using a biodegradable lipid nanoparticle, results in a 75% reduction of plasma methylmalonic acid and increased MCM activity in the liver of *Mut*^{-/-} mice, and that repeated dosing led to weight gain and improved survival. To the best of our knowledge, no mRNA treatment for PA has been reported.

Jorge-Finnigan et al.⁷⁵ reported that some pharmacological chaperones may stabilize the enzyme adenosyltransferase (encoded by *MMAB*) in patients with missense mutations in *MMAB* that destabilize the enzyme. They demonstrate that co-administration of some pharmacological chaperones and cobalamin resulted in increased adenosyltransferase stability in both *MMAB* patient fibroblasts and wild-type mice.⁷⁵

Enzyme replacement therapies have been studied in both MMA and PA. For PA, in both *PCCA*-defective and *PCCB*-defective lymphoblasts it was demonstrated that PCC subunits could effectively be delivered to the mitochondria, using cell penetrating peptides and mitochondria targeting sequences, resulting in an apparent improvement of PCC activity.⁷⁷ A single intraperitoneal injection of PCC in a PCC defective mouse model, directed towards mitochondria, resulted in a substantial improvement of the biochemical phenotype.⁷⁸ Similarly, for MMA, in both patient fibroblasts and in CRISPR/Cas9-engineered HepG2 *Mut*^{-/-} liver cells it was demonstrated that MCM could be effectively delivered to the mitochondria, enhancing cell viability, reducing methylmalonic acid levels, and enhancing albumin and urea secretion in the liver cells.⁷⁶

As an alternative for solid organ transplantation, to bypass the donor organ shortage, hepatocyte transplantation has been performed in – amongst others – urea cycle disorders in order to postpone liver transplantation.¹²¹⁻¹²⁴ For MMA, transplantation of fetal liver cells in a *Mut*^{-/-} mouse model attained donor cell engraftment in the liver, bone marrow and spleen, resulting in some correction of the biochemical phenotype. To realize greater disease correction, higher levels of engraftment are required.⁷⁹ Limitations of hepatocyte transplantation however still comprise limited supply of (good quality) donor livers, insufficient engraftment of hepatocytes and allogeneic rejection¹²⁵ Moreover, in line with solid organ transplantation, hepatocyte transplantation would most likely still not be a curative treatment.

Aiming to prevent any residual disease requiring other treatment strategies,⁵ presumably the biggest challenge is to design a drug that is delivered to the mitochondria of all tissues that require enzymatic activity (including the brain) without inducing any off-target effects. While some studies might be ongoing, to the best of our knowledge, no studies have yet reported results of a clinical trial with gene therapy, mRNA supplementation or enzyme replacement therapy in PA or MMA patients, nor are there any case reports of hepatocyte transplantation in PA or MMA. Despite the fact that we assume that these reports will be published in the coming years and that the results will be positive, it will still take some time before these treatment strategies can be incorporated in standard clinical care for PA and MMA patients.

Unexplored options

In Figure 1 we demonstrate that several therapeutic targets have remained unexplored.

For example, to decrease the third supply route that comprises approximately 25% of the total load of propionyl-CoA,^{13,14} odd-chain fatty acid and/or cholesterol restriction can be explored. To increase disposal of toxic metabolites, we could try to identify compounds that induce glycine N-acetyltransferase activity. In addition, we could search for nontoxic scavengers of 2-methylcitric acid, methylmalonic acid, propionic acid and possibly 3-hydroxypropionic acid. For therapeutic targets that already have been explored, there might be additional treatment options. For example, due to side effects of varying severity, treatment with metronidazole is sometimes (temporarily) discontinued in PA and MMA patients. Investigation of antibiotics with less severe side effects that effectively reduce the production of propionyl-CoA derived from anaerobic bacterial fermentation, could serve more continuous reduction of the propionyl-CoA load originating from the gut.

Treatment strategy 2: prevent or treat mitochondrial energetic failure and increase of ROS formation

Current treatment strategies

There are no current treatment strategies specifically aiming to prevent or treat energetic failure and increase of ROS formation described in the guideline for PA and MMA patients⁴⁹ (Table 1).

Experimental treatment strategies

Several experimental treatment strategies aim to prevent or treat mitochondrial failure. This aim can be attained by supplementation of anaplerotic substances, supplementation of cofactors for enzymes with decreased activities, supplementation of anti-oxidants and supplementation of electron transfer mediators. Regarding anaplerotic substances, citric acid (Figure 2, Table 1, TT#9) has been used in a clinical trial with PA and MMA patients,⁸⁵ resulting in increased citric acid intermediates and possibly also in a reduced number of hospitalizations. In addition, succinate (TT#8) has been tested for neuroprotection in methylmalonic acid-induced cognitive problems⁸⁴ and seizures⁸³ in rats, resulting in complete reduction of the induced phenotype. The energetic substrate creatine (TT #10) attained similar effects as succinate, possibly due to restoring intra-mitochondrial high energy phosphate levels.⁸⁴

Efficiency of cofactor supplementation for enzymes with decreased activities has also been explored. Pyridoxine (vitamin B6) was used in rats with methylmalonic acid-induced seizures,⁴⁵ resulting in complete reduction of the phenotype by preventing methylmalonic acid-induced inhibition of glutamic acid decarboxylase (TT#11). Thiamine (vitamin B1) is used in patients with lactic acidosis due to a (relative) thiamine deficiency,^{86,87} resulting in reduced lactate levels by increasing pyruvate dehydrogenase activity (TT#12).

In addition, the effects of many anti-oxidants are explored (TT#14). Ascorbic acid (vitamin C) was used in methylmalonic acid-induced glutathione reduction in rats with no effect.⁹¹ However, in methylmalonic acid-induced seizures,⁹² in cognitive problems induced by propionic acid and methylmalonic acid^{33,93} and in a patient suffering from lactic acidosis due to glutathione deficiency,⁹⁴ ascorbic acid did partially alleviate the phenotype. α -Tocopherol (Vitamin E) was also used in methylmalonic acid-induced glutathione reduction in rats, but also with no effect.⁹¹ It has been explored in methylmalonic acid-induced seizures^{92,95} and in methylmalonic acid-induced ROS formation and lipid peroxidation,⁴⁷ resulting in reduction of the induced phenotype. α -Tocopherol in combination with coenzyme Q10 is used in patients with optic atrophy aiming to improve their sight with varying effects.^{96,97}

Coenzyme Q10 has been reported to reverse cardiomyopathy in one PA patient.⁸⁸ It has also been used – with varying effects – in MMA patients with optic atrophy^{89,90} and in *Mut*^{-/-} mice with renal failure¹²⁶ (TT#13). Other explored anti-oxidants are CB agonist WIN and S-allylcysteine,⁹⁸ glutathione,⁴² GM1 ganglioside,¹⁰⁰ melatonin,⁴⁷ mitoQ and resveratrol,^{101,102} tiron and trolox,¹⁰¹ in most cases resulting in a partial or complete reduction of the induced phenotype (TT#15). Methylene blue, an electron transfer mediator, is successfully used in methylmalonic acid-induced seizures.¹⁰³

The use of NMDA-receptor antagonists is explored specifically for the brain. Celecoxib is a known COX-2 inhibitor which acts as an indirect NMDA-receptor antagonist by preventing prostaglandin E2 production, a metabolite that induces decreased Na⁺/K⁺-ATPase activity. It has been successfully used in methylmalonic acid-induced seizures.¹⁰⁴ Fish oil has also been investigated for neuroprotection in methylmalonic acid-induced seizures, in rats.¹⁰⁵ Its positive effects are attributed to the interference with the convulsive activity of prostaglandin E2. Kynurenic acid, a direct NMDA-receptor antagonist is investigated for neuroprotection in propionic and methylmalonic acid-induced, and NMDA-receptor agonist co-induced ROS formation, lipid peroxidation and mitochondrial failure, leading to a partial reduction.⁹⁹ MK-801, also a direct NMDA-receptor antagonist successfully reversed methylmalonic acid and propionic acid-induced seizures^{37,45,83} and methylmalonic acid and propionic acid-induced ROS formation,^{47,99} but it had no effect on methylmalonic acid-induced cognitive problems.⁸⁴ The fact that on one hand both anaplerotic substrates and cofactors result in reduction of methylmalonic acid and propionic acid-induced phenotypes, and on the other hand anti-oxidants attain the same effects, underlines an important aspect of PA and MMA pathophysiology: toxic metabolites induce both mitochondrial energetic failure and an increase of mitochondrial ROS formation, leading to lipid peroxidation and oxidative stress.

Unexplored options

In terms of treatment strategies, the three most important approaches are currently being explored: supplementation of anaplerotic substrates, supplementation of cofactors and supplementation of anti-oxidants. While the most important cofactors are already tested, the effects of some anaplerotic substances and anti-oxidant candidates are yet to be explored, such as fumarate, malate or α -ketoglutarate as anaplerotic substances and lipoic acid, retinol (vitamin A), β -carotene or uric acid (only when glomerular filtration rate is normal, Haijes et al.⁵), as anti-oxidants. However, it is not to be expected that these substances will achieve much better effects than the ones already investigated.

A final unexplored option is glutamate supplementation, which could provide α -ketoglutarate as anaplerotic substance for the citric acid cycle. Glutamine, but not glutamate, is found to be decreased in plasma of PA and MMA patients which has been attributed to shortage of α -ketoglutarate.^{29,30} Glutamine supplementation is controversial in critically ill patients, given the associated high rate of adverse outcomes that raised the hypothesis that low glutamine levels are an adaptive response.¹²⁷ Therefore, glutamate supplementation, which was for example demonstrated to improve postischaemic heart function in rats,¹²⁸ might be a better option to consider.

CONCLUSION

In this review we provide a systematic overview on current, experimental and unexplored treatment strategies in PA and MMA in order to provide insight in what we have to offer PA and MMA patients, now and in the future. We discerned two main treatment strategies:

treat the cause, by reducing the amount of toxic metabolites, and treat the effects, by preventing or treating mitochondrial energetic failure and increase of ROS formation. It is encouraging that within these two treatment strategies, many therapy targets have already been identified (Figure 1, Figure 2), and many of these have been or are being explored, in various ways and to a greater or lesser extent. Unfortunately, available evidence on the effectiveness of treatment strategies is often scarce, since none of them were tested in randomized clinical trials. This raises concerns, since the consensus on best practice treatment for PA and MMA, which includes a protein restricted diet with or without amino acid supplementation, a high caloric diet during illness, an antibiotic regimen, laxatives in case of constipation, hydroxycobalamin in case of cobalamin responsive MMA and possibly solid organ transplantation for severely affected patients, is not without controversy. In addition, treatment strategies that aim to prevent or treat mitochondrial failure and increase of ROS formation, demonstrate promising, but varying and limited effects.

To attain a curative treatment for PA and MMA patients, gene therapy, messenger RNA therapy and enzyme replacement therapy are most promising. If the accumulation of toxic metabolites is permanently reduced, the mitochondrial function should theoretically remain undisturbed. This allows for a less strict therapeutic regime and not only prevents mitochondrial-associated complications, but also complications that are due to protein restriction or the accumulation of acidic compounds. However, it is still a long way to go from bench to bedside. It is challenging to design a drug that is delivered to the mitochondria of all tissues that require enzymatic activity, including the brain, without inducing any off-target effects. Moreover, the therapeutic window of opportunity and the target tissue(s) are, to date, still not sufficiently understood.⁵

In summary, to further improve survival rate and, equally important, quality of life of PA and MMA patients, there is a need for systematic (re-)evaluation of each and everyone of the accepted and potential treatment strategies, ideally in (large) randomized clinical trials¹⁰⁹ but if that is not feasible, in smaller trials⁸⁵ or on an individual patient basis,^{1,3} so that we can better determine *who* will benefit *when* and *how* from *which* treatment strategy.

REFERENCES

- Childs B, Nyhan WL, Borden M, Bard L, Cooke RE. Idiopathic hyperglycinemia and hyperglycinuria: a new disorder of amino acid metabolism I. *Pediatrics*. 1961;27:522-538.
- Matsui SM, Mahoney MJ, Rosenberg LE. The natural history of the inherited methylmalonic acidemias. *N Engl J Med*. 1983;308: 857-861.
- Nyhan WL, Borden M, Childs B. Idiopathic hyperglycinemia: a new disorder of amino acid metabolism. II. The concentrations of other amino acids in the plasma and their modification by the administration of leucine. *Pediatrics*. 1961;27:539-550.
- Roe CR, Millington DS, Maltby DA, Bohan TP, Hoppel CL. LCarnitine enhances excretion of propionyl coenzyme a as propionylcarnitine in propionic acidemia. *J Clin Invest*. 1984;73: 1785-1788.
- Haijes HA, Jans JJM, Tas SY, Verhoeven-Duif NM, van Hasselt PM. Pathophysiology of propionic and methylmalonic acidemias. Part 1: Complications. *J Inherit Metab Dis*. 2019;42(5):745-761.
- Takahashi-Iñiguez T, González-Noriega A, Michalak C, Flores ME. Human MMAA induces the release of inactive cofactor and restores methylmalonyl-CoA mutase activity through their complex formation. *Biochimie*. 2017;142:191-196.
- Froese DS, Kopec J, Fitzpatrick F et al. Structural insights into the MMACHC-MMADHC protein complex involved in vitamin B12 trafficking. *J Biol Chem*. 2015;290(49):167-177.
- Hörster F, Baumgartner MR, Viardot C et al. Long-term outcome in methylmalonic acidurias is influenced by the underlying defect (mut0, mut-, cIbA, cIbB). *Pediatr Res*. 2007;62:225-230.
- Manoli I, Myles JG, Sloan JL, Shchelochkov OA, Venditti CP. A critical reappraisal of dietary practices in methylmalonic acidemia raises concerns about the safety of medical foods. Part 1: isolated methylmalonic acidemias. *Genet Med*. 2016;18(4):386-395.

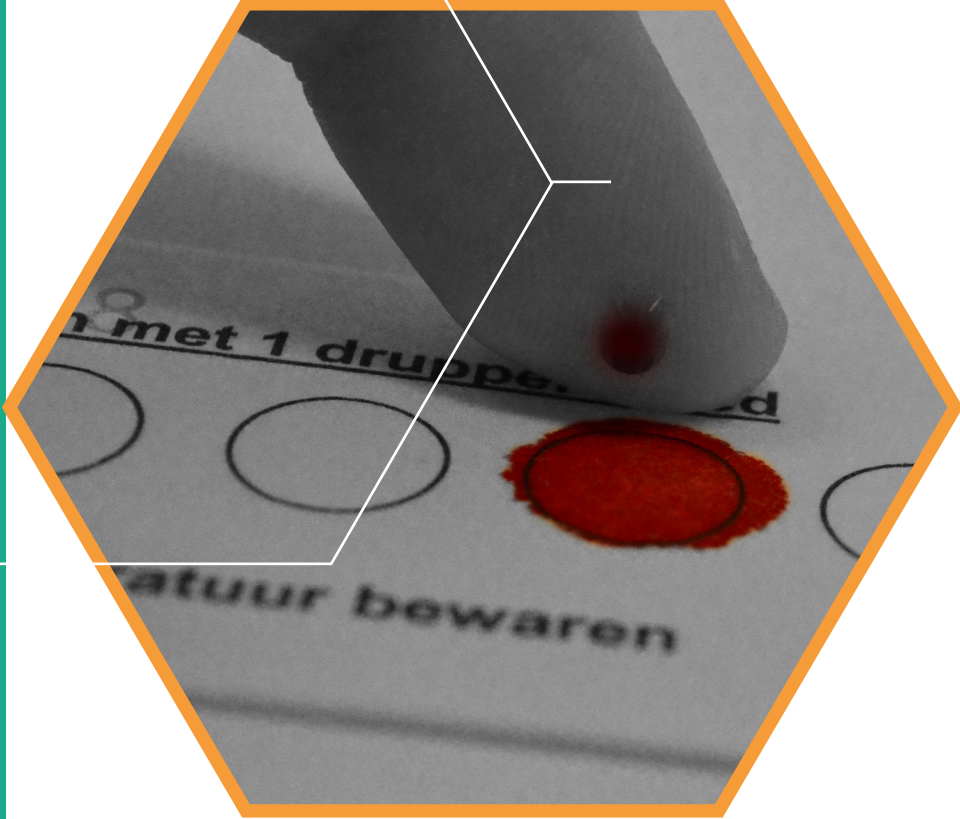
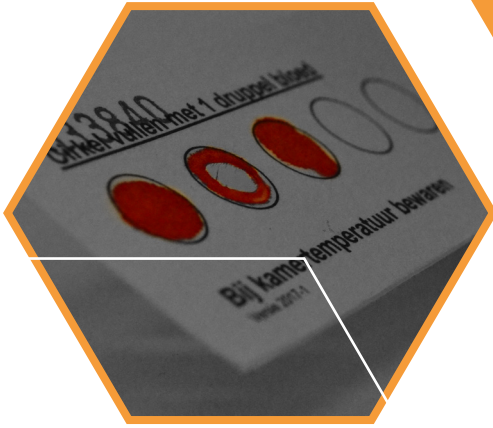
10. Manoli I, Sloan JL, Venditti CP. Isolated methylmalonic acidemia. In: Adam MP, Ardinger HH, Pagon RA et al., eds. GeneReviews®. Seattle, WA: University of Washington, Seattle; 1993-2019. Updated: 2016, December 1.
11. Parini R, Furlan F, Brambilla A et al. Severe neonatal metabolic decompensation in methylmalonic acidemia caused by CblD defect. *JIMD Rep.* 2013;11:133-137.
12. Abily-Donval L, Torre S, Samson A et al. Methylmalonyl-CoA epimerase deficiency mimicking propionic aciduria. *Int J Mol Sci.* 2017;18(11):2294.
13. Leonard JV. Stable isotope studies in propionic and methylmalonic acidemia. *Eur J Pediatr.* 1997;156(1):67-69.
14. Thompson GN, Walter JH, Bresson KL et al. Sources of propionate in inborn errors of propionate metabolism. *Metabolism.* 1990;39:1133-1137.
15. Coude FX, Sweetman L, Nyhan WL. Inhibition by propionylcoenzyme A of N-acetylglutamate synthetase in rat liver mitochondria. A possible explanation for hyperammonemia in propionic and methylmalonic acidemia. *J Clin Invest.* 1979;64:1544-1551.
16. Fowler B, Leonard JV, Baumgartner MR. Causes of and diagnostic approach to methylmalonic acidurias. *J Inherit Metab Dis.* 2008;31:350-360.
17. Hayasaka K, Tada K. Effects of the metabolites of the branched-chain amino acids and cysteamine on the glycine cleavage system. *Biochem Int.* 1983;6:225-230.
18. Olson MS, Hampson RK, Craig F. Regulation of the hepatic glycine-cleavage system. *Biochem Soc Trans.* 1986;14(6):1004-1005.
19. Bremer J. Pyruvate dehydrogenase, substrate specificity and product inhibition. *Eur J Biochem.* 1969;8(4):535-540.
20. Gregersen N. The specific inhibition of the pyruvate dehydrogenase complex from pig kidney by propionyl-CoA and isovaleryl-CoA. *Biochem Med.* 1981;26:20-27.
21. Stumpe DA, McAfee J, Parks JK, Eguren L. Propionate inhibition of succinate:CoA ligase (GDP) and the citric acid cycle in mitochondria. *Pediatr Res.* 1980;14:1127-1131.
22. Brock M, Buckel W. On the mechanism of action of the antifungal agent propionate. *Eur J Biochem.* 2004;271(15):3227-3241.
23. Schwab MA, Sauer SW, Okun JG et al. Secondary mitochondrial dysfunction in propionic aciduria: a pathogenic role for endogenous mitochondrial toxins. *Biochem J.* 2006;398:107-112.
24. Cheema-Dhadli S, Leznoff CC, Halperin ML. Effect of 2-methylcitrate on citrate metabolism: implications for the management of patients with propionic acidemia and methylmalonic aciduria. *Pediatr Res.* 1975;9:905-908.
25. Jafari P, Braissant O, Zavadakova P, Henry H, Bonafé L, Ballhausen D. Brain damage in methylmalonic aciduria: 2-methylcitrate induces cerebral ammonium accumulation and apoptosis in 3D organotypic brain cell cultures. *Orphanet J Rare Dis.* 2013;8:4.
26. Cudré-Cung HP, Zavadakova P, do Vale-Pereira S et al. Ammonium accumulation is a primary effect of 2-methylcitrate exposure in an *in vitro* model for brain damage in methylmalonic aciduria. *Mol Genet Metab.* 2016;119:57-67.
27. Amaral AU, Cecatto C, Castilho RF, Wajner M. 2-Methylcitric acid impairs glutamate metabolism and induces permeability transition in brain mitochondria. *J Neurochem.* 2016;137:62-75.
28. Braissant O, McLin VA, Cudalbu C. Ammonia toxicity to the brain. *J Inherit Metab Dis.* 2013;36(4):595-612.
29. Zwickler T, Haegge G, Riderer A et al. Metabolic decompensation in methylmalonic aciduria: which biochemical parameters are discriminative? *J Inherit Metab Dis.* 2012;35(5):797-806.
30. Zwickler T, Riderer A, Haegge G, Hoffmann GF, Kölker S, Burgard P. Usefulness of biochemical parameters in decisionmaking on the start of emergency treatment in patients with propionic acidemia. *J Inherit Metab Dis.* 2014;37(1):31-37.
31. Wyse AT, Brusque AM, Silva CG, Streck EL, Wajner M, Wannmacher CM. Inhibition of Na⁺, K⁺-ATPase from rat brain cortex by propionic acid. *Neuroreport.* 1998;9:1719-1721.
32. Fontella FU, Pulrolnik V, Gassen E et al. Propionic and methylmalonic acids induce oxidative stress in brain of young rats. *Neuroreport.* 2000;11:541-544.
33. Pettenuzzo LF, Schuck PF, Fontella F et al. Ascorbic acid prevents cognitive deficits caused by chronic administration of propionic acid to rats in the water maze. *Pharmacol Biochem Behav.* 2002;75:623-629.
34. Trindade VM, Brusque AM, Raasch JR et al. Ganglioside alterations in the central nervous system of rats chronically injected with methylmalonic and propionic acids. *Metab Brain Dis.* 2002; 17:93-102.
35. de Mattos-Dutra A, Meirelles R, Bevilacqua da Rocha B et al. Methylmalonic and propionic acids increase the *in vitro* incorporation of ³²P into cytoskeletal proteins from cerebral cortex of young rats through NMDA glutamate receptors. *Brain Res.* 2000; 856:111-118.
36. Brusque AM, Borba Rosa R, Schuck PF et al. Inhibition of the mitochondrial respiratory chain complex activities in rat cerebral cortex by methylmalonic acid. *Neurochem Int.* 2002;40:593-601.

37. Rigo FK, Pasquetti L, Malfatti CRM et al. Propionic acid induces convulsions and protein carbonylation in rats. *Neurosci Lett.* 2006;408:151-154.
38. Ribas GS, Manfredini V, de Marco MG et al. Prevention by L-carnitine of DNA damage induced by propionic and methylmalonic acids in human peripheral leukocytes *in vitro*. *Mutat Res.* 2010;702:123-128.
39. Wilson KA, Han Y, Zhong M et al. Inter-relations between 3-hydroxypropionate and propionate metabolism in rat liver: relevance to disorders of propionyl-CoA metabolism. *Am J Physiol Endocrinol Metab.* 2017;313:413-428.
40. Martin-Requero A, Corkey BE, Cerdan S, Walajtys-Rode E, Parrilla RL, Williamson JR. Interactions between alpha-ketoglutarate metabolism and the pathways of gluconeogenesis and urea synthesis in isolated hepatocytes. *J Biol Chem.* 1983; 258(6):3673-3681.
41. Dutra JC, Dutra-Filho CS, Cardozo SE, Wannmacher CM, Sarkis JJ, Wajner M. Inhibition of succinate dehydrogenase and beta-hydroxybutyrate dehydrogenase activities by methylmalonate in brain and liver of developing rats. *J Inher Metab Dis.* 1993;16:147-153.
42. Wyse AT, Streck EL, Barros SV, Brusque AM, Zugno AI, Wajner M. Methylmalonate administration decreases Na⁺, K⁺-ATPase activity in cerebral cortex of rats. *Neuroreport.* 2000;11: 2331-2334.
43. Schuck PF, Rosa RB, Pettenuzzo LF et al. Inhibition of mitochondrial creatine kinase activity from rat cerebral cortex by methylmalonic acid. *Neurochem Int.* 2004;45:661-667.
44. Mirandola SR, Melo DR, Schuck PF, Ferreira GC, Wajner M, Castillo RF. Methylmalonate inhibits succinate-supported oxygen consumption by interfering with mitochondrial succinate uptake. *J Inher Metab Dis.* 2008;31:44-54.
45. Malfatti CRM, Perry MLS, Schweigert ID et al. Convulsions induced by methylmalonic acid are associated with glutamic acid decarboxylase inhibition in rats: a role for GABA in the seizures presented by methylmalonic acidemia patients? *Neuroscience.* 2007;146:1879-1887.
46. Melo DR, Mirandola SR, Assunção NA, Castilho RF. Methylmalonate impairs mitochondrial respiration supported by NADH-linked substrates: involvement of mitochondrial glutamate metabolism. *J Neurosci Res.* 2012;90(6):1190-1199.
47. Fernandes CG, Borges CG, Seminotti B et al. Experimental evidence that methylmalonic acid provokes oxidative damage and compromises antioxidant defenses in nerve terminal and striatum of young rats. *Cell Mol Neurobiol.* 2011;31:755-785.
48. Schuck PF, Alves L, Pettenuzzo LF et al. Acute renal failure potentiates methylmalonate-induced oxidative stress in brain and kidney of rats. *Free Radic Res.* 2012;47:233-240.
49. Baumgartner MR, Hörster F, Dionisi-Vici C et al. Proposed guidelines for the diagnosis and management of methylmalonic and propionic acidemia. *Orphanet J Rare Dis.* 2014;9:130.
50. Childs B, Nyhan WL. Further observations of a patient with hyperglycinemia. *Pediatrics.* 1964;33:403-412.
51. Saudubray JM, Amédée-Manesme O, Lavaud J. Emergency treatment of inborn errors of amino acid metabolism detected in the neonatal period. *Arch Fr Pediatr.* 1979;36(10):969-980.
52. Mellon AF, Deshpande SA, Mathers JC, Bartlett K. Effect of oral antibiotics on intestinal production of propionic acid. *Arch Dis Child.* 2000;82:169-172.
53. Prasad C, Nurko S, Borovoy J, Korson MS. The importance of gut motility in the metabolic control of propionic acidemia. *J Pediatr.* 2004;144:532-535.
54. Schlenzig JS, Poggi-Travert F, Laurent J et al. Liver transplantation in two cases of propionic acidemia. *J Inher Metab Dis.* 1995;18:448-461.
55. Hoff V t, WG DM, Taylor J et al. Combined liver-kidney transplantation in methylmalonic acidemia. *J Pediatr.* 1998;132:1043- 1044.
56. Sawada T, Ledley FD. Correction of methylmalonyl-CoA mutase deficiency in Mut0 fibroblasts and constitution of gene expression in primary human hepatocytes by retroviral-mediated transfer. *Somat Cell Mol Genet.* 1992;18(6):507-516.
57. Stankovics J, Crane AM, Andrews E, Wu CH, Wu GY, Ledley FD. Overexpression of human methylmalonyl CoA mutase in mice after *in vivo* gene transfer with asialoglycoprotein/polylysine/DNA complexes. *Hum Gene Ther.* 1994;5 (9):1095-1104.
58. Chandler RJ, Tsai MS, Dorko K et al. Adenoviral-mediated correction of methylmalonyl-CoA mutase deficiency in murine fibroblasts and human hepatocytes. *BMC Med Genet.* 2007;30: 8-24.
59. Chandler RJ, Venditti CP. Adenovirus-mediated gene delivery rescues a neonatal lethal murine model of mut(0) methylmalonic acidemia. *Hum Gene Ther.* 2008;19(1):53-60.
60. Chandler RJ, Venditti CP. Long-term rescue of a lethal murine model of methylmalonic acidemia using adeno-associated viral gene therapy. *Mol Ther.* 2010;18:11-16.
61. Carrillo-Carrasco N, Chandler RJ, Chandrasekaran S, Venditti CP. Liver-directed recombinant adeno-associated viral gene delivery rescues a lethal mouse model of methylmalonic acidemia and provides long-term phenotypic correction. *Hum Gene Ther.* 2010;21:1147-1154.

62. Chandler RJ, Venditti CP. Pre-clinical efficacy and dosing of an AAV8 vector expressing human methylmalonyl-CoA mutase in a murine model of methylmalonic acidemia (MMA). *Mol Genet Metab.* 2012;107:617-619.
63. Senac JS, Chandler RJ, Sysol JR, Li L, Venditti CP. Gene therapy in a murine model of methylmalonic acidemia using rAAV9-mediated gene delivery. *Gene Ther.* 2012;19:385-391.
64. Harrington EA, Sloan JL, Manoli I et al. Neutralizing antibodies against adeno-associated viral capsids in patients with methylmalonic acidemia. *Hum Gene Ther.* 2016;27:345-353.
65. Wong ESY, McIntyre C, Peters HL, Ranieri E, Anson DS, Fletcher JM. Correction of methylmalonic aciduria *in vivo* using a codon-optimized lentiviral vector. *Hum Gene Ther.* 2014;25: 529-538.
66. Hofherr SE, Senac JS, Chen CY, Palmer DJ, Ng P, Barry MA. Short-term rescue of neonatal lethality in a mouse model of propionic acidemia by gene therapy. *Hum Gene Ther.* 2009;20: 169-180.
67. Chandler RJ, Chandrasekaran S, Carrillo-Carrasco N et al. Adeno-associated virus serotype 8 gene transfer rescues a neonatal lethal murine model of propionic acidemia. *Hum Gene Ther.* 2011;22(4):477-481.
68. Guenzel AJ, Hofherr SE, Hillestad M et al. Generation of a hypomorphic model of propionic acidemia amenable to gene therapy testing. *Mol Ther.* 2013;21(7):1316-1323.
69. Guenzel AJ, Hillestad ML, Matern D, Barry MA. Effects of adeno-associated virus serotype and tissue-specific expression on circulating biomarkers of propionic acidemia. *Hum Gene Ther.* 2014;25:837-843.
70. Guenzel AJ, Collard R, Kraus JP, Matern D, Barry MA. Longterm sex-biased correction of circulating propionic acidemia disease markers by adeno-associated virus vectors. *Hum Gene Ther.* 2015;26(3):153-160.
71. Buck NE, Wood L, Hu R, Peters HL. Stop codon read-through of a methylmalonic aciduria mutation. *Mol Genet Metab.* 2009;97 (4):244-249.
72. Buck NE, Wood LR, Hamilton NJ, Bennett MJ, Peters HL. Treatment of a methylmalonyl-CoA mutase stopcodon mutation. *Biochem Biophys Res Commun.* 2012b;427(4):753-757.
73. Sánchez-Alcudia R, Pérez B, Ugarte M, Desviat LR. Feasibility of nonsense mutation readthrough as a novel therapeutical approach in propionic acidemia. *Hum Mutat.* 2012;33:973-980.
74. An D, Schneller JL, Frassetto A et al. Systemic messenger RNA therapy as a treatment for methylmalonic acidemia. *Cell Rep.* 2018;21:3548-3558.
75. Jorge-Finnigan A, Brasil S, Underhaug J et al. Pharmacological chaperones as a potential therapeutic option in methylmalonic aciduria cblB type. *Hum Mol Genet.* 2013;22:3680-3689.
76. Erlich-Hadad T, Hadad R, Feldman A, Greif H, Lichtenstein M, Lorberboum-Galski H. TAT-MTS-MCM fusion proteins reduce MMA levels and improve mitochondrial activity and liver function in MCM-deficient cells. *J Cell Mol Med.* 2018;22:1601-1613.
77. Darvish-Damavandi M, Ho HK, Kang TS. Towards the development of an enzyme replacement therapy for the metabolic disorder propionic acidemia. *Mol Genet Metab Rep.* 2016;8:51-60.
78. Collard R, Majtan T, Park I, Kraus JP. Import of TAT-conjugated propionyl coenzyme a carboxylase using models of propionic acidemia. *Mol Cell Biol.* 2018;38(6):e00491-e00417.
79. Buck NE, Pennell SD, Wood LR, Pitt JJ, Allen KJ, Peters HL. Fetal progenitor cell transplantation treats methylmalonic aciduria in a mouse model. *Biochem Biophys Res Commun.* 2012;427: 30-35.
80. Gebhardt B, Vlaho S, Fischer D, Sewell A, Böhles H. N-Carbamylglutamate enhances ammonia detoxification in a patient with decompensated methylmalonic aciduria. *Mol Genet Metab.* 2003;79:303-304.
81. Gebhardt B, Dittrich S, Parbel S, Vlaho S, Matsika O, Böhles H. N-Carbamylglutamate protects patients with decompensated propionic aciduria from hyperammonaemia. *J Inherit Metab Dis.* 2005;28:241-244.
82. Walter JH, Wraith JE, Cleary MA. Absence of acidosis in the initial presentation of propionic acidemia. *Arch Dis Child.* 1995;72: 197-199.
83. Royes LFF, Figuera MR, Furian AF et al. Creatine protects against the convulsive behavior and lactate production elicited by the intrastriatal injection of methylmalonate. *Neuroscience.* 2003; 118:1079-1090.
84. Vasques V, Brinco F, Viegas CM, Wajner M. Creatine prevents behavioral alterations caused by methylmalonic acid administration into the hippocampus of rats in the open field task. *J Neurol Sci.* 2006;244:23-29.
85. Longo N, Price LB, Gappmaler E et al. Anaplerotic therapy in propionic acidemia. *Mol Genet Metab.* 2017;122:51-59.
86. Matern D, Seydewitz H, Lehnert W, Niederhoff H, Leititis JU, Brands M. Primary treatment of propionic acidemia complicated by acute thiamine deficiency. *J Pediatr.* 1996;129:758-760.
87. Mayatepek E, Schulze A. Metabolic decompensation and lactic acidosis in propionic acidemia complicated by thiamine deficiency. *J Inherit Metab Dis.* 1999;22:189-190.
88. Baruteau J, Hargreaves I, Krywawych S et al. Successful reversal of propionic acidemia associated cardiomyopathy: evidence for low myocardial coenzyme Q10 status and secondary mitochondrial dysfunction as an underlying pathophysiological mechanism. *Mitochondrion.* 2014;17:150-156.
89. Williams ZR, Emmet Hurley P, Altiparmak UE et al. Late onset optic neuropathy in methylmalonic and propionic acidemia. *Am J Ophthalmol.* 2009;147:929-933.
90. Martinez Alvarez L, Jameson E, Parry NR, Lloyd C, Ashworth JL. Optic neuropathy in methylmalonic acidemia

- and propionic acidemia. *Br J Ophthalmol.* 2016;100:98-104.
91. Viegas CM, Zanatta Â, Grings M et al. Disruption of the redox homeostasis and brain damage caused *in vivo* by methylmalonic acid and ammonia in cerebral cortex and striatum of developing rats. *Free Radic Res.* 2014;48:659-669.
 92. Figuera MR, Queiroz CM, Stracke MP et al. Ascorbic acid and alpha-tocopherol attenuate methylmalonic acid-induced convulsions. *Neuroreport.* 1999;10:2039-2043.
 93. Petteuzo LF, Schuck PF, Wyse ATS et al. Ascorbic acid prevents water maze behavioral deficits caused by early postnatal methylmalonic acid administration in the rat. *Brain Res.* 2003;976: 234-242.
 94. Treacy E, Arbour L, Chessex P et al. Glutathione deficiency as a complication of methylmalonic acidemia: response to high doses of ascorbate. *J Pediatr.* 1996;129:445-448.
 95. Ribeiro MCP, de Avila DS, Schneider CYM et al. α -Tocopherol protects against pentylentetrazol- and methylmalonate-induced convulsions. *Epilepsy Res.* 2005;66:185-194.
 96. Pinar-Sueiro S, Martínez-Fernández R, Lage-Medina S, Aldamiz-Ecchevarria L, Vecino L. Optic neuropathy in methylmalonic acidemia: the role of neuroprotection. *J Inherit Metab Dis.* 2010; 33:199-203.
 97. Traber G, Baumgartner MR, Schwarz U, Pangalu A, Donath MY, Landau K. Subacute bilateral visual loss in methylmalonic acidemia. *J Neuroophthalmol.* 2011;31:344-346.
 98. Colin-González AL, Paz-Loyola AL, Serratos IN et al. The effect of WIN 55,212-2 suggests a cannabinoid-sensitive component in the early toxicity induced by organic acids accumulating in glutaric acidemia type I and in related disorders of propionate metabolism in rat brain synaptosomes. *Neuroscience.* 2015a;310: 578-588.
 99. Colin-González AL, Paz-Loyola AL, Serratos IN et al. Toxic synergism between quinolinic acid and organic acids accumulating in glutaric acidemia type I and in disorders of propionate metabolism in rat brain synaptosomes: relevance for metabolic acidemias. *Neuroscience.* 2015b;12:64-74.
 100. Figuera MR, Bonini JS, de Oliveira TG et al. GM1 ganglioside attenuates convulsions and thiobarbituric acid reactive substances production induced by the intrastriatal injection of methylmalonic acid. *Int J Biochem Cell Biol.* 2003;35:465-473.
 101. Gallego-Villar L, Pérez B, Ugarte M, Desviat LR, Richard E. Antioxidants successfully reduce ROS production in propionic acidemia fibroblasts. *Biochem Biophys Res Commun.* 2014;452: 457-461.
 102. Rivera-Barahona A, Alonso-Barroso E, Pérez B, Murphy MP, Richard E, Desviat LR. Treatment with antioxidants ameliorates oxidative damage in a mouse model of propionic acidemia. *Mol Genet Metab.* 2017;122:43-50.
 103. Furian AF, Figuera MR, Oliveira MS et al. Methylene blue prevents methylmalonate-induced seizures and oxidative damage in rat-striatum. *Neurochem Int.* 2007;50:164-171.
 104. Salvadori MGSS, Banderó CRR, Jesse AC et al. Prostaglandin E2 potentiates methylmalonate-induced seizures. *Epilepsia.* 2012;53:189-198.
 105. Banderó CRR, Salvadori MGSS, Teixeira Gomes A et al. Fish oil attenuates methylmalonate-induced seizures. *Epilepsy Res.* 2013;105:69-76.
 106. Brassier A, Boyer O, Valayannopoulos V. Renal transplantation in 4 patients with methylmalonic aciduria: a cell therapy for metabolic disease. *Mol Genet Metab.* 2013;110(1-2):106-110.
 107. Chalmers RA, Roe CR, Stacey TE, Hoppel CL. Urinary excretion of L-carnitine and acylcarnitines by patients with disorders of organic acid metabolism: evidence for secondary insufficiency of L-carnitine. *Pediatr Res.* 1984;18(12):1325-1328.
 108. Arbeiter AK, Kranz B, Wingen AM et al. Continuous venovenous haemodialysis (CVVHD) and continuous peritoneal dialysis (CPD) in the acute management of 21 children with inborn errors of metabolism. *Nephrol Dial Transplant.* 2010;25 (4):1257-1265.
 109. Ah Mew N, Cnaan A, McCarter R. Conducting an investigator-initiated randomized double-blinded intervention trial in acute decompensation of inborn errors of metabolism: lessons from the N-carbamylglutamate consortium. *Transl Sci Rare Dis.* 2018;3 (3-4):157-170.
 110. Nyhan WL. Treatment of hyperglycemia. *Am J Dis Child.* 1967;113(1):129-133.
 111. Nyhan WL, Fawcett N, Ando T, Rennert OM, Julius RL. Response to dietary therapy in B12 unresponsive methylmalonic acidemia. *Pediatrics.* 1973;51(3):539-548.
 112. Touati G, Valayannopoulos V, Mention K et al. Methylmalonic and propionic acidurias: management without or with a few supplements of specific amino acid mixture. *J Inherit Metab Dis.* 2006;29:288-298.
 113. Yannicelli S. Nutrition therapy of organic acidemias with amino acid-based formulas: emphasis on methylmalonic and propionic acidemia. *J Inherit Metab Dis.* 2006;29(2-3):281-287.
 114. Myles JG, Manoli I, Venditti CP. Effects of medical food leucine content in the management of methylmalonic and propionic acidemias. *Curr Opin Clin Nutr Metab Care.* 2018;21(1):42-48.
 115. Niemi AK, Kim IK, Krueger CE. Treatment of methylmalonic acidemia by liver or combined liver-kidney transplantation. *J Pediatr.* 2015;166(6):1455-1461.
 116. Sloan JL, Manoli I, Venditti CP. Liver or combined liver-kidney transplantation for patients with isolated

- methylmalonic acidemia: who and when? *J Pediatr.* 2015;166(6):1346-1350.
117. Neidich AB, Neidich E. Elective transplantation for MMA patients: how ought patients' needs for organs to be prioritized when transplantation is not their only available treatment? *AMA J Ethics.* 2016;18(2):153-155.
 118. Tummulo A, Melpignano L, Carella A et al. Long-term continuous N-carbamylglutamate treatment in frequently decompensated propionic acidemia: a case report. *J Med Case Rep.* 2018;12 (1):103.
 119. Valayannopoulos V, Baruteau J, Delgado MB. Carglumic acid enhances rapid ammonia detoxification in classical organic acidurias with a favourable risk-benefit profile: a retrospective observational study. *Orphanet J Rare Dis.* 2016;31(11):32.
 120. Levrat V, Forest I, Fouilhoux A, Acquaviva C, Vianey-Saban C, Guffon N. Carglumic acid: an additional therapy in the treatment of organic acidurias with hyperammonemia? *Orphanet J Rare Dis.* 2008;30(3):2.
 121. Meyburg J, Das AM, Hoerster F et al. One liver for four children: first clinical series of liver cell transplantation for severe neonatal urea cycle defects. *Transplantation.* 2009;87(5): 636-641.
 122. Mitry RR, Dhawan A, Hughes RD et al. One liver, three recipients: segment IV from split-liver procedures as a source of hepatocytes for cell transplantation. *Transplantation.* 2004;77(10): 1614-1616.
 123. Stéphanne X, Najimi M, Smets F, Reding R, de Ville de Goyet J, Sokal EM. Cryopreserved liver cell transplantation controls ornithine transcarbamylase deficient patient while awaiting liver transplantation. *Am J Transplant.* 2005;5(8):2058-2061.
 124. Stéphanne X, Najimi M, Sibille C, Nassogne MC, Smets F, Sokal EM. Sustained engraftment and tissue enzyme activity after liver cell transplantation for argininosuccinate lyase deficiency. *Gastroenterology.* 2006;130(4):1317-1323.
 125. Iansante V, Mitry RR, Filippi C, Fitzpatrick E, Dhawan A. Human hepatocyte transplantation for liver disease: current status and future perspectives. *Pediatr Res.* 2018;83(1-2):232-240.
 126. Manoli I, Sysol JR, Li L et al. Targeting proximal tubule mitochondrial dysfunction attenuates the renal disease of methylmalonic acidemia. *Proc Natl Acad Sci U S A.* 2013;110: 13552-13557.
 127. Smedberg M, Wernerman J. Is the glutamine story over? *Crit Care.* 2016;20(1):361.
 128. Kimose HH, Randsbaek F, Christensen TD, Valen G, Bøtker HE, Vaage J. A dose-response study of glutamate supplementation in isolated, perfused rat hearts undergoing ischaemia and cold cardioplegia. *Eur J Cardiothorac Surg.* 2018;53(3):664-671.



Retrospective evaluation of the Dutch pre-newborn screening cohort for propionic acidemia and

isolated methylmalonic acidemia: what to aim, expect, and evaluate from newborn screening?

*Journal of Inherited Metabolic Diseases 2019, Epub ahead of print
DOI: 10.1002/jimd.12193*

Hanneke A. Haijes^{†,*}, Femke Molema[†], Mirjam Langeveld,
Mirian C. Janssen, Annet M. Bosch, Francjan van Spronsen,
Margot F. Mulder, Nanda M. Verhoeven-Duif, Judith J.M. Jans,
Ans T. van der Ploeg, Margreet A. Wagenmakers, M. Estela Rubio-Gozalbo,
Martijn C.G.J. Brouwers, Maaïke C. de Vries, Janneke G. Langendonk,
Monique Williams[#], Peter M. van Hasselt^{#,*}

[†] These authors contributed equally to this article

[#] These authors contributed equally to this article

* Corresponding authors

ABSTRACT

Background: Evidence for effectiveness of newborn screening (NBS) for propionic acidemia (PA) and isolated methylmalonic acidemia (MMA) is scarce. Prior to implementation in the Netherlands, we aim to estimate the expected health gain of NBS for PA and MMA.

Methods: In this national retrospective cohort study, the clinical course of 76/83 Dutch PA and MMA patients, diagnosed between January 1979 and July 2019, was evaluated. Five clinical outcome parameters were defined: adverse outcome of the first symptomatic phase, frequency of acute metabolic decompensations (AMD), cognitive function, mitochondrial complications and treatment-related complications. Outcomes of patients identified by family testing were compared with the outcomes of their index siblings.

Results: An adverse outcome due to the first symptomatic phase was recorded in 46% of the clinically diagnosed patients. Outcome of the first symptomatic phase was similar in 5/9 sibling pairs and better in 4/9 pairs. Based on the day of diagnosis of the clinically diagnosed patients and sibling pair analysis, a preliminary estimated reduction of adverse outcome due to the first symptomatic phase from 46% to 36-38% was calculated. Among the sibling pairs, AMD frequency, cognitive function, mitochondrial and treatment-related complications were comparable.

Discussion: These results suggest that the health gain of NBS for PA and MMA in overall outcome may be limited, as only a modest decrease of adverse outcomes due to the first symptomatic phase is expected. With current clinical practice, no reduced AMD frequency, improved cognitive function or reduced frequency of mitochondrial or treatment-related complications can be expected.

KEY MESSAGE

Implementation of newborn screening for propionic acidemia and methylmalonic acidemia may result in only a modest decrease of adverse outcomes due to the first symptomatic phase. With current clinical practice, no reduced frequency of acute metabolic decompensations, improved cognitive function, reduced frequency of mitochondrial complications or treatment-related complications can be expected.

INTRODUCTION

Propionic acidemia (PA, MIM #6060054) and isolated methylmalonic acidemia (MMA, MIM #251000, #251100, #251110, #277400 and #277410) are caused by enzyme and cofactor deficiencies involved in propionyl-CoA breakdown. The clinical course usually starts with an acute metabolic decompensation (AMD) in the neonatal period (early onset, EO) or thereafter (late onset, LO).¹ The first symptomatic phase frequently causes irreversible neurological damage, manifesting as movement disorders in varying severity and/or psychomotor retardation. This neurological damage is often reflected by white matter lesions and/or basal ganglia hyperintensities on brain imaging. In addition, the clinical course is characterized by frequent AMD, cognitive deficits and long-term complications.² A diagnosis before the first symptomatic phase, feasible through newborn screening (NBS), could theoretically prevent the neurological damage.³ However, the majority of patients is symptomatic well before NBS results can be available, limiting the potential gain.^{4,5} Four studies described the potential additional value of NBS, but each with limited sample sizes and follow-up time,⁶⁻⁹ resulting in controversy about the potential effectiveness of NBS for PA and MMA.

Many efforts have been made to achieve consensus on which diseases are suitable for screening, both on a global level by the World Health Organization (WHO)¹⁰⁻¹¹ (Supplemental Notes 1), and on European level.¹²⁻¹⁴ Despite these efforts, it is still debatable which diseases to screen for and it is not clear on what criteria decisions should be based, resulting in divergent conclusions. Regarding PA and MMA, NBS implementation has been recommended in the United States of America¹⁵, but PA and MMA were not included in the European list of 26 disorders to be considered for NBS expansion.¹³ Nevertheless, several European countries implemented NBS for PA and MMA.⁵

In the Netherlands, the Health Council decided based on the expected health gain for LO patients that NBS for PA and MMA met the screening criteria and will start in October 2019.¹⁶ NBS will be performed based on increased C3-carnitine and increased C3/C2 carnitine ratio, complemented with a second-tier test on increased 2-methylcitric acid and methylmalonic acid. As the heel prick is performed within 3-7 days after birth, the aim is to report a positive second-tier test within 11-21 days after birth.

For the addition of new diseases to NBS, three WHO criteria seem of particular importance: clearly defined objectives (WHO#2), evidence for effectiveness (WHO#4) and careful evaluation (WHO#9)¹¹ (Supplemental Notes 1). To date, for PA and MMA these three criteria are not sufficiently met. Also, despite statements that good long-term outcome is the ultimate goal and that monitoring is necessary to evaluate NBS programmes, long-term outcome is rarely monitored in a standardized manner.¹³

We performed a national retrospective cohort study including 76/83 Dutch PA and MMA patients. We aim to define which objectives could be attained with NBS implementation. Hereto, we estimate the expected health gain in the Netherlands by comparing siblings diagnosed via family testing with their older index sibling. In addition, we explore how evaluation of NBS implementation can be performed by assessing newly defined clinical outcome parameters. Lastly, we use insights obtained from studying this pre-NBS cohort to guide counseling and surveillance of NBS cohorts.

METHODS

Patient inclusion

In this nationwide retrospective cohort study, patients clinical records from all six Dutch

metabolic centers were analyzed. Patients were eligible for inclusion if PA or MMA was confirmed by enzymatic activity analysis or mutation analysis of *PCCA*, *PCCB*, *MUT*, *MMAA*, *MMAB*, *MCEE* or *MMADHC*. Patients or their legal guardians signed an informed consent form, approving analysis of their clinical records and publication of the anonymous data, in agreement with institutional and national legislation. The study was approved by the Ethical Committees of the University Medical Centers Utrecht (17-490/C) and Rotterdam (MEC-2018-1312), on behalf of all Ethical Committees of involved University Medical Centers.

Data collection

Data collection was performed by two investigators (HH, FM). Data was extracted from both paper and electronic patient files. Data was collected from the first symptomatic phase until the last follow-up visit. Data collection was focused on patient and family characteristics, outcome of the first symptomatic phase, AMD, hospital admissions, cognitive and psychomotor development and long-term complications. All data was entered in OpenClinica open source software, version 3.12.2.

EO was defined as an episode of severely reduced clinical condition starting in the first 28 days of life, and LO as symptoms starting after 28 days of life¹. Patients identified through family testing based on an affected older (index) sibling were regarded a separate category.

Outcome parameters

To evaluate clinical outcomes, five grouped outcome parameters were defined (Supplemental Notes 2). “Adverse outcome (AO) of the first symptomatic phase” was categorized based on the presence of movement disorders that developed during or right after the first symptomatic phase, objectified during follow-up examinations by pediatric neurologists and physiotherapists shortly after the first symptomatic phase, and/or the presence of basal ganglia hyperintensities or white matter abnormalities detected at the first time of brain imaging after the first symptomatic phase (Supplemental Notes 2). “AMD frequency” was defined based on the frequency of (impending) AMD requiring hospital admission per patient year (PY) in the first four years of life, other than the first symptomatic phase (Supplemental Notes 2). “Cognitive function” was distinguished in three categories based on neuropsychological test results, or in the absence of neuropsychological test results on educational level or professional employment (Supplemental Notes 2).¹⁷ Long-term complications were divided into mitochondrial, treatment-related and miscellaneous complications. Patients were categorized into six categories based on the number of mitochondrial complications present at a certain age. These mitochondrial complications included 21 complications likely to be caused by mitochondrial failure (Supplemental Notes 2).² Complications with potential treatment-related etiology included decreased bone mineral density (BMD), growth retardation and obesity (Supplemental Notes 2).² Growth retardation was defined present when height to weight was < -2 SD at any moment during follow-up. Other complications, with no evidence for a sole mitochondrial or treatment-related etiology, were regarded miscellaneous complications. These complications included pes planovalgus, port-a-cath infections, teeth enamel defects, urolithiasis and gout.²

Data-analysis

Each outcome parameter was evaluated in the complete cohort, separate for both PA and MMA patients and separate for both EO and LO patients. In addition, for all AMDs age at decompensation, admission duration, need for intensive care unit admission and AMD

triggers were evaluated. For each complication assessed, prevalence was calculated. As a proxy for the potential health gain of NBS, all five clinical outcome parameters were compared between patients identified by family testing and their index siblings. The expected health gain was calculated by extrapolating findings of the sibling comparison on AO of the first symptomatic phase to the entire cohort, if NBS would have been implemented. Calculations were performed for six possible days that definitive NBS results could become available: day 0, 3, 7, 11, 15 and 21 after birth.

Assessment of risk factors for each outcome parameter was performed by comparing disease types, for both PA and MMA presentation types and for MMA vitamin B12 responsiveness. All statistical analyses were performed in R programming language. Results are expressed as either means or medians with standard deviations and ranges for quantitative data and as number and percentage for qualitative data. Student's t-tests were performed for quantitative data and Fisher's exact tests for qualitative data. P-values were adjusted according to the Bonferroni method when multiple testing was performed, adjusted p-values < 0.05 were considered statistically significant. P-values solely reported in the text for the assessment of risk factors of clinical outcome parameters were calculated using Fisher's exact tests and were not adjusted, as no multiple testing was performed.

RESULTS

Patient characteristics

Of all 83 PA and MMA patients in the Netherlands diagnosed between January 1979 and July 2019, 76 patients were included. Five patients refused to participate and clinical records of 2 deceased MMA patients could not be retrieved. For nearly all patients, data was available from the first symptomatic phase to the last moment of follow-up. The cohort included 31 PA patients from 24 families and 45 MMA patients from 40 families. Between 01-01-1998 and 31-12-2017, 46/76 patients (PA: $n = 19$, MMA: $n = 27$) were diagnosed, with a median of 2 patients per birth year (range: 1 – 5). In this period 3.729.128 live births were registered, providing an estimated incidence in the Netherlands of 1:81.000 for PA and MMA combined, 1:196.000 for PA and 1:138.000 for MMA. Presentation type was EO in 29, LO in 34, family testing in 12 and unknown in one patient (Table 1). Clinical data of 5 PA sibling pairs and 1 trio, and 3 MMA sibling pairs ($n = 9$) was available for sibling comparison (Table S1). Two MMA patients identified through family testing could not be compared with their index siblings, because medical records of the index sibling were not available.

Mutation analysis was available in 52/76 patients and revealed 24 previously unreported mutations, including 7 mutations in *PCCA*, 5 in *PCCB*, 8 in *MUT*, 2 in *MMAA* and 2 in *MMAB* (Table S2). Pregnancy and delivery were uncomplicated in the majority of the patients' mothers. Birth weight of MMA patients was significantly lower compared to PA patients, in line with previous reports (Table S3).¹ In most patients, the first symptomatic phase was characterized by lethargy and anorexia. Significantly more LO patients presented with vomiting. Plasma ammonia at presentation was significantly higher in EO patients, resulting in significantly more EO patients requiring dialysis (Table S4).

Adverse outcome of the first symptomatic phase

An AO of the first symptomatic phase was recorded in 36/76 (47%) of all patients and in 30/64 (47%) of the clinically diagnosed patients (Figure 1). Movement disorders were recorded in 24/36 patients. Basal ganglia hyperintensities were observed in 18, white matter abnormalities in 14 and both in 6 patients. In 19/26 patients in whom white matter

abnormalities and/or basal ganglia hyperintensities were observed, brain imaging was performed within 3 days to 6 months after the first symptomatic phase and in 7/26 patients later in life (range: 9 months to 23 years). In 3 of these patients also a movement disorder was recorded, and in all 7 patients the observed abnormalities were considered to be long-existent based on unchanged clinical symptoms and imaging characteristics.

Table 1. Baseline characteristics of the Dutch cohort of PA and MMA patients

	Propionic acidemia (<i>n</i> = 31)		Methylmalonic acidemia (<i>n</i> = 45)	
Presentation type	Early onset Late onset Family testing Unknown	<i>n</i> = 15; 48% <i>n</i> = 8; 26% <i>n</i> = 7; 23% <i>n</i> = 1; 3%	Early onset Late onset Family testing	<i>n</i> = 14; 31% <i>n</i> = 26; 56% <i>n</i> = 5; 11%
Presentation age	Early onset Late onset Family testing	6.05 ± 6.12 days 14.1 ± 22.9 years 0.07 ± 0.19 years	Early onset Late onset Family testing	2.07 ± 1.77 days 1.41 ± 2.74 years 0.32 ± 0.72 years
Genotype	PCCA PCCB No mut. analysis	<i>n</i> = 8; 26% <i>n</i> = 7; 23% <i>n</i> = 16; 52%	MUT MMAA MMAB No mut. analysis	<i>n</i> = 26; 58% <i>n</i> = 8; 18% <i>n</i> = 7; 16% <i>n</i> = 4; 9%
Enzyme activity	0.0 – 0.4 nmol/h/mg 0.5 – 2.0 nmol/h/mg Not measured	<i>n</i> = 10; 32% <i>n</i> = 5; 16% <i>n</i> = 16; 52%		
Vitamin B12 responsiveness			Responsive Not responsive	<i>n</i> = 21; 47% <i>n</i> = 24; 53%
Age at last follow-up		19.2 ± 15.1 years		17.3 ± 12.1 years
Mortality		<i>n</i> = 7; 23% (4 EO, 1 LO, 2 FT)		<i>n</i> = 2; 4% (1 LO, 1 FT)

Early onset: presentation ≤28 days of life; Late onset: presentation >28 days of life. Qualitative data are expressed as number and percentage, quantitative data as mean ± standard deviation. Abbreviations: EO: early onset; LO: late onset; FT: family testing.

In EO patients an AO due to the first symptomatic phase was either absent or, more often, mild, whereas in LO patients most often no AO due to the first symptomatic phase was recorded. If an AO was recorded in LO patients it was either mild or severe, which is represented by a significant difference in mild AO due to the first symptomatic phase in EO versus LO patients (Table 2, Figure S1). AO due to the first symptomatic phase tended to be less frequent in patients identified through family testing than in their siblings (better outcome of the first symptomatic phase in 4/9 sibling pairs, similar in 5/9) (Table S1). Symptoms or signs present during the first symptomatic phase, nor presentation type in PA or MMA, nor vitamin B12 responsiveness in MMA, was associated with an increased risk for an AO (Table S5).

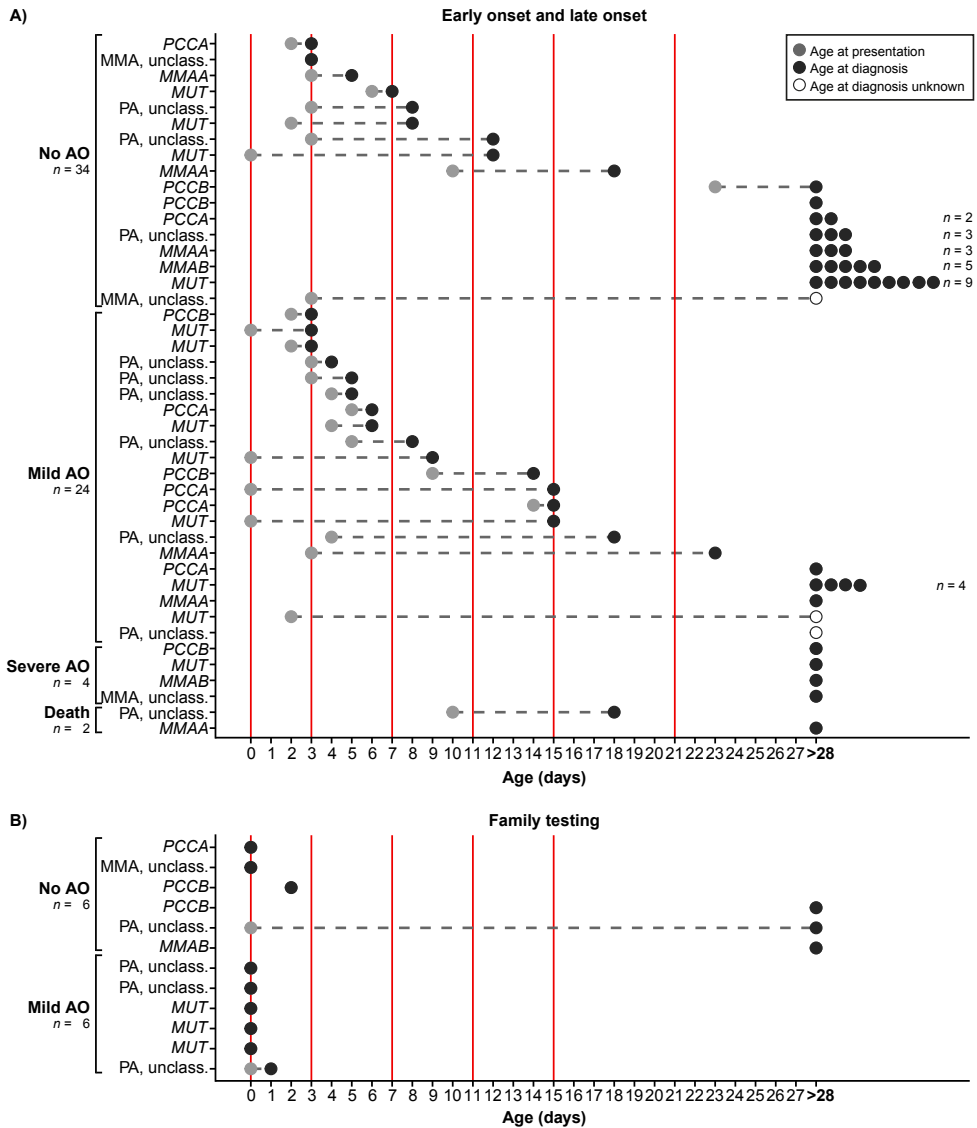
The expected health gain of NBS for PA and MMA in the Netherlands was estimated based on the moment of presentation of all EO and LO patients in this cohort and based on analysis of sibling pairs (Figure 1, Table S1, Table 3). Theoretically, the earlier NBS results are available, the more patients could be protected from an AO due to the first symptomatic phase (Figure 1, Table 3). In this cohort, NBS results available at day 0 of life could have prevented an AO in 14 patients, reducing the percentage of an AO during the first symptomatic phase from 46% to 23%. NBS results available between day 11 and 21 could have prevented an AO in 6 or 5 patients, reducing the percentage from 46% to 36-38% (Table 3).

Table 2. Grouped outcome parameters according to presentation type

	Early onset (n = 29)	Late onset (n = 34)	P-value	Bonferroni correction
Adverse outcome of first sympt. phase				
No adverse outcome	n = 11; 38%	n = 23; 64%	0.024	NS
Mild adverse outcome	n = 17; 59%	n = 6; 21%	0.001	0.006
Severe adverse outcome	n = 0; 0%	n = 4; 12%	0.118	NS
Death due to first presentation	n = 1; 3%	n = 1; 3%	1.000	NS
AMD frequency				
None: no AMD in first four years	n = 3; 10%	n = 13; 38%	0.019	NS
Mild: >0.0 < 0.5 AMD/PY	n = 1; 3%	n = 3; 9%	0.618	NS
Moderate: >0.5 ≤ 1.0 AMD/PY	n = 2; 7%	n = 2; 6%	1.000	NS
Severe: >1.0 ≤ 2.0 AMD/PY	n = 6; 21%	n = 3; 9%	0.280	NS
Very severe: >2.0 AMD/PY	n = 11; 38%	n = 5; 15%	0.045	NS
Death: during or due to AMD	n = 3; 10%	n = 1; 3%	0.326	NS
NA	n = 3; 10%	n = 7; 21%	0.319	NS
Cognitive function				
Group 1: IQ >90 or regular education	n = 4; 14%	n = 15; 44%	0.013	NS
Group 2: IQ 60-90 or special education	n = 10; 34%	n = 8; 24%	0.407	NS
Group 3: IQ <60 or no education	n = 10; 34%	n = 5; 15%	0.081	NS
NA	n = 5; 17%	n = 6; 18%	1.000	NS
Mitochondrial complications				
None	n = 1; 3%	n = 5; 15%	0.205	NS
Mild	n = 6; 21%	n = 19; 56%	0.005	0.034
Moderate	n = 5; 17%	n = 5; 15%	1.000	NS
Severe	n = 9; 31%	n = 2; 6%	0.017	NS
Very severe	n = 8; 28%	n = 3; 9%	0.093	NS
Death	n = 0; 0%	n = 0; 0%	1.000	NS
NA	n = 0; 0%	n = 0; 0%	1.000	NS
Treatment-related complications				
None	n = 9; 31%	n = 17; 50%	0.199	NS
Mild	n = 10; 34%	n = 13; 38%	0.798	NS
Severe	n = 6; 21%	n = 3; 9%	0.280	NS
Very severe	n = 4; 14%	n = 1; 3%	0.171	NS
NA	n = 0; 0%	n = 0; 0%	1.000	NS

Early onset: presentation ≤28 days of life; Late onset: presentation >28 days of life. Statistical significance was determined by Fisher's exact tests. All p-values were adjusted according to the Bonferroni method. Adjusted p-values < 0.05 were considered statistically significant and are depicted in bold. Abbreviations: AMD/PY: acute metabolic decompensations per patient year; NA: not assessed; NS: not significant.

Figure 1. Age at onset and age at diagnosis for PA and MMA patients



A) Patients with early or late onset presentation. B) Patients identified through family testing. The y-axis depicts the patients, ordered on type of adverse outcome and age at diagnosis. The x-axis depicts the patient age in days, with a maximum of 28 days (early onset). Light gray circles depict age at presentation, dark gray circles depict age at diagnosis, open circles depict in which patients the exact age at diagnosis is unknown. For all ages at presentation and ages at diagnosis ≥ 28 days of age (late onset), the circles have been placed at 28 days. The vertical red solid lines depict the potential moments NBS results could become available, in line with Table 3. On the left the severity of adverse outcomes (AO) due to the first symptomatic phase are listed: no adverse outcome, mild, severe or death due to the first symptomatic phase.

Table 3. Expected effect of NBS implementation on occurrence of adverse outcomes due to the first symptomatic phase

Patients	Group	ID	Formula	Day 0 (% (n))	Day 3 (% (n))	Day 7 (% (n))	Day 11 (% (n))	Day 15 (% (n))	Day 21 (% (n))
Potentially diagnosed through NBS (after NBS implementation)	Total	A,a		100% (61)	84% (51)	61% (37)	56% (34)	54% (33)	54% (33)
	Without AO	B,b	A-C, a-c	54% (33)	59% (30)	65% (24)	68% (23)	70% (23)	70% (23)
Potentially diagnosed after first symptomatic phase (after NBS implementation)	With AO	C,c	A-B, a-b	46% (28)	41% (21)	35% (13)	32% (11)	30% (10)	30% (10)
	Total	D,d		0% (0)	16% (10)	39% (24)	44% (27)	46% (28)	46% (28)
Index siblings of patients identified through family testing	Without AO	E,e	D-F, d-f	0% (0)	30% (3)	38% (9)	37% (10)	36% (10)	36% (10)
	With AO	F,f	D-E, d-e	0% (0)	70% (7)	62% (15)	63% (17)	64% (18)	64% (18)
Siblings identified through family testing	Total	G,g		100% (9)	100% (9)	100% (9)	100% (9)	100% (9)	100% (9)
	Without AO	H,h		11% (1)	11% (1)	11% (1)	11% (1)	11% (1)	11% (1)
Siblings identified through family testing	With AO	I,i		89% (8)	89% (8)	89% (8)	89% (8)	89% (8)	89% (8)
	Without AO	J,j		56% (5)	56% (5)	56% (5)	56% (5)	56% (5)	56% (5)
Estimated effectivity	With AO	K,k		44% (4)	44% (4)	44% (4)	44% (4)	44% (4)	44% (4)
	L		k / i	50%	50%	50%	50%	50%	50%
Protected from AO (after NBS implementation)	m		L * c	n = 14	n = 11	n = 7	n = 6	n = 5	n = 5
Percentage AO first symptomatic phase (after NBS implementation)	N,n		$n / (a+d)$ $c + f - m$	23% n = 14	28% n = 17	34% n = 21	36% n = 22	38% n = 23	38% n = 23

AO: adverse outcome; ID: identifier; NBS: newborn screening. Total number of patients included is 61; excluding patients identified through family testing $n = 12$, excluding patients for whom the exact day of diagnosis is unknown, $n = 3$ (Figure 1). The column listing the identifiers indicates the identifier of the percentage in capitals, or the number of patients in lowercases, for the interpretation of the formula. The formula indicates how the percentages and numbers of patients were calculated. The five time points indicate the days that NBS results could become available when NBS would be implemented. All percentages and patient numbers were rounded.

AMD frequency

In total, 962 AMD requiring hospital admission were reported. Hospitalization duration was significantly shorter in MMA than in PA patients. AMD triggers were similar, with the exception of significantly more frequent feeding problems in MMA patients and constipation in PA patients (Table S6).

Among the sibling pairs, AMD frequency was similar in 4/9 pairs. The index patients of 4/9 sibling pairs died following an AMD, whereas all but one of the siblings identified through family testing are still alive, although currently only P6.3 survived his sibling in age (Table S1). AMD frequency tended to be shifted towards a more severe frequency in EO patients compared to LO patients (Table 2, Figure S1). Between PA and MMA patients no difference in AMD frequency was recorded. (Table S6). Among PA patients, EO patients experienced significantly more AMD/PY ($p = 0.002$) and among MMA patients, vitamin B12 unresponsive patients experienced significantly more AMD/PY (Table S6).

Cognitive function

A total of 139 neuropsychological test results were recorded in 46/76 patients, with a median of 3 tests per patient (range: 1 – 10). In 17 patients, cognitive function was based on the patient's educational level and in 13 patients, cognitive function was not assessed (yet). An IQ >90 was noted in 24/63 patients, an IQ between 60 and 90 in 20/63 patients and an IQ <60 in 19/63 patients (Table S7).

Cognitive function was comparable among the sibling pairs (similar in 3, better in 2, worse in 1, not assessed in 3) (Table S1), as well as between EO and LO patients (Table 2, Figure S1). An IQ <60 was significantly more prevalent in PA patients (Table S7). Among PA patients, EO was significantly associated with cognitive function (IQ >90: EO 0%, LO 63%, $p = 0.002$). Among MMA patients, presentation type nor vitamin B12 responsiveness were associated with cognitive function.

Complications with potential mitochondrial etiology

Mitochondrial complications were present in 70/76 patients, and were mild in 30, moderate in 13, severe in 12 and very severe in 14 patients. One PA patient with very severe mitochondrial complications died due to cardiomyopathy. Prevalence of mitochondrial complications was compared with the literature and was fairly comparable for most complications (Table S7).² For quite some complications, especially for MMA, prevalence was here assessed for the first time in a cohort study (Table S7). Renal failure was significantly more prevalent among MMA patients than among PA patients (Table S7).

For mitochondrial complications with acute onset, age at onset was assessed (Table S7, Figure 2). The earliest manifestation of renal failure was already reported at the age of 1.2 years in an *MMAB* patient and in 5/20 patients age of onset was < 6 years (2 *MUT*, 2 *MMAB*, one unclassified). The first manifestation of prolonged QTc interval was shortly after birth in PA, and at 3.6 years in MMA. Cardiomyopathy in PA was noted at 7.5 years, optic atrophy at 11.8 years in PA and at 12.6 years in MMA (Table S7). Age at onset of hepatomegaly, epilepsy and sensorineural hearing loss ranged from birth to ten years, while most other complications typically arose from late infancy to adolescence (Table S7, Figure 2).

Mitochondrial complications were comparable among sibling pairs (similar in 1, better in 4, worse in 4) (Table S1). LO patients were significantly more frequently recorded to have only mild mitochondrial complications than EO patients (Table 2, Figure S1). PA patients had more very severe mitochondrial complications than MMA patients (Table S7), and all

of these PA patients were EO patients (EO 53%, LO 0%, $p = 0.019$). Among MMA patients, mitochondrial complications were comparable between EO and LO patients but the prevalence of moderate to very severe mitochondrial complications was significantly higher in vitamin B12 unresponsive patients (unresponsive 63%, responsive 24%, $p = 0.016$). EO for PA and vitamin B12 unresponsiveness for MMA were also found to be significantly associated with a higher risk for mitochondrial complications with acute onset (Figure 3). In addition, EO in PA tended to be associated with the occurrence of hepatomegaly, prolonged QTc interval, psychoses and sensorineural hearing loss (Figure S2). Vitamin B12 unresponsiveness tended to be associated with the occurrence of optic atrophy, pancreatitis and prolonged QTc interval in MMA, and was significantly associated with the occurrence of renal failure (Figure S3). One of the first occurring mitochondrial complications with acute onset was hepatomegaly (Figure 2). Intriguingly, hepatomegaly was significantly associated with the onset of other mitochondrial complications with acute onset later in life, for PA and MMA as a group and for both PA and MMA separately (Figure 3).

Complications with potential treatment-related etiology

Reduced BMD was noted in 27, growth retardation in 21 and obesity in 16 patients. Treatment-related complications were absent in 33, mild in 28, severe in 9 and very severe in 6 patients (Table S8).

Treatment-related complications were comparable among sibling pairs (similar in 2, better in 5, worse in 2) (Table S1), as well as among EO and LO patients (Table 2, Figure S1), nor were there any differences between PA and MMA, or among PA patients between EO and LO patients (Table S8). Among MMA patients, the rate of mild, severe and very severe treatment-related complications was significantly higher in vitamin B12 unresponsive patients (unresponsive 71%, responsive 33%, $p = 0.017$).

Complications with miscellaneous etiology

A prevalence of 29% pes planovalgus, a feature so far only described in MMA,¹⁸ was noted in PA. In one MMA and one PA patient urolithiasis was recorded. In both patients, calculi developed due to hypercalciuria, although dehydration, chronic acidotic state and a low-protein diet might have contributed. Two MMA patients (*MUT* and *MMAA*) were found to have juvenile gout (Table S8). The *MMAA* patient had chronic renal failure when exhibiting gout, whereas the *MUT* patient did not.

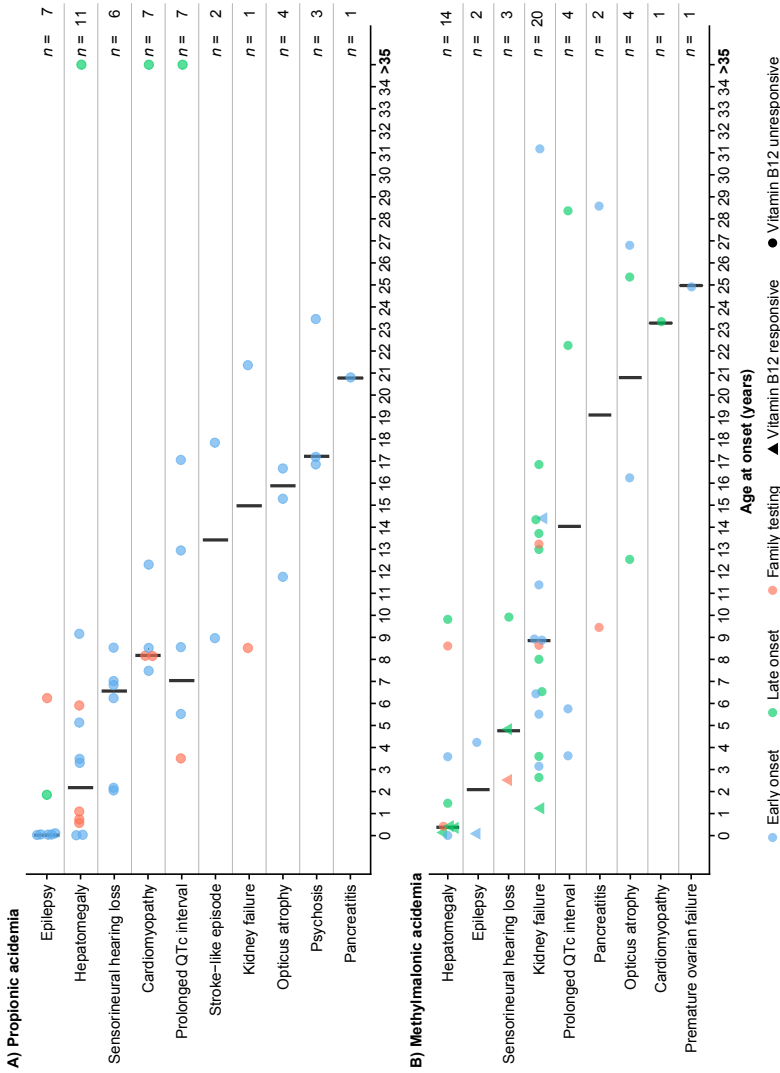
DISCUSSION

Expected health gain of NBS for PA and MMA in the Netherlands (WHO#4)

Here we present an extensive, nationwide cohort study, describing the clinical course of 76/83 Dutch PA and MMA patients. We demonstrated that the expected health gain of introducing NBS for PA and MMA in the Netherlands in overall outcome may be limited. Patients can already present shortly after birth and even if patients are diagnosed pre-symptomatically, they can still develop an adverse outcome. We calculated an expected reduction from 46% to 36-38% AO due to the first symptomatic phase and we consider it unlikely that NBS could result in reduced AMD frequency, improved cognitive function or a reduced frequency of mitochondrial and therapy-related complications.

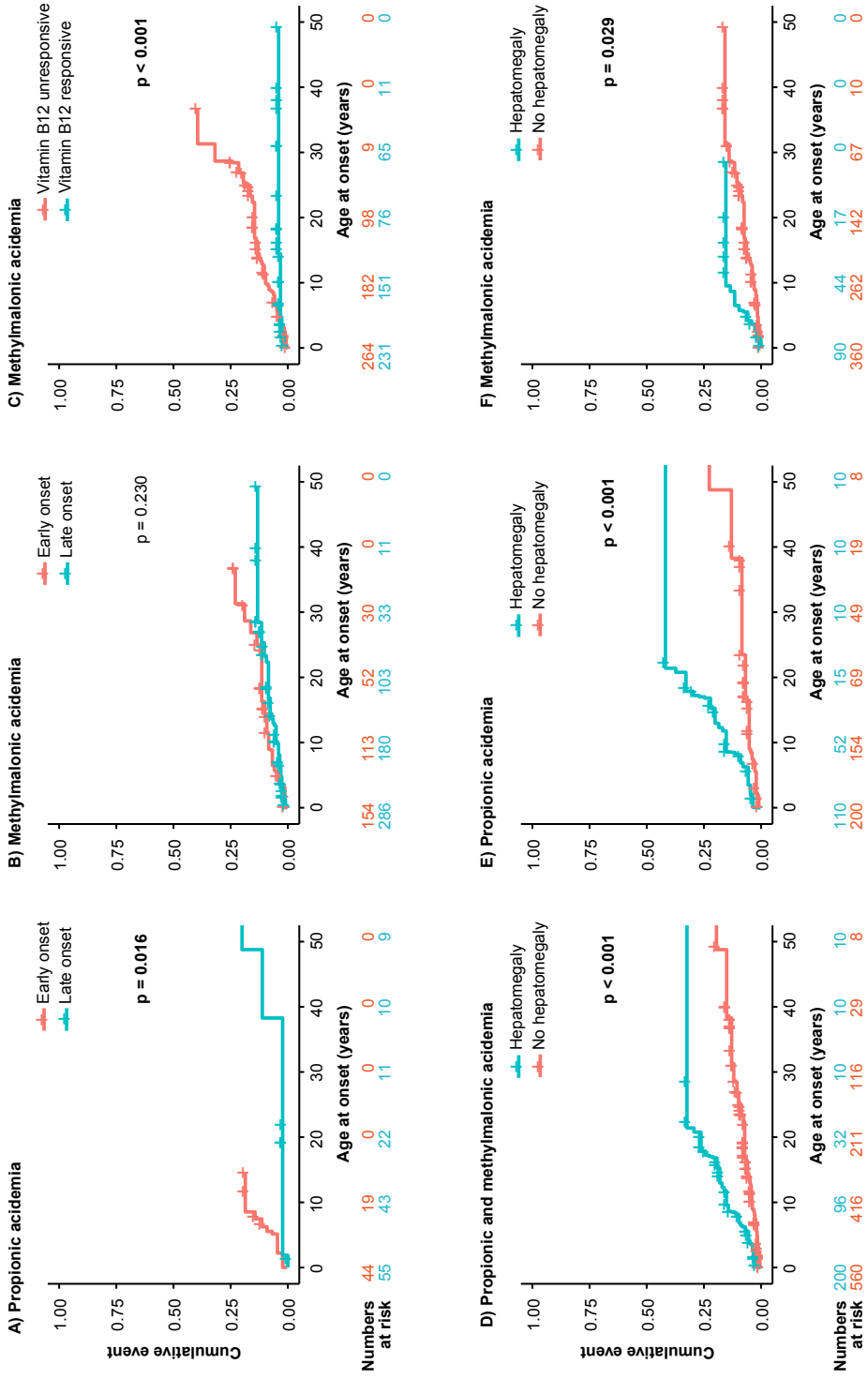
These findings are in line with previous reports. Although time to diagnosis is reduced in patients identified by NBS,⁹ NBS is unlikely to identify more than 59-72% of PA and MMA patients before the first symptomatic phase.⁸⁻⁹

Figure 2. Age at onset of mitochondrial complications with acute onset



Panel A depicts propionic acidemia, panel B depicts methylmalonic acidemia. The y-axis depicts the mitochondrial complications with acute onset, ordered on median age at onset. The x-axis depicts patient age in years, with a maximum of 35 years of age. For all ages > 35 years, the circles have been placed at 35 years. The black vertical lines depict the median age at onset. The filled circles and triangles depict the individual patient age at onset of a complication. Circles depict no vitamin B12 responsiveness, triangles depict vitamin B12 responsiveness of methylmalonic acidemia patients. Blue circles and triangles depict early onset, green circles and triangles depict late onset, orange circles and triangles depict diagnosis through family testing. Early onset: presentation \leq 28 days of life; Late onset: presentation >28 days of life.

Figure 3. Factors associated with increased risks for mitochondrial complications with acute onset



[Figure 3 continued] Kaplan-Meier plots wherein the y-axis depicts the cumulative percentage and the x-axis depicts patient age in years. Numbers at risk for the subgroups, indicating for how many complications the patients are at risk, are depicted below the panels, in corresponding colors. Panel A-B demonstrate late onset in blue versus early onset in orange for propionic acidemia (PA) in panel A and for methylmalonic acidemia (MMA) in panel B. Early onset: presentation ≤ 28 days of life; late onset: presentation > 28 days of life. Panel C demonstrates vitamin B12 responsiveness in blue versus vitamin B12 unresponsiveness in orange for MMA. Panel D-F depicts the association of the presence of hepatomegaly to other mitochondrial complications with acute onset in blue, versus no hepatomegaly in orange, in panel D for both PA and MMA, in panel E for PA and in panel F for MMA.

One study described no decreased AMD frequency, no better neurological outcome and no reduced frequency of long-term complications in PA patients,⁸ although another study found that PA patients identified by NBS had lower cardiac manifestations,⁹ but follow-up time in these patients was limited. In MMA patients, besides improved attainment of motor milestones and reduced manifestations of movement disorders in vitamin B12 unresponsive patients, NBS implementation did not result in other improved outcome parameters.⁹ Thus, as evidence supporting improved outcomes if treatment can be initiated in the asymptomatic phase is limited, despite reasonable consensus on therapeutic strategies for PA and MMA,¹⁹⁻²⁰ it is questionable whether the criterion regarding an accepted (effective) treatment for patients with recognized disease is met (WHO#2). As a consequence, it remains debatable whether the criteria requesting effectiveness (WHO#4) and benefits outweigh harm (WHO#10), are met (Supplemental Notes 1). We advocate that the (now limited) health gain of NBS can only be improved if treatment strategies are identified that can effectively prevent AMD, cognitive impairment and mitochondrial complications, such as innovative therapies aiming to increase enzyme activity.²⁰

Evaluation of NBS implementation for PA and MMA (WHO #9)

Insight in NBS efficacy is still limited, due to factors complicating proper evaluation, such as timing of evaluation. Follow-up time of the four studies describing the potential additional value of NBS for PA and MMA was relatively short, resulting in uncertainty when drawing conclusions.⁶⁻⁹ We propose that these countries reassess their NBS cohorts when a longer follow-up time is available. For the Netherlands, assuming a similar incidence in the NBS cohort as in the here presented cohort, but taking into account the slightly decreasing birth rate, it will take at least till 2050 before an NBS cohort similar in size and follow-up time as the pre-NBS cohort is available for evaluation. More timely evaluation can only be achieved by composing larger NBS cohorts through data sharing initiatives, within Europe or worldwide. Even if timing of evaluation is adequate, proper evaluation of the presumed effect of NBS remains challenging given the many factors that can influence the clinical course of PA and MMA. This includes genotypic factors as mutation type, residual enzyme activity and vitamin B12 responsiveness (MMA). Also, a high variability in clinical management existed between the different metabolic centers and metabolic physicians (data not shown). Next, compliance of parents and patients to clinical management, and disease insight could influence clinical outcomes. Moreover, pre-NBS cohorts are diagnosed and treated in the era before NBS cohorts, with NBS cohorts taking advantage of general advances in clinical care, and possibly increased insights and improved therapies for PA and MMA patients.

To aid evaluation of NBS efficacy, we suggest the five clinical outcome parameters here presented and we advocate the introduction of continuation and stop criteria. We propose that NBS for PA and MMA should be continued when it results in a statistically significant and clinically relevant reduction of AO due to the first symptomatic phase, and that it should be stopped otherwise. While based on our results, NBS may be unlikely to result in reduced

AMD frequency, improved cognitive function and reduced mitochondrial complications, these outcome parameters should be assessed to gain insight in the effects of improved treatment strategies. If NBS would unexpectedly result in improvement of these parameters, this would be a supportive argument to continue NBS. NBS evaluation should also include assessment of treatment-related complications, to gain knowledge regarding risks and harm of screening.

In NBS cohorts, patients in whom the disease is mild and who would not become symptomatic during infancy, could be detected as has been reported in Japan, where a ten times higher incidence of PA was found during preparatory studies for NBS implementation.²¹ These mildly affected patients will probably be treated according to the current treatment guidelines,¹⁹ inducing a risk for developing treatment-related complications. One could advocate that these patients should not be treated in order to prevent treatment-related complications. However, in our cohort, two PA patients presented at 48 and 56 years of age with cardiomyopathy as first presenting symptom,²² indicating that even in very mild, untreated patients, mitochondrial complications can still occur. It is presently unknown whether earlier initiation of adequate treatment could have prevented this complication. Even if this would alter the clinical course, it is questionable whether these patients should be exposed to life-long protein restriction, to prevent complications occurring well into adulthood. We consider overtreatment of mildly affected patients, that might or might not develop late complications,²¹⁻²² a serious risk of NBS.

Lessons learned from the pre-NBS cohort, to guide follow-up of NBS cohorts

We demonstrated that mitochondrial complications with acute onset can already develop before monitoring should be initiated according to recent guidelines¹⁹ and we thus propose to adapt these guidelines. Specifically, we suggest to assess renal function in *MUT* and *MMAB* patients from one year of age, to regularly check QTc intervals in PA and MMA patients starting at birth, and to maintain yearly cardiac ultrasounds and ophthalmologic assessments from six years onwards. Importantly, as we demonstrate that hepatomegaly is associated with the occurrence of other acute onset mitochondrial complications later in life, we advise to perform physical examination to check for hepatomegaly during every outpatient visit starting at birth, to be able to study the relevance of this finding. Lastly, we advocate awareness of all complications assessed in this cohort, including rarely described complications as exercise intolerance, acute psychosis, premature ovarian failure, pes planovalgus, gout and urolithiasis.

For surveillance and counseling of patients in NBS cohorts, we stress the importance to take into account disease severity. For MMA patients we demonstrated that vitamin B12 unresponsiveness increases the risk of a higher AMD frequency, mitochondrial complications and treatment-related complications. This is in line with previous reports, that demonstrate that vitamin B12 unresponsiveness is associated with a decreased survival rate in EO patients, a higher frequency of AMD, an increased rate of developmental delay in EO patients and an increased rate of disability.²³ In addition, a tendency towards an increased rate of chronic renal failure has been reported.²⁴ For PA patients, EO is associated with a higher risk for an AO of the first symptomatic phase, a higher AMD frequency, more severe cognitive impairment and more mitochondrial complications. While this still holds true for patients that are symptomatic before NBS results are available, presentation type will be unknown for PA patients diagnosed via NBS, complicating surveillance and counseling of these patients. This augments the need for systematic determination of PCC activity in PA

patients and illustrates the imminent need for a metabolic marker that can predict the risks for AMD frequency, cognitive function and mitochondrial complications.²⁵⁻²⁶

We could not identify specific genotype-phenotype correlations due to the variation of the identified mutations. However, we did note that whereas patients with *MMAB* type MMA are generally reported to be vitamin B12 unresponsive¹⁹, 6/7 of our *MMAB* patients were responsive. In 5 of these, we identified the *MMAB* c.556C>T missense mutation in either homozygous or heterozygous fashion (Table S2). We speculate that this mutation might be related to the observed vitamin B12 responsiveness of *MMAB* patients, but we cannot prove this hypothesis.

Limitations and strengths

We note a few limitations. First, due to the retrospective nature of this study and variable follow-up schedules, missing data could have affected the reliability of the analyses. We expect missing data to be random and consider it unlikely to have resulted in confounding. Nevertheless, to facilitate reliable analyses and conclusions on NBS effectivity, we advocate precise and structured prospective follow-up of NBS cohorts. Minimum requirements for evaluation are listed in Table S9. Centers participating in data-sharing initiatives should agree on the items to be recorded and on the timing of diagnostics studies (Table S9). Second, sample size of the sibling comparison is limited, hampering solid conclusions on the expected health gain of NBS for PA and MMA, but consolidating the urge for thorough assessment of NBS cohorts. The potential health gain might have been overestimated 1) due to the unknown number of EO patients that died undiagnosed, 2) since families with an index child are prepared for the diagnosis, and can minimize the risk for AMD more efficiently than families from individuals identified by NBS, 3) since calculations were performed with a potential overestimation of AO due to the first symptomatic phase, as we assumed that all observed brain imaging abnormalities were caused by the first symptomatic phase instead of being caused by AMD occurring later in life (and thus under treatment). Conversely, the potential health gain of NBS might have been underestimated as the clinical course between siblings may vary and it is not known whether the sibling diagnosed through family testing would have stayed in the same condition if diagnosed later in life.

Important strengths of our study are that we provide a comprehensive overview of a nationwide cohort spanning over four decades, by systematically assessing nearly all PA and MMA patients in the Netherlands in great detail. We designed five clinical outcome parameters to guide evaluation of implementation NBS and we provide an extensive description of a pre-NBS cohort to compare NBS cohorts with. Moreover, due to the systematic assessment of AMD, complications and risk factor analysis, we were able to establish recommendations regarding surveillance and counseling of NBS cohorts. Lastly, continuation and stopping criteria for NBS were provided, as well as minimum requirements for follow-up of NBS cohorts to facilitate data sharing initiatives.

CONCLUSION

The objective of NBS for PA and MMA in the Netherlands is to protect LO patients from irreversible neurological damage due to the first symptomatic phase. Implementation in the Netherlands may result in a reduction of AO due to the first symptomatic phase from 46% to 36-38%, if NBS results become available between day 11 and 21. We consider reduced AMD frequency, improved cognitive function and reduced mitochondrial and treatment-related complications unlikely given the currently available therapies.

REFERENCES

1. Kölker S, Garcia Cazorla A, Valayannopoulos V et al. The phenotypic spectrum of organic acidurias and urea cycle disorders. Part 1: the initial presentation. *J Inherit Metab Dis.* 2015;38:1041-1057.
2. Haijes HA, Jans JJM, Tas SY, Verhoeven-Duif NM, van Hasselt PM. Pathophysiology of propionic and methylmalonic acidemias. Part 1: Complications. *J Inherit Metab Dis.* 2019;42(5):730-744.
3. Sass JO, Hofmann M, Skladal D, Mayatepek E, Schwahn B, Sperl W. Propionic acidemia revisited: a workshop report. *Clin Pediatr (Phila).* 2004;43(9):837-43.
4. Leonard JV, Vijayaraghavan S, Walter JH. The impact of screening for propionic and methylmalonic acidemia. *Eur J Pediatr.* 2003;612:S21-4.
5. Hörster F, Kölker S, Loeber JG, Cornel MC, Hoffmann GF, Burgard P. Newborn screening programmes in Europe, arguments and efforts regarding harmonisation: focus on organic acidurias. *JIMD Rep.* 2016;32:105-115.
6. Dionisi-Vici C, Deodato F, Röschinger W, Rhead W, Wilcken B. "Classical" organic acidurias, propionic aciduria, methylmalonic aciduria and isovaleric aciduria: long-term outcome and effects of expanded newborn screening using tandem mass spectrometry. *J Inherit Metab Dis.* 2006;29(2-3):383-9.
7. Couce ML, Castiñeiras DE, Bóveda MD et al. Evaluation and long-term follow-up of infants with inborn errors of metabolism identified in an expanded newborn screening programme. *Mol Genet Metab.* 2011;104(4):470-5.
8. Grünert SC, Müllerleile S, de Silva L et al. Propionic acidemia: neonatal versus selective metabolic screening. *J Inherit Metab Dis.* 2012;35:41-49.
9. Heringer J, Valayannopoulos V, Lund AM et al. Impact of age at onset and newborn screening on outcome in organic acidurias. *J Inherit Metab Dis.* 2016;39(3):341-53.
10. Wilson JMG, Jungner G. Principles and practice of screening for disease. *Bol Oficina Sanit Panam.* 1968;65(4):281-393.
11. Andermann A, Blancquaert I, Beauchamps S, Déry V. Revisiting Wilson and Jungner in the genomic age: a review of screening criteria over the past 40 years. *Bulletin of the World Health Organization.* 2008;86(4):317-319.
12. Cornel MC, Rigter T, Weinreich SS et al. Newborn screening in Europe: expert opinion document. 2011.
13. Burgard P, Rupp K, Lindner M et al. Newborn screening programmes in Europe; arguments and efforts regarding harmonization. Part 2. From screening laboratory results to treatment, follow-up and quality assurance. *J Inherit Metab Dis.* 2012;35(4):613-25.
14. Cornel MC, Rigter T, Weinreich SS. A framework to start the debate on neonatal screening policies in the EU: an Expert Opinion Document. *Eur J Hum Gen.* 2014;22:12-17.
15. American College of Medical Genetics Newborn Screening Expert Group. Newborn screening: toward a uniform screening panel and system, executive summary. *Pediatrics.* 2006;117:S296-307.
16. Health Council of the Netherlands. Neonatal screening: new recommendations. The Hague: Health Council of the Netherlands. 2015; publication no. 2015/08.
17. Hörster F, Baumgartner MR, Viardot C et al. Long-term outcome in methylmalonic acidurias is influenced by the underlying defect (mut0, mut-, cblA, cblB). *Pediatr Res.* 2007;62(2):225-230
18. Ktena YP, Paul SM, Hauser NS, Sloan JL, Gropman A, Manoli I, Venditti CP. Delineating the spectrum of impairments, disabilities and rehabilitation needs in methylmalonic acidemia (MMA). *Am J Med Genet.* 2015;167A(9):2075-84.
19. Baumgartner MR, Hörster F, Dionisi-Vici C et al. Proposed guidelines for the diagnosis and management of methylmalonic and propionic acidemia. *Orphanet J Rare Dis.* 2014;9:130.
20. Haijes HA, van Hasselt PM, Jans JJM, Verhoeven-Duif NM. Pathophysiology of propionic and methylmalonic acidemias. Part 2: Treatment strategies. *J Inherit Metab Dis.* 2019;42(5):745-761.
21. Yorifuji T, Kawai M, Muroi J et al. Unexpectedly high prevalence of the mild form of propionic acidemia in Japan: presence of a common mutation and possible clinical implications. *Hum Genet.* 2002;111(2):161-5.
22. Riemersma M, Hazebroek MR, Helderma-van den Enden ATJM et al. Propionic acidemia as a cause of adult-onset dilated cardiomyopathy. *Eur J Hum Genet.* 2017;25(11):1195-1201.
23. Hörster F, Garbade SF, Zwickler T et al. Prediction of outcome in isolated methylmalonic acidurias: combined use of clinical and biochemical parameters. *J Inherit Metab Dis* 2009;32:630-639.
24. Kölker S, Valayannopoulos V, Burlina AB et al. The phenotypic spectrum of organic acidurias and urea cycle disorders. Part 2: the evolving clinical phenotype. *J Inherit Metab Dis* 2015;38:1059-1074.
25. Manoli I, Sysol JR, Epping MW et al. FGF21 underlies a hormetic response to metabolic stress in methylmalonic acidemia. *JCI Insight* 2018;3(23).
26. Molema F, Jacobs EH, Onkenhout W, Schoonderwoerd GC, Langendonk JG, Williams M. Fibroblast growth factor 21 as a biomarker for long-term complications in organic acidemias. *J Inherit Metab Dis* 2018;41(6):1179-1187.

SUPPLEMENTAL DATA

Supplemental Notes 1. Screening criteria

1968, Wilson and Jungner, ten criteria to guide selection of conditions suitable for screening

- (1) The condition sought should be an important health problem.
- (2) There should be an accepted treatment for patients with recognized disease.
- (3) Facilities for diagnosis and treatment should be available.
- (4) There should be a recognizable latent or early symptomatic stage.
- (5) There should be a suitable test or examination.
- (6) The test should be acceptable to the population.
- (7) The natural history of the condition, including development from latent to declared disease, should be adequately understood.
- (8) There should be an agreed policy on whom to treat as patients.
- (9) The cost of case-finding (including diagnosis and treatment of patients diagnosed) should be economically balanced in relation to possible expenditure on medical care as a whole.
- (10) Case-finding should be a continuing process and not a "once and for all" project.

2008, World Health Organization, ten criteria additional to the Wilson and Jungner criteria

- (1) The screening programme should respond to a recognized need.
- (2) The objectives of screening should be defined at the outset.
- (3) There should be a defined target population.
- (4) There should be scientific evidence of screening programme effectiveness.
- (5) The programme should integrate education, testing, clinical services and programme management.
- (6) There should be quality assurance, with mechanisms to minimize potential risks of screening.
- (7) The programme should ensure informed choice, confidentiality and respect for autonomy.
- (8) The programme should promote equity and access to screening for the entire target population.
- (9) Programme evaluation should be planned from the outset.
- (10) The overall benefits of screening should outweigh the harm.

Supplemental Notes 2. Definition of grouped outcome parameters

Definition of "Adverse outcome (AO) of the first symptomatic phase" as clinical outcome parameter

No AO:	No basal ganglia hyperintensities, or white matter abnormalities or movement disorder
Mild AO:	Basal ganglia hyperintensities or white matter abnormalities or movement disorder that can be most likely attributed to the first symptomatic phase, but not wheelchair-bound
Severe AO:	Basal ganglia hyperintensities or white matter abnormalities or movement disorder, wheelchair-bound due to movement disorders that most likely arose due to the first symptomatic phase
Death:	Death during or due to the first symptomatic phase

Definition of "AMD frequency" as clinical outcome parameter

None:	No episode of AMD during first four years of life
Mild:	$>0.0 \leq 0.5$ AMD/PY during first four years of life
Moderate:	$>0.5 \leq 1.0$ AMD/PY during first four years of life
Severe:	$>1.0 \leq 2.0$ AMD/PY during first four years of life
Very severe:	>2.0 AMD/PY during first four years of life
Death:	Death during or due to AMD, at any moment in life
Not assessed (NA):	If death during or due to first presentation

Definition of "Cognitive function" as clinical outcome parameter

Group 1:	IQ >90 or regular education
Group 2:	IQ 60-90 or special education
Group 3:	IQ <60 or no education
Not assessed (NA):	Last moment of follow-up <4 years of age

Definition of "Mitochondrial complications" as clinical outcome parameter

Twenty-one complications considered to be potentially caused by mitochondrial failure based on an extensive

literature review² were included: hepatomegaly, epilepsy, cardiomyopathy, optic atrophy, pancreatitis, renal failure, sensorineural hearing loss, acute psychosis, stroke-like episodes, prolonged QTc interval, premature ovarian insufficiency, exercise intolerance, autism, feeding disorders, muscular hypotonia, constipation, attention deficit hyperactive disorder, anemia, leukopenia, thrombocytopenia and pancytopenia.

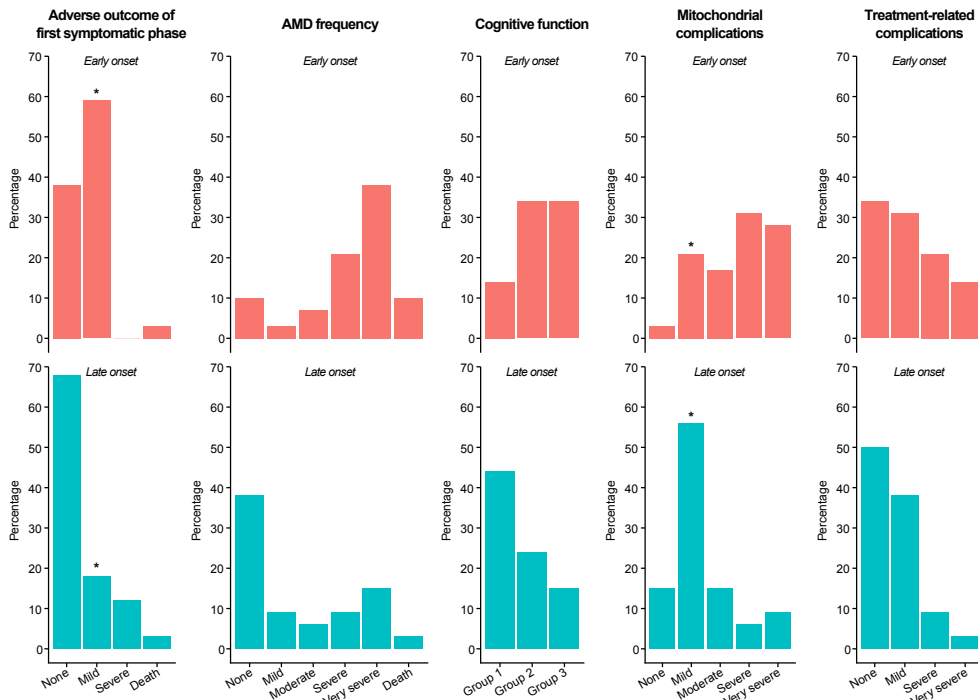
Severity is based on the number of complications recorded at the last moment of follow-up, as follows:

	0-12 year	13-18 year	19-24 year	>25 years
None:	0	0	0	0
Mild:	1-2	1-4	1-6	1-8
Moderate:	3-4	5-6	7-8	9-10
Severe:	5-6	7-8	9-10	11-12
Very severe:	≥7	≥9	≥11	≥13
Death:	Death due to mitochondrial complication			
Not assessed (NA):	If death during or due to first presentation			

Definition of “Treatment-related complications” as clinical outcome parameter

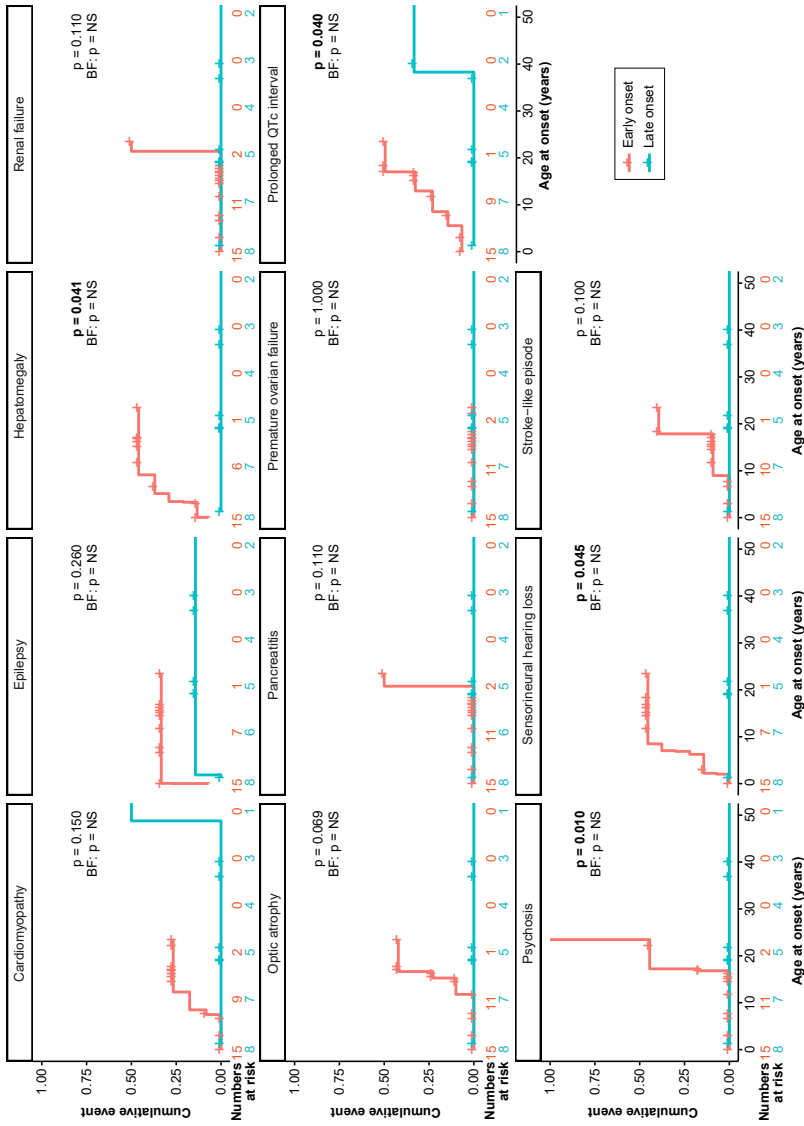
None:	No decreased BMD, no growth retardation, no obesity
Mild:	1 of the following: decreased BMD, growth retardation, obesity
Severe:	2 of the following: decreased BMD, growth retardation, obesity
Very severe:	Decreased BMD and growth retardation and obesity
Not assessed (NA):	If death during or due to first presentation

Figure S1. Grouped outcome parameters according to presentation type



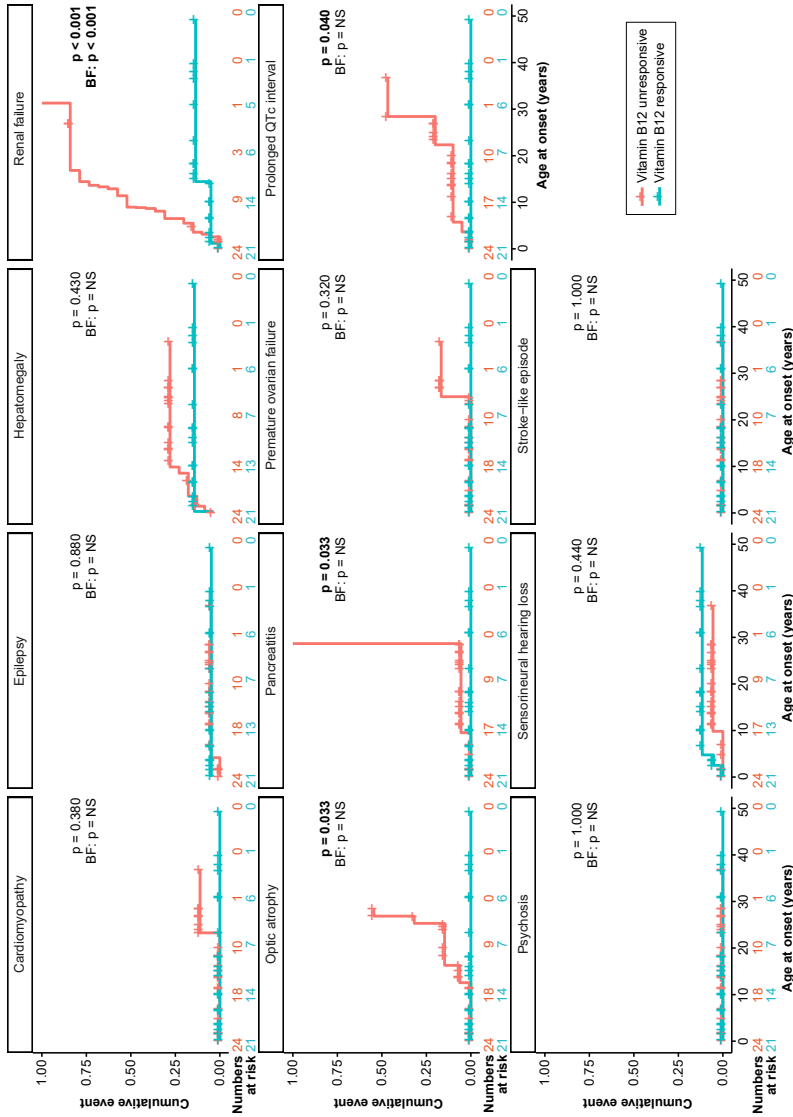
Visual representation of Table 2. Categories of the outcome parameters are depicted on the x-axis, percentages are depicted on the y-axis. Early onset (presentation ≤28 days of life) is depicted in orange, late onset (presentation >28 days of life) is depicted in blue. Statistical significance was determined by Fisher’s exact tests. All p-values were adjusted according to the Bonferroni method. Adjusted p-values < 0.05 were considered statistically significant and are depicted with bold asterisks, as in Table 2.

Figure S2. Early onset presentation in PA tends to be an independent predictor for four mitochondrial complications with acute onset



Kaplan-Meier plots wherein the y-axis depicts the cumulative percentage and the x-axis depicts patient age in years. The panels demonstrate the different mitochondrial complications with acute onset, for patients with late onset presentation in blue versus patients with early onset presentation in orange. Numbers at risk, indicating the number of patients at risk for a certain complication are depicted below the panels, in corresponding colors. Early onset: presentation ≤ 28 days of life; Late onset: presentation >28 days of life. All p-values were adjusted according to the Bonferroni method. Adjusted p-values < 0.05 were considered statistically significant and are depicted in bold. Abbreviations: BF: Bonferroni; NS: not significant.

Figure S3. Vitamin B12 unresponsiveness in MMA tends to be an independent predictor for three mitochondrial complications with acute onset and is a significant predictor for the occurrence of renal failure



Kaplan-Meier plots wherein the y-axis depicts the cumulative percentage and the x-axis depicts patient age in years. The panels demonstrate the different mitochondrial complications with acute onset, for vitamin B12 responsive patients in blue versus vitamin B12 unresponsive patients in orange. Numbers at risk, indicating the number of patients at risk for a certain complication are depicted below the panels, in corresponding colors. All p-values were adjusted according to the Bonferroni method. Adjusted p-values < 0.05 were considered statistically significant and are depicted in bold. Abbreviations: BF: Bonferroni; NS: not significant.

Table S1. Comparison of baseline characteristics and outcome parameters of patients identified through family testing and their index siblings

	P1.1	P1.2	P2.1	P2.2	P3.1	P3.2	P4.1	P4.2	P5.1	P5.2	P6.1	P6.2	P6.3
Gene	PCCA	PCCA	PCCB	PCCB	PCCB	PCCB	PA, uncl	PA, uncl	PA, uncl	PA, uncl	PA, uncl	PA, uncl	PA, uncl
Sex	M	F	M	M	M	M	F	M	M	F	F	M	M
Age at diagnosis	Day 15	Day 0	0.7 y	Day 2	Day 3	Day 0	Day 18	Day 1	5.0 y	2.0 y	Day 8	Day 4	Day 1
Age at death (y)	18.4	8.6	19.1	19.0	7.0	5.6	12.1	9.7	37.0	33.4	2.9	1.4	11.4
Age last follow-up (y)	EO	Family	LO	Family	EO	Family	EO	Family	LO	Family	EO	Family	Family
AO first sympt. phase	Mild	No	Severe	No	Mild	No	Mild	Mild	No	No	Mild	Mild	Mild
AMD irrefractory	Severe	Severe	Death	Stable	Death	Very s.	Death	Severe	Stable	Stable	Death	Death	Very s.
Cognitive function	Gr. 3	Gr. 3	Gr. 3	Gr. 1	NA	Gr. 3	Gr. 2	Gr. 3	Gr. 1	Gr. 1	NA	NA	Gr. 3
Mitochondrial compl.	Very s.	Death	Moder.	Mild	Very s.	Severe	Severe	Very s.	None	Mild	Very s.	Very s.	Very s.
Treatment-rel. compl.	Very s.	Mild	Mild	Mild	None	Mild	Very s.	None	None	None	None	None	Mild

	P7.1	P7.2	P8.1	P8.2	P9.1	P9.2
Gene	MUT	MUT	MUT	MUT	MMAB	MMAB
Sex	M	M	M	F	F	M
Age at diagnosis	Day 3	Day 0	0.2 y	Day 0	3.9 y	1.6 y
Age at death (y)	13.9	1.7	18.5	13.7	18.3	16.1
Age last follow-up (y)	EO	Family	LO	Family	LO	Family
Presentation type	No	No	No	No	Yes	Yes
AO first sympt. phase	Mild	Mild	Mild	Mild	Severe	No
AMD irrefractory	Severe	NA	Severe	Severe	Stable	Stable
Cognitive function	Group	NA	Group	Group	Group	Group
Mitochondrial compl.	3	Moder.	3	2	1	1
Treatment-rel. compl.	Very s.	Mild	Very s.	Mild	Mild	None

Early onset: presentation ≤28 days of life; Late onset: presentation >28 days of life. Cognitive function group 1: IQ >90 or regular education, group 2: IQ 60-90 or special education, group 3: IQ <60 or no education. Abbreviations: AMD: acute metabolic decompensation; AO first sympt. phase: Adverse outcome of the first symptomatic phase; compl: complications; EO: early onset; Family: family testing; F: female; Gr.: group; LO: late onset; M: male; NA: Not assessed; Very s.: very severe; y: years.

Table S2. All mutations detected in PA and MMA related genes in the Dutch patient cohort

Gene	Mutation (c.)	Mutation (p.)	Mutation type	Reported	Alleles	Origin	Remarks
PCCA	c.625G>C	p.Ala209Pro	Missense/Nonsense	No	1	Dutch	
PCCA	c.923dup	p.Leu308Phefs*35	Duplication	No	1	Dutch	
PCCA	c.1409T>G	p.Leu470Asg	Missense/Nonsense	No	6	Moroccan	2 sibs HO, not reported consanguine; 1 ind.HO, consanguine, not knowingly related to the 2 sibs
PCCA	c.2077A>C	p.Met693Leu	Missense/Nonsense	No	1	Dutch	
PCCA	Exon 2 del.		Gross deletion	No	1	Dutch	
PCCA	Exon 5 and 6 del.		Gross deletion	No	1	Dutch	
PCCA	Exon 10 del.		Gross deletion	No	1	Dutch	
PCCA	c.1900-1G>A		Splicing	Yang et al. 2004 ¹	2	Afghan	HO, consanguine
PCCA	c.2127delT	p.Val710Cysfs*43	Small deletion	Campeau et al. 1999 ²	1	Dutch	
PCCB	c.644G>C	p.Gly222Ayg	Missense/Nonsense	No	2	Turkish	HO, consanguine
PCCB	c.671C>T	p.Ala224Val	Missense/Nonsense	No	1	Dutch	
PCCB	c.703A>C	p.Thr235Pro	Missense/Nonsense	No	4	Moroccan	2 sibs HO, not reported consanguine
PCCB	c.883_885del	p.Phe295del	Small deletion	No	1	Dutch	
PCCB	c.1127G>A	p.Arg376His	Missense/Nonsense	No	4	Turkish	2 sibs HO, consanguine
PCCB	c.337C>T	p.Arg113*	Missense/Nonsense	Brosch et al. 2008 ³	2	Turkish	HO, consanguine
MUT	c.623_624del		Small deletion	No	1	Dutch	
MUT	c.730A>C	p.Gln213His	Missense/Nonsense	No	2	Dutch	HO, consanguinity unknown
MUT	c.1022dupA	p.Asn341fs*	Duplication	No	1	Surinamese	
MUT	c.1280G>T	p.Gly427Val	Missense/Nonsense	No	2	Egyptian	HO, consanguine
MUT	c.1311_1312insA	p.Val438Serfs*3	Small insertion	No	4	Turkish/ Dutch	1 ind. HO, consanguine; 1 ind.HO, consanguinity unknown, not knowingly related
MUT	c.1690G>T	p.Glu564*	Missense/Nonsense	No	2	Turkish	HO, consanguine
MUT	c.1962_1963delTC	p.Arg655*	Missense/Nonsense	No	4	Turkish	2 sibs HO, consanguine
MUT	c.2078delG	p.Gly693Aspfs*12	Small deletion	No	2	Moroccan	HO, consanguine
MUT	c.322C>T	p.Arg108Cys	Missense/Nonsense	Worgan et al. 2006 ⁴	4	Dutch	HE, 2 sibs; 2 ind., not knowingly related
MUT	c.454C>T	p.Arg152*	Missense/Nonsense	Martinez et al. 2005 ⁵	3	Turkish/ Dutch	1 ind.HO, consanguine; 1 ind.HE, not knowingly related
MUT	c.654A>C	p.Gln218His	Missense/Nonsense	Fuchshuber et al. 2000 ⁶	6	Dutch	2 ind.HO, 2 ind.HE, not reported
MUT	c.655A>T	p.Asn219Tyr	Missense/Nonsense	Acquaviva et al. 2005 ⁷	7	Turkish/ Dutch	consanguine, not knowingly related
MUT	c.1106G>A	p.Arg369His	Missense/Nonsense	Janata et al. 1997 ⁸	3	Turkish/ Dutch	2 sibs HO (1 consanguine); 3 ind. (2 sibs) HE, not knowingly related
MUT	c.1160C>T	p.Thr387Ile	Missense/Nonsense	Dündar et al. 2012 ⁹	2	Syrian	1 ind.HO, consanguine; 1 ind.HE, not knowingly related
MUT	c.1531C>T	p.Arg511*	Missense/Nonsense	Acquaviva et al. 2005 ⁷	1	Dutch	HO, consanguine
MUT	c.1677-1G>C		Splicing	Acquaviva et al. 2005 ⁷	1	Dutch	
MUT	c.2150G>T	p.Gly717Val	Missense/Nonsense	Crane et al. 1992 ¹⁰	1	Surinamese	

MMAA	c.202C>T	p.Gln68*	Missense/Nonsense	No	1	Dutch	2 siblings, 1 cousin, HO, consanguine
MMAA	c.455del	p.Pro152Leufs*9	Small deletion	No	6	Turkish	2 ind.HO (1 consanguine); 1 HE, not
MMAA	c.433C>T	p.Arg145*	Missense/Nonsense	Yang et al. 2004 ¹	5	Dutch	knowingly related
MMAA	c.733+1G>A		Splicing	Lerner-Ellis et al. 2004 ¹¹	4	Dutch	1 ind.HO (not reported consanguine); 2 ind.HE, not knowingly related
MMAB	c.556C>T	p.Arg186Trp	Missense/Nonsense	Lerner-Ellis et al. 2006 ¹²	5	Dutch	1 ind.HO (not reported consanguine); 3 ind.HE (2 siblings), patients not knowingly related (except the siblings)
MMAB	c.565_577del	p.Cys189A _{rgfs} *	Small deletion	No	1	Hindi	
MMAB	c.655T>C	p.Tyr219His	Missense/Nonsense	No	1	Hindi	
MMAB	c.569G>A	p.Arg190His	Missense/Nonsense	Lerner-Ellis et al. 2006 ¹²	1	Dutch	
MMAB	c.197-1G>A		Splicing	Lerner-Ellis et al. 2006 ¹²	2	Dutch	HE, 2 siblings
MMAB	c.700C>T	p.Gln234*	Missense/Nonsense	Lerner-Ellis et al. 2006 ¹²	2	Dutch	HE, 2 ind., not knowingly related

Mutation (c.) depicts the genetic change in the DNA coding sequence, mutation (p.) depicts the resulting change in the protein coding sequence. HO: homozygous, HE: heterozygous. In one patient with a mutation in PCCA, no other mutation at the other allele was identified. References:

1. Yang X, Sakamoto O, Matsubara Y et al. Mutation spectrum of the PCCA and PCCB genes in Japanese patients with propionic acidemia. *Mol Genet Metab* 2004;81(4):335-42
2. Campeau E, Dupuis L, León-Del-Río A, Gravel R. Coding sequence mutations in the alpha subunit of propionyl-CoA carboxylase in patients with propionic acidemia. *Mol Genet Metab* 1999;67(1):11-22.
3. Brosch S, Rauffeisen A, Baur M, Michels L, Trefz FK, Pfister M. Propionic acidemia and sensorineural hearing loss: is there a connection at the molecular genetics level? *HNO* 2008;56(1):37-42.
4. Worgan LC, Niles K, Tirone JC et al. Spectrum of mutations in mut methylmalonic acidemia and identification of a common Hispanic mutation and haplotype. *Hum Mutat* 2006;27(1):31-43.
5. Martínez MA, Rincón A, Desviat LR, Merinero B, Ugarte M, Pérez B. Genetic analysis of three genes causing isolated methylmalonic acidemia: identification of 21 novel allelic variants. *Mol Genet Metab* 2005;84(4):317-25.
6. Fuchshuber A, Mucha B, Baumgartner ER, Völlmer M, Hildebrandt F. Mut0 methylmalonic acidemia: eleven novel mutations of the methylmalonyl-CoA mutase including a deletion-insertion mutation. *Hum Mutat*. 2000;16(2):179.
7. Acquaviva C, Benoist JF, Pereira S, Callebaut I, Koskas T, Porquet D, Elion J. Molecular basis of methylmalonyl-CoA mutase apoenzyme defect in 40 European patients affected by mut(0) and mut- forms of methylmalonic acidemia: identification of 29 novel mutations in the MUT gene. *Hum Mutat*. 2005;25(2):167-76.
8. Janata J, Kogekar N, Fenton WA. Expression and kinetic characterization of methylmalonyl-CoA mutase from patients with the mut- phenotype: evidence for naturally occurring interallelic complementation. *Hum Mol Genet* 1997;6(9):1457-64.
9. Dündar H, Özgül RK, Güzel-Ozantürk A et al. Microarray based mutational analysis of patients with methylmalonic acidemia: identification of 10 novel mutations. *Mol Genet Metab* 2012;106(4):419-23.
10. Crane AM, Martin LS, Valle D, Ledley FD. Phenotype of disease in three patients with identical mutations in methylmalonyl-CoA mutase. *Hum Genet*. 1992;89(3):259-64.
11. Lerner-Ellis JP, Dobson CM, Wai T et al. Mutations in the MMAA gene in patients with cblIA disorder of vitamin B12 metabolism. *Hum Mutat*. 2004;24(6):509-16.
12. Lerner-Ellis JP, Gradinger AB, Watkins D et al. Mutation and biochemical analysis of patients belonging to the cblB complementation class of vitamin B12-dependent methylmalonic aciduria. *Mol Genet Metab* 2006;87(3):219-25.

Table S3. Pregnancy, delivery and birth parameters

	Propionic acidemia (n = 31)	Methylmalonic acidemia (n = 45)	P-val.	Bonf. corr.
Maternal health problems during pregnancy	n = 2; 6%	n = 3; 7%	1.000	NS
Delivery via caesarean section	n = 4; 13%	n = 2; 4%	0.218	NS
Gemelli	n = 1; 3%	n = 1; 2%	1.000	NS
Gestational age				
Prematurity (<36 weeks)	n = 0; 0%	n = 5; 11%	0.075	NS
Serotinity (>42 weeks)	n = 0; 0%	n = 5; 11%	0.075	NS
Abnormal APGAR scores	n = 2; 6%	n = 4; 9%	1.000	NS
Birth weight (median ± SD; (n))	0.38 ± 1.61 SDS (23)	-1.48 ± 1.19 SDS (32)	<0.001	<0.001
Birth weight < -2 SDS	n = 2; 9% (23)	n = 10; 31% (32)	0.055	NS

Student's t-tests were performed for quantitative data and Fisher's exact tests were performed for qualitative data. All p-values were adjusted according to the Bonferroni method. Adjusted p-values < 0.05 were considered statistically significant and are depicted in bold. Abbreviations: NS: not significant; SDS: standard deviation score.

Table S4. Symptoms and signs, laboratory tests and interventions during the first symptomatic phase

	Early onset (n = 29)	Late onset (n = 34)	P-val.	Bonf. corr.
Symptoms and signs				
Lethargy	n = 21; 72%	n = 19; 56%	0.199	NS
Anorexia	n = 20; 69%	n = 18; 53%	0.211	NS
Vomiting	n = 6; 21%	n = 26; 76%	<0.001	<0.001
Hypotonia	n = 14; 48%	n = 12; 35%	0.318	NS
Dehydration	n = 11; 38%	n = 8; 24%	0.275	NS
Kussmaul breathing	n = 9; 31%	n = 10; 29%	1.000	NS
Tachypnea	n = 9; 31%	n = 2; 6%	0.017	NS
Weight loss	n = 5; 17%	n = 5; 15%	1.000	NS
Hypothermia	n = 7; 24%	n = 1; 3%	0.019	NS
Coma	n = 1; 3%	n = 5; 15%	0.205	NS
Failure to thrive	n = 0; 0%	n = 6; 18%	0.027	NS
Global develop. delay	n = 0; 0%	n = 3; 9%	0.243	NS
Laboratory tests				
Glucose	Median ± SD [Min-Max] (N) 5.5 ± 6.2 [1.6 – 25.4] (22)	Median ± SD [Min-Max] (N) 7.2 ± 7.6 [1.2 – 34.0] (23)	0.465	NS
pH	7.33 ± 0.14 [6.89 – 7.43] (26)	7.28 ± 0.17 [6.81 – 7.42] (27)	0.179	NS
pCO ₂	28.1 ± 14.0 [12.0 – 62.3] (23)	18.7 ± 12.5 [10.0 – 60.0] (22)	0.023	NS
Bicarbonate	16.1 ± 6.3 [3.2 – 24.9] (25)	7.5 ± 6.7 [2.8 – 23.0] (22)	0.006	NS
Base excess	-9.0 ± 8.5 [-30.0 – 0.1] (23)	-19.1 ± 8.9 [-28.2 – -1.0] (25)	0.052	NS
Lactate	2.2 ± 1.2 [1.0 – 6.0] (19)	2.2 ± 2.0 [0.7 – 6.8] (19)	0.353	NS
Ammonia	934 ± 629 [170 – 2767] (20)	137 ± 104 [49 – 400] (19)	<0.001	<0.001
Haemoglob.	9.1 ± 1.7 [5.8 – 13.7] (22)	6.9 ± 1.0 [5.2 – 9.0] (25)	<0.001	<0.001
Thrombocyt.	*10 ⁹ /L 292 ± 103 [6 – 358] (22)	321 ± 158 [98 – 892] (22)	0.027	NS
Leukocyt.	*10 ⁹ /L 6.2 ± 4.8 [1.8 – 21.0] (23)	8.0 ± 7.4 [0.8 – 33.6] (25)	0.108	NS
Interventions				
Intensive care admission	n = 18; 62%	n = 15; 44%	0.208	NS
Mechanical ventilation	n = 13; 45%	n = 10; 29%	0.294	NS
Dialysis (any type) due to hyperammonemia	n = 11; 38%	n = 0; 0%	<0.001	<0.001

Early onset: presentation ≤28 days of life; Late onset: presentation >28 days of life. Student's t-tests were performed for quantitative data and Fisher's exact tests were performed for qualitative data. All p-values were adjusted according to the Bonferroni method. Adjusted p-values < 0.05 were considered statistically significant and are depicted in bold. Abbreviations: Min.: minimum value; Max.: maximum value; NS: not significant.

Table S5. Adverse outcome due to the first symptomatic phase

	Propionic acidemia (n = 31)			Methylmalonic acidemia (n = 45)		P-val.	Bonf. corr.
Disease type							
No AO	n = 14; 45%			n = 26; 58%		0.352	NS
Mild AO	n = 15; 48%			n = 15; 33%		0.235	NS
Severe AO	n = 1; 3%			n = 3; 7%		0.641	NS
Death due to AO	n = 1; 3%			n = 1; 2%		1.000	NS
Presentation type	Early onset (n = 15)	Late onset (n = 8)	P-val.	Early onset (n = 14)	Late onset (n = 26)	P-val.	
No AO	n = 4; 27%	n = 6; 75%	0.039	n = 7; 50%	n = 17; 65%	0.500	NS; NS
Mild AO	n = 10; 67%	n = 1; 13%	0.027	n = 7; 50%	n = 5; 19%	0.071	NS; NS
Severe AO	n = 0; 0%	n = 1; 13%	0.348	n = 0; 0%	n = 3; 12%	0.539	NS; NS
Death due to AO	n = 1; 7%	n = 0; 0%	1.000	n = 0; 0%	n = 1; 4%	1.000	NS; NS
Vitamin B12 responsiveness				Vitam. B12 unresp. (n = 24)	Vitam. B12 resp. (n = 21)	P-val.	
No AO				n = 12; 50%	n = 14; 67%	0.366	NS
Mild AO				n = 11; 46%	n = 4; 19%	0.068	NS
Severe AO				n = 1; 4%	n = 2; 10%	0.592	NS
Death due to AO				n = 0; 0%	n = 1; 5%	0.467	NS

Early onset: presentation ≤ 28 days of life; Late onset: presentation > 28 days of life. Statistical significance was determined by performing Fisher's exact tests. All p-values were adjusted according to the Bonferroni method. Adjusted p-values < 0.05 were considered statistically significant. Abbreviations: AO: adverse outcome; NS: not significant.

Table S6. Acute metabolic decompensations

	Propionic acidemia (n = 31) n = ; median ± SD /PY [range]	Methylmalonic acidemia (n = 45) n = ; median ± SD /PY [range]	P-val.	Bonf. corr.
Total	394; 0.7 ± 1.6 [0.0 – 7.3]	568; 0.4 ± 1.1 [0.0 – 4.7]	0.257	NS
Early onset	293; 1.2 ± 1.3 [0.0 – 4.2]	254; 0.9 ± 1.4 [0.0 – 4.7]	0.604	NS
Late onset	22; 0.2 ± 0.2 [0.0 – 0.7]	242; 0.2 ± 0.9 [0.0 – 3.5]	0.032	NS
Family testing	79; 0.8 ± 2.7 [0.0 – 7.3]	72; 0.6 ± 1.1 [0.0 – 2.8]	0.327	NS
Vitamin B12 unresp.		504; 1.0 ± 1.1 [0.0 – 4.7]		
Vitamin B12 resp.		64; 0.1 ± 0.8 [0.0 – 3.5]	0.001	0.001
Age				
<1 years	55; 1.0 ± 2.0 [0.0 – 7.0]	38; 0.0 ± 1.4 [0.0 – 5.0]	0.032	NS
1-3 years	136; 1.0 ± 2.0 [0.0 – 8.3]	156; 0.3 ± 1.7 [0.0 – 6.7]	0.485	NS
4-11 years	146; 0.3 ± 0.9 [0.0 – 3.5]	206; 0.1 ± 1.0 [0.0 – 5.0]	0.940	NS
12-17 years	40; 0.0 ± 0.5 [0.0 – 2.0]	85; 0.0 ± 0.8 [0.0 – 4.0]	0.483	NS
>18 years	17; 0.0 ± 0.4 [0.0 – 1.8]	73; 0.0 ± 1.2 [0.0 – 9.9]	0.145	NS
Admission duration				
1 – 3 days	110; 28%	207; 36%	0.006	0.026
4 – 7 days	143; 36%	164; 29%	0.017	NS
8 – 14 days	80; 20%	96; 17%	0.203	NS
≥ 15 days	51; 13%	45; 8%	0.012	0.047
NA	10; 3%	56; 10%		
ICU admission	23; 5.8%	18; 3.1%	0.051	NS
Triggers				
Upper RTI	114; 29%	154; 27%	0.559	NS
Unknown	77; 20%	141; 25%	0.060	NS
Gastro-enteritis	75; 19%	111; 20%	0.868	NS
Feeding problems	16; 4%	50; 9%	0.004	0.033
Bacterial infection	24; 6%	32; 6%	0.781	NS
Constipation	39; 10%	4; 1%	<0.001	<0.001
Chronic instability	13; 3%	9; 2%	0.123	NS
Protein overload	4; 1%	4; 1%	0.723	NS
Other	16; 4%	11; 2%	0.072	NS
NA	16; 4%	52; 9%		
AMD frequency				
None	7; 23%	14; 31%	0.448	NS
Mild	2; 6%	2; 4%	1.000	NS
Moderate	1; 3%	3; 7%	0.641	NS
Severe	6; 19%	6; 13%	0.532	NS
Very severe	8; 26%	10; 22%	0.787	NS
Death	5; 16%	1; 2%	0.038	NS
NA	2; 6%	9; 20%		

Early onset: presentation ≤28 days of life; Late onset: presentation >28 days of life. Student's t-tests were performed for quantitative data and Fisher's exact tests were performed for qualitative data. All p-values were adjusted according to the Bonferroni method. Adjusted p-values < 0.05 were considered statistically significant and are depicted in bold. Abbreviations: AMD: Acute metabolic decompensation; ICU: intensive care unit; NA: not assessed; NS: not significant; PY: patient year; RTI: respiratory tract infection.

Table S7. Complications with potential mitochondrial etiology

Mitochondrial pathophysiology ^a		Propionic acidemia (n = 31)		Methylmalonic acidemia (n = 45)		P-val.	Bonf. corr.
		This cohort	Lit.	This cohort	Lit.		
Mitochondrial complications during first presentation							
Basal ganglia hyp.	Probably	n = 10; 32%	22%	n = 8; 18%	28%	0.175	NS
White matter lesions		n = 6; 19%	39%	n = 8; 18%	32%	1.000	NS
Complications related to first presentation							
Cerebral atrophy		n = 13; 42%		n = 11; 24%		0.135	NS
Movement disorders		n = 10; 32%	16%	n = 14; 31%	32%	1.000	NS
Psychomotor retardation		n = 19; 61%	49%	n = 24; 53%	53%	0.638	NS
Cognitive dysfunction		n = 20; 65%	69%	n = 19; 42%	58%	0.066	NS
Group 1: IQ >90/regular ed.		n = 7; 23%		n = 17; 38%		0.212	NS
Group 2: IQ 60-90/spec. ed.		n = 7; 23%		n = 13; 29%		0.604	NS
Group 3: IQ <60/no ed.		n = 13; 42%		n = 6; 13%		0.007	0.021
NA		n = 4; 13%		n = 9; 20%			
Mitochondrial complications with acute onset							
Hepatomegaly or hyperechog. liver	Probably	n = 11; 35%	78%	n = 14; 31%	33%	0.805	NS
Epilepsy	Probably	3.3 y (0.1–57.1) n = 7; 23%	23%	0.4 y (0.0–9.9) n = 2; 4%	13%	0.027	NS
Cardiomyopathy	Probably	0.0 y (0.0–6.3) n = 7; 23%	14%	2.1 y (0.0–4.2) n = 1; 2%	5%	0.007	NS
Optic atrophy	Probably	8.5 y (7.5–56.3) n = 4; 13%	5%	23.3 y n = 4; 9%	6%	0.709	NS
Pancreatitis	Probably	15.9 y (11.8–16.7) n = 1; 3%	5%	20.8 y (12.6–26.9) n = 2; 4%	4%	1.000	NS
Renal failure	Possibly	20.8 y n = 1; 3%	1%	19.1 y (9.5–28.7) n = 20; 44%	29%	<0.001	<0.001
Sensorineural hearing loss	Possibly	21.4 y n = 6; 19%	4%	8.9 y (1.2–31.3) n = 3; 7%	2%	0.434	NS
Acute psychosis	Possibly	6.6 y (2.0–8.5) n = 3; 10%		4.8 y (2.5–9.8) n = 0; 0%		0.064	NS
Stroke-like episodes	Possibly	17.2 y (16.8–23.5) n = 2; 7%	14%	n = 0; 0%	17%	0.163	NS
Prolonged QTc interval	Unkn.	13.4 y (9.0–17.9) n = 7; 23%	31%	n = 4; 9%	2%	0.300	NS
Premature ovarian insuffic.	Unkn.	8.5 y (0.0–38.3) n = 0; 0%		14.0 y (3.6–28.4) n = 1; 2%		1.000	NS
				19.1 y			
Mitochondrial complications with chronic onset							
Exercise intoler.	Probably	n = 15; 48%		n = 10; 22%		0.025	NS
Autism	Probably	n = 2; 6%	9%	n = 4; 9%		1.000	NS
Feeding problems	Possibly	n = 18; 58%		n = 22; 49%		0.488	NS
Muscular hypot.	Possibly	n = 13; 42%	45%	n = 21; 47%		0.815	NS
Constipation	Unkn.	n = 14; 45%		n = 9; 20%		0.024	NS
Attention deficit hyperactive dis.		n = 1; 3%	15%	n = 1; 2%		1.000	NS
Mitochondrial complications with intermittent occurrence							
Anemia	Possibly	n = 21; 68%	51%	n = 28; 62%		0.807	NS
Leukopenia	Possibly	n = 19; 61%	31%	n = 16; 36%		0.036	NS
Thrombocytopenia	Possibly	n = 19; 61%	28%	n = 23; 51%		0.483	NS
Pancytopenia	Possibly	n = 13; 42%	19%	n = 9; 20%	0%	0.044	NS
Mitochondrial complications							
None		n = 3; 10%		n = 3; 7%		0.683	NS
Mild		n = 8; 26%		n = 22; 49%		0.057	NS
Moderate		n = 3; 9%		n = 10; 22%		0.219	NS
Severe		n = 5; 16%		n = 7; 16%		1.000	NS
Very severe		n = 11; 35%		n = 3; 7%		0.002	0.013
Death		n = 1; 3%		n = 0; 0%		0.408	NS

a: Likelihood of mitochondrial pathophysiology²; Lit: percentage reported in literature². Statistical significance was determined by performing Fisher's exact tests. All p-values were adjusted according to the Bonferroni method. Adjusted p-values < 0.05 were considered statistically significant and are depicted in bold. Abbreviations: ed.: education, hyp.: hyperintensities, hypot.: hypotonia, NA: not assessed; NS: not significant.

Table S8. Prevalence of treatment-related and miscellaneous complications

	Propionic acidemia (n = 31)	Methylmalonic acidemia (n = 45)	P-val.	Bonf. corr.
<i>Treatment-related complications</i>				
Reduced bone mineral density	n = 9; 29%	n = 18; 40%	0.465	NS
Growth retardation/short stature	n = 8; 26%	n = 13; 29%	0.801	NS
Obesity	n = 10; 32%	n = 6; 13%	0.084	NS
Treatment-related complications				
None	n = 12; 39%	n = 21; 47%	0.638	NS
Mild	n = 13; 42%	n = 15; 33%	0.477	NS
Severe	n = 4; 13%	n = 5; 11%	1.000	NS
Very severe	n = 2; 6%	n = 4; 9%	1.000	NS
<i>Miscellaneous complications</i>				
Pes planovalgus	n = 9; 29%	n = 13; 29%	1.000	NS
Port-a-cath infections	n = 3; 10%	n = 2; 4%	0.393	NS
Enamel defects	n = 1; 3%	n = 3; 7%	0.641	NS
Urolithiasis	n = 1; 3%	n = 1; 2%	1.000	NS
Gout	n = 0; 0%	n = 2; 4%	0.511	NS

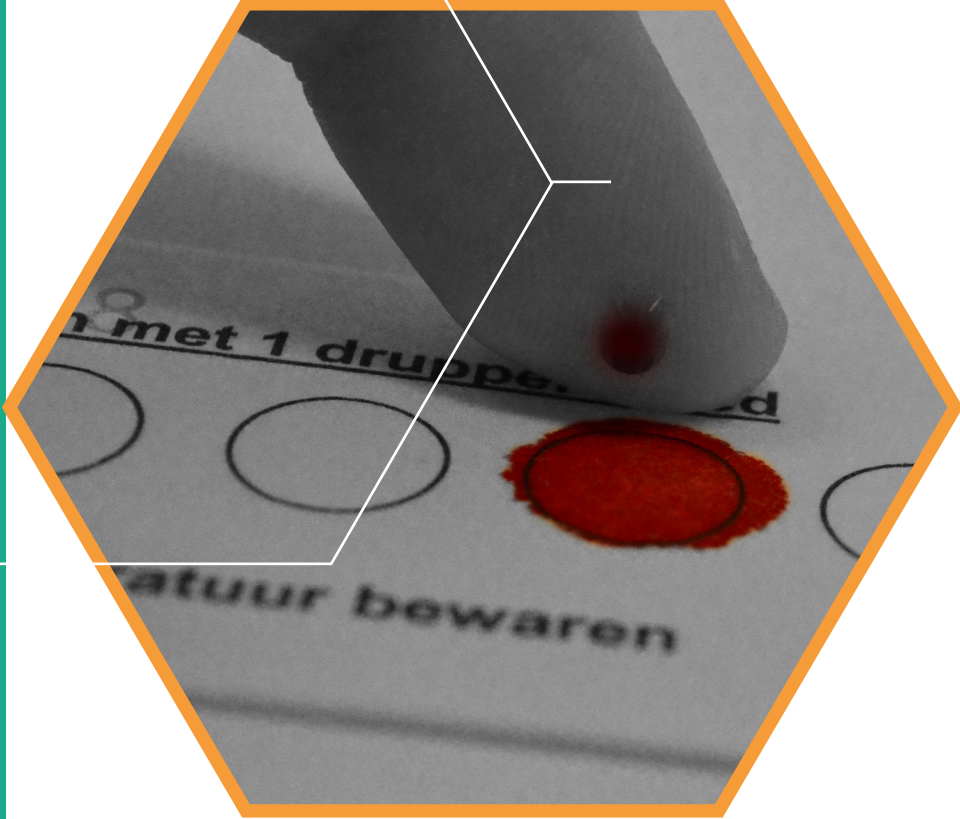
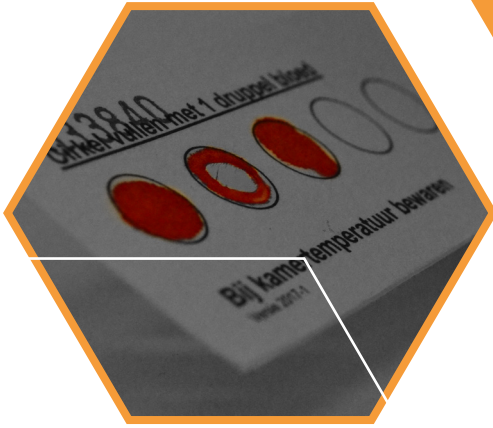
Statistical significance was determined by performing Fisher's exact tests. All p-values were adjusted according to the Bonferroni method. Adjusted p-values < 0.05 were considered statistically significant and are depicted in bold. Abbreviations: NS: not significant.

Table S9. Minimum requirements for follow-up of the post-NBS cohort

	Items to record	Diagnostics to perform
Patient characteristics		
Patient	Day of birth Sex	
Family	Ancestry Consanguinity	
Mutation	<i>g. / c. / p.</i> coding sequence	Genetic testing
Vitamin B12 responsiveness	Type enzymatic assay Results enzymatic assay	Enzymatic assay B12 respons.
PCC activity	Type enzymatic assay Results enzymatic assay	Enzymatic assay PCC activity
Death	Day of death Cause of death	
Follow-up	Age at last follow-up	
AO of first sympt. phase		
First presentation	Symptomatic/asymptomatic Day of first symptoms Day of diagnosis	
AO first presentation	Day of brain MRI Brain MRI results Movement disorder	Brain MRI at set times Consult neurologist
AMD frequency		
Number of AMD	Day of admission Day of release Reason of admission	
Cognitive function		
Cognition	Day of neuropsychological tests Neuropsychological test type Neuropsych. test results; IQ	Neuropsychological tests at set times
Education	School career Type of employment	
Mitochondrial complications		
Hepatomegaly	Day of diagnostic study	Liver ultrasound at set times
Epilepsy	Results of diagnostic study	EEG at set times
Cardiomyopathy	Presence complication yes/no	Cardiac ultrasound at set times
Prolonged QTc interval		ECG at set times
Optic atrophy		Consult ophthalmologist at set times
Renal failure		Urine kidney function biochemistry at set times
Pancreatitis		Complete blood count at set times
Sensorineural hearing loss		
Acute psychosis		
Stroke-like episodes		On indication: consult ENT doctor, gastro-enterologist, neurologist, gynecologist, psychiatrist, physical therapist
Premature ovarian insufficiency		
Exercise intolerance		
Muscular hypotonia		
Feeding problems		
Constipation		
Autism		
Attention deficit hyperactive dis.		
Anemia, leukopenia, thrombocytopenia, pancytopenia		
Treatment-related complications		
Bone mineral density	Day of diagnostic study	DEXA-scan at set times
Growth retardation	Results of diagnostic study	
Obesity	Presence complication yes/no Visit date each visit Weight and length each visit	

Abbreviations: AO of first sympt. phase: Adverse outcome of the first symptomatic phase. DEXA: dual-energy X-ray absorptiometry; ECG: electrocardiogram; EEG: electroencephalogram; ENT: ear-nose-throat; MRI: magnetic resonance imaging; PCC: propionyl-CoA carboxylase; IQ: intelligence quotient. *g./c./p.* coding sequence: genetic change in the DNA coding sequence and resulting change in the protein coding sequence.

Retrospective evaluation of the Dutch pre-newborn screening cohort for propionic acidemia and isolated methylmalonic acidemia: what to aim, expect, and evaluate from newborn screening?



High protein prescription in methylmalonic and propionic acidemia patients and its negative association with long-term outcome

Femke Molema^{†,*}, Hanneke A. Haijes[†], Mirian C. Janssen, Annet M. Bosch, Francjan van Spronsen, Margot F. Mulder, Nanda M. Verhoeven-Duif, Judith J.M. Jans, Ans T. van der Ploeg, Margreet A. Wagenmakers, M. Estela Rubio-Gozalbo, Martijn C.G.J. Brouwers, Maaïke C. de Vries, Sabine A. Fuchs, Janneke G. Langendonk, Dimitris Rizopoulos, Peter M. van Hasselt[#], Monique Williams^{#,*}

† These authors contributed equally to this article

These authors contributed equally to this article

* Corresponding authors

ABSTRACT

Background: While survival of methylmalonic (MMA) and propionic acidemia (PA) patients has improved in recent decades, outcome is still unsatisfactory. It is presently unknown to what extent long-term outcome is influenced by dietary treatment.

Methods: We performed a nationwide retrospective cohort study and evaluated both longitudinal dietary treatment and clinical course of 76 Dutch MMA and PA patients. Protein prescription was compared to the recommended daily allowances (RDA) as provided by the World Health Organization. The association of longitudinal dietary treatment with four outcome parameters: frequency of acute metabolic decompensations (AMD), number of long-term (mitochondrial) complications, cognitive function and height, was evaluated.

Results: Seventy-five out of 76 patients received a protein restriction. The median retrospective follow-up period was 15 years (range: 0-48 years). Natural protein prescription exceeded RDA in 37% (470/1287) and total protein in 84% (1070/1277) of all prescriptions. Natural protein prescription mainly exceeded RDA in patients from 1 year of age till adolescence and after the age of 20 years. Amino acid mixtures (AAM) were prescribed in 85% of patients. In 32% (343/1087) of the AAM prescriptions, natural protein prescription exceeded RDA. In PA early onset patients a higher natural:total protein ratio prescription was associated with more frequent AMD. In MMA vitamin B12 unresponsive and responsive patients, a higher total protein prescription and AAM protein prescription were associated with more mitochondrial complications. A higher AAM protein prescription was associated with increased frequency of cognitive impairment in the entire cohort, and with decreased height in the entire cohort, except for PA EO patients.

Discussion: A high natural protein, protein from AAM and total protein prescription are negatively associated with patient outcome in MMA and PA patients, reflected by more frequent AMD and mitochondrial complications, and reduced cognitive function and height.

KEY MESSAGE

Despite a protein restricted diet, protein prescribed to methylmalonic and propionic acidemia patients exceeds WHO recommendations, and this is negatively associated with long-term patient outcome.

INTRODUCTION

Methylmalonic acidemia (MMA, MIM: #251000, #251100, #251110, #277400 #277410 and #251120) and propionic acidemia (PA, MIM: #6060054) are inborn errors of metabolism caused by deficiencies of enzymes or cofactors that contribute to the breakdown of the branched-chain amino acids (BCAA) L-isoleucine and L-valine.

While survival of MMA and PA patients has greatly improved in recent decades, overall outcome remains poor. Despite currently available treatment, patients continue to have frequent acute metabolic decompensations (AMD), often requiring hospitalization or even intensive care unit admission. They also frequently develop severe mitochondrial long-term complications such as cardiomyopathy and renal failure, and several patients have reduced cognitive function and impaired height.¹⁻⁶ Newborn screening in MMA and PA patients is not expected to improve these complications substantially,³ and therefore evaluation and potential improvement of currently applied dietary treatment is essential.

For several decades, a protein-restricted diet has been the mainstay of treatment for patients suffering from MMA and PA. The current guideline for MMA and PA advises a natural protein requirement, i.e. an intake of 100% of the protein safe levels defined by the World Health Organization (WHO),⁷ and to supplement amino acid mixtures (AAM) when the tolerated natural protein intake is below 100%.⁸

However, the current guideline advices are not yet based on studies that evaluate the effect of dietary treatment on specific outcome measures. Only the effect of dietary treatment on height has previously been studied, and minimum and maximum values for the prescribed protein-to-energy ratio (P:E ratio) to achieve optimal height have been provided.⁹ Without this crucial evidence-based corroboration of the guideline advices, clinicians continue to compose their own approach to optimize the protein-restricted diet for MMA and PA patients. This is illustrated by a recent study evaluating dietary treatment – among patients included in the European registry and network for Intoxication type Metabolic Diseases – which demonstrated that several patients with a natural protein prescription of 100% RDA received additional AAM. This is against guideline advices and may be harmful.⁸⁻¹³

In order to determine the influence of currently prescribed dietary treatment on long-term outcome of MMA and PA patients, this study evaluated the association of longitudinal dietary treatment, comprising natural protein, AAM protein, total protein and kilocalorie prescription – with patient outcome, defined as: (1) AMD episodes, (2) long-term mitochondrial complications, (3) cognitive development and (4) height.^{8,14}

METHODS

Patient inclusion, data collection and outcome parameters

Patient inclusion, informed consent, data collection and definition of outcome parameters of this study cohort have been described before.³ Patients were grouped according to disease severity: PA early onset (EO) (disease onset before day 28 of life), PA late onset (LO) (disease onset beyond day 28 of life), MMA vitamin B12 (vitB12) unresponsive and MMA vitB12 responsive.³ PA patients identified by family testing were grouped as either EO or LO based on the disease course of their index sibling.³ For this study, data collection also included dietary prescriptions and plasma BCAA levels at outpatient visits. Plasma BCAA levels were available for patients from the University Medical Center Utrecht and the Erasmus Medical Center ($n = 41$ patients). Cognitive function was classified in three categories (IQ >90, IQ 60-90, IQ <60) based on neuropsychological test results, or in the absence of neuropsychological test results on educational level or professional employment.^{3,15} Adolescence was defined

according to the WHO as patient age between 10-19 years.¹⁶

Data analysis

Prescription of natural protein in gram/kg and protein from AAM supplementation in gram/kg were compared to the protein requirement as mentioned in the MMA and PA guideline based on gender- and age-specific safe levels of protein intake.^{7,8} For this study we interpreted these safe levels as recommended daily allowances (RDA). Total protein prescription in gram/kg was calculated by combining natural protein prescription and protein from AAM supplementation. The natural:total protein ratio was calculated by dividing natural protein over the total amount of protein prescribed. The AAM:total protein ratio was calculated by dividing protein from AAM supplementation over the total amount of protein prescribed. Energy prescription in kilocalories (kcal) per day was compared to the RDA.⁷ The total P:E ratio was defined as the total amount of protein prescribed in grams per prescription of 100 kcal per day. Standard deviation scores of height, indicated by height Z-scores, were calculated according to the LMS method,¹⁷ using reference data.^{18,19} Plasma BCAA levels were compared with reference values.²⁰ A ratio of 1:2:4 for L-isoleucine:L-leucine:L-valine was considered normal.^{20,21}

Statistical analysis

The association of natural protein, AAM protein, total protein prescription, natural:total protein ratio, AAM:total protein ratio, kcal prescription and total P:E ratio with AMD, mitochondrial complications and cognitive function as outcome measures were tested in all four patient subgroups and in the entire cohort.

To determine the association of protein and energy prescription with the occurrence of AMD a recurrent event analysis using a Cox regression model was performed using the R package survival. To determine the association of protein and energy prescription with mitochondrial complications, poisson regression analysis with age of follow-up as offset was performed using the R glm() function. To determine the association of protein and energy prescription with the category of cognitive functioning, ordinal regression analysis was performed using the R polr() function. For both Poisson and ordinal regression, a mean area under the curve (AUC) was calculated using the AUC() function of the R DescTools package, to calculate a weighted mean of protein and energy prescription during a patient's follow-up time. A linear mixed-effects model analysis was performed using SPSS to determine the association of protein and energy prescription with the patient's height. In particular, we used this model first to study the longitudinal evolutions of the height Z-score, and then to investigate the association of dietary treatment with height. In our model the three fixed effects were 1) the total P:E ratio; 2) prescription of AAM protein as % RDA; 3) age at each visit. For the random-effects structure we used a build-up approach, starting from random intercepts, and including linear and nonlinear random slopes for the age variable. The appropriate random-effects structure was selected using the Akaike Information Criterion. Pearson correlation tests were performed to assess correlations between the mean AUC of natural protein RDA as well as the mean AUC of the AAM:total protein ratio and the mean AUC of the plasma levels of valine, isoleucine and leucine throughout life. In addition, Pearson correlation tests were performed to assess the correlation between the frequency of AMD per patient year during the first four years of life and the mean AUC of the plasma levels of valine, isoleucine and leucine during the first four years of life. A Kendall-tau correlation test was performed to assess the association between the mean AUC AAM:total protein ratio

prescription and the mean AUC natural protein prescription. The Holm-Bonferroni method was used to correct for familywise error rates for multiple testing. All statistical analyses were discussed with a statistician (prof. dr. D. Rizopoulos).

RESULTS

Baseline characteristics

The nationwide cohort consisted of 76 MMA and PA patients.³ Of these patients, 75 were prescribed a protein-restricted diet at some point in life. In 79% (59/75) a protein-restricted diet was prescribed at all evaluated time points during outpatient visits. During a median retrospective follow-up period of 15 years (range: 0-48 years) details of protein prescription were available from 1,287 time points (Table S1). IQ was determined in 63 patients and could not be determined in 13 patients due to early death ($n = 5$) and due to a too young age for reliable evaluation ($n = 8$).

As expected based on disease severity, AMD were frequent in MMA vitB12 unresponsive and PA EO patients (Figure S1). A mean of 6.7 mitochondrial complications per patient was noted in the entire cohort, 30% of the patients had an IQ <60 (19/63) (Table S1) and the majority of patients had impaired height growth (Figure S2).

Dietary protein prescription and outcome

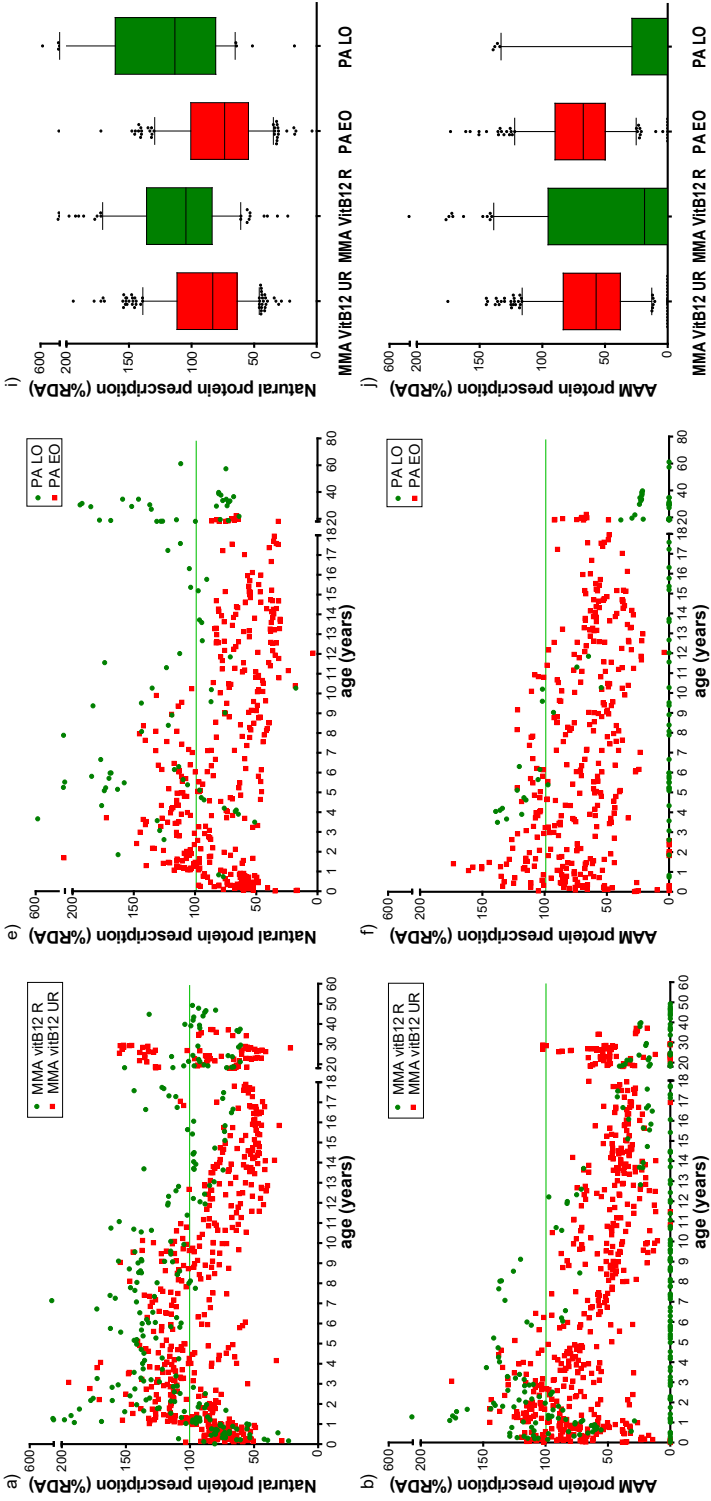
Entire cohort

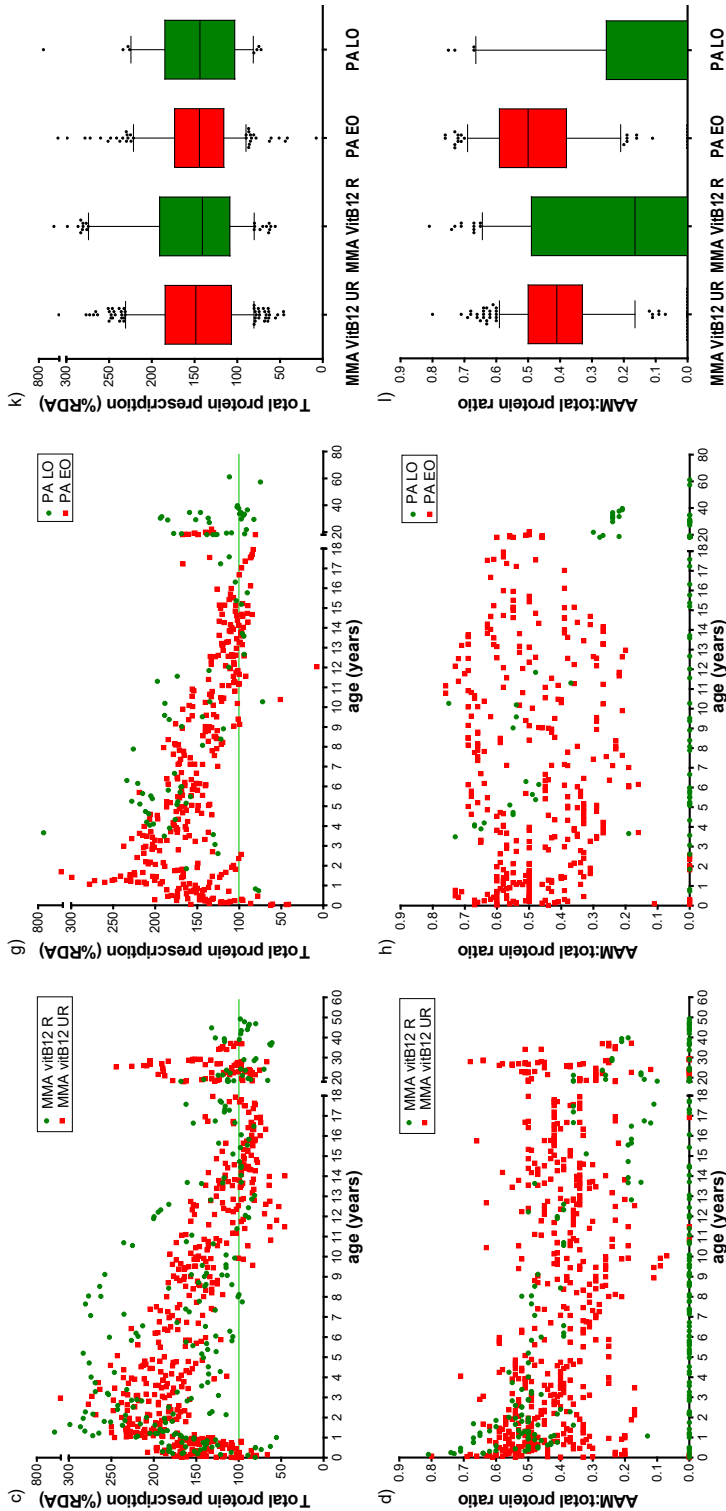
In 37% (470/1,287 measurements in 75 patients) of all prescriptions, natural protein prescription exceeded RDA. Natural protein prescription mainly exceeded RDA in patients from 1 year of age till adolescence and after the age of 20 years, in all subgroups (Figure 1a, 1e and 1i). AAM were prescribed in 85% (64/75) of patients with a protein-restricted diet (Figure 1b, 1f and 1j, Table S1). In 31% (343/1,089) of the time points that AAM was prescribed, natural protein prescription was already above RDA. The additional AAM supplementation resulted in a total protein prescription exceeding RDA in 84% of the measurements (1,070/1,277) (mean \pm SD: 150 ± 52 %RDA) (Figure 1c, 1g and 1k). Overall, the AAM:total protein ratio prescription differed widely (mean \pm SD AAM:total protein ratio: 0.36 ± 0.20) (Figure 1d, 1h and 1l). A higher AAM protein prescription, as well as a higher AAM:total protein ratio prescription were associated with a higher frequency of impaired cognition in the entire cohort (Table 1, Figure S3a,b) and a higher natural:total protein ratio prescription with a lower frequency of impaired cognition (Table 1). A higher AAM protein, total protein, and AAM:total protein ratio prescription were associated with more frequent mitochondrial complications (Table 1). A higher natural protein and a higher natural:total protein ratio prescription were associated with less frequent mitochondrial complications (Table 1). Furthermore, a higher AAM protein prescription was negatively associated with height Z-scores in the entire cohort, except for PA EO patients (Table 1).

MMA vitB12 unresponsive patients

Natural protein prescription was above RDA in 34% (174/518) (mean \pm SD: 87 ± 30 %RDA) (Figure 1a, i) and total protein prescription was above RDA in 80% (416/517) (mean \pm SD: 149 ± 48 %RDA) of all prescriptions (Figure 1c, k). Of all time points that AAM was prescribed, natural protein prescription was already above RDA in 34% (167/498) and total protein prescription was above RDA in 82% (410/498). Both a higher total protein and a higher AAM protein prescription were associated with more frequent mitochondrial complications (Figure 3a-b, Table 1).

Figure 1. Protein prescription according to the patient's age, and according to disease subgroup





Panel a-h: dots/squares represent one measurement per patient. Red squares indicate the more severely affected patients, namely MMA vitB12 unresponsive and PA EO patients, and green dots indicate the less severely affected patients, namely MMA vitB12 responsive and PA LO patients. Horizontal green lines in panel a-c and e-g indicate an RDA of 100%. Panel i-l: boxplots based on all measurements per patient, indicating median, 25th – 75th percentile and 95% CI. Black dots indicate outliers. Abbreviations: AAM: amino acid mixtures; EO: early onset; LO: late onset; MMA: methylmalonic acidemia; PA: propionic acidemia; R: responsive; RDA: recommended daily allowances; UR: unresponsive; vitB12: vitamin B12.

Table 1.: Dietary intake and risk on certain outcome in disease severity groups

	Outcome parameter	Age	Natural protein RDA	AAM protein RDA	Total protein RDA	Natural:total protein ratio	AAM:total protein ratio	kcal RDA	Total P:E ratio
MMA vitB12 UR	AMID	ND	NS	NS	NS	NS	NS	NS	NS
	Mitochondrial complications	ND	NS	1.02	1.01	NS	NS	NS	NS
	Cognitive func.	ND	NS	<0.001	<0.001	NS	NS	NS	NS
	Height Z-score	-0.13	NS	-0.02	ND	ND	ND	NS	0.76
MMA vitB12 R	AMID	<0.001	<0.001	<0.001	NS	NS	NS	NS	0.002
	Mitochondrial complications	ND	NS	NS	NS	NS	NS	NS	NS
	Cognitive func.	ND	NS	1.01	1.01	0.08	12.0	1.01	NS
	Height Z-score	-0.17	NS	0.003	0.011	<0.001	<0.001	<0.001	NS
PA EO	AMID	<0.001	NS	-0.01	ND	ND	ND	ND	NS
	Mitochondrial complications	ND	NS	0.003	NS	NS	NS	NS	NS
	Cognitive func.	ND	NS	-0.01	ND	ND	ND	ND	NS
	Height Z-score	<0.001	NS	0.003	NS	77.4	0.01	NS	NS
PA LO	AMID	ND	NS	NS	NS	NS	NS	NS	NS
	Mitochondrial complications	ND	NS	NS	NS	NS	NS	NS	0.57
	Cognitive func.	ND	NS	NS	NS	NS	NS	NS	0.010
	Height Z-score	-0.11	NS	NS	NS	NS	NS	NS	NS
Entire cohort	AMID	<0.001	NS	-0.01	ND	ND	ND	ND	NS
	Mitochondrial complications	ND	NS	0.010	NS	NS	NS	NS	NS
	Cognitive func.	ND	NS	NS	NS	NS	NS	NS	NS
	Height Z-score	0.023	NS	-0.01	NS	NS	NS	NS	NS
Entire cohort	AMID	ND	NS	NS	NS	NS	NS	NS	NS
	Mitochondrial complications	ND	NS	1.01	1.01	0.10	9.26	1.01	0.73
	Cognitive func.	ND	<0.001	<0.001	<0.001	<0.001	<0.001	<0.001	0.003
	Height Z-score	ND	NS	1.03	NS	0.01	75.43	NS	NS
Entire cohort	AMID	ND	NS	0.012	NS	<0.001	0.022	NS	NS
	Height Z-score	ND	NS	NS	NS	NS	NS	NS	NS

Abbreviations: AAM: amino acid mixtures; AMD: acute metabolic decompensation; coef: coefficient; EO: early onset; exp: exponential; kcal: kilocalorie; LO: late onset; MMA: methylmalonic acidemia; ND: not determined; NS: not significant; PA: propionic acidemia; P:E ratio: protein-to-energy ratio; R: responsive; RDA: recommended daily allowance; UR: unresponsive; vitB12: vitamin B12.

PA EO patients

Natural protein prescription was above RDA in 26% (109/423) (mean \pm SD: 78 \pm 30 %RDA), (Figure 1e, i) and total protein prescription was above RDA in 91% (383/421) (mean \pm SD: 154 \pm 49 %RDA) of all prescriptions (Figure 1g, k). Of all time points that AAM was prescribed, natural protein prescription was already above RDA in 25% (105/413) and total protein prescription was above RDA in 92% (397/413). A higher natural:total protein ratio prescription was associated with more frequent AMD and a higher AAM:total protein ratio prescription was associated with less frequent AMD (Figure 3c-d, Table 1).

MMA vitB12 responsive patients

In 53% (120/227) of all prescriptions natural protein prescription was above RDA (mean \pm SD: 109 \pm 35 %RDA) (Figure 1a, i) and total protein prescription was above RDA in 79% (179/226) (median, range: 141, 56-432 %RDA) (Figure 1c, k). In 45% (56/125) of time points that AAM was prescribed, natural protein prescription was already above RDA. A higher AAM protein, a higher AAM:total protein ratio and a higher total protein prescription were associated with more frequent mitochondrial complications (Figure S3c-e, Table 1) and a higher natural:total protein ratio prescription was associated with less frequent AMD (Table 1).

PA LO patients

In 44% (52/119) of all prescriptions natural protein prescription was above RDA (median, range: 110, 18-558 %RDA) (Figure 1e, i) and total protein prescription was above RDA in 81% (92/113) (median, range: 142, 65-689 %RDA) (Figure 1c, k). No statistically significant associations were found between dietary protein and energy prescription and the outcome parameters (Table 1).

Dietary energy prescription and outcome

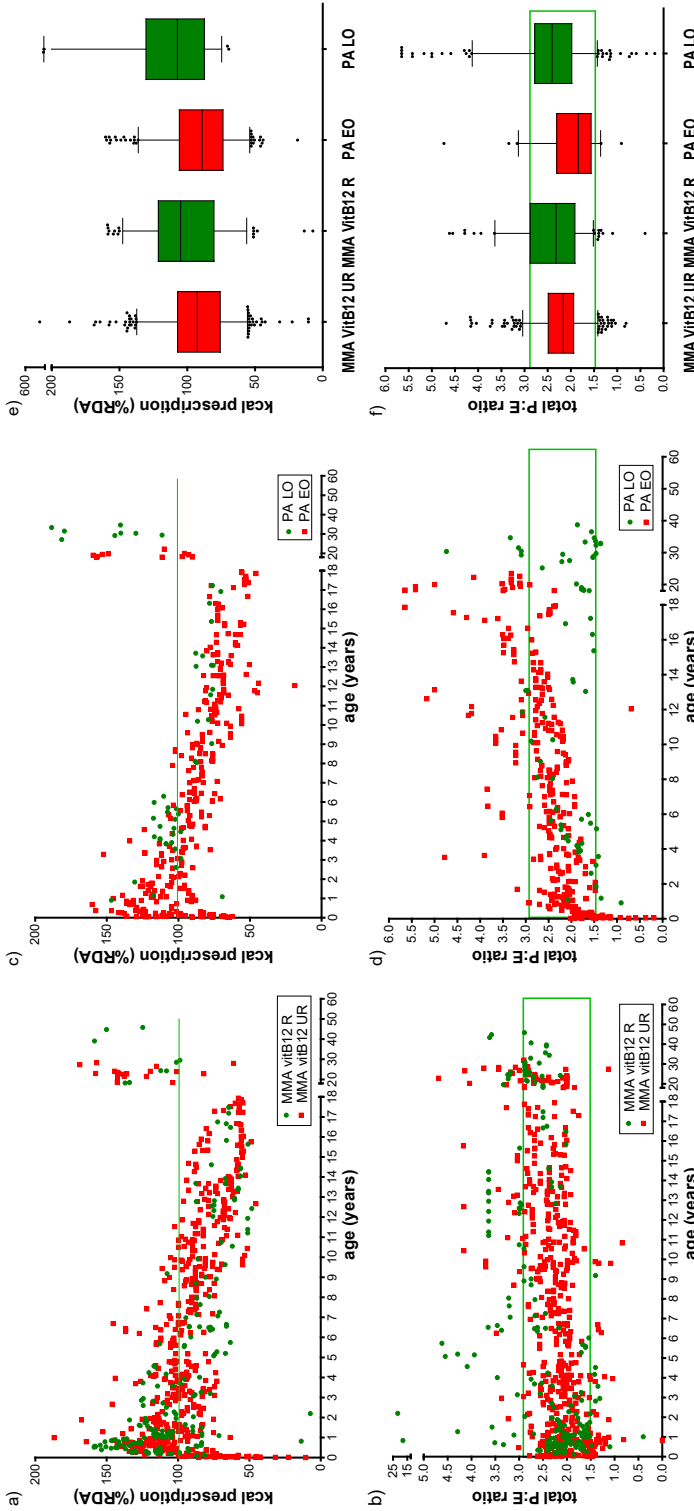
Energy prescription decreased with age and was below RDA in all subgroups during adolescence, while increasing thereafter (Figure 2). Total P:E ratio prescription increased with age and was prescribed according to recommendations⁹ in the majority of patients (Figure 2).

The higher the energy prescription, the higher the frequency of mitochondrial complications in MMA vitB12 responsive patients (Figure S3f, Table 1) and in the entire cohort (Table 1). A higher total P:E ratio prescription was associated with increased height Z-score in MMA vitB12 unresponsive patients and with decreased mitochondrial complications in PA EO and PA LO patients (Figure S3g-h, table 1) and in the entire cohort (Table 1).

Plasma BCAA levels

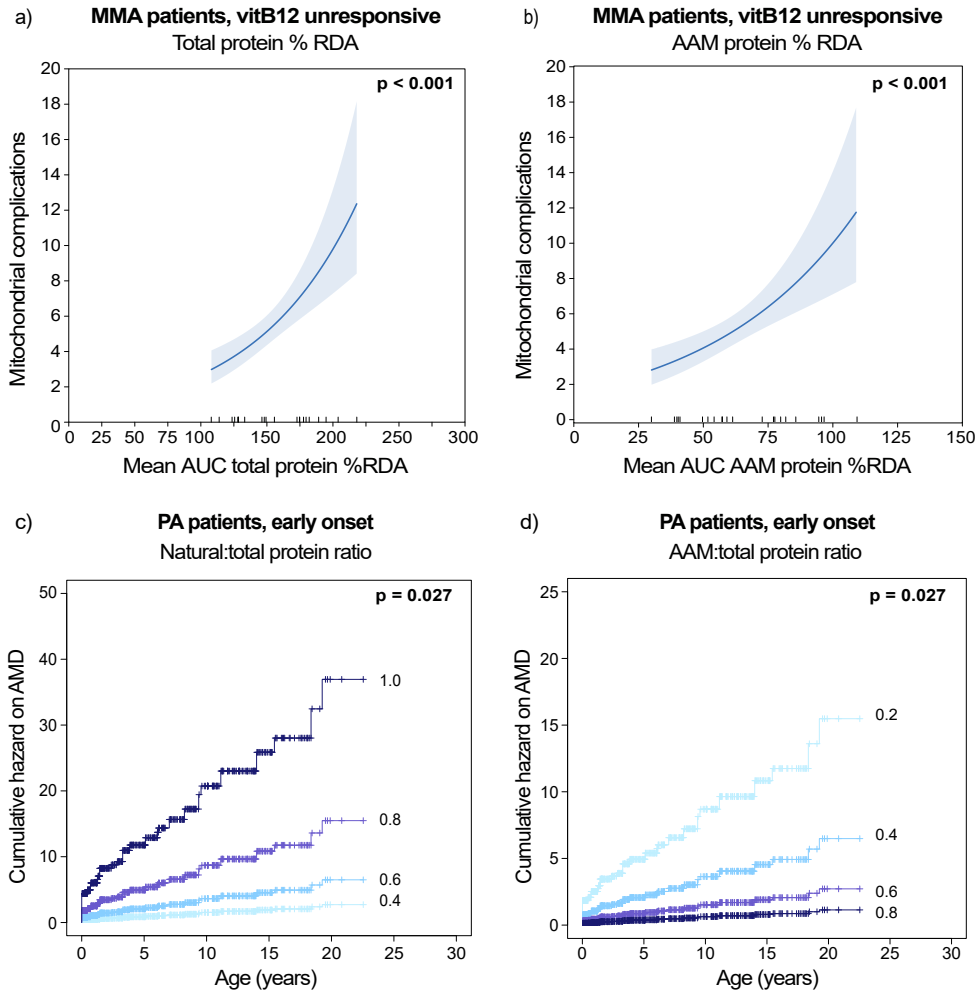
Plasma BCAA levels were low in almost all assessed patients ($n = 41$) (Figure S4). This included the valine:leucine ratio (mean: 1.2, reference value: 2.0) and the isoleucine:leucine ratio (mean: 0.37, reference value: 0.50) (Figure S4). No associations were found between natural protein prescription and plasma BCAA levels in any subgroup. In PA EO patients, a higher AAM:total protein ratio prescription was associated with lower plasma valine levels ($r = -0.89$, $p < 0.001$). In PA LO patients, a higher mean AUC plasma valine, isoleucine, and valine:isoleucine ratio were associated with less frequent mitochondrial complications (Table S2).

Figure 2. Kilocalorie and total P:E ratio prescription according to patient's age, and according to disease subgroup.



Panel a-d: dots/squares represent one measurement per patient. Red squares indicate the more severely affected patients, namely MMA vitB12 unresponsive and PA EO patients, and green dots indicate the less severely affected patients, namely MMA vitB12 responsive and PA LO patients. Panel e-f: boxplots based on all measurements per patient, indicating median, 25th – 75th percentile and 95% CI. Black dots indicate outliers. Horizontal green lines in panel a and c indicate an RDA of 100%, the horizontal green square in panel b and d indicates the dispersion of the recommended total P:E ratio. Abbreviations: EO: early onset; LO: late onset; kcal: kilocalorie; LO: late onset; MMA: methylmalonic acidemia; P:E ratio: protein-to-energy ratio; PA: propionic acidemia; R: responsive; RDA: recommended daily allowances; UR: unresponsive; vitB12: vitamin B12.

Figure 3. Associations between protein prescription and outcome in vitamin B12 unresponsive MMA patients and early onset PA patients



Panels a and b show the association between total protein and AAM protein prescription and the risk of mitochondrial complications in MMA vitB12 unresponsive patients. Panels c and d show the association between natural:total protein ratio and AAM:total protein ratio and the cumulative hazard on an AMD in PA EO patients. Abbreviations: AAM: amino acid mixtures; AUC: area under the curve; MMA: methylmalonic acidemia; PA: propionic acidemia; RDA: recommended daily allowances; vitB12: vitamin B12.

In MMA vitB12 responsive patients, a higher mean AUC plasma valine level and a higher mean AUC isoleucine:leucine ratio were associated with less frequent mitochondrial complications (Table S2). No clear associations between the mean AUC of valine, isoleucine, and leucine (first four years) and AMD (per patient year in first four years) were found.

DISCUSSION

The aim of this study was to evaluate longitudinal dietary treatment in MMA and PA patients. Through a concise retrospective study we demonstrated that on average the prescribed amount of protein in MMA and PA patients grossly exceeded the RDA. In addition, AAM was often applied when natural protein was already sufficient according to the RDA. More importantly, we revealed that this high natural, AAM protein and total protein prescription is associated with adverse patient outcomes (AMD, mitochondrial complications, cognitive development and height).

The observation in our nationwide cohort that more than one fourth of patients received a natural protein prescription exceeding the RDA aligns with previous studies.²²⁻²⁴ Excessive prescription of AAM protein resulted in a total protein prescription exceeding the RDA in almost all patients, as also observed in the European cohort.¹⁰ Reasons for providing patients on a protein-restricted diet with a protein prescription above 100% RDA might be (1) adjusting protein prescription due to impaired height growth, (2) compensating for the inferior quality of the protein that patients consume, (3) adjusting protein prescription based on low BCAA levels or (4) use of other guidelines or protein calculation methods (g/kg) than the RDA of the WHO.

Our data suggest that PA EO patients who receive a higher natural:total protein prescription are at risk of AMD. In PA EO patients in whom not enough natural protein is tolerated (i.e. below the RDA), additional AAM should be applied in amounts that lead to a total protein prescription which approximates, but not exceeds, the RDA. MMA patients (vitB12 unresponsive and responsive patients) who receive a high total protein and a high AAM protein prescription are at risk of mitochondrial complications. In the entire cohort potential harmful associations of AAM were also observed with respect to impaired cognitive development, mitochondrial complications and impaired height growth. Intriguingly, additional AAM was often applied when natural protein already complied to the RDA, despite the fact that guidelines suggest to only apply AAM when natural protein is below the RDA.⁸ This resulted in total protein largely exceeding the RDA, while this might be harmful regarding patient outcome. In MMA and PA patients urea-cycle function is impaired^{25,26} and a high protein intake can overload the urea-cycle, resulting in chronic hyperammonemia and thereby affecting patient outcome. Importantly, adverse effects on plasma BCAA levels induced by the addition of AAM products to natural protein prescription have previously been reported. AAM supplementation can be a major cause of disturbed BCAA ratios as well as decreased valine and isoleucine (plasma) levels.^{9,11-13} This could be due to the high leucine content in AAM products, and consequently BCAA interaction on the large-neutral amino acid transporter (LAT) affecting cellular uptake (also at the blood brain barrier level). The lack of an association between natural protein prescription and plasma BCAA levels observed in this study can be due to the addition of AAM and thereby BCAA competition at the LAT transporter level. Low BCAA levels may be harmful as they can increase the risk of an AMD²⁷ and since BCAA are essential for growth and development.²⁸⁻³⁰ Furthermore, BCAA supplementation can support mitochondrial biogenesis.³¹ (Over)supplementation of AAM (lacking isoleucine and valine) and consequential low and disturbed BCAA levels

can potentially increase the risk of mitochondrial complications and impaired cognitive development and height growth. Therefore, we advise caution with the prescription of AAM. High energy intake is generally prescribed to prevent catabolism (especially in younger children). However, we observed that a high energy prescription was associated with increased risk of mitochondrial complications in MMA vitB12 responsive patients. High energy prescription can be harmful, and caloric restriction can reduce burden of mitochondrial function by increased mitochondrial biogenesis.³²⁻³⁵ The relative high caloric intake prescribed to prevent catabolism, can lead to a lower P:E ratio. We observed that a higher total P:E ratio prescription in PA EO and LO patients was associated with a lower frequency of AMD and, as previously reported, with increased height Z-score.^{9,36} Regarding the P:E ratio in MMA and PA patients it is important that protein can be efficiently metabolized. In order to achieve optimal protein utilization sufficient energy supply is essential. However, several factors play a role: energy intake does not always equal energy uptake (gut mobility is important and can be impaired in MMA and PA patients), energy requirement is highly dependent on physical activity (often impaired in MMA and PA patients), the optimal P:E ratio is hard to define in children and depends on growth, and mitochondrial dysfunction can disturb the energy balance in MMA and PA.⁷ Furthermore, it is important to acknowledge that the P:E ratio can appear optimal when high protein as well as high energy is prescribed. However, an increased energy intake could result in deleterious effects on the already compromised mitochondria. Before adjusting the P:E ratios, further studies are necessary to determine the optimal ratio in MMA and PA patients, with respect to all outcome measures (AMD, mitochondrial complications, cognitive development and growth).

The main study limitations are inherent to the retrospective design. It could be that other factors than diet, such as viral infections, genetic variation within subgroups, the first severe AMD (high ammonia) or introduction of new therapies are associated with the studied outcome parameters (AMD, mitochondrial complications, IQ). Infection, as a potential confounder for AMD, does not seem to explain the association between higher protein prescription and AMD, since protein intake is often decreased during infectious episodes. Genetic variation within the subgroups (phenotypically either reflected by more frequent AMD, more mitochondrial complications or lower IQ) does not seem to be a potential confounder either, because more severe patients received a high natural and total protein prescription instead of lower. Additionally, a positive association was found between this higher natural and total protein prescription and the outcome parameters. In the analyses of the entire cohort, disease severity within the subgroups (MMA vitB12 responsive, MMA vitB12 unresponsive, PA EO and PA LO) may partially contribute to the observed association due to a potential higher AAM protein prescription in the more severely affected patients. However, the harmful effects of AAM have previously been well reported and we add additional evidence. Disease severity subgroups are likely to explain the identified association between a higher natural protein and less frequent mitochondrial complications. Regarding the effect of the first severe AMD on cognitive development, we have previously shown that siblings identified through family testing and protected from severe hyperammonemic crises still have a cognitive development comparable to their sibling that presented with a severe AMD.³ This implies that our care, rather than disease presentation only, is important for cognitive development. Due the long follow-up period, new therapies may have been introduced which might act as confounders for the observed associations. However, we expect this effect to be limited, as N-carbamylglutamate for example was only prescribed in a few patients.

Next to potential confounders, a limitation of our study is that our results are based on dietary prescription rather than actual intake, which might be different. This is likely to affect size, but it is unlikely to affect direction of the identified effects. Additionally, AMD that were managed at home were often not registered in the patients' medical records, and were therefore not included. This could give an underestimation of AMD frequencies in this cohort, although the more severe AMD are likely accounted for. Lastly, sampling interval between the last intake and sampling for BCAA plasma levels was not known. Since possibly, sampling was not performed simultaneously with dietary treatment prescription and height recording, we could not correlate these measures directly, potentially affecting the observed correlations.

An important strength of our study is that, while over the past decades no clear effects of dietary treatment on patient outcome have been reported, we describe clear correlations between dietary prescriptions and patient outcomes. This was possible by describing an entire national cohort with a large follow-up time and very detailed information on dietary prescriptions and patient outcome parameters.³ More personalized dietary treatment advice is necessary to provide protein sufficient for that specific patient, and hereby patient characteristics such as physical activity, estimated ideal weight, and growth to target height should be taken into account. Also, determining protein requirement by amino acid oxidation method or nitrogen balance studies in MMA and PA patients could provide additional information.^{37,38} Prospective studies are necessary to evaluate our observations and substantiate our suggestions.

CONCLUSION

Natural protein prescription exceeded the RDA in one third of MMA and PA patients. Numerous patients were prescribed additional AAM protein, even when natural protein prescription already met the RDA, resulting in a very high total protein prescription. Excessive natural protein, AAM protein and total protein prescription were negatively associated with patient outcome – AMD, mitochondrial complications, cognition and height growth – in MMA and PA patients. We therefore advise to reduce protein prescription in (mainly severely affected) patients for whom more protein than recommended is prescribed and to be cautious with the prescription of AAM.

REFERENCES

1. Kölker S, Valayannopoulos V, Burlina AB et al. The phenotypic spectrum of organic acidurias and urea cycle disorders. Part 2: the evolving clinical phenotype. *J Inherit Metab Dis.* 2015b;38:1059-1074.
2. Haijes HA, Jans JJM, Tas SY, Verhoeven-Duif NM, van Hasselt PM. Pathophysiology of propionic and methylmalonic acidemias. Part 1: Complications. *J Inherit Metab Dis.* 2019;42(5):745-761.
3. Haijes HA, Molema F, Langeveld M et al. Retrospective evaluation of the Dutch pre-newborn screening cohort for propionic acidemia and isolated methylmalonic acidemia: what to aim, expect, and evaluate from newborn screening? *J Inherit Metab Dis.* 2019; *Epub ahead of print.*
4. Hörster F, Garbade SF, Zwickler T et al. Prediction of outcome in isolated methylmalonic acidurias: combined use of clinical and biochemical parameters. *J Inherit Metab Dis.* 2009;32:630-639.
5. De Baulny HO, Benoist JF, Rigal O, Touati G, Rabier D, Saudubray JM. Methylmalonic and propionic acidemias: management and outcome. *J Inherit Metab Dis.* 2005;28(3):415-23.
6. Grünert SC, Müllerleile S, de Silva L et al. Propionic acidemia: neonatal versus selective metabolic screening. *J Inherit Metab Dis.* 2012;35:41-49.
7. Joint FAO/WHO/UNU Expert Consultation on Protein and Amino Acid Requirements in Human Nutrition, 2002 : Geneva, Switzerland. Food and Agriculture Organization of the United Nations, World Health Organization & United Nations University, 2007. Protein and amino acid requirements in human nutrition: report of a joint FAO/WHO/UNU expert consultation. World Health Organization.
8. Baumgartner MR, Hörster F, Dionisi-Vici C et al. Proposed guidelines for the diagnosis and management of

- methylmalonic and propionic acidemia. *Orphanet J Rare Dis.* 2014;9:130.
9. Evans M, Truby H, Boneh A. The relationship between dietary intake, growth, and body composition in inborn errors of intermediary protein metabolism. *J Pediatr.* 2017;188:163-172.
 10. Molema F, Gleich F, Burgard P et al. Evaluation of dietary treatment and amino acid supplementation in organic acidurias and urea-cycle disorders: on the basis of information from a European multicenter registry. *J Inher Metab Dis.* 2019;42(6):1162-1175.
 11. Manoli I, Myles JG, Sloan JL, Shchelochkov OA, Venditti CP. A critical reappraisal of dietary practices in methylmalonic acidemia raises concerns about the safety of medical foods. Part 1: isolated methylmalonic acidemias. *Genet Med.* 2016;18(4):386-395.
 12. Manoli I, Myles JG, Sloan JL et al. A critical reappraisal of dietary practices in methylmalonic acidemia raises concerns about the safety of medical foods. Part 2: cobalamin C deficiency. *Genet Med.* 2016;18(4):396-404.
 13. Myles JG, Manoli I, Venditti CP. Effects of medical food leucine content in the management of methylmalonic and propionic acidemias. *Curr Opin Clin Nutr Metab Care.* 2018;21(1):42-48.
 14. Southeast regional genetic network and Genetic metabolic dietitians international. PROP Nutrition management guidelines, version 1.2, September 2017.
 15. Hörster F, Baumgartner MR, Viardot C et al. Long-term outcome in methylmalonic acidurias is influenced by the underlying defect (mut0, mut-, clbA, clbB). *Pediatr Res.* 2007;62:225-230.
 16. Patton GC, Sawyer SM, Santelli JS et al. Our future: a Lancet commission on adolescent health and wellbeing. *Lancet.* 2016;387(10036):2423-2478.
 17. Cole TJ. The LMS method for constructing normalized growth standards. *Eur J Clin Nutr.* 1990;44:45-60.
 18. Cole TJ, Freeman JV, Preece MA. British 1990 growth reference centiles for weight, height, body mass index and head circumference fitted by maximum penalized likelihood. *Stat Med.* 1998;17:407-429.
 19. Cole TJ, Williams AF, Wright CM, Group RGCE. Revised birth centiles for weight, length and head circumference in the UK-WHO growth charts. *Ann Hum Biol.* 2011;38:7-11.
 20. Duran, M. Amino acids. In: Blau N, Duran M, Gibson KM, eds. *Laboratory guide to the methods in biochemical genetics.* Berlin, Heidelberg. Springer Verlag, 53-89.
 21. Strauss KA, Wardley B, Robinson D et al. Classical maple syrup urine disease and brain development: principles of management and formula design. *Mol Genet Metab.* 2010;99:333-345.
 22. Daly A, Evans S, Gerrard A, Santra S, Vijay S, MacDonald A. The nutritional intake of patients with organic acidemias on enteral tube feeding: can we do better? *JIMD Rep.* 2015;28:29-39.
 23. Hauser NS, Manoli I, Graf JC, Sloan J, Venditti CP. Variable dietary management of methylmalonic acidemia: metabolic and energetic correlations. *Am J Clin Nutr.* 2011;93:47-56.
 24. Daly A, Pinto A, Evans S et al. Dietary practices in propionic acidemia: a European survey. *Mol Genet Metab Rep.* 2017;13:83-89.
 25. Gebhardt B, Vlaho S, Fischer D, Sewell A, Bohles H. N-carbamylglutamate enhances ammonia detoxification in a patient with decompensated methylmalonic aciduria. *Mol Genet Metab.* 2003;79(4):303-304.
 26. Nashabat M, Obaid A, Al Mutairi F et al. Evaluation of long-term effectiveness of the use of carnitine in patients with propionic acidemia (PA) or methylmalonic acidemia (MMA): study protocol for a randomized controlled trial. *BMC Pediatr.* 2019;19(1):195.
 27. Scaglia F. New insights in nutritional management and amino acid supplementation in urea cycle disorders. *Mol Genet Metab.* 2010;100:S72-76.
 28. Novarino G, El-Fishawy P, Kayserili H et al. Mutations in BCKD-kinase lead to a potentially treatable form of autism with epilepsy. *Science.* 2012;338:394-397.
 29. Garcia-Cazorla A, Oyarzabal A, Fort J et al. Two novel mutations in BCKDK (branched-chain keto-acid dehydrogenase kinase) gene are responsible for a neurobehavioral deficit in two pediatric unrelated patients. *Hum Mut.* 2014;35:470-477.
 30. Semba RD, Shardell M, Sakr Ashour FA et al. Child stunting is associated with low circulating essential amino acids. *EBioMedicine.* 2016;6:246-252.
 31. Valerio A, D'Antona G, Nisoli E. Branched-chain amino acids, mitochondrial biogenesis, and healthspan: an evolutionary perspective. *Aging (Albany NY).* 2011;3(5):464-478.
 32. Singh G, Krishan P. Dietary restriction regimens for fighting kidney disease: insights from rodent studies. *Exp Gerontol.* 2019;128:110738.
 33. Weir HJ, Yao P, Huynh FK et al. Dietary restriction and AMPK increase lifespan via mitochondrial network and peroxisome remodeling. *Cell Metab.* 2017;26:884-896.
 34. Zhang R, Wang X, Qu JH et al. Caloric restriction induces microRNAs to improve mitochondrial proteostasis. *iScience.* 2019;17:155-166.
 35. Gottlieb RA, Carreira RS. Autophagy in health and disease. 5. Mitophagy as a way of life. *Am J Physiol Cell Physiol.* 2010;299(2):C203-10.
 36. Molema F, Gleich F, Burgard P et al. Decreased plasma L-arginine levels in organic acidurias (MMA and PA)

and decreased plasma branched-chain amino acid levels in urea cycle disorders as a potential cause of growth retardation: options for treatment. *Mol Genet Metab.* 2019;126:397-405.

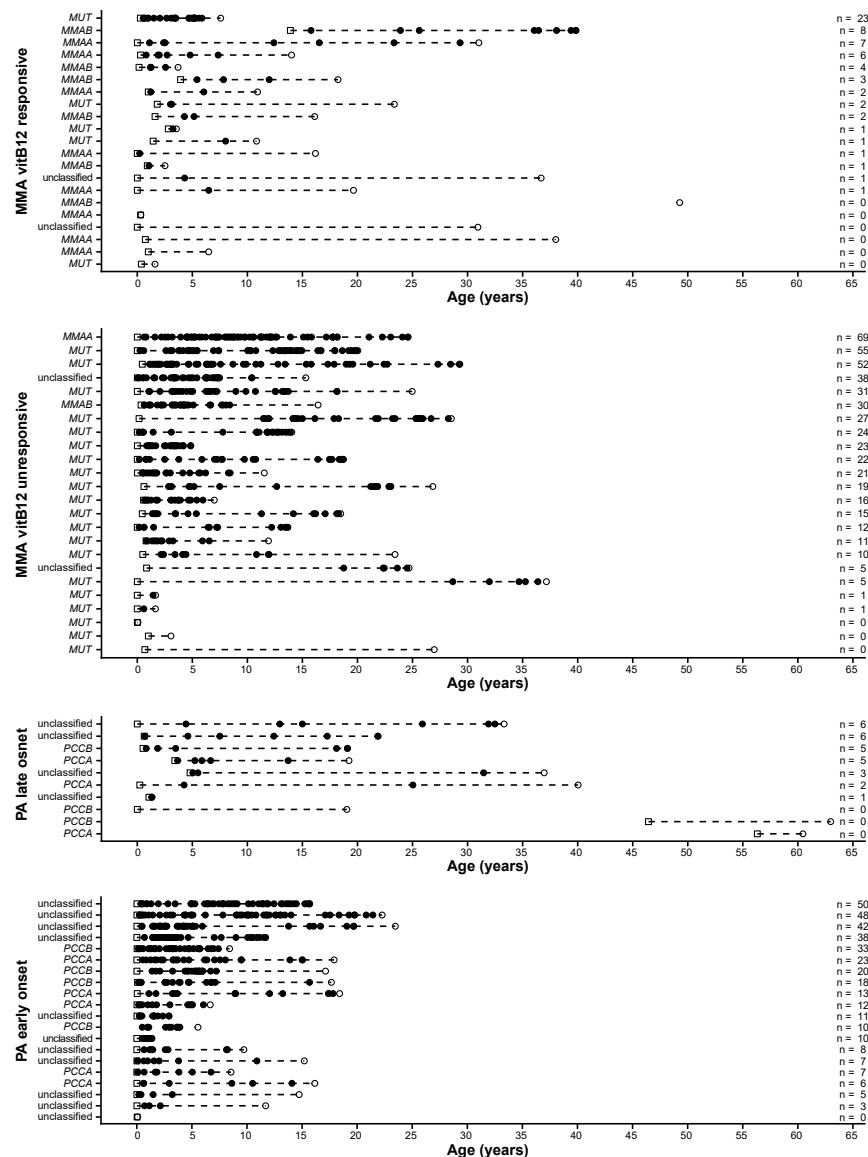
37. Elango R, Ball RO, Pencharz PB. Indicator amino acid oxidation: concept and application. *J Nutr.* 2008;138:243-246.
38. Tome D. Criteria and markers for protein quality assessment – a review. *Br J Nutr.* 2012;108:S222-229.

WEB RESOURCES

OMIM <https://www.omim.org>

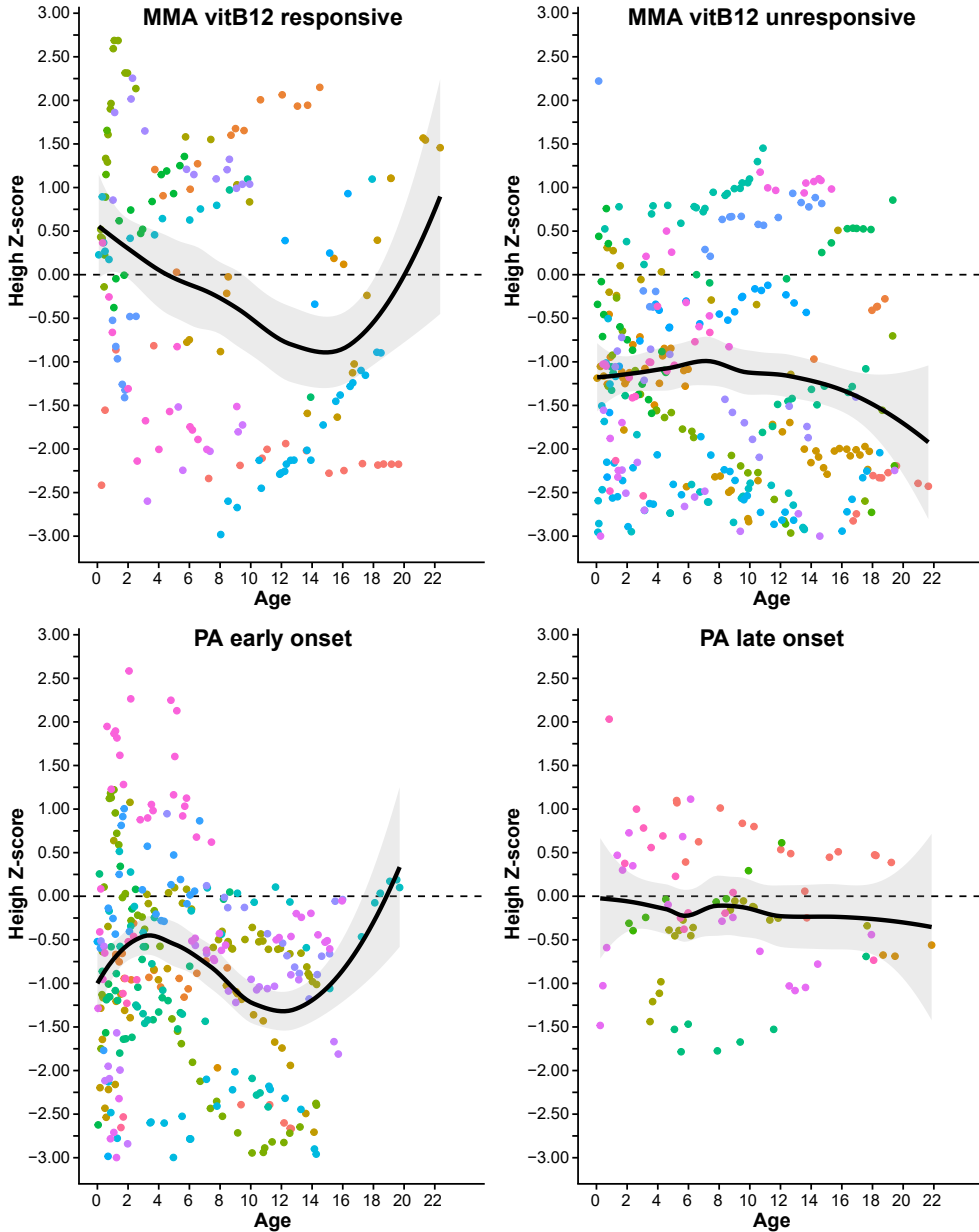
SUPPLEMENTAL DATA

Figure S1. Frequencies of acute metabolic decompensations according to patient's age



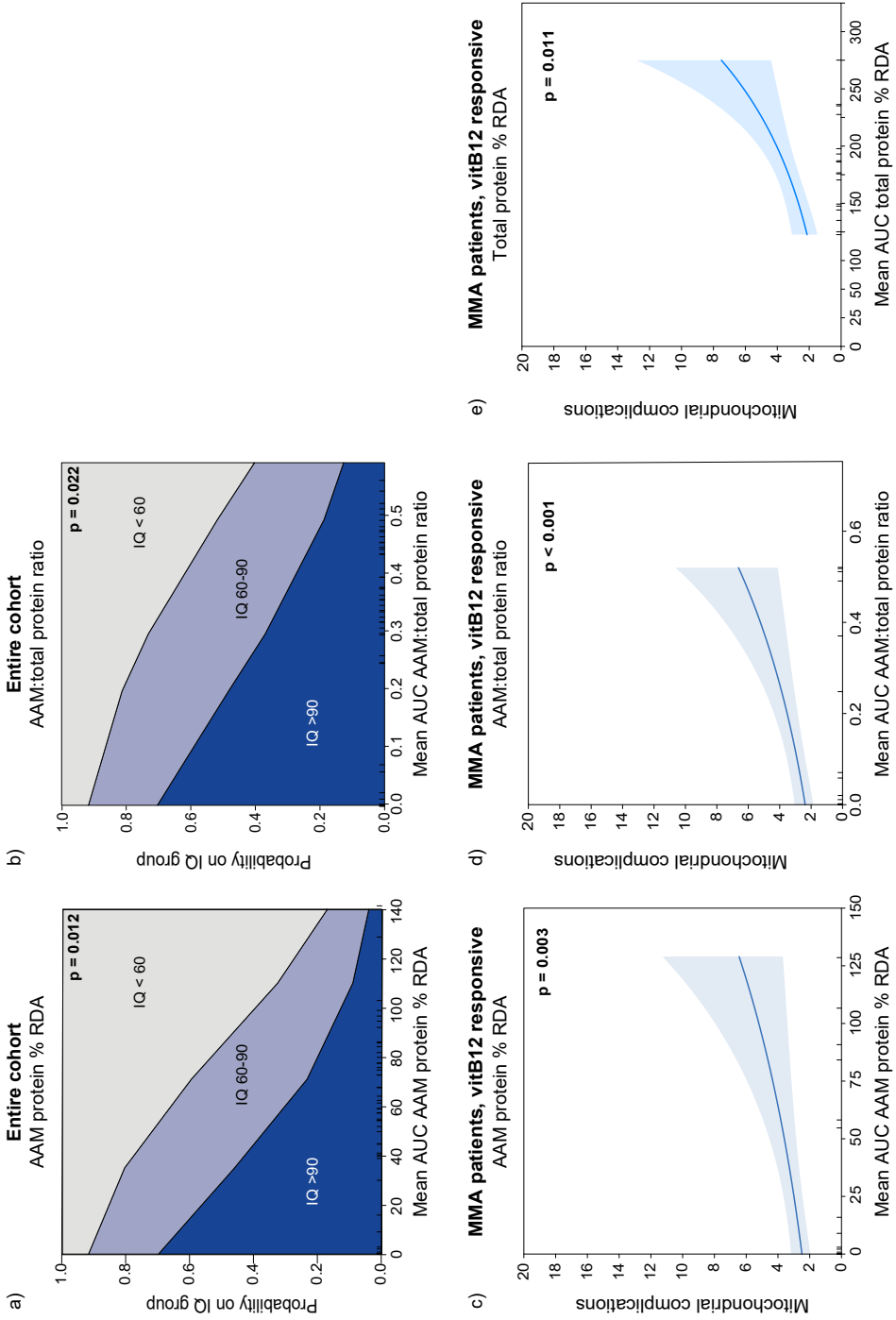
[Figure S1 continued] White squares represent the time at diagnosis, white dots the time at last follow-up for each patient. Each black dot indicates an acute metabolic decompensation requiring hospitalization. n = total number of acute metabolic decompensations. Abbreviations: MMA: methylmalonic acidemia; PA: propionic acidemia.

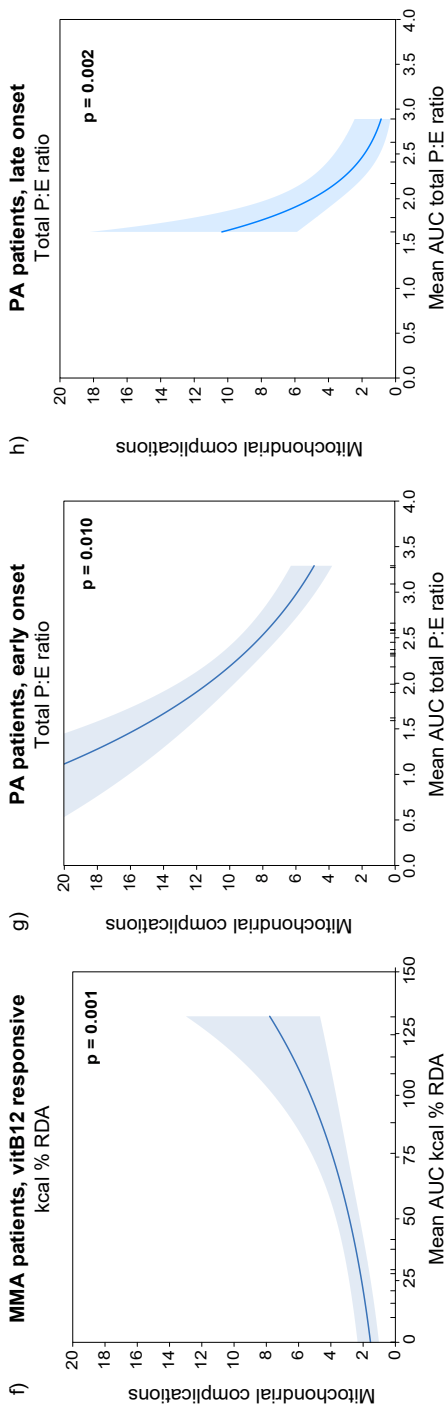
Figure S2. Height Z-scores



Each dot indicates one measurement per patient, each color indicates one individual patient. The black dotted line indicates a height Z-score of 0.00. The black bold line indicates the median height Z-score of the total group, the gray plane indicates the 95% confidence interval of the black line. Abbreviations: MMA: methylmalonic acidemia; PA: propionic acidemia.

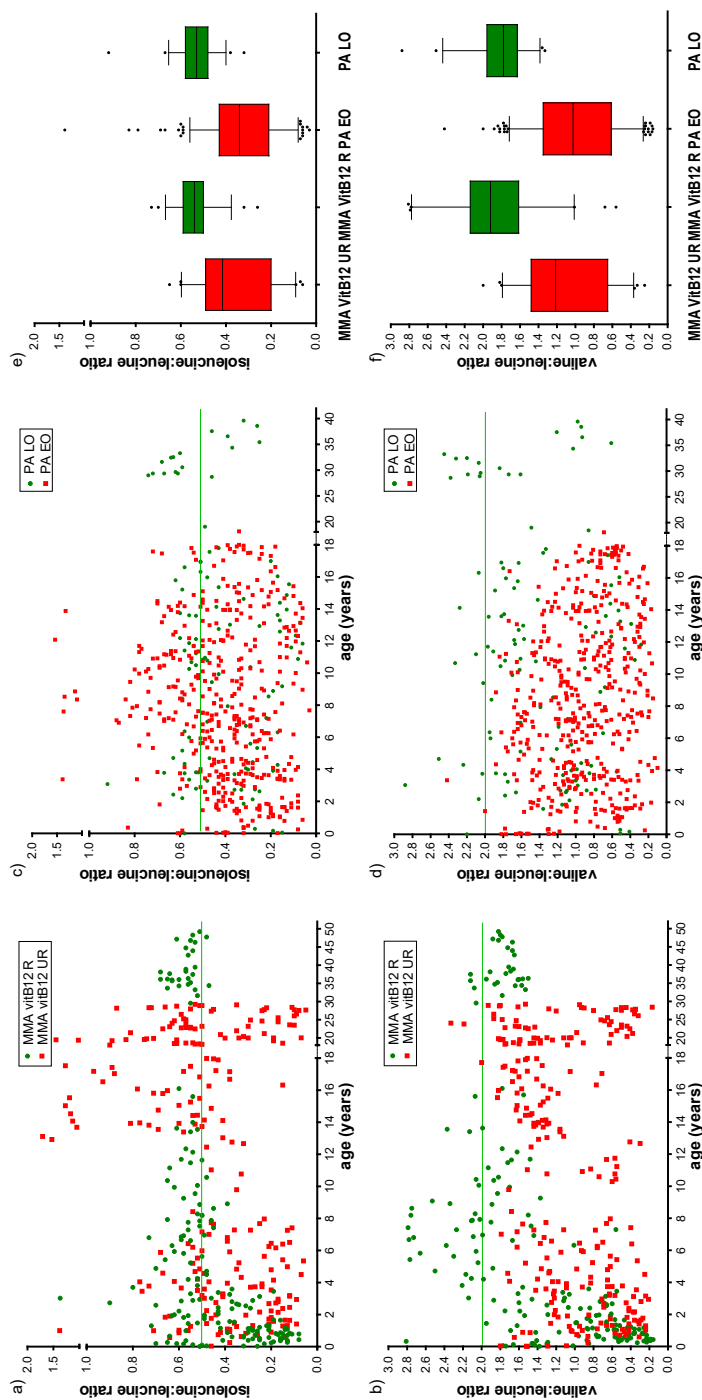
Figure S3. Associations between protein and energy prescription and mitochondrial complications and cognitive development

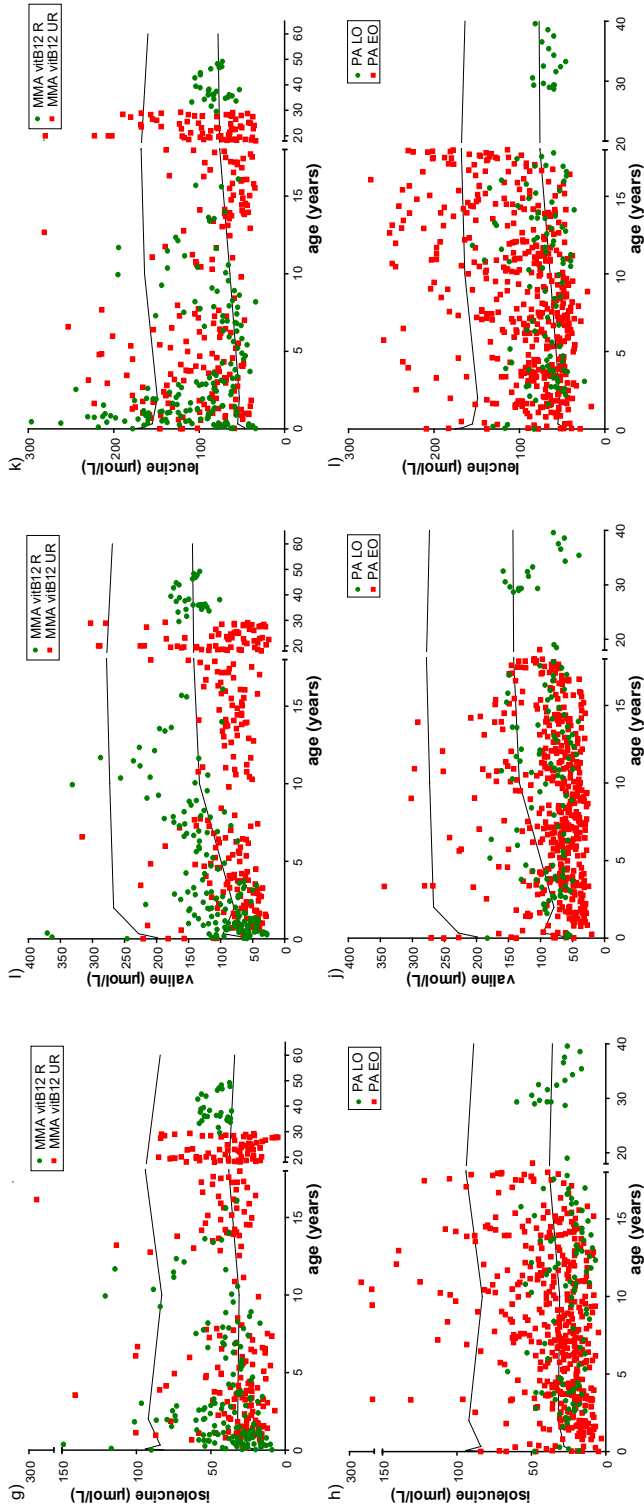




Panel a and b show the association between AAM protein and AAM:total protein ratio prescription and the probability of being in one of the three categories of cognitive functioning for the entire cohort. Panel c, d, e and f show the association between AAM protein, AAM:total protein ratio, total protein and kcal prescription and the risk on mitochondrial complications in MMA vit B12 responsive patients. Panel g and h show the association between total P:E ratio prescription and the risk on mitochondrial complications in PA early onset and late onset patients. Abbreviations: AAM: amino acid mixtures; AUC: area under the curve; kcal: kilocalorie; MMA: methylmalonic acidemia; P:E ratio: protein-to-energy ratio; PA: propionic acidemia; RDA: recommended daily allowances; vitB12: vitamin B12.

Figure S4. Plasma BCAA levels and plasma BCAA ratios according to patient's age





Panel a-d and g-l: dots/squares represent one measurement per patient. Red squares indicate the more severely affected patients, namely MMA vitB12 unresponsive and PA EO patients, and green dots indicate the less severely affected patients, namely MMA vitB12 responsive and PA LO patients. Panel a-d: horizontal green lines indicate the reference value of the ratio. Panel g-j: upper and lower black horizontal lines indicate the age-adjusted upper and lower reference values of the amino acid concentrations. Panel e-f: boxplots based on all measurements per patient, indicating median and 95% CI. Black dots indicate outliers. Abbreviations: EO: early onset; LO: late onset; MMA: methylmalonic acidemia; PA: propionic acidemia; R: responsive; UR: unresponsive; vitB12: vitamin B12.

Table S1. Baseline characteristics

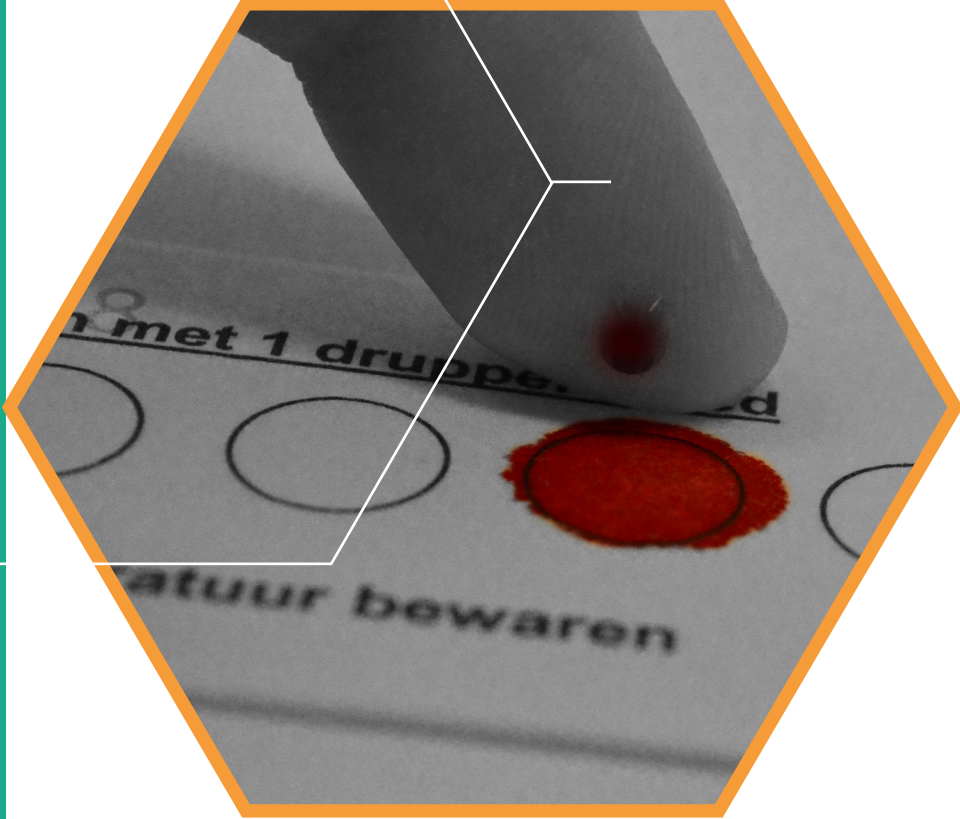
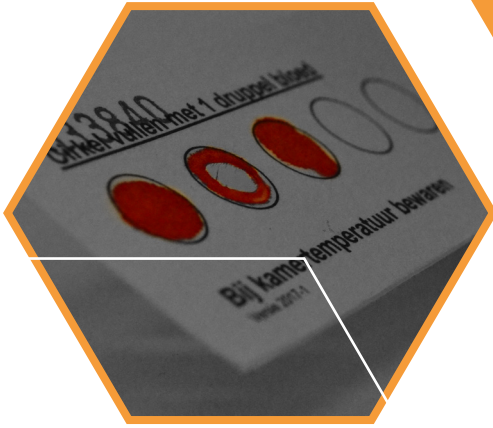
	MMA vitB12 unresponsive	MMA vitB12 responsive	PA EO	PA LO	Entire cohort
Number of patients	24	21	20	10	76*
Age at last follow-up (mean \pm SD)	16.9 \pm 10.2	18.1 \pm 14.4	12.3 \pm 6.7	31.4 \pm 19.4	18.2 \pm 13.5
Natural protein prescribed (measurements)	518	227	423	112	1287
AAM protein prescribed (measurements)	498	126	414	50	1089
Kilocalorie prescribed (measurements)	543	220	415	88	1266
Height (measurements)	429	184	359	87	1061
Number of AMD (mean; min-max)	18.2; 0-50	2.8; 0-6	20.3; 0-69	3.0; 0-23	12.4; 0-69
Cognitive development (number of patients)					
IQ >90	8	9	0	7	24
IQ 60-90	9	4	4	2	20
IQ <60	3	3	12	1	19
Number of mitochondrial complications (mean \pm SD)	6.7 \pm 3.3	4.9 \pm 3.1	9.8 \pm 4.9	4.1 \pm 4.1	6.7 \pm 4.3

*Including 1 PA patient for whom disease onset is unknown. Abbreviations: AAM: amino acid mixture; AMD: acute metabolic decompensation; EO: early onset; LO: late onset; SD: standard deviation; vitB12: vitamin B12.

Table S2. Mean AUC plasma BCAA levels and risk on mitochondrial complications

	MMA vitB12 unresponsive	MMA vitB12 responsive	PA EO	PA LO
Mean AUC plasma valine	NS	p = 0.002	NS	p = 0.010
Mean AUC plasma isoleucine	NS	p = 0.040	NS	p = 0.006
Mean AUC plasma leucine	NS	NS	NS	NS
Isoleucine:leucine ratio	NS	NS	NS	p < 0.001
Valine:leucine ratio	NS	p = 0.001	NS	p = 0.040

Abbreviations: AUC: area under the curve; EO: early onset; LO: late onset; NS: not significant; vitB12: vitamin B12.



Understanding acute metabolic decompensation in

propionic and methylmalonic acidemias: a deep
metabolic phenotyping approach

Orphanet Journal of Rare Diseases 2020, 15(1): 68
DOI: 10.1186/s13023-020-1347-3

Hanneke A. Haijes*, Judith J.M. Jans, Maria van der Ham,
Peter M. van Hasselt, Nanda M. Verhoeven-Duif*

* Corresponding authors

ABSTRACT

Background: Pathophysiology of life-threatening acute metabolic decompensations (AMD) in propionic acidemia (PA) and isolated methylmalonic acidemia (MMA) is insufficiently understood. Here, we study the metabolomes of PA and MMA patients over time, to improve insight in which biochemical processes are at play during AMD.

Methods: Longitudinal data from clinical chemistry analyses and metabolic assays over the life-course of 11 PA and 13 MMA patients were studied retrospectively. Direct-infusion high-resolution mass spectrometry was performed on 234 and 154 remnant dried blood spot and plasma samples of PA and MMA patients, respectively. In addition, a systematic literature search was performed on reported biomarkers. All results were integrated in an assessment of biochemical processes at play during AMD.

Results: We confirmed many of the metabolite alterations reported in literature, including increases of plasma valine and isoleucine during AMD in PA patients. We revealed that plasma leucine and phenylalanine, and urinary pyruvic acid were increased during AMD in PA patients. 3-hydroxyisovaleric acid correlated positively with plasma ammonia. We found that known diagnostic biomarkers were not significantly further increased, while intermediates of the branched-chain amino acid (BCAA) degradation pathway were significantly increased during AMD.

Discussion: We revealed that during AMD in PA and MMA, BCAA and BCAA intermediates accumulate, while known diagnostic biomarkers remain essentially unaltered. This implies that these acidic BCAA intermediates are responsible for metabolic acidosis. Based on this, we suggest to measure plasma 3-hydroxyisovaleric acid and urinary ketones or 3-hydroxybutyric acid for the biochemical follow-up of a patient's metabolic stability.

KEY MESSAGE

During AMD in PA and MMA, BCAA and BCAA intermediates accumulate, while known diagnostic biomarkers remain essentially unaltered, implying that these acidic BCAA intermediates are responsible for metabolic acidosis.

INTRODUCTION

Propionic acidemia (PA) and isolated methylmalonic acidemia (MMA) are disorders affecting the catabolic pathway of the branched-chain amino acids (BCAA) L-isoleucine and L-valine, and the amino acids L-threonine and L-methionine. PA is caused by a deficiency of propionyl-CoA carboxylase (encoded by *PCCA* and *PCCB*), and isolated MMA is either caused by a deficiency of methylmalonyl-CoA mutase, methylmalonyl-CoA epimerase or by a defect in the metabolism of the cofactor of methylmalonyl-CoA mutase, 5'-deoxyadenosylcobalamin (encoded by *MUT*, *MCEE*, *MMAA*, *MMAB* or *MMADHC*, respectively).

The clinical course of PA and MMA is characterized by life-threatening acute metabolic decompensations (AMD). Clinically, AMD result in lethargy, anorexia, vomiting, dehydration, hypotonia, Kussmaul breathing and potentially coma and even death. Biochemically, AMD are characterized by hyperammonemia, metabolic acidosis with a high anion gap and lactic acidosis.^{1,2} AMD are held responsible for the neurological deficits that patients present with, such as psychomotor retardation, cognitive impairment, movement disorders and epilepsy.³ AMD are thought to arise as a result of a catabolic stressor, which induces protein catabolism and increases the load of toxic metabolites, causing clinical distress. However, despite increasing knowledge on specific metabolite alterations during these decompensations, pathophysiology of AMD is not entirely understood. Plasma ammonia for example, is considered the best available biochemical read-out of AMD, but does not provide insight in other pathophysiological processes that may occur during AMD. Increased insight in the exact pathophysiological events during AMD could potentially pave the way towards optimized clinical care and better neurological outcomes.^{4,5}

To increase pathophysiological understanding of AMD, we here study the metabolomes throughout life of twenty-four PA and MMA patients. Hereto, longitudinal results from targeted biochemical assays and from untargeted metabolomics were analyzed, and integrated with the results of a systematic search for biomarkers reported in literature.

METHODS

Patient inclusion

Patients were eligible for inclusion when PA or isolated MMA was enzymatically or genetically confirmed (patients with combined methylmalonic aciduria and homocystinuria were excluded), and when targeted metabolic analyses had been performed or when remnant samples were available at the University Medical Centre Utrecht. All twenty-four included patients or their legal guardians provided written approval for the analysis of their medical records and the use of their remnant samples for this research. All procedures followed were in accordance with the ethical standards of the University Medical Centre Utrecht (17-490/C) and with the Helsinki Declaration of 1975, as revised in 2000.

Eleven patients were diagnosed with PA and thirteen with MMA, of whom four were nonresponsive and nine were responsive to cobalamin supplementation (Table 1). Median age at follow-up was 17.9 and 11.9 years for PA and MMA patients, respectively (Table 1). Three PA patients and one MMA patient died (Table 1). Patients were treated in line with current treatment protocols.³

Targeted biochemical analyses

Available results of all targeted analyses performed throughout the patient's life in the clinical chemical laboratory and in the metabolic diagnostic laboratory of the University Medical Centre Utrecht were systematically retrieved (Table 1).

Table 1. Patient and sample inclusion

Patient	Sex	Age (y)	Gene	Cobalamin resp.	Pre-sen-tation	Number of AMD per patient year	Targeted analysis clinical laboratory		Targeted metabolic assays		NUMBER OF SAMPLES in plasma		Untargeted DI-HRMS in DBS					
							Total	No AMD	Total	No AMD	Total	No AMD	Total	No AMD				
P.01	F	19.6	MUT	No	Early	0.4	217	46	19	96	43	5	20	11	1	15	0	1
P.02	M	11.9	MUT	No	Late	0.9	43	28	0	69	59	0	20	19	0	11	10	0
P.03	F	11.0	MUT	Yes	Late	0.1	6	6	0	18	17	1	8	8	0	7	7	0
P.04	F	7.2	MUT	No	Late	0.5	1	1	0	2	2	0	1	1	0	0	0	0
P.05	M	7.5	MUT	Yes	Late	2.1	1	0	0	6	0	0	0	0	0	0	0	0
P.06	F	20.2	MM/AA	Yes	Early	0.1	79	52	1	76	59	1	18	14	0	7	7	0
P.07*	F	16.2	MM/AA	Yes	Early	0.1	87	37	2	57	41	0	6	4	0	3	3	0
P.08*	M	t, 0.3	MM/AA	Yes	Late	0	0	0	0	2	0	0	0	0	0	0	0	0
P.09	M	13.9	MM/AA	Yes	Late	0.1	7	7	0	7	7	0	2	2	0	2	2	0
P.10	F	11.1	MM/AA	Yes	Late	0.1	44	0	3	60	1	1	13	0	1	19	1	1
P.11	F	40.6	MM/AB	Yes	Late	0.0	25	10	0	16	11	0	2	1	0	0	0	0
P.12	M	0.1	MM/AA#	No	Early	0	0	0	0	7	0	0	0	0	0	0	0	0
P.13	M	37.3	MM/AA#	Yes	Early	0.0	0	0	0	19	0	0	0	0	0	0	0	0
							510	187	25	435	240	8	90	60	2	64	30	2
P.14	F	23.1	PA#		Early	0.6	369	18	38	106	3	14	18	0	2	7	0	1
P.15*	F	t, 2.9	PA#		Early	4.1	33	28	3	0	0	0	1	1	0	0	0	0
P.16*	M	12.5	PA#		Family	2.4	92	6	19	21	3	3	9	1	2	13	0	2
P.17	F	17.6	PCCB		Early	0.7	206	6	23	92	0	9	29	9	4	24	0	4
P.18	F	17.9	PCCA		Early	0.7	251	64	31	128	50	12	37	11	4	30	0	4
P.19	F	8.6	PCCB		Early	2.6	157	5	36	14	1	3	9	1	3	7	0	2
P.20	M	t, 7.5	PCCB		Early	0.3	0	0	0	19	0	0	0	0	0	0	0	0
P.21	F	24.6	PCCA		Late	0.2	16	0	0	7	0	0	1	0	0	0	0	0
P.22*	M	t, 19.1	PCCB		Late	0.3	80	1	2	72	2	0	12	0	0	0	0	0
P.23*	M	19.1	PCCB		Family	0.1	62	32	4	61	32	1	19	9	0	11	0	0
P.24	M	20.4	PCCA		Late	0.2	11	0	1	7	0	0	4	0	0	3	0	0
							1277	160	157	527	91	42	139	23	15	95	0	13

Subtotals are depicted in bold. Early onset: presentation <28 days of life; Late onset: presentation >28 days of life. Family: diagnosis at birth through an affected sibling. Abbreviations: AMD: acute metabolic decompensation; F: female; M: male; (S): sibling; (V): years; *P.07 and P.08, P.15 and P.16, and P.22 and P.23 are pairs of siblings; #: genetic defect is unclassified; t: passed away.

Untargeted biochemical analyses: Direct-infusion high-resolution mass spectrometry

Blood samples were drawn and stored as described before.⁶ Direct-infusion high-resolution mass spectrometry (DI-HRMS) was performed on 234 remnant DBS and plasma samples of PA patients and on 154 remnant DBS and plasma samples of MMA patients (Table 1), as described before.⁶ DI-HRMS analysis resulted in the identification of 1,905 mass peaks that could be annotated as 3,929 metabolites that are expected to occur endogenously. For each mass peak per patient sample, the deviation from the intensities in the thirty control samples was indicated by a Z-score⁶. Z-scores were calculated for both patient and control samples and were considered aberrant when > 2.0 or < -1.5 .

Data analysis

A sample was classified as “no AMD” when the sample was obtained at an outpatient, scheduled visit that did not result in hospitalization. A sample was classified as “AMD” when the sample was drawn on the first day of admission, when the patient was hospitalized for an (impending) AMD. All other samples, for example samples drawn during hospitalizations but not on the first day, were considered neither “no AMD” nor “AMD” (Table 1).

To identify diagnostic biomarkers in targeted analyses, a metabolite was considered a biochemical disease marker when the median was below the lower limit of the reference range (RR), or above the upper limit of the RR. For DI-HRMS, Mann-Whitney U tests were performed comparing samples classified as “no AMD” to control samples, for PA and MMA separately.

To identify metabolites associated with metabolic instability, Mann-Whitney U tests were performed comparing samples classified as “AMD” with samples classified as “no AMD”, for both PA and MMA separately. In addition, Spearman correlation tests were performed comparing concentrations and Z-scores of every measured metabolite in every patient in this study to plasma ammonia concentrations.

P-values were adjusted according to the Bonferroni method, and considered statistically significant when < 0.05 . R^2 values were considered biologically relevant when > 0.50 or < -0.50 . Data analysis was performed in R programming language. Data and R code are available on request.

Supervised clustering analyses were performed using the software of MetaboAnalyst 4.0.⁷ Z-score tables with unpaired samples in columns were uploaded. No missing value estimation, data filtering or normalization was performed. The analysis paths “Partial Least Squares – Discriminant Analysis” (PLS-DA) including the 2D scores plot and the variable importance in projection score, and heatmaps were analyzed.

Literature study

To obtain an overview on known diagnostic biomarkers and on biochemical parameters reported to be associated with AMD in PA and MMA, we performed an extensive literature search.^{4,5} All reports discussing biomarkers were systematically evaluated and results were tabulated in Table S1.^{1,2,8-31} This table lists, to the best of our knowledge, the first reports of diagnostic biomarkers, of biochemical parameters associated with the presence of AMD and of biochemical parameters that correlate with plasma ammonia in PA and MMA.^{1,2,8-31}

Integration of findings reported in literature and study results

Findings reported in the reviewed literature as listed in Table S1^{1,2,8-31} were combined with the results obtained in this study and visualized in an overview of the catabolic pathway of

L-isoleucine, L-valine, L-threonine and L-methionine, derived from figure 1 and 2 of Haijes et al. 2019,⁵ to obtain an overview of the all known metabolite alterations during AMD in PA and MMA. For each of the alterations, the significance for the pathophysiology of AMD was assessed.

Since we did not quantify propionyl-CoA or acetyl-CoA, propionylcarnitine and acetylcarnitine were used as proxy to estimate these concentrations. In healthy individuals, acetylcarnitine is ten-fold higher than propionylcarnitine (RR 0.7 – 9.7 $\mu\text{mol/L}$ for acetylcarnitine, RR 0.0 – 0.8 $\mu\text{mol/L}$ for propionylcarnitine). Extrapolation of these concentrations suggests that the C2/C3 ratio in healthy individuals approximates 10. The C2/C3 ratio in PA and MMA patients was calculated based on targeted quantification of acetylcarnitine and propionylcarnitine.

RESULTS

Confirmation of metabolite alterations already reported in literature

Targeted metabolic assays in the included samples confirmed abnormalities in thirteen diagnostic biomarkers reported in the reviewed literature, of which six are shared between PA and MMA, three were only observed in PA patients and four were only observed in MMA patients (Table S2, Figure S1). Untargeted DI-HRMS confirmed six disease biomarkers, three of which are shared between PA and MMA, two were only observed in PA patients and one was only observed in MMA patients (Table S2, Figure S2-S3). PLS-DA of untargeted DI-HRMS data from both DBS and plasma confirmed propionylcarnitine, propionylglycine, glycine, 3-dehydroxycarnitine and 2-methylcitric acid as biomarkers for PA (Figure S4-S11), and methylmalonic acid, propionylcarnitine, glycine, 2-methylcitric acid, 3-dehydroxycarnitine and methylmalonyl-carnitine as biomarkers for MMA (Figure S12-S17).

With respect to the samples obtained during AMD, clinical chemistry tests confirmed that urea was increased in MMA patients (Table 2, Figure S18-S19) and that ammonia was increased in PA patients (Table 2, Figure S18, S20). Targeted metabolic assays confirmed the increases of valine and isoleucine, the decreases of glutamine, citrulline and free carnitine in plasma, and the increase of lactic acid and 3-hydroxybutyric acid in urine, in PA patients during AMD (Table 2, Figure S21-S29). Untargeted DI-HRMS confirmed 3-hydroxyisovaleric acid (10 isomers) as a biochemical marker increased during AMD in PA patients (Table 2, Figure S30-S31).

Targeted metabolic assays and untargeted DI-HRMS disclosed that 2-methylcitric acid, 3-hydroxypropionic acid and propionylglycine correlated positively with plasma ammonia (Table 3, Figure S32-S33).

Identification of novel metabolite alterations

Targeted analysis of amino acids revealed that histidine was significantly decreased in (treated) PA patients and glutamine was significantly decreased in (treated) MMA patients (Table S2, Figure S1, S24, S34). Histidine was also relatively decreased in MMA, and glutamine in PA, although the medians were not below the lower limit of the RR (Table S2, Figure S1, S24, S34). Untargeted DI-HRMS showed that histidine and glutamine were significantly decreased in both PA and MMA patients (Table S2, Figure S2). In addition, untargeted DI-HRMS unveiled 17 unreported potential diagnostic biomarkers (Table S2, Figure S2-S3) including increased lysoPC(15:0) (2 isomers), lysoPC(17:0) (2 isomers) and 2-amino-3-phosphonopropionic acid, especially in PA patients, and increased propionic acid (2 isomers) in MMA patients (Table S2, Figure S35-S39). PLS-DA of untargeted DI-HRMS data from both DBS and plasma confirmed 2-amino-3-phosphopropionic acid and lysoPC(15:0)

as biomarkers for PA, and propionic acid as biomarker for MMA (Figure S4, S12), supporting that these three metabolites could serve as diagnostic biomarkers.

Investigation of biochemical parameters associated with AMD disclosed that urea, as already reported for MMA, was increased in PA patients during AMD (Table 2, Figure S18-S19). In addition, glucose was slightly increased in both PA and MMA patients (Table 2, Figure S18, S20) and ionized calcium was decreased in PA patients during AMD (Table 2, Figure S18). Targeted metabolic assays uncovered six unreported biochemical parameters altered during AMD in PA patients. Leucine and phenylalanine in plasma and pyruvic acid in urine were increased (Table 2, Figure S21, S39-S42), and C8- and C10-carnitine in plasma and homovanillic acid were decreased (Table 2, Figure S21). Untargeted DI-HRMS revealed an increase of acetylcysteine and cortisol, and a normalization of fructoseglycine during AMD in PA patients (Table 2), but PLS-DA of untargeted DI-HRMS data from both DBS and plasma demonstrated that AMD could not be distinguished clearly from no AMD, based on the patients' metabolomes (Figure S43-S44).

Both targeted metabolic assays and untargeted DI-HRMS showed that 3-hydroxyisovaleric acid correlated positively with plasma ammonia (Table 3, Figure S30-S33). In addition, two biochemical parameters for mitochondrial disease were found to negatively correlate with ammonia: alanine/lysine ratio and alanine/(phenylalanine+tyrosine) ratio (Table 3, Figure S32).

Integration of findings reported in literature and study results

Metabolite alterations during AMD, either reported in the reviewed literature or reported here, are visualized in Figure 1. Contrary to what is often expected, diagnostic biomarkers such as propionylglycine, propionylcarnitine, methylmalonylcarnitine, propionic acid and methylmalonic acid remained essentially unaltered during AMD (Figure 1 – Part 2, Table 4), although for methylmalonic acid, the non-significant test results could be due to the small number of samples drawn during AMD ($n = 2$, Table 4). Rather, AMD appeared to induce an increase of BCAA and BCAA intermediates, all upstream metabolites of propionyl-CoA (Figure 1 – Part 1). Based on this observation, we propose that the acidic BCAA intermediates are responsible for the metabolic acidosis in PA and MMA patients during AMD.

Interestingly, intermediates of the leucine degradation pathway were elevated as well, even though leucine is not degraded via propionyl-CoA (Figure 1 – Part 1). The increase of leucine and 2-oxoisocaproate could be explained by inhibition of the branched-chain α -ketoacid dehydrogenase complex (BCKDC) by -CoA esters, including propionyl-CoA.^{2,32} BCKDC is the rate-limiting enzyme in the BCAA catabolism pathway and is responsible for the irreversible step that converts branched-chain α -ketoacids into isobutyryl-CoA, 2-methylbutyryl-CoA and isovaleryl-CoA. Increases of valine and isoleucine, as well as increases of 2-oxoisovalerate and 2-oxo-methylvalerate, have also been explained by inhibition of BCKDC (Figure 1 – Part 1). However, inhibition of BCKDC cannot explain all reported increases of BCAA intermediates. Reasons for accumulation of metabolites downstream of BCKDC, such as 3-hydroxyisovaleric acid, 2-methylbutyric acid and 3-methylglutaconic acid await further elucidation.

Next, the increase of plasma ammonia, and the relative decrease of plasma citrulline can be explained as follows. Propionyl-CoA inhibits N-acetylglutamate synthase and consequently, there is a lack of stimulation of carbamoylphosphate synthase.³³ This process might be aggravated by the relative decrease of acetyl-CoA and glutamine (Figure 1 – Part 2). The result is decreased detoxification of ammonia³³ and also a relative lack of carbamoylphosphate.

Table 2A. Biochemical parameters associated with presence of AMD for PA

Analyte	Matrix	No AMD Median \pm SD [Min-Max] (N)	AMD Median \pm SD [Min-Max] (N)	P-value	Known
Clinical chemistry					
Urea	Plasma	3.5 \pm 1.8 [0.4-8.0] (84)	6.3 \pm 2.9 [0.6-15.3] (103)	<0.0001	No
Glucose	Plasma	5.1 \pm 1.1 [3.8-10.9] (104)	6.2 \pm 5.4 [1.2-44.8] (194)	<0.0001	Yes
Ammonia	Plasma	75 \pm 41 [9-222] (107)	115 \pm 221 [21-1807] (170)	<0.0001	Yes
Calcium ionized	Plasma	1.30 \pm 0.06 [1.09 - 1.38] (33)	1.22 \pm 0.08 [0.91 - 1.32] (75)	0.0001	No
Targeted metabolic assays					
Leucine	Plasma	59 \pm 23 [31 - 152] (73)	113 \pm 65 [16 - 318] (34)	<0.0001	No
Phenylalanine	Plasma	37 \pm 8 [26 - 61] (73)	54 \pm 22 [32 - 146] (34)	0.0001	No
Valine	Plasma	66 \pm 26 [20 - 183] (73)	121 \pm 72 [25 - 344] (34)	0.0019	Yes
Isoleucine	Plasma	21 \pm 9 [7 - 48] (73)	40 \pm 28 [8 - 131] (29)	0.0104	Yes
Lactic acid	Urine	46 \pm 206 [18 - 1067] (30)	878 \pm 3462 [201 - 11273] (16)	<0.0001	Yes
3-Hydroxybutyric acid	Urine	10 \pm 190 [2 - 766] (16)	366 \pm 1311 [152 - 5284] (15)	0.0052	Yes
Pyruvic acid	Urine	29 \pm 24 [4 - 121] (24)	103 \pm 180 [23 - 712] (15)	0.0115	No
Glutamine	Plasma	494 \pm 105 [252 - 793] (73)	383 \pm 110 [189 - 698] (34)	0.0066	Yes
Citrulline	Plasma	28 \pm 8 [6 - 50] (73)	17 \pm 11 [4 - 53] (34)	0.0073	Yes
C10-carnitine	Plasma	0.08 \pm 0.02 [0.04 - 0.14] (31)	0.04 \pm 0.03 [0.02 - 0.15] (22)	0.0296	No
Free carnitine	Plasma	38.9 \pm 16.8 [7.0 - 93.3] (56)	22.0 \pm 12.4 [8.0 - 70.1] (25)	0.0370	Yes
C8-carnitine	Plasma	0.05 \pm 0.01 [0.03 - 0.09] (29)	0.03 \pm 0.02 [0.01 - 0.10] (22)	0.0446	No
Homovanillic acid	Urine	8.3 \pm 7.5 [4.0 - 35.0] (22)	2.0 \pm 1.9 [1.0 - 7.0] (15)	0.0166	No
Untargeted DI-HRMS					
Acetylcysteine	Plasma	-0.2 \pm 1.6 [-1.6 - 4.2] (23)	3.9 \pm 10.1 [0.5 - 41.6] (15)	0.0031	No
Cortisol (2 isomers)	Plasma	0.1 \pm 0.9 [-1.8 - 0.8] (23)	1.6 \pm 1.1 [-0.8 - 4.0] (15)	0.0208	No
3-Hydroxyisovaleric acid (10 isomers)	Plasma	0.0 \pm 7.5 [-1.9 - 33.8] (23)	12.3 \pm 13.6 [4.3 - 58.7] (12)	0.0412	Yes
Fructoseglycine	Plasma	7.6 \pm 5.7 [-0.8 - 25.8] (23)	0.9 \pm 2.6 [-1.3 - 6.2] (15)	0.0073	No

Results of clinical chemistry are presented in mmol/L, except for ammonia for which results are presented in $\mu\text{mol/L}$. Results of targeted metabolic assays in plasma are presented in $\mu\text{mol/L}$, results of targeted metabolic assays in urine are presented in mmol/mol creatinine. All p-values were adjusted according to the Bonferroni method. A p-value < 0.05 was considered statistically significant. Abbreviations: DI-HRMS: direct-infusion high-resolution mass spectrometry; Max: maximum value; Min: minimum value; (N): number of samples; NS: not significant; SD: standard deviation.

Table 2B. Biochemical parameters associated with presence of AMD for MMA

Analyte	Matrix	No AMD Median \pm SD [Min-Max] (N)	AMD Median \pm SD [Min-Max] (N)	P-value	Known
Clinical chemistry					
Urea	Plasma	3.0 \pm 1.6 [1.0 – 8.2] (93)	9.1 \pm 8.0 [1.8 – 25.3] (10)	0.0043	Yes
Glucose	Plasma	5.2 \pm 1.1 [3.7 – 11.2] (86)	6.1 \pm 1.2 [4.8 – 9.5] (27)	0.0288	No
Ammonia	Plasma	45 \pm 22 [13 – 97] (66)	49 \pm 33 [20 – 161] (22)	NS	
Calcium ionized	Plasma	1.27 \pm 0.05 [1.07 – 1.35] (40)	1.22 \pm 0.06 [1.14 – 1.32] (10)	NS	
Targeted metabolic assays					
Leucine	Plasma	77 \pm 40 [34 – 223] (77)	97 \pm 11 [89 – 104] (2)	NS	
Phenylalanine	Plasma	45 \pm 14 [24 – 110] (77)	77 \pm 16 [65 – 88] (2)	NS	
Valine	Plasma	107 \pm 42 [41 – 217] (77)	143 \pm 11 [135 – 150] (2)	NS	
Isoleucine	Plasma	32 \pm 15 [7 – 84] (77)	43 \pm 12 [34 – 51] (2)	NS	
Lactic acid	Urine	41 \pm 314 [2 – 3424] (149)	123 \pm 133 [40 – 425] (7)	NS	
3-Hydroxybutyric acid	Urine	9 \pm 503 [0 – 3377] (50)	14 \pm 2867 [9 – 6436] (5)	NS	
Pyruvic acid	Urine	15 \pm 12 [0 – 76] (72)	33 \pm 13 [11 – 45] (5)	NS	
Glutamine	Plasma	380 \pm 126 [190 – 736] (77)	303 \pm 13 [294 – 312] (2)	NS	
Citrulline	Plasma	24 \pm 16 [8 – 133] (77)	19 \pm 6 [14 – 23] (2)	NS	
C10-carnitine	Plasma	0.16 \pm 0.79 [0.03 – 5.09] (68)	0.10 \pm 0.07 [0.04 – 0.18] (3)	NS	
Free carnitine	Plasma	42.8 \pm 21.2 [3.0 – 105.7] (89)	45.5 \pm 66.4 [18.1 – 144.3] (3)	NS	
C8-carnitine	Plasma	0.11 \pm 0.59 [0.03 – 3.69] (68)	0.09 \pm 0.04 [0.04 – 0.12] (3)	NS	
Homovanillic acid	Urine	5.0 \pm 4.9 [1.0 – 27.5] (71)	1.0-5.0 [1.0 – 12.0] (5)	NS	
Untargeted DI-HRMS					
Acetylcysteine	Plasma	0.2 \pm 1.0 [-2.2 – 2.7] (51)	0.9 \pm 1.6 [-0.3 – 2.1] (2)	NS	
Cortisol (2 isomers)	Plasma	0.1 \pm 1.0 [-1.8 – 2.8] (51)	0.2 \pm 2.9 [-1.9 – 2.2] (2)	NS	
3-Hydroxyisovaleric acid (10 isomers)	Plasma	0.0 \pm 0.7 [-0.6 – 3.4] (51)	1.9 \pm 2.7 [-0.1 – 3.8] (2)	NS	
Fructoseglycine	Plasma	2.2 \pm 2.2 [-1.2 – 7.6] (51)	3.0 \pm 1.6 [1.8 – 4.1] (2)	NS	

Results of clinical chemistry are presented in mmol/L, except for ammonia for which results are presented in $\mu\text{mol/L}$. Results of targeted metabolic assays in plasma are presented in $\mu\text{mol/L}$, results of targeted metabolic assays in urine are presented in mmol/mol creatinine. All p-values were adjusted according to the Bonferroni method. A p-value < 0.05 was considered statistically significant. Abbreviations: DI-HRMS: direct-infusion high-resolution mass spectrometry; Max: maximum value; Min: minimum value; (N): number of samples; NS: not significant; SD: standard deviation.

Table 3. Biochemical parameters that correlate with plasma ammonia for PA and MMA

Analyte	Matrix	N	R ²	P-value	Known
Targeted metabolic assays					
Ketones	Plasma	5	1.00	<0.0001	No
2-Methylcitric acid*	Plasma	42	0.77	<0.0001	Yes
Arachidonic acid	Plasma	44	0.72	<0.0001	No
3-Hydroxyisovaleric acid	Plasma	39	0.70	0.0058	No
2-Methylcitric acid*	Plasma	79	0.67	<0.0001	Yes
3-Hydroxyisovaleric acid	Urine	163	0.67	<0.0001	No
3-Hydroxypropionic acid	Plasma	46	0.66	<0.0001	Yes
Glutaric acid	Urine	149	0.64	<0.0001	No
Pipicolinic acid	Plasma	68	0.52	0.0432	No
Alanine/lysine ratio	Plasma	94	-0.68	<0.0001	No
C4-DC carnitine	Plasma	225	-0.55	<0.0001	No
C14:1 carnitine/C2 carnitine ratio	Plasma	88	-0.53	0.0011	No
Alanine/(phenylalanine+tyrosine) ratio	Plasma	94	-0.51	0.0013	No
Untargeted DI-HRMS					
2-Methylcitric acid (3 isomers)	Plasma	157	0.68	<0.0001	Yes
Alanyl-Isoleucine (3 isomers)	Plasma	157	0.65	<0.0001	No
3-Hydroxyisovaleric acid (10 isomers)	Plasma	157	0.64	<0.0001	No
3-Methyl-2-oxovaleric acid (7 isomers)	DBS	122	0.56	<0.0001	No
Isobutyrylglycine (6 isomers)	Plasma	157	0.55	<0.0001	No
Indole-5,6-quinonez	DBS	122	0.53	<0.0001	No
Propionylglycine (9 isomers)	DBS	122	0.52	<0.0001	Yes
3-Hydroxyphenylacetic acid (3 isomers)	Plasma	157	0.51	<0.0001	No
Indole-5,6-quinone	Plasma	157	0.51	<0.0001	No
Pyrocatechol sulfate	DBS	122	-0.65	<0.0001	No
Threonic acid	DBS	122	-0.60	<0.0001	No
Trimethylamine N-oxide	DBS	122	-0.59	<0.0001	No
Stearoylcarnitine	DBS	122	-0.58	<0.0001	No
Methylmalonic acid (3 isomers)	DBS	122	-0.57	<0.0001	No
Ergothioneine	DBS	122	-0.55	<0.0001	No

All p-values were adjusted according to the Bonferroni method. A p-value < 0.05 was considered statistically significant. An R² value of > 0.50 or < -0.50 was considered biologically relevant. *Due to methodological developments over time, two different diagnostic assays for 2-methylcitric acid were included in the analysis, both demonstrating a solid positive correlation with plasma ammonia. Abbreviations: DI-HRMS: direct-infusion high-resolution mass spectrometry; N: number of samples.

Table 4A. Diagnostic biomarkers for PA that are not significantly altered during AMD

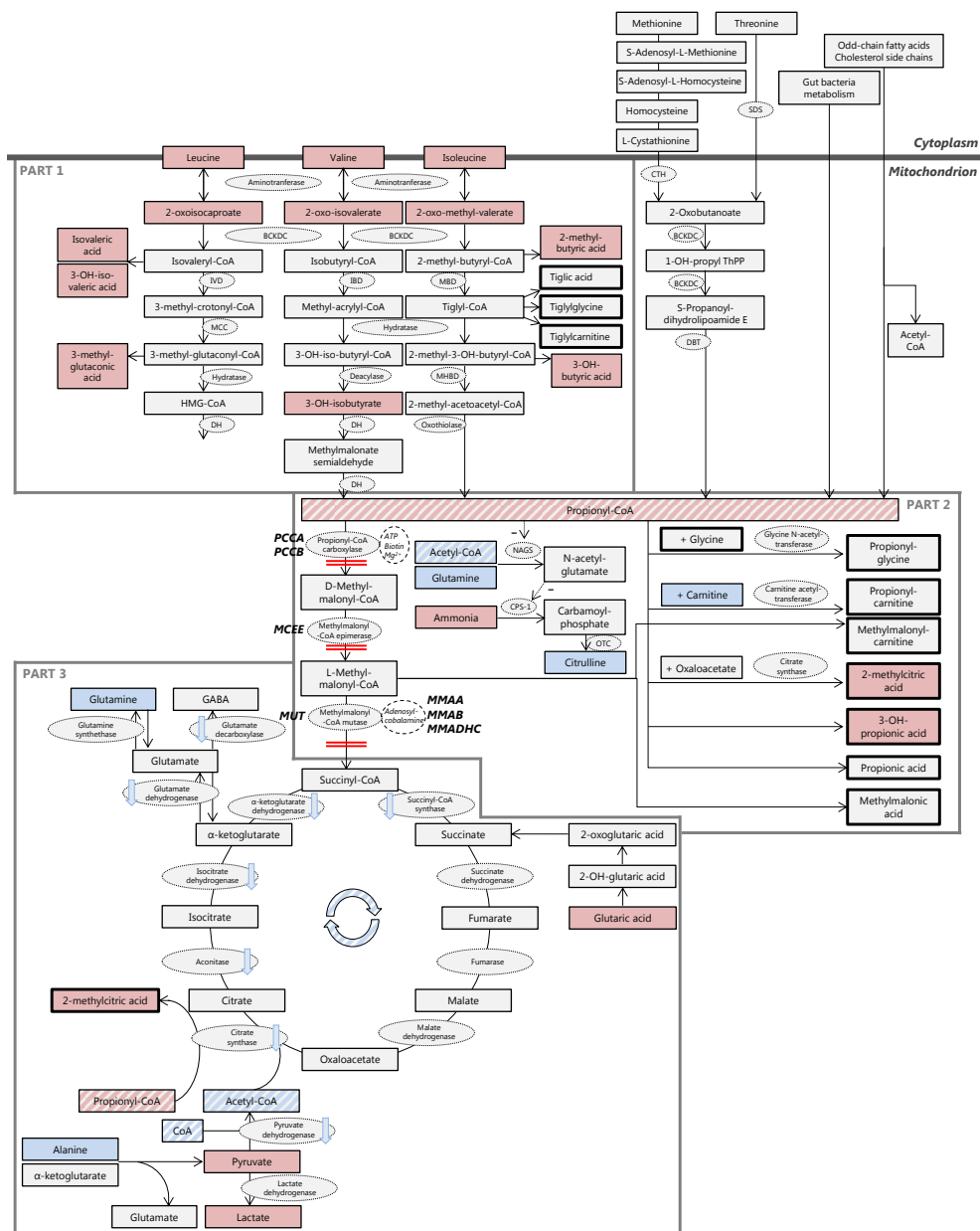
Analyte	Matrix	No AMD	AMD	P
		Median \pm SD [Min-Max] (N)	Median \pm SD [Min-Max] (N)	
Targeted metabolic ass.				
Propionylcarnitine	Plasma	54.4 \pm 19.6 [23.0 – 99.5] (34)	49.7 \pm 25.6 [24.0 – 128.0] (23)	NS
Glycine	Plasma	1381 \pm 362 [350 – 1962] (73)	1160 \pm 514 [265 – 2051] (35)	NS
Methylcitric acid	Plasma		49.5 \pm 14.8 [24.9 – 78.9] (12)	NS
Methylcitric acid	Urine	697 \pm 383 [425 – 968] (3)		NS
3-OH-propionic acid	Urine	232 \pm 99 [89 – 349] (10)	738 \pm 355 [184 – 1534] (13)	NS
Acetylcarnitine	Plasma	10.1 \pm 7.5 [1.6 – 42.2] (34)	10.9 \pm 9.5 [1.3 – 43.9] (23)	NS
Untargeted DI-HRMS				
Propionylcarnitine	Plasma	12.0 \pm 80.8 [-2.8 – 363] (23)	272 \pm 193 [1.5 – 730] (15)	NS
Glycine	Plasma	9.5 \pm 4.8 [-2.4 – 18.5] (23)	4.9 \pm 4.1 [-0.4 – 14.7] (15)	NS
2-Methylcitric acid (3 isomers)	Plasma	57.4 \pm 43.1 [-1.8 – 147] (23)	93.7 \pm 31.4 [30.4 – 139] (15)	NS
Propionylglycine (9 isomers)	Plasma	28.5 \pm 29.3 [-3.0 – 91.1] (23)	80.6 \pm 50.1 [4.0 – 177.1] (15)	NS

Table 4B. Diagnostic biomarkers for MMA that are not significantly altered during AMD

Analyte	Matrix	No AMD	AMD	P
		Median \pm SD [Min-Max] (N)	Median \pm SD [Min-Max] (N)	
Targeted metabolic ass.				
Propionylcarnitine	Plasma	21.0 \pm 21.7 [2.7 – 83.7] (68)	78.0 \pm 81.0 [14.8 – 175.5] (3)	NS
Glycine	Plasma	492 \pm 369 [168 – 1916] (77)	334 \pm 152 [226 – 441] (2)	NS
Methylcitric acid	Plasma	2.2 \pm 2.8 [1.0 – 10.9] (11)		NS
Methylcitric acid	Urine			NS
3-OH-propionic acid	Urine	13.0 \pm 18.6 [0. – 86.0] (57)	9.5 \pm 76.8 [4.0 – 161.0] (4)	NS
Methylmalonylcarnitine	Plasma	7.6 \pm 7.7 [3.4 – 20.2] (5)		NS
Methylmalonic acid	Plasma	74 \pm 346 [3 – 1327] (52)		NS
Methylmalonic acid	Urine	727 \pm 4651 [64 – 21587] (174)	4062 \pm 3200 [536 – 9044] (7)	NS
Acetylcarnitine	Plasma	9.2 \pm 5.8 [2.1 – 29.9] (68)	12.6 \pm 24.4 [3.9 – 49.9] (3)	NS
Untargeted DI-HRMS				
Propionylcarnitine	Plasma	37.9 \pm 171 [-1.4 – 684] (61)	596 \pm 835 [5.7 – 1186] (2)	NS
Glycine	Plasma	1.8 \pm 2.2 [-1.1 – 8.5] (61)	2.7 \pm 3.0 [0.5 – 4.8] (2)	NS
2-Methylcitric acid (3 isomers)	Plasma	9.0 \pm 9.5 [-0.6 – 41.3] (61)	41.1 \pm 27.0 [22.1 – 60.2] (2)	NS
Propionylglycine (9 isomers)	Plasma	1.6 \pm 3.1 [-2.3 – 10.4] (61)	5.8 \pm 5.3 [2.0 – 9.6] (2)	NS
Methylmalonic acid (3 isomers)	Plasma	25.3 \pm 77.5 [-0.0 – 376] (61)	150 \pm 175 [26.3 – 274] (2)	NS
Methylmalonylcarnitine	Plasma	2.4 \pm 9.1 [-2.3 – 29.7] (61)	22.9 \pm 31.7 [0.4 – 45.3] (2)	NS

Results of targeted metabolic assays in plasma are presented in $\mu\text{mol/L}$, results of targeted metabolic assays in urine are presented in mmol/mol creatinine. All p-values were adjusted according to the Bonferroni method. A p-value < 0.05 was considered statistically significant. Abbreviations: DI-HRMS: direct-infusion high-resolution mass spectrometry; Max: maximum value; Min: minimum value; (N): number of samples; NS: not significant; P: p-value; SD: standard deviation.

Figure 1. Alterations of the propionate pathway in times of acute metabolic decompensation



Metabolites are depicted in rectangles. Metabolites with significantly increased values during acute metabolic decompensations (AMD) are depicted in red, metabolites with normal values during AMD are depicted in light gray and metabolites with significantly decreased values during AMD are depicted in blue. The potential blockages of the pathway, due to enzyme deficiencies in PA and MMA, are depicted by double red lines. Genes involved in PA and MMA are depicted in bold capitals. Propionyl-CoA and acetyl-CoA, central metabolites in the pathway, are highlighted by diagonal stripes. Enzymes are depicted in light gray ovals, cofactors are depicted in white ovals. Decreased activity of enzymes is depicted by light blue arrows. The pathway is distinguished in three parts, indicated by dark gray lines. Cytoplasm is distinguished from the mitochondrion, indicated by a broad dark gray

[Figure 1 continued] line. Abbreviations: BCKDC: branched-chain α -ketoacid dehydrogenase complex; CPS-1: carbamoyl phosphate synthase I; CTH: cystathionine gamma-lyase; DBT: dihydrolipoamide branched chain transacylase E2; DH: dehydrogenase; IBD: isobutyryl-CoA dehydrogenase; IVD: isovaleryl-CoA dehydrogenase; MBD: 2-methylbutyryl-CoA dehydrogenase; MCC: 3-methylcrotonyl-CoA carboxylase; MHBD: 2-methyl-3-hydroxybutyryl-CoA dehydrogenase; NAGS: N-acetylglutamate synthase; OTC: ornithine transcarbamylase; SDS: L-serine dehydratase.

As carbamoylphosphate is the precursor of citrulline, we hypothesize that the observed decrease of plasma citrulline is caused by hampered citrulline formation by ornithine transcarbamylase (Figure 1 – Part 2).

Downstream consequences of accumulation propionyl-CoA appear to be centered around a relative shortage of acetyl-CoA (Figure 1 – Part 3). The median value of propionylcarnitine is five-fold higher than the median value of acetylcarnitine (Table 4) in PA and MMA patients. Hence, the C2/C3 carnitine ratio, which we use as proxy for the ratio of acetyl-CoA over propionyl-CoA, approximates 0.5, which is a twenty-fold decrease compared to healthy individuals. We hypothesize that as a consequence of this relative shortage, the high levels of propionyl-CoA compete with the relatively low levels of acetyl-CoA for citrate synthase, resulting in formation of excessive amounts of 2-methylcitric acid formed from propionyl-CoA and oxaloacetate, rather than citrate (Figure 1 – Part 3). Reduced conversion of acetyl-CoA and oxaloacetate into citrate could augment, in turn, depletion of citric acid cycle intermediates, potentially causing an energy deficiency (Figure 1 – Part 3).

To replenish the citric acid cycle, we hypothesize that two different routes are being utilized. Firstly, in line with others, we hypothesize that glutamine, and possibly glutamate, might be used to replenish α -ketoglutarate, and that for this reason glutamine is decreased (Figure 1 – Part 3).^{1,2,28,34} Secondly, alanine might be used for anaplerosis as well. In combination with a propionyl-CoA induced decreased activity of pyruvate dehydrogenase⁵ this could result in the observed increase of both pyruvate and lactate (Figure 1 – Part 3), which could explain the observed lactic acidosis.

DISCUSSION

Through an extensive literature study and a longitudinal analysis of the metabolomes of a cohort of PA and MMA patients, we revealed that during AMD, BCAA and BCAA intermediates accumulate, while known diagnostic biomarkers remain essentially unaltered. This implies that these acidic metabolites are responsible for metabolic acidosis. In addition, we speculated that downstream consequences of accumulating propionyl-CoA are centered around a relative shortage of acetyl-CoA, potentially resulting in depletion of citric acid cycle intermediates and thereby explaining the observed energy deficiency in PA and MMA patients. A relative shortage of acetyl-CoA could also explain the decrease of glutamine, decrease of alanine and the increases of pyruvate and lactate, thereby explaining the observed lactic acidosis.

Biochemical analyses to perform during AMD

This study presents an overview of what is currently known on the biochemical processes during AMD in PA and MMA. More insight in the metabolic stability of a patient at a certain point in time can be attained by measuring plasma ammonia and lactate, pH, $p\text{CO}_2$, bicarbonate and base excess. To improve insight in the metabolic consequences of AMD, we suggest to measure 2-methylcitric acid and 3-hydroxyisovaleric acid in plasma, as these parameters are significantly correlated to plasma ammonia and since 3-hydroxyisovaleric

acid is significantly increased during AMD. In addition, we suggest to measure urinary ketones – which is already common practice by many clinicians – or specifically urinary 3-hydroxybutyric acid, as this metabolite is also significantly increased during AMD. Altogether, quantification of these markers could increase insight in the patient's current metabolic stability. Conversely, we conclude that quantification of diagnostic biomarkers does not contribute to insight in the current metabolic stability of a patient.

Although concentrations were often still in the normal range, isoleucine, valine and leucine, as well as glutamine, citrulline and alanine could also be determined in times of AMD, as a trend analysis on an individual patient basis could increase insight in the biochemical processes during AMD in that patient. In addition, we advise to determine free carnitine concentrations to monitor whether carnitine supplementation is sufficient during AMD, as free carnitine is relatively decreased during AMD.

Therapeutic interventions during AMD

Since free carnitine is relatively decreased during AMD, increasing free carnitine might improve scavenging of propionyl-CoA and methylmalonyl-CoA. This could be achieved by emergency (increase of) carnitine supplementation, possibly in a much earlier stage than at the time of hospital admission.

In addition, during AMD there is also a significant decrease of plasma citrulline, although the lack of citrulline is not as distinct as in urea cycle disorders. We speculate that citrulline supplementation, as provided during AMD in urea cycle disorders as N-acetylglutamate synthase deficiency, carbamoyl phosphate synthase I deficiency and ornithine transcarbamylase deficiency to maximize ammonia excretion through the urea cycle,³⁵ might also contribute to ammonia detoxification in severely decompensated PA and MMA patients, but this hypothesis requires further study.

Potential novel diagnostic biomarkers

Untargeted DI-HRMS revealed four metabolites that could potentially be new diagnostic biomarkers for PA and MMA. However, as diagnosing PA and MMA is often quite straightforward, the added value of these four metabolic markers for diagnostic purposes is limited. Though, these markers could point towards important pathophysiological processes in PA and MMA, and thereby they could potentially serve as markers for certain disease conditions, such as long-term metabolic control or neurological damage.

Firstly, lysoPC(15:0) and lysoPC(17:0), phospholipids with an odd-chain tail, were unveiled as potential disease biomarkers, especially in PA patients. It has been reported that increased intracellular concentration of propionyl-CoA leads to a relative abundance of odd-numbered long-chain fatty acids in body lipids, for example in erythrocyte membrane lipids. These odd-numbered long-chain fatty acids seem to be increased even higher in patients with a more severe clinical course.³⁶ It has been hypothesized that odd-numbered long-chain fatty acids are a reflection of continuous burden of propionyl-CoA toxicity within the cells, and that this might serve as a reliable tool for evaluating the quality of the long-term metabolic control.³⁷ In line with this, we observed that lysoPC(15:0) and lysoPC(17:0) were higher in patients that experienced AMD more frequently.

Secondly, in PA patients, 2-amino-3-phosphonopropionic acid (AP3) was found to be increased. It could not be distinguished whether this increase was caused by L-AP3, D-AP3 or a combination thereof. Yuan et al. found that D-AP3 does not induce any neurotoxic effects,³⁸ but, in contrast, that L-AP3 is a stereoselective metabotropic excitatory glutamate

receptor antagonist that blocks activation of excitatory glutamate receptors³⁸ and thereby increases activity of the *N*-acetyl-D-aspartate receptor.³⁸⁻⁴⁰ Activation of the *N*-acetyl-D-aspartate receptor by propionic acid and methylmalonic acid has been described as an important pathophysiological process in inducing apoptosis of neurons and thereby causing neurological complications in PA and MMA,^{4,5,41} although the exact cascade is not fully understood. L-AP3 could be an intermediate in this process. This is further supported by a study demonstrating that intracaudal injection of L-AP3 in rats caused a neurotoxic effect, characterized by vasogenic brain edema and neuronal degeneration, processes that are also described in PA and MMA.⁴ An *N*-acetyl-D-aspartate receptor antagonist attenuated this effect. Although a potential role of L-AP3 in inducing neural degeneration is interestingly, this is still speculative.

Thirdly, a metabolite with a molecular weight corresponding to propionic acid and its endogenous isomers lactaldehyde and hydroxyacetone and its exogenous isomers ethyl formate, 3-hydroxypropanal and methyl acetate, was found to be markedly increased in MMA. Unexpectedly, this feature was not increased in PA. However, for none of the possible annotations of this *m/z*, a role in MMA but not in PA could be hypothesized. Since a very consistent correlation between methylmalonic acid and this metabolite was identified, both in DBS and plasma, especially for Z-scores > 50, we hypothesize that this metabolite could be a potential biomarker for MMA, and that this yet unannotated compound is a derivative of methylmalonic acid.

Limitations and strengths

An important limitation of this study, inherent to studying rare diseases, is the limited sample cohort (Table 1). Almost all samples were drawn during dietary and/or pharmacological treatment, complicating pathophysiological interpretation. In addition, identification of metabolic markers characterizing AMD was affected by a smaller sample size, especially for MMA, for which no significant results were obtained for both targeted and untargeted analyses. Also, due to the retrospective design, samples were not obtained for every patient at similar time points. Moreover, our limited understanding of metabolic stability in PA and MMA patients impeded classification of samples as drawn during AMD or in times of metabolic stability. This may have contributed to the fact that we were not able to detect metabolic markers that could clearly distinguish AMD from no AMD. Furthermore, interpretation of historical data was affected by methodological developments, leading to different assays performed to quantify one metabolite, for example for 2-methylcitric acid. Lastly, the fact that due to direct-infusion an observed mass can account for multiple metabolite annotations, hampered solid conclusions on for example L-AP3 as potential biomarker for PA patients, and a metabolite with an *m/z* corresponding to propionic acid as potential biomarker for MMA patients. Therefore, the implications of these findings remain to be further elucidated.

Due to the limited sample size and variation in assays performed at each time point, we were not able to calculate the fraction of the anion gap of the accumulating BCAA intermediates during an AMD. To test our hypothesis that accumulation of BCAA intermediates is responsible for metabolic acidosis during AMD, we suggest to determine the fraction of the anion gap of BCAA intermediates during AMD in a prospective study.

Despite these limitations, important strengths of this study are that historical, longitudinal results from both clinical chemistry and targeted metabolic assays were combined with untargeted analyses in remnant samples, in order to search for potential disease biomarkers

as broad as possible. Our approach accurately verified the findings of previous studies and we identified potentially novel diagnostic biomarkers for both PA and MMA. By combining our results with an extensive literature search on biomarkers for PA and MMA during AMD, we generated new hypotheses regarding which biochemical processes could be at play in the pathophysiology of AMD in PA and MMA.

CONCLUSION

In conclusion, we here verify and expand reported findings on altered metabolites during AMD in PA and MMA. We illustrate in detail what could be important pathophysiological processes during AMD. Based on our findings, we propose that accumulating acidic BCAA intermediates may be held responsible for inducing metabolic acidosis during AMD, instead of propionic acid and methylmalonic acid, which are essentially unaltered during AMD.

REFERENCES

- Zwickler T, Haege G, Riderer A, Hörster F, Hoffmann GF, Burgard P, Kölker S. Metabolic decompensation in methylmalonic aciduria: which biochemical parameters are discriminative? *J Inherit Metab Dis.* 2012;35:797-806.
- Zwickler T, Riderer A, Haege G, Hoffmann GF, Kölker S, Burgard P. Usefulness of biochemical parameters in decision-making on the start of emergency treatment in patients with propionic acidemia. *J Inherit Metab Dis.* 2014;37:31-7.
- Baumgartner MR, Hörster F, Dionisi-Vici C et al. Proposed guidelines for the diagnosis and management of methylmalonic and propionic acidemia. *Orphanet J Rare Dis.* 2014;9:130.
- Haijes HA, Jans JJM, Tas SY, van Hasselt PM, Verhoeven-Duif NM. Pathophysiology of propionic and methylmalonic acidemias. Part 1: Complications. *J Inherit Metab Dis.* 2019;42(5):730-744.
- Haijes HA, van Hasselt PM, Jans JJM, Verhoeven-Duif NM. Pathophysiology of propionic and methylmalonic acidemias. Part 2: Treatment strategies. *J Inherit Metab Dis* 2019;42(5):745-761.
- Haijes HA, Willemsen M, van der Ham M et al. Direct infusion based metabolomics identifies metabolic disease in patients' dried blood spots and plasma. *Metabolites* 2019;9.
- Chong J, Soufan O, Li C et al. *MetaboAnalyst 4.0: towards more transparent and integrative metabolomics analysis.* *Nucl. Acids Res.* 2018; 46:486-484.
- Childs B, Nyhan WL, Borden M, Bard L, Cooke RE. Idiopathic hyperglycinemia and hyperglycinuria: a new disorder of amino acid metabolism. I. *Pediatrics* 1961;27:522-38.
- Gompertz D, Storrs CN, Bau DC, Peters TJ, Hughes EA. Localisation of enzymic defect in propionicacidaemia. *Lancet* 1970; 1:1140-1143.
- Rosenberg LE, Lilljehqvist AC, Hsia YE. Methylmalonic aciduria – an inborn error leading to metabolic acidosis, long-chain ketonuria and intermittent hyperglycinemia. *N Engl J Med.* 1968;278:1319-1322.
- Hommes FA, Kuipers JR, Elema JD, Jansen JF, Jonxis JH. Propionicacidemia, a new inborn error of metabolism. *Pediatr Res.* 1968;2:519-24.
- Ando T, Rasmussen K, Nyhan WL, Donell GN, Barnes ND. Propionic acidemia in patients with ketotic hyperglycinemia. *J Pediatr.* 1971;78:827-32.
- Ando T, Rasmussen K, Wright JM, Nyhan WL. Isolation and identification of methylcitrate, a major metabolic product of propionate in patients with propionic acidemia. *J Biol Chem.* 1972; 247:2200-4.
- Chalmers RA, Lawson AM, Watts RW. Studies on the urinary acidic metabolites excreted by patients with beta-methylcrotonylglycinuria, propionic acidemia and methylmalonic acidemia, using gas-liquid chromatography and mass spectrometry. *Clin Chim Acta* 1974;52:43-51.
- Ando T, Rasmussen K, Nyhan WL, Hull D. 3-hydroxypropionate: significance of –oxidation of propionate in patients with propionic acidemia and methylmalonic acidemia. *Proc Natl Acad Sci U S A* 1972;69:2807-11.
- Rasmussen K, Ando T, Nyhan WL et al. Excretion of propionylglycine in propionic acidemia. *Clin Sci.* 1972;42:665-71.
- Thompson GN, Chalmers RA. Increased urinary metabolite excretion during fasting in disorders of propionate metabolism. *Pediatr Res.* 1990;27:413-6.
- Rasmussen K, Ando T, Nyhan WL, Hull D, Cottom D, Kilroy AW, Wadlington W. Excretion of tiglylglycine in propionic acidemia. *J Pediatr.* 1972;81:970-2.
- Imen M, Hanene B, Ichraf K, Aida R, Ilhem T, Naziha K, Neziha GK. Methylmalonic acidemia and hyperglycemia: an unusual association. *Brain Dev.* 2012;34:113-4.
- Duran M, Bruinvis L, Ketting D, Kamerling JP, Wadman SK, Schutgens RB. The identification of (E)-2-

- methylglutaconic acid, a new isoleucine metabolite, in the urine of patients with beta-ketothiolase deficiency, propionic acidemia and methylmalonic acidemia. *Biomed Mass Spectrom.* 1982;9:1-5.
21. Wikoff WR, Gangoi JA, Barshop BA, Siuzdak G. Metabolomics identifies perturbations in human disorders of propionate metabolism. *Clin Chem.* 2007;53:2169-76.
 22. Roe CR, Hoppel CL, Stacey TE, Chalmers RA, Tracey BM, Millington DS. Metabolic response to carnitine in methylmalonic aciduria. An effective strategy for elimination of propionyl groups. *Arch Dis Child.* 1983;58:916-20.
 23. Malvagia S, Haynes CA, Grisotto L et al. Heptadecanoylcarnitine (C17) a novel candidate biomarker for newborn screening of propionic and methylmalonic acidemias. *Clin Chim Acta* 2015;23:342-8.
 24. Nyhan WL, Ando T, Rasmussen K, Wadlington W, Kilroy AW, Cottom D, Hull D. Tiglicaciduria in propionicacidemia. *Biochem J.* 1972;126:1035-7.
 25. Oberholzer VG, Levin B, Burgess EA, Young WF. Methylmalonic aciduria. An inborn error of metabolism leading to chronic metabolic acidosis. *Arch Dis Child.* 1967;42:492-504.
 26. van den Berg H, Boelkens MT, Hommes FA. A case of methylmalonic and propionic acidemia due to methylmalonyl-CoA carboxylmutase apoenzyme deficiency. *Acta Paediatr Scand.* 1976;65:113-8.
 27. Maeda Y, Ito T, Suzuki A et al. Simultaneous quantification of acylcarnitine isomers containing dicarboxylic acylcarnitines in human serum and urine by high-performance liquid chromatography/electrospray ionization tandem mass spectrometry. *Rapid Commun Mass Spectrom.* 2007;21:799-806.
 28. Kuhara T, Shinka T, Matsuo M, Matsumoto I. Increased excretion of lactate, glutarate, 3-hydroxyisovalerate and 3-methylglutaconate during clinical episodes of propionic acidemia. *Clin Chim Acta* 1982;123:101-9.
 29. Kølvrå S, Gregersen N, Christensen E, Rasmussen K. Excretion pattern of branched-chain amino acid metabolites during the course of acute infections in a patient with methylmalonic acidemia. *J Inherit Metab Dis.* 1980;3:63-6.
 30. Filipowicz HR, Ernst SL, Ashurst CL, Pasquali M, Longo N. Metabolic changes associated with hyperammonemia in patients with propionic acidemia. *Mol Genet Metab.* 2006;88:123-30.
 31. de Sain-van der Velden MG, van der Ham M, Verhoeven-Duif NM, Visser G, van Hasselt PM. Comment on Zwickler et al.: usefulness of biochemical parameters in decision-making on the start of emergency treatment in patients with propionic acidemia. *J Inherit Metab Dis.* 2014;37:651-2.
 32. Brosnan JT, Brosnan ME. Branched-chain amino acids: enzyme and substrate regulation. *J Nutr.* 2006;136:207S-11S.
 33. Coude FX, Sweetman L, Nyhan WL. Inhibition by propionyl-coenzyme A of N-acetylglutamate synthetase in rat liver mitochondria. A possible explanation for hyperammonemia in propionic and methylmalonic acidemia. *J Clin Invest.* 1979;64:1544-51.
 34. Scholl-Bürgi S, Sass JO, Heinz-Erian P et al. Changes in plasma amino acid concentrations with increasing age in patients with propionic acidemia. *Amino Acids* 2010;38:1473-81.
 35. Häberle J, Burlina A, Chakrapani A et al. Suggested guidelines for the diagnosis and management of urea cycle disorders: First revision. *J Inherit Metab Dis.* 2019; 42(6):1192-1230.
 36. Sperl W, Murr C, Skladal D, Sass JO, Suormala T, Baumgartner R, Wendel U. Odd-numbered long-chain fatty acids in propionic acidemia. *Eur J Pediatr.* 2000;159:54-8.
 37. Wendel U, Eissler A, Sperl W, Schadewaldt P. On the differences between urinary metabolite excretion and odd-numbered fatty acid production in propionic and methylmalonic acidemias. *J Inherit Metab Dis.* 1995;18:584-591.
 38. Yuan F, Wang TY, Xu LX, Sun YL, Luo L, Qu BQ. Neurotoxic effect of high dose of L-(+)-2-amino-3-phosphonopropionic acid in rats after intracaudal injection. *Acta Pharmacol Sin.* 2001;22:556-60.
 39. Schoepp DD, Johnson BG, Smith EC, McQuaid LA. Stereoselectivity and mode of inhibition of phosphoinositide-coupled excitatory amino acid receptors by 2-amino-3-phosphonopropionic acid. *Mol Pharm.* 1990;38:222-228.
 40. Ambrosini A, Bresciani L, Fracchia S, Brunello N, Racagni G. Metabotropic glutamate receptors negatively coupled to adenylate cyclase inhibit N-methyl-D-aspartate receptor activity and prevent neurotoxicity in mesencephalic neurons in vitro. *Mol Pharm.* 1990;47:1057-1064.
 41. Malfatti CRM, Perry MLS, Schweigert ID et al. Convulsions induced by methylmalonic acid are associated with glutamic acid decarboxylase inhibition in rats: a role for GABA in the seizures presented by methylmalonic acidemia patients? *Neuroscience.* 2007;146:1879-1887.

SUPPLEMENTAL DATA

[Figure S1 – S44](#)

Due to the sizes of the figures, these figures are only available online.

Table S.1. Reported biochemical parameters associated with PA or MMA, with the presence of AMD and with plasma ammonia in PA and MMA

Analyte	Matrix	Alteration	PROPIONIC ACIDURIA References	Alteration	METHYLMALONIC ACIDURIA References
General disease biomarkers					
Glycine	Plasma, urine	Increase	Chids et al. 1961, Gompertz et al. 1970 Hommes et al. 1968, Ando et al. 1971	Increase	Rosenberg, Lilljeqvist and Hsia 1968 Ando et al. 1971
Propionic acid	Plasma	Increase	Ando et al. 1972a, Chalmers et al. 1974	Increase	Chalmers et al. 1974
2- Methylcitric acid	Urine	Increase	Ando et al. 1972b	Increase	
3-Hydroxypropionic acid	Urine	Increase	Rasmussen et al. 1972a	Increase	Ando et al. 1972b
Propionylglycine	Urine	Increase	Rasmussen et al. 1972b	Increase	Thompson and Chalmers 1990 Imen et al. 2012
Tiglylglycine	Plasma, urine	Increase	Duran et al. 1982, Wikoff et al. 2007	Increase	Duran et al. 1982, Wikoff et al. 2007
Tiglylcarnitine (C5:1-carn.)	Plasma	Increase	Roe et al. 1983	Increase	Roe et al. 1983
Propionylcarnitine (C3-carn.)	DBS	Increase	Malvagia et al. 2015	Increase	Malvagia et al. 2015
Heptadecanoylcarnitine	Plasma	Increase	Wikoff et al. 2007	Increase	Wikoff et al. 2007
γ-butyrobetaine (C0-carn.)	Plasma	Increase	Wikoff et al. 2007	Increase	Wikoff et al. 2007
Acetylcarnitine (C2-carn.)	Plasma	Increase	Wikoff et al. 2007	Increase	Wikoff et al. 2007
Hexanoylcarnitine (C6-carn.)	Plasma	Increase	Wikoff et al. 2007	Increase	Wikoff et al. 2007
2-Hexenoylcarnitine (C6:1-carn.)	Plasma	Increase	Wikoff et al. 2007	Increase	Wikoff et al. 2007
3-OH-tetradecanoylcarnitine (C14-OH-carn.)	Plasma	Increase	Wikoff et al. 2007	Increase	Wikoff et al. 2007
Tiglic acid	Urine	Increase	Nyhan et al. 1972	Increase	Wikoff et al. 2007
Methylmalonic acid	Plasma, urine	Increase		Increase	Oberholzer et al. 1967, van den Berg, Boelkens and Hommes 1976
Methylmalonylcarnitine (C4-DC-carn.)	Plasma, urine			Increase	Maeda et al. 2007
Isovalerylcarnitine (C5-carn.)	Plasma			Increase	Wikoff et al. 2007
Biochemical parameters altered during AMD					
Ammonia	Plasma	Increase	Zwicker et al. 2014	Increase	Zwicker et al. 2012
Isoleucine	Plasma	Increase	Zwicker et al. 2014	Increase	Zwicker et al. 2012
Valine	Plasma	Increase	Zwicker et al. 2014	Increase	Zwicker et al. 2012
3-Hydroxyisovaleric acid	Urine	Increase	Kuhara et al. 2012	Increase	Kølvraa et al. 1980
Lactic acid	Urine	Increase	Kuhara et al. 2012	Increase	Kølvraa et al. 1980
pH	ABG	Decrease	Zwicker et al. 2014	Decrease	Zwicker et al. 2012
pCO ₂	ABG	Decrease	Zwicker et al. 2014	Decrease	Zwicker et al. 2012
Bicarbonate	Plasma	Decrease	Zwicker et al. 2014	Decrease	Zwicker et al. 2012
Base excess	Plasma	Decrease	Zwicker et al. 2014	Decrease	Zwicker et al. 2012
Glutamine	Plasma	Decrease	Zwicker et al. 2014	Decrease	Zwicker et al. 2012
Lactate	Plasma	Increase	Zwicker et al. 2014	Decrease	Zwicker et al. 2012
Anion gap	Plasma	Increase	Zwicker et al. 2014	Decrease	Zwicker et al. 2012
Glucose	Plasma	Increase	Zwicker et al. 2014	Decrease	Zwicker et al. 2012
Alanine	Plasma	Decrease	Zwicker et al. 2014	Decrease	Zwicker et al. 2012
Citrulline	Plasma	Decrease	Zwicker et al. 2014	Decrease	Zwicker et al. 2012

Glutamine + glutamate	Plasma			
Free carnitine	Plasma	Decrease	Zwickler et al. 2014	
3-Methylglutaconic acid	Urine	Decrease	Zwickler et al. 2014	
Glutaric acid	Urine	Increase	Kuhara et al. 2012	
Ketone bodies (3-OH-butyric acid, acetoacetate)	Urine	Increase	Kuhara et al. 2012	
Urea	Plasma	Increase	Zwickler et al. 2014	
Uric acid	Plasma	Increase	Zwickler et al. 2012	Zwickler et al. 2012
Alanine aminotransferase	Plasma	Increase	Zwickler et al. 2012	Zwickler et al. 2012
2-Methylcitric acid	Urine	Increase	Zwickler et al. 2012	Zwickler et al. 2012
3-Hydroxypropionic acid	Urine	Increase	Kølvraa et al. 1980	Kølvraa et al. 1980
Isovaleric acid	Urine	Increase	Kølvraa et al. 1980	Kølvraa et al. 1980
2-Methylbutyric acid	Urine	Increase	Kølvraa et al. 1980	Kølvraa et al. 1980
Isobutyric acid	Urine	Increase	Kølvraa et al. 1980	Kølvraa et al. 1980
2-Oxo acids	Urine	Increase	Kølvraa et al. 1980	Kølvraa et al. 1980
3-Hydroxybutyric acid	Urine	Increase	Kølvraa et al. 1980	Kølvraa et al. 1980
3-Hydroxyisobutyric acid	Urine	Increase	Kølvraa et al. 1980	Kølvraa et al. 1980
Biochemical parameters correlated to plasma ammonia				
2-Methylcitric acid	Urine, plasma	Positive	Filipowicz et al. 2006	
Propionylglycine	Urine	Positive	de Sain et al. 2014	
3-Hydroxypropionic acid	Urine	Positive	Filipowicz et al. 2006	
Free carnitine	Urine	Positive	Filipowicz et al. 2006	

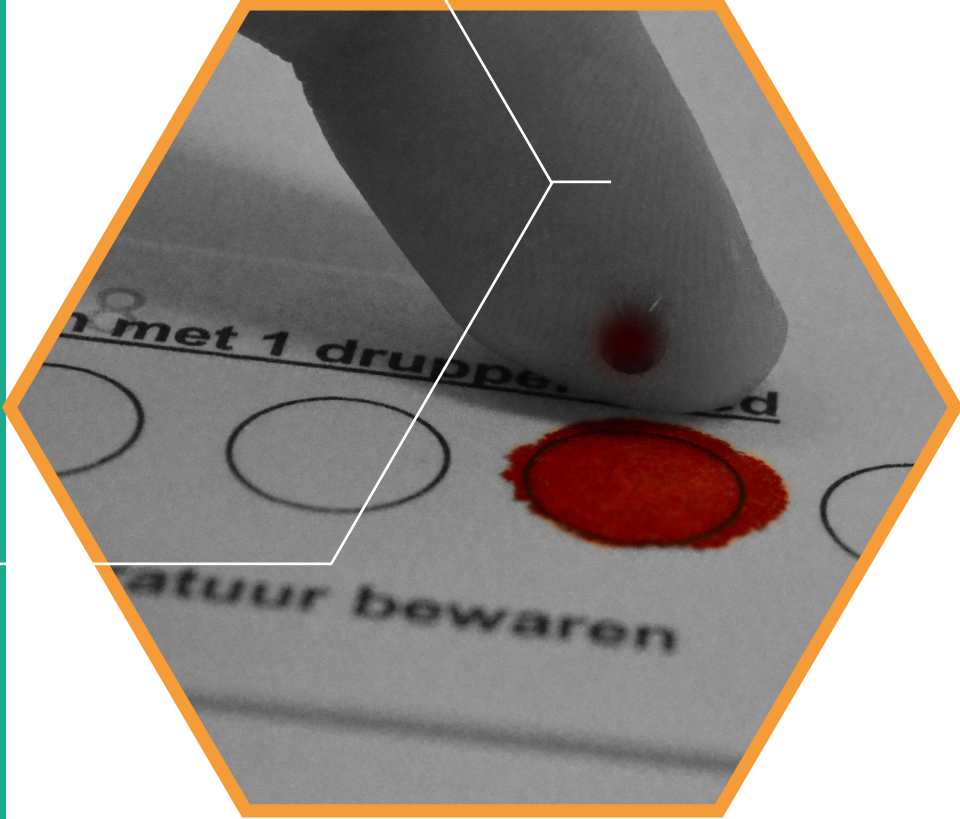
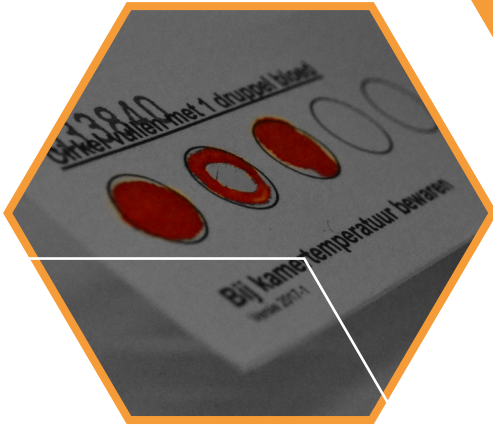
The table lists, to the best of our knowledge, the first reports of general disease biomarkers for PA and MMA, of biochemical parameters associated with presence of AMD in PA and MMA and of biochemical parameters that correlate with plasma ammonia in PA and MMA. Analytes can have been reported also in other body fluids, and can have been reported also in other studies than the ones referred to. Abbreviations: ABG: arterial blood gas.

Table S2. Diagnostic biomarkers for PA and isolated MMA

Analyte	Matrix	PROPIONIC ACIDURIA						METHYLMALONIC ACIDURIA							
		N	Med.	SD	Min	Max	RR	Known	N	Med.	SD	Min	Max	RR	Known
Targeted metabolic assays															
Propionylcarnitine	Plasma	34	54.4	19.6	23.0	99.5	0.00-0.81	Yes	68	21.0	21.7	2.7	83.7	0.00-0.81	Yes
Glycine	Plasma	73	1381	362	350	1962	166-330	Yes	77	492	369	168	1916	166-330	Yes
Isoleucine	Plasma	73	21	9	7	48	34-106	Yes, TH	77	32	15	7	84	34-106	Yes, TH
Valine	Plasma	73	66	26	20	183	155-343	Yes, TH	77	107	42	41	217	155-343	Yes, TH
Leucine	Plasma	73	59	23	31	152	86-206	Yes, TH	77	77	39	34	223	86-206	Yes, TH
Threonine	Plasma	73	72	29	29	212	102-246	Yes, TH	77	80	31	36	174	102-246	Yes, TH
Acetylcarnitine	Plasma	34	10.1	7.5	1.6	42.2	0.69-9.72	Yes	68	9.2	5.8	2.1	29.9	0.69-9.72	Yes
Methylcitric acid	Urine	3	697	383	426	968		Yes	0						
3-OH-propionic acid	Urine	10	232	99	89	349	0-20	Yes	57	13	19	0	86	0-20	Yes
Histidine	Plasma	73	65	14	32	107	68-108	No	77	72	15	45	142	68-108	Yes
Methylmalonic acid	Urine	12	2.0	3.1	1.0	10.0	0-20		174	727	4651	64	21587	0-20	Yes
Methylmalonic acid	Plasma	0					0.12-0.29		52	73.8	345.8	2.9	1327.4	0.12-0.29	Yes
Methylmalonylcarn.	Plasma	26	0.01	0.01	0.01	0.04	0.00-0.07	Yes	68	0.34	0.52	0.10	2.69	0.00-0.07	Yes
Methylcitric acid	Plasma	0					0.00-0.83		11	2.2	2.8	1.0	10.9	0.00-0.83	Yes
Glutamine	Plasma	73	494	105	252	793	457-857		77	380	126	190	736	457-857	No
Untargeted DI-HRMS analysis															
2-Methylcitric acid (3 is.)	Plasma	23	57.4	43.1	-1.8	146.9	P-value <0.0001	Yes	51	6.1	7.6	-0.6	25.5	P-value <0.0001	Yes
3-Dehydroxycarnitine	Plasma	23	15.9	53.2	0.4	203.4	<0.0001	Yes	51	3.2	7.0	-0.6	26.6	<0.0001	Yes
Propionylcarnitine	Plasma	23	12.0	80.8	-2.8	362.6	<0.0001	Yes	51	27.9	80.0	-1.4	368.0	<0.0001	Yes
Fructoseglycine	Plasma	23	7.6	5.7	-0.8	25.8	<0.0001	No	51	2.2	2.2	-1.2	7.6	<0.0001	No
Isoleucyl-isoleucine (3 is.)	Plasma	23	5.7	3.8	-0.6	13.9	<0.0001	No	51	3.4	2.8	-1.0	10.8	<0.0001	No
LysoPC(15:0) (2 is.)	Plasma	23	5.5	4.6	-2.9	16.0	<0.0001	No	51	2.5	4.1	-1.7	20.5	<0.0001	No
Glucosamine (2 is.)	Plasma	23	5.1	8.9	-2.5	31.1	<0.0001	No	51	2.2	4.8	-0.7	22.2	<0.0001	No
Threonic acid	Plasma	23	2.1	1.6	-2.8	3.6	0.0009	No	51	2.5	2.4	-1.4	8.0	<0.0001	No
DL-2-Aminoocctanoic acid	Plasma	23	-1.6	0.1	-1.7	-1.3	<0.0001	No	51	-1.5	0.5	-1.7	0.4	<0.0001	No
2-Methyl-3-keto-valeric acid (7 is.)	Plasma	23	-1.8	0.3	-2.8	-1.3	<0.0001	No	51	-2.1	0.9	-2.8	1.9	<0.0001	No
L-Glutamine (4 is.)	Plasma	23	-1.8	0.1	-1.9	-1.6	<0.0001	No	51	-1.5	0.9	-2.1	1.5	<0.0001	No
L-Methionine	Plasma	23	-2.0	0.5	-2.5	-0.5	<0.0001	No	51	-1.5	0.5	-2.1	1.0	<0.0001	No
L-Histidine	Plasma	23	-2.8	1.4	-5.6	-0.6	<0.0001	No	51	-1.7	1.3	-5.2	1.6	<0.0001	No
Propionylglycine (9 is.)	Plasma	23	28.5	29.3	-3.0	91.1	<0.0001	Yes	51	1.1	2.4	-2.4	8.7	<0.0001	No
Glycine	Plasma	23	9.5	4.8	-2.4	18.5	<0.0001	Yes	51	1.5	2.2	-1.1	8.5	<0.0001	No
2-Amino-3-phosphonopropionic acid	Plasma	23	6.2	6.5	-1.9	23.7	<0.0001	No	51	0.8	1.3	-1.3	7.1	<0.0001	No
1-(sn-Glycero-3-phospho)-1D-myo-inositol	Plasma	23	5.3	3.9	-0.6	10.8	<0.0001	No	51	0.3	4.8	-2.7	25.5	<0.0001	No

LysoPC(17:0) (2 is.)	Plasma	23	4.1	5.3	-2.3	17.3	<0.0001	No	51	1.5	3.4	-2.5	14.4
Homocysteine	Plasma	23	-1.7	1.2	-3.5	2.1	0.0002	No	51	-0.9	1.2	-3.0	4.1
L-Isoleucine (6 is.)	Plasma	23	-1.7	0.7	-2.8	0.1	<0.0001	Yes	51	-1.3	0.9	-2.8	2.6
Methylmalonic acid (3 is.)	Plasma	23	0.1	1.7	-2.2	7.0			51	10.0	50.7	0.0	228.6
Propionic acid (2 is.)	Plasma	23	-0.3	4.4	-2.4	20.1			51	6.9	79.1	-1.1	344.9
3-Hydroxy-9-hexadecenoylecarnitine	Plasma	23	3.1	3.1	-1.7	8.8			51	3.6	7.6	-0.9	40.0

Results of targeted metabolic assays in plasma are presented in $\mu\text{mol/L}$, results of targeted metabolic assays in urine are presented in $\text{mmol/mol creatinine}$. All p-values were adjusted according to the Bonferroni method. A p-value <0.05 was considered statistically significant. Abbreviations: DI-HRMS: direct-infusion high-resolution mass spectrometry; is.: isomers; Max: maximum value; Min: minimum value; N: number of samples; Ref. range: reference range; SD: standard deviation; TH: therapy related.



General discussion

The in-depth study of pathophysiology in rare inborn errors of metabolism (IEM) is important, as pathophysiological insights aid a better understanding and prediction of a patient's disease course and create increased opportunities for conceiving and rethinking treatment strategies. However, pathophysiologic research in IEM is complicated by the rarity of each individual disease and by the inherent scarcity of available data.

In this thesis, we developed different approaches and explored their use for the study of pathophysiology in rare diseases, that can be used despite the small number of patients and limited data. We have shown how these approaches resulted in the recognition of discrete details, originating either from the patient's phenotype or metabolome and we demonstrated how these details led to important insights in pathophysiology of different IEM.

The final chapter of this thesis consists of four parts. First, we discuss the implications of our findings. In addition, we consider some of the challenges that we came across, we reflect on a few methodological questions that touch upon philosophical questions and we describe future prospects.

IMPLICATIONS OF OUR FINDINGS

Phenomics

Detailed phenotypic descriptions can aid the understanding of pathophysiology. In the first part of this thesis, we developed four approaches to use deep phenotyping to gain insight in pathophysiology of genetic diseases. The choice for a specific approach depends on the type of data available and on the desired type of pathophysiological insight. We summarized the characteristics of the four deep phenotyping approaches in Table 1.

Table 1. Deep phenotyping approaches for the elucidation of pathophysiology of IEM

Approach	Pathophysiological insight	Application	Required data	Open access databases	Example
Phenotypic severity	Severity of phenotypic consequences of a certain genetic variant	Prediction Treatment	Individual patients, comparable genetic defects		Chapter 2 Chapter 4
Phenotypic specificity	Shared pathophysiology between diseases that share clinical similarities, etiology of a feature	Treatment	Individual patients, comparable genetic defects	Human Phenotype Ontology GeneCards	Chapter 3
Phenotypic overlap between patients	Interpretation of pathogenicity of VUS	Diagnosis Prediction Treatment Reproduction	Individual patients, comparable genetic defects		Chapter 4
Phenotypic overlap between IEM	Etiology of a certain clinical feature	Treatment	Well-characterized or well-grouped IEM	Human Phenotype Ontology	Chapter 11

Abbreviations: IEM: inborn error of metabolism.

First, the quantification of phenotypic severity, rather than a more qualitative assessment, can provide insight into the severity of the phenotypic consequences of a certain genetic variant (**chapter 2 and 4**). Quantification of phenotypic severity can be performed when deep phenotyping data is available for individual patients with comparable genetic defects, for example originating from detailed case-reports and case-series. Insight into the severity of the phenotypic consequences of a certain genetic variant can aid prediction of a patient's disease course and can aid decisions on the need for therapeutic interventions (Table 1). The potential predictive value of genetic variants has also been illustrated by others for

patients with medium-chain acyl-CoA dehydrogenase deficiency¹. After implementation of newborn screening (NBS), variants in *ACADM* were identified that had not been identified in clinically diagnosed patients. Patients harboring these novel variants presented with a much milder phenotype and, in contrast to severely affected patients, do not have to be advised to prevent prolonged fasting.¹

Second, determining phenotypic specificity can provide insights in shared pathophysiology between diseases that share clinical similarities (**chapter 3**). This approach also relies on the availability of deep phenotyping data of individual patients with comparable genetic defects. To study occurrence in other genetic diseases, and to study potential pathophysiological overlap between genetic diseases that share a certain phenotypic feature, open access databases as the Human Phenotype Ontology and GeneCards can be used. Insights in shared pathophysiology between diseases that share clinical similarities could elucidate pathophysiology of a certain phenotypic feature, which could allow for conceiving treatment strategies (Table 1). This has also been illustrated by a reported case-series on four patients with Niemann-Pick type C, of whom three had elevated liver transaminases.² In mice and in post-mortem liver samples of patients, suppression of hepatic cytochrome P450 was detected. In line with other diseases that present with cholestasis and suppressed cytochrome P450 activity, for which supplementation with a bile acid has proven effective – such as for example cerebrotendinous xanthomatosis – the patients were treated with ursodeoxycholic acid. Surprisingly, not only liver transaminases nearly normalized, but also alertness, appetite and activity of patients was reported to be improved.²

Third, ascertaining phenotypic overlap between patients with pathogenic mutations and patients with variant(s) of unknown significance (VUS) can serve as a line of evidence in the appraisal of the pathogenicity of these VUS (**chapter 4**). Phenotypic overlap between patients can be assessed if deep phenotyping data of individual patients with comparable genetic defects or from a well-described cohort study is available. Establishment of the pathogenicity of a VUS results in a diagnosis, which could provide clarity for clinicians, parents and patients on what to expect from the disease course. In addition, it may allow for the initiation of treatment strategies and it could provide guidance on decision-making about reproduction (Table 1).

Fourth and final, determining phenotypic overlap between mitochondrial diseases supported a mitochondrial etiology of a set of complications observed in propionic acidemia (PA) and isolated methylmalonic acidemia (MMA) patients (**chapter 11**). This approach can serve as a line of evidence in the appraisal of the etiology of a certain clinical feature. Phenotypic overlap between diseases or disease groups can be assessed if these disorders are well characterized and well-grouped based on their pathophysiology, for example using the nosology of Ferreira et al.,³ and when deep phenotyping data is available for these individual disorders, from well-described cohort studies or as provided by the Human Phenotype Ontology. In line with the determination of phenotypic specificity, elucidation of the etiology of a certain clinical feature could allow for rethinking of treatment strategies (Table 1).

The accuracy of deep phenotyping approaches is directly dependent on the reliability of the phenotypic data available. To aid reliable determination of phenotypic severity, phenotypic specificity and phenotypic overlap between patients and IEM, we advocate the use of unambiguous vocabulary as provided by the Human Phenotype Ontology, to describe a patient's phenotype as detailed as possible in case-series and case-reports (**chapter 3**). The more detail, the better.

Metabolomics

Untargeted metabolomics is finding its way to clinical applications and to date, seven different applications can be discerned. For each of these applications, several examples have been reported and throughout this thesis, we demonstrated examples of four clinical applications of untargeted metabolomics methods. First, the diagnostic value of untargeted metabolomics methods for next-generation metabolic screening platforms has been demonstrated for dried blood spots (**chapter 5**), for plasma (**chapter 5**)^{4,5}, for urine⁶ and for cerebrospinal fluid (**chapter 6**). To date, the diagnostic values of the reported untargeted metabolomics approaches are not yet sufficient to replace targeted diagnostic assays. Therefore, we consider untargeted metabolomics methods only applicable in the metabolic diagnostic laboratory as add-on assay: either as a first-tier screening test in patients suspected for an IEM to guide which targeted assays should be performed, or as a final option for patients that have had a diagnostic odyssey to obtain clues that could ultimately lead to a diagnosis. To this aim, dried blood spots, plasma, urine and cerebrospinal fluid are all suitable biological fluids, as they do not show any differences in diagnostic value (**chapter 5 and 6**).⁴⁻⁶

Second, untargeted metabolomics methods are used for the elucidation of novel biomarkers (**chapter 9**) or biochemical profiles. Biomarkers can either be diagnostic, allowing for the biochemical identification of an IEM, or informative on disease severity, or associated with certain phenotypic features. Many examples of the use of untargeted metabolomics for the identification of biomarkers have been reported. Some studies even identified diagnostic biomarkers for IEM that would be missed when only routine targeted assays are applied (**chapter 9**).^{5,7-9} Ideally, diagnostic biomarkers are pathognomonic: specific for only one IEM and clearly distinguishing patients from control individuals. However, this is not feasible for most diseases since pathophysiology of IEM can overlap, as exemplified by increased aspartylglucosamine in both NGLY1-CDDG and aspartylglucosaminuria (**chapter 9**). It has been demonstrated that calculation of diagnostic ratios could further improve specificity of NBS for IEM for which clear biomarkers already were available, such as phenylketonuria¹⁰ and very long chain acyl-CoA dehydrogenase deficiency.¹¹ Thus, a clearer differentiation of IEM can be attained by calculating diagnostic ratios (**chapter 5 and 10**). The reliability of finding a biomarker for an IEM can be improved by inclusion of more patients and more samples. However, for rare diseases, these samples are not readily available. For cerebrospinal fluid we revealed that minor difference in storage conditions do not affect stability of small-molecule metabolites (**chapter 8**) and therefore we consider historical and multicenter cohorts with small differences in pre-analytical storage conditions suitable for studies into new small-molecule biomarkers. This conclusion provides opportunities to increase the number of samples available for testing, through systematic sample collection (biobanking) and collaborations with other institutes.

Third, untargeted metabolomics can support pathogenicity of VUS (**chapter 4**).^{5,12} Thereby, it could serve as an additional line of evidence in establishing pathogenicity of an identified variant. We discuss this application in more detail in the paragraph “dealing with uncertainty”. In the fourth place, untargeted metabolomics can be used for attaining new insights in pathophysiology (**chapter 15**). These pathophysiological insights could lead to suggestions for clinical management of patients, either with respect to the biochemical follow-up (**chapter 15**) or with regard to new or adjusted treatment strategies (**chapter 15**).¹³⁻¹⁴ Likewise, the added value of pathophysiological insights, attained through untargeted metabolomics approaches for clinical patient care, was also supported by a study investigating

asymptomatic individuals with urocanic aciduria.¹⁵ Metabolic profiling resulted in the assumption that urocanic aciduria is a benign biochemical phenotype, which was followed by the recommendation to further search for the underlying cause of the phenotype in symptomatic individuals with urocanic aciduria.¹⁵

Next to these four applications, metabolomics approaches can also be used for detection of novel IEM¹⁶⁻¹⁷, for monitoring of therapeutic effects and for integration with other –omics techniques.¹⁸ As of now, examples of these three applications are still scarce, but we expect that many will follow in the coming years.

Deep metabolic phenotyping: propionic acidemia and methylmalonic acidemia

We performed deep metabolic phenotyping in PA and MMA to attain more insight into pathophysiology of AMD and long-term complications, with the ultimate aim of providing clinicians with more knowledge to predict, prevent or treat clinical problems arising in these destructive IEM.

First, our visual overview of all known information on the biochemical hallmarks of PA and MMA (**chapter 12**), integrated with the results of a detailed study of the metabolomes throughout the life of PA and MMA patients, helped us realize that known diagnostic markers remain essentially unaltered, contrasting with branched-chain amino acid intermediates which do accumulate during AMD. This insight resulted in new recommendations for the biochemical follow-up of PA and MMA patients to evaluate a patient's metabolic stability (**chapter 15**).

Second, our overview of the reported prevalence of all common and rare complications occurring in PA and MMA, in combination with the assessed prevalence among all Dutch patients resulted in more insight into which complications can be expected during the clinical course of PA and MMA patients (**chapter 13**). Moreover, this overview combined with the study of all hypotheses and available evidence on underlying pathophysiology of these complications, led to the differentiation of a specific set of complications likely to be caused by mitochondrial impairment, and a set of complications likely to be induced by the protein-restricted diet (**chapter 11**). Based on this set of complications, we disclosed that PA patients with early onset and MMA vitamin B12 unresponsive patients are more at risk for these mitochondrial complications than PA patients with late onset and MMA vitamin B12 responsive patients. We also provided adjusted advices for the initiation of monitoring of mitochondrial complications (**chapter 13**).¹⁹

Third, our overview of all current, experimental and unexplored treatment strategies in PA and MMA resulted in the conclusion that evidence for treatment strategies considered best practice treatment is often scarce and not without controversy (**chapter 12**). Among all Dutch patients, we revealed that clinicians tend to prescribe more protein than recommended by the current guidelines,¹⁹ and that this is associated with an increased frequency of AMD, cognitive impairment and mitochondrial complications. We therefore advocated awareness of the guidelines for dietary treatment, and extreme caution for exceeding these recommendations (**chapter 14**).¹⁹

Lastly, although NBS for PA and MMA has been initiated aiming to improve overall outcome, we demonstrated the expected health gain is likely limited (**chapter 13**) and we advocated that the protective effect of NBS can only be increased by improved treatment strategies that can effectively prevent AMD, cognitive impairment and mitochondrial complications. In summary, with our research we contributed to improved clinical management of these rare and destructive IEM. We provided thorough overviews of the biochemical hallmarks,

prevalence of complications and available treatment strategies that can be used as a quick reference in daily clinical practice. Moreover, we reported additional insights enabling clinicians better to (1) counsel patients and families on what to expect from their clinical disease course (**chapter 13**), (2) establish more meaningful outpatient follow-up, both biochemically and for monitoring onset of complications (**chapter 15** and **13**) and (3) prevent prescription of more protein than recommended by the current guidelines (**chapter 14**).¹⁹ More in general, we demonstrate that a thorough assessment of many different aspects of certain IEM, through the integration of extensive literature searches and deep metabolic phenotyping studies, can truly provide progress in better prediction and improved prevention and treatment strategies for IEM, in line with the success story of the elucidation of pathophysiology of phenylketonuria that eventually resulted in remarkably improved outcomes (**chapter 1**, BOX I).

CHALLENGES

Dealing with data

The validity of a study conclusion is, amongst others, determined by the amount of data, the specificity of the data, and the type of data collected.

Data scarcity

In rare genetic diseases, including IEM, scarcity of data and scarcity of patients to collect data from, greatly complicates studies on natural history, treatment strategies, metabolic markers and pathophysiology of diseases. There are many examples. First, regarding natural history, previous cohort studies for PA and MMA, which often had limited sample sizes, did not report important but infrequent complications like acute psychosis, premature ovarian failure, gout and urolithiasis (**chapter 13**). Second, randomized clinical trials to assess treatment strategies for rare IEM are scarce, as we discussed for PA and MMA (**chapter 12**). This is, next to a shortage of resources, mainly due to limited availability and a wide dispersion of study participants.²⁰ Third, with respect to metabolic markers, confirmation of aspartylglucosamine as biomarker for NGLY1-CDDG in additional patients is still required, as a sample size of four patients is too small to draw solid conclusions from (**chapter 9**). Fourth and final, identification of metabolic markers and assessment of pathophysiology during AMD in PA and MMA was complicated by the limited availability of remnant samples drawn during AMD (**chapter 15**).

In this thesis we strived to overcome this challenge of data scarcity. We advocate that this obstacle can be dealt with by increasing data specificity and by intelligible use of available data, as we demonstrated by our deep phenotyping approaches (**chapter 2-4**). In addition, integrating extensive literature searches with clinical studies, as demonstrated in **chapter 11** and **12** which served as groundwork for **chapter 13** and **14**, and as demonstrated in **chapter 15**, can improve the validity of the conclusions to a great extent.

Data specificity

Regarding data specificity, conclusions on the prevalence of complications and effectiveness of treatment strategies among the different types of isolated MMA (*mut⁰* or *mut*, *MMAA*, *MMAB*, *MMADHC* or *MCEE* type) were hampered by the reality that many of the studies assessed, considered isolated MMA as a single disease entity and assembled all data, despite the fact that cause and range of accumulation of toxic metabolites, natural history and prognosis differ between the different types of isolated MMA (**chapter 11** and **12**).²¹

Demonstrating the power of data specificity, we could determine highly specific phenotypic features by using the Human Phenotype Ontology, which allowed for improved specificity of the phenotypic descriptions so that slightly different symptoms could be better distinguished (**chapter 3**). Likewise, evaluation of specific developmental milestones of the individuals with heterozygous *de novo* variants in *POLR2A* allowed for calculations of developmental Z-scores (**chapter 4**). This semi-quantitative parameter aided the discovery that individuals with variants predicted to cause haploinsufficiency presented with mild developmental delays, whereas individuals with variants expected to cause a dominant-negative effect presented with more severe delays. Finally, exact quantification of urinary amino acid values instead of qualitative assessment allowed for a reliable differentiation of Hartnup disorder from generalized aminoaciduria (**chapter 10**). As we are convinced that the more specific the data are, the more value they have for attaining insights into pathophysiology, in this thesis we demonstrated several useful approaches to increase the specificity of the data in order to increase pathophysiological understanding.

Data types

The validity of the conclusion can also be influenced by the type of data. Retrospective data is often considered less valuable than prospectively collected data since it relies on accurate recordkeeping by others and since valuable information is often missing. This can introduce significant information bias. However, retrospective data may contain a wealth of information and if the risk of information bias is kept in mind when drawing conclusions, retrospective data can provide unsuspected, valuable insights. This is illustrated by the thorough, retrospective, evaluation of the complete medical records of almost all Dutch PA and MMA patients (**chapter 13 and 14**). We assumed that missing data occurred randomly and we considered it to be minimally confounding. Still, since conclusions on for example propionyl-CoA carboxylase activity were hampered by missing data, we advocated precise and structured prospective follow-up of NBS cohorts and therefore we listed minimum requirements for evaluation to facilitate reliable analyses and conclusions on NBS effectivity. Thus, despite risking information bias, we emphasize that retrospective data should not be discarded thoughtlessly. Oftentimes, it is the only available information and therefore we should strive to get the most out of this type of data .

A second challenge that we came across is related to longitudinal data (**chapter 14 and 15**). Longitudinal data could provide more insight in pathophysiology than cross-sectional data, but the validity of the conclusions relies heavily on accurate statistical analyses, which are much more complicated for longitudinal data than for cross-sectional data. Nevertheless, when performed properly, statistical analyses of longitudinal data can provide unsuspected insights, even when the number of patients is rather small, as evidenced by adjusted advices regarding dietary treatment of PA and MMA patients, and by adjusted advices regarding the assessment of biochemical parameters as indicator of metabolic stability in PA and MMA (**chapter 14 and 15**).

Dealing with uncertainty

John Allen Paulos, professor in mathematics at the University of Philadelphia and writer, once said: *“In science, the only certainty is uncertainty”*. In science we have to handle varying levels of uncertainty, while aiming to demonstrate the likelihood of a certain claim. Here, we discuss how we dealt with genetic VUS and metabolites of unknown significance throughout this thesis.

Genetic variants of unknown significance

Whole-exome sequencing and whole-genome sequencing often reveal VUS, for which the degree of pathogenicity is unclear. To aid interpretation of genetic variants, the American College of Medical Genetics and Genomics reported standards and guidelines (Table 2).²² We applied these guidelines throughout this thesis to establish pathogenicity of observed genetic variants. More than just applying these guidelines, we studied some additional lines of evidence that can be used to establish pathogenicity of observed genetic variants.

Table 2. Lines of evidence to support pathogenicity of a variant of unknown significance

Type of data	Criterion	Strength
Inheritance	De novo variant, paternity and maternity confirmed De novo variant, paternity and maternity not confirmed Co-segregation with disease in multiple affected family members For recessive disorders, detected in trans with an established pathogenic variant	PS2 PM6 PP1 PM3
Prediction software	Variant resulting in loss of function Same amino acid change as established pathogenic variant Novel missense change, but at amino acid residue of established pathogenic missense change Protein length changing variant Lines of computational evidence support deleterious effect on gene or gene product: evolutionary conservation, splicing impact	PVS1 PS1 PM5 PM4 PP3
Population data	Prevalence in affected statistically increased over controls Variant absent in population databases Mutational hot-spot or well-studied functional domain without benign variation Missense in gene with low rate of benign missense variants, and established pathogenic missense variants common Variant intolerance according to gnomAD (chapter 2 and 4) CADD score (chapter 4) Desert Z-score (chapter 4)	PS4 PM2 PM1 PP2
Functional data	Well-established functional studies show a deleterious effect	PS3
Phenotypic data	Patient's phenotype or family history highly specific for a disease with a single genetic etiology	PP4
Reputable source	Reputable source recently reports variant as pathogenic, but evidence is not available to the laboratory to perform an independent evaluation	PP5

Criteria in regular font were derived from the American College of Medical Genetics and Genomics standards and guidelines for the interpretation of sequence variants³. Criteria in bold are not reported in the guidelines, but are discussed in this thesis as potential additional lines of evidence to support pathogenicity of an observed genetic variant. Abbreviations: GnomAD: Genome aggregation database; PM: Pathogenic moderate; PP: Pathogenic supporting; PS: Pathogenic strong; PVS: Pathogenic very strong.

We evaluated almost all lines of evidence listed in Table 2 to establish pathogenicity of sixteen *de novo* heterozygous *POLR2A* variants (Table 2, Inheritance, PS2) (**chapter 4**). Next to these lines of evidence, we argued that the CADD score, a score that predicts whether a variant is among the most deleterious substitutions that can be present in the human genome, could not serve as an indicator of pathogenicity for *POLR2A*, as CADD scores of variants observed in the gnomAD cohort in individuals without severe pediatric disease were also above the cut-off value for pathogenicity. We investigated an alternative score and introduced the desert Z-score, a score that unveils gene regions intolerant to genetic change. These regions are devoid of protein-changing variants observed in the gnomAD cohort. Strikingly, almost all *POLR2A* protein-changing variants described in the individuals were positioned within these regions. Moreover, these regions were found to be of functional importance to the protein, indicating that the desert Z-score is capable of disclosing regions within a gene that are intolerant to change and of functional importance, in line with criteria PM1 and PP2

(Table 2, Population data). Therefore, we advocate that this score can serve as a supporting line of evidence in establishing pathogenicity of a genetic variant (Table 2, Population data). Other potential indicators of pathogenicity are indicators of the tolerance to genetic variability of a gene, like the observed/expected ratios of variants reported in gnomAD. We demonstrated that genes encoding lobe A COG proteins were less tolerant to variation, as the number of observed variants is much lower than the number of expected variants, resulting in a very low observed/expected ratio (**chapter 2**). In line with this, also *POLR2A* is less tolerant to variation compared to genes encoding the other subunits of the RNA polymerase II complex (**chapter 4**). We advocate that these indicators of tolerance to genetic variability of a gene could also serve as an extra line of evidence in establishing pathogenicity of genetic variants (Table 2, Population data). Next, we demonstrated that our untargeted metabolomics method can serve as a well-established functional study demonstrating a deleterious effect and thus can serve as a line of evidence in the establishment of pathogenicity (**chapter 5**) (Table 2, Functional data, PS3). Finally, we demonstrated that determining the degree of phenotypic overlap could serve as line of evidence supporting pathogenicity (**chapter 4**) (Table 2, Phenotypic data, PP4).

Metabolites of unknown significance

Just like genomics may come along with uncertainty about the pathogenicity of a genetic variant, untargeted metabolomics introduces uncertainty about the significance of altered metabolites: metabolites of unknown significance. In **chapter 5-9** and **chapter 15** we used direct-infusion high-resolution mass spectrometry to perform non-quantitative metabolomics studies. However, data interpretation is challenging due to the novelty of this approach. Standards and guidelines, such as those available for interpretation of genetic variants,²² are lacking. Uncertainty about the significance of metabolite alterations is based on several factors, of which we will discuss three.

First, the amount of data gained through untargeted metabolomics methods is much higher than the amount of data originating from targeted assays and, as a consequence, it is much more data than laboratory specialists are familiar with. To allow interpretation, we narrowed down the amount of data. We selected only the mass to charge ratio (m/z) peaks that could be annotated. Thereafter, we selected the most common adduct ions, and subsequently, we selected m/z peaks corresponding to metabolites with an endogenous function, based on information present in the Human Metabolome Database and manually curated by four trained laboratory specialists clinical genetics. These selection steps reduced the amount of metabolites of unknown significance from >160,000 unannotated m/z peaks to ~1,800 m/z peaks corresponding to ~3,800 endogenous metabolites (**chapter 5**). Although these selection steps certainly ease data interpretation, they also introduce a risk of missing interesting findings. The researchers that developed two other next-generation metabolic screening methods also felt the need to narrow down the amount of data.^{4,5} In both approaches similar selection steps were introduced, resulting either in the analysis of 489 endogenous metabolites⁴ or 340 clinically relevant metabolites.⁵ As expected, the selection steps introduced in these two approaches resulted in the missing of at least three⁵ and four⁴ important biochemical hallmarks for IEM, such as guanidinoacetic acid.^{4,5} Using our slightly less rigorous selection process, we correctly identified these metabolites, but we missed 3-hydroxyisovaleryl-carnitine, another important biochemical hallmark for IEM. To overcome the risk of missing important biochemical hallmarks, Coene et al. introduced “open the metabolome”, in order to study the data without applying any selection process.⁵

They demonstrated that this more untargeted approach resulted in the detection of an unknown feature that might serve as biomarker for histidinemia⁵ and of two that might serve as biomarkers for phenylketonuria.^{5,23} Moreover, they even demonstrated that detection of an unknown feature in an undiagnosed patient led to the diagnosis of a novel IEM.^{5,16} Although the amount of metabolites of unknown significance is immense and data interpretation is extremely laborious, these examples do demonstrate the added value of performing an “open the metabolome” approach in addition to the more feasible approach in which only endogenous metabolites are analyzed.

The second factor that could complicate data interpretation is the selection of control samples, which we use to compare the patient samples to. In line with Miller et al., our control samples consist of samples of individuals in whom an IEM is excluded based on targeted diagnostics.⁴ Our control samples are selected in such a way that they vary in age, gender, time of day at sampling, diets, supplements, the use of drugs and storage times. Moreover, for plasma samples the degree of hemolysis varies and for cerebrospinal fluid samples the fraction varies (**chapter 5** and **6**). Hereby, we take into account considerable variation in factors that might influence a patient's metabolome, to ensure that observed variation is more likely due to a metabolic defect than due to other factors. Although this reduces the number of metabolites of unknown significance to some extent, the inevitable consequence is that we miss more subtle variations in metabolite concentrations, as evidenced in **chapter 8**. It could be that the risk of missing subtle variations is reduced when matched control samples were used. Coene et al. match control samples based on age and gender,⁵ but they do not take into account time of day at sampling, diets, supplements, the use of drugs, storage times and degree of hemolysis, since it is unfeasible to match samples on all these factors. To match or not to match – and to what extent – that is the question.

The third factor that can complicate data interpretation is that in direct-infusion, an observed *m/z* can account for multiple isomers. Theoretically, this introduces more metabolites of unknown significance, but in practice this did not result in data interpretation problems or incorrect diagnoses in **chapter 5-7**. In addition, as the *m/z* of aspartylglucosamine does not account for any other metabolite annotation, data interpretation was unambiguous in **chapter 9** as well. However, the annotation of multiple isomers to a single *m/z* peak did create a challenge in data interpretation in **chapter 15**, as some intermediates of the branched-chain amino acid degradation pathway share the same *m/z*. This complicated solid conclusions on which intermediates are truly increased during AMD, and thus the assessment of pathophysiological mechanisms at play during an AMD. The challenge of observed *m/z* accounting for multiple isomers could be overcome by using gas chromatography and/or liquid chromatography approaches^{4,5}, as retention times^{4,5} and fragmentation signatures⁴ allow for distinguishing isomers. When using direct-infusion, results of non-quantitative metabolomics can be confirmed with targeted second-tier tests, to ensure correct interpretation of the results.

REFLECTIONS

Definition of disease

In the introduction we mentioned the definition of an IEM: “any condition in which the impairment of a biochemical pathway is intrinsic to the pathophysiology of the disease”.³ Genetic disorders are defined as “a disease that is caused by a genetic variation in an individual's DNA sequence” and can be grouped into single gene disorders, chromosome disorders and multifactorial disorders. Essential to both these definitions is the causal

link between genotype and phenotype, hence pathophysiology, which is the scope of this thesis. The discussed lines of evidence supporting pathogenicity of a genetic variant and the potential of all –omics technologies to link genotype and phenotype aid in the understanding of rare genetic diseases. However, the insights that these –omics technologies have provided also shake up our current perspectives on health and disease. The paradigm that in one patient, one affected gene leads to one genetic disease, which explains all the symptoms of a patient, is faltering. When should we call the consequences of a genetic variant a disease? When should we call an individual a patient?

One gene, one disease?

According to the Online Mendelian Inheritance in Men (OMIM), an increasing number of disease-associated genes (1,278/4,132, 31%) is recorded to have multiple associated phenotypes. For example, according to OMIM, mutations in *COG6* are associated with two phenotypes: COG6-CDG²⁴ and Shaheen syndrome.²⁵ At OMIM it is mentioned that we argued that Shaheen syndrome should not be considered a separate syndrome, but rather a mild variant of COG6-CDG due to the presence of some residual COG6 protein.²⁶ Therefore, we included the patient described by Shaheen et al. as COG6-CDG patient (**chapter 2 and 3**). Recently, COG6-CDG has indeed been considered one disease entity, based on criterium 2 of the nosology of Ferreira et al., that severity alone is not considered sufficient for separation into different entries when a single gene product is involved (**chapter 1, BOX II**).³

An example of the opposite, in which indeed two different phenotypes and two different pathomechanisms are at play, is *GLS*, encoding glutaminase. Glutaminase hyperactivity results in glutamate accumulation and causes infantile cataract, skin abnormalities and impaired intellectual development,²⁷ whereas glutaminase deficiency results in glutamine accumulation and causes epileptic encephalopathy, volume loss of the brain and infantile death²⁸ or early-onset global developmental delay and progressive ataxia.²⁹

One disease, one gene?

Conversely, mutations in many different genes may underlie a phenotype considered a single disease. For example, in this thesis we deem isolated MMA one disease entity (**chapter 11-15**), while mutations in five genes may underlie this diagnosis and natural history and prognosis differ between the different types of isolated MMA.^{3,21} Most researchers would argue that ideally, the different types should be distinguished, and in most studies this is clearly mentioned. Interestingly, PA is always considered one disease and this is never questioned, although also for PA mutations in two genes may underlie the disease. The difference between PA and isolated MMA in this aspect, is that the gene product of both *PCCA* and *PCCB* is propionyl-CoA carboxylase, a protein complex containing these two subunits. Thus, for PA there is one pathomechanism causing the disease, while for MMA there are five (criterium 4 according to the nosology of Ferreira et al. 2019,³ **chapter 1, BOX II**). Thus, rather than one gene, one disease, we advocate in line with Ferreira et al., that the new paradigm should be: one pathomechanism, one disease.³

One patient, one diagnosis?

An increasing number of patients, especially the offspring of consanguineous parents, is being diagnosed with multiple single gene disorders.^{18,30} It is expected that this may explain some phenotypic variation observed in historically reported patients. The possibility of multiple single gene disorders or multiple VUS in one patient complicates assessment of

pathophysiology and interpretation of the pathogenicity of VUS. We reported an individual in whom we identified a missense mutation in *POLR2A* with no line of evidence supporting pathogenicity other than *de novo* occurrence, conservation across species and a severe phenotype (**chapter 4**). The genetic variant was not located in a functionally important domain, functional studies did not support pathogenicity and the phenotype did not match the phenotype of all other individuals. We therefore classified this variant as VUS. In this patient, multiple VUS were identified, but none of the other genetic variants was considered to be potentially disease-causing. Future studies should confirm or exclude pathogenicity of this *POLR2A* VUS, and these studies also might elucidate whether this patient has another, or a second, genetic disease.

The presence of multiple single gene disorders can also complicate treatment. In our Dutch national cohort study we included a patient in whom diagnosis of the first single gene disorder impeded diagnosis of isolated MMA, *MMAA* type (**chapter 13**). The patient developed an AMD at three months of age on protein enriched tube feeding (while he would have been fed a protein-restricted diet if timely diagnosed with MMA) during a hospital admission for failure to thrive. He died within two days, despite immediate diagnosis and adequate treatment. The patient's phenotype did not seamlessly fit the first single gene disorder, but despite consanguinity of the parents, this did not raise the question whether it was the only genetic disorder in this patient.

It would be logical and easy to start advocating awareness of the possibility of a second (or third) genetic disorder in patients with a slightly different phenotype than what has been described, but we acknowledge the complexity of deciding whether this difference should be interpreted as an expansion of the known phenotypic spectrum, or as a sign of a second (genetic) disorder. Theoretically, other genetic defects could be identified by whole-exome or whole-genome sequencing, but as these techniques often reveal VUS, interpretation of these results will remain difficult, impeding definitive conclusions on which diseases a patient should be diagnosed with.

Disease or risk factor? Patient or individual?

As mentioned, many diseases can present with a wide phenotypic spectrum, ranging from mild to severe. Are all these individuals patients? Do they all have a disease? Textual definitions of “disease” and “patient” are presented in BOX I.

BOX I. Definitions according to the Merriam-Webster Dictionary

Disease is and impairment of the normal state of the living animal or plant body or one of its parts, that interrupts or modifies the performance of the vital functions, is typically manifested by distinguishing signs and symptoms, and is a response to environmental factors, to specific infective agents, to inherent defects of the organisms or to combinations of these factors.

Patient is an individual awaiting or under medical care and treatment.

To date, many individuals with Hartnup disorder remain asymptomatic due to a high intake of protein, tryptophan or vitamin B3 (**chapter 10**). Are these individuals, that never experienced any “impairment of the normal state” (BOX I), patients? As they would probably only demonstrate symptoms from their disease under specific circumstances, like fasting due to illness, should we not merely consider Hartnup disorder in these individuals a risk factor, rather than a disease?

This question, whether IEM should be considered risk factors or diseases, is relevant for more IEM¹ than Hartnup disorder alone. In **chapter 13** we describe NBS for PA and MMA.

In Japan, preparatory studies for the implementation of NBS resulted in a ten times higher incidence of PA patients than previously reported.³¹ Although patients were only in early childhood at time of reporting (1-3 years), all patients detected through screening were asymptomatic. These patients may develop symptoms later in life, like the two adult PA patients who developed cardiomyopathy in their fifth decade of life (**chapter 13**).³² To date, it is not known whether current treatment strategies allow us to prevent these complications (**chapter 13**), but we will certainly try, without being completely sure that we will not do these patients more harm than good by treating them. At present, we do not know how many patients we will identify by NBS for PA and MMA in the Netherlands. Will we identify asymptomatic or mild individuals that would not have been diagnosed otherwise? Is that a good thing, and can we protect them from potentially severe consequences of their IEM? Or will we, unintentionally, introduce “impairment of the normal state”, and thus, disease? Will we make them patients?

How to define disease severity?

When diagnosed with a disease, either through NBS or after a symptomatic presentation, patients, families and doctors want to know what to expect. What symptoms will develop when, how ill will the patient be? Although natural history of, for example, PA and MMA is increasingly understood on a group-level, it is still hard to paint a picture of the future for one specific patient. To do this, predictors of severity are needed, but how can severity be defined?

Definitions of severity based on genomic or molecular indicators are considered most objective and thus reliable. However, to identify genomic and molecular predictors of severity, clinical outcome parameters on a phenomic level are required. This is feasible for diseases for which no treatment is available, but once patients are treated, clinical outcome parameters as indicators of disease severity become less reliable, as treatment (as well as other interventions, such as implementation of NBS) interferes with the patient’s phenotype. This intrinsic interrelatedness cannot be solved easily.

For COGx-CDG and *POLR2A* deficiency, two diseases for which no treatment is available, we demonstrated that phenotypic severity can be linked to genetic variants. We established that comparable genetic variants are more detrimental in lobe A COG-CDG than in lobe B COG-CDG (**chapter 2**) and we showed that heterozygous loss of function mutations in *POLR2A* lead to a milder phenotype than missing mutations (**chapter 4**), providing some clues on what can be expected regarding the future course of the disease. Despite these links on group-level, similar genotypes do not predict similar outcomes of individual patients, especially not regarding mortality, since a patient’s phenotype is also determined by many context-dependent factors. For example, patients P4.1 and P4.2 with COG6-CDG, whom we report in the paper of Rymen et al.,²⁴ are brothers with the same genotype and a similar phenotypic severity score (P4.1: 10 points, P4.2: 14 points, **chapter 2**). Despite these more or less objective similarities, subjectively the patient’s outcome could not differ more, as P4.1 is 21 years of age and is able to work in a sheltered workshop, while his younger brother, P4.2, suffered from fulminant hepatic failure and died at 14 months of age due to complications of a liver transplantation. Likewise, a patient with PA identified through family testing was treated from birth, but died due to cardiomyopathy at 8.6 years of age, while her brother who presented symptomatically, is still alive at 18.4 years of age (**chapter 13**). Thus, genomic predictors of severity can only predict risks, but not outcomes of individual patients.

For PA and MMA, treatment strategies are available. The predictive value of a patient's genotype is low and biochemical predictors of severity are scarce. Although suboptimal for predicting a patient's prognosis due to the potential influence of treatment, we defined clinical outcome parameters for both diseases (**chapter 13**), to serve identification of more objective predictors of severity and to evaluate the effectiveness of dietary treatment strategies. Based on these outcome parameters we could demonstrate that for MMA vitamin B12 unresponsiveness, which can be determined at birth, increases the risk of metabolic instability, mitochondrial complications and treatment-related complications (**chapter 13**). Based on a patient's vitamin B12 responsiveness, we could inform patients, parents and doctors to some extent on what the future might hold. For PA however, metabolic markers are lacking, possibly due to missing information regarding PCC activity. We could demonstrate that for PA, early onset presentation increases the risk of an adverse outcome of the first symptomatic phase, metabolic instability, cognitive impairment and mitochondrial complications (**chapter 13**). However, while this still holds true for patients that are symptomatic before NBS results are available, presentation type will be unknown for PA patients diagnosed via NBS, complicating counseling of these patients. Based on these risk groups and based on the clinical outcome parameters, we could demonstrate that in severely affected patients the prescription of more protein than guidelines recommend¹⁹ is associated with an increased frequency of AMD, cognitive impairment and mitochondrial complications, resulting in adjusted dietary treatment advices for PA and MMA patients (**chapter 14**). Thus, although the reliability of clinical outcome parameters might be limited when assessed in patients undergoing treatment, we demonstrate that it could aid in the identification of more objective predictors of severity.

How to find something better?

Medicine always strives for improvement. However, especially in diagnostic studies, potential improvements are extremely hard to study and to validate. If what we today consider best practice is not good enough, and what we pose as new best practice correlates with that, is it equally insufficient? And if it correlates less, it is worse than what we had, or better? Exemplifying this practically unsolvable paradox, we consider ammonia a fairly good indicator of metabolic instability in PA and MMA patients. However, in some patients who clinically seem metabolically stable, ammonia is increased. If we find a marker that correlates better with the clinical symptoms, but worse with ammonia, is it a better indicator of metabolic stability? Or is it a worse indicator, since we miss our only read-out of cellular metabolic instability that does not lead to clinical symptoms at that moment, but that might induce complications later in life?

Due to this paradox, current best practice is, understandably, not easily deserted. However, this attitude might also preclude improvements. For example, if to date 2-methylcitric acid and 3-hydroxyisovaleric acid would be considered the best available biochemical indicators of metabolic stability instead of plasma ammonia, based on the available evidence we would not replace these parameters for plasma ammonia. Though, now that we consider plasma ammonia the best available indicator, we are skeptical to replace it for 2-methylcitric acid and 3-hydroxyisovaleric acid (**chapter 15**). Since we do not easily abandon concepts we are familiar with and since we are unable to prove the additional value of the new, we tend to stick to the things that came first. How evidence-based is that?

PROSPECTS

Phenomics

To support future attainment of new pathophysiological insights, we advocate the use of deep phenotyping, as we greatly value the insights that thorough assessment of a patient's phenotype can provide. These insights can be gained either through quantification of phenotypic severity, through assessment of phenotypic overlap between patients and between genetic diseases, or through determination of phenotypic specificity (Table 1). We are looking forward to see more examples, provided by us or by others, of deep phenotyping leading to new insights in pathophysiology of rare genetic diseases.

The use of deep phenotyping approaches can be aided by a wider use of the Human Phenotype Ontology, as this unambiguous nomenclature could serve univocal interpretation of case-series and case-reports, but also of patients' medical records. The use of the Human Phenotype Ontology could be promoted by editors, in refresher courses for medical doctors and in curricula of medical students. We advocate that broader publicity will serve a more extensive use, and that a more extensive use will improve both the completeness of the nomenclature and the validity of the deep phenotyping approaches that we present here.

Metabolomics

We are truly convinced of the potential of untargeted metabolomics for each of its seven main purposes, and in particular for next-generation metabolic screening, for biomarker identification, as line of evidence in the interpretation of VUS and for obtaining insights in pathophysiology of IEM. We work hard to realize a permanent place for untargeted metabolomics in the metabolic diagnostic laboratory by improving, amongst others, standardization of the method and quality assessment to obtain ISO-15189 certification. We foresee untargeted metabolomics to serve both as a first-tier screening test and as a last resort, to study yet undiagnosed patients. In this light, we are currently studying the value of the automated data interpretation of untargeted metabolomics as described in **chapter 7** as first-tier screening test in patients referred for metabolic diagnostic screening, and we are also studying the value of "open untargeted metabolomics" as final option to find a diagnosis in patients with often very long diagnostic odysseys. Furthermore, in patients with these long diagnostic odysseys we are performing a health technology assessment to explore, amongst others, what the economic value of untargeted metabolomics might be. Lastly, the laboratory is exploring the diagnostic value of untargeted metabolomics in combination with genomics (called: "crossomics"), in which untargeted metabolomics findings are matched to genetic VUS to establish a diagnosis. All these initiatives also relate to the Dutch nationwide initiative of United for Metabolic Diseases that was recently set up, to search for a diagnosis for 500 patients through the combination of genomics, metabolomics and other functional studies, to which our laboratory is contributing by using the untargeted metabolomics method for dried blood spots which we present in this thesis.

Next to these studies and developments regarding the untargeted metabolomics method, we will expand our work on the potential biomarker we found for NGLY1-CDDG. In collaboration with the worldwide patient organization, we are developing a method for the quantitative measurement of aspartylglycosamine, which we will validate in samples of the patients who joined the patient organization.

Propionic acidemia and methylmalonic acidemia

For PA and MMA, there is an urgent need for treatment strategies that can prevent

metabolic instability, cognitive impairment and mitochondrial complications, without introducing treatment-related complications. Most promising are the innovative therapies that aim to increase enzyme activity, such as gene addition therapies,³³ mRNA therapies,³³ enzyme replacement therapies, hepatocyte transplantation or solid organ transplantation (**chapter 12**). Next to effective treatment strategies, solid predictors of severity are required, ideally not based on phenotype but on genomic, molecular or biochemical markers that are definable at birth. If both treatment strategies and severity predictors are available, NBS should be performed as early as possible, ideally around birth, to be able to diagnose every patient before symptoms develop. In this perfect, but at present unrealistic scenario, we would be able to decide which patient needs which treatment, to optimally protect patients with severe disease from metabolic instability, cognitive impairment and mitochondrial complications, and to protect patients with mild disease and asymptomatic individuals from treatments, treatment-associated complications and from being patients. The closer these three requirements are met, the better we will be able to enable patients, parents and clinicians to handle the extremely difficult task of balancing doing good versus doing harm in the clinical management of PA and MMA patients.

CONCLUSION

With the introduction of –omics technologies, medicine has entered a new era. This era is full of new possibilities for the in-depth study of pathophysiology of rare IEM, but also full of new challenges, due to the enormous detail of the data that –omics technologies can provide. At the level of the data, challenges complicating data interpretation include, amongst others, the amount, the specificity and the type of data collected, and the uncertainty within the data. At the level of interpretation challenges comprise, amongst others, the definition of disease, the definition of severity and the question whether a new discovery is truly an improvement or not.

Throughout this thesis, we came across these challenges. We described and discussed them, we discussed to what extent they might have complicated data interpretation, we explored potential solutions and we suggested approaches to handle them. Hereby, we contributed to strengthening the potential of the –omics technologies. We propose that more awareness of these challenges, more experience in handling them and more solutions to face them, will strengthen the unprecedented potential of the –omics technologies even more.

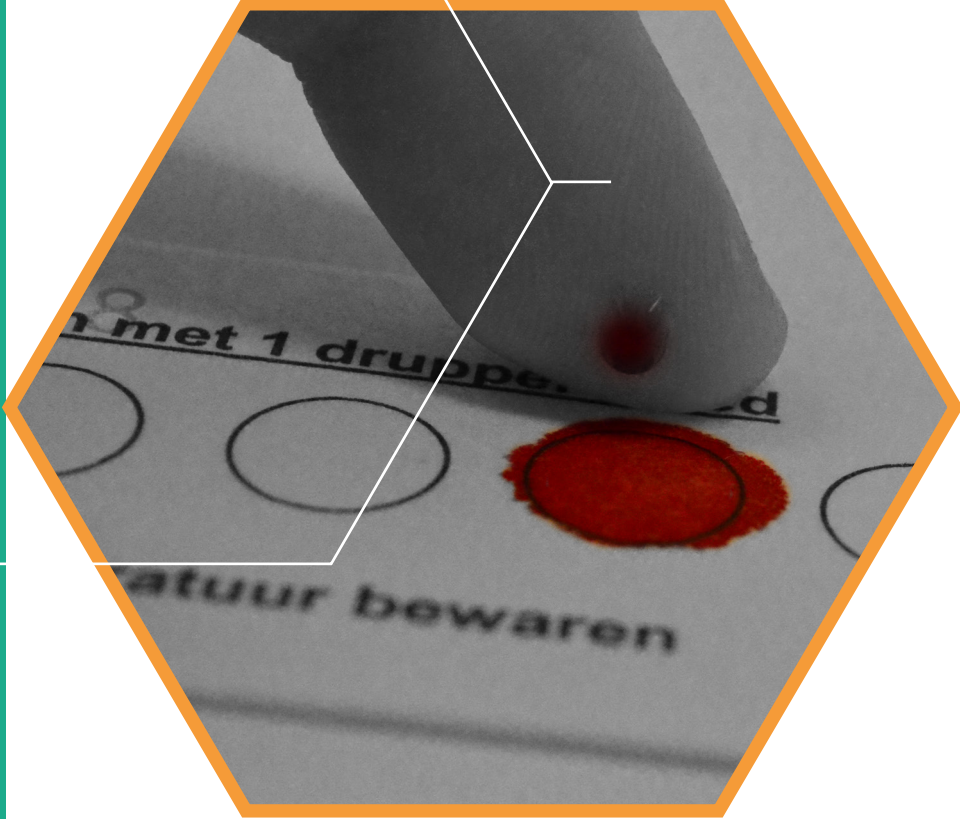
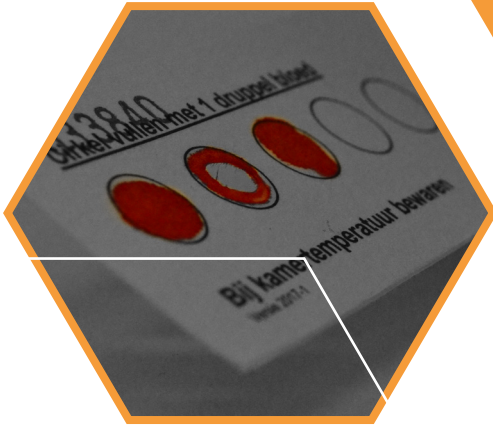
In this thesis, while we might only have scratched the surface of the true potential of the –omics technologies, we demonstrated approaches for the in-depth study of pathophysiology of IEM. We showed how discrete details can lead to important insights in pathophysiology and how these insights have the potential of serving improvements in clinical patient care. Only time will tell what the future may hold, when –omics technologies might reach their full potential.

REFERENCES

1. Touw CM, Smit GP, Niezen-Koning KE, Bosgraaf-de Boer C, Gerding A, Reijngoud DJ, Derks TG. In vitro and in vivo consequences of variant medium-chain acyl-CoA dehydrogenase genotypes. *Orphanet J Rare Dis.* 2013;20(8):43.
2. Evans WRH, Nicoli ER, Wang RY, Movsesyan N, Platt FM. Case report: ursodeoxycholic acid treatment in Niemann-Pick disease type C; clinical experience in four cases. *Wellcome Open Res.* 2017;31(2):75.
3. Ferreira CR, van Karnebeek CDM, Vockley J, Blau N. A proposed nosology of inborn errors of metabolism. *Genet Med.* 2019;21:102-106.
4. Miller MJ, Kennedy AD, Eckhart AD et al. Untargeted metabolomics analysis for the clinical screening of

- inborn errors of metabolism. *J Inher Metab Dis.* 2015;38(6):1029-39.
5. Coene KLM, Kluijtmans LAJ, van der Heeft E et al. Next-generation metabolic screening: targeted and untargeted metabolomics for the diagnosis of inborn errors of metabolism in individual patients. *J Inher Metab Dis.* 2018;41(3):337-353.
 6. Kennedy AD, Miller MJ, Beebe K et al. Metabolic profiling of human urine as a screen for multiple inborn errors of metabolism. *Genet Test Mol Biomarkers* 2016;20(9):485-95.
 7. Peretz H, Watson DG, Blackburn G et al. Urine metabolomics reveals novel physiological functions of human aldehyde oxidase and provides biomarkers for typing xanthinuria. *Metabolomics* 2012;8(5):951-9.
 8. Kennedy AD, Pappan KL, Donti T et al. 2-pyrrolidinone and succinimide as clinical screening biomarkers for GABA-transaminase deficiency: anti-seizure medications impact accurate diagnosis. *Front Neurosci.* 2019;8(13):394.
 9. Broeks MH, Shamseldin HE, Alhashem A et al. MDH1 deficiency is a metabolic disorder of the malate-aspartate shuttle associated with early onset severe encephalopathy. *Hum Genet.* 2019; 138(11-12):1247-1257.
 10. Eastman JW, Sherwin JE, Wong R, Liao CL, Currier RJ, Lorey F, Cunningham G. Use of the phenylalanine:tyrosine ratio to test newborns for phenylketonuria in a large public health screening programme. *J Med Screen.* 2000;7(3):131-5.
 11. Diekman E, de Sain-van der Velden M, Waterham H et al. The newborn screening paradox: sensitivity versus overdiagnosis in VLCAD deficiency. *JIMD Rep* 2016;27:101-6.
 12. Atwal PS, Donti TR, Cardon AL et al. Aromatic L-amino acid decarboxylase deficiency diagnosed by clinical metabolomic profiling of plasma. *Mol Genet Metab* 2015;115(2-3):91-4.
 13. Ramos RJ, Pras-Raves ML, Gerrits J et al. Vitamin B6 is essential for serine de novo biosynthesis. *J Inher Metab Dis.* 2017;40(6):883-891.
 14. Cappuccio G, Pinelli M, Alagia M et al. Biochemical phenotyping unravels novel metabolic abnormalities and potential biomarkers associated with treatment of GLUT1 deficiency with ketogenic diet. *PLoS One* 2017;12(9):e0184022.
 15. Glinton KE, Levy HL, Kennedy AD, Pappan KL, Elsea SH. Untargeted metabolomics identifies unique though benign biochemical changes in patients with pathogenic variants in *UROCL1*. *Mol Genet Metab Rep* 2018;29(18):14-18.
 16. Van Karnebeek CD, Bonafé L, Wen XY et al. NANS-mediated synthesis of sialic acid is required for brain and skeletal development. *Nat Genet.* 2016;48(7):777-84.
 17. Rodan LH, Anyane-Yeboah K, Chong K et al. Gain-of-function variants in the *ODC1* gene cause a syndromic neurodevelopmental disorder associated with macrocephaly, alopecia, dysmorphic features, and neuroimaging abnormalities. *Am J Med Genet A.* 2018;176(12):2554-2560.
 18. Tarailo-Graovac M, Shyr C, Ross CJ et al. Exome sequencing and the management of neurometabolic disorders. *N Engl J Med.* 2016;374(23):2246-55.
 19. Baumgartner MR, Hörster F, Dionisi-Vici C et al. Proposed guidelines for the diagnosis and management of methylmalonic and propionic acidemia. *Orph J Rare Dis* 2014; 9:130.
 20. Ah Mew N, Cnaan A, McCarter R et al. Conducting an investigator-initiated randomized double-blinded intervention trial in acute decompensation of inborn errors of metabolism: lessons from the N-Carbamylglutamate Consortium. *Transl Sci Rare Dis.* 2018;3(3-4):157-170.
 21. Manoli I, Sloan JL, Venditti CP. Isolated methylmalonic acidemia. In: Adam MP, Ardinger HH, Pagon RA et al., eds. *GeneReviews*®. Seattle, WA: University of Washington, Seattle; 1993-2019. Updated: 2016, December 1.
 22. Richards S, Aziz N, Bale S et al. Standards and guidelines for the interpretation of sequence variants: a joint consensus recommendation of the American College of Medical Genetics and Genomics and the Association for Molecular Pathology. *Genet Med* 2015;17(5):405-24.
 23. Václavík J, Coene KLM, Vrobel I et al. Structural elucidation of novel biomarkers of known metabolic disorders based on multistage fragmentation mass spectra. *J Inher Metab Dis.* 2018;41(3):407-414.
 24. Rymen D, Winter J, van Hasselt PM et al. Key features and clinical variability of COG6-CDG. *Mol Genet Metab.* 2015;116(3):163-70.
 25. Shaheen R, Ansari S, Alshammari MJ, Alkhalidi H, Alrukban H, Eyaid W, Alkuraya FS. A novel syndrome of hypohidrosis and intellectual disability is linked to COG6 deficiency. *J Med Genet.* 2013;50(7):431-6.
 26. Haijjes HA, Prinsen HC, Thiel C, Koerner C, Verhoeven-Duif NM, van Hasselt PM. Expanding the clinical phenotype of COG6 deficiency. *J Med Genet.* 2014;51(6):425.
 27. Rumping L, Tessadori F, Pouwels PJW et al. GLS hyperactivity causes glutamate excess, infantile cataract and profound developmental delay. *Hum Mol Genet.* 2019;28(1):96-104.
 28. Rumping L, Büttner B, Maier O et al. Identification of a loss-of-function mutation in the context of

- glutaminase deficiency and neonatal epileptic encephalopathy. *JAMA Neurol.* 2018;76(3):342-350.
29. van Kuilenburg ABP, Tarailo-Graovac M, Richmond PA et al. Glutaminase deficiency caused by short tandem repeat expansion in *GLS*. *N Engl J Med.* 2019;380(15):1433-1441.
 30. Reid ES, Papandreou A, Drury S et al. Advantages and pitfalls of an extended gene panel for investigating complex neurometabolic phenotypes. *Brain* 2016;139(11):2844-2854.
 31. Yorifuji T, Kawai M, Muroi J et al. Unexpectedly high prevalence of the mild form of propionic acidemia in Japan: presence of a common mutation and possible clinical implications. *Hum Genet.* 2002;111(2):161-5.
 32. Riemersma M, Hazebroek MR, Helderma-van den Eenden ATJM et al. Propionic acidemia as a cause of adult-onset dilated cardiomyopathy. *Eur J Hum Genet.* 2017;25(11):1195-1201.
 33. Chandler RJ, Venditti CP. Gene therapy for methylmalonic acidemia: past, present, and future. *Hum Gene Ther.* 2019;30(10):1236-1244.





Appendices

Samenvatting
Summary
List of abbreviations
List of publications
Dankwoord
Curriculum vitae

SAMENVATTING

DOEL VAN DIT PROEFSCHRIFT

Het onderwerp van dit proefschrift is de ontwikkeling van diverse benaderingen om pathofysiologie van metabole ziekten gedetailleerd te kunnen bestuderen. Pathofysiologie is de verklaring van de functionele veranderingen in fysiologische processen in een persoon, die optreden als gevolg van een ziekte. Voor metabole ziekten, die genetische ziekten zijn, hebben we geprobeerd meer inzicht te verkrijgen in hoe variatie in het genoom (genotype) kan leiden tot de symptomen waarmee een patiënt zich presenteert (fenotype). Metabole ziekten zijn ziekten waarin een verstoorde biochemische route een belangrijke rol speelt. Deze biochemische routes kunnen de eiwit-, vet- en koolhydraatstofwisseling betreffen, maar ook de stofwisseling van vitaminen en mineralen. Genen die zijn aangedaan in metabole ziekten coderen vaak voor enzymen die de omzetting van bepaalde substraten in producten faciliteren. Klinische consequenties van enzymdeficiënties ontstaan door ophoping van het substraat of door een tekort van het product. Metabole ziekten kunnen ook worden veroorzaakt door een deficiëntie van een transporteiwit. In deze ziekten kan een substraat niet getransporteerd worden naar het juiste weefsel, de juiste cel of het juiste organel, waar het zijn functie in een biochemische route moet uitoefenen. Ook deze locatie-specifieke tekorten kunnen leiden tot een variëteit aan klinische problemen.

Aangezien metabole ziekten zeldzaam zijn, wordt de mogelijkheid om de pathofysiologie te bestuderen beperkt door het kleine aantal patiënten en de daarmee gepaard gaande gelimiteerde beschikbaarheid van gegevens over de ziekte. In dit proefschrift hebben we diverse benaderingen laten zien om pathofysiologie van zeldzame metabole ziekten toch te kunnen bestuderen. Deze benaderingen kunnen gebruikt worden ondanks de beperkte beschikbaarheid van gegevens over de ziekte. We laten zien hoe schijnbaar onopvallende details, ofwel in het fenotype ofwel in het metabooloom van de patiënt, kunnen leiden tot belangrijke inzichten. Deze onopvallende details hebben we gevonden door *phenomics*, wat het systematisch bestuderen van het fenotype van een patiënt is, door *metabolomics*, wat het systematisch meten van metabolieten met een kleine massa in een biologisch monster van een patiënt is, of door *deep metabolic phenotyping*, wat de integratie van zowel de *phenomics* als de *metabolomics* benadering is.

In **hoofdstuk 1** hebben we uitgelegd wat pathofysiologie is en wat metabole ziekten zijn. Daarnaast hebben we elk van de metabole ziekten die in dit proefschrift behandeld worden besproken. We hebben ook de drie delen van dit proefschrift geïntroduceerd door per hoofdstuk te beschrijven wat de vraagstelling van dat hoofdstuk is.

PHENOMICS

In het eerste deel van dit proefschrift laten we het belang en de mogelijkheden van het gebruiken van de *phenomics* benadering zien. We hebben beschreven hoe we de schaarse hoeveelheid beschikbare data met een zo groot mogelijke efficiëntie kunnen gebruiken om de pathofysiologie van zeldzame ziekten te ontrafelen.

In **hoofdstuk 2** vermoeden we dat genetische defecten in lob A van het COG-complex tot een ernstiger fenotype leiden dan vergelijkbare genetische defecten in lob B van het COG-complex doen. We hebben overtuigend bewijs geleverd om dit vermoeden te staven door alle studies die de fenotypes van gemuteerde COG cellijnen beschrijven te bestuderen en

door de ernst van het fenotype van alle in de literatuur gerapporteerde COG-CDG patiënten te kwantificeren.

We hebben het fenotype van COG-CDG patiënten ook systematisch bestudeerd in **hoofdstuk 3**. Hier hebben we de hypothese getoetst dat overlap in symptomen tussen patiënten met verschillende ziektes kan betekenen dat er ook overlap in pathofysiologie is tussen deze ziektes. We hebben de specificiteit van de fenotypische kenmerken bepaald voor alle fenotypische kenmerken die gerapporteerd zijn in COG-CDG patiënten. Daarnaast hebben we de pathofysiologie bestudeerd van andere genetische ziekten die ook gepaard gaan met de meest specifieke fenotypische kenmerken van COG-CDG patiënten. We hebben gevonden dat het prioriteren van kenmerken op basis van de specificiteit niet alleen leidde tot het identificeren van kenmerken die geassocieerd zijn met CDG, maar dat er ook een symptoom uitsprong dat niet in andere CDG gezien wordt, namelijk episodische koorts. Dit laat mogelijk zien dat er nog meer, onbekendere, functies zijn van het COG complex. Het COG complex blijkt geassocieerd te zijn met autofagie, net als meer dan de helft van alle andere ziektes die zich presenteren met episodische koorts. Dit suggereert dat episodische koorts mogelijk veroorzaakt wordt door verstoorde autofagie. Met deze bevindingen hebben we laten zien dat het bepalen van de specificiteit van een fenotypisch kenmerk inderdaad kan bijdragen aan het begrijpen van de pathofysiologie van zeldzame genetische ziekten.

In **hoofdstuk 4** hebben we tot slot het fenotype van zestien patiënten systematisch bestudeerd om het pathogene effect van zestien nieuw ontstane, heterozygote varianten in *POLR2A* te bepalen. We hebben functioneel bewijs gekregen voor het pathogene effect van de verschillende varianten door op een iteratieve manier informatie over de structuur van het eiwit, massa spectrometrie metingen, een gist modelsysteem en bepaling van de levensvatbaarheid van cellen in cellijnen te combineren. We hebben vervolgens de mate van overlap in fenotype bepaald, tussen patiënten met varianten waarvoor veel functioneel bewijs was voor een pathogeen effect en patiënten met varianten waarvoor middelmatig functioneel bewijs was voor een pathogeen effect. Op basis van de geobserveerde overeenkomsten in het fenotype kwamen we voor vijftien van de zestien gevonden varianten tot de conclusie dat de genetische variant waarschijnlijk of mogelijk de oorzaak van het fenotype van de patiënt is.

METABOLOMICS

In **hoofdstuk 5** hebben we de ontwikkeling van een nieuwe kwalitatieve methode voor diagnostiek naar metabole ziekten beschreven. Voor deze methode maken we gebruik van directe infusie hoge resolutie massaspectrometrie. We hebben laten zien dat deze methode zeer consistente resultaten geeft, veel monsters snel achter elkaar kan analyseren en dat de methode niet selectief is in het meten van de verschillende metaboliëten. De methode kan gebruikt worden voor bloedspots en voor bloedplasma. In **hoofdstuk 6** hebben we aangetoond dat de methode ook het biochemisch profiel van hersenvocht betrouwbaar meet. In **hoofdstuk 7** staat beschreven dat ons op kennis gebaseerde algoritme met geautomatiseerde data-interpretatie voor diagnostiek naar metabole ziekten veel verschillende metabole ziekten correct kan diagnosticeren. Dit gaat zeer snel en er is slechts één bloedspot of bloedplasma monster voor nodig. Dit algoritme zou de implementatie van niet-selectieve *metabolomics* methoden voor diagnostiek naar metabole ziekten enorm kunnen faciliteren.

In **hoofdstuk 8** hebben we onderzocht of de concentraties metaboliëten met een kleine massa in hersenvocht veranderen als gevolg van verschillende manieren van het bewaren

van het hersenvocht. Kleine verschillen in de manier van bewaren beïnvloeden de stabiliteit van de metaboliëten niet. Op basis hiervan hebben we geconcludeerd dat historische cohorten en cohorten uit verschillende ziekenhuizen, met slechts kleine verschillen in de manier van het bewaren van monsters, geschikt zijn voor studies naar nieuwe biomarkers met een kleine moleculaire massa.

We hebben in **hoofdstuk 9** beschreven dat aspartylglucosamine een biomarker is voor NGLY1-CDDG. We hebben aangetoond dat het de eerste potentiële biomarker in bloedspots is voor NGLY1-CDDG. Dit maakt een biochemische diagnose voor deze ziekte haalbaarder.

We hebben de waarde van exacte kwantificering van aminozuren in de urine gedemonstreerd in **hoofdstuk 10**. Hier hebben we geprobeerd de ziekte van Hartnup te onderscheiden van andere aminoacidurieën. Het berekenen van de ratio van concentratieverdubbelingen van aminozuren geassocieerd met de ziekte van Hartnup ten opzichte van andere aminozuren, is een geschikt diagnostisch hulpmiddel om de ziekte van Hartnup betrouwbaar te onderscheiden van andere aminoacidurieën.

DEEP METABOLIC PHENOTYPING

We hebben de resultaten van een systematische evaluatie van de literatuur over de pathofysiologie van propionacidurie (PA) en methylmalonacidurie (MMA) gerapporteerd in **hoofdstuk 11** en **12**. We hebben de huidige hypothesen en het beschikbare ondersteunende bewijs voor de pathofysiologie van verschillende complicaties samengevat in **hoofdstuk 11**. We hebben in dit hoofdstuk ook de rol van mitochondrieel falen in het ontstaan van deze complicaties bediscussieerd. In **hoofdstuk 12** hebben we de huidige, experimentele en nog niet geëxploreerde behandelstrategieën beschreven. Hierin konden we twee strategieën onderscheiden: (1) behandel de oorzaak, door de hoeveelheid toxische metaboliëten te verminderen en (2) behandel de effecten, door energietekort in het mitochondrion en het ontstaan van zuurstofradicalen te voorkomen of te behandelen.

Hoofdstuk 13 beschrijft de resultaten van een nationale, retrospectieve cohort studie. Het fenotype van alle PA en MMA patiënten is systematisch in kaart gebracht om de gezondheidswinst van de hieprikscreening in te kunnen schatten. We hebben beargumenteerd dat de gezondheidswinst waarschijnlijk beperkt is, omdat patiënten al kort na de geboorte ziek worden en zelfs als ze gediagnosticeerd worden voor de eerste symptomatische fase, er vaak al onherstelbare schade is opgetreden. We hebben daarnaast ook laten zien dat er naar alle verwachting geen vermindering van het aantal decompensaties, geen verbetering van de cognitieve functie en geen vermindering van het aantal mitochondriële complicaties optreedt.

In **hoofdstuk 14** hebben we de huidige behandelstrategie ten aanzien van het eiwitbeperkte dieet geëvalueerd, uitgesplitst naar ziekte-ernst. We hebben aangetoond dat patiënten over het algemeen meer eiwit krijgen voorgeschreven dan wordt aanbevolen, en dat dit overschot aan eiwit geassocieerd is met een verhoogde frequentie van decompensaties, meer cognitieve dysfunctie en meer mitochondriële complicaties, met name in ernstig aangedane patiënten. Op basis hiervan hebben we het belang van kennis van de richtlijnen benadrukt en hebben we geadviseerd zeer terughoudend te zijn met het overschrijden van de aanbevolen hoeveelheden eiwit.

In **hoofdstuk 15** hebben we het metabooloom van PA en MMA patiënten bestudeerd om meer inzicht te krijgen in de pathofysiologie van acuut optredende decompensaties door de biochemische processen tijdens een decompensatie te bestuderen. We hebben laten zien dat intermediairen in de afbraakroute van de vertakte-keten aminozuren mogelijk

verantwoordelijk zijn voor het optreden van de metabole verzuring van het bloed van patiënten, in tegenstelling tot de bekende ziektemarkers propionzuur en methylmalonzuur. Op basis van deze bevindingen hebben we een set metabolieten aanbevolen voor het biochemisch vervolgen van de metabole stabiliteit van een patiënt.

CONCLUSIE

In **hoofdstuk 16** bediscussiëren we tot slot de implicaties van onze bevindingen. Ook bediscussiëren we een aantal uitdagingen die we tegen zijn gekomen, reflecteren we op enkele methodologische vraagstukken en bespreken we de toekomstperspectieven. We concluderen dat de geneeskunde, met de introductie van de *-omics* technologieën, een nieuw tijdperk is ingegaan vol mogelijkheden voor het bestuderen van de pathofysiologie van zeldzame metabole ziekten, maar dat deze mogelijkheden ook gepaard gaan met uitdagingen. Zelfs al hebben we het volledige potentieel van de *-omics* technologieën mogelijk slechts aangeraakt in dit proefschrift, door verschillende benaderingen te presenteren om met de uitdagingen om te gaan hebben we een bijdrage kunnen leveren aan de ongekende mogelijkheden van de *-omics* technologieën.

SUMMARY

SCOPE OF THIS THESIS

The focus of this thesis is the development of different approaches for the in-depth study of pathophysiology of inborn errors of metabolism (IEM). Pathophysiology is the explanation of functional changes in physiological processes that are occurring within an individual, due to a disease. As IEM are genetic diseases, we aimed to gain insight into how a variation in the genome (genotype) can lead to the symptoms and signs that a patient presents with (phenotype). IEM are conditions in which the impairment of a biochemical pathway is intrinsic to the pathophysiology of a disease. These biochemical pathways concern protein, fat and carbohydrate metabolism, but also metabolism of vitamins and minerals. The genes affected in IEM mostly encode enzymes that facilitate conversion of metabolic substrates into products. Clinical problems of enzyme deficiencies can either arise from accumulation of the substrate or from a deficiency of the product. IEM can also be caused by transporter deficiencies. In these IEM, a specific metabolite cannot be transported into the tissue, cell or organelle where it is supposed to perform its function in a biochemical pathway. Also these location-specific deficiencies can lead to a variety of clinical problems.

As IEM are rare diseases, study of pathophysiology is impeded by the small number of patients and the inherent scarcity of available data. In this thesis we demonstrated different approaches to study of pathophysiology of rare IEM, that can be used despite this limitation of data scarcity. We showed how discrete details, originating either from the patient's phenotype or metabolome, can lead to important insights in pathophysiology of several different IEM. These discrete details were revealed either by phenomics, which is the systematic study of the phenotype of the patient, by metabolomics, which is the study of small- molecule metabolites in a biological sample of the patient, or by deep metabolic phenotyping, which is the integration of phenomics and metabolomics approaches.

In **chapter 1** we introduced pathophysiology and IEM, including the different IEM addressed throughout this thesis. We also presented the three parts of this thesis, by providing an outline of the chapters in this thesis.

PHENOMICS

In part I of this thesis we illustrated the power of the use of deep phenotyping as an approach for using scarce data with utmost efficiency, in order to reveal pathophysiology of rare genetic diseases.

In **chapter 2** we hypothesized that genetic defects in subunits of lobe A of the COG-complex cause a more severe phenotype than comparable genetic defects in subunits of lobe B of the COG-complex. We provided convincing evidence supporting this hypothesis by reviewing all studies that assessed phenotypes of mutant COG cell lines, and by quantification of phenotypic disease severity of all reported COG-CDG patients.

We also performed deep phenotyping of COG-CDG patients in **chapter 3**. Here, we hypothesized that clinical similarities may be indicative of shared pathophysiology. We determined phenotypic specificity for all phenotypic features reported in COG-CDG patients, and we studied pathophysiology of other genetic diseases sharing highly specific phenotypic features. We found that prioritization of phenotypic features based on phenotypic specificity not only captured phenotypic features commonly associated with glycosylation disorders,

but also a feature not seen in any other glycosylation disorder: episodic fever, likely reflecting other, underappreciated, cellular functions of the COG complex. Indeed, the COG complex has been implicated in the autophagy pathway, as more than half of the genes underlying disorders that present with episodic fever, suggesting that episodic fever might be caused by disrupted autophagy. Hereby, we demonstrated that determining phenotypic specificity could indeed facilitate understanding of pathophysiology in rare genetic disorders.

Lastly, in **chapter 4**, we performed deep phenotyping to support pathogenicity of sixteen *de novo* heterozygous variants in *POLR2A*. We obtained functional support for pathogenicity of the variants through an iterative process combining structural evaluation, mass spectrometry analyses, a yeast model system and cell viability assessment in cell lines. By demonstrating the degree of phenotypic overlap between variants with strong functional support for pathogenicity and variants with moderate functional support for pathogenicity, we concluded that the genetic variant is probably or possibly disease-causing in fifteen of these variants.

METABOLOMICS

In **chapter 5** we described the development of a non-quantitative direct-infusion high-resolution mass spectrometry method for next-generation metabolic screening. We demonstrated that this method is a very consistent, high-throughput and nonselective method for investigating the metabolome in both dried blood spots and plasma. In addition, in **chapter 6** we demonstrated that this method accurately captures the biochemical profile of several IEM in cerebrospinal fluid, and in **chapter 7** we disclosed that our diagnostic knowledge-based algorithm with automated data interpretation for next-generation metabolic screening can correctly diagnose many different IEM, very rapidly and using only a single dried blood spot or plasma sample. We argued that this algorithm could potentially facilitate implementation of untargeted metabolomics for next-generation metabolic screening to a great extent.

In **chapter 8** we assessed whether small-molecule metabolites in cerebrospinal fluid are affected by changes in storage conditions and we revealed that minor differences in storage conditions do not affect stability. Therefore, we concluded that historical and multicenter cohorts with small differences in pre-analytical storage conditions are suitable for studies into new small-molecule biomarkers.

We described that aspartylglucosamine is a biomarker for NGLY1-CDDG in **chapter 9**. We showed that it is the first potential small-molecule biomarker in dried blood spots for NGLY1-CDDG, which makes a biochemical diagnosis for this disease potentially feasible.

We reported the value of exact quantification of urinary amino acid excretion in **chapter 10**, in which we aimed to distinguish Hartnup disorder from other aminoacidurias. We showed that calculation the ratio of fold changes of amino acids associated with Hartnup disorder over other amino acids could serve as diagnostic tool that enhances correct discrimination of Hartnup disorder from other aminoacidurias.

DEEP METABOLIC PHENOTYPING

We reported the results of a systematic review into the pathophysiology of propionic acidemia (PA) and isolated methylmalonic acidemia (MMA) in **chapter 11** and **12**. We summarized current hypotheses and available evidence on underlying pathophysiology of complications in **chapter 11**, and discussed the role of mitochondrial impairment in pathophysiology of these complications. In **chapter 12** we delineated all current, experimental and unexplored

treatment strategies, discerned in two strategies: (1) treat the cause, by reducing the amount of toxic metabolites and (2) treat the effects, by preventing or treating mitochondrial energetic failure and increase of reactive oxygen species formation.

In **chapter 13**, we performed deep phenotyping on a national, retrospective cohort including almost all Dutch PA and MMA patients, to estimate the expected health gain of newborn screening. We argued that the health gain of introducing newborn screening for PA and MMA in the Netherlands in overall outcome is expected to be limited, since patients already present shortly after birth and even if diagnosed before symptoms occur, patients still develop adverse outcomes due to the first symptomatic phase. In addition, we demonstrated that newborn screening is not expected to result in a reduced frequency of acute metabolic decompensations (AMD), improved cognitive function or a reduced number of mitochondrial complications.

In **chapter 14** we evaluated best-practice treatment strategies with respect to the protein-restricted diet for PA and MMA, stratified based on disease severity. We demonstrated that patients are generally prescribed more protein than recommended, and that this exceedance is associated with an increased frequency of AMD, cognitive dysfunction and mitochondrial complications, especially in severely affected patients. Based on our findings, we advocated awareness of the guidelines for dietary treatment, and we advised to be cautious with exceeding these recommendations.

In **chapter 15** we studied the metabolome of PA and MMA patients to improve insight in pathophysiology of AMD, by evaluating the biochemical processes at play during an AMD. We revealed that intermediates in the pathway of the branched-chain amino acid degradation may be held responsible for inducing metabolic acidosis during AMD, instead of the known disease biomarkers propionic acid and methylmalonic acid. Based on these findings, we suggested a set of metabolites to be measured for the biochemical follow-up of a patient's metabolic stability.

CONCLUSION

Finally, in **chapter 16**, we discuss the implications of our findings, we discuss some of the challenges that we came across, we reflect on a few methodological questions and we discuss future prospects of our research. We conclude that medicine, with the introduction of –omics technologies, has entered an era full of new possibilities for the in-depth study of pathophysiology of rare IEM, but also of new challenges that these opportunities come along with. Although we might only have scratched the surface of the true potential of –omics technologies throughout this thesis, by suggesting approaches to handle some of these challenges we contributed to strengthening the unprecedented potential of –omics technologies.

LIST OF ABBREVIATIONS

AAM:	Amino acid mixtures
AAM:total protein ratio	Ratio of protein from AAM over the total protein prescription
AAV:	Adenoassociated viral
AMD:	Acute metabolic decompensation(s)
ANOVA:	Analysis of variance
AO:	Adverse outcome
AP3:	2-amino-3-phosphonopropionic acid
Asn-N:	Neu5Ac1Hex1GlcNAc1-Asn
AUC:	Area under the curve
BCAA:	Branched-chain amino acids
BCKDC:	Branched-chain α -ketoacid dehydrogenase complex
BMD:	Bone mineral density
CDG:	Congenital disorders of glycosylation
CDDG:	Congenital disorders of deglycosylation
COG:	Conserved oligomeric Golgi
CPT:	Carnitine palmitoyltransferase
CSF:	Cerebrospinal fluid
CTD:	C-terminal domain
DBS:	Dried blood spots
DD:	Differential diagnosis
DI-HRMS:	Direct-infusion high-resolution mass spectrometry
EO:	Early onset
ExAC:	Exome Aggregation Consortium
FC:	Fold change
GC-MS:	Gas chromatography mass spectrometry
GnomAD:	Genome Aggregation Database
HAA:	Hartnup amino acids, classically related to Hartnup disorder
HMDB:	Human Metabolome Database
HPO:	Human Phenotype Ontology
IEM:	Inborn error(s) of metabolism
IF:	In-frame
Kcal:	Kilocalorie
LC-MS:	Liquid chromatography mass spectrometry
LO:	Late onset
LoF:	Loss of function
LPI:	Lysinuric protein intolerance
MCE:	Methylmalonyl-CoA epimerase
MCM:	Methylmalonyl-CoA mutase
MIM:	Mendelian Inheritance in Man
MMA:	Isolated methylmalonic acidemia/aciduria
MPA:	Mycophenolic acid
MRI:	Magnetic resonance imaging
MS:	Mass spectrometry
MTHFR:	Methylenetetrahydrofolate reductase
MTT:	(3-(4,5-dimethylthiazolyl-2)-2,5-diphenyltetrazoliumbromide

m/z:	Mass to charge ratio
NA:	Not assessed
Natural:total protein ratio	Ratio of natural protein over the total protein prescription
NBS:	Newborn screening
ND:	Not determined
NGLY1-CDDG:	Congenital disorder of glycosylation caused by non-functional peptide: <i>N</i> -glycanase, encoded by <i>NGLY1</i>
NGMS:	Next-generation metabolic screening
NMDA:	<i>N</i> -methyl-D-aspartate
NS:	Not significant
OAA:	Other amino acids, not classically related to Hartnup disorder
(O)MIM:	(Online) Mendelian Inheritance in Man
PA:	Propionic acidemia/aciduria
PCC:	Propionyl-CoA carboxylase
P:E ratio	Protein-to-energy ratio
PKU:	Phenylketonuria
pLI:	Probability of intolerance to loss of function
PLS-DA:	Partial Least Squares Discriminant Analysis
PNG:	Peptide: <i>N</i> -glycanase
Pol II:	RNA polymerase II complex
PY:	Patient year
(r)AAV:	(Recombinant) adenoassociated virus
RDA:	Recommended daily allowances
REE:	Resting energy expenditure
ROS:	Reactive oxygen species
RR:	Reference range
RSD:	Relative standard deviation
<i>S. cerevisiae</i>	<i>Saccharomyces cerevisiae</i>
SCT:	Stem cell transplantation
SD:	Standard deviation
sILC:	Stable isotope-labeled compounds
TMLHE:	Trimethyllysine hydroxylase
TT:	Therapy target
vitB12:	Vitamin B12
VUS:	Variant(s) of unknown significance
WES:	Whole-exome sequencing
WGS:	Whole-genome sequencing
WHO:	World Health Organization
WT:	Wild-type
YPD:	Yeast peptone dextrose

LIST OF PUBLICATIONS

- **Haijes HA**, Jans JJM, van der Ham M, van Hasselt PM, Verhoeven-Duif NM. Understanding acute metabolic decompensation in propionic and methylmalonic acidemias: a deep metabolic phenotyping approach. *Orphanet J Rare Dis.* 2020;15(1):68.
- **Haijes HA**, van der Ham M, Prinsen HCMT, Broeks MH, van Hasselt PM, de Sain-van der Velden MGM, Verhoeven-Duif NM, Jans JJM. Untargeted metabolomics for metabolic diagnostic screening with automated data interpretation using a knowledge-based algorithm. *Int J Mol Sci.* 2020;21:3.
- **Haijes HA**, Prinsen HCMT, de Sain-van der Velden MGM, Verhoeven-Duif NM, van Hasselt PM, Jans JJM. Accurate discrimination of Hartnup disorder from other aminoacidurias using a diagnostic ratio. *Mol Genet Metab Rep.* 2019; eCollection March 2020.
- **Haijes HA**, Molema F, Langeveld M, Janssen MC, Bosch AM, van Spronsen F, Mulder MF et al. Retrospective evaluation of the Dutch pre-newborn screening cohort for propionic acidemia and isolated methylmalonic acidemia: What to aim, expect, and evaluate from newborn screening? *J Inherit Metab Dis.* 2019; *Epub ahead of print.*
- **Haijes HA**, Jaeken J, van Hasselt PM. Hypothesis: could determining phenotypic specificity facilitate understanding of pathophysiology in rare genetic disorders? *J Inherit Metab Dis.* 2019. *Epub ahead of print.*
- **Haijes HA**, Willemsse EAJ, Gerrits J, van der Flier WM, Teunissen CE, Verhoeven-Duif NM, Jans JJM. Assessing the pre-analytical stability of small-molecule metabolites in cerebrospinal fluid using direct-infusion metabolomics. *Metabolites* 2019;9:10.
- **Haijes HA**, Koster MJE, Rehmann H, Li D, Hakonarson H, Cappucio G, Hancarova M et al. *De novo* heterozygous *POLR2A* variants cause a neurodevelopmental syndrome with profound infantile-onset hypotonia. *Am J Hum Genet.* 2019;105(2):283-301.
- **Haijes HA**, de Sain-van der Velden MGM, Prinsen HCMT, Willems AP, van der Ham M, Gerrits J, Couse MH et al. Aspartylglycosamine is a biomarker for NGLY1-CDDG, a congenital disorder of deglycosylation. *Mol Genet Metab.* 2019;127(4):368-372.
- **Haijes HA**, Jans JJM, Tas SY, Verhoeven-Duif NM, van Hasselt PM. Pathophysiology of propionic and methylmalonic acidemias. Part 1: Complications. *J Inherit Metab Dis.* 2019;42(5):730-744.
- **Haijes HA**, van Hasselt PM, Jans JJM, Verhoeven-Duif NM. Pathophysiology of propionic and methylmalonic acidemias. Part 2: Treatment strategies. *J Inherit Metab Dis.* 2019;42(5):745-761.
- **Haijes HA**, van der Ham M, Gerrits J, van Hasselt PM, Prinsen HCMT, de Sain-van der Velden MGM, Verhoeven-Duif NM, Jans JJM. Direct-infusion based metabolomics unveils biochemical profiles of inborn errors of metabolism in cerebrospinal fluid. *Mol Genet Metab.* 2019;127(1):51-57.
- **Haijes HA**, Willemsen M, van der Ham M, Gerrits J, Pras-Raves ML, Prinsen HCMT, van Hasselt PM, de Sain-van der Velden MGM, Verhoeven-Duif NM, Jans JJM. Direct-infusion based non-quantitative metabolomics identifies metabolic disease in patients' dried blood spots and plasma. *Metabolites* 2019;9:12.
- **Haijes HA**, Jaeken J, Foulquier F, van Hasselt PM. Hypothesis: Lobe A (COG1-4)-CDG causes a more severe phenotype than lobe B (COG5-8)-CDG. *J Med Genet.* 2018;55:137-142.

- **Haijes HA**, van Thiel GJ. Participatory methods in paediatric participatory research: a systematic review. *Pediatr Res.* 2016;79(5):676-83.
- Rymen D, Winter J, van Hasselt PM, Jaeken J, Kasapkara C, Gokçay G, **Haijes HA** et al. Key features and clinical variability of COG6-CDG. *Mol Genet Metab.* 2015;116(3):163-170.
- **Haijes HA**, Prinsen HCMT, Thiel C, Koerner C, Verhoeven-Duif NM, van Hasselt PM. Expanding the clinical phenotype of COG6 deficiency. *J Med Genet.* 2014;51(6):425.

DANKWOORD

Slechts één naam op de voorkant, maar wat is promoveren een team effort! Gelukkig staan van velen van jullie de namen wel op de artikelen die we samen geschreven hebben. Ik wil iedereen die bijgedragen heeft aan al het werk dat we samen verzet hebben bedanken. Ik ben ontzettend blij met wat we hebben bereikt, maar ik vind het ook erg jammer dat het afgelopen is, want ik heb er ontzettend van genoten!

Allereerst een woord van dank voor de leescommissie: prof. dr. Peter van Tintelen, prof. dr. Saskia van Mil, prof. dr. Manon Benders, prof. dr. Dirk Lefeber en prof. dr. Tom de Koning. Dank dat jullie de tijd genomen hebben om mijn proefschrift te lezen en te beoordelen. Ik ben benieuwd naar jullie vragen en kijk uit naar de discussies die we zullen hebben tijdens de verdediging.

Nanda, dank voor alle kansen en mogelijkheden die ik van je heb gekregen vanaf het eerste moment dat ik bij jullie de afdeling op stapte. Dank, dat ik zo verschrikkelijk veel van jullie allemaal heb mogen leren. Ik had me geen betere promotieplek kunnen wensen en ik had me geen betere promotor kunnen wensen. Ik stapte met diep ontzag de eerste keer de kamer van “de professor” binnen, en ik heb je leren kennen als een warme en aandachtige promotor, een hele goede en kritische wetenschapper en een leidinggevende met oog voor iedereen. Ik zou graag, op velerlei manieren, in je voetsporen treden!

Peter, dank voor je begeleiding. Je gaf me een kans binnen het onderzoek toen ik als derdejaars student werd “aangeprezen” als “wel enthousiast, maar nog veel te leren” en liet me vrij om zelf uit te vogelen wat wetenschap eigenlijk is. Je bracht me bij de afdeling metabole diagnostiek, omdat je dacht dat dat wel een goede plek voor me zou zijn, en wat had je daar gelijk in! Ik ben blij dat we de afgelopen jaren samen opgetrokken zijn. Ik werd soms wel een beetje zenuwachtig als iets bijna af was en jij binnen liep of belde: “ik heb een goed idee”, en ik heb er ook wel eens van gebaald als het inderdaad écht een goed idee bleek en dat betekende dat ik alles opnieuw moest doen. Toch had ik je creativiteit en goede ideeën voor geen goud willen missen, en wist ik ook naar wie ik toe wilde als ik zélf een goed idee had. Ik waardeer je enthousiasme voor nieuwe inzichten en hoe je iedereen meekrijgt in je ideeën. Ik hoop nog veel van je te leren!

Judith, dank voor alles. Ik bewonder wie je bent als wetenschapper, als persoon, als collega. Ik bewonder je enthousiasme, je interesse en dat je de spanning van het wachten op de resultaten écht deelt. Je wist altijd precies wat ik nodig had, qua begeleiding en qua feedback. Altijd duidelijk, dat was in het begin even wennen, maar heb ik ontzettend gewaardeerd, ik wist precies wat ik aan je had (heel veel!). Dank voor je steun, voor je gezelligheid, voor je interesse ook in als er privé iets speelde. Dank voor de ruimte die ik kreeg, voor dat ik altijd bij je binnen kon lopen, voor duidelijke antwoorden op vragen, of gewoon voor het kletsen over schoolreisjes of paaseitjes verstoppertje. Ik ga je missen.

Lisan en Paul, dank voor wie jullie zijn en voor wat jullie hebben gemaakt van het Alexandre Suerman stipendium. Lisan, ik heb genoten van elke masterclass en intervisie, en ik heb er ontzettend veel van geleerd. Dank dat ik altijd naar je toe kon komen. Paul, dank voor je kritische blik op onze voortgang, en voor de gezellige alumniborrels! Anneloes, dank voor

de gezellige samenwerking in het bouwen van de website en het organiseren van de borrels. Willemiek, Nicola, Zonne, Rob, Eelco, Jasmijn, Anneloes, Mimount, Tobias, Wouter, Suze, Maartje, Marijke, Floris en Arjan, dank voor jullie aanmoediging, inspiratie en gezelligheid tijdens de masterclasses en interviews. Dank voor het delen van de struggles en het delen van de successen! Ik had dit niet willen missen!

Jeroen en Tom, dank voor het in de gaten houden van mijn voortgang. Dank dat jullie op de achtergrond beschikbaar waren, het was een geruststelling te weten dat ik op jullie terug kon vallen als dat nodig was geweest.

Maria, dank voor al je werk! Voor het opzetten en optimaliseren van de metabolomics methode, de eindeloze hoeveelheid samples die je hebt geanalyseerd, het samen nadenken over de kwaliteitseisen, dat je beschikbaar was om het draaien van de bioinformatica pijplijn over te nemen, voor je geduld en je inzet toen ik je heel veel nieuwe dingen mocht leren. Ik vond het leuk en gezellig met je en ook al geloof je het niet, zonder jou was het écht niet gelukt. Voor mij was jij onmisbaar!

Mia en Marcel, dank voor jullie werk aan de bioinformatica pijplijn voor de metabolomics methode. Dank voor het wegwijs maken in de wereld van de bioinformatica, en voor jullie hulp wanneer het niet lukte. Martin, dank dat je verscheen toen het heel erg nodig was. Marten en Nienke, dank dat jullie het werk hebben voortgezet en verder optimaliseren. Ik vind het ontzettend tof dat we samen verder (hebben) kunnen werken aan de definitieve inbedding van metabolomics in de diagnostiek!

Berthil en Monique, ik wil jullie bedanken dat ik altijd binnen mocht lopen voor wat biochemische bijscholing. Dank voor jullie kritische blik op het werk dat ik deed, en voor jullie hulp, inzicht en kennis bij het ontrafelen van problemen of het uitdenken van hypotheses. Anke, ik vind het gezellig dat jij er nu ook bent, dank voor je frisse inzichten!

Lieve collega's van de afdeling metabole diagnostiek, dank dat ik me zo thuis mocht voelen bij jullie! Mirjam, bedankt voor het leren kweken, jammer dat mijn enige echte lab-project niets is geworden, maar ik vond het wel erg leuk! Suzana en Astrid, dank voor het eindeloos bij elkaar zoeken van alle samples. Arda, dank voor alle ondersteuning die je hebt geleverd en voor je vrolijkheid en bemoedigende woorden. Johan, Birgit en Melissa, ik ben jullie ook veel dank verschuldigd voor het analyseren van alle samples! Johan, jou wil ik ook graag bedanken voor je assistentie bij het maken van de foto's voor dit proefschrift! Ik vind dat ze erg mooi geworden zijn, dank daarvoor! Ruben, Lynne, Jolita, Melissa, Marjolein, Fried, Denise, Sanne en Glen, dank voor de leuke, zinvolle en gezellige researchbesprekingen, ik vond het leuk om jullie mee te nemen in wat ik aan het doen was en ik vond het nog leuker om te horen waar jullie mee bezig waren! Aafke, Eduard, Jeanette, Jolita, Loek, Marit en Suzan: dank voor de gezelligheid op de kamer. Samen kwamen we de dagen goed door, ook toen het daglicht "uit" ging! Aan iedereen: dank voor jullie gezelligheid tijdens de koffie, lunch, de speciale paas-, herfst-, kerst- of zomerlunches, de kerst- of nieuwjaarsborrel, tijdens het maken van de fimpjes of gewoon tussendoor. Ik had me geen betere werkplek kunnen wensen!

Jaak, ik was er tijdens mijn stage bij Peter al erg van onder de indruk dat ik mocht samenwerken met degene die in 1980, twaalf jaar voor ik geboren werd, al publiceerde over CDG, dat eerst “Jaeken syndrome” werd genoemd. Ik heb uw kritische commentaar en bemoedigende woorden zeer gewaardeerd, en ik ben blij met het resultaat!

Femke en Monique, dank voor de samenwerking! Samen hebben we heel veel kennis en inzicht gegenereerd over propion- en methylmalonacidemie in Nederland. Femke, het was fijn dat we deze enorme hoeveelheid (monniken)werk konden (ver)delen. Ik ben trots op wat we samen bereikt hebben! Ook dank aan de internisten en kinderartsen metabole ziekten, fijn dat wij jullie patiënten in kaart konden brengen en dank voor jullie bijdrage! Uiteraard gaat mijn dank ook uit naar de patiënten en hun ouders. Zonder jullie vertrouwen in ons onderzoek en toestemming voor het lezen van jullie dossiers, was dit niet gelukt.

Eline en Charlotte, dank voor het inschakelen van Nanda bij jullie stabiliteitsstudies. Ik vond het leuk dat ik met jullie mocht samenwerken en ben trots op het resultaat dat we samen hebben neergezet.

Frank, Bram en Simone, ook jullie bedankt voor jullie bijdragen aan dit proefschrift. Ik vond het leuk jullie te begeleiden en ik wens jullie veel succes met jullie carrières!

A big thanks to the co-authors of the other papers, through inspiring collaborations we were able to add some beautiful work to the metabolic/genetic field.

Leden van de ESN, fietsers van de Stofwisseltour, en in het bijzonder Leo, Hans, Henk en Herman, ik vond het een feest jullie te leren kennen en met jullie Nederland rond te fietsen! Tof om te zien hoe jullie ook in je vrije tijd toegewijd zijn om stofwisselingsziekten onder de aandacht te brengen, een mooi voorbeeld!

Tot slot, dank aan alle lieve vrienden om ons heen. Dank voor de mooie vriendschappen, al opgebouwd in Beekbergen en Apeldoorn of later in Utrecht, en inmiddels voortgezet door heel Nederland. Dank voor de eindeloze koppen thee en oneindige hoeveelheid spelletjes. Dank voor alle etentjes, dagjes uit en weekendjes weg. We genieten van deze mooie vriendschappen. Dit blijven we voortzetten!

Rozemarijn en Anouk, lieve paranimfen, en ook jullie wederhelften Maarten en Jos, dank voor wie jullie zijn. Er is altijd een reden om samen te eten, te varen, of erop uit te trekken. Roos en Anouk, dank dat jullie aan een paar woorden genoeg hebben. We hebben dezelfde ambities en dromen, en ook dezelfde twijfels. Dank voor jullie meeleven, jullie luisterend oor, jullie goede ideeën en jullie steun. Ik ben blij dat jullie naast me staan.

Veel dank aan het thuisfront. Dank aan mijn lieve ouders en schoonouders voor hun aandacht en zorg voor mij en voor de hele familie. Lieve pap, dank voor de biologielessen, de kritische blik en het doorzetten om iets te leren, al is het de hele encyclopedie. Lieve mam, dank voor je voorbeeld in het hebben van zorg en aandacht voor de mensen om ons heen, in werk of in privésituaties. De bioloog en de mensenmens maken mij tot de persoon, wetenschapper en dokter die ik ben! Anne en Karin, lieve pap en mam, dank voor jullie voorbeeld, in hoe toegewijd je kunt zijn aan datgene waaraan je je verbonden hebt.

Ik heb grote bewondering voor hoe jullie in het leven staan. Anika, grote zus, dank voor je voorbeeld, de drive van vroeger om ook te kunnen wat jij kunt heb ik altijd vast gehouden. Ik bewonder je ambitie en je lef om je eigen pad te kiezen, en hoe je dat ook ogenschijnlijk probleemloos altijd voor elkaar krijgt. Veel dank ook voor de schitterende cover die je voor me hebt ontworpen, en voor je hulp bij de verdere vormgeving van dit proefschrift! Rik, broertje, dank voor je eeuwige vrolijkheid die me altijd weer blij maakt, je kunt overal een grap van maken (en lacht er zelf in elk geval altijd hard om) en zorgt ervoor dat ik niet te serieus word. Jeroen, Maaïke, Nienke en ook Wouter, wat heb ik er leuke (bonus)broers en zussen bij gekregen! Ik ben ontzettend blij met alle dingen die we samen doen, van whiskeyproeverijen en concerten tot vakanties in Drenthe of op de fiets en op de ski's. Kyara, Jimmie en Sylvano, dank voor jullie gezelligheid en voor alle logeerpartijtjes! Ik ben blij dat ik jullie grote zus mag zijn.

Wouter, ja, wat kan ik zeggen. Dank voor alles, voor wie je bent, voor wie je voor mij bent. Zonder jou was dit nooit zo leuk geweest. Ik geniet elke dag het meest van jou, en nu ook van onze kleine Joas, en ik hoop dat nog heel lang te mogen doen.

CURRICULUM VITAE



Hanneke Haijes (Siepel) was born in Beekbergen on the 11th of March in 1992. She grew up in Beekbergen, with an older sister and a younger brother. Being the daughter of a professor in biology and a dedicated youth health care worker, Hanneke's enthusiasm for fundamental research (how does the world work) and youth health care (how do we care for our children) were combined in a fascination for pediatrics. Hanneke graduated from "CSG de Heemgaard" in 2010 (cum laude). In the same year she started her Medicine studies at the Utrecht University. As a student she joined the both the Honours Program Bachelor and Master, which she successfully completed. Being intrigued by pathophysiology (the development of disease), her research during the Master's phase was focused on genotype-phenotype correlation in COG6-CDG, a rare inborn error of metabolism, under the supervision of dr. Peter van Hasselt. Her graduation research was on the design of a

metabolomics workflow, a new tool providing opportunities to study inborn errors of metabolism in more detail. She performed this research under the supervision of dr. Judith Jans and prof. dr. Nanda Verhoeven-Duif. Hanneke graduated from her Master's study in 2016 (cum laude), and she received two awards for her Master's thesis. Hanneke was granted an Alexandre Suerman scholarship, which gave her the opportunity to combine pathophysiological research and metabolomics research during a PhD at the metabolic diagnostic laboratory, under the supervision of dr. Peter van Hasselt, dr. Judith Jans and prof. dr. Nanda Verhoeven-Duif. During her PhD, Hanneke completed her training from the Graduate School of Life Sciences in the program "Cancer, Stem Cells and Developmental Biology". The result of her PhD, on different approaches for increasing pathophysiological insights in inborn errors of metabolism, are presented in this thesis. With her unwavering passion for pathophysiology, Hanneke pursues a career in child health, aiming to combine clinical care and pathophysiological research for pediatric patients.

